IFERP®
connecting engineers... developing research

ICRCEST-2021

VIRTUAL CONFERENCE

INTERNATIONAL CONFERENCE ON

RECENT CHALLENGES IN ENGINEERING SCIENCE AND TECHNOLOGY

09th - 10th April 2021

Organized By

Department of Electronics & Communication Engineering

Ramachandra College of Engineering, Eluru, AP

in Association with

Institute For Engineering Research and Publication (IFERP)

ISBN : 978-93-90214-20-4

ICRCEST 2K21

International Conference on Recent Challenges in Engineering Science and Technology

Virtual Conference

Andhra Pradesh, India

09th - 10th April, 2021

Organized By

Department of Electronics and Communication Engineering,
Ramachandra College of Engineering, Eluru,
Andhra Pradesh, India

in Association with

Institute For Engineering Research and Publication (IFERP)

Publisher: IFERP Explore

Rudra Bhanu Satpathy
Chief Executive Officer
Institute For Engineering Research and Publication.

Message

On behalf of **Institute For Engineering Research and Publication (IFERP)** in association with **Ramachandra College of Engineering, Eluru, AP, India.** I am delighted to welcome all the delegates and participants around the globe to **Ramachandra College of Engineering, Eluru, AP, India** for the **"International Conference on Recent Challenges in Engineering Science and Technology (ICRCEST 2K21)"** Which will take place from **09th-10th April, 2021.**

It will be a great pleasure to join with Engineers, Research Scholars, academicians and students all around the globe. You are invited to be stimulated and enriched by the latest in engineering research and development while delving into presentations surrounding transformative advances provided by a variety of disciplines.

I congratulate the reviewing committee, coordinator **(IFERP & RCE)** and all the people involved for their efforts in organizing the event and successfully conducting the International Conference and wish all the delegates and participants a very pleasant stay at **Eluru, Andhra Pradesh, India**

Sincerely,

Rudra Bhanu Satpathy

Preface

The **"International Conference on Recent Challenges in Engineering Science and Technology (ICRCEST 2K21)"** is being Organized jointly by **Department of Electronics and Communication Engineering, Ramachandra College of Engineering, Eluru, AP, India** in Association with **IFERP-Institute For Engineering Research and Publication** on the 09^{th} –10^{th} April, 2021.

Ramachandra College of Engineering, Eluru has a sprawling student – friendly campus with modern infrastructure and facilities which complements the sanctity and serenity of the major city of Guntur in Andhra Pradesh.

The **"International Conference on Recent Challenges in Engineering Science and Technology (ICRCEST 2K21)"** was a notable event which brings Academia, Researchers, Engineers, Industry experts and Students together.

The purpose of this conference is to discuss applications and development in area of **"Recent Challenges in Engineering Science and Technology"** which were given International values by **Institute for Engineering Research and Publication (IFERP).**

The International Conference attracted over 130 submissions. Through rigorous peer reviews 63 high quality papers were recommended by the Committee. The Conference aptly focuses on the tools and techniques for the developments on current technology.

We are indebted to the efforts of all the reviewers who undoubtedly have raised the quality of the proceedings. We are earnestly thankful to all the authors who have contributed their research works to the conference. We thank our Management for their wholehearted support and encouragement. We thank our Principal for his continuous guidance. We are also thankful for the cooperative advice from our advisory Chairs and Co-Chairs. We thank all the members of our local organizing Committee, National and International Advisory Committees.

ICRCEST 2K21

ICRCEST 2K21

International Conference on Recent Challenges in Engineering Science and Technology

Andhra Pradesh, India - 09th-10th April, 2021

Organizing Committee

CHIEF PATRON

Sri Ganta Ramachandra Rao
Chairman, Ramachandra College of Engineering, Eluru, AP

Prof. Sri K.Venu Gopal
Secretary, Ramachandra College of Engineering, Eluru, AP

PATRON

Prof. Sri DrDola Sanjay S
Principal, Ramachandra College of Engineering, Eluru, AP

CONVENERS

Prof. Dr. L Bharathi
HOD – ECE, Ramachandra College of Engineering, Eluru, AP

COORDINATORS

Prof. Mr J Prasanth Kumar
Associate Professor – ECE, Ramachandra College of Engineering, Eluru, AP

Prof. Mr R Durga Prasad
Associate Professor – ECE, Ramachandra College of Engineering, Eluru, AP

STEERING COMMITTEE MEMBERS

Prof. Dr S Jagan Mohan Rao
Professor – ECE, Ramachandra College of Engineering, Eluru, AP

Prof. Dr. N SangeethaPriya
Associate Professor – ECE, Ramachandra College of Engineering, Eluru, AP

Prof.Dr V Surya Narayana
Professor – CSE, Ramachandra College of Engineering, Eluru, AP

Prof. Dr S JayaLakshmi
Professor – EEE, Ramachandra College of Engineering, Eluru, AP

Prof. Dr J Ranga
Professor – EEE, Ramachandra College of Engineering, Eluru, AP

Prof. Dr Shameena Begum
Professor – CSE, Ramachandra College of Engineering, Eluru, AP

NATIONAL ADVISORY COMMITTEE

Dr. D. Muruganandam
Principal, Department Of Mechanical Engineering, Sri Venkateswaraa College of Technology, Chennai, Tamil Nadu, India

Dr. K.B.V.S.R. Subrahmanyam
Dean & Professor, Department Of Electrical And Electronics Engineering, DNR College of Engineering and Technology, Bhimavaram, Andhra Pradesh, India

Dr. M. Vijaya Sekhara Babu
Dean & Professor, Department Of Mechanical Engineering, Godavari Institute Of Engineering And Technology, Rajahmundry, Andhra Pradesh, India

Dr. Mahesh Kr. Porwal
Dean & Professor, Department Of Electronics And Communication Engineering, Sree Chaitanya College Of Engineering, Karimnagar, Telangana, India

Dr. N. Kumaraswamy
Dean & Professor, Department Of Civil Engineering, Vasireddy Venkatadri Institute of Technology, Guntur, Andhra Pradesh, India

Dr Abdul Majid
Professor & Head, Department Of Computer Science And Engineering, Dr. Sri Shivkumara Mahaswamy College Of Engineering, Bangalore, Karnataka, India

Dr K. Balaji
Professor & Head, Department Of Computer Applications, Surana College, Bangalore, Karnataka, India

INDEX

INDEX

INDEX

INDEX

INDEX

INDEX

INDEX

INDEX

ICRCEST 2K21

International Conference on Recent Challenges in Engineering Science and Technology

Andhra Pradesh, India

09th - 10th April, 2021

ABSTRACTS

ICRCEST 2K21

Organized By

Ramachandra College of Engineering, Eluru, AP, India

in Association with

Institute For Engineering Research and Publication (IFERP)

An Artificial Neural Network-Based System for the Classification of Ripeness State of Fruits

[1] Rajitha Laxmi CH, [2] V Naresh, [3] Y Lavanya, [4] N Srikanth, [5] Y Naveen Kumar

[1][2][4] Assistant Professor, Dept. of ECE, Rama Chandra College of Engineering, Eluru, AP, India
[3][4] Associate Professor, Dept. of ECE, Rama Chandra College of Engineering, Eluru, AP, India

Abstract:

The quality of fresh banana fruit is a main concern for consumers and fruit industrial companies. The effectiveness and fast classification of bananas maturity stage are the most decisive factors in determining its quality. It is necessary to design and implement image processing tools for correct ripening stage classification of the different fresh incoming banana bunches. Ripeness in banana fruit generally affects the eating quality and the market price of the fruit. In this paper, an automatic computer vision system is proposed to identify the ripening stages of bananas. First, a four- class homemade database is prepared. Second, with the help of raspberry-pi we and image processing technique we can find the freshness of the fruit. After purchasing we have to cut the fruit and keep it in one bowl by sending the fresh air into it we should have to measure the freshness of the fruit. an artificial neural network-based framework which uses color, development of brown spots, and Tamura statistical texture features is employed to classify and grade banana fruit ripening stage.

Keywords:

Raspberry-Pi, LCD, Buzzer, Gas Sensors, Air Pumps, Relay boards

1. INTRODUCTION

Banana is one of the most consumed fruits globally. It contributes about 16% of the worlds fruit production according to FAO. Maturity stage of fresh banana fruit is a principal factor that affects the fruit quality during ripening and market ability after ripening. The ability to identify maturity of fresh banana fruit will boost farmers to optimize harvesting phase which helps to avoid harvesting either over-matured or under-matured banana. Early in the ripening process ,the banana fruit synthesizes compounds such as alkaloid sand tannins. These fight infections and cause the under-ripe banana fruit to taste bitter and astringent. As banana fruit continues to grow, its storage cells expand, engorging it with water, sugars, starches, organic acids, vitamins, and minerals, and its skin turns from green to yellow with brown spots. Starch and acid contents decrease, while sugar content increases, and alkaloids and tannins disappear. Aromas develop as the acid and protein composition changes, and the fruits texture softens as the substances that hold up its cell walls begin to break down. All these changes make the banana fruit ripe and ready to eat. Ripening treatment of banana is accomplished globally with controlled humidity, suitable temperature, time, air flow, and using ethylene gas. To ensure the productivity, competitively, quality standards ,and reliability of banana fruit products, automatic image processing tools based upon intelligent techniques are paramount over visual features methods. Such machine vision system has the advantage in making decisions at a very fast rate. This paper is intended first to generate a database for the Egyptian banana species with different ripening levels such as unripe, ripe, and overripe. Then, new efficient ripening level determination algorithms are presented. The proposed techniques are based on HSV color, development of brown spots, and texture analysis of the banana fruit.

2. LITERATURE SURVEY

In the literature, a lot of methods, which depend on shape, size, color, and texture features, have been developed for banana fruit ripening classification. First of these are the color moments and the color histogram [1,2]. The mean and the variance of the RGB, the HSV, and the CIELAB colors paces of the banana fruit intensity histograms are extracted and analyzed. The system was able to correctly predict with more than 94% the seven ripening stages of the banana bunch. The seven ripening stages are the green, the green with traces of yellow, more green than yellow, more yellow than green, green tip and yellow, all yellow, and yellow flecked with brown. Secondly, the third and the fourth statistical moments [3] can be used to classify the under-mature, mature, and over-mature banana fruit classes. The classification accuracy of this technique for the three classes reaches99.1%. The accuracy of the banana fruit ripening classification class depends upon the used preprocessing segmentation algorithm. Segmentation is a vital step for many computer visions tasks. The technology of image segmentation is widely used in medical image processing, fruit industry, face recognition ,pedestrian detection, etc. Discrete wavelet transforms (DWT) and wavelet packet transform (WPT) have proven to be effective in image compression, de-noising, segmentation, and classification [4–6]. They span many disciplines. It is demonstrated that

 ISBN: 978-93-90214-20-4

DWT and WPT could be used for 2Dimages surface segmentation and 3D images volume segmentation [7–11]. Two-dimensional DWT is used as a multi-resolution analysis tool for segmenting and classifying healthy and damaged Fruits while they are moving in a conveyor belt [9,11]. It has demonstrated that DWT distinguishes the healthy green olive fruits from the damaged fruits with accuracy of 90% [9], while the recognizer can identify the healthy brown, light or deep, or the healthy black olive fruits with accuracy of about78% [9]. Texture homogeneity measuring technique, which is based on measuring the degree of homogeneity of adjacent pixels, and the special image convolution algorithm, which uses special kernels or masks to perform image convolution, are another 2D texture feature algorithms for detecting, classifying ,and calculating automatically the external defects of fruits and its area [12]. It is shown that [12] the classification accuracy of these algorithms is higher than the 2D fuzzy C means algorithm by 7%, for the healthy olives, whereas it is higher by 9% for defected olives. Additionally, it is illustrated that 3D DWT and WPT could be used for medical 3D images volume segmentation and for tumor quantification and measurement and thus radio therapy planning and cancer diagnosis [7,8]. Three-dimensional volume segmentation aims at partitioning the voxels into 3D objects (sub-volumes) which represent meaningful physical entities. The 3D wavelet domain detected the objects with better accuracy and reduces the percentage error by several percent more than the traditional 2Dsegmentation techniques [8]. Besides the 3D DWT volume segmentation, unsupervised 3D fuzzy C-means clustering algorithm to extract region of interest, ROI, for objects in3D volumes reveals that the algorithm detects accurately the ROI [13]. Besides DWT, independent component analysis (ICA) is another feature extraction technique for detection and classification[14]. ICA maximizes the absolute value of the normalized kurtosis. It aims at capturing the statistical structure in images that is beyond second-order information, by exploiting higher-order statistical structure in data. It has proven a useful tool for finding structure and changes in fruits images. ICA seeks basis vectors that best fit the variance of the fruits images. In contrast, local binary pattern (LBP) is considered as a high-performance texture features technique [15]. It transforms an image into an array or image of integer labels describing small-scale textures of the image.LBP and its variants produce long histograms, which slowdown the recognition speed. Local gradient code (LGC), which is based on the relationship of neighboring pixels ,is proved to be more stable to local intensity variation, less influenced by local color variation, and more distinctive than LBP [16]. The LGC is able to capture the locally changing gradient information, while LBP is globally invariant, since it only compares the central pixel value with the neighboring pixel value. On the other hand, learning-/trained-based classifiers require an intensive training phase of the classifier parameters ,and hence a higher recognition rate is obtained. Examples are the support vector machine [17] (SVM), the hidden Markov model [16] (HMM), and the artificial neural network [18–22] (ANN).As an application of the supervised classification techniques, it was demonstrated that laser light back scattering imaging (LLBI) with five laser diodes emitting at wavelengths532, 660, 785, 830, and 1060nm could be employed for predicting quality attributes of banana fruit [23,24]. The predicted attributes were chlorophyll, elasticity, and soluble solids content (SSC). A correct classification accuracy of92.5% and 95.5% was claimed using the ANN model and the SVM model, respectively. In [19,20], a computer vision system that uses gray-level co-occurrence matrix (GLCM)texture features is proposed to train an artificial neural network. The system can be used to sort banana at an accuracy of 98.8%. SVMs, HMMs, and ANNs are used for supervised learning tasks and classification. However, deep learning models can be trained in an unsupervised manner for unsupervised learning tasks. Convolutional neural network [18] (CNN) is a class of deep learning neural networks and has acquired a broad application in image classification. It is a powerful visual model that yields hierarchies of features. It is demonstrated that CNN architecture of 17,312 images of bananas produces a classification accuracy of 94.4% [18].In this paper, we propose a novel ANN adapted to fine grained feature-based representation for classifying ripening stages of the Egyptian bananas species. To show the power of the proposed classification system, we create a database,1comprising of 300 Egyptian banana images, with different ripening levels such as unripe (green banana), yellowish green, mid-ripe, and overripe. The proposed scheme makes use of the Tamuras contrast, coarseness, and the direction visual perceptual texture features to correct labeling the data [25,26]. The rest of the paper is organized as follows: Sect. 3 illustrates the basic principles of the proposed system for classifying the different bananas ripening stages. In Sect. 4, the proposed classification system is tested and compared against other supervised classification algorithms, such as SVM, naive Bayes, KNN, decision tree, and discriminant.

3. BLOCK DIAGRAM

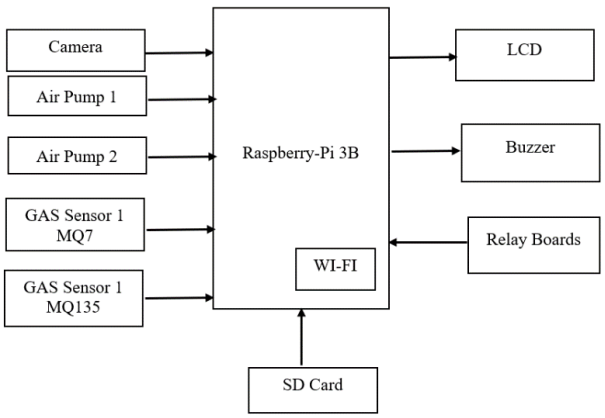

Fig 1.1 Block Diagram

RASPBERRY PI-3

The Raspberry Pi is a progression of little single-board PCs created in the United Kingdom by the Raspberry Pi Foundation to advance the instructing of essential software engineering in schools and in creating nations. The first model wound up much more prominent than foreseen, offering outside its objective market for utilizations, for example, mechanical technology. It does exclude peripherals, (for example, consoles, mice and cases). Be that as it may, a few frills have been incorporated into a few official and informal packs. As indicated by the Raspberry Pi Foundation, more than 5 million Raspberry-Pi were sold by February 2015, making it the top of the line British PC. By November 2016 they had sold 11 million units, and 12.5m by March 2017, making it the third top rated "broadly useful PC". In July 2017, deals came to almost 15 million. In March 2018, deals achieved 19 million. Raspberry Pi 3 Model B was discharged in February 2016 with a 64-bit quad center processor, and has on-load up Wi-Fi, Bluetooth and USB boot capabilities [18]. On Pi Day 2018 model 3B+ showed up with a quicker 1.4 GHz processor and a 3 times speedier system in view of gigabit Ethernet (300 Mbit/s) or 2.4/5 GHz double band Wi-Fi (100 Mbit/s) [1]. Other choices are: Power over Ethernet (POE), USB boot and system boot (a SD card is never again required). This permits the utilization of the Pi in difficult to-achieve places (perhaps without power).

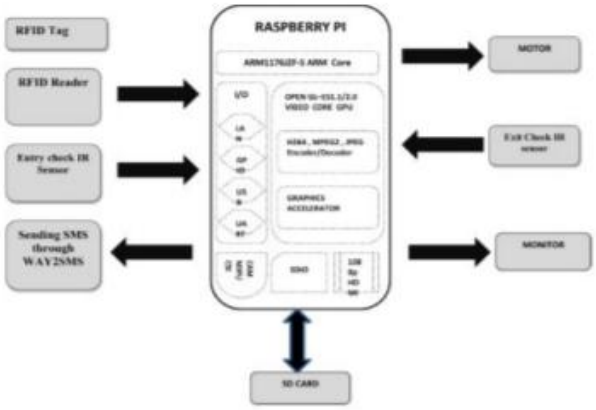

Fig 1.2: Raspberry Pi 3 Based Diagram

IOT

The Internet of Things (IOT) is a system of interrelated devices are digital machines, objects, animals or people that are provided with unique identifiers and the ability to transfer data over a network without requiring human-to-human or human-to-computer interaction

ARM 11 Processor

ARM11 is a group of older 32-bit RISC ARM processor cores licensed by ARM Holdings. The ARM11 core family consists of ARM1136J (F)-S, ARM1156T2 (F)-S, RM1176JZ (F)-S, and ARM11MPCore. Since ARM11 cores were released from 2002 to 2005, they are no longer recommended for new IC designs, instead ARM Cortex-A and ARM Cortex-R cores are preferred.

- ARM stands for Advanced RISC Machine
- The ARM11 is based on the ARMv6 Instruction set architecture
- Bi-endian – can operate in either littleendian or big-endian format
- Most devices today use little-endian
- Actually, uses two instruction sets – the 32-bit ARM and the 16-bit Thumb

ANDROID MOBILE

Android's default UI is primarily in view of direct control, utilizing contact inputs that freely compare to true activities, such as swiping, tapping, squeezing, and invert squeezing to control on-screen objects, alongside a virtual keyboard. Game controllers and full-measure physical consoles are bolstered by means of Bluetooth or USB. The reaction to client include is intended to be prompt and gives a liquid touch interface, frequently utilizing the vibration capacities of the gadget to give haptic criticism to the client. Inward equipment, for example, accelerometers, whirligigs and vicinity sensors are utilized by a few applications to react to extra client activities, for instance altering the screen from picture to scene contingent upon how the gadget is situated, or enabling the client to guide a vehicle in a hustling amusement by pivoting the gadget, reproducing control of a directing wheel. Android gadgets boot to the home screen, the essential route and data "center point" on Android gadgets, practically equivalent to the work area found on PCs. Android home screens are commonly comprised of application symbols and gadgets; application symbols dispatch the related application, while gadgets show live, auto refreshing substance, for example, a climate conjecture, the client's email inbox, or a news ticker straightforwardly on the home screen. A home screen might be comprised of a few pages, between which the client can swipe forward and backward. Outsider applications accessible on Google Play and other application stores can broadly re-subject the home screen, and even copy the look of other working frameworks, for example, Windows Phone. Most producers tweak the look and highlights of their Android gadgets to separate themselves from their rivals. Along the highest point of the screen isa status bar, indicating data about the gadget and its network. This status bar can be "pulled" down to uncover a notice screen where applications show essential data or updates. Warnings are "short, auspicious, and pertinent data about your application when it's not being used", and when tapped, clients are coordinated to a screen inside the application identifying with the notice. Starting with Android 4.1 "Jam Bean", "expandable warnings" enable the client to tap a symbol on the notice with the end goal for it to extend and show more data and conceivable application activities ideal from the notice.

Capturing Module

The Logitech C270 HD Webcam is a high utility device that helps you to enjoy seamless video calling. This device comes with easy installation process that offers a hassle-free set up. The ergonomic design and sleek body helps in saving space and makes it easy to install the webcam on your PC or laptop. The adjustable design makes it easy to tilt and use it according to your needs. It features 'Logitech Fluid Crystal Technology' and has a 3 MP camera which enhances picture quality while the integrated microphone delivers perfect sound quality. It supports video calling and enables you to record videos in HD quality. This webcam comes with Logitech Fluid Crystal Technology that offers high quality video calling. This feature records visuals with complete detailing and allows you to enjoy vivid colors and more depth.

Fig 1.3Capturing Module

Specifications

- HD video calling (1280 x 720 pixels) with recommended system, Video capture: Up to 1280 x 720 pixels
- Logitech Fluid Crystal Technology, Photos: Up to 3.0 megapixels (software enhanced)
- Built-in mic with noise reduction, Hi-Speed USB 2.0 certified (recommended)
- Universal clip fits laptops, LCD or CRT monitors
- You can be heard loud and clear thanks to a built-in microphone that reduces background noise.
- Interface: USB2.0, compatible with USB1.1
- Transmission speed:
- 320*240_25 frames/second
- 640*480_15frames/second
- 2560*1920_15 frames/second
- Imaging Distance: 5CM to infinity
- Built –in image Compression
- Automatic White Balance
- Automatic Color Compression
- Win XP / VISTA/ 7/ 8/ 8.1/ 10 system
- Manual snapshot

MQ137 Gas Sensor

A gas detector is a device that detects the presence of gases in an area, often as part of a safety system. This type of equipment is used to detect a gas leak or other emissions and can interface with a control system so a process can be automatically shut down. A gas detector can sound an alarm to operators in the area where the leak is occurring, giving them the opportunity to leave. This type of device is important because there are many gases that can be harmful to organic life, such as humans or animals. Gas detectors can be used to detect combustible, flammable and toxic gases, and oxygen depletion. This type of device is used widely in industry and can be found in locations, such as on oil rigs, to monitor manufacture processes and emerging technologies such as photovoltaic. They may be used in fire fighting. Gas leak detection is the process of identifying potentially hazardous gas leaks by sensors. Additionally a visual identification can be done using a thermal camera These sensors usually employ an audible alarm to alert people when a dangerous gas has been detected. Exposure to toxic gases can also occur in operations such as painting, fumigation, fuel filling, construction, excavation of contaminated soils, landfill operations, entering confined spaces, etc. Common sensors include combustible gas sensors, photo ionization detectors, infrared point sensors, ultrasonic sensors, electrochemical gas sensors, and metal-oxide-semiconductor sensors (MOS sensors). More recently, infrared imaging sensors have come into use. All of these sensors are used for a wide range of applications and can be found in industrial plants, refineries, pharmaceutical manufacturing, fumigation facilities, paper pulp mills, aircraft and shipbuilding facilities, hazmat operations, waste-water treatment facilities, vehicles, indoor air quality testing and homes.

Fig 1.4 MQ137 Gas Sensor

4. RESULTS

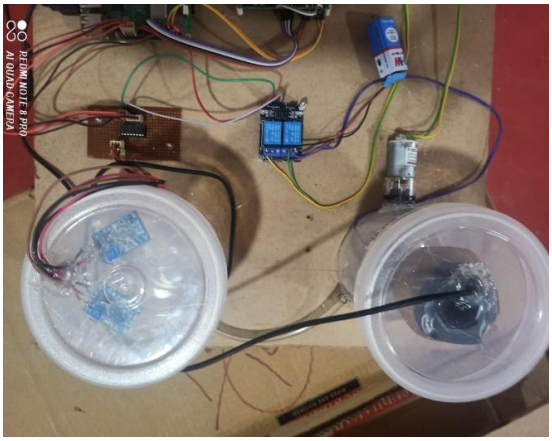

Fig 1.5 Circuit with Vapour measuring sensor

 ISBN: 978-93-90214-20-4

Fig 1.6 Overall circuit

Fig 1.7 Measuring Freshness of the fruit

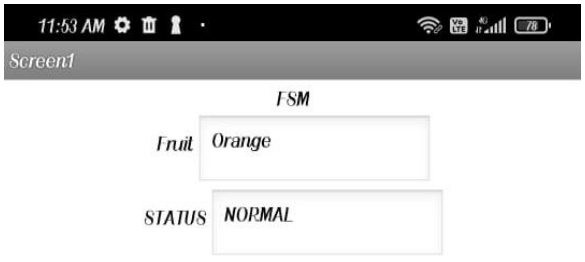

Fig 1.8 status of the fruit

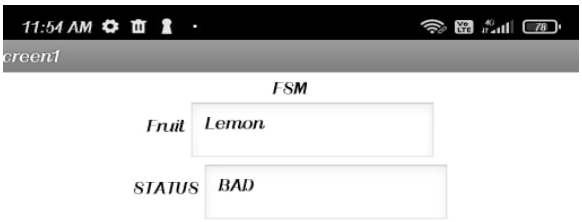

Fig 1.8 Status of unhealthy fruit

Fig1.9 Initializing the system

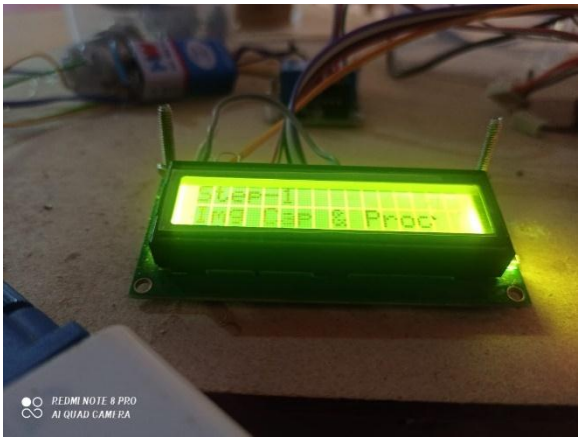

Fig 1.10 Step 1 Procedure

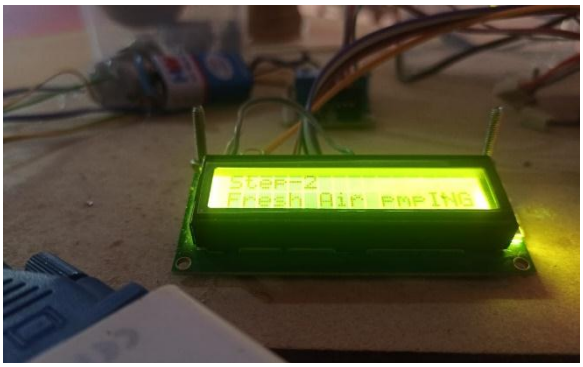

Fig 1.11 Step fresh air pump

 ISBN: 978-93-90214-20-4

Fig 1.12 Step 3 Air to sensor

Fig 1.13 Final Raspberry-pi out put

5. CONCLUSION

An artificial neural network-based system for the classification of ripeness state of banana fruits has been discussed. The proposed model uses Tamura's texture features and anew feature defined as ripening factor to properly discriminate between the four banana fruits classes. The system has optimal performance as compared with other supervised classification algorithms as the SVM, the naive Bayes, the KNN, the decision tree, and the discriminant analysis classifiers. The overall class recognition accuracy of 100% is obtained for the green and over ripen classes, while it is 97.75% for the yellowish green and mid-ripen classes. The simplicity ,the high recognition rate, and the speed of the classification model, 18 s for the 89 test bananas, make it appropriate for implementing a productive and profitable computer vision machine for the food processing industry. Future directions will focus on applying 3D volume segmentation techniques, transfer learning, and deep learning methods to supervised/semi-supervised machine learning algorithms to enhance the classification rate and to minimize the training and the testing run time for banana fruits classification application.

REFERENCE

[1] Mendoza, F.;Dejmek, P.;Aguilera, J.M.: Predicting ripening stages of bananas (Musa cavendish) by computer vision. ActaHortic.682(183), 1363–1370 (2005)

[2] Mendoza, F.; Aguilera, J.M.: Application of image analysis for classification of ripening bananas. J. Food Sci. 69(9), 471–477(2004)

[3] Prabha, D.S.; Kumar, J.S.: Assessment of banana fruit maturity byimage processing technique. J. Food Sci. Technol. 52(3), 1316–1327 (2015). https://doi.org/10.1007/s13197-013-1188-3

[4] AlZubi, S.; Islam, N.; Abbod, M.: Multiresolution analysis usingwavelet, ridgelet, and curvelet transforms for medical image segmentation .J. Biomed.Imaging(2011) .https://doi.org/10.1155/2011/136034

[5] Schelkens, P.; Munteanu, A.; Barbarien, J.; Galca, M.; Giro-Nieto,X.; Cornelis, J.: Wavelet coding of volumetric medical data sets.IEEE Trans. Med. Imaging 22(3), 441–458 (2003)

[6] Alzu'bi, S.; Amira, A.: 3D medical volume segmentation usinghybrid multiresolution statistical approaches. Adv. Artif. Intell.(2010). https://doi.org/10.1155/2010/520427

[7] AlZubi, S.; Sharif, M.S.; Abbod, M.: Efficient implementationand evaluation of wavelet packet for 3D medical image segmentation.In: IEEE InternationalSymposiumonMedicalMeasurementsand Applications(2011). https://doi.org/10.1109/MeMeA.2011.5966667

[8] AlZubi, S.; Jararweh, Y.; Shatnawi, R.: Medical volume segmentationusing 3D multiresolution analysis. In: InternationalConference on Innovations in Information Technology (IIT) (2012)

[9] Nashat, A.A.; Hussain Hassan, N.M.: Automatic segmentationand classification of olive fruits batches based on discrete wavelettransform and visual perceptual texture features. Int. J. WaveletsMultiresolut. Inf. Process. 16(1), 1850003 (2018) .https://doi.org/10.1142/S0219691318500030

[10] Kumar, H.C.S.; Raja, K.B.; Venugopal, K.R.; Patnaik, L.M.: Automaticimage segmentation using wavelets. Int. J. Comput. Sci.Netw. Secur.9(2), 305–313 (2009).

[11] Khoje, S.A.; Bodhe, S.K.; Adsul, A.: Automated skin defectidentification system for fruit grading based on discrete curvelettransform. Int. J. Eng. Technol. 5(4), 3251–3256 (2013)

[12] Hussain Hassan, N.M.; Nashat, A.A.: New effective techniquesfor automatic detection and classification of external olive fruitsdefects based on image processing techniques. Multidimens.Syst. SignalProcess.(2018). https://doi.org/10.1007/s11045-018-0573-5

[13] Al-Zu'bi, S.; Al-Ayyoub, M.; Jararweh, Y.; Shehab, M.A.:Enhanced 3D segmentation techniques for reconstructed 3D medicalvolumes: robust and accurate intelligent system. Proc. Comput.Sci. 113, 531–538 (2017)

[14] Déniz, O.; Castrillon, M.; Hernández, M.: Face recognition usingindependent component analysis andsupportvectormachines.PatternRecogn.Lett.24(13), 2153–2157 (2003)

[15] Zhao, G.; Pietikainen, M.: Dynamic texture recognition using localbinary patterns with an application to facial expressions. IEEETrans. Pattern Anal. Mach. Intell. 29(6), 915–928 (2007)

[16] Nashat, A.A.: Facial expression recognition using best tree RDLGPencoded features and HMM. Int. J. Wavelets Multiresolut.Inf. Process. 16(6), 1850047 (2018) .https://doi.org/10.1142/S0219691318500479

[17] Juncai, H.; Yaohua, H.; Lixia, H.; Kangquan, G.; Satake, T.: Classificationof ripening stages of bananas based on support vectormachine. Int. J. Agric. Biol. Eng. 8(6), 99–103 (2015)

[18] Zhang, Y.; Lian, J.; Fan, M.; Zheng, Y.: Deep indicator for finegrainedclassification of banana's ripening stages. EURASIP J.Image Video Process.46, 1–10 (2018). https://doi.org/10.1186/s13640-018-0284-8

[19] Olaniyi, E.O.; Adekunle, A.A.; Odekuoye, T.; Khashman, A.:Automatic system for grading banana using GLCM texture featureextraction and neural network arbitrations. J. Food Process Eng. 40(4), 1–10 (2017)

[20] Olaniyi, E.O.; Oyedotun, O.K.; Adnan, K.: Intelligent grading systemfor banana fruit using neural network arbitration. J. FoodProcess Eng. 40, 1–9 (2017). https://doi.org/10.1111/jfpe.12335

[21] Espinoza, E.M.L.; Duran, M.T.; Morales, R.A.L.; Yepez, E.C.;Robles,N.S.: Determination of the ripeness state of guavas using anartificial neural network. Res. Comput. Sci. 121, 105–111 (2016)

[22] Sabzi, S.; Gilandeh,Y.A.;Mateos, G.G.:Anewapproach for visualidentification of orange varieties using neural networks and metaheuristicalgorithms. Inf. Process. Agric. 5, 162–172 (2018)

[23] Adebayo, S.E.; Hashim, N.; Abdan, K.; Hanafi, M.; Mollazade,K.: Prediction of quality attributes and ripeness classification ofbananas using optical properties. Sci. Hortic.212, 171–182 (2016)

[24] Adebayo, S.A.; Hashim, N.; Abdan, K.; Hanafi, M.; Zude-Sasse,M.: Prediction of banana quality attributes and ripeness classificationusing artificial neural network. In: ActaHorticulturae,Proceedings of the III InternationalConference on Agricultural andFood Engineering, pp. 335–343 (2017). https://doi.org/10.17660/ActaHortic.2017.1152.45

[25] Bagri, N.; Johari, P.: A comparative study on feature extractionusing texture and shape for content-based image retrieval. Int. J.Adv. Sci. Technol. 80, 41–52 (2015)

[26] Kebapci, H.; Yanikoglu, B.; Unal, G.: Plant image retrieval usingcolor, shape, and texture features. Comput. J. 54(9), 1475–1490(2011).

Smart Agricultural System Analysis Using IoT

[1] Velivela Naresh, [2] Rajitha Lakshmi CH, [3] Y Naveen Kumar, [4] P Bhuvana Sri

[1][2][3][4] Assistant Professor, ECE, Ramachandra College Of Engineering Eluru, AP, India

Abstract:

Agriculture based IOT is considered as one of the major sources in maintaining a nation's GDP. Many countries are interested on cultivation to improve their economic wealth. Now a day's technology plays a major role in the agriculture sector. The latest technology has the capability to improve various cultivation phases like watering, fertilizing, harvesting etc.., To make the cultivation phases easier, we deploy smart sensors in the fields to sense the water level, photo sensors to ensure sufficient sunlight is available for plant's growth, sensors to sense the nitrogen content and thereby to inform the farmer to initiate steps for proper fertilizing, etc. There are so many works has been done in this area, and much more is progressing in the labs now. We analyze the various standard IoT techniques used in Agriculture sector based on hardware and software so that deriving the existing challenges for making farming much smarter and efficient.

Keywords:

Agricultural, IoT

1. INTRODUCTION

1.1 Introduction

India is the country of village and agriculture plays an important role for development of country. In our country, agriculture depends on the monsoons which has insufficient source of water. So, the irrigation is used in agriculture field. In Irrigation system, depending upon the soil type, water is provided to plant. In agriculture, two things are very important, first to get information of about the fertility of soil and second to measure moisture content in soil. Nowadays, for irrigation, different techniques are available which are used to reduce the dependency of rain. And mostly this technique is driven by electrical power and on/off scheduling. In this technique, water level indicator placed in water reservoir and soil moisture sensors are placed root zone of plant and near the module and gateway unit handles the sensor information and transmit data to the controller which in turns the control the flow of water through the valves.

To improve the agricultural yield with fewer resources and labor efforts, substantial innovations have been made throughout human history. Nevertheless, the high population rate never let the demand and supply match during all these times. According to the forecasted figures, in 2050, the world population is expected to touch 9.8 billion, an increase of approximately 25% from the current figure [1]. Almost the entire mentioned rise of population is forecasted to occur among the developing countries [2]. On the other side, the trend of urbanization is forecasted to continue at an accelerated pace, with about 70% of the world's population predicted to be urban until 2050 (currently 49%) [3]. Furthermore, income levels will be multiples of what they are now, which will drive the food demand further, especially in developing countries. As a result, these nations will be more careful about their diet and food quality; hence, consumer preferences can move from wheat and grains to legumes and, later, to meat. In order to feed this larger, more urban, and richer population, food production should double by 2050. Particularly, the current figure of 2.1 billion tons of annual cereal production should touch approximately 3 billion tons, and the annual meat production should increase by more than 200 million tons to fulfill the demand of 470 million tons.

Not only for food, but crop production is becoming equally critical for industry; indeed crops like cotton, rubber, and gum are playing important roles in the economies of many nations. Furthermore, the food-crops-based bioenergy market started to increase recently. Even before a decade, only the production of ethanol utilized 110 million tons of coarse grains (approximately 10% of the world production). Due to the rising utilization of food crops for bio-fuel production, bio-energy, and other industrial usages, food security is at stake. These demands are resulting in a further increase of the pressure on already scarce agricultural resources.

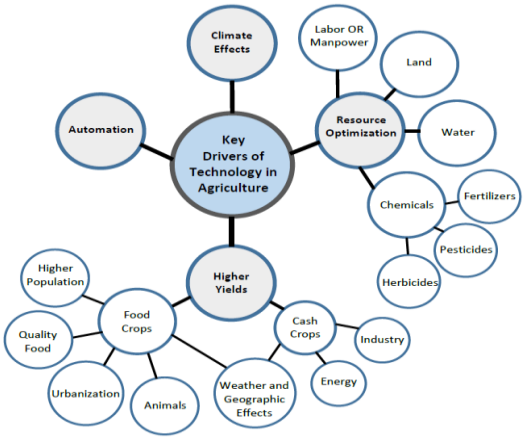

FIGURE 1: Key Drivers of Technology in Agriculture Industry

 ISBN: 978-93-90214-20-4

Unfortunately, only a limited portion of the earth‘s surface is suitable for agriculture uses due to various limitations, like temperature, climate, topography, and soil quality, and even most of the suitable areas are not homogenous. When zooming the versatilities of landscapes and plant types, many new differences start to emerge that can be difficult to quantify. Moreover, the available agricultural land is further shaped by political and economic factors, like land and climate patterns and population density, while rapid urbanization is constantly posing threats to the availability of arable land. Over the past decades, the total agriculture land utilized for food production has experienced a decline [9]. In 1991, the total arable area for food production was 19.5 million square miles (39.47% of the world‘s land area), which was reduced to approximately 18.6 million square miles (37.73% of the world‘s land area) in 2013 [10]. As such, the gap between demand and supply of food is becoming more significant and alarming with the passage of time.

1.2 Motivation

For continuously increasing demand and decrease in supply of food necessities, it’s important to rapid improvement in production of food technology. Agriculture is only the source to provide this. This is the important factor in human societies to growing and dynamic demand in food production. Agriculture plays the important role in the economy and development, like India. Due to lack of water and scarcity of land water result the decreasing volume of water on earth, the farmer use irrigation. Irrigation may be defined as the science of artificial application of water to the land or soil that means depending on the soil type, plant is to be provided with water.

1.3 Area of Utility

The primary focus of this project is to help the farmers and reduce their work. This module can be implemented in perennial plant irrigation land and gardening land.

2. MAJOR APPLICATIONS

By implementing the latest sensing and IoT technologies in agriculture practices, every aspect of traditional farming methods can be fundamentally changed. Currently, seamless integration of wireless sensors and the IoT in smart agriculture can raise agriculture to levels which were previously unimaginable. By following the practices of smart agriculture, IoT can help to improve the solutions of many traditional farming issues, like drought response, yield optimization, land suitability, irrigation, and pest control. Figure 3 lists a hierarchy of major applications, services and wireless sensors being used for smart agriculture applications. While, major instances in which the advanced technologies are helping at various stages to enhance overall efficiency are discussed below.

A. SOIL SAMPLING AND MAPPING

Soil is the ―stomach‖ of plants, and its sampling is the first step of examination to obtain field-specific information, which is then further used to make various critical decisions at different stages. The main objective of soil analysis is to determine the nutrient status of a field so that measures can be taken accordingly when nutrient deficiencies are found. Comprehensive soil tests are recommended on an annual basis, ideally in Spring; however, based on soil conditions and weather consents, it may be done in in Fall or Winter. The factors that are critical to analyze the soil nutrient levels include soil type, cropping history, fertilizer application, irrigation level, topography, etc. These factors give insight regarding the chemical, physical, and biological statuses of a soil to identify the limiting factors such that the crops can be dealt accordingly. Soil mapping opens the door to sowing different crop varieties in a specific field to better match soil properties accordingly, like seed suitability, time to sow, and even the planting depth, as some are deep-rooted and others less. Furthermore, growing multiple crops together could also lead to smarter use of agriculture, simply making the best use of resources.

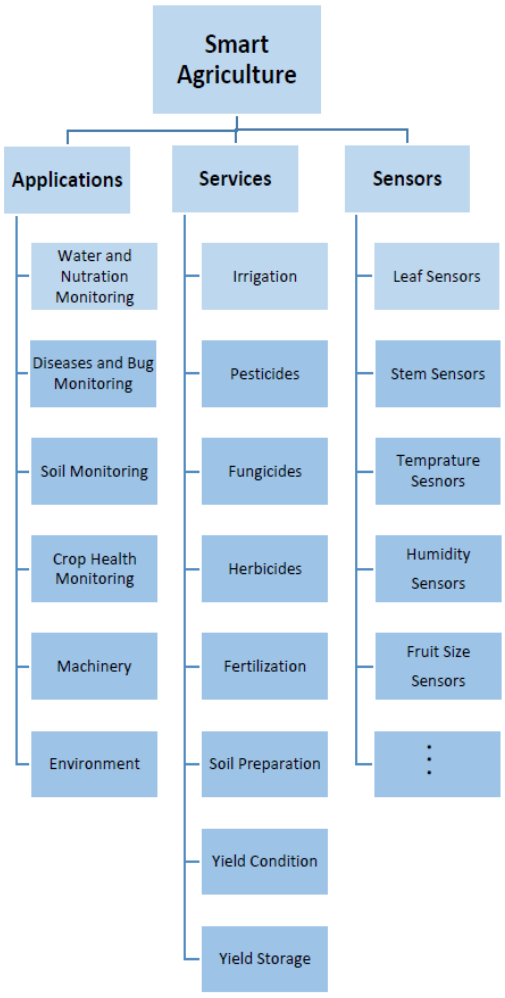

FIGURE 2: General Hierarchy of Possible Applications, Services and Sensors for Smart Agriculture

 ISBN: 978-93-90214-20-4

B. IRRIGATION

About 97% of Earth‘s water is salt-water held by oceans and seas, and only the remaining 3% is fresh water—more than two-third of which is frozen in the forms of glaciers and polar ice caps. Only 0.5% of the unfrozen fresh water is above the ground or in the air, as the rest lies underground. In short, humanity relies on this 0.5% to fulfill all its requirements and to maintain the ecosystem, as enough fresh water must be kept in rivers, lakes, and other similar reservoirs to sustain it. It is worth mentioning that solely the agriculture industry uses approximately 70% of this accessible fresh water. In many countries, situation rises to 75% e.g. Brazil, further in some underdeveloped countries, even it exceeds 80%. The main reason for this high water consumption is the monitoring procedure as even in 2013, crops visual inspection for irrigation decision-making was very common, as nearly 80% of farms in United States were observed. According to the UN Convention to Combat Desertification (UNCCD) estimates in 2013 show that there were 168 countries affected by desertification and by 2030, almost half of the world population will be living in areas with high water shortages. Considering the figures of water crises around the globe, same time its increasing demands in agriculture and many other industries, it should be provided to places only where it is needed, most importantly, in required quantities. For this purpose, increased awareness has been implemented to conserve the existing under-stress water resources by employing more efficient irrigation systems.

C. CROP DISEASE AND PEST MANAGEMENT

The Great Famine, also known as the Irish Potato Famine, in which approximately one million Irish people died around 1950, resulted due to crop failure and yield reduction caused by ―potato blight‖ disease. Even today, corn growers in the US and southern Canada are facing an economic loss of approximately one billion USD due to ―southern corn leaf blight‖ disease. The Food and Agriculture Organization (FAO) estimates that 20–40% of global crop yields are lost annually due to pests and diseases. To control such vast production losses, pesticides and other agrochemicals became an important component of the agriculture industry during the last century. It is estimated that, in each year, around half a million tons of pesticide are used in the US alone, while more than two-million tons are used globally. Most of these pesticides are harmful to human and animal health, leaving severe, even irreversible, impact to the environment, ultimately causing significant contamination to entire ecosystems.

3. BLOCK DIAGRAM AND DESCRIPTION

3.1 Block Diagram

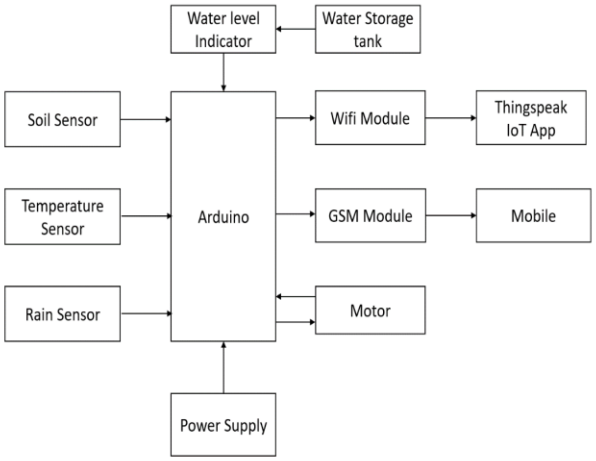

Fig 3.1 Block Diagram

3.2 Schematic Diagram

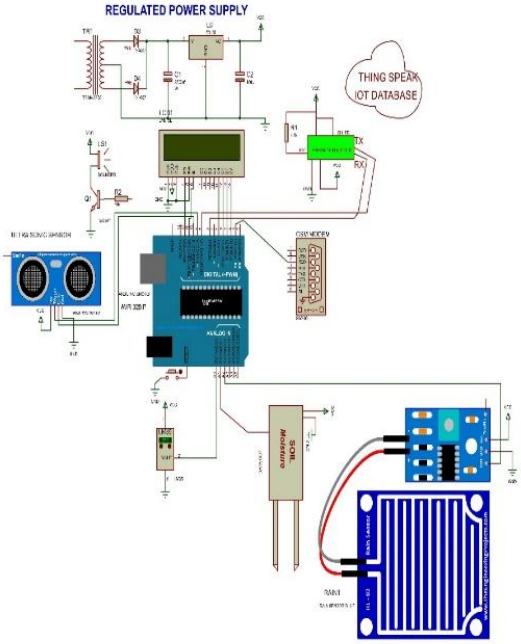

Fig 3.2 Schematic diagram

3.3 WORKING

Initially the sensors like temperature, soil moisture, rain sensor capture the data from the field and is sent to the controller. Now the controller compares the received data with that of pre-existing data and if the values are beyond the threshold point the corresponding devices is in ON state. Initially temperature inside the farm is compared with that of the pre-defined value in the micro controller and if it is beyond the threshold point the fan gets ON. Later soil moisture inside the farm is compared with that of the pre-defined value in the micro controller and if it is beyond the

threshold point the water motor gets ON. When it's raining, rain sensor inside the farm is compared with that of the pre-defined value in the micro controller and if it is beyond the threshold point the motor gets ON and the values obtained from the sensors are sent to the thingspeak IOT web page through Wi-Fi module and is represented in a graphical format. After reaching the desired level these devices automatically turn OFF. Usually it takes 15 seconds to upload data of each and every sensor and this is a cyclic process.

4. APPLICATIONS AND ADVANTAGES

4.1 APPLICATIONS

Livestock Monitoring

Livestock monitoring is all about animal husbandry and cost savings. Ranchers are able to use wireless IoT applications to gather data regarding the health, well-being, and location of their cattle. This information saves them money in two ways:

- This data helps identify sick animals so they can be pulled from the herd, thus preventing a larger number of sick cattle.
- Ranchers who know where their cattle are located can lower labour costs.

There are some specific challenges when instrumenting livestock with sensors. Specifically, it's quite difficult to outfit cattle with a collar. An alternate option is to use a wireless retrofitted bolus in the cow's stomach, which can communicate via Bluetooth to an ear tag.

Conservation Monitoring

While it doesn't strictly fall under the heading of "agriculture," monitoring for endangered rhinos is one of the most interesting animal IoT use cases out there. Knowing where rhinos in large game facilities are located can help conservationists protect them and keep poachers from killing the rhinos for their horn.As one may imagine, collaring a rhino isn't easy and we've found it isn't often successful. The collars get ripped off from fighting, and they've been known to cause behavioural changes in the rhinos. To solve for this, we are currently examining the idea of a putting Symphony Link devices inside a rhinoceros's horn.

Plant & soil monitoring

Monitoring plant and soil conditions is a simple use case, but it can lead to a fantastic return on investment for farmers utilizing sensing technology. We've seen three great general uses for agriculture IoT in this space:

1. Sensing for soil moisture and nutrients.
2. Controlling water usage for optimal plant growth.

4.2 ADVANTAGES

- Reducing the risk of electric shocks, deaths due to poisonous creatures in the fields.
- Watering depends on the moisture level present in the field.
- All the farm parameters can view through online in graphical notation.
- Efficient and low-cost design.
- Fast response.
- User friendly

5. RESULT ANALYSIS

5.1 Hardware Equipment

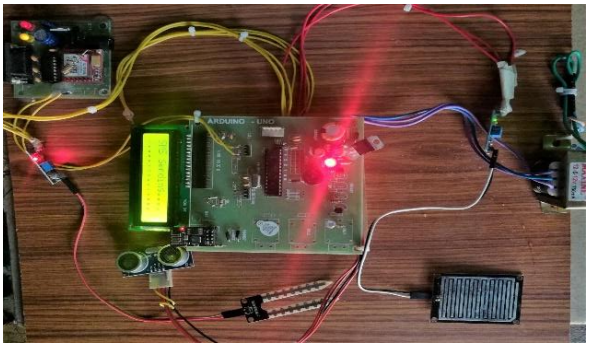

Fig 5.1 Hardware kit

Fig 5.2 LCD Displaying Project Title

Fig 5.3 Agricultural Parameters

 ISBN: 978-93-90214-20-4

Fig 5.4 Sending SMS

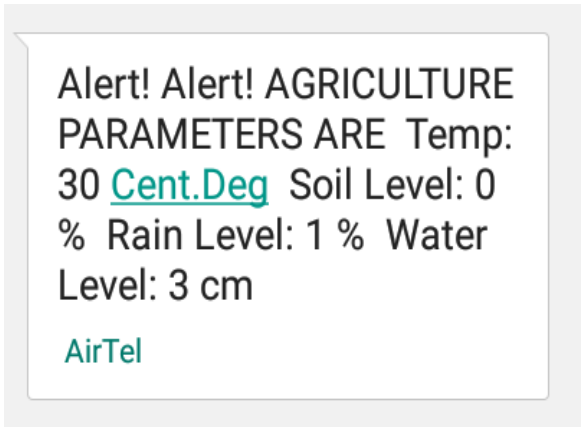

Fig 5.5 GSM Agricultural Parameters message

Step 1 This is the Hardware Equipment of the project. First we intialize the kit by using a toggle switch.

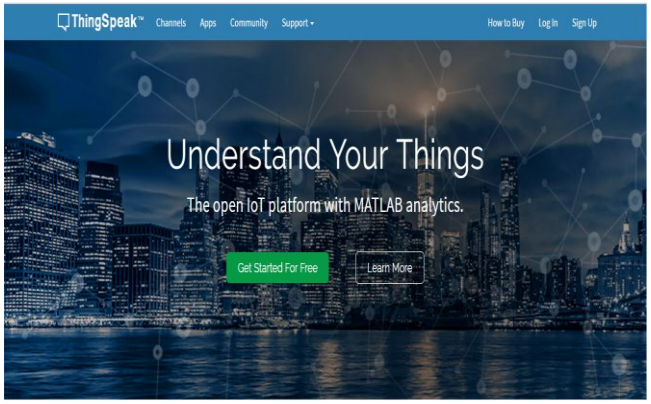

Fig 5.6 Thingspeak web page

step 2 Initially we have to sign up in thingspeak iot web page by using an email id and later we have to create channel on it based upon our project title.

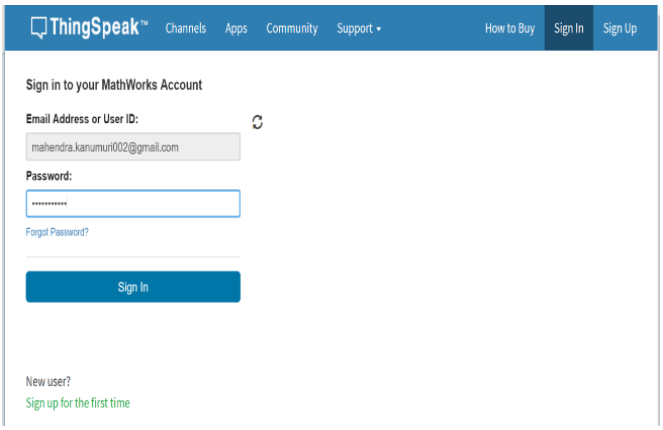

Fig 5.7 Thingspeak sign in

Step 3 This is an IOT ThingSpeak web page. we have to login the thingspeak by using an email address and we can connect to the Aurdino which is present in the equipment through WI-FI module.

5. CONCLUSION AND FUTURE SCOPE

CONCLUSION

The main advantage is that the system's action can be changed according to the situation (crops, weather conditions, soil etc). By implementing this agricultural, horticultural lands, parks, gardens, golf courses can be irrigated, and this is cheaper and efficient when compared to other type of automation system. In large scale applications, high sensitivity sensors can be implemented for large areas of agricultural lands. Also, with this kind of implementation we can be able to reduce the soil erosion and wastage of water

FUTURE SCOPE

By using this IoT system here it will be much useful for farmers where they can perform different tasks like plucking weeds and also for spraying pest controllers.
It can also be used to protect the field from bird and animal scaring by keeping vigilance etc.
For the fore coming days, we have an idea to monitor the water level with flow level and can be displayed in the Web Portal and intimate in Mobile.

REFERENCE

[1] S. R. Nandurkar, V. R. Thool, R. C. Thool, "Design and Development of Precision Agriculture System Using Wireless Sensor Network", IEEE International Conference on Automation, Control, Energy and Systems (ACES), 2014

[2] 2. Joaquin Gutierrez, Juan Francisco Villa-Medina, Alejandra Nieto-Garibay, and Miguel Ángel Porta-Gándara, "Automated Irrigation System Using a Wireless Sensor Network and GPRS Module", IEEE TRANSACTIONS ON INSTRUMENTATION AND MEASUREMENT, 0018-9456,2013

[3] Dr. V. Vidya Devi, G. Meena Kumari, "Real- Time Automation and Monitoring System for Modernized Agriculture", International Journal of Review and Research in Applied Sciences and Engineering (IJRRASE) Vol3 No.1. PP 7-12, 2013

[4] Y. Kim, R. Evans and W. Iversen, "Remote Sensing and Control of an Irrigation System Using a Distributed Wireless Sensor Network", IEEE Transactions on Instrumentation and Measurement, pp. 1379–1387, 2008.

[5] Q. Wang, A. Terzis and A. Szalay, "A Novel Soil Measuring Wireless Sensor Network", IEEE Transactions on Instrumentation and Measurement, pp. 412–415, 2010.

[6] Yoo, S.; Kim, J. Kim, T. Ahn, S.; Sung, J.; Kim, D. A2S: Automated agriculture system based on WSN. In ISCE 2007. IEEE International Symposium on Consumer Electronics, 2007, Irving, TX, USA, 2007.

[7] Arampatzis, T. Lygeros, J. Manesis, S. A survey of applications of wireless sensors and Wireless Sensor Networks. In 2005 IEEE International Symposium on Intelligent Control & 13th Mediterranean Conference on Control and Automation. Limassol, Cyprus, 2005, 1-2, 719-724.

Implementation of an Advanced and Low Power Linear Built-In-Self-Test Using Linear Feedback Shift Register

[1] Yadlapalli Naveen Kumar, [2] Rajitha Lakshmi CH, [3] Velivela Naresh, [4] S Bhanu Keerthi

[1][2][3] Assistant Professor, ECE, Ramachandra College of Engineering, Eluru, AP, India
[4] PG Scholor, Ramachandra College of Engineering, Eluru, AP, India

Abstract:

This project plays vital role in all type of communication applications. It presents a novel low-transition linear feedback shift register (LFSR) that is based on some new observations of LBIST. Security of a hardware implementation can be compromised by a random fault or a deliberate attack. The traditional testing methods are good at detecting random faults, but they do not provide to secure all type of attacks. It requires a small set of deterministic tests to cover maximum percentage of single stuck-at faults. Thus, the test execution time is much shorter (at least two orders of magnitude).It has a higher resistance against stuck-at fault type of hardware Trojans. In this algorithm, all test patterns to circuit are generated using low power LFSR and, generated patterns are reordered, in such a way; power will be decreased while testing application.

Keywords:

Low Power Linear, Feedback Shift Register, Self-Test

1. INTRODUCTION

The growing demand of portable battery-operated systems has made energy efficient processors a necessity. For applications like wearable computing energy efficiency takes top most priority. These embedded systems need repeated charging of their batteries. The problem is more severe in the wireless sensor networks which are deployed for monitoring the environmental parameters. These systems may not have access for recharging of batteries. We know that on chip memories determine the power dissipation of Sock chips. Hence it is very important to have low power and energy efficient and stable SRAM which is mainly used for on chip memories. There are various approaches that are adopted to reduce power dissipation, like design of circuits with power supply voltage scaling, power gating and drowsy method. Lower power supply voltage reduces the dynamic power in quadratic fashion and leakage power in exponential way. But power supply voltage scaling results in reduced noise margin. Many SRAM arrays are based on minimizing the active capacitance and reducing the swing voltage. In sub-100nm region leakage currents are mainly due to gate leakage and sub threshold leakage current. High dielectric constant gate technology decreases the gate leakage current. Forward body biasing methods and dual TV techniques are used to reduce sub threshold leakage current. In sub threshold SRAMs power supply voltage (VDD) is lower than the transistor threshold voltage (TV) and the sub threshold leakage current is the operating current. The energy loss during writing is more than the energy loss during reading in conventional SRAM since there is full swing of voltage in bit lines whereas the bit line voltage swing is very less during reading. It is known that the energy stored in the bit lines of the conventional SRAM is lost to ground in each write operation during '1' to '0' transition and this is the main source of energy loss. The power dissipated in bit lines represents about 60% of the total dynamic power consumption during a write operation. The power consumption by bit lines during writing is proportional to the bit line capacitance, square of the bit line voltage and the frequency of writing. Energy loss is reduced by limiting voltage differences across conducting devices. This is accomplished through the use of time-varying voltage waveforms. This is also called Adiabatic charging technique. The SRAM working purely on adiabatic charging principles need multiple phase power clocks. Although there is huge saving in energy during writing as well as reading, the design of the SRAM circuit is complex and not same as the design of conventional SRAM. The latency of operation is more. There is a powerful approach in which the energy stored in the bit line capacitance that is normally lost to ground is collected and pumped back into the source. This is known as energy recovery approach. Based on the phase of the charging source, pre charging techniques, sense amplifier, the complexity and area of the pumping circuit there are variants. To overcome the design complexity and latency of complete adiabatic SRAMS, SRAMs that make use of adiabatic charging technique partially have been designed. Based on whether adiabatic charging is applied to only power supply line or ground line or bit lines and word lines or only bit lines, there are many

types of adiabatic SRAMs. High resistivity switches are also used to vary the power supply voltage slowly . Energy stored in the bit lines is recycled by the help of switches to adjacent bit lines in order to save energy in bit line charge-recycle method. This method reduces the swing voltages to a low swing voltage. Based on whether energy recycling is done only during writing cycle or during both writing and reading cycles, there are variants. It is necessary that in addition to saving energy in SRAMs care should be taken to see the performance parameters are not much affected. In this Thesis an attempt has been made to recover energy stored in the bit lines and reused it by adiabatic principles. This has been made possible by using a very simple, small and efficient adiabatic driver for charging and discharging the bit lines. The adiabatic driver is driven by a D.C shifted single phase sinusoidal power clock which enables the charging and discharging of the bit lines based on the signal which is 'DATA' AND 'WE' input. Hence the loss of energy to the ground during '1'to'0' transition in SRAM is reduced to a great extent. No separate pre charging circuit is used before or after reading. No synchronization circuit is needed as only bit lines are concerned. Low power sense amplifier is utilized to sense the data. The design of the conventional SRAM can be retained except the write driver and the pre charge circuit. With this adiabatic driver circuit working in conjunction with conventional 6T SRAM cell other performance characteristics like read stability, write ability, read and write delay etc have been found by simulation in addition to energy saving under varied conditions of memory operations. The effect of device parameters of the driver on total energy of the SRAM cell has been investigated. Further studies covered proposed SRAM cell arrays. In addition to recovering the energy from both bit lines the possibility of operating the SRAM cell with single bit line driven by an adiabatic driver is examined to save energy. This effort has resulted in realizing adiabatic 5T SRAM cell which consumes significantly lower energy than adiabatic 6T SRAM cell with reduction in bit line leakage power and with better Static Noise Margin (SNM). Single ended reading is employed and this does not need pre charging, which saves energy. Further the design of adiabatic 5T SRAM is modified to get Feat SRAM which has better speed of operation in addition to other performance parameters remaining almost the same.

2.1 Static Random Access Memory (SRAM) [1] Static memory cells [1] basically consist of two back to back connected inverters as seen in Fig. 2.1. The output of the second inverter (Vo2) is connected to the input of the first inverter (Vi1). If we consider the voltage transfer characteristics of the first inverter (Vo1 vs.Vi1) and that of the second consideringVi2=Vo1 as shown in Fig. 2.2a and Fig. 2.2b respectively, there are three possible operating points (A, B and C) obtained by intersection as shown in Fig. 2.2c. It may be seen that operation points A, B are stable as loop gain is less than 1. Point A shows that the output of inverter1 is high and the output of the inverter2 is low. Point B shows that the output of inverter1 is low and the output of inverter 2 is high. This shows that the outputs of two inverters are complementary in any stable condition. This property is made use of to realize static random access memory SRAM. Point C is a meta stable operating point as the loop gain at point C is much larger than 1. When a small deviation is applied to the input of the first inverter when the operating point is C, it gets amplified by the gain of the first inverter and is applied to the input of the second inverter and again amplified by the gain of the second inverter. The values of Vo1 and Vo2 (Vi2) increases and the bias point moves away from C until it reaches either A or B. Fig. 2.3 shows

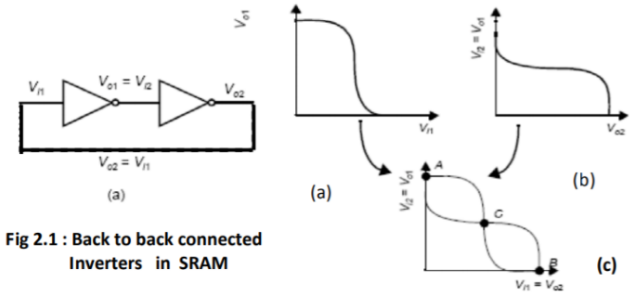

Fig 2.1 : Back to back connected Inverters in SRAM

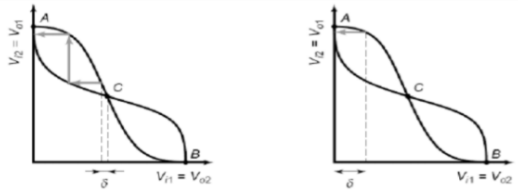

Fig 2.2 : Transfer characterstics of Inverters (a) Vo1 vs Vi1 (Vo2) (b) Vo1 vs Vo2 (c)Butterfiy curve

The actual SRAM architecture based on CMOS inverters is shown in Fig.2.1. It consists of two back to back connected inverters A and B and two access transistors PG1 and PG2. The access transistors are connected between inverters and bit lines BL and BLB and their gates are connected to word line WL. The access transistors are turned on through the word line to enable writing and reading operation and turned off during hold condition. Same ports are used for read and write operation. To operate the cell reliably, the sizes of the transistors should be properly designed. Since sense amplifiers (which are basically differential amplifiers) are used to read the data quickly, the conventional 6T SRAM is balanced and double ended. 2.2 Basic operations of SRAM and design considerations. The various operations of SRAM cell can be understood considering the circuit diagram of conventional SRAM system shown in Fig. 2.2. There are three operations associated with SRAM namely hold, read and write. The sequence of steps in which these operations are carried out are given below. Hold: The access transistors are disabled by applying word line signal WL equal to '0' to their gates. The data is held in the latch. The bit lines (BL and BLB) are charged to the supply

 ISBN: 978-93-90214-20-4

voltage. Read: The Bit lines (BL and BLB) of the cell are pre charged as given in the above step if reading is done just after write operation.

2. PROPOSED SYSTEM

It is very important to choose the proper LFSR architecture for achieving the appropriate fault coverage. Every architecture consumes different power even for same polynomial. Another problem associated with choosing LFSR is LFSR design issue, which includes LFSR partitioning, in this the LFSR are differentiated on the basis of hardware cost and testing time cost. A typical BIST architecture consists of a test pattern generator (TPG), usually implemented as a linear feedback shift register (LFSR), a test response analyzer (TRA), implemented as a multiple input shift register (MISR), and a BIST control unit (BCU), all implemented on the chip. This approach allows applying at-speed tests and eliminates the need for an external tester. The BIST architecture components are given below.

Circuit Under Test (CUT):
It is the portion of the circuit tested in BIST mode. It can be sequential, combinational or a memory. Their Primary Input (PI) and Primary output (PO) delimit it.

Test pattern generator (TPG):
It generates the test patterns for the CUT. It is a dedicated circuit or a microprocessor. The patterns may be generated in pseudorandom or deterministically.

Multiple input signatures register (MISR):
It is designed for signature analysis, which is a technique for data compression. MISR are frequently implemented in portability of alias. MISR are frequently implemented in BIST designs, in which output response are compressed by MISR.

Test Response Analysis (TRA):
It analyses the value sequence on PO and compares it with the expected output.

BIST controller Unit (BCU):
It controls the test execution; it manages the TPG, TRA and reconfigures the CUT and the multiplexer. It is activated by the Normal/Test signal and generates Go/No go.

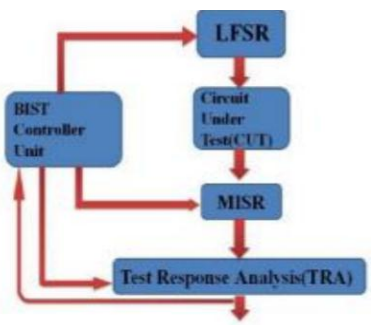

Fig : BIST Architecture

LFSR is used to generate test patterns for BIST. In this, test patterns are generated externally by LFSR, which is inexpensive and high speed. LFSR is a circuit consists of flip-flops in series. LFSR is a shift register where output bit is an XOR function of some input bits. The initial value of LFSR is called seed value. LFSR's seed value has a significant effect on energy consumption

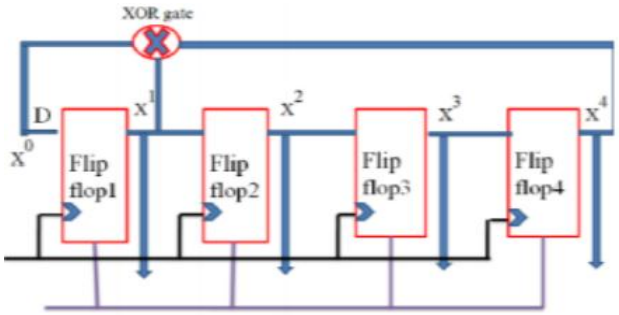

Fig 4.2 : LFSR, in which input of first flip-flop is cored with last flip-flop

The output that influence the input are called tap. A LFSR is represented by as polynomial, which is also known as characteristic polynomial used to determine the feedback taps, which determine the length of random pattern generation. The output of LFSR is combination of 1's and 0's. A common clock signal is applied to all flip-flops, which enable the propagation of logical values from input to output of flip-flops. Increasing the correlation between bits reduces the power dissipation. This can be achieved by adding more number of test vectors, which decreases the switching activity.

Proposed Algorithm

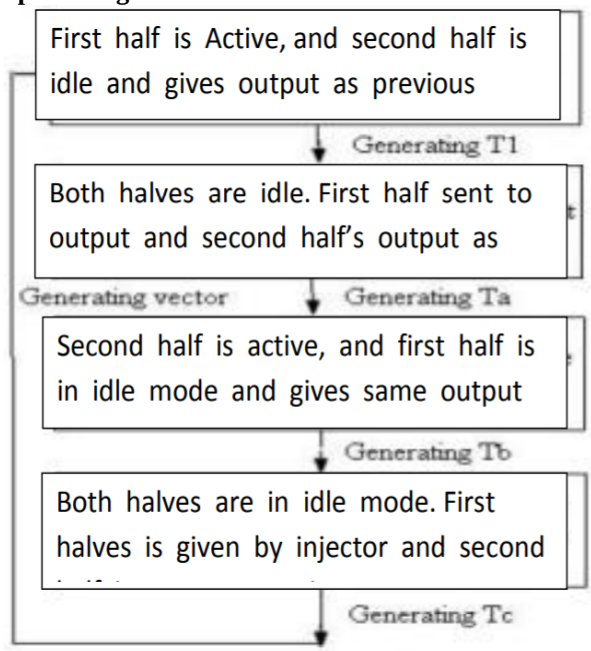

LFSR is characterized by the polynomial by its characteristics polynomial and inverse of characteristics polynomial is generated polynomial. In this approach the 3 intermediate test vectors are generated between every two successive vectors (say TI, T2). The total number of signal transition occurs between these 5 vectors are equivalent to the number of transition occurs between the 2 vectors. Hence the power consumption is reduced. Additional circuit is used for few logic gates in order to generate 3 intermediate vectors. The 3 intermediate vectors (Ta, Tb, Tc) are achieved by modifying conventional flip-flops outputs and low power outputs. The first level of hierarchy from top to down includes logic circuit design for propagation either the present or next state of flip-flop to second level of hierarchy. Second level of hierarchy is implementing Multiplexed (MUX) function i.e. selecting two states to propagate to output as shown in flow. Second level of hierarchy is implementing Multiplexed (MUX) function i.e. selecting two states to propagate to output as shown in flow:

3. RESULTS

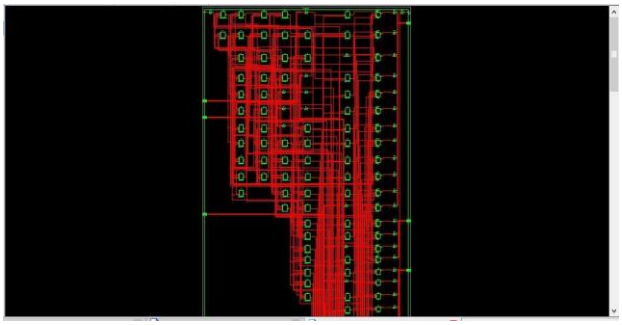

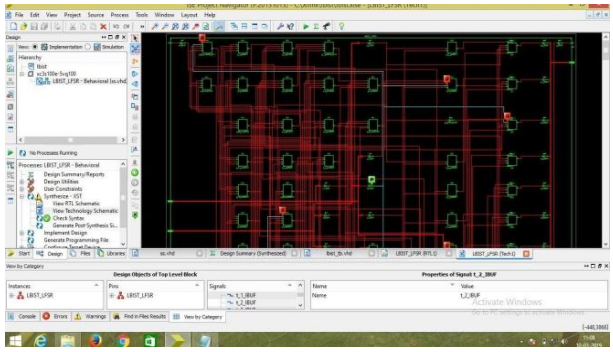

Fig6.1: RTLSCHEMATIC

wherer,t,daretheinputs
xisoutput.S,zareino

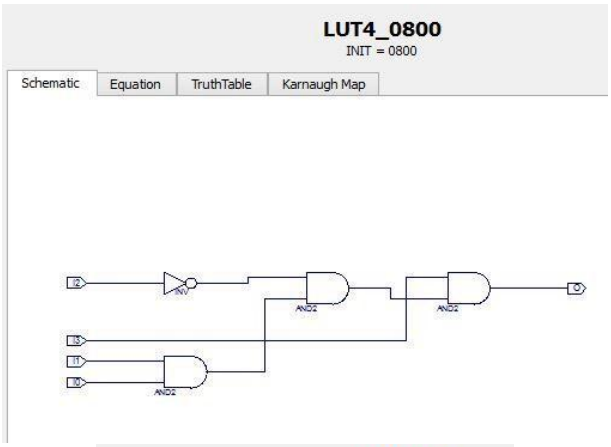

I3	I2	I1	I0	O
0	0	0	0	1
0	0	0	1	1
0	0	1	0	1
0	0	1	1	1
0	1	0	0	1
0	1	0	1	1
0	1	1	0	1
0	1	1	1	1
1	0	0	0	1
1	0	0	1	1
1	0	1	0	1
1	0	1	1	0
1	1	0	0	1
1	1	0	1	1
1	1	1	0	1
1	1	1	1	1

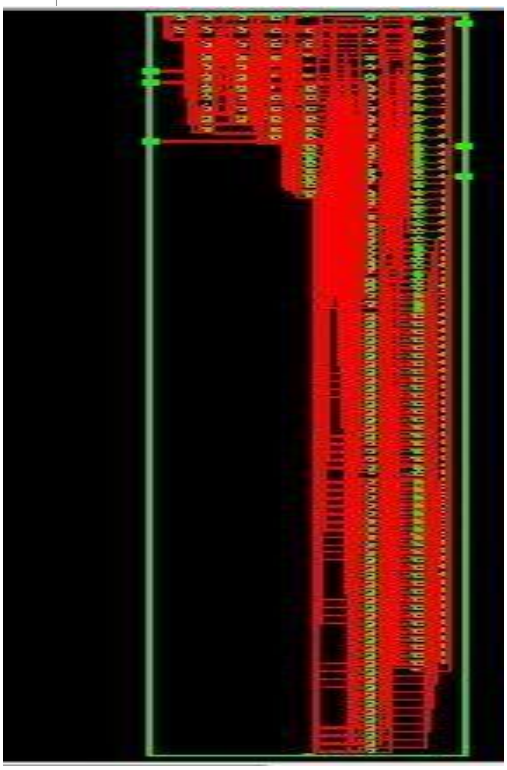

 ISBN: 978-93-90214-20-4

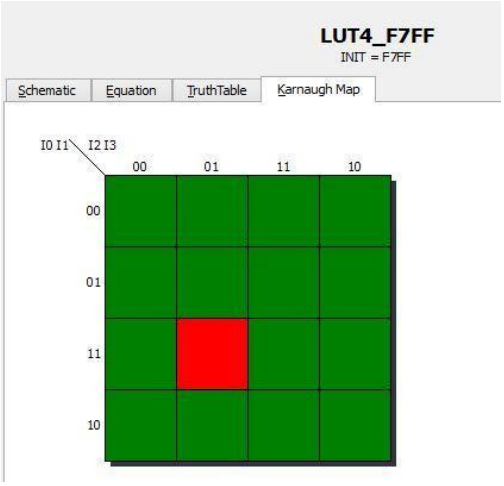

Fig6.4:SchematicdiagramofLUT4_F7FF

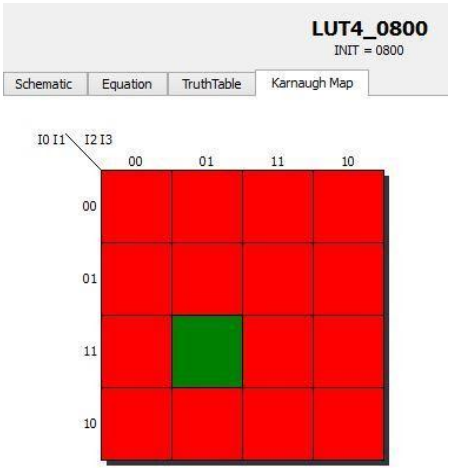

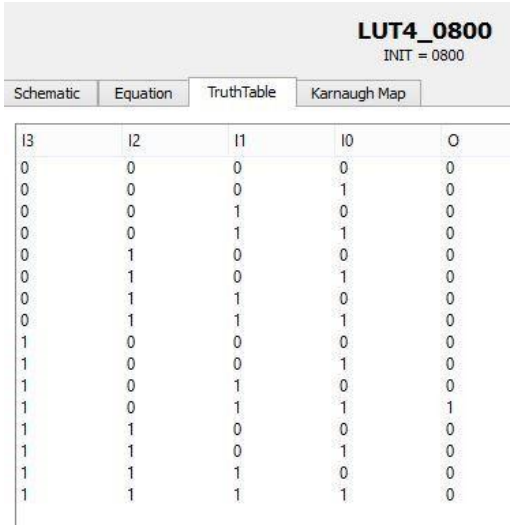

I3	I2	I1	I0	O
0	0	0	0	0
0	0	0	1	0
0	0	1	0	0
0	0	1	1	0
0	1	0	0	0
0	1	0	1	0
0	1	1	0	0
0	1	1	1	0
1	0	0	0	0
1	0	0	1	0
1	0	1	0	0
1	0	1	1	1
1	1	0	0	0
1	1	0	1	0
1	1	1	0	0
1	1	1	1	0

Simulation Part:

Forinput0011

If both address lines ‘r’ and ‘t’ are matched complementally then output data will flow.

Fig6.10: Simulation Output

If input address lines ‘r’ and ‘t’ are doesn’t matched complementally then data ‘d’ doesn’t pass through output(‘x’).

Figure6.11:Output error

Forinput1110

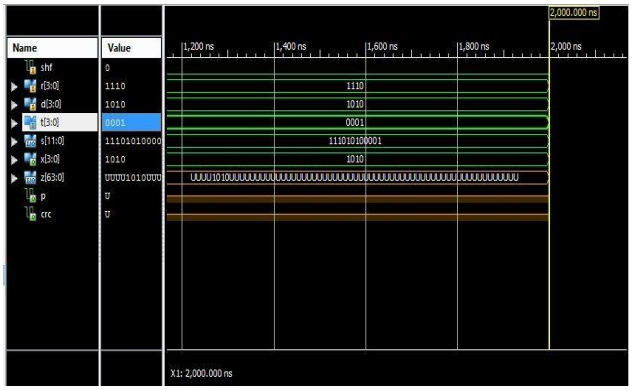

Fig6.12:Simulationoutput for next inputs

Fig6.13 Error output

4. CONCLUSION & FUTURESCOPE

LFSR based Pseudo random test pattern generator is used in the testing of ASIC chips which generates random sequences of test patterns. This project deals with the design of LFSR and also how to multiplex the Test inputs with the ASIC inputs to reduce the additional test input pins required for the ASIC. This project presents a novel low-transition Linear Feedback Shift Register (LFSR) that is based on some new observations about the output sequence of a conventional LFSR. It is observed that the total power consumed in modified LFSR is less than the power consumed with normal LFSR and output dynamic power is decreased. It is concluded that low power LFSR is very useful for BIST implementation in which the CUT may be Combinational, sequential and memory circuits. Using low power LFSR technique we can further decrease the power in BIST implementation.

FutureScope:

In this present project we use 4-bit LFSR in Future it will be increased upto 8-bit, 16-bit and 32-bit LFSR is used By increasing the number of bits Performance of the circuit will increase. Further it will be testing for DRAM.

REFERENCE

[1] N.Ahmed, M.H. Tehran pour, M. Neurone" Low Power Pattern Generation for BIST Architecture"

[2] Bal winder Singh, Arum Kholo, Sakhalin Bandar" Power Optimization of Linear Feedback Shift Register(LFSR)f or Low Power BIST"

[3] E. Atoofian, S. Hatami, Z. Navabi, M. Alisaface and A. Afzali-Kusha," A New Low-PowerScan-Path Architecture," IEEE International Symposium, Vol.5, pp.5278 - 5281, 23-26 May2005

[4] Dr.K.Gunavathi, Mr.K.ParamasivaM, Ms.P.Subashini Lavanya, M.Umamageswaran, "Anovel BIST TPG for testing of VLSI circuits", IEEE International Conference on Industrial and Information Systems, pp.8-11,August2006.

[5] Mohammad Tehranipoor, Mehrdad Nourani, NisarAhmed, "Low-Transition LFSR for BIST-Based Applications, "14th Asian Test Symposium, pp.138-143,18-21Dec.2005.

[6] F. Najm, "Transition Density, A New Measure of Activity in Digital Circuits", in IEEE Transaction on computer Aided Design no.2,vol.12, pp.310-323,February1993.

[7] A.Chandrakaran, T.Shengand R.Brodersen, "LowPower CMOS Digital Design",inIEEE Jounal of Solid State Circuits,

[8] Mohammad Tehranipoor,MehrdadNourani,NearAhmed,"LowTransitionLFSRforBISTBasedApplications

[9] FulvioCorno, Paolo Prinettom, Matteo SonzarForda "testability Analysis and ATPG on Behavioral al RT-LevelVHDL".

[10] F.Corno, M.Rebaudengo,M.SonzaReorda,"ATestPatternGenerationMethodologyfor LowPowerConsumption",pp.1-5,2008.

[11] Dr.K.Gunavathi, Mr.K.Paramasiva, Ms.P.SubashiniLavanya, M.Umamageswaram, "A Novel BISTTPG for Testing of VLSI Circuits".

[12] BalwinderSingh, ArunKhosla, SukhleenBindra, "poweroptimization of LFSR for LowPower BIST", IEEE International conference 2009, pp.311-314.

[13] A.Crouch,"Design-for-Test for Digital IC's and Embedded Core Systems",PrenticeHall,1999

[14] WeiPei,Wen-BenJoneandYi-MingHu"FaultModelingandDetectionforDrowsy SRAM Caches" IEEE Trans.on CAD of Integrated CircuitsandSystems26(6):1084-1100(2007)

Computing Capital Budgeting for Banking Sector

[1] Sushain Koul, [2] Dr. Parag Ravikant Kaveri

[1] Student, Symbiosis Institute of Computer Studies and Research, Pune, India
[2] Department of Computer, Symbiosis Institute of Computer Studies and Research, Pune, India

Abstract:

Perhaps the most difficult hurdle which companies come across is the selection of the project which is beneficial to the organization in the long-run and also increases the present value of the shareholders. This is where Capital Budgeting comes into play. Capital Budgeting is one of the most important areas of financial management. This paper gives an overview of what capital budgeting is, what different types of techniques comes under capital budgeting and how to represent capital budgeting technique algorithmically. In this paper we also throw some light on what the results of various capital budgeting techniques will be if any banking organization follows these techniques and compare those results. These techniques namely as Payback Period (PP), Average Rate of Return (ARR), Net Present Value (NPV), Profitability Index (PI) and Internal Rate of Return (IRR) are used to evaluate projects.

Keywords:

Capital Budgeting, Cash Flow, Discount Rate, Time Value of Money

1. INTRODUCTION

An organizaton's success or failure depends on capital budgeting decisions. Capital budgeting decisions among several costly long-term investments play a profound impact on the organization and long-term performance. A capital budgeting decision can be stated as the process that companies use for making decisions on long-term projects. Such type of decisions are generally taken in line with the goal of maximizing shareholders value. A firm's investment decisions would generally include expansion, acquisition, modernisation and replacement of long-term assets. The decisions to invest in fixed assets are made by the managers as these are one of the major judgements. Capital budgeting involves various techniques which give a clear picture about which project is profitable. When a project is finalized, initial investment is made and then it is expected that future cash flows are calculated and discounted to the present value. If all the expected future discounted cash flows when combined together is greater than initial investment the project is said to be profitable.

2. OBJECTIVE

To understand the practical use of capital budgeting methods in a banking organization for decision- making.
To learn the significance of capital budgeting in valuing the project for financing.

3. METHODOLOGY

The information of this research paper has been compiled through Primary and Secondary Sources.

4. ALGORITHM

A. Payback Period

Step1: Start
Step2: Read initial_inv (initial investment) value from the user
Step3: Set pbdt (profit before depreciation and tax), pbt (profit before tax), np (net profit), ci (cash inflow) as the empty list
Step4: Set sum1 and c variable as zero
Step5: Read sal_value (salvage value), l (expected life) and tax from the user
Step6: For i=0 to l Do
Step7: Read Profit Before Depreciation and Tax for each year
from the user and append it in pbdt list
Step8: End For
Step9: Compute Depreciation= (initial_inv-sal_value)/l
Step10: For i=0 to l Do
Step11: Compute pbdt[i]-Depreciation and append each value in pbt list
Step12: End For
Step13: For i=0 to l Do
Step14: Compute pbt[i]-(pbt[i]*(tax/100)) and append each value in np list
Step15: End For
Step 16: For i=0 to l Do
Step17: Compute np[i]+Depreciation and append each value in ci list
Step18: End For
Step19: For i=0 to l Do
Step20: Compute sum1=sum1+ci[i]
Step21: Check If sum1 is less than initial_inv
Step22: If True, Compute c=c+1

Step23: If False, Compute pb=c+((initial_inv-(sum1-ci[i]))/ci[i]) and break out of the loop
Step25: Print pb
Step26: Stop

B. Average Rate of Return

Step1: Start
Step2: Read initial_inv (initial investment) value from the user
Step3: Set pbdt (profit before depreciation and tax), pbt (profit before tax), np (net profit), ci (cash inflow) as the empty list
Step4: Set sum1, avp and avi variable as zero
Step5: Read sal_value (salvage value), l (expected life) and tax from the user
Step6: For i=0 to l Do
Step7: Read Profit Before Depreciation and Tax for each year from the user and append it in pbdt list
Step8: End For
Step9: Compute Depreciation= (initial_inv-sal_value)/l
Step10: For i=0 to l Do
Step11: Compute pbdt[i]-Depreciation and append each value in pbt list
Step12: End For
Step13: For i=0 to l Do
Step14: Compute pbt[i]-(pbt[i]*(tax/100)) and append each value in np list
Step15: End For
Step 16: For i=0 to l Do
Step17: Compute sum1=sum1+np[i]
Step18: End For
Step19: Compute avp=sum1/l
Step20: Compute avi= (initial_inv+sal_value)/2
Step21: Compute arr= (avp/avi)*100
Step22: Print arr
Step23: Stop

C. Discounted Payback Period

Step1: Start
Step2: Import math Library
Step3: Read initial_inv (initial investment) value from the user
Step4: Read pbdt (profit before depreciation and tax), pbt (profit before tax), pvf (present value factor), pv (present value), np (net profit) and ci (cash inflow) as the empty list
Step5: Set sum1, dpb and c variable as zero
Step6: Read sal_value (salvage value), l (expected life), dr (discount rate) and tax from the user
Step7: Compute dr=dr/100
Step8: For i=0 to l Do
Step9: Read Profit Before Depreciation and Tax for each year from the user and append it in pbdt list
Step10: End For
Step11: Compute Depreciation= (initial_inv-sal_value)/l
Step12: For i=0 to l Do
Step13: Compute pbdt[i]-Depreciation and append each value in pbt list
Step14: End For
Step15: For i=0 to l Do
Step16: Compute pbt[i]-(pbt[i]*(tax/100)) and append each value in np list
Step17: End For
Step 18: For i=0 to l Do
Step19: Compute np[i]+Depreciation and append each value in ci list
Step20: End For
Step21: For i=0 to l Do
Step22: Compute 1/(math.pow((1+dr),i+1)) and append each value in pvf list
Step23: End For
Step24: For i=0 to l Do
Step25: Compute ci[i]*pvf[i] and append each value in pv list
Step26: End For
Step27: For i=0 to l Do
Step28: Compute sum1=sum1+pv[i]
Step29: Check If sum1 is less than initial _inv
Step30: If True, Compute c=c+1
Step31: If False, Compute dpb=c+((initial_inv-(sum1-pv[i]))/pv[i])
Step32: End For
Step33: Print dpb
Step34: Stop

D. Net Present Value

Step1: Start
Step2: Import math Library
Step2: Read initial_inv (initial investment) value from the user
Step3: Set pbdt (profit before depreciation and tax), pbt (profit before tax), np (net profit), pv (present value), pvf (present value factor), ci (cash inflow) as the empty list
Step4: Set sum1 variable as zero
Step5: Read sal_value (salvage value), l (expected life), dr (discount rate) and tax from the user
Step7: Compute dr=dr/100
Step6: For i=0 to l Do
Step7: Read Profit Before Depreciation and Tax for each year from the user and append it in pbdt list
Step8: End For
Step9: Compute Depreciation= (initial_inv-sal_value)/l
Step10: For i=0 to l Do
Step11: Compute pbdt[i]-Depreciation and append each value in pbt list
Step12: End For
Step13: For i=0 to l Do
Step14: Compute pbt[i]-(pbt[i]*(tax/100)) and append each value in np list
Step15: End For
Step 16: For i=0 to l Do
Step17: Compute np[i]+Depreciation and append each value in ci list
Step18: End For
Step19: For i=0 to l+1 Do

 ISBN: 978-93-90214-20-4

Step20: Compute 1/(math.pow((1+dr),i+1)) and append each value in pvf list
Ste21: End For
Step22: Insert at 0th position of ci list –initial_inv
Step19: For i=0 to l+1 Do
Step20: Compute ci[i]*pvf[i] and append each value in pv list
Step22: End For
Step21: For i=0 to l+1 Do
Step22: Compute sum1=sum1+pv[i]
Step23: End For
Step25: Print sum1
Step26: Stop

E. Profitability Index

Step1: Start
Step2: Import math Library
Step3: Read initial_inv (initial investment) value from the user
Step4: Read pbdt (profit before depreciation and tax), pbt (profit before tax), pvf (present value factor), pv (present value), np (net profit) and ci (cash inflow) as the empty list
Step5: Set sum1 variable as zero
Step6: Read sal_value (salvage value), l (expected life), dr (discount rate) and tax from the user
Step7: Compute dr=dr/100
Step8: For i=0 to l Do
Step9: Read Profit Before Depreciation and Tax for each year from the user and append it in pbdt list
Step10: End For
Step11: Compute Depreciation= (initial_inv-sal_value)/l
Step12: For i=0 to l Do
Step13: Compute pbdt[i]-Depreciation and append each value in pbt list
Step14: End For
Step15: For i=0 to l Do
Step16: Compute pbt[i]-(pbt[i]*(tax/100)) and append each value in np list
Step17: End For
Step 18: For i=0 to l Do
Step19: Compute np[i]+Depreciation and append each value in ci list
Step20: End For
Step21: For i=0 to l+1 Do
Step22: Compute 1/(math.pow((1+dr),i+1)) and append each value in pvf list
Step23: End For
Step24: Insert at 0th position of ci list –initial_inv
Step25: For i=0 to l+1 Do
Step26 Compute ci[i]*pvf[i] and append each value in pv list
Step27: End For
Step28: For i=1 to l+1 Do
Step29: Compute sum1=sum1+pv[i]
Step30: End For
Step31: Compute pi=sum1/initial_inv
Step32: Print pi
Step33: Stop

F. Internal Rate of Return

Step1: Start
Step2: Import math Library
Step3: Read initial_inv (initial investment) value from the user
Step4: Read pbd (profit before depreciation), pbt (profit before tax), pvf1 (present value factor1), pvf2 (present value factor2), pv (present value), np (net profit), pv1 (present value1), pv2 (present value2) and ci (cash inflow) as the empty list
Step5: Set sum1, sum2 variable as zero
Step6: Read sal_value (salvage value), l (expected life), dr1 (discount rate1), dr2 (discount rate2) and tax from the user
Step7: For i=0 to l Do
Step8: Read Profit Before Depreciation for each year from the user and append it in pbd list
Step9: End For
Step10: Compute Depreciation= (initial_inv-sal_value)/l
Step11: For i=0 to l Do
Step12: Compute pbd[i]-Depreciation and append each value in pbt list
Step13: End For
Step14: For i=0 to l Do
Step15: Compute pbt[i]-(pbt[i]*(tax/100)) and append each value in np list
Step16: End For
Step17: For i=0 to l Do
Step18: Compute np[i]+Depreciation and append each value in ci list
Step19: End For
Step20: For i=0 to l+1 Do
Step21: Compute 1/(math.pow((1+dr1/100),i)) and append each value in pvf1 list
Step22: End For
Step23: Insert at 0th position of ci list –initial_inv
Step24: For i=0 to l+1 Do
Step25: Compute ci[i]*pvf1[i] and append each value in pv1 list
Step26: End For
Step27: For i=1 to l+1 Do
Step28: Compute sum1=sum1+pv1[i]
Step29: End For
Step30: For i=0 to l+1 Do
Step31: Compute 1/(math.pow((1+dr2/100),i)) and append each value in pvf2 list
Step32: End For
Step30: For i=0 to l+1 Do
Step33: Compute ci[i]*pvf2[i] and append each value in pv2 list
Step34: End For
Step35: For i=1 to l+1 Do
Step36: Compute sum2=sum2+pv2[i]
Step37: End For
Step38: Check If dr1 is less than dr2 and sum1 is greater than dr2

Step39: If True, Compute irr=dr1+((sum1/(sum1-sum2))*(dr2-dr1)
Step40: Else Check If dr2 is less than dr1 and sum2 is greater than sum1
Step41: If True, Compute irr=dr2+((sum2/(sum2-sum1))*(dr1-dr2)
Step42: Print irr
Step43: Stop

5. FORMULAS

Payback Period=$\frac{Initial\ Cash\ Outflow}{Annual\ Cash\ Inflows}$ (1)

Average Rate of Return=$\frac{Average\ Annual\ Profits(after\ dep\ \&\ tax)}{Average\ Investment} * 100$ (2)

Net Present Value (NPV)=Present Value of Cash Inflow-Present Value of Cash Outflow (3)

Profitability Index=$\frac{PV\ of\ cash\ inflows}{Initial\ investment\ or\ Cash\ Outflows}$ (4)

Net profitability index=Profitability Index-1 (5)

IRR=Lower Rate+$\frac{PV\ at\ lower\ rate}{PV\ at\ lower\ rate - PV\ at\ higher\ rate} * difference\ in\ rates$ (6)

6. CALCULATIONS

The bank is making an allowance for investment in a project that costs Rs. 2,00,000. The project's expected life is 5 years and has zero salvage value. The company practices straight line technique of depreciation. The company's tax rate is 40% and the interest rate is 10%. The expected earnings before depreciation and before tax from the business are as follows:

YEAR	1	2	3	4	5
CASH FLOW BEFORE TAX	70000	80000	120000	90000	60000

6.1 Pay Back Period

Table 6.1 Showing the Calculation of Payback Period

YEARS	EARNINGS BEFORE DEPRICIATION & TAX	DEPRECIATION	EARNINGS BEFORE TAX	TAX	EARNINGS AFTER TAX	NET PROFIT
1	70000	40000	30000	12000	18000	18000
2	80000	40000	40000	16000	24000	24000
3	120000	40000	80000	32000	48000	48000
4	90000	40000	50000	20000	30000	30000
5	60000	40000	20000	8000	12000	12000

Preliminary Investment=200000

Depreciation=$\frac{Initial\ Investment - Salvage\ Value}{Number\ of\ years}$ (6)

Since salvage value is zero, substituting the values we get,

Depreciation=$\frac{200000}{5}$ =Rs. 40,000/-

Amount received till 2nd year=Rs. 1,22,000/-

Amount expected in 3rd year (Rs. 2,00,000 - Rs. 1,22,000) =Rs. 78,000/-

Cash Inflows after tax in 3rd year= Rs. 88,000/-

PBP=2 Yrs+$\frac{78000}{88000}$

=2+0.8863=2 years 10 months and 23 days

6.2 Average Rate of Return

Table 6.2 Showing the calculation of Average Rate Of Return

YEARS	EARNINGS BEFORE DEPRECIATION & TAX	DEPRECIATION	EARNING S BEFORE TAX	TAX	EARNIN GS AFTER TAX	CASH INFLOWS (EARNINGS AFTER TAX+DEPRECIATIO N)	CUMULATIVE CASH INFLOWS
1	70000	40000	30000	12000	18000	58000	58000
2	80000	40000	40000	16000	24000	64000	(58000+64000)
3	120000	40000	80000	32000	48000	88000	(122000+88000)
4	90000	40000	50000	20000	30000	70000	(210000+70000)
5	60000	40000	20000	8000	12000	52000	(280000+52000)

Preliminary Investment=200000

Depreciation=$\frac{Initial\ Investment - Salvage\ Value}{Number\ of\ years}$

Since salvage value is zero, substituting the values we get,

Depreciation=$\frac{200000}{5}$ =Rs. 40,000/-

Net Profit= (Rs.8,000 + Rs.24,000 + Rs.48,000 + Rs.30,000 + Rs.12,000)= Rs.1,32,000/-

Average Annual Profit=$\frac{132000}{5}$ =Rs. 26,400

Average Investment= $\frac{Initial\ Investment + Scrap\ Value}{2}$ =$\frac{200000}{2}$

=Rs. 1,00,000/-

Average rate of return=$\frac{Average\ Annual\ Profit}{Average\ Investment} * 100$ =$\frac{26400}{100000} * 100$ =26.4%

 ISBN: 978-93-90214-20-4

6.3 Discounted Pay Back Period

Table 6.3 Showing the calculation of Discounted Payback Period

YEA RS	EARNINGS BEFORE DEPRICIATION & TAX	DEPRECIATION	EARNINGS BEFOR E TAX	TAX	EARNINGS AFTER TAX	CASH FLOWS (EAT+ DEP.)	PV @ 10%	DISCOUNTED CASH FLOWS	CUMULATIVE DISCOUNTED CASH FLOWS
1	70000	40000	30000	12000	18000	58000	0.909	52722	52722
2	80000	40000	40000	16000	24000	64000	0.826	52864	(52722+52864)
3	120000	40000	80000	32000	48000	88000	0.751	66088	(105586+66088)
4	90000	40000	50000	20000	30000	70000	0.683	47810	(171674+47810)
5	60000	40000	20000	8000	12000	52000	0.621	32292	(219484+32292)

Preliminary Investment=200000

Depreciation=$\frac{Initial\ Investment-Salvage\ Value}{Number\ of\ years}$

Since salvage value is zero, substituting the values we get,

Depreciation=$\frac{200000}{5}$ =Rs. 40,000/-

Amount received till 3rd year = Rs. 1,71,674/-

Amount expected in 4th year = (Rs.2,00,000 - Rs.1,71,674) = Rs.28,326/-

Cumulative Discounted Cash Inflows after tax in 4th year = Rs.47,810/-

PBP=3Yrs+$\frac{28326}{48710}$ =3+0.5924 =3.5924 =3 years 7 months and 16 days

6.4 Net Present Value Method

Table 6.4 Showing the calculation of Net Present Value

YEARS	EARNINGS BEFORE DEPRICIATION & TAX	DEPRECIATIO N	EARNINGS BEFORE TAX	TAX	EARNIN GS AFTER TAX	CASH FLOWS (EAT+ DEP.)	PV @ 10%	PV of CASH FLOW S
1	70000	40000	30000	12000	18000	58000	0.909	52722
2	80000	40000	40000	16000	24000	64000	0.826	52864
3	120000	40000	80000	32000	48000	88000	0.751	66088
4	90000	40000	50000	20000	30000	70000	0.683	47810
5	60000	40000	20000	8000	12000	52000	0.621	32292

Total Present Value of Cash Inflow = Rs.2,51,776.00

Present Value of Cash Outflow=Rs.2,00,000.00

NPV =Present Value of Cash Influx-Present Value of Cash Outlay = Rs.2,51,776 - Rs.2,00,000 = Rs.51,776.00

6.5 Profitability Index

Table 6.5 Showing the calculation of Profitability Index

YEARS	EARNINGS BEFORE DEPRICIATION & TAX	DEPRECIATION	EARNINGS BEFORE TAX	TAX	EARNINGS AFTER TAX	CASH FLOWS (EAT+DEP.)	PV @ 10%	PV of CASH FLOWS
1	70000	40000	30000	12000	18000	58000	0.909	52722
2	80000	40000	40000	16000	24000	64000	0.826	52864
3	120000	40000	80000	32000	48000	88000	0.751	66088
4	90000	40000	50000	20000	30000	70000	0.683	47810
5	60000	40000	20000	8000	12000	52000	0.621	32292

Net Present Value of Cash Inflows = Rs.2,51,776/-

Present Value of Cash Outflow = Rs.2,00,000/-

Profitability Index= $\frac{Present\ value\ of\ Cash\ Inflow}{Present\ value\ of\ Cash\ Outflow}$ =$\frac{251776}{200000}$

=1.2588

 ISBN: 978-93-90214-20-4

6.6 Internal Rate of Return

Table 6.6 Showing the calculation of Internal Rate of Return

YEARS	EARNING S BEFORE DEPRICIATION & TAX	DEPRECIATION	EARNINGS BEFORE TAX	TAX	EARNINGS AFTER TAX	CASH FLOWS(EAT+DEP.)	PV @ 10%	DISCOUNTED CASH FLOWS	PV @ 20%	DISCOUNTED CASH FLOWS
1	70000	40000	30000	12000	18000	58000	0.909	52722	0.833	48314
2	80000	40000	40000	16000	24000	64000	0.826	52864	0.694	44416
3	120000	40000	80000	32000	48000	88000	0.751	66088	0.578	50864
4	90000	40000	50000	20000	30000	70000	0.683	47810	0.482	33740
5	60000	40000	20000	8000	12000	52000	0.621	32292	0.401	20852

Net Discounted Cash Flows @ 10%=Rs. 2,51,776/-
Net Discounted Cash Flows @ 20 %=Rs. 1,98,186/-

IRR=Lower Rate + $\frac{Present\ Value\ at\ lower\ rate}{Present\ Value\ at\ lower\ rate - Present\ Value\ at\ higher\ rate} * Difference\ in\ Rates$

$=10\% + \frac{251776}{251776-198186} * (20-10)\%$

=56.98%

7. RESULTS & DISCUSSIONS

The Payback Period is 2 years 10 months and 23 days i.e. the initial investment can be recovered in the calculated time.

The Average Rate of Return is 22.40%.

The Net Present Value i.e. NPV =Rs. 51,776 is satisfactory.

The Internal Rate of Return i.e. IRR =56.98% is good to an extent.

The Profitability Index is fairly good. As PI (i.e 1.2588) is greater than 1, hence the project can be accepted.

The above calculations can be performed for different techniques and get results for the same techniques for any project where the banking organization would like to invest in and foresee whether the project they are going to invest in reaps benefits to them in future. This helps in taking the call as to choose and go with the project that is most profitable.

Generally, the calculations are done manually but the same steps can be done through automation or programmatically using python language. The above given algorithm steps when written and compiled using python language can ease the tedious task of manually updating cash flows for different successive years and computing the results for different techniques.

Most of the large organizations consider all the measures because each one provides somewhat different piece of relevant information to the decision makers and yet an impression has been created that the firms should use NPV method for decision making.

The reason why NPV is considered as superior method because it helps the organization to decide as to which project is the most profitable by ranking projects of different sizes over varying period of time.

8. CONCLUSION

All the methodologies of capital budgeting postulate that several investment offers under concern are mutually exclusive which may not essentially be accurate in certain situations. Ambiguity and threat pose major restrictions to the methods of capital budgeting. Urgency is another check in the valuation of capital investment judgements. The method of capital budgeting involves valuation of future cash inflows and outflows. The future is always undefined and the data collected may not be precise. Clearly the outcomes based upon incorrect data may not be respectable.

REFERENCE

[1] Capital Budgeting Concept at: https://youtu.be/ZOaGNDmKpzo

[2] Capital Budgeting at: https://en.m.wikipedia.org/wiki/Capital_budgeting

[3] An Introduction to Capital Buddgeting at: https://www.investopedia.com/articles/financial-theory/11/corporate- project-valuation-methods.asp

[4] Taylor, G.A. (1964). Managerial and Engineering Economy. Van Nostrand Reinhold Cp., New York

[5] Rishi, D., & Rao, N. (2005). Capital Budgeting Practices: A Perceptual Study, Sri Lankan Journal of Management, 10(1&2), 93-97

[6] Mao, J.C.T. (1970). Survey of Capital Budgeting: Theory and Practice, Journal of Finance, 349-360

[7] Miller, E. (1987). The Competitive Market Assumption and Capital Budgeting Criteria, Financial Management, 16(44), 22-28

[8] Solomon, E. (1956). The Arithmetic of Capital-Budgeting Decisions, Journal of Business, 124-129

[9] Capital Budgeting Theory and Practice at: https://academized.com/samples/capital-budgeting-theory-and-practice

[10] https://ieeexplore.ieee.org/document/5974625

[11] Capital budgeting: a systematic review of the literature at: https://www.scielo.br/scielo.php?script=sci_arttext&pid=S0103-65132020000100402

[12] Arya, A., Fellingham, J.C. and Glover, J.C. (1998) 'Capital budgeting: some exceptions to the

netpresent rule', Issues in Accounting Education, Vol 13, No. 3, pp.499-508.
[13] Block, S. (1997) 'Capital budgeting techniques used by small business firms', Engineering Economist, Vol. 42, pp.289-302
[14] Brealey, R.A., Myers, S.C. and Allen, F. (2011) Principles of Corporate Finance, 10 ed., McGraw Hill.
[15] Brounen, D., De Joung, A. and Koedijk, K. (2004) 'Corporate finance in Europe: confronting theory with practice', Financial Management, Vol. 33, pp. 71-101
[16] Brennan, M. J. and Trigeorgis, L, 2000. Project Flexibility, Agency and Competition, Oxford University Press, Oxford and New York.
[17] Busby, J. S., and Pitts C. G. C., 1998. Assessing Flexibility in Capital Investment, London: The Chartered Institute of Management Accountants
[18] Butler, R., Davies, L. Pike, R., and Sharp, J., 1993. Strategic Investment Decision-Making: Theory, Practice and Process, London/New York: Routledge
[19] Drury, C., 2003. Cost and Management Accounting, 5th edition, Thomson.
[20] Gitman, L.J. (2008) Principles of Managerial Finance, 12th ed., Pearson International.
[21] Horngren, C.T., Bhimani, A., Datar, S.M, and Foster, G., 2002. Management and Cost Accounting, 2nd edition, Hemel Hempstead: Prentice Hall.
[22] Lazaridis, I.T. (2004) 'Capital budgeting practices: a survey in the businesses of Cyprus', Journal of Small BusinessManagement, Vol. 42, No. 4, pp.427-433.
[23] Maccarone, P. (1996) 'Organizing the capital budgeting process in large firms', Management Decision, Vol. 34, No. 6, pp.43-56.
[24] Louderback, J.G., Holmen, J. S. and Dominiak, G. F., 2000. Managerial Accounting, 9th edition, South-Western College Publishing.
[25] Northcott, D., 1998. Capital Investment Decision-Making, London: International Thomson Business Press.
[26] Trigeorgis, L., 1999. Real Options and Business Strategy: Applications to Decision-Making Risk Books. Pinches, G E., 1998. Real Options: Developments and Applications, The Quarterly Review of Economics and Finance, 38, 533-536.

Test Case Reduction Using Statement Coverage Based Antcolony System

[1] Dr.C.P.Indumathi, [2] Dr.N.Suguna, [3] P.Subhavarshini, [4] V.Dharani

[1] Assistant Professor, DCSE, BIT Campus, Anna University, Tirchirappalli, Tamil Nadu, India
[2] Associate Professor, Department of CSE, GCE, Sengipatti, Tanjavur, Tamilnadu, India
[3] Department of CSE, Jeepiar Engineering College, Chennai, Tamilnadu, India
[4] UCE, BIT Campus, Anna University, Tirchirappalli, Tamil Nadu, India

Abstract:

Prioritization of test cases and ordering them for improving the performance of regression testing has become an important researchsubject in recent technology. This paper presents an appropriate method for the Ant Colony System (ACS) to address the problem ofcoverage-based test case priority setting. A tour-based heuristic mechanism and a tree-shaped updation of pheromone rule are used inthis method. The underlying logic is in their later journey, the partially built solutions of the antsare used, and their search is variedsimultaneously. To improve the algorithm's convergence speeda sorting based local search mechanism was used. The propound method is tested and the experimental results have shown that this technique will surpass other state-of-the-artmethods in terms of Average Percentage of Statement Coverage(APSC).Subsequently ,reduced significant number of test cases and help the software testers for immediate testing process.

Keywords:

Test suite reduction, Test case prioritization, control flow graph, Ant Colony Optimization

1. INTRODUCTION

Regression testing was time-consuming task and it is very costly. This accounts for as much as half of the total cost of maintaining apps. The quantity of regression testing has also increased with the ongoing development of the software systems. Also, the number of test cases is getting much greater. If all test cases were made tore-run,it might can take days , weeks or even months. [1]. Thus researchers have suggested numerous methods to enhance the efficiency of regression testing and make it cost-effective. Such methods are listed in the analysis carried out by Yoo and Harman as test suite
minimization, test case selection and test case prioritization [2]. In this project, our aim is to eliminate the redundant test cases in the regression testing suite and thus minimizing the cost of regression testing. It is achieved by solving statement cover-age-based sequence of a control flow graph CFG (Singh, 2012) and prioritize them as per the combined pheromone level and heuristic value on the path. The CFG is a schematic representation of the program's source code. The program statements are represented by the nodes and the flow of control by the edges(Singh, 2012). Throughout our work, we have focused on decision to decision (DD) paths in CFG, a directed graph with program statements as nodes and control flow between those nodes are represented through edges. Bio-inspired algorithms are used to solve complex optimization problems in an optimal manner. The Test Case Prioritization-ANT (TCP-ANT), is used here with ant colony optimization[3] as the basis.Nonetheless ,by using pheromones the current approaches for TCP problems are relied to direct the search while dismissing the heuristic function. We designed the ACO to speed up the search on the basis of a particular problem.Therefore, to boost search performance we can use domain information but,in the existing Ant Colony Optimization(ACO) for the coverage based TCP there is a issues to use domain information.In this paper, to effectively address the TCP-related coverage issues we suggest an expanded Ant Colony Optimization (ACO) architecture, it is capable of using domain-specific expertise and historical search information to direct the finding process. To aid the suggested ACO system we develop an ACB-Heuristic(Additional Coverage-Based Heuristic) method and proved it to be a deciding factor of TCP-related coverage problems to a certain degree and developed a new local search system based on theoverhead described mechanism. The considerable findings are as follows:

i) To help artificial ants to select the states to transmit next according to problem-specific information we propound an ACB-Heuristic approach, i.e. the remaining test cases coversthe number of uncovered statements. This heuristic blends the quest for the efficiency of the state-of-the-art additional greedy approach with the global search ability of the ACO method, such that the theoretical scheme avoids the downside of existing techniques

ii)We are suggesting a sorting-based local search (SB-LS)method to refine the answers of artificial ants. Depending upon a coverage-based TCP problem's solution key property, thissearch method boosts solution consistency and the finding performance. In addition, this finding is universal and to be extended to the consistency of answers

of coverage-based TCP problems produced by several other approaches.

iii) We also perform detailed studies to test the conceptual structure for the ACO. In contrast,multiple stateoftheart approaches are introduced. The research uses a variety of comparison problems and functional issues. The findings have shown that the new ACO has high effectiveness and generality.

The remaining portion of this article is structured as follows. Section II discusses the overtures ofthe coverage-based and the ACO approach, and reviews several relevant works. Section III provides the basis for the propound ACO. The experiments are provided for in Section IV. Section V addresses threats to the study's validity. This report is eventually concluded in Section VI.

2. RELATED WORK

Throughout the last few years, we have gone across the effects and usefulness of Ant Colony Optimizatiom(ACO) and swarm-based methods to automate the different phases of software testing. N.Sethiet's.Al. in [7] used ACO in regression testing to reduce test suite. S. Yang et al. Al.[8] implemented a updated ACO approach for automatic testing of applications. We introduced new update coefficient for local pheromones and con-trasted the findings with current approaches focused on random and genetic algo-rithms. In their research they report increased performance and test coverage [9]C. Lu et.Al. by using tree-shaped function for pheromone updates for statements cover-age-based test case prioritization.Mukesh Mann et al.[10] al-so ACO to automate the program development processes by adding it to flow graph control and decision graphs.

3. PROBLEM DEFINITION

TCP problem inregression testing are defined in Rothermel et al.[4] as follows:

Problem in Test Case Prioritization is defined as follows:

Given: A test suite T, PT, the set of permutations of T and f , a function from PT to real numbers. Problem: Find T′ ∈ PT such that (∀T″) (T″ ∈ PT) (T″ , T′) [f (T′)≥ f (T″)].

PT denotes the set of all possible ordering of T and f is a function that yields an award value when applied to any such ordering. Proposed by Li et al. [5], the Average Percentage of Statement Coverage (APSC) metric is calculated using below formula (1),

$$APSC\left(T'\right) = 1 - \frac{TS_1 + TS_2 + \cdots + TS_m}{mn} + \frac{1}{2n} \quad (1)$$

Here, m=total number of statements being evaluated in this program, n=number of test cases in T and TSi - is the first test case in T′ covering a statement.

4. ANT COLONY ALGORITHM

AS algorithm used to solve a travelling salesperson problem but it does not delt with the progressive(state-of-the-art)algorithms.AS algorithm is the first algorithm,inspired by the action of real ants.AS algorithm has the benefit of implementing Ant Colony Optimization algorithms and demonstrating the promise of using artificial pheromone and ants to accelerate the search for ever fitter solutions to compounded problems of optimization. The forthcoming work was driven by two objectives:Theinitial objectiveis to enhance it's efficiency and then second was to analyze and describe its behaviour. A simpler version was transpired that retained approximately the balanced level of efficiency, calculated by sophistication of algorithms and numerical tests described in 1996 Ant Colony System (ACS)[6]. Because ACS is one of the basis of several algorithms described in following years, we concentrate on ACS rather than AS. Three major aspects varies ACS from the previous AS:

4.1 Pheromone

In ACS, after all of the ants have measured their tour (i.e. at the end of each iteration) AS updates the pheromone trail using all the solutions generated by the ant colony. Growing edge of one of the calculated solutions shall be changed by a pheromone quantity equal to its solution value. By the conclusion of this step, the pheromone of the whole system evaporates and the building and upgrading process is iterated. In the opposite, ACS uses the best solution computed after the beginning of the calculation to update pheromone globally. Like in the case of AS, global updates are meant to improve the attractiveness of the desirable path, but the ACS approach is more successful because it prevents long convergence time by specifically focusing the search in the neighborhood of the best route to the current iteration of the algorithm.

In ACS, the final evaporation phase is substituted by a local updation of the pheromone applied during the construction phase. Every time an ant moves from the current to the next, the edge-associated pheromone is changed as follows (2):

$$\tau(r,s) \leftarrow (1-\rho)\cdot\tau(r,s) + \rho\cdot\tau_0 \quad (2)$$

here $0 \le \rho \le 1$ is a parameter (set at 0.9) and the starting pheromone value is $\tau 0$.Theresult of local updation is to dynamically adjust the eligibility of the edges.When each time an ant is use an edge, this becomes moderately less preferable and pheromone remains $\tau 0$ just for the edges that were never part of a global best tour. A significant trait of local updating and global updating process at every edge's pheromone $\tau ij(t)$ is inferior constrained by $\tau 0$.

4.2 State transition rule

This rule was used during the development of upto date answer, each ant agrees on the state to transit next by state transition rule step. A new state transition rule is introduced in ACS called pseudo-random-proportional. Byusing the random-proportional rule of AS, the next state is automatically chosen with a distribution of probabilities based on ηij and τij. Then the upcoming state is randomly chosen based on ηij and τij weighted by α (equal to 1) and β (equal to 2) with a probability distribution.

 ISBN: 978-93-90214-20-4

5. PROPOSED APPROACH

The proposed algorithm is constructed based on the Ant Colony System (ACS)[3] and is called the Coverage Based ACS(CB-ACS). A test suite T = {t1, t2, ..., tn} containing n test cases covering a total of m statements in a program tested is translated to a graph G = {V, E}. V is the set of vertices with n real vertices corresponding to the n test cases and one virtual vertex v-1.All ants start their traversal from virtual vertex. Ants are aimed at stopping when complete coverage of statements is obtained and are discouraged from unnecessary traversals to all vertices. Start index was one virtual vertex v-1 and n real vertices, in graph G we transform the n unordered test cases. The heuristic of CRP is extended to discover the first history better solution TH0. The quantity of τ0= APSC(TH0) pheromone is deposited on each common edge and also on the virtual edge in G, then all the artificial ants are initialized at v-1.

S is a set consisting of all statements. Sak denotes the set of statements this statement was already covered by an artificial ant k. The heuristic function is denoted by η, From vertex vr to vs, the heuristic value for ant k defined below using the formula(3):

$$\eta k(r,s)=|(S\backslash Sak)\cap Svs| \quad (3)$$

Where Svs is the covered statement sets of vertex vs, S\Sak obtains the complementary set of Sak within S. The above formulation returns the input set elements ηk(s) and determines the cost of moving ant k to s. k will consider and transfers to s at the stage of a candidate vertex s contains statements that was never covered by k at that iteration. Otherwise, ηk(s) becomes zero if Sakcontain all the elements in Svs, and k was constant. A vertex yields a larger heuristic if k covers more additional statements by moving to it, and yields smaller heuristics if it provides comparatively fewer additional statements for k. At the end of each transition, Sak value is updated by by using formula(4):

$$Sak \leftarrow Sak(Svs\backslash Sak) \quad (4)$$

computes the difference of Svs and Sak ,WhereSvs is the set of statements covered by the selected vertex s.

Using the PRP rule [11] defined below(5),

$$P_k(r,s)=\begin{cases}\frac{[\tau(r,s)]\cdot[\eta(r,s)]^{\beta}}{\sum_{u\in J_k(r)}[\tau(r,u)]\cdot[\eta(r,u)]^{\beta}}, & \text{if } s\in J_k(r)\\ 0, & \text{otherwise}\end{cases} \quad (5)$$

Ants attempt to transit vertices both with a larger number of statements and belong to the initial answer, with a biased probability escaping local optima. After each transition by LPU rule, on G all ants deposit the pheromone. Finally, all artificial ants are stop at a vertex, the full statement coverage is attained place.The sorting based local search(SB-LS) mechanism was applied by which the constructed solutions are fine-tuned and their fitness values are calculated. The GBT tree was revised by comparing the iteration-best fitness value and the historybest one accordingly. Finally,to update the amount of pheromone on G we use the proposed GBT tree was used which uses the GPU rule.

```
#include<stdio.h>
#include<math.h>
1.  void main()
2.  {
3.  double a,b,c;
4.  double a1,a2,a3;
5.  int valid=0;
6.  clrscr();
7.  printf("enter first side of triangle");
8.  scanf("%f",&a);
9.  printf("enter second side of triangle");
10. scanf("%f",&b);
11. printf("enter third side of ttriangle");
12. scanf("%f",&c);
13. if(a>0&&a<100&&b>0&&b<=100&&c>
    0&&c<100){
14. if((a+b)>c&&(b+c)>a&&(c+a)>b){
15. valid=1;
16. }
17. else{
18. valid=-1;
19. }
20. }
21. if(valid==1){
22. a1=(a*a+b*b)/(c*c);
23. a2=(b*b+c*c)/(a*a);
24. a3=(c*c+a*a)/(b*b);
25. if(a1<=1||a2<=1||a3<=1){
26. printf("obtuse angled triangle");
27. }
28. else if(a1==1||a2==1||a3==1){
29. printf("right angled triangle");
30. }
31. else{
32. printf("acute angled triangle");
33. }
34. }
35. else if(valid==-1){
36. printf("\ninvalid triangle");
37. }
38. else{
39. printf("\ninput values are out of range");
40. }
41. getch();
42. }
```

Fig.1.Triangle program

 ISBN: 978-93-90214-20-4

As in Fig 1, Triangle classification program[12] is used and we generated a CFG with each node covering different number of statements shown in Fig 2. Initially the program consists of 25 test cases each with different statement coverage represented graphically in(). Applying our proposed approach using Conditional Random Push method we can obtain an initial solution with which τ0 is calculated [].

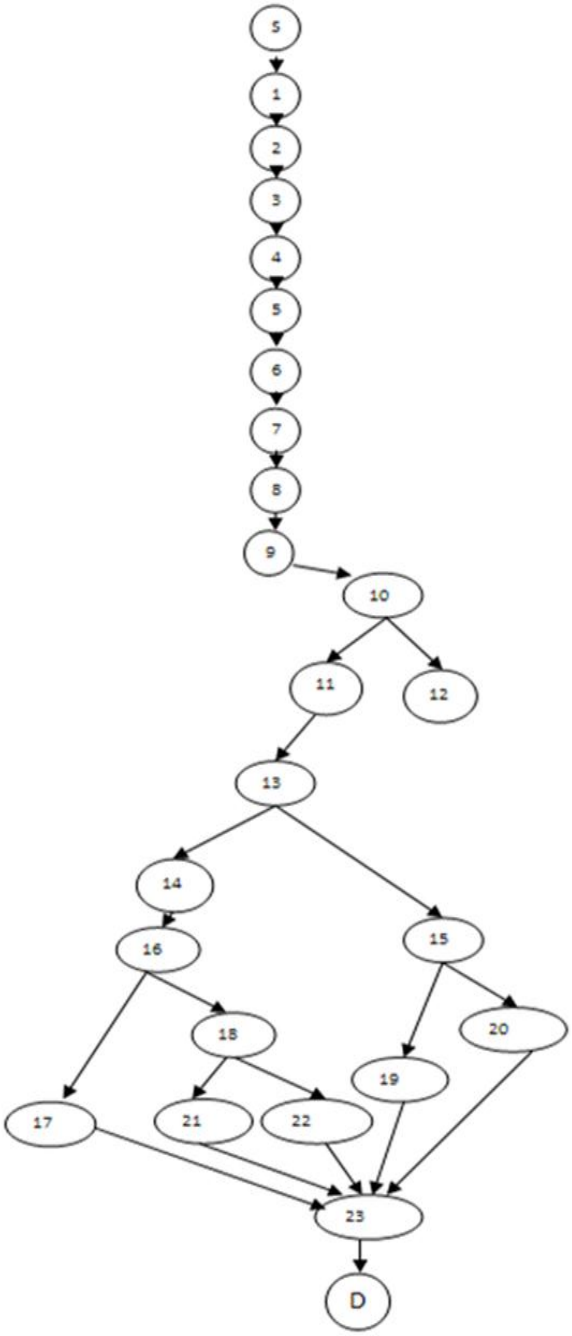

Fig. 2.CFG for Triangle program

According to our algorithm, ants traverse to each node with highest statement coverage and pheromone strength thereby achieving prioritization.The statement covered by each node is shown in table 1.The statement covered by each test case is shown in table 2.The highest priority is given to the node having the maximum combined strength of pheromone and heuristic. The traversal of nodes ends when full statement coverage is achieved that results in the reduction of the test suite size drastically.The graphical representation of test suite and reduced test suite shown in Fig 4 and Fig 5.. The resulting test suite size for the considered program is 5.

Table.1.Statements covered by each node

S.NO	NODES	STATEMENTS COVERED
1	S	1
2	1	2
3	2	3
4	3	4
5	4	5
6	5	6
7	6	7,8
8	7	9,10
9	8	11,12
10	9	13
11	10	14
12	11	15,16
13	12	17,18,19,20
14	13	21
15	14	22,23,24
16	15	35
17	16	25
18	17	28
19	18	26,27
20	19	36,37
21	20	38,39,40
22	21	29,30
23	22	31,32,33,34
24	23	41
25	D	42

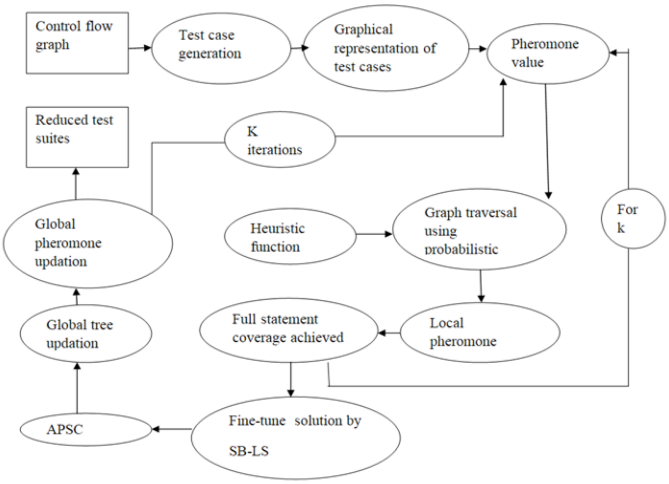

Fig 3.System Architecture Design

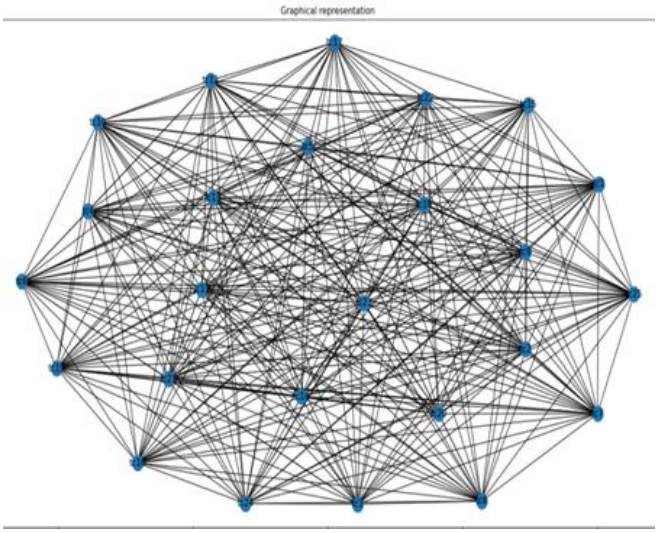

Fig4. Graphical representation of Test Suite

Table.2.Statements covered by each Test case

TEST CASES	INPUT	OUTPUT	NODES COVERED	STATEMENTS COVERED
T1	(101,88,63)	Input value out of range	1-9,20,23,D	(1-13,38-42)
T2	(3,4,6)	Obtuse angled	1-11,13,14,16,18,23,D	(1-15,21-27,41,42)
T3	(3,4,5)	Right angled	1-11,13,14,16,17,21,23,D	(1-15,21-25,28-30,41,42
T4	(2,3,4)	Obtuse angled	1-11,13,14,16,18,23,D	(1-15,21-27,41,42)
T5	(3,3,6)	Acute angled	1-10,22,23,D	(1-14,31-34,41,42)
T6	(10,3,4)	Invalid triangle	1-10,12,15,19,23,D	(1-14,17-20,35-37,41,42)
T7	(4,2,2)	Acute angled	1-10,22,23,D	(1-14,31-34,41,42)
T8	(98,108,201)	Input value out of range	(1-9,20,23,D)	(1-13,38-42)
T9	(0,0,0)	Invalid triangle	1-10,12,15,19,23,D	(1-14,17-20,35-37,41,42)
T10	(2,0,2)	Invalid triangle	1-10,12,15,19,23,D	(1-14,17-20,35-37,41,42)
T11	(7,2,2)	Invalid triangle	1-10,12,15,19,23,D	(1-14,17-20,35-37,41,42)
T12	(5,6,7)	Right angled	1-11,13,14,16,17,21,23,D	(1-15,21-25,28-30,41,42
T13	(5,12,13)	Right angled	1-11,13,14,16,17,21,23,D	(1-15,21-25,28-30,41,42
T14	(8,15,8)	Obtuse angled	1-11,13,14,16,18,23,D	(1-15,21-27,41,42)
T15	(11,18,15)	Obtuse angled	1-11,13,14,16,18,23,D	(1-15,21-27,41,42)
T16	(10,12,12)	Acute angled	1-10,22,23,D	(1-14,31-34,41,42)
T19	(15,20,8)	Obtuse angled	1-11,13,14,16,18,23,D	(1-15,21-27,41,42)
T20	(7,2,3)	Invalid triangle	1-10,12,15,19,23,D	(1-14,17-20,35-37,41,42)
T21	(10,5,5)	Acute angled	1-10,22,23,D	(1-14,31-34,41,42)
T22	(8,9,15)	Obtuse angled	1-11,13,14,16,18,23,D	(1-15,21-27,41,42)
T23	(4,1,1)	Invalid triangle	1-10,12,15,19,23,D	(1-14,17-20,35-37,41,42)
T24	(2,4,201)	Input value out of range	(1-9,20,23,D)	(1-13,38-42)
T25	(20,10,10)	Acute angled	1-10,22,23,D	(1-14,31-34,41,42)

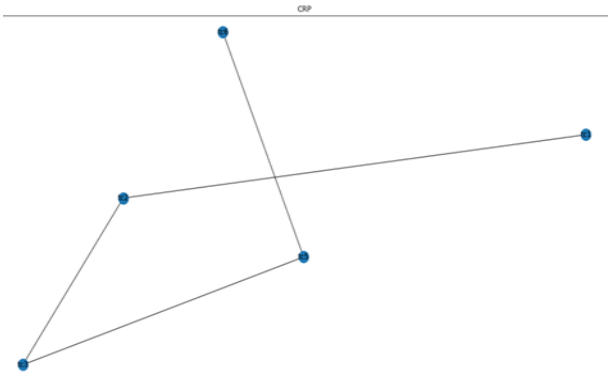

Fig 5. Graphical Representation of Reduced Test Suite

6. RESULTS AND CONCLUSION

This paper used ACS for reducing the test suite, which automatically selects the optimum test path in a control flow graph by making use of CB-ACS. An Ant can effectively discover the CFG states and reduces the test suite for testing automatically. CB-ACS prioritize and the number of test cases for execution will be reduce according to the normal foraging action of ants and thus helps software testers to a great degree. In Ant Colony Optimization(ACO), Artificial Bee Colony Optimization (ABC), Particle Swarm Optimization (PSO), Genetic Algorithm, Simulated Annealing and are only a few other meta heuristic methods on which work can be done to harness species' natural intelligence and solve NP problems**.**

REFERENCE

[1] R.Wang, B.Qu, Y.Lu.(2015).“Empirical study of the effects of different profiles on regression test case reduction”.IETSoftw, 9(2), pp.29–38.

[2] Yoo, S., & Harman, M.(2012). Regression testing minimization, selection and prioritization: a survey. Software Testing, Verification and Reliability, 22(2), 67-120. https://doi.org/10.1002/stv.430

[3] S.Karma, Y.Singh, S.Dalal and P.R.Srivastava, Test case prioritization: A approach based on modified ant colony optimization, In Proc.Int.Conf,Emerg.Res.Comput(2016)

[4] Y.Singh, a.Kaur and B.Suri, Test case prioritization using ant colony optimization, ACM SIGSOFT Eng.(2010)

[5] Dorigo, M., Gambardella, L.: Ant colony system: a cooperative learning approach to the traveling salesmanproblem. IEEE Trans. Evol. Comput. 1(1), 53–66 (1997)

[6] G. Rothermel; R. H. Untch; Chengyun Chu; M. J. Harrold. 2001. Prioritizing Test

[7] Cases for Regression Testing. IEEE Trans. on Soft. Eng. 27, 10 (2001), 929–948.

[8] Zheng Li; Mark Harman; Robert M. Hierons. 2007. Search Algorithms for Regression Test Case Prioritization. IEEE Trans. on Soft. Eng. 33, 4 (2007), 225–237

[9] Dorigo, M., Maniezzo, V., und Colorni, A.: The Ant System: Optimization by a colony of cooperating agents. IEEE Transactions on Systems, Man, and Cybernetics Part B: Cybernetics. 26(1):29–41. 1996.

[10] N. Sethi, S. Rani, and P. Singh, "Ants Optimization for Minimal Test Case Selection and Prioritization as to Reduce the Cost of Regression Testing," Int. J. Comput. Appl., vol. 100, no. 17, pp. 48– 54, 2014.

[11] S. Yang, T. Man, and J. Xu, "Improved ant algorithms for software testing cases generation," Sci. World J., vol. 2014, 2014.

[12] C. Lu, J. Zhong, and C. Author, "An Efficient Ant Colony System For Coverage Based Test Case Prioritization," in GECCO '18 Companion, 2018, pp. 91–92.

[13] M. Mann and O. P. Sangwan, "Generating optimization and prioritizing optimal paths using ant colony," vol. 5, no. 1, pp. 1–15, 2015.

[14] O.Dhaiya and K.Solanki, "A Systematic literature study of regression test case prioritization approaches," Int.J.eng,Technol

[15] D.Yamuna, Dr.N.Sasirekha, An overview on test case reduction methods for data mining techniques, International Journal of Contemporary Research in Computer Science and Technology(IJCRCST)(2017)

[16] Marwah Allah, Dima Suleiman, Adnan S, Test case reduction Technique Survey(IJACSA)International Journal of Advanced Computer Science and Applications(2016).

Socio - Economic Background of Women Entrepreneurs in Thoothukudi District

[1] D. Shakila, [2] Dr. A.M.Tony Melwyn

[1] Kamaraj College (Affiliated to Manonmaniam Sundaranar University, Tirunelveli), Thoothukudi, India
[2] Associate Professor and Director of Self-Financing Courses, Kamaraj College (Affiliated to Manonmaniam Sundaranar University, Tirunelveli), Thoothukudi, India

Abstract:

Women entrepreneurship play a energetic role in the economic development of a country. Economic development of a country depends essentially on its entrepreneurs. Women are highly empowered and dynamic nowadays. So they also participate in all such activities to raise the economic status and economical prosperity of the country. Women entrepreneurs run business more efficiently than men nowadays. This shows they are highly entitled in this society. Women entrepreneurs are those who bring about business idea, strengthen an organization, amalgamate the factors of production, operate the unit, undertake risks and handle problems involved in operating a business enterprise.Economic affluenceand social fortune of a nation always depends on the cooperate strength of innovation, creativity and cognitive aid and effort of both men and women. The success of the entrepreneur depends on the environmental factors such as social, economic, legal, political and technology which influence their activities thus leading to successful entrepreneurship. The present article, focuses on the demographic profile of the women entrepreneurs and their socio-economic background of women entrepreneurs in Thoothukudi district.

Keywords:

Women Entrepreneurs, Demographic Profile, Socio Economic Background, Women Empowerment

1. INTRODUCTION

Women entrepreneur is a person who accepts arduous role to meet her own consumption and become economically independent. Economic independence makes women aware of their rights. Nowadays women have slowly come out of their home to earn something for substance of their families, as the earnings of a single individual is not sufficient. Women have taken hold in agronomy operations, home industries, trade and commerce and other related economic activities. It leads to economic independence of women and women empowerment.

Socio economic conditions play important role in the formation of stratified business policies. The socio environment of a person strongly affects the entrepreneurial behavior and it includes the values, attitudes, beliefs, customs religion and habits of the people. On the other hand economic environment is not easily controllable, it includes factors like economic condition, economic policies, state of various resources and facilities like capital, raw materials, infrastructure so on.

Women entrepreneurship play a pivotal role in women empowerment. Empowering women through entrepreneurship influence women development, economic growth, social stability. Women can invest capital, run the business, take risk and get the profits of the business carried on by them. Visibly, their socio-economic status increases in the society.

2. OBJECTIVES OF THE STUDY

The research paper has the following objectives:

1. To study about women Entrepreneurs involved in the various business activities and employment opportunities provided by them especially to the women in the study area.
2. To understand the economic activities created by the women entrepreneur and their empowerment.

3. STATEMENT OF THE PROBLEM

Women have a good merger of entrepreneurial psyche, ambition, discipline and tenacity. All these help them to succeed in these highly evaporative markets. Entrepreneurship can permit women not only to participate in the activity of economic development, but also empower them. The 21st century women are victorious, yet a many face hurdles and challenging constraints. Many women face challenging constraints in the form of finance, scarcity of raw materials, stiff competition, mobility, family restriction, lack of education, lack of mental strength, unfavorable business environment and lack of risk-bearing ability. At this juncture, an attempt has been made by the researcher to study the Socio Economic background of women entrepreneurs in Thoothukudi District.

4. SCOPE OF THE STUDY

The study covers entrepreneurial skills of entrepreneurs in the enterprises such as Palm products, Tailoring, Food Items, and Handicrafts in Thoothukudi District and also

focuses on the Socio Economic conditions of Women entrepreneurs in Thoothukudi District. The study analyses a broad scope strategy to understand the realistic status and treatment provided to women entrepreneurs in the present socio-economic environment.

5. METHODOLOGY

Data was collected from 30 women entrepreneurs in Thoothukudi district. Primary data was collected using structured questionnaire prepared and administered among the women entrepreneurs to collect data. Secondary data was collected from books, internet, websites, journals, etc.

6. SAMPLE FOR THE STUDY

Stratified random sampling method was adopted. The sample size for the present study is 30 respondents.

7. TOOLS FOR ANALYSIS

Appropriate statistical tools like Percentage Analysis and Garrett Ranking technique were applied to analyses the data and to draw valid conclusions.

8. LIMITATIONS OF THE STUDY

The study is based on women entrepreneurs, hence has the limitation of generalization. The constraint of limited time has forced the researcher to restrict the size of the sample to only 30. It is presumed that whatever data disclosed by the entrepreneur is true.

9. ANALYSIS

The researcher has analysed the Socio economic background of women entrepreneurs and has collected data with the help of questionnaire subjected to a critical interpretation. The interpretation and analysis have been carried out by assessing different types of women entrepreneurs. The socio factors related to the family and communities have a bearing on entrepreneurship. The economic factors related to financial support and develop entrepreneurship.

TABLE 1.1: Personal profile of women entrepreneurs

Socio Economic Problems	1	2	3	4	5	Total	Garrett Mean Score	Rank
High price of Raw materials	750	420	300	160	75	1705	56.83	III
Mobility Constraints	375	360	250	240	200	1425	47.5	VI
Financial Problem	900	420	150	160	100	1730	57.66	I
Lack of support from family Members	600	720	250	80	75	1725	57.5	II
Stiff Competition	675	660	150	80	125	1690	56.33	IV
Lack of entrepreneurial skill among women	450	300	200	280	200	1430	47.66	V

Marital Status	Married	21	70
	Unmarried	9	30
	Total	30	100
Type of Family	Joint family	12	40
	Nuclear family	18	60
	Total	30	100
Size of the Family	Up to 3 members	3	10
	4 members	9	30
	5 members	8	26.6
	More than 5 member	10	33.3
	Total	30	100
Type of Business	Palm products	6	20
	Tailoring	5	16.6
	Food Items	10	33.3
	Handicrafts	4	13.3
	Others	5	16.6
	Total	30	100
Net Monthly Income From Business	Upto 5,000	4	13.3
	5,000-10,000	8	26.6
	10,000-15,000	4	13.3
	15,000-20,000	5	16.6
	Above 20,000	9	30
	Total	30	100
No. Of. Workers Employed	2 workers	5	16.6
	3 to 6 workers	8	26.6
	7 to 10 workers	11	36.6
	More than 10 workers	6	20
	Total	30	100

 ISBN: 978-93-90214-20-4

It is inferred from Table1.1 highlights the fact that (23.3%) of the women entrepreneurs belong to the age group of 20 to 30 years, followed by (33.3%) belonging to the age group of 30 to 40 years. Thus it is clear that young women aged 20 to 40 years have the capability to work hard, desire for high achievement and high degree of optimism form a greater proportion of women entrepreneurs in the study area. Majority of the women entrepreneurs (46.6%) belong to Hindu family followed by (13.3%) of Christian families and the least contribution (20%) is by muslim. Women entrepreneur due to the rigid religious custom followed by muslim. Most of the women entrepreneurs hail from Backward community (43.3%), 26.6% from other castes and (23.3%) from Most backward community, due to their financial and social background SC/ST constitute a very meagre percentage of 6.6. In the case of educational qualification, women who have completed their (Undergraduate courses) degree are in carrying out a new venture, their contribution is more (33.3%) when compare to SSLC educated women. (26.6%), women whose education is upto higher secondary level and below SSLC constitute only (20%) respectively. It is revealed that education gives confidence and courage and has motivated these women entrepreneurs to take up entrepreneurial activities. Majority of the women entrepreneurs (70%) are married. A greater proportion of women entrepreneurs (33.3%) have a family which consists of 5 members. From the table it is clearly evident that in the study area, 20 percent of the respondents are engaged in Palm Products , 16.6 percent in tailoring, 33.3 percent are involved in Food items, 13.3 percent are engaged in sales of Handicraft products and (16.6%) are involved in other business activity. The table shows that out of 30 women entrepreneurs a majority of (13.3%) earn a monthly income of upto Rs.5000 followed by (26.6%) earning Rs.5000-10000. 13.3 percent of women entrepreneurs earn Rs.10000-15000 and 16.6 percent of the women entrepreneurs earn Rs.15000-20000 and 30 percent of the women entrepreneurs earn above Rs.2000. It is also found that (36.6%) of the women entrepreneurs have employed 7 to 10 workers.

Table 1.2: Ranking of Socio Economic Problems Faced by women Entrepreneurs

Socio Economic Problems	1	2	3	4	5	Total	Garrett Mean Score	Rank
High price of Raw materials	750	420	300	160	75	1705	56.83	III
Mobility Constraints	375	360	250	240	200	1425	47.5	VI
Financial Problem	900	420	150	160	100	1730	57.66	I
Lack of support from family Members	600	720	250	80	75	1725	57.5	II
Stiff Competition	675	660	150	80	125	1690	56.33	IV
Lack of entrepreneurial skill among women	450	300	200	280	200	1430	47.66	V

Table 1.2 reveals that the most important problem faced by women entrepreneurs is Financial Problem which scores 57.66 points and gets I rank. The second major problem faced by the women entrepreneurs is Lack of support from family Members which scores 57.5 points and gets the II rank. High price of Raw materials occupies III rank with 56.83 points. Stiff competition is faced by majority of the women entrepreneurs which scores 56.33 points. As a result of stiff competition,the demand for the products/ services tend to decrease. Lack of entrepreneurial skill among women and Mobility Constraints score V and VI ranks respectively.

10. TEST FINDINGS

- Most of the women entrepreneurs in Thoothukudi District are young aged between 20 to 40 years form a greater proportion of women entrepreneur while the majority of them were married and were living in Nuclear family.
- 33.3 percent of the women entrepreneurs carry on entrepreneurial activities in Food items followed by 20 percent of the women entrepreneurs who deal with Palm products.
- Majority of the women entrepreneurs (30%) earn a net monthly income of above Rs.20,000.
- It is identified that women entrepreneurs employ 7 to 10 workers in the study area which contributes 36.6%
- Financial Problem, Lack of support from family Members and high price of raw materials are some of the most important Socio Economic problems faced by women entrepreneurs in the study area.

11. CONCLUSION

The researcher showed in evident to study the socio-economic background of women entrepreneurs in Thoothukudi District. Women entrepreneurs in the study area have self assurance in life. The results of the study show that the socio-economic status of women entrepreneurs have increased to a considerable extent. Government and various agencies should provide adequate support – technically, financially and psychologically to women entrepreneurs to help them handle in this ruthless business environment. Today, business is a composite and hazardous venture, so women entrepreneurs should keep face with the newest trends and technological developments and take their business to the next level.

REFERENCE

Books:

[1] Khanka S. S. Entrepreneurial Development, S Chand and Company Limited, New Delhi, (1999).

[2] Vasanthagopal R. and Santha S. Women Entrepreneurship In India, New Century Publications. (2008)[1].

Journals:

[3] ChitraChellam K. Indian Journal of Applied Research, Volume 7 September 2017.

[4] BeaulahSucharitha P. Indian Journal of Research, Volume 3, March 2014.

[5] Websites:

[6] www.womenentrepreneurship.com

[7] www.entrepreneur.com

Pomegranate Fruit Diseases Detection Using Image Processing Techniques: A Review

[1] Jayashri Patil, [2] Sachin Naik

[1] Research scholar at Symbiosis Institute of Computer Studies and Research (SICSR), Symbiosis International University (Deemed University) Pune, India
[2] Assistant Professor at Symbiosis Institute of Computer Studies and Research (SICSR), Symbiosis International University (Deemed University) Pune, Maharashtra, India

Abstract:

The Agriculture plant diseases are responsible for farmer economic losses. These diseases affect on plant root, fruit, leaf, and stem. Detection of disease at early stages helps the farmer to improve productivity. In the traditional system agriculture experts and experienced farmer can recognize the plant diseases at the lower accuracy which causes losses to farmers. Currently several researchers are proposing soft computing and expert systems to recognize plant diseases. Plant disease identification by visual way is less accurate because some diseases do not have any visible symptoms or some of the diseases appear too late at the time of harvesting. The modern technology in agriculture sector can substantially improve the agriculture production & sustainability. This paper provides a review for fruit disease detection techniques for pomegranate plants. This study includes preprocessing, segmentation, feature extraction and classification techniques for pomegranate fruit diseases detection systems. This paper also states the comparison and limitations of existing fruit disease detection techniques.

Keywords:

Plant disease detection, Classification, Feature extraction, segmentation, pre-processing, SVM

1. INTRODUCTION

Fruit agriculture play important role in every country economy. In India agricultural practices carried out in traditional manner. Agriculture has become uncertain with weather, water scarcity and pesticides are the major player in it. In 21st Century to compete the world the improved and advanced techniques should be used and implemented in farming. Developing country like India there is need of adapting new technology for increase the yield of farmer meet to requirement of customer also financial growth of farmers.

In agriculture every crop need proper management of fertilizer, irrigation, pesticides and early disease detection. Modern technology is playing important role in development of country. To achieve the highest economic growth of farmer there is need of adoption of modern technology for sustainable farming system. It is hard to detect and classify the types of disease and pests which cannot be detected by farmer. Only agriculture expert or very experienced farmers can know the type of diseases and pests on plant. So, farmers have to invite the agriculture expert to their farms or farmers need take the sample from the farm to agriculture research center. Diseases are responsible for economic, social and ecological losses. These diseases need to be control at initial stage of infection. Some of the diseases very hard to control in next stage of infection. Plant disease detection system first capturing image by image sensor devices, preprocessing technique on diseased plant leaf or fruit image, Split the image into different segments using segmentation technique, feature selection and extraction , fruit or leaf disease identification using classification. The plant leaf, fruit or stem are main visual parts of plant shown the disease symptoms. Therefore use of soft computing technique to find and classify diseases in agricultural applications is useful. Pomegranate is one of the commercial and drought tolerant crops. Pomegranate growers are essential part of the agriculture sector in India where they present significant share in agriculture economy. Pomegranate Belongs to the family of Punicaceae [1] with botanical name Punica granatum L., As per Report of National Horticulture Board of India are of pomegranate cultivation is an increasing from 2014-15 to 2018-19; similarly, the productivity has decreased from 12.15 (MT/HA) to 11.64(MT/HA) thousand tons during the same period. Pomegranate farmers are suffering from low productivity and low quality. [Source: Horticultural Statistics at a Glance, 2017].

2. POMEGRANATE PLANT DISEASES

Pomegranate plants get affected by fungi, Bacteria and pests every year. Pomegranate farmer facing a huge damage because of these diseases. Due to these diseases 60% pomegranate plant may die in the field. This section describes Pomegranate plants get affected by fungi, Bacteria and virus.

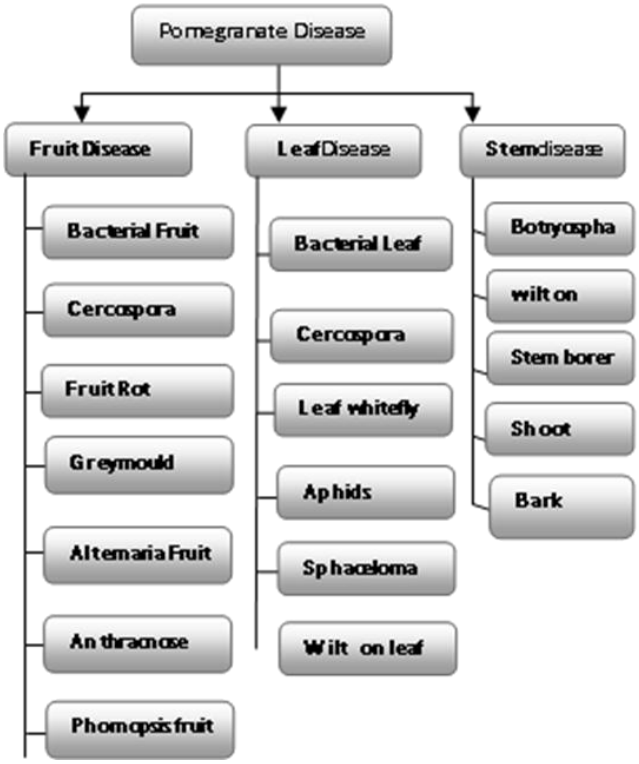

Fig. 1 Pomegranate Plant Diseases

3. POMOGRANATE PLANT FRUIT DISEASAE DETECTION STEPS USING IMAGE PROCESSING TECHNIQUES

Plant leaf detection systems follows following generic steps for leaf detection systems.

1. Pomegranate fruit image Acquisition
2. Preprocessing techniques for diseased fruit
3. Fruit segmentation with respect to disease sections
4. Retrieving interest disease section from fruit segments.
5. Extracting features from the fruit segment
6. Disease prediction using classification techniques.

3.1 Pomegranate fruit Image Acquisition

Pomegranate plant fruit image acquisition includes three ways: reflective mode imaging, Emissive imaging and transmissive imaging. This image capturing is usually carried out using image sensing devices such as cameras, radar, infrared, X-Ray, ultrasound or computer generated. After capturing this image is converted into digitization.

Bacterial Blight

Anthracnose

Cercospora

Alternaria

Fruit rot

Fruit mold

Fig. 2. Pomegranate Diseases. Source of Images [2]

3.2 Preprocessing techniques for diseased fruit

Preprocessing techniques are used to improve the quality of captured image. In this steps remove noise caused by dust, dewdrops, insect be present on the plant.

In image enhancement enhance the whole image or enhance interested region of the image. Image restoration in this process we are trying to restore blur or missing part of the image in further processing. This preprocessing step includes normalizing the intensity, removing background noise, masking portion of image, contrast improvement, image resizing, image smoothing, brightness enhancement, Histogram equalization and shadow removal activities etc.

3.3 Fruit segmentation with respect to disease sections

Fruit Image is split into different regions is called segment. Region based techniques. In segmentation mask the interested pixels in the image. In fruit disease detection most of the researchers used three techniques K-means clustering, Fuzzy C-means and Thresholding.

K-means clustering: In k-means clustering image is divide in to k-clusters. According to the future set k-means algorithm classify the image pixel in to k clusters. Initially randomly select the cluster centroid. "During classification minimizing the sum of distance squares between the data objects and the corresponding k cluster. Euclidean distance is used to measure the distance between observed value and centroid value of clustered" [3].

$$\sqrt{(Xo - Xc)2 + (Yo - Yc)2} \qquad (1)$$

Fuzzy C-means: it is soft clustering. In case of fuzzy c means allow the pixel point in more than cluster. In Fuzzy c means assign membership node to each cluster.

Algorithm:

Step 1: initializing the data point randomly.

Step 2: find out the centroid of data point following equation.

Step 3: find out the distance between observed value and centroid value.

Step 4: Updating the membership value.

Step 5: repeat the step 2 and 4 until the forming constant cluster.

Thresholding: Thresholding is segmentation technique used for converting foreground and background. In some image has dark background and light object. In this case retrieve the object from dark background.This thresholding technique are used for converting grayscale image into

 ISBN: 978-93-90214-20-4

binary image. There are two types of thresholding applied for image segmentation depending upon application.

Algorithm:
Step I: Select the initial element for threshold T.
Step II: whole image is segment using T
A1 is all the pixels with intensities >T
A2 is all the pixels with intensities<=T
Step III: compute average p1 and p2 for the pixels in A1 and A2
Step IV: Let T= (p1+p2)/2
Step V: Repeat the step 1 and 4 until constant cluster will form.

Different segmentation techniques are applied for locate object and their boundaries

3.4 Retrieving interest disease section from fruit segments.

After segmentation of image next step is retrieving interest disease section. Extracted infected part of disease on fruit. In this step future selection and feature extraction techniques are applied. In fruit image futures usually consist of morphology, color, shape, texture, spatial and wavelet transformation. Morphology is one of the most important feature in image classification and feature retrieving. Accuracy of classification is highly depend on which feature set extracted from fruit image.

3.5 Extracting the Feature from fruit segment

"Feature extraction is the process of deriving a set of values called features from an image, which provides information about the image for further processing."[4]
Different feature extraction techniques used to extract features in infected disease segment of plant leaf, stem and fruit. Feature extraction methods applied on infected region of fruit disease image are GLCM, GLRM, standard deviation, entropy, variance, smoothness, skewness, kurtosis, contrast, fuzzy c-means and k-means.

3.6 Disease prediction using classification techniques

In this step assigning Pixels in the image to categories or classes of interest. Classify a set of data into different classes. Classification is done by two methods supervised learning and unsupervised learning. There are many image classification techniques used for plant disease detection. All these classifier tested using combination of various features extracted by feature extraction techniques. Most commonly used classification techniques for classifying pomegranate fruit diseases are SVM, ANN, KNN, PNN , Minimum distance classifier. The SVM classifier achieve highest accuracy 98.5%. When you multiclassifier techniques some of the author apply KNN,SVM and PNN classifier with fuzzy c- means for disease classification this achieved 99% accuracy. The 99% accuracy is achieved closed capturing system, with high resolution camera is used. There is need of fusion of more than one feature extraction technique will achieved.

4. COMPARATIVE ANYALYSI POMEGRANATE FRUIT DISEASE DETECTION USING VARIOUS SOFT COMPUTING TECHNIQUES.

Fruit horticulture is backbone of every country. According to annual report of APEDA Maharashtra is leading state production of Pomegranate. Now a day's Indian farmer facing problem of fruit disease. "In pomegranate common fruit diseases are Bacterial Blight, Alternaria, Cercospora fruit rot, fruit rot, fruit borer, fruit mold. In India main reason of decreasing production of pomegranate is bacterial blight disease (Telya in Marathi)."[1] In this oily dark brown spot scattered on fruit. Fruit spot disease caused by fungi symptoms on fruit is light brown spot patches in fruit. Fruit rot actually this disease occurs on flowering stages they fails the process conversion of flowering to fruit. New young fruit drop on the plant. Early disease detection is essential so farmer can easily prevent theses disease at primary stage of infection. This disease detection achieved by image processing techniques.

Sr.no	Ref	Fruit Disease	Preprocessing	Segmentation	Feature Extraction	Classification	Accuracy
1	[5]	Bacterial diseases	resize, filtering, morphological operations,	K-means	HCI color model, erosion dilation operation for morphology, Gabor filter for texture feature	Minimum distance classifier (MDC).	Not specified
2	[6]	Bacterial Blight	image resizing	Not specify	Color Coherence Vector feature vectors	SVM	82%
3	[7]	Fruit rot, Fruit spot, Bacterial Blight	Removing noise	K-means	GLCM	Back-propagation algorithm	90%
4	[8]	Bacterial Blight	removes noise, smoothen the image also	K-means	Not Specify	Calculating plant leaf area and diseased	Not specified

 ISBN: 978-93-90214-20-4

			perform resizing of images			area on leaf	
7	[9]	Anthracnose, Bacterial Blight, Scab	background is removed using thresholding	Fuzzy C means	fuzzy C mean and K means	KNN, PNN and SVM with Fuzzy C Means	99%
8	[10]	Anthracnose	Canny edge detector and Median filter	K-menas	GLCM and GLRM	Nearest Neighbor and Euclidian distance	94.85%
9	[11]	Bacterial Blight, Alternaria and Scab	contrast enhancement	fuzzy C mean and K means	fuzzy C mean and K means	KNN, PNN and SVM classifier	98.3%
10	[12]	Cercospora, Bacterial Blight, Alternaria	contrast enhancement	K-means	standard deviation, entropy, variance, smoothness,	SVM	Not pecified
11	[13]	Scab, Bacterial Blight, Anthracnose	Gaussian low pass channel, Resizing	Not Specifed	standard deviation, entropy, variance, smoothness, skewness, kurtosis, contrast	KNN, PNN and SVM classifier	KNN-84.84% PNN-80% SVM-54.54%
12	[14]	Bacterial Blight, Alternaria	Removing noise	K-means	Color and texture features are extracted	BPNN classifier	97.30%
13	[15]	bacterial blight, wilt, thrip, fruit borer and scab	Image resized to 400*400	K-Means	Morphology, color and CCV	Multi-class Support Vector Machine	84%
14	[16]	Bacterial Blight, Fruit rot, Anthronous	Histogram equalization.	Not Specified	Spatial and Wavelet features extracted wavelet transform (DWT) is used for feature extraction	SVM training and Testing and Feed Forward Artificial Neural Network	SVM 76.483% ANN 92.65%

Table 1: comparative analysis of image processing techniques applied on pomegranate fruit disease detection technique.

This section presents a survey of 16 papers of pomegranate fruit disease detection including criteria such as pomegranate diseases name, Pre-processing, Segmentation, Feature Extraction, classification and accuracy. Table 1 presents the comparative analysis of image processing techniques applied on pomegranate fruit disease detection. Generally, to identify the disease from a fruit one of the most important thing is dataset. In case of pomegranate no standard dataset is available. All the dataset is created by own by capturing healthy and unhealthy fruit images from farmer field. At each step of image processing steps author applied different techniques out of which most of the author applied SVM classifier. SVM classifier gives better result. K-Means clustering techniques is widely applied for segmentation. "Fuzzy C means segmentation technique gives highest accuracy. Some of the author classify the data using multiple classifier SVM, KNN, PNN" [9]. Classification accuracy is depends upon which feature set extracted from infected region. There is need of fusion of one and more future extraction techniques applied on extracting features in disease interested area.

5. DISCUSSION AND SUMMARY

This review articles summarizes various pomegranate disease detection and classification techniques. The literature survey shows extensive computer vision techniques in pomegranate disease detection there so immense of research in this area is possible in future.

Here are some points for future research to boost current state of art.

- Most of the research on disease detection was done manually collected database. The lack of availability of

dataset remains a major challenge for enabling vision based plant disease detection. The few existing databases are either too limited or not accessible to the scientific community. There is a need to develop standard dataset for Pomegranate disease detection.

- Sometime two disease present on same fruit or Different disorders with similar symptoms challenging to identify investigate one or more diseases in same fruit accurately along with the stage of the disease.
- The research conducted till date with available techniques detects few diseases only. There is need to develop techniques which identify and classify recent pomegranate fruit disease therefore study number of more diseases.
- Some of the existing system uses manual dataset every disease having different stages Different stages having different symptoms. No one yet detect different stages of disease and exact solution of those diseases.
- Most of the existing systems are semi-automatic. There is need to develop fully automated system with collaboration of agriculture universities and research centers for upgrading the system with new diseases and checking the disease detection accuracy.
- A real time system for Pomegranate plant disease detection is not yet proposed in the existing literature. Need of exploring algorithms for image segmentation, fusion of more than one disease feature extraction selection methods to improve the output of the proposed method.
- There is need to develop decision support system/app which will easily and widely available to farmer, just by capture the plant query image of fruit captured by sensor devices and send it to the DSS system. DSS system detect the plant diseases at initial stages of infection provide plant treatments prescribed by the decision support system.
- Existing plant disease detection system having limitations in terms of techniques, size of database, captured image quality, disease symptoms varies according to variety of pomegranate plant

6. CONCLUSION

In this paper, we present a review of pomegranate plant disease detection using image processing techniques. From literature during feature extraction color, texture and morphology features are used to identify and classify the pomegranate fruit diseases. Among these techniques morphological features gives best result as compared to all other features. SVM and ANN, KNN, PNN classifier used to detect bacterial and fungal and viral diseases in fruit of pomegranate. K-means clustering for image segmentation Fuzzy c means gives highest accuracy. In existing system very few diseases are covered. There are need to cover maximum disease which are existing in pomegranate fruit. This paper is helpful for the study of existing system and work on research gaps finding and development of new technology for pomegranate fruit and plant disease. This will helpful for pomegranate farmers to increase the yield. Most of the existing systems are semi-automatic. There is need to develop fully automated system with collaboration of agriculture universities and research centers for upgrading the system with new diseases.

REFERENCE

[1] Pawar, R., & Jadhav, A. (2017, September). Pomegranate disease detection and classification. In 2017 IEEE International Conference on Power, Control, Signals and Instrumentation Engineering (ICPCSI) (pp. 2475-2479). IEEE.

[2] http://vikaspedia.in/agriculture/crop-production.

[3] Dhanashree Gadkari, "Image quality analysis using glcm", Thesis, University of Central Florida , Orlando, Florida, 2000.

[4] Bharate, A. A., & Shirdhonkar, M. S. (2017, December). A review on plant disease detection using image processing. In 2017 International Conference on Intelligent Sustainable Systems (ICISS) (pp. 103-109). IEEE.

[5] Khot, S. T., Supriya, P., Gitanjali, M., & Vidya, L. (2016). Pomegranate disease detection using image processing techniques. Pune, International Journal of Advanced Research in Electrical, Electronics and Instrumentation Engineering.

[6] Bhange, M., & Hingoliwala, H. A. (2015). Smart farming: Pomegranate disease detection using image processing. Procedia Computer Science, 58, 280-288.

[7] Dhakate, M., & Ingole, A. B. (2015, December). Diagnosis of pomegranate plant diseases using neural network. In 2015 fifth national conference on computer vision, pattern recognition, image processing and graphics (NCVPRIPG) (pp. 1-4). IEEE.

[8] Deshpande, T., Sengupta, S., & Raghuvanshi, K. S. (2014). Grading & identification of disease in pomegranate leaf and fruit. International Journal of Computer Science and Information Technologies, 5(3), 4638-4645.

[9] Shivanand B Lamani, Ravikumar K, Arshi Jamal (2018) . Pomegranate Fruits Disease Classification with Fuzzy C Mean ClusteringInternational Journal of Advance Engineering and Research Development(IJAERD) Volume 5, Issue 02, February -2018.

[10] Pujari, J. D., Yakkundimath, R., & Byadgi, A. S. (2015). Image processing based detection of fungal diseases in plants. Procedia Computer Science, 46, 1802-1808.

[11] Noola, D. (2018). Disease Identification of Pomegranate Fruit using Image Processing. Asian Journal For Convergence In Technology (AJCT), 4(3).

[12] Gaikwad, D., Karande, K., & Deshpande, H. (2016, December). Pomegranate Fruit Diseases Identification and Grading. In International Conference on

Communication and Signal Processing 2016 (ICCASP 2016). Atlantis Press.

[13] Purvimath, M. K., & Patil, P. B. POMEGRANATE FRUIT DISEASE DETECTION AND CLASSIFICATION.

[14] Sannakki, S. S., & Rajpurohit, V. S. (2015). Classification of pomegranate diseases based on back propagation neural network. International Research Journal of Engineering and Technology (IRJET), Vol2, (02).

[15] More, S., & Nighot, M. (2016, March). Agrosearch: A web based search tool for pomegranate diseases and pests detection using image processing. In Proceedings of the Second International Conference on Information and Communication Technology for Competitive Strategies (pp. 1-6).

[16] Kumar, A., Rajpurohit, V. S., & Jirage, B. J. (2018). Pomegranate fruit quality assessment using machine intelligence and wavelet features. Journal of Horticultural Research, 26(1), 53-60.

Comparative Analysis of LSTM based Deep Learning Models for Abnormal Action Prediction in Surveillance Videos

[1] Mrs. Manju D, [2] Dr. Seetha M, [3] Dr. Sammulal P

[1] Assistant Professor, Dept.of CSE., GNITS, Hyderabad, India
[2] Professor & HOD, Dept. of CSE, GNITS, Hyderabad, India
[3] Professor, Dept.of CSE, JNTUH CEJ, Hyderabad, India

Abstract:

Video surveillance is being increasingly adopted for ensuring safety and security both in public and private places. Automated prediction of abnormal events like theft, robbery, murder etc from continuous observation of surveillance videos is a multidisciplinary study involving computer vision, deep learning and artificial intelligence. Deep learning based video analysis and categorization is a most researched topic. Many deep learning models based on LSTM (Long Short Term Memory) are proposed for automated prediction of abnormal events. This work does a comparative analysis of four LSTM based deep learning models for abnormal event prediction from surveillance videos. Deep learning models of Resnet, VGG16, VGG19 and 3DCNN are combined with LSTM for prediction of abnormal event from past observation of events in the video stream. These four models are run against different benchmarked abnormal event detection datasets and performance is compared in terms of accuracy, loss and execution time.

Keywords:

Surveillance Videos, Abnormal Action Prediction, Deep Learning Models, LSTM

1. INTRODUCTION

Video surveillance systems are being increasingly deployed in many places like roads, stations, airport, malls etc for public safety. Detecting abnormal events from video surveillance systems is very important for security applications. Detecting abnormal activities can provide better security to the individuals. People and their interactions must be constantly monitored for longer duration and any abnormal activity must be predicted. It is difficult for trained personnel to reliably monitor videos for longer duration and predict abnormal events. With the need to automate this activity with high accuracy, many autonomous abnormal activity detection systems are proposed. The goal of any autonomous anomaly recognition system is to detect/predict any offensive or disruptive activities in the surveillance video in real time. The conventional systems extract various features of appearance, dynamic relationship and interactions between the entities in the video and classify them to detect any abnormal activity. The accuracy is limited in this approach due to insufficiency of hand crafted features to detect the abnormal activity. As abnormality is context dependent, identification of features which represent the activity in the relevant context is challenging. Recently deep learning algorithms are being used for many computer vision problems. Deep learning algorithms learn features automatically and provide better accuracy. Deep learning use discriminative feature representations of both appearance and motion patterns to model the event patterns. In this work, a comparative analysis of four deep learning LSTM based models for abnormal event prediction is presented. With capability of learning long term dependencies and ability to extrapolate temporarily sequential data, long short term memory (LSTM) are best suited for abnormal event prediction. LSTM combined with deep learning event classification can provide a better accuracy of abnormal event prediction. This work explores four different deep learning models of Resnet[1], VGG16[2],VGG19[2] and (3DCNN)3D deep convolutional neural network [3] in combination with LSTM for abnormal event prediction. The performance of these four models is compared against benchmarking datasets in terms of accuracy, loss and execution time.

2. DEEP LEARNING BASED LSTM MODELS

The four deep learning based LSTM models used for abnormal activity prediction is detailed in this section. LSTM is combined with Resnet, VGG16, VGG19 and 3DCNN.

LSTM is an adapted version of recurrent neural networks to solve the problem of vanishing gradient. LSTM has a memory unit. This memory unit encodes the knowledge learnt. It learns when to forget and update hidden states when new information is provided as input. Memory unit functionality is controlled by three gates: input gate(i),

forget gate(f) and output gate(o). The update and output functions are defined as below

$i_t = \sigma(W_{ix}x_t + W_{im}m_{t-1} + b_i)$ $f_t = \sigma(W_{fx}x_t + W_{fm}m_{t-1} + b_f)$

$o_t = \sigma(W_{ox}x_t + W_{om}m_{t-1} + b_o)$ $g_t = \sigma(W_{cx}x_t + W_{cm}m_{t-1} + b_c)$

$c_t = f_t \odot c_{t-1} + i_t \odot g_t \quad h_t = o_t \odot c_t$

$\sigma(x) = (1 + e^{-x})^{-1}$

$\sigma(x)$ is input mapping sigmoid nonlinearity function. W is the matrix representing the parameters of the gates. $\odot$ represents product operation with values of gate. LSTM control multiple gates to mitigate vanishing gradient problem and capture temporal dependencies. The overall architecture of the proposed comparison model is given in Figure 1.

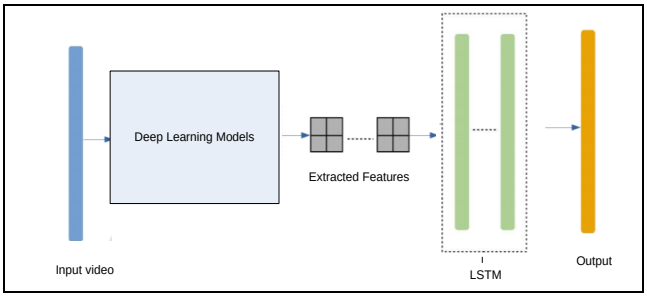

Figure 1 Deep learning LSTM model

Deep learning models extract features and provide to LSTM for prediction of abnormality. Four different deep learning models of Resnet, VGG16, VGG19 and 3DDCNN are used for extracting features.

A. Resnet with LSTM

Resnet or Residual Network was proposed by Microsoft researchers in 2015 as a solution to the problem of vanishing/exploding gradient with the increase in number of layers in deep convolutional neural network. Resnet adopts a skip-connection strategy to reinforce feature learning ability and therefore effectively expands the depth of the network, improving model feature learning ability. Skip connection between stacked cells sends useful information directly to the next layer which is an effective way to avoid gradient vanishing.

Resnet with LSTM abnormality prediction model uses Resnet50 for spatial feature extraction and LSTM for prediction using temporal feature extraction. The Resnet-50 model used for spatial feature extraction is of following configuration.

Table 1 Resnet 50 Configuration

Layer name	Output size	Type
Input	224*224*3	None
Conv1	112*112	7 × 7, 64, stride 2 3 × 3 max pool, stride
Conv2	56*56	$\begin{bmatrix} 1*1 & 64 \\ 3*3 & 64 \\ 1*1 & 256 \end{bmatrix} * 3$
Conv3	28*28	$\begin{bmatrix} 1*1 & 128 \\ 3*3 & 128 \\ 1*1 & 512 \end{bmatrix} * 4$
Conv4	14*14	$\begin{bmatrix} 1*1 & 256 \\ 3*3 & 256 \\ 1*1 & 1024 \end{bmatrix} * 6$
Conv5	7*7 1*1	$\begin{bmatrix} 1*1 & 512 \\ 3*3 & 512 \\ 1*1 & 2048 \end{bmatrix} * 3$ Avg pool,1000-d FC

The detailed structure of RestNet-50 is given in Figure 2

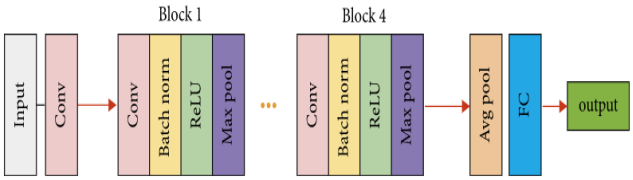

Figure 2 Resnet 50 architecture

The Resnet with LSTM model for abnormality prediction is given in Figure 3.

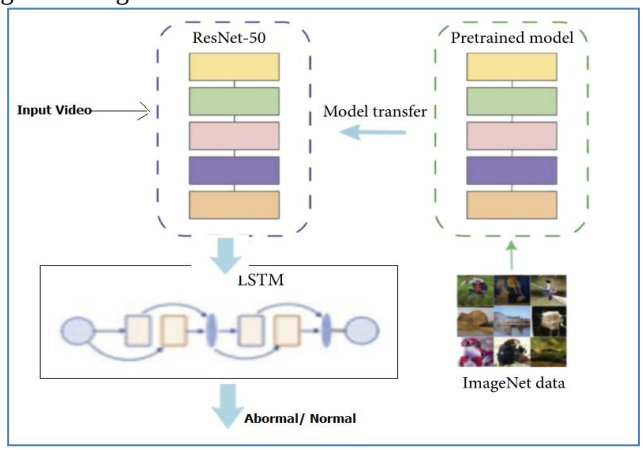

Figure 3 Resnet-with LSTM Model

The Resnet-50 is trained using transfer learning strategy to boost the training performance. Compared to training from scratch, transfer learning reduces the number of parameters that need to be trained and enables the model to converge faster.

B. VGG16 with LSTM

VGG16 is a simple deep convolutional neural network. It has deep stacked layered CNN by two fully connected layers having 4096 neurons on each of them.

In VGG16 with LSTM model, VGG16 network [4] prepares the input feature vector for LSTM which predicts abnormality. The network structure of VGG16 is given in Figure 4.

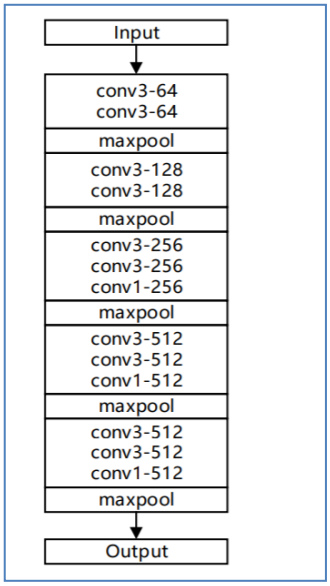

Figure 4 VGG16 network structure

Input frames from the video are sized to 224*224. The features are extracted using VGG16 and provided to LSTM in a time sequence, to provide abnormal or normal class as output. The overall flow of VGG16 with LSTM is adapted from [5] and given in Figure 4.

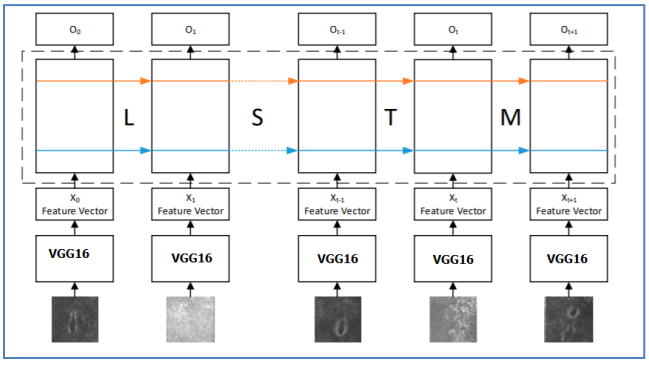

Figure 5 VGG16 with LSTM

The dimension of the extracted features are (7,70,512). The feature vector is sliced into a set of 10 samples with each of size {7,7*512}. This feature vector is given as input to LSTM with 10 time steps. The output of the last cell in LSTM is a binary output which gives as 1 for abnormal and 0 for normal.

C. VGG19 with LSTM

VGG19 is similar to VGG16 but it is deeper than VGG16. Due to this depth, VGG19 is able to extract more low level features from a frame than VGG16. VGG19 has 16 layers for convolution, 3 layers fully connected, 5 Max pool layer, and 1 softmax layer. The architecture of VGG19 is given in Figure 6.

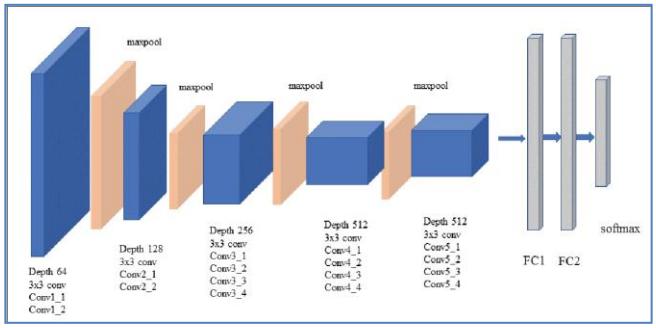

Figure 6 VGG19

From the input layer to the last max pooling layer (labeled by 7 x 7 x 512) is regarded as **feature extraction part** of the model. The feature extracted from VGG19 model is passed to LSTM to learn the long term dependencies between the video frames and predict abnormal activity. The pipelining of VGG19 with LSTM is same as that used for VGG16 shown in Figure 5.

D. 3DCNN with LSTM

The architecture of 3DCNN with LSTM is given in Figure 7.

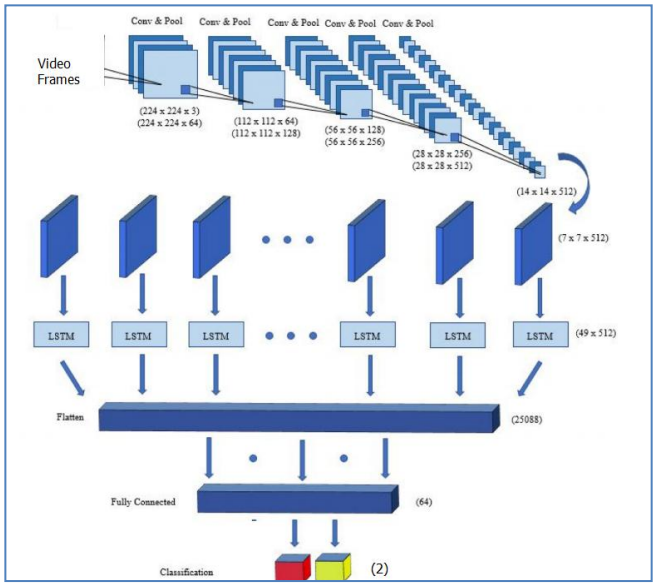

Figure 7 3DCNN with LSTM

The network has 20 layers: 12 convolutional layers, five pooling layers, one FC layer, one LSTM layer, and one output layer with the softmax function. Each convolution block is combined with two or three 2D CNNs and one pooling layer, followed by a dropout layer characterized by a 25% dropout rate. The convolutional layer with a size of 3 × 3 kernels is used for feature extraction that is activated by the ReLU function. The max-pooling layer with a size of 2 × 2 kernels is used to reduce the dimensions of an input image. In the last part of the architecture, the function map is transferred to the LSTM layer to extract time information. After the convolutional block, the output shape is found to

be (none, 7, 7, 512). Using the reshape method, the input size of the LSTM layer has become (49, 512).
After analyzing the time characteristics, the architecture sorts the video frames through a fully connected layer to predict whether they belong under any of the two categories (Abnormal/Normal).

3. RESULTS

The performance comparison of the four deep learning based LSTM models was done using following setup.

Table 2 Performance configuration

PC configuration	Intel i7, 8 GB RAM, Nvidia MX350
Software tools	Python 3.7, Keras, tensor flow
Dataset	UCSD Anomaly detection dataset [10]
Number of Training samples	34 videos
Number of Test samples	36 videos

The train and test accuracy over various epochs for Resnet with LSTM is given below

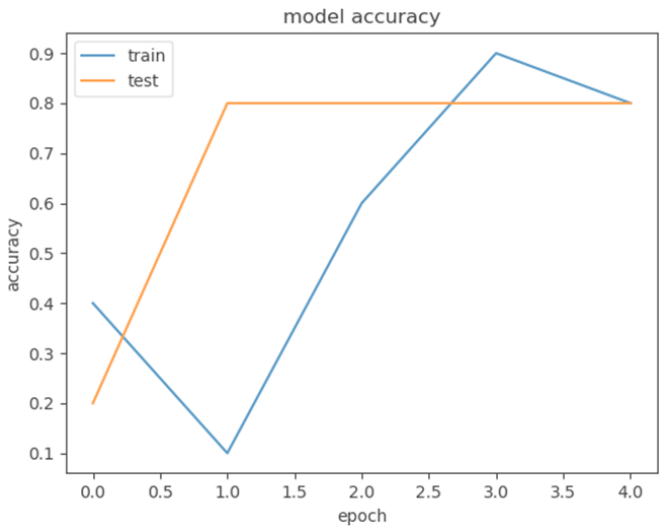

Figure 8 Accuracy in Resnet with LSTM

The Resnet with LSTM model is able to achieve a accuracy of 80% at epoch of 4 seconds. The loss in the Resnet with LSTM model for various epochs is given below

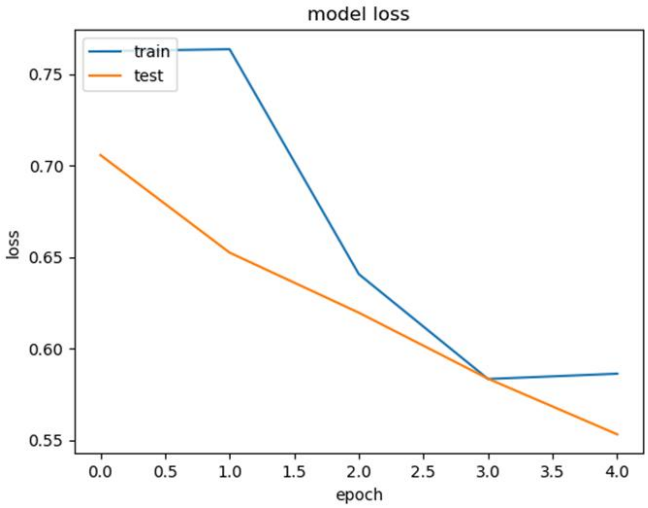

Figure 9 Loss in Resnet with LSTM

The loss achieves it minimal value of 56% at epoch of 4 seconds.
The train and test accuracy over various epochs for VGG16 with LSTM is given below

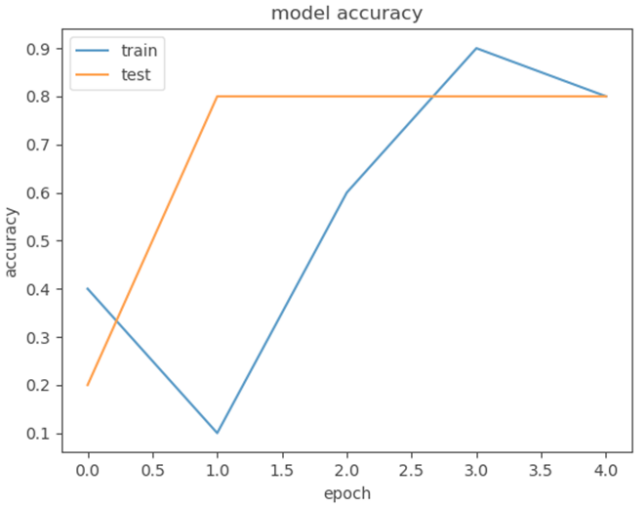

Figure 10 Accuracy in VGG16 with LSTM

The VGG16 with LSTM model is able to achieve an accuracy of 80% at epoch of 4 seconds. The loss in the VGG16 with LSTM model for various epochs is given below

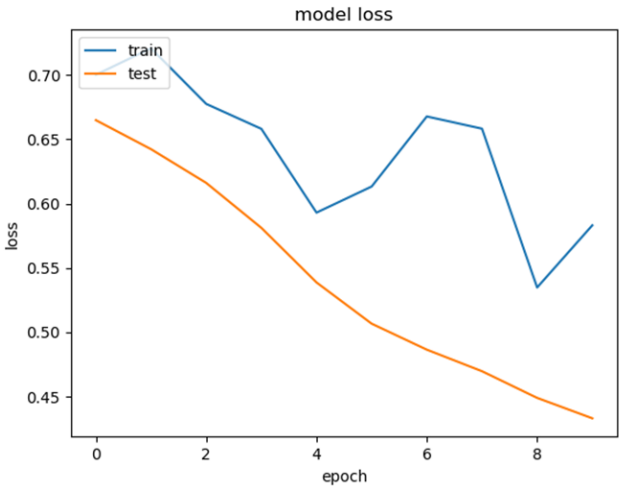

Figure 11 Loss in VGG16 with LSTM

The loss achieves it minimal value of 44% at epoch of 9 seconds.
The train and test accuracy over various epochs for VGG19 with LSTM is given below

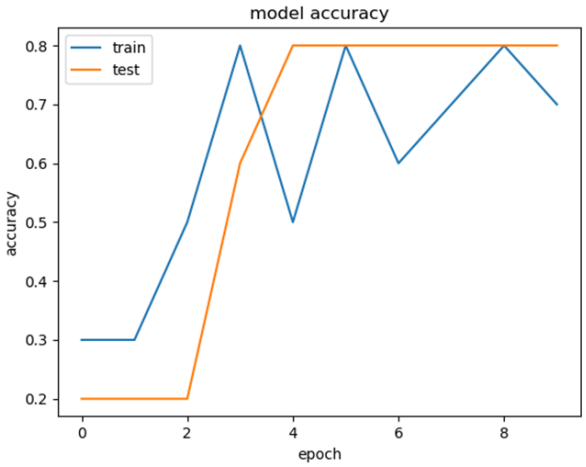

Figure 12 Accuracy in VGG19 with LSTM

The VGG19 with LSTM model is able to achieve an accuracy of 80% at epoch of 8 seconds. The loss in the VGG19 with LSTM model for various epochs is given below

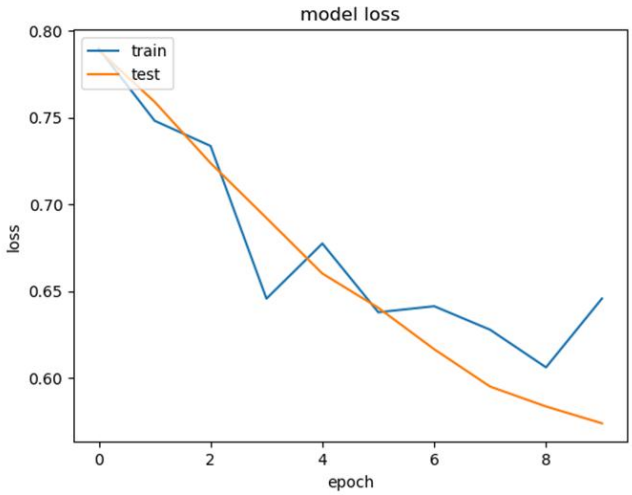

Figure 13 Loss in VGG19 with LSTM

The loss achieves it minimal value of 56% at epoch of 9 seconds. The comparison of training and test accuracy and loss across the four models are given below

Table 3 Comparison of Loss and accuracy

Model	Training		Test	
	Loss	Accuracy	Loss	Accuracy
Resnet with LSTM	0.59	0.70	0.56	0.80
VGG16 with LSTM	0.64	0.70	0.60	0.80
VGG19 with LSTM	0.64	0.70	0.57	0.80
3DCNN with LSTM	0.60	0.68	0.54	0.76

The result shows that three models of Resnet, VGG16 and VGG19 with LSTM are able to achieve same accuracy of 80%. The accuracy of 3DDCNN is 76% which is lower compared to rest of three models but the loss is lower in 3DDCNN with LSTM model at 54%.
The average execution time is compared against all the four different models and the result is given below.

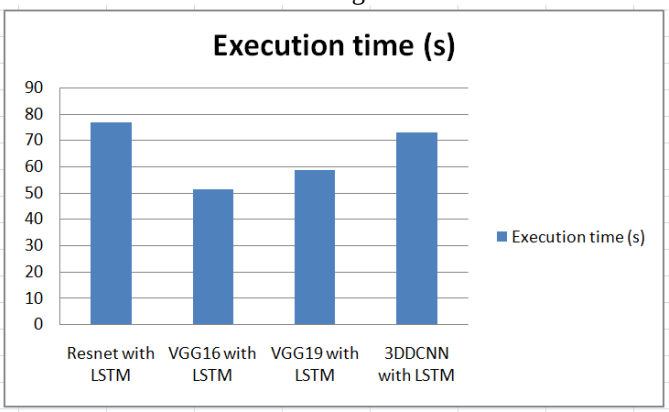

Figure 14 Comparison of execution

 ISBN: 978-93-90214-20-4

The execution time is lower in VGG16 compared to VGG19 and Resnet due to lower depth. 3DCNN feature extraction takes almost same execution time as that of Resnet with LSTM even though layers is less due to 3D feature complexity.

4. CONCLUSION

A comparative analysis of four deep learning based LSTM models for abnormal activity prediction is presented in this work. Resnet, VGG16 and VGG19 when combined with LSTM are able to provide an accuracy of 80%. VGG16 with LSTM is able to provide a higher accuracy of 80% with a lower execution time of 51.33 seconds compared to other deep learning with LSTM models. In the current work, the activities were classified into one two classes of normal and abnormal. Extending to more classes of anomalies is a part of future scope of work.

REFERENCE

[1] Kaiming He, Xiangyu Zhang, Shaoqing Ren, and Jian Sun. Deep residual learning for image recognition. arXiv preprint arXiv:1512.03385, 2015.

[2] Simonyan, Karen & Zisserman, Andrew. (2014). Very Deep Convolutional Networks for Large-Scale Image Recognition. arXiv 1409.1556.

[3] S. Ji, W. Xu, M. Yang and K. Yu, "3D Convolutional Neural Networks for Human Action Recognition," in *IEEE Transactions on Pattern Analysis and Machine Intelligence*, vol. 35, no. 1, pp. 221-231, Jan. 2013, doi: 10.1109/TPAMI.2012.59

[4] Qassim, H.; Verma, A.; Feinzimer, D. Compressed residual-VGG16 CNN model for big data places image recognition. In Proceedings of the 2018 IEEE 8th Annual Computing and Communication Workshop and Conference (CCWC), Las Vegas, NV, USA, 8–10 January 2018

[5] Liu, Yang & Xu, Ke & Xu, Jinwu. (2019). Periodic Surface Defect Detection in Steel Plates Based on Deep Learning. Applied Sciences. 9. 3127. 10.3390/app9153127.

[6] Shakil Ahmed Sumon et al., Violence Detection by Pretrained Modules with Different Deep Learning Approaches, Vietnam Journal of Computer Science, doi: 10.1142/S2196888820500013

[7] Sumon, S. A., Shahria, M. T., Goni, M. R., Hasan, N., Almarufuzzaman, A. M., & Rahman, R. M. (2019, April). Violent Crowd Flow Detection Using Deep Learning. In Asian Conference on Intelligent Information and Database Systems (pp. 613-625). Springer

[8] Baccouche, M. M. (2010, September). Action classification in soccer videos with long shortterm memory recurrent neural networks. In International Conference on Artificial Neural Networks (pp. 154-159). Berlin, Heidelberg. Springer

[9] Li, Qing & Qiu, Zhaofan & Yao, Ting & Mei, Tao & Rui, Yong & Luo, Jiebo. (2017). Learning hierarchical video representation for action recognition. International Journal of Multimedia Information Retrieval. 6. 10.1007/s13735-016-0117-4.

[10] http://www.svcl.ucsd.edu/projects/anomaly/dataset.html

High Gain Luo Converter Based Grid Connected Hybrid Solar Wind Energy System

[1] R. Aswin, [2] Dr. Lakshmi

[1] Student, Electrical and electronics Engg, ME Power System, AMET University, Tamilnadu, India
[2] Associate professor, AMET University, Tamilnadu, India

Abstract:

This project presents a control of a micro-grid at an isolated location fed from wind and solar based hybrid energy sources. The machine used for wind energy conversion is doubly fed induction generator (DFIG) and a battery bank is connected to a common DC bus of them. A solar photovoltaic (PV) array is used to convert solar power, which is evacuated at the common DC bus of DFIG using a DC-DC Luo converter in a cost effective way. The voltage and frequency are controlled through an indirect vector control of the line side converter, which is incorporated with droop characteristics. It alters the frequency set point based on the energy level of the battery, which slows down over charging or discharging of the battery. The system is also able to work when wind power source is unavailable. Both wind and solar energy blocks, have maximum power point tracking (MPPT) in their control algorithm. The system is designed for complete automatic operation taking consideration of all the practical conditions. The system is also provided with a provision of external power support for the battery charging without any additional requirement. Neuro Fuzzy logic algorithm is used to track the power from PV system. A simulation model of system is developed in Matlab environment and simulation results are presented for various conditions e.g. unviability of wind or solar energies, unbalanced and nonlinear loads, low state of charge of the battery.

Keywords:

Luo, Grid, Hybrid Solar, Wind Energy

1. INTRODUCTION

1. Tyler J. Formica *et al*[2017] discussed the challenges with the reliability of current solar photovoltaic systems and the key reliability bottlenecks, with a focus on the ROI. In this paper, the different warranty structures offered by companies, the return on investment (ROI) challenges, the reliability concerns, and candidate solutions to these concerns associated with solar energy systems. However, the failures could also be attributed to hardware components since there was no investigation beyond restarting the inverter, and hardware failures are also capable of inducing software shutdowns.

2. Sandeep Anand *et al*[2014] proposed a transformer-less grid feeding current source inverter for solar photovoltaic system. In this paper, an inverter that suppresses the earth leakage current without using an isolation transformer, thereby increasing the efficiency and reducing cost as compared to conventional current source based solar inverter is proposed. However, if significant unbalance in capacitor voltages is observed, a zero sequence based controller can be designed.

3. Albert Alexander Stonier *et al*[2018] proposed an intelligent based fault tolerant system for solar fed cascaded multilevel inverters. This research proposes an efficient power electronic interface whose switching action is stimulated by the intelligent controller. The fault detection given requires monitoring devices for the individual panels, which makes the system more complex and expensive.

4. Andreas Spring *et al*[2016] proposed a grid influences from reactive power flow of photovoltaic inverters with a power factor specification of one.In this paper ,the understanding of the impact of a high number of renewable energy systems on the distribution network, and the new conditions that arise due to the high number of renewable energy systems. The utilization rate of the cables and transformers is increased. This means that the real utilization rates are higher than the simulated ones.

5. M. Nawaz *et al*[2017] presented a model predictive control strategy for a solar-based series-resonant inverter in domestic heating. In this paper, control techniques do not predict the response of the system in advance; hence, a feed-forward model predictive control (MPC) strategy is proposed. Overshoot may occur in a high order system if prediction horizon is too short.

6. Mohamed A. Awadallah *et al*[2016] presented a paper on the effects of solar panels on distribution transformers. This paper presents a two-step study on the effects of SP on distribution transformers via simulation and experiments. Experimental results conclude that under the worst case loading scenario (i.e., full load with active power flow reversed), the transformer lifetime expectancy is anticipated to decrease by 8.3%.

7. Aditya Shekhar *et al*[2018] proposed a harvesting roadway solar energy—performance of the installed infrastructure integrated PV bike path.In this paper, the incident solar energy from roadways, it is possible to maximize the utilization of land dedicated toward transportation . However, the ability to generate useful

energy from solar irradiation is limited by the land constraint due to its dispersed nature.

8. Seyed Ali Arefifar *et al*[2017]implemented an improving solar power pv plants using multivariate design optimization. In this paper, a detailed multivariate study of PV plant design is presented, resulting in an improved technique to increase the potential benefits of solar plants with lower capital costs. However, there are still issues remaining for solar power plant designers to reflect on for improvements.

9. F. Karbakhsh *et al*[2017] presented A two-switch flyback inverter employing a current sensorless MPPT and scalar control for low cost solar powered pumps. This paper mitigates the problem of high-voltage transients at switch turn off which commonly exists in single switch flyback inverters.A lower cost microcontroller would be more than adequate to implement the proposed control algorithm.

10. Rajiv K. Varma, *et al*[2017]implemented SSR Mitigation with a New Control of PV Solar Farm as STATCOM (PV-STATCOM). This paper has proposed a novel fast method of reconnection of PV solar farm while keeping the PV-STATCOM SSR damping function activated. Mechanisms should also be evolved for compensating the PV solar farms financially for this very important service of SSR mitigation.

11. Sumit K. *et al*[2017] proposed a new asymmetric multilevel inverter topology suitable for solar pv applications with varying irradiance. In this paper , A roof-top 9.4kWp solar PV installation is used for the purpose. If the voltage is dropped, the overlap will be further increased and there will not be any unreachable vectors inside the space-vector plane.

12. Namwon Kim *et al*[2018] proposed a PV-battery series inverter architecture: a solar inverter for seamless battery integration with partial-power DC-DC Optimizer. In this integration, the architecture uses the partial-power processing universal DC-DC optimizer to have flexible system power control by regulating the T-node compensation current. The battery current is also changed unless the universal optimizer regulates enough.

13. Yoash Levron *et al*[2016] discussed High Weighted Efficiency in Single Phase Solar Inverters by a Variable Frequency Peak Current Controller. This paper enables a low-cost design that operates with a small inductor and achieves a peak efficiency of 99.5 % and a weighted efficiency of 99.15 %. This controller only senses the peak inductor current.

14. Rajan Kumar *et al*[2017] proposed single stage solar PV fed brushless dc motor driven water pump. The proposed control eliminates the BLDC motor phase current sensors. No supplementary control is associated for the speed control of motor-pump and its soft start. A small ripple in the torque appears because of phase current commutation and phase current sensor-less operation of the motor.

15. M. J. E. Alam *et al*[2014] proposed a multi-mode control strategy for VAr support by solar PV inverters in distribution networks. In this paper is the development of a multimode VAr control strategy that can provide an appropriate reactive power support to meet various conditions associated with PV power generation, including the absence of PV generation in the evening and the high ramp rate operation during passing cloud. However, proposing any incentive/penalty scheme or subsidies based on VAr generation/consumption would be a complex task and will need ancillary market oriented detailed studies.

16. M. Flota *et al*[2016] proposed a passivity-based control for a photovoltaic inverter with power factor correction and night operation. In this work a double-loop control scheme is presented to facilitate this improvement**.**

17. Mathieu D'amours *et al*[2018] proposed a planning solar in energy-managed cellular networks. In this paper, A hybrid solar-grid system for a single base station that is less costly than pure solar is proposed. Base station 0 is almost always in the sleep mode except during the two traffic peaks from 10:00 to 12:00 and 16:00 to 18:00. Base station 1 is almost always on except during the peak period at 16:00 where the traffic is taken up by base station 0.

18. Qingzeng Yan *et al*[2016] proposed an improved grid-voltage feedforward strategy for high-power three-phase grid-connected inverters based on the simplified repetitive predictor. The grid-voltage full-feedforward strategy for single-phase *LCL* based grid-connected inverters is proposed, dealing with the distorted grid voltage conditions. However, in digital control systems, *id, iq, ed, eq* , and *u*dc are not the real values but the measured (sampled) values from the power circuit; *vd* and *vq* are not the output voltages of the inverter but the reference voltages given to the PWM.

19. Yam P. Siwakoti *et al*[2017] proposed a common-ground-type transformerless inverters for single-phase solar photovoltaic systems This paper unveils three new single-phase transformerless inverters for a grid-connected PV system. However, the two-stage charge transfer process (Vin to C1 and C1 to C2) increases the number of power components and losses in the system.

20. Rajiv K. Varma *et al*[2015] proposed a New Control of PV Solar Farm as STATCOM (PV-STATCOM) for Increasing Grid Power Transmission Limits During Night and Day.In this paper , novel concept of utilizing PV solar farm inverter as STATCOM, termed PV-STATCOM, for improving stable power transfer limits of the interconnected transmission system is proposed . This proposed control utilizes only the inverter capacity left after the maximum power point operation of both the solar DG and wind DG.

2. OBJECTIVES

- To implement Energy management system based on Hybrid energy system for improving grid integration.
- To implement Energy management system based on Artificial Neural Network with Bidirectional Battery converter.
- To achieve Grid Synchronization using D-Q theory and extract maximum power from PV system using Neuro Fuzzy logic algorithm with Luo converter.

3. PROPOSED SYSTEM BLOCK DIAGRAM

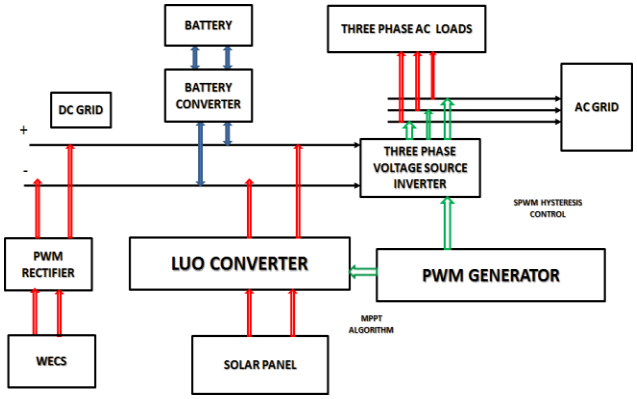

REFERENCE

[1] Formica, T. J., Khan, H. A., & Pecht, M. G. ,2017,'The Effect of Inverter Failures on the Return on Investment of Solar Photovoltaic Systems', IEEE Access ,Vol.5 ,pp.21336-21343.

[2] Anand, S., Gundlapalli, S. K., & Fernandes, B. G. ,2014,' Transformer-Less Grid Feeding Current Source Inverter for Solar Photovoltaic System', IEEE Transactions on Industrial Electronics, vol. 61,no.10,pp. 5334–5344.

[3] Stonier, A. A., & Lehman, B.,2017,' An Intelligent Based Fault Tolerant System for Solar Fed Cascaded Multilevel Inverters', IEEE Transactions on Energy Conversion,vol.33,no.3,pp.1047-1057.

[4] Spring, A., Wirth, G., Becker, G., Pardatscher, R., & Witzmann, R. ,2016,' Grid Influences From Reactive Power Flow of Photovoltaic Inverters With a Power Factor Specification of One', IEEE Transactions on Smart Grid, vol.7,no.3, pp.1222–1229.

[5] Nawaz, M., Saqib, M. A., & Kashif, S. A. R., 2017,' Model predictive control strategy for a solar-based series-resonant inverter in domestic heating'. Electronics Letters, vol.53,no.8,pp. 556–558.

[6] Awadallah, M. A., Xu, T., Venkatesh, B., & Singh, B. N.,2016, 'On the Effects of Solar Panels_newline on Distribution Transformers', IEEE Transactions on Power Delivery,vol. 31,no.3,pp.1176–1185.

[7] Shekhar, A., Kumaravel, V. K., Klerks, S., de Wit, S., Venugopal, P., Narayan, N., … Zeman, M., 2018,' Harvesting Roadway Solar Energy—Performance of the Installed Infrastructure Integrated PV Bike Path', IEEE Journal of Photovoltaics,vol. 8,no.4,pp. 1066–1073.

[8] Arefifar, S. A., Paz, F., & Ordonez, M., 2017,'Improving Solar Power PV Plants Using Multivariate Design Optimization', IEEE Journal of Emerging and Selected Topics in Power Electronics, vol.5,no.2, pp. 638–650.

[9] Karbakhsh, F., Amiri, M., & Abootorabi Zarchi, H. ,2017,'Two-switch flyback inverter employing a current sensorless MPPT and scalar control for low cost solar powered pumps', IET Renewable Power Generation, vol.11,no.5, pp.669–677.

[10] Varma, R. K., & Salehi, R. , 2017, 'SSR Mitigation With a New Control of PV Solar Farm as STATCOM (PV-STATCOM)' , IEEE Transactions on Sustainable Energy, vol.8,no.4,pp.1473–1483.

[11] Chattopadhyay, S. K., & Chakraborty, C., 2017,' A New Asymmetric Multilevel Inverter Topology Suitable for Solar PV Applications With Varying Irradiance', IEEE Transactions on Sustainable Energy, vol.8,no.4,pp.1496–1506.

[12] Kim, N., & Parkhideh, B. , 2018, 'PV-Battery Series Inverter Architecture: A Solar Inverter for Seamless Battery Integration with Partial-Power DC-DC Optimizer', IEEE Transactions on Energy Conversion, Vol.34 , no.1 ,pp.478-485.

[13] Levron, Y., & Erickson, R. W. , 2016,' High Weighted Efficiency in Single-Phase Solar Inverters by a Variable-Frequency Peak Current Controller', IEEE Transactions on Power Electronics, vol.31,no.1,pp.248–257.

[14] Kumar, R., & Singh, B., 2017, 'Single Stage Solar PV Fed Brushless DC Motor Driven Water Pump', IEEE Journal of Emerging and Selected Topics in Power Electronics,vol.5,no.3,pp.1377–1385.

[15] Alam, M. J. E., Muttaqi, K. M., & Sutanto, D., 2015,'A Multi-Mode Control Strategy for VAr Support by Solar PV Inverters in Distribution Networks', IEEE Transactions on Power Systems, vol.30,no.3,pp.1316–1326

[16] Flota Banuelos, M. I., Ali, B., Villanueva, C., & Perez Cortes, M., 2016, 'Passivity-Based Control for a Photovoltaic Inverter with Power Factor Correction and Night Operation', IEEE Latin America Transactions, vol.14,no.8,pp.3569–3574.

[17] D'Amours, M., Girard, A., & Sanso, B., 2018, 'Planning Solar in Energy-Managed Cellular Networks' ,IEEE Access, vol.6,pp. 65212–65226.

[18] Yan, Q., Wu, X., Yuan, X., & Geng, Y., 2016,' An Improved Grid-Voltage Feedforward Strategy for High-Power Three-Phase Grid-Connected Inverters Based on the Simplified Repetitive Predictor', IEEE Transactions on Power Electronics,vol.31,no.5,pp.3880–3897.

[19] Siwakoti, Y. P., & Blaabjerg, F., 2018, 'Common-Ground-Type Transformerless Inverters for Single-Phase Solar Photovoltaic Systems', IEEE Transactions on Industrial Electronics, vol.65, no.3,pp.2100–2111.

[20] Varma, R. K., Rahman, S. A., & Vanderheide, T. , 2015, 'New Control of PV Solar Farm as STATCOM (PV-STATCOM) for Increasing Grid Power Transmission Limits During Night and Day', IEEE Transactions on Power Delivery, vol.30, no.2,pp.755–763.

Monitoring Bio Parameters of Sea Researchers Using Visible Light in Underwater Wireless System

[1] Dr. Sankara Gomathi S, [2] Dinesh Babu K, [3] Shalini P, [4] Sakthi Vel S, [5] Abinaya B

[1] Professor, Electronics and Communication Department, Adhi college of Engineering and Technology, Tamil Nadu, India
[2] Assistant Professor, Electronics and Communication Department, Adhi college of Engineering and Technology, Tamil Nadu, India
[3][5] Student, Electronics and Communication Department, Adhi college of Engineering and Technology, Tamil Nadu, India
[4] Student, Biotech Department, Sri Venkateshwara College of Engineering, Sriperumbudur, Tamil Nadu, India

Abstract:

Water data communication is an expected innovation to acknowledge underwater communication. The analysis of underwater communication in the laboratory is distinctive with that in the real seawater because, the physical scale is limited. In recent several decades, artificial scattering agents are used to recreate underwater data communication through water channels under different communication medium conditions, but the similarity between experimental water and natural water is not reliable, such as the similarity in frequency domain characteristics.

In this paper, we have added some kinds of impurities to change the coefficients of experimental water precisely. Then, the frequency domain characteristic of data communication through water channel in experimental water is measured and compared. The results show that the type and particle size of the agents will significantly affect its water properties, and the frequency domain component of the water communication signal gets affected by the agents' concentration. By having a separate transmitter and receiver module in the water, we can transmit the sea researcher's biomedical conditions and the interactions to the monitoring end available on the ship.

Keywords:

sea researchers, underwater networks, Li Fi, wireless sensor networks, underwater optical communication, scattering agents

1. INTRODUCTION

Underwater Optical Wireless Communication is important to our continued development of the underwater environment and also, it plays a significant role in military, industry and also in scientific researches and these fields requires high data rates with low power consumption. Within the last few years, the event of optical communication is increased because it provides high data rates with low power consumption. The foremost disadvantage of reliable underwater communication is that the variations of underwater environment from coastal water to deep ocean water. There are many underwater wireless communication systems are available which uses sonar, piezoelectric elements etc. But these devices emit radio signals which may affect the oceanographer's or driver's health condition.

To account this problem, Underwater Optical Wireless Communication (UOWC) was introduced in contrast of RF communication. And also, UOWC carries more information and overcomes the limitation of RF Bandwidth. In this paper, the Under Water Optical Communication is achieved by the appropriate design of transmitter and receiver using Li Fi (Light Fidelity) module [8].

Usually, the sea navigators or fisherman requires an additional support from the land whenever something unusual things happen within the sea. The sea researcher cannot inform this to anyone immediately, whenever any needs arise. In order to avoid these issues, we have introduced a health monitoring system for sea researchers. For that, we have used Li Fi module as the underwater communication system to monitor the health conditions of the oceanographers.

2. RELATED WORK

In the last few years, the interest towards optical wireless communication has increased for terrestrial, space and underwater links as it is capable of providing high data rates with low power and mass requirement. Many of researchers have carried out work for terrestrial and space links [3]. In recent years the submerged acoustic correspondence assumes an essential job in the field of remote correspondence. In the earlier systems, electromagnetic waves were used, which was found to be with less efficiency [4,7]. The atmospheric conditions under the sea will be changing tremendously. It affects the sea navigators in too much trouble. It is difficult to monitor the health conditions of sea navigator after diving. Even if he dives below 20 meters his heart beat becomes uncontrollably changing. So even if his blood pressure lows dangerously it may lead to death. And there is no idea to save those navigators in those conditions [2]. Hence, the wireless

optical communication system for data transfer in the underwater networks has been developed [9,10], in order to facilitate the communication link in free space and as well as in under water [1]. The authors in [11] describes a system in which the underwater communication is done by visible light and this system provides only the transmitting and receiving of data like image, audio and text between the Underwater Autonomous Vehicle (UAV) and does not provides the communication between the sea researcher [4].

Wei Wei et.al [5] introduced a system, which is a LED based underwater wireless communication system, conducted a study of the efficiency of that system in highly turbid water. The underwater communication is achieved by many methods, one such is achieved the underwater communication by using piezoelectric elements [5,6]. This radiation affects the health of the sea researcher and also the cost and speed of transmission of data is also become a significant factor.

Hence, we proposed a visible light-based underwater communication system which monitors the bio parameters of the sea researcher. The bio sensors will sense the temperature, blood pressure and humidity of the sea researcher and processed by the processor and displayed on the LCD which is in the transmitter section. Then the processed data are encoded according to their specification and the data are converted to the light energy and sent to the photodetector which receives the light at the receiver end. The receiver converts the light energy into electrical energy and the data are viewed on the computer for further communication.

3. PROPOSED SYSTEM

Today, underwater sensors cannot share data with the ashore, as both the end will be using different wireless signal, that only work in their corresponding mediums. The acoustic signals, or electromagnetic signals used in underwater wireless communication system causes inefficiencies and other problems for a variety of applications, like ocean exploration and submarine-to-plane communication, etc.

The disadvantage of earlier systems uses underwater wired communications which limits the length of a cable and hence long-distance propagation can't be achieved. Whereas, in our concept of wireless communication, is having the capability to communicate within the appropriate range with less difficulty. And hence the drawback of the earlier concepts has been suppressed to the extent possible. The advantage of this system is that a person who is above the water surface can observe the health conditions of a person who is under the water.

As shown in the block diagram in figure1, our system comprises two Microcontrollers, temperature sensor, gauge pressure sensor which are used to measure the ex-vivo blood pressure and humidity sensor and Li-Fi module. The system has two sections such as transmitter section and receiver section. The transmitter section comprises of a microcontroller (PIC16F877A), LCD Display, Humidity sensor (DHT11), Temperature sensor (LM35), gauge pressure sensor (KEN843A) and data communication module (Li-Fi transmitter module). The receiver section consists of Microcontroller (PIC16F877A), LCD display and data communication receiver module (LiFi receiver module). With the help of the proposed model, we can able to monitor the temperature, pressure and humidity level of the sea researcher. These mentioned bio parameters are taken with the help of appropriate sensors and displayed on LCD display and the data are encoded by 8-bit encoding method.

For experimental purpose a fish tank is placed between the transmitter end and the receiver end. Li fi transmitting and receiving modules are placed outside the tank. Once we turn on the device, the bio parameters of the oceanographers are sensed and the controller in the transmitter side transmits the data to the receiver side through water via visible light using Li Fi Transmitter Module. Here the data are transmitted via water.

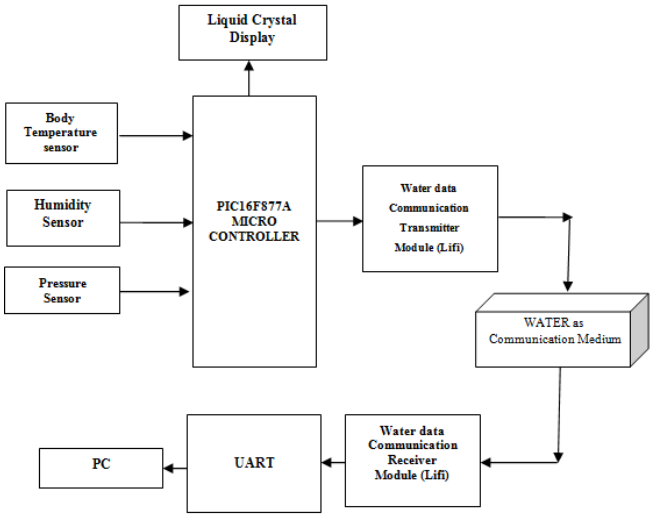

Figure 1. Block diagram of Li Fi transmission model

A photodetector is placed at the receiver end and it will receive the data and decode it. Then the decoded data will be sent to the UART board and results are viewed on the Computer. This has been given as shown in Figure 1. This system allows the navigator to move freely. Through this system the condition of the sea researcher can be monitored and we can help the navigator before something happen to him.

A. TRANSMISSION SECTION

The main part of designing an underwater wireless system is to choose the appropriate source for transmitting the data and it should transmit the data with high speed, low cost and with low complexity. The detail bout transmitter section is elaborately given in the below figure 2.

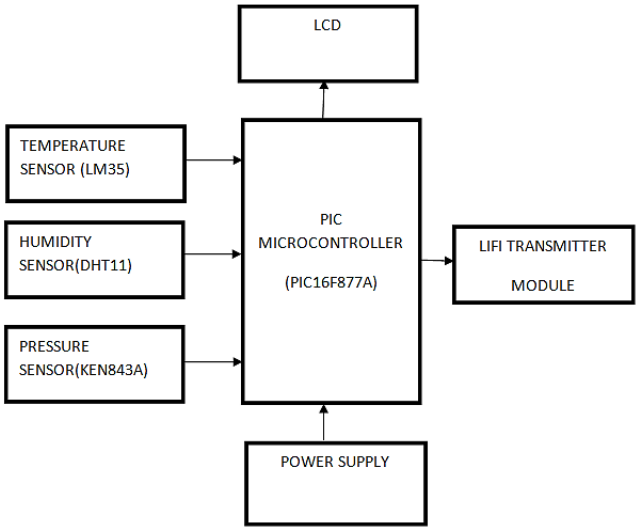

Figure 2. Block diagram of transmitter section

The Optical communication in the underwater is achieved by using various light sources like LED, laser etc. Both of the sources have its own advantages and disadvantages. Laser sources are mostly not used for underwater optical wireless communication. Because, to obtain the full efficiency of the laser source, there should be a proper alignment of transceivers in the Autonomous Underwater Vehicles (AUV). This is practically impossible in case of AUV's due to its floating nature. The design of underwater wireless system needs simplicity, reliability, smaller size, cost efficiency and high speed. Hence, we have chosen LED as a source for data transmission. Thereby the various parameters of optical communication like attenuation, scattering and propagation losses should be considered which depends on the turbidity and impurities present on the water. The bio parameters like temperature, pressure and humidity are sensed using appropriate selection of the sensors. Thereby all the data are processed by the Programmable Interrupt Controller (PIC) Microcontroller. This will process the data which are then encoded and converted into optical energy, and then transmitted using Li Fi Module.

B. RECEIVER MODULE

The block diagram of the receiver module is as stated below in figure 3. In this the visible light is used for transmitting the data over the water, photodetector is used at the receiver section to detect the optical signal.

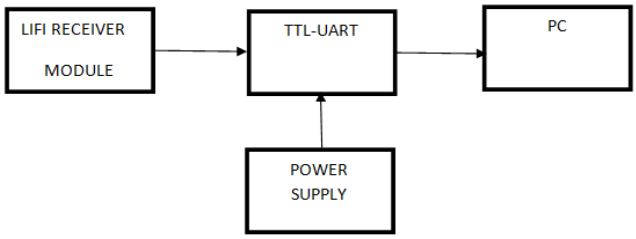

Figure 3. Block diagram of Receiver Section

Here, photodiode is used as photodetector and once the data are detected, the optical signal from the transmitter module is decoded and the signal gets amplified. The results can be viewed by the computer using UART Board.

4. RESULT AND ANALYSIS

In this we have represented the data observed from spectrum analyser of optical signal with respect to the concentration of dust particles like attenuation, scattering, absorption are measured and given as shown in the graph Figure. From this we can conclude that the dust particles gets linearly increases with respect to optical coefficients.

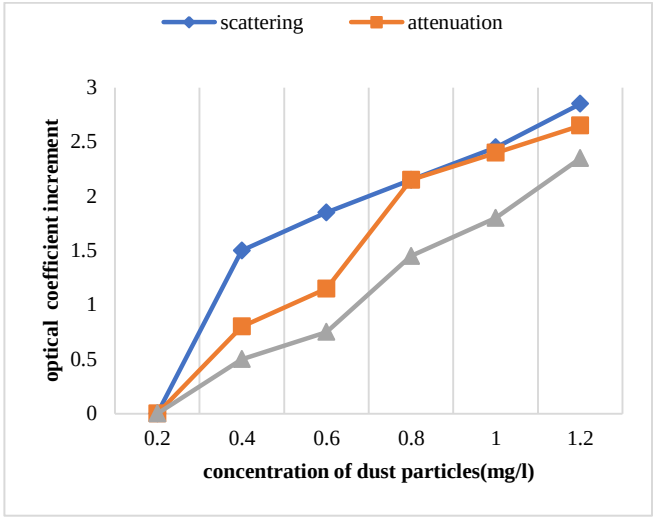

Figure 4. Effect of Dust particles in water

Similarly we analysed the parameter with respect to the effect of black ink in the water and its incremental factor of optical coeefficient as shown in figure 5. From this it jis observed that, the scattering effect is as low as possible or very minimal compared to attenuation and absorption.

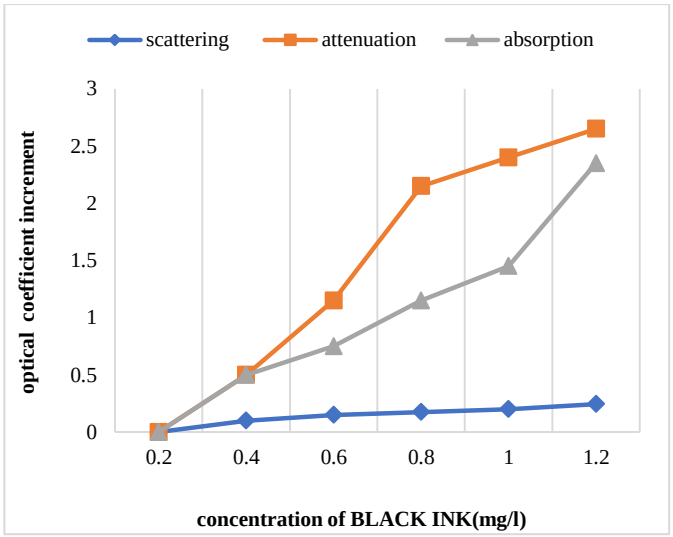

Figure 5. Effect of Black ink in water

Figure 6. Bio parameters viewes in PC

Figure 6 shows the result of the received bio parameters at the receiver section. The optical parameters of the experimental water can be tested by adding different kinds of impurities in it to make it as reliable as real sea water in future. We present a prototype which covers the distance of 2m with the baud rate of 9600/sec.

5. CONCLUSION

High speed underwater optical communication has an increasing demand on nowadays and deployed in different underwater environments ranging from coastal water to sea water. In this paper, we have proved that the proposed prototype constantly monitors the various impurity parameters which enable the sea researchers to concentrate on their health condition and used to help the oceanographer from the emergency situation. While implementing this prototype in the real scenario, the intensity of the light in the Li Fi Module can be increased depends on the nature of the water and the distance between the transmitter and receiver. This system can be further improved by having data transmission option between the sea researchers while they are in the sea. The health monitoring system can be further developed by adding artificial intelligent techniques like data mining

REFERENCE

[1] Narmatha.M, Portia Sahayam. J, Prabavathi. M, Tharani. T, K S. Hepzibhai, "Optical data transfer in underwater system using Li Fi" *International Journal of Research and Technology* in 2017.

[2] Prof. Ranjitha Rajan, Ms. Elizabeth P.T, Ms. Amala Susan Roy, Ms. Aiswarya K.S , Ms. Christymol Bousally, "underwater wireless communication system", *International Journal of Engineering and Technology* in 2020.

[3] Kaushal H and Kaddoum G. "Underwater optical wire-less communication". *IEEE Access* 2016, URL: *Digital Object Identifier 10.1109/ACCESS.2016.2552538*

[4] Arun Kumar P, Naresh Subray Harikant, Malashree A V, Dr.Sridhar N, Dr. K.Venkateswaran, "Development of Data Transmission Model for Under Water Communication using Li-Fi Technologys" *IEEE Fifth International Conference on Communication and Electronics Systems* (ICCES 2020).

[5] Wei Wei , Chunlei Zhang, Wei Zhang, Wei Jiang, Chang Shu, and Giao Xiaorui "Led-based underwater wireless optical communication for small mobile platforms experimental channel study in highly-turbid lake water", *IEEE Access* in 2020

[6] Puvvadi Manideep, Vusa Pavan Kumar, Snehith Reddy Kota, Dr.M.N.Vimal Kumar, "Feasibility Study and Implementation of Sea Researcher's Bio-Parameters Monitoring by Water Channel Model", *International Journal of Innovative Research In Technology* in 2020.

[7] Li Ma, Min Fu, Zhaorui Gu, Mengnan Sun, Hua Yang, Xinmin Ren, Bing Zheng, Xuefeng Liu, "*Experiments of Recreating the Frequency Domain Properties of Seawater Channel for Underwater Optical Communication"*, IEEE Conference in 2019.

[8] Balaji K, S.Shakthivel Murugan, "*Implementing IoT in Underwater communication using Li-Fi*", International Journal of Recent Technology and Engineering in 2019.

[9] Clifford Pontbriand, Norman Farr, Jonathan Ware, James Preisig, Hugh Popenoe, "*Diffuse High-Bandwidth Optical Communications*", IEEE Conference in 2008.

[10] Ms. A. Shyamalaprasanna, Ms. B. Ragavi, Ms. L. Pavithra, Ms. K.Mohanapriya, Mrs. P. Santhiyadevi, "*Achieve High Data Rate By Using Optical Modem In Under Water Wireless Communication*", International Conference on Innovative Trends in Information Technology in 2020.

[11] Hemonth G. Rao, Catherine E. DeVoe, Andrew S. Fletcher, Igor D. Gaschits, Farhad Hakimi, Scott A. Hamilton, Nicholas D. Hardy, John G. Ingwersen, Richard D. Kaminsky, Marvin S. Scheinbart, and Timothy M. Yarnall, "*Turbid-Harbor Demonstration of Transceiver Technologies for Wide Dynamic Range Undersea Laser Communications*" IEEE in 2016.

Seasonal Variation in the Groundwater Quality & Irrigation Suitability of Water in a Rural Area of Andhra Pradesh

Dr.Babu Rao Gudipudi

Associate Professor, Department of Civil Engineering, Narasaraopeta Engineering College(Autonomous), Narasaraopet, Guntur, India

Abstract:

To assess the suitability of groundwater for drinking, domestic and irrigation purposes, a total of one hundred groundwater samples (fifty during pre-monsoon & fifty during post monsoon) were collected and analyzed in Nuzendla mandal of Guntur District, Andhra Pradesh. Hydrochemical data of groundwater of study area were compared with the standards of WHO (2004) and (BIS 2003). Most of the groundwater samples of the study area fall in the category of brackish waters in pre- and post-monsoon seasons periods based on Total Dissolved Solids (>500 mg/L) and all are unsuitable for drinking purpose. The Concentration of major ions during pre- and post-monsoon periods are exceeding the safe limit (Na^+ (86% and 88%), Ca^{2+} (80% and 72%), Mg^{2+} (92 and 72%), K^+ (98% and 92%), HCO_3^- (96% and 100%), Cl^- (66% and 74%), SO_4^{2-} (18% and 8%), NO_3^- (64% and 74%) and F^- (64% and 72%)) and indicates the groundwater of study area is alkaline nature and it is not potable for drinking and domestic uses without proper treatment. USSLs diagram also indicates the poor water quality of major groundwater samples in both the seasons for irrigation purpose. Based on Permeability Index groundwater samples come under Class I and class II types, implying the safe and marginally safe categories respectively suggests that the most of groundwater is suitable for irrigation use in both the seasons. Kellys Ratio also indicates the poor quality of water in both the seasons (70% and 68% during pre-and post-monsoons) for irrigation purpose. The seasonal variations in the quality of groundwater are influenced mostly by the geogenic and partially by anthropogenic sources including the domestic and agricultural activities through infiltration and percolation during monsoon. The groundwater quality in the study area is not potable for drinking and domestic purpose. The groundwater in the most of the study area is unfit for agriculture practices. Therefore, the long duration of intake of this of water can cause many types of public health problems.

Keywords:

Groundwater, Nuzendla, Water Quality, Irrigation, Permeability Index

1. INTRODUCTION

The agricultural development is the main factor in the economic development of a country like India, as the agriculture is the main source of nourishment for the majority of the population in the country and contributes 19.9% to the gross national product. Utilization of groundwater has augmented greatly for agricultural purpose, because large parts of the country have little access to rainfall due to frequent failures of monsoon and variable flow of surface water sources (rivers, lakes and artificial basins). There was gradual increase in groundwater irrigation from past to present meeting about 70% of the irrigation water requirements of the country. This clearly indicates the growing pressure on groundwater resources. Groundwater quality is important besides the quantity. Poor quality of water may adversely affect the growth of plant and also the human health (Wilcox 1948; US Salinity Laboratory Staff 1954; Holden 1971; Todd 1980). Adverse conditions may increase the investment in irrigation sector and which in turn, reduces agrarian economy and decrease agricultural production. This may lead to human health disorders which may affect the sustainable development of the particular region. A number of studies on ground water quality with respect to drinking and irrigation purposes have been carried out in the different parts of the country (Sreedevi 2004; Subba Rao and John Oevadas 2005; Babu Rao and Sai Ramya, 2018; Babu Rao et al. 2019), but little work on this aspect has so far been done in the rural area of Guntur district, Andhra Pradesh, India.

2. STUDY AREA

The study area is Nuzendla mandal of Narasaraopet Revenue Division of Guntur district, Andhra Pradesh, India (Fig. 1). It lies in between the latitudes 79^0 33' 28" - 79^0 52' 51" E, and longitudes 15^0 49' 26" and 16^0 01' 42" N, falling in the Survey of India toposheets 56P/12, 56P/16, 57M/9 and 56M/13. The area extents of about 350 km^2 and is distributed in 20 rural villages. The population is 52,853 (2011 Census). The area is well connected by road and rail network to all important towns in Andhra Pradesh.

 ISBN: 978-93-90214-20-4

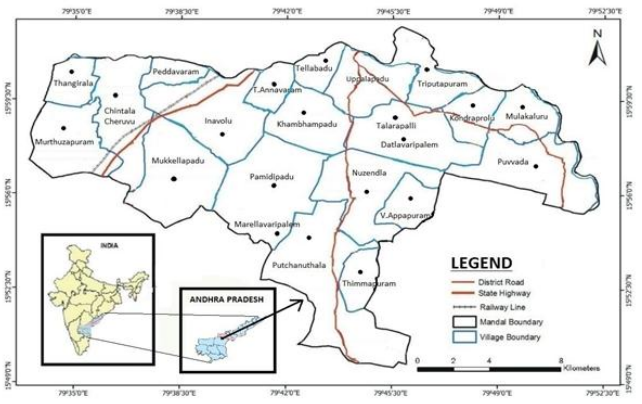

Fig. 1 Location of the study area

The area experiences a semi-arid climate, with minimum and maximum temperatures of 16.8^0C and 48.5^0C, respectively. Rentachintala of Guntur district (nearest IMD station) records the highest temperatures (48.5^0C) during summer (March to May). Loamy to clayey skeletal deep reddish brown soils are the dominant type of the soils in the study area. Geomorphologically, the study area comprises of mainly pediplain, pediments, inselbergs, residual hills and floodplains. The study area is underlain by the rock formations ranging from Archaean to Permo-carboniferous age. The rock formations include quartz-mica-schist, banded-biotite-hornblende-gneiss/granite and coarse grained sandstone. Groundwater occurs under phreatic conditions in the weathered and fractured rocks at shallow depths and under semi-confined to confined conditions in the deeper fractured rocks.

3. METHODOLOGY

Fifty groundwater samples were collected in pre- (May) and post-monsoon (November) seasons during the year 2012 in the study area. Prior to water sampling, sampling bottles soaked in 1:1 HCl for 24 hours were rinsed with distilled water, followed by deionized water. They were washed again prior to each sampling of the filtrates. The bottles were tightly capped to protect the samples from atmospheric CO_2, adequately labeled and preserved in the refrigerator till they were taken to laboratory for measurement. The collected groundwater samples from the field were analyzed for chemical variables, using the standard water quality methodology of American Public Health Association (APHA, 2005). The chemical variables include pH, electric conductivity (EC), total dissolved solids (TDS), calcium (Ca^{2+}), magnesium (Mg^{2+}), sodium (Na^{+}), potassium (K^{+}), bicarbonate (HCO_3^{-}), chloride (Cl^{-}), sulphate (SO_4^{2-}), nitrate (NO_3^{-}) and fluoride (F^{-}). The pH and EC of the groundwater samples were measured in the field, using a portable pH and EC meters. The TDS was calculated from EC adhering to the procedure of Hem (1991). The rest of the chemical variables were determined in the laboratory immediately after the groundwater sampling. A summary of the analytical procedures are listed in Table 1. All concentrations of chemical parameters are expressed in milligrams per litre (mg/L), except pH (units) and EC (µS/cm at 25°C).

Table 1 Methods used for chemical analysis of groundwater

Chemical parameters	Methods
Hydrogen ion concentration (pH)	pH meter
Specific electrical conductivity (SEC)*	SEC meter
Total dissolved solids (TDS)	SEC X Conversion factor (0.55 to 0.75)
Calcium (Ca^{2+})	Titration with EDTA
Magnesium (Mg^{2+})	Calculation (TH- Ca^{2+})
Sodium (Na^{+})	Flame photometer
Potassium (K^{+})	Flame photometer
Bicarbonate (HCO_3^{-})	Titration with HCl
Carbonate (CO_3^{2-})	Titration with HCl
Chloride (Cl^{-})	Titration with $AgNO_3$
Sulphate (SO_4^{2-})	Spectrophotometer
Nitrate (NO_3^{-})	Colorimeter
Fluoride (F^{-})	Spectrophotometer
Silica (Si)	Spectrophotometer

Various types of contaminants released from soil salts, domestic, sewage, and industrial wastes, agricultural runoff etc., reach the water table and consequently they change chemical characteristics of groundwater. The chemical composition of groundwater controls many interrelated processes and understanding of such processes is a pre-requisite to water quality control and improvement. Therefore, the fundamental knowledge of processes that control the groundwater composition is required for rational management of water quality (Hem, 1991). Groundwater quality deterioration and supply of safe drinking water is a major concern throughout the world.

4. RESULTS

The pH in the study area varies from 7.3 to 8.8, with a mean of 8.20 in the pre-monsoon groundwater, while it is in between 7.3 and 8.9 with a mean of 8.16 in the post-monsoon groundwater, indicating an alkaline condition. The EC is in the range of 1,078.18 to 3, 182 and 1548 to 3,524 µS/ cm in the pre- and post- monsoon seasons with a mean of 2,102.95 µS/cm and 2,373.38 µS/cm respectively indicating a wide variation in the activities of geochemical processes. The Total Dissolved Solids (TDS) ranges from 690 to 2,036 with a mean of 1,345.89 mg/L in the pre-monsoon groundwater, while it is in between 991 and 2,255 mg/L with a mean of 1,518.96 mg/L in the post-monsoon

 ISBN: 978-93-90214-20-4

groundwater indicating more brackish water in the study area.

CATIONS: The Ca^{2+} content is in between 32 and 193 mg/L in the pre-monsoon, while it is from 16 mg/L to 197 mg/L in the post-monsoon groundwater with their mean values are 97.74 and 96.98, which contribute to 5.54 to 51.23% and 2.27 to 56.28%, respectively to the total cations. The Mg^{2+} varies from 19 to 98 mg/L in the pre-monsoon and 5 to 112 mg/L in the post-monsoon, with a mean of 44.92 and 43.20 mg/L, respectively. The contribution of Mg^{2+} to the total cations is 2.01 to 33.98% and 0.84 to 25.45% in the pre- and post-monsoon respectively. The concentration of Na^{+} is in between 72 and 544 mg/L in the pre-monsoon and its mean is 286.84 mg/L in the study area. It is in between 98 and 776 mg/L with a mean of 360.02 mg/L in the post-monsoon groundwater. The contribution of Na^{+} to the total cations varies from 20.54 to 88.74% in the pre- monsoon and is from 20.62 to 94.93% in post-monsoon which reflects a silicate weathering and/or dissolution of soil salts stored by the influences of evaporation and anthropogenic activities and also it indicates man-made pollution (Chemical fertilizers, drainage wastes etc.;(Stallard and Edmond, 1983). The higher concentration of Na^{+} than the Ca^{2+} to the total cations is attributable to the influence of ion exchange (Todd, 1980; Hem, 1991). The concentration of K^{+} varies from 9 to 107 with a mean of 26.42 mg/L in pre-monsoon and from 5 to 221 with a mean of 45.31 mg/L in post-monsoon. Its contribution to the major cations is 2.04 to 16.26% (pre-monsoon) and 0.92- 35.41% (post-monsoon). In contrast to the concentrations of Ca^{2+}, Na^{+} and Mg^{2+} ions, a lower concentration of K^{+} is observed in both the seasons indicating its lesser geochemical mobility.

ANIONS: The Bicarbonates in the study area ranges from 246 to 787 mg/L, with a mean of 464.36 mg/L in the pre-monsoon and is from 353 to 866 mg/L with a mean of 497.96 mg/L in post-monsoon in the study area. The contribution of HCO_3^- to the total anions is 28.11 to 69.10% and 33.62 to 62.20% during pre-and post-monsoon periods respectively. The dominance of HCO_3^- classifies the area as a recharge zone (Ophori and Toth, 1989). This infers a dominance of mineral dissolution (Stumm and Morgam, 1996). The concentration of Cl^- ranges from 59 to 398 mg/L during pre-monsoon and is in between 86 and 522 mg/L during post-monsoon in the present study area. Their mean values are 224.82 and 266.20 mg/L respectively. The concentration of Cl- was higher in post-monsoon compared to pre-monsoon because of leaching process from upper soil layers due to domestic sewage activities and dry climates (Srinivasamoorthy, 2008). This is the second largest anion, after HCO_3^- contributing 8.82% to 38.16% (pre-monsoon) and 10.91% to 38.07% (post-monsoon) to the total anionic concentration. This is due to the influences of irrigation-return-flow and chemical fertilizers in the study area as the agricultural activity is intensive and long term and no other sources are evident (Srinivasamoorthy et al., 2010). The content of SO_4^{2-} is from 32 to 288 mg/L with a mean of 137.94 mg/L in the pre-monsoon groundwater, which contributes 4.37 to 29.87% to the total anions. The content of SO_4^{2-} ranges from 78 to 312 mg/L with a mean of 143.20 mg/L during post-monsoon, which contributes about 1.32-28.21% of total anions. The $SO_4^{2-}$is higher in post-monsoon compared to pre- monsoon indicates the leaching of sulphate from anthropogenic sources (Miller, 1979; Craig and Anderson, 1979; Srinivasamoorthy et al., 2010). The NO_3^- content is in between 5 and 174 mg/L in the pre-monsoon groundwater and is in between 16 and 187 mg/L during the post-monsoon in the study area. Their mean values are 60.38 and 73.40 mg/L respectively. The contribution of NO_3^- to the total anions is 0.36 to 19.39% during pre-monsoon and is 1.47 to 21.55% during post-monsoon. The NO_3^- was higher in post-monsoon (73.40 mg/L) compared to pre-monsoon (60.38 mg/L) indicating the dilution of NO_3^- content from plant nutrient and NO_3^- fertilizers such as urea and ammonium nitrate (Freeze and Cherry, 1979; Madison and Brunett, 1984). In natural conditions, it comes from the non-lithological sources (Hem, 1991), where it does not exceed 10 mg/L in the water (Cushing et al., 1993; Ritzit al., 1993). A higher concentration (>10 mg/L) of NO_3^- in waters of study area reflects the man-made pollution such as application of fertilizers, waste disposal etc. (Reddy 2010, 2012b, 2014; Reddy et al., 2012) and also atmospheric nitrite fixation on soils (Handa, 1975). The concentration of F^- ranges from 0.5 to 12.4 mg/L with a mean of 2.54 mg/L in the pre-monsoon of the study area. This contributes 0.07 to 1.06 % to the total anions. During post-monsoon, it varies from 0.14 to 16 with a mean 2.97 mg/L. The contribution of F- is 0.02 to 1.28% to the total anions during post-monsoon. The source of F- in groundwater of the study area is due to occurrence of various F- bearing minerals (fluorite, apatite, hornblende, biotite, sphene) in crystalline aquifers of study area.

Table 2: Compliance of groundwater quality of study area to drinking water quality standards of WHO (2004) and BIS (2003)

Chemical Parameters	WHO (2004)	BIS (2003)	% of samples BDL	% of samples BDL
P^H (units)	6.5-8.5	7.0-8.5	16	16
TDS (mg/L)	500	500	100	100
Ca^{2+} (mg/L)	75	75	80	72
Mg^{2+} (mg/L)	30	30	92	72
Na^{+} (mg/L)*	200	200	86	88
HCO_3^- (mg/L)	-	300**	96	100
Cl^- (mg/L)	200	250	66	74
SO_4^- (mg/L)	200	150	18	8
NO_3^- (mg/L)	45	45	64	74
F^- (mg/L)	1.5***	1.2	64***	72***

*Holden (1970), **BIS (1991); ***Maximum permissible limit; BDL- Beyond the Desirable limit

5. SUITABILITY FOR DRINKING AND DOMESTIC USES

To assess the suitability for drinking, general domestic and public health purposes, the hydrochemical data of groundwater of study area were compared with the standards of WHO (2004) and (BIS 2003) as in given Table 2. According to Fetter (1990) and Caroll (1962), the TDS values of study area fall in the category of fresh (10%; 8%) and brackish (90%; 92%) waters in pre- and post-monsoon seasons respectively. In the present study area, 100% of total groundwater samples in both the seasons are considered as unsuitable (>500 mg/L) for drinking purpose. At room temperature the prescribed limit for Na^+ concentration in drinking water is 200 mg/L (Holden, 1970). Concentration of Na^+ exceeding the prescribed limit of 200 mg/L in 86% and 88% of water samples in pre- and post-monsoon seasons respectively. Na+ makes the unsuitable for drinking because it causes severe health problems like hypertension (Holden, 1970). Therefore, Na^+ restricted diet is recommended to the heart patients. The Ca^{2+} concentration beyond the specified limit of 75 mg/L in 80% and 72% groundwater samples of pre- and post-monsoon seasons. Similarly, Mg^{2+} concentration exceeds the safe limits of 30 mg/L in 92% and 72% of total pre- and post-monsoon groundwater samples. These cations are the main contributors of the total hardness of water, which can prevent formation lather with soap and increases boiling point of water. In the study area, 98% and 92% of pre- and post-monsoon groundwater samples have K^+ concentration more than 10 mg/L. It indicates that the population of study area does not effected by health complications related to K^+ intoxication. However, it is recommended that the high risk health individual may seek medical advice while they consuming the groundwater treated by water softening using potassium chloride. The concentrations of HCO_3^- and Cl^- have no known adverse effect on health. However, it should not exceed the safe limits of 300 mg/L and 250 mg/L respectively in drinking water. The chemical analyses show that HCO_3^- exceeds the safe limits about 96% and 100% and Cl^- in 66% and 74% of pre- and post- monsoon samples. Higher concentration of Cl- in drinking water gives a salty taste and has a laxative effect balances the electrolytes in blood plasma and develop hypertension, renal stones and risk of stroke (Mc Carthy et al., 2004). The SO_4^{2-} is considered as one of the inorganic ions, which deteriorate the quality of drinking water. Concentration of SO_4^{2-} exceeds the desirable limit of 200 mg/L in 18% and 8% of pre- and post- monsoon samples. High concentration of SO_4^{2-} may cause diarrhea, catharsis, dehydration and gastrointestinal irritation (Garg et al., 2009). In the present study, 64% and 74% of total groundwater samples from the pre- and post- monsoon seasons have NO_3^- content beyond the desirable limit (45 mg/L). High concentration NO_3^- (>45 mg/L) in drinking water also causes methemoglobinemia (Bouwer, 1978) and cancer (Dissanayake and,Weerasooriya, 1987). The desirable limit of F- concentration is 1.2 mg/L and maximum permissible limit is 1.5 mg/L in drinking water. In the study area, 64% and 72% of total analyzed samples of pre- and post-monsoon exceeds the maximum permissible limit (>1.5 mg/L). However, 2% and 4% of total groundwater samples from the pre- and post-monsoon samples show <0.60 mg/L concentration of F^-. Excess F^- concentration causes dental and skeletal fluorosis, while the lower F^-concentration causes dental caries. The above results indicate the groundwater of study area is alkaline nature and it is not potable for drinking and domestic uses without proper treatment.

Table 3 Compliance of groundwater quality to irrigational standards of salinity and sodium hazards

Class	Salinity hazard	Sodium hazard	% of Samples (pre-monsoon)	% of Samples (post-monsoon)	Groundwater Quality
C_3S_1	High	Low	8	2	Moderate
C_3S_2	High	Medium	2	6	Moderate
C_3S_3	High	High	6	6	Poor
C_3S_4	High	Very high	44	26	Poor
C_4S_2	Very high	Medium	2	8	Poor
C_4S_3	Very high	High	6	10	Poor
C_4S_4	Very high	Very high	32	42	Poor

Table 4 Classification of groundwater of preset study for irrigational purpose

Classification	Range	% of samples (Pre-monsoon)	% of samples (Post- monsoon)	Water Quality
RSC	1.25	64	60	Safe
	1.25- 2.5	6	6	Marginally safe
	>2.5	30	34	Unsafe
PI	>75	48	44	Safe
	75- 25	52	56	Marginally
	< 25	-	-	-
MH	< 50	74	84	Suitable
	>50	26	16	Unsuitable

 ISBN: 978-93-90214-20-4

Na%	< 60	54	58	Suitable
	>60	46	42	Unsuitable
KR	< 1.0	30	32	Suitable
	>1.0	70	68	Unsuitable

6. QUALITY CRITERIA FOR IRRIGATION USE

The suitability of water for irrigation can be assessed by many determined parameters like Sodium Absorption Ratio (SAR), Percent Sodium (Na%), Permeability Index (PI), Residual Sodium Carbonate (RSC) and Magnesium Hazard (MZ). The results of irrigational parameters are presented in Tables 3 and 4.

Sodium Absorption Ratio

Sodium Absorption Ratio (SAR) is a measure of the degree to which irrigation water enters into cation exchange reacting in soil. The Na^+ replacing adsorbed Ca^{2+} and Mg^{2+} is a hazard as it causes damage to the soil texture such as compact and impervious. SAR is defined as;

$$SAR = \frac{Na^+}{\sqrt{\frac{(Ca^{2+} + Mg^{2+})}{2}}} \quad (1)$$

Where, the concentrations are reported in meq/L.

Sodium hazard is expressed in terms of SAR and Na%, while the salinity hazard is expressed in terms of EC. The values of SAR (6.70-104.62; 8.32-203.78) and EC (1078-3182; 1548-3524 (µS/cm) in the pre-and post-monsoon seasons respectively are plotted in US Salinity Laboratory Staff diagram (Richards, 1954) for rating of the irrigation water (Fig. 2). It is observed from the figure that most of the pre- and post-monsoon water samples fall in the categories of C3S4 (44% & 26%), C¬4S4 (32% & 42%) and C4 S3 (6% & 10%) respectively, indicating the high to very high salinity and sodium hazards (Table 3) This implies the quality of water is poor for irrigation purpose. High saline water cannot be used on soils with restricted drainage and needs special treatment for salinity control. Salt tolerant crops/plants should be selected in such regions.

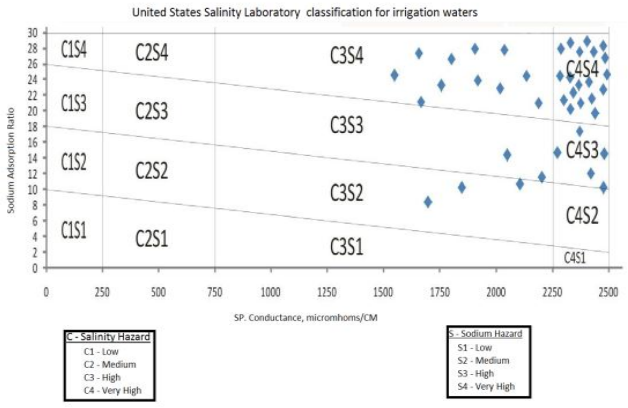

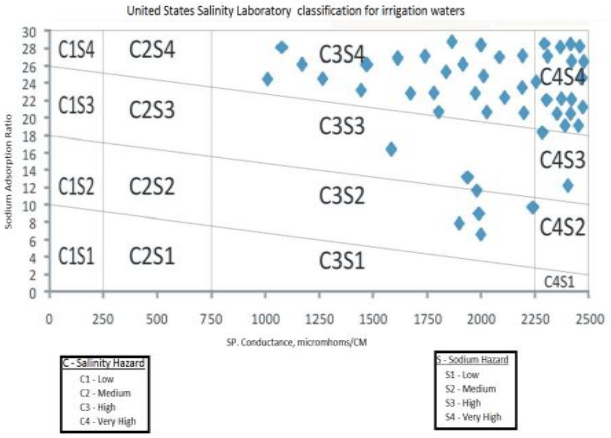

Fig. 2 USSL'S diagram of groundwater during the pre-monsoon (left) and post-monsoon (right) season

Percent Sodium

The Percent Sodium (Na%) in the irrigation water is usually expressed as percent sodium and can be determined by the following equation;

$$\%Na^+ = \left[\frac{(Na^+ + K^+)}{(Ca^{2+} + Mg^{2+} + Na^+ + K^+)}\right] \times 100 \quad (2)$$

Where, the concentrations of Na, Ca, Mg and K are taken meq/L.

The Na% in groundwater samples of study area ranges from 22.61 to 76.90 in the pre-monsoon and 29.43 to 95.35 in post-monsoon (Table 4). According to the classification of irrigation water based on the Na% (Wilcox, 1967) is assessed as permissible to unsuitable quality. As per the BIS (1991; Subba Rao and John Devadas, 2005), the maximum Na% of 60 is recommended for irrigation water, which indicates 54% and 58% of water samples in the pre- and post-monsoon seasons are suitable and remaining water samples from the study area are unsuitable for irrigation purpose. High Na% causes deflocculation and impairment of the permeable soils (Karanth, 1987).

Residual Sodium Carbonate

Richards (1954) used Residual Sodium Carbonate (RSC) for assessing the quality of water for irrigation purpose. In water having high concentration HCO_3^-, there is a tendency for Ca^{2+} and Mg^{2+} there may be possibility of complete precipitation of Ca and Mg (Karanth, 1987). As a result the water in soil becomes more concentrated and relative proportion of sodium in the water is increased in the form of sodium carbonate. To quantify the effects of $CO_3^{\neg}$-, HCO_3^-

as RSC has been computed as per the following equation (Eaton, 1950);

RSC = (HCO3- + CO3¬-¬) – (Ca2+ + Mg2+) (3)

Where, the concentrations are reported in meq/L.

A high concentration of RSC in water leads to increase in the adsorption of Na in soil. This influences the suitability of groundwater for irrigation use.

Health coat classified the irrigation water based on RSC as suitable (<1.25), marginal (1.25-2.5) and not suitable (>2.5). In the study area, RSC values from -9.70 to 7.44 in pre-monsoon and -4.35 to 14.50 in the post-monsoon, suggesting that the groundwater quality for irrigation is safe in 64%, marginally safe in 6% and unsafe in 30% of total samples in the pre-monsoon season (Table 4). During the post-monsoon season, the water quality is safe in 60%, marginally safe in 6% and unsafe in 34% of total samples.

Permeability Index

The Permeability Index (PI) also indicates whether the groundwater is suitable for irrigation. If the soil contains high salts (alkaline earths and carbonates), they destroy the soil permeability.

$$PI = \frac{Na\sqrt{HCO3}}{(Ca+Mg+Na)} X\ 100 \quad (4)$$

Where, the concentrations are reported in meq/L.

Donnen (1964) classified the irrigation water as class I (>75), class II (75-25) and class III (< 25). The PI values in the study area ranges from 82.10 to 85.97 in the pre-monsoon, while it is from 41.06 to 109.20 in the post-monsoon. Accordingly, 48% and 52% of total water samples in pre-monsoon indicates class I (>75) and class II (75-25) whereas 44% and 56% of total water samples in the post-monsoon come under Class I and class II types, implying the safe and marginally safe categories respectively (Table 4).

Magnesium Hazard

Magnesium Hazard (MH) values are also computed by Scaboles and Darab, 1964) equation;

MH = Mg/ (Ca+ Mg) x 100 (5)

MH value is > 50 are considered as harmful and unsuitable for irrigation use. The water samples of study area, the MH values ranges from 25.14 to 65.35 and 13.11 to 69.78 in pre- and post-monsoon seasons respectively, which accounting the 74% and 84% of samples having MH values below 50 (Table 4). This suggests that the most of groundwater is suitable for irrigation use in both the seasons.

Kelly Ratio

Kelly Ratio (KR) is measured for the concentration levels of Na^+ against Ca^{2+} and Mg^{2+}. KR is also used for classification of groundwater for irrigation purpose (Kelly, 1946; Paliwal, 1967). KR is computed by using the following equation;

$KR = Na^+ / (Ca^{2+} + Mg^{2+})$ (6)

Concentration of Na^+ in irrigation water is considered to be in excess (KR; >1.0), thereby the water is unsuitable. If the KR is < 1.0 is suitable for irrigation. 70% and 68% of total groundwater sample in the pre- and post-monsoon of study area record KR >1.0, indicating the poor quality of water for irrigation purpose (Table 4).

The seasonal variations in the quality of groundwater are influenced mostly by the geogenic and partially by anthropogenic sources including the domestic and agricultural activities through infiltration and percolation during monsoon. The groundwater quality in the study area is not potable for drinking and domestic purpose. The groundwater in the most of the study area is unfit for agriculture practices. Therefore, the long duration of intake of this of water can causes many types of public health problems

REFERENCE

[1] Wilcox, L.V. (1967). Classification and use of irrigation water, USDACirc., 969, Washington DC, USA, 19p.

[2] U.S. Salinity Laboratory Staff 1954. Diagnosis and Improvement of Saline and Alkali Soils, U.S. Dept. Agriculture Hand Book, 160p.;

[3] Holden, W, S (1970) Water treatment and examination. J & Churchill Publishers, London, p 513.

[4] Domenico PA, Schwartz FW (1990) Physical and chemical hydrogeology. Wiley, New York

[5] Todd, D. K (1980). Groundwater Hydrology. 2ndEdn., New York.

[6] Sreedevi PD (2004) Groundwater quality Pageru River Basin, Cuddapah district, Andhra Pradesh. J Geol Soc India 64(5):619–636

[7] Subba Rao, N., & John Devadas, D. (2005). Quality criteria for groundwater use for development of an area. Journal of Applied Geochemistry, 7, 9–23.

[8] Babu Rao, G and Sai Ramya, B (2018). Suitability of groundwater for irrigation purpose in the Ipur and Rompicherla mandals of the Guntur District, Andhra Pradesh, IJCRT, Volume 6, Issue 1 March 2018.

[9] Babu Rao Gudipudi , M. Srinivasa Rao , K. Dinesh Kumar (2019). Application of Water Quality Index (WQI) for Assessment of Groundwater Quality in Narasaraopet Mandal of Guntur District, Andhra Pradesh, India, International Journal Of Engineering Research & Technology (IJERT) Volume 08, Issue 06.

[10] Hem JD (1991) Study and interpretation of the chemical characteristics of natural water. Book 2254, 3rd edn. Scientific Publishers, Jodhpur, India

[11] American Public Health Association (2005). Standard methods for the examination of water and waste water, 21st edn., APHA, Washington, DC.

[12] Stallard, R.F. and Edmond, J.M. (1983) Geochemistry of the Amazon: 2. The Influence of Geology and Weathering Environment on the Dissolved Load. Journal of Geophysical Research: Oceans, 88, 9671-9688. http://dx.doi.org/10.1029/JC088iC14p09671

[13] Todd, D. K (1980). Groundwater Hydrology. 2ndEdn., New York.

[14] Hem, J. D. (1991). Study and interpretation of the chemical characteristics of natural Water. U S G S Professional Paper Book- 2254.Scientific Publishers, Jodhpur, India.

[15] Ophori D. U. and Toth, J. (1989). Patterns of groundwater chemistry, Ross Creek basin, Alberta, Canada. Ground Water, V.27, pp. 20–26.

[16] Stumm, W. and Morgan, J. J. (1996). Aquatic Chemistry. Wiley- Inter Science, New York.

[17] Srinivasamoorthy, K. Chidambaram, S., Prasanna, M,V., Vasanthavihar, M., Peter, J. and Anandhan, P. (2008). Identification of major sources controlling groundwater chemistry from a hard rock terrain - a case study from Metturtaluk, Salem district, Tamil Nadu, India. Jour. Earth Sys. Sci., v. 117(1), pp. 49–58.

[18] Srinivasamoorthy, K., Vijayaraghavan, K., Vasanthavihar, M., Sarma, S., Chidambaram, S., Anandhan, P and Manivannan, R (2010). Assessment of groundwater quality with special emphasis on fluoride contamination in crystalline bed rock aquifers of Mettur region, Tamil Nadu, India. Arb. Jour. GeoSci., v.5, pp. 83-94.

[19] Miller, G. T. (1979). Living in the Environment. 2ndEdn., Belmont, C.A. (Ed.) Wadsworth Publishing Company, Belmond California.

[20] Craig, E. and Anderson, M. P. (1979). The effects of urbanization of groundwater quality. A case study of ground water ecosystems. Environ. Conserv., v. 30 (2), pp. 104–130.

[21] Cushing et al., 1993;

[22] Ritzi, R.W., Wright, S.L., Mann, B. and Chen, M. (1993). Analysis of temporal variability in hydrogeochemical data used for multivariate analyses. Groundwater, v.31, pp. 221 - 229.

[23] Reddy, A. G. S. (2010). A comprehensive study on nitrate contamination of water resources. In: Laughton R (Ed.) Aquifers: formation, transport and pollution. Nova Science Publishers, USA, p. 500. (ISBN 978-1-61668-051-0).

[24] Reddy, A. G. S. (2012b). Evaluation of hydrogeochemical characteristics of phreatic alluvial aquifers in South eastern coastal belt of Prakasam district, South India. Environ. Earth Sci. DOI:10.1007/s12665-012-1752-6.

[25] Reddy, A. G. S. (2014). Geochemical evaluation of nitrate and fluoride contamination in varied hydrogeological environs of Prakasam district, Southern India. Environ. Earth Sci., v. 71(10), pp. 4473–4495.

[26] Reddy, A. G. S., Saibaba, B. and Sudarshan, G. (2012). Hydrogeochemical characterization of contaminated groundwater in Patancheru industrial area, Southern India. Environ. Monit. Assesst., v. 184(6), pp. 3557–3576.

[27] Handa, B. K (1975). Geochemistry and genesis of fluoride containing groundwaters in India. Groundwater, v. 13 (3), pp. 275–281.

[28] Fetter CW (1990) Applied hydrogeology. CBS Publishers & Distributors, New Delhi, India

[29] Carroll. D., (1962) Rainwater as a chemical agent of geologic processes – A review,U.S. Geological Survey Water – Supply Paper 1535 – G, pp 18.

[30] Holden, W, S (1970) Water treatment and examination. J & Churchill Publishers, London, p 513.

[31] Bureau of Indian Standards (BIS) (1991) Indian Standard Specification for drinking water, IS:10500. New Delhi

[32] WHO (1996) Guidelines for Drinking-water Quality. Volume 2. Health Criteria and Other Supporting Information. 2nd edition, World Health Organization, Geneva (BIS 2003)

[33] Mccarthy, J., T. Gumbricht, T. S. Mccarthy, P. E. Frost, K. Wessels and F. Seidel. (2004). Flooding patterns in the Okavango Wetland in Botswana between 1972 and 2000. Ambio, v. 7, pp.453–457.

[34] Garg, V.K., Suthar, S., Singh,S, Sheoran, A., Garima, Meenakshi And Jai,S. (2009) Drinking water quality in villages of southwestern Haryana, India: assessing human health risks associated with hydrogeochemistry. Environ. Geol., v. 58, pp. 1329-1340.

[35] Bouwer, H (1978). Groundwater hydrology. McGraw-Hill Book Company, New York.

[36] Dissanayake, C.B. (1991). The fluoride problems in the groundwaters of Srilanka- environmental management and health. Int. Jour. Environ. Studies, v. 38, pp. 137-156.

[37] Richard, L.A (U.S. Salinity Laboratory Staff) (1954). Diagnosis and improvement of saline and alkali soils. U. S. Department of Agriculture Hand Book, 60, 160 p.

[38] KARANTH, K.R. (1987) Groundwater Assessment and Development and Management, Tata McGraw Hills Publ. Co. Ltd. New Delhi.

[39] Eaton, F.M. (1950) Significance of carbonates in irrigation waters, Soil Sci., v.39, pp. 123-133.

[40] Doneen, L, D (1964). Notes on Water Quality in Agriculture, Department of Water Science and Engineering, University of California, Water Science and Engineering, p. 400.

[41] Kelley, W, P (1946). Permissible composition and concentration of irrigation waters. In: Proceedings of American Society of Civil Engineering 607.

[42] Paliwal, K.V (1967). Effect of gypsum application on the quality of irrigation waters. Madras Agricul. Jour., 59: 646-647.

[43] Scaboles, L. and Darab, C. (1964). The influence of irrigation water of high sodium carbonate content of soils. In: Proc. 8th Intern. Congress of Isss, Trans., II: 803-812.

A Study on Going Cashless With Cryptocurrency in India and Its Impact in Banking Industry

[1] Dr R.B.Ayeswarya, [2] Ms. Reema Varghese

[1][2] Assistant Professor, Department Of Commerce, Stella Maris College, Chennai, Tamil Nadu

Abstract:

India is a developing country and one such development is transforming to be a Digital India. With the announcement of demonetisation in 2016, India took a huge step of transforming to Cashless Economy. The idea of transforming into digitalization was to eliminate black money in the country. Banking system has faced a major change in this transformation by introducing Net Banking, Mobile Banking. Being the industry with the most leading financial sector of the country and one of the most important reasons for economic development, with the innovation of certain digital currencies the banks was not satisfied. One of the digital transformations is the evolution of Crypto currency. Cryptocurrency is a digital or virtual currency which is moulded to use as a medium of exchange used by a strong cryptography (used for solving codes) to secure financial transactions and verify the transfer of assets. They are considered to be one such future development of Block chain technology. But the awareness regarding to cryptocurrencies is not appreciated. The Banking sector is opposing to investment or transactions with cryptocurrencies as the banks do not earn much profits with the innovation of cryptocurrency. The objective of the study is (i)To assess the level of awareness among the investors on investment in crypto currency (ii) To suggest measures on bringing new form of crypto currencies for progressing towards a cashless society.

Keywords:

Digital India, Block Chain Technology, Cryptography, financial transactions

1. INTRODUCTION

India's one kind of development was the announcement of Demonetisation to evade black currency and to make every citizens of the country by paying regular taxes. Thus, Digital India movement was initiated in order to make the society a Cashless society. Through Digital movement, many Banks, Corporate companies, Educational institutions and many other profit making organisations started with the usage on online transactions.

Through the adoption of digitalization in banking sector, it has helped them in converting data into digital format and also provides enhanced customer services and helps in saving time. Many banks introduced Mobile banking applications as they could make digital payments easy and customer could track their investments. Google Pay, UPI and many more of these applications were made in support of this banking system to make payments and transactions in much easier way. Many public and private sector banks have linked themselves with certain applications for easy transactions and to track proper transactions.

With more usage of digitalization, Artificial Intelligence was introduced to make more technology prone and easier for working environment. Through AI, banks introduced many facilities like robots, Chat – bots and many virtual currencies. One such virtual currency was Crypto currency.

1.1 Crypto Currency

Crypto currency is a digital based function that allows secure payments through online in terms of virtual 'tokens' represented by ledger entries to the system. It is a digital money created from code and operates as a medium of exchange. The first ever crypto currency was Bitcoin invented by Satoshi nakamoto in 2009. This invention was not to create a currency but for a decentralized cash system. Satoshi wanted to invent this as this could help payment network with account, balances and transactions. But this invention is not been encouraged by many as it involves a lot of illegal activities like tax evasion and money laundering. This technology is been welcomed with advantages, disadvantages and criticisms by many. Indian banks are not comfortable is introducing crypto currencies in India and has always been a debate to encourage these virtual currencies or not.

2. REVIEW OF LITERATURE

Singh Aarti and Nidhi Chawla (2016)in their study titled **Review on Strategies for growing E commerce in India,** predicted that emerging new technologies, awareness regarding new technology and frauds, Reduced search and transaction cost, Reduced lead-time and faster time to market, Increased customer service, Improved convenience and shopping experience, Increased information transparency, Knowledge generation, Novel products and services will be the trends that will be followed in crypto currency

Dr. Alka Mittal.(2017) on his study titled **"An analytical study of present position of bitcoins."** focuses on merchants and traders who accept this digital currency as a medium of exchange to overcome its problem of volatility. This will boost the market of Bitcoins not only in India but also in other developing economies. This emphasizes that to

survive in the system; Bitcoin has to adapt itself to the required technical and operational innovations. In addition to this, government should impose proper legal framework, to protect the consumers or users of these digital currencies, as the progress seen in the transactions in this currency during the past few months is tremendous**.**

Dr. Anita Sharma (2018) in their study titled **"Crypto currency: Evolution, Impacts and Future in India"** focuses on the introduction of Crptocurrency and its impacts at the present. The study clearly states the positive and the negative sides of the virtual currency and has predicted the future of crypto currency in India. This emphasis encourage individuals to earn profits and make more investments. The legal position of crypto currency in India is neither accepted nor denied.

C.V Smalley (2017) on article **Crypto currency and taxes** explains about the workings of Crypto currency and the process to transact the currency with the miners, traders and investors involved. It also clearly specifies about trading with crypto currency as a Taxable event but converting cash to virtual currency to be Money Laundering.The article also mentioned the IRS notice about the recommendations on updating the guidance for requirements and its tax treatments.

Xin Li and Chong Alex Wang (2017) in their study titled **"The technology and economic determinants of crypto currency exchange rates: The case of Bitcoin"** details on one particular crypto currency, Bitcoin. The study explains on Bitcoin exchange rates against USD, its technology and economic factors. It has also analyzed that the bitcoin exchange rates has adjusted to economic fundamentals and market conditions and also identified the significant impact of mining technology and difficulty in Bitcoin exchange price determination.

3. RESEARCH METHODOLOGY

3.1 Research Design

The study prefers to use Descriptive Research design to project the insights of cashless economy and crypto currencies

3.2 Sources of Data

Primary and secondary data are to be used in the study. The primary data is to be tested through a structured questionnaire, Secondary data is obtained from internet websites and links, Journals to develop an insight into research problem.

3.3 Sampling Method

The study has preferred to use Convenience Sampling Technique.

3.4 Sample Size

Sample is a subset of population which meets the inclusion criteria for participation in the study. The study has collected response from 91 respondents.

4. ANALYSIS AND INTERPRETATION

The study has used percentage analysis and Chi-square for interpretation of results.

Hypotheses 4.1 Ho: There is no association between Gender and the opinion to divide the crypto currencies according to locations for the purpose of creating awareness

H1: There is an association between Gender and the opinion to divide the crypto currencies according to locations for the purpose of creating awareness

Table 4.1 Case Processing Summary

	Cases					
	Valid		Missing		Total	
	N	Percent	N	Percent	N	Percent
Gender * Do you think currencies should get divided by Geographical locations?	91	100.0%	0	0.0%	91	100.0%

Table 4.2 Gender * Do you think currencies should get divided by Geographical locations? Crosstabulation

			Do you think currencies should get divided by Geographical locations?			Total
			No	No opinion	Yes	
Gender	Female	Count	14	10	21	45
		Expected Count	13.4	4.9	26.7	45.0
	Male	Count	13	0	33	46
		Expected Count	13.6	5.1	27.3	46.0
Total		Count	27	10	54	91
		Expected Count	27.0	10.0	54.0	91.0

Table 4.3 Chi-Square Tests			
	Value	df	Asymp. Sig. (2-sided)
Pearson Chi-Square	12.694[a]	2	.002
Likelihood Ratio	16.578	2	.000
N of Valid Cases	91		

Opinion on division of currencies according to Geographical Locations

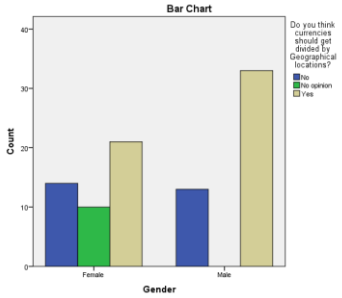

Decision: The calculated Pearson Chi-square value is 12.694 and the corresponding p-value is 0.002 which is less than 0.05. Hence the Ho is rejected.

Conclusion: There is an association between Gender and the opinion to divide the crypto currencies according to locations for the purpose of creating awareness

Hypotheses 4.2 Ho: There is no association between Gender and level of trust in crypto currency technology.
H1: There is an association between Gender and level of trust in crypto currency technology .

Table 4.4 Gender and level of trust in technology

			No	No opinion	Yes	Total
Gender	Female	Count	20	10	15	45
		Expected Count	20.8	5.4	18.8	45.0
	Male	Count	22	1	23	46
		Expected Count	21.2	5.6	19.2	46.0
Total		Count	42	11	38	91
		Expected Count	42	11.0	38.0	91.0

Table 4.5 Chi-Square Tests			
	Value	df	Asymp. Sig. (2-sided)
Pearson Chi-Square	11.438[a]	3	.010
Likelihood Ratio	13.406	3	.004
N of Valid Cases	91		
a. 2 cells (25.0%) have expected count less than 5. The minimum expected count is .99.			

Decision: The calculated Pearson Chi-square value is 11.438 and the corresponding p-value is 0.010 which is less than 0.05. Hence the Ho is rejected.
Conclusion: There is an association between Gender and level of trust in crypto currency technology.

5. FINDINGS

- Out of 91 respondents, 49.5% of respondents were female and 50.5% were male respondents.
- Relating to the nature of work, 14.3% of respondents work for Public sector, 35.2% of respondents work for Private sector, 16.5% are self-employed and 34.1% belong to employees other than public, private and self-employed category.
- Among the respondents participated in the survey, 48.4% are of the age group of 20-30 and 29.7% are in the age group of 30-40.
- 42% of the respondents have an understanding of crypto currency.
- 79% of respondents are of the view that the authorities should involve in monetary policy regulation prior to inception of various types of crypto currency.
- 59.3% of respondents are of the opinion that currency should be divided by Geographical locations
- 70% of respondents stated that crypto currency should be regulated by public authorities.
- Only 40% of the respondent are willing to invest in crypto currency.
- Speculation and intention in faster multiplication of money had made respondents to invest in crypto currency
- 32% of the respondents consider extreme volatility as a main constraint to invest in crypto currency
- 40% of the respondents are of the view that bitcoin will be a predominant currency in a couple of years.
- 55% of the respondents are of the view that bitcoin will be a predominant currency in a decade.
- 43% of the respondents has a trust on the technology of the crypto currency
- 52% of the respondents are of the view that crypto currencies will be an acceptable mode of currency in the day to day transactions of individuals.
- 64% are of the view that the currencies should be regulated by authorities to protect theft and loss
- 36% of the respondents consider bitcoin as a currency.

6. SUGGESTIONS

- Measures should be taken through awareness programs to facilitate investment in crypto currency
- Regulatory measures and conditions should be in an understandable manner to promote and create a path for investment in crypto currency
- Security and trust factors should be strengthened with the help of banks and regulatory authorities to create confidence in the minds of investors to invest in crypto currencies
- Complexities should be simplified and more literacy level will have to be increased to enhance awareness.
- Investment and use relating to crypto currency(purchase and sale) should be made easy to facilitate the use of currency in day to day transactions
- Protection aspect should be strengthened to prevent theft and loss.
- Steps should be taken to make bitcoin as a currency first and as an asset in subsequent stages.

7. CONCLUSION

From India's perspective, an important point is to introduce virtual currency. This further brings focus on a big question that why can't India not regulate these currencies similar to other countries by amending taxation laws, Foreign Exchange Management Act (FEMA), etc, and also appointing an authority like RBI or (Securities and Exchange Board of India) SEBI over this business, as just the introduction of digital rupee does not guarantee that there will be no frauds or laundering. The future of crypto currency lies totally in the hands of legislature, whether to ban the currency or not. Apart from this, a decision to be taken for the way forward is the introduction of digital rupee or to regularize the sector. This is the need of the hour to make it a viable opportunity for investors and consumers.

REFERENCE

[1] Anna Olesko, o. t. (2018, Vol 4, No 2). Formation of Cashless economy in the Ukraine and in the world. Baltic Journal of Economic Studies , 147-150.

[2] Banwari, D. V. (Vol 8, Issue 12, 2017). Cryptocurrency scope in India. International Research Journal of Management Sociology and Humanity , 82-92.

[3] Jain, V. (2017). A Journey towards a Cashless society. Research gate , 61-73.

[4] Sanjay Jha, S. K. Application of Block chain technology. Sixteenth AIMS International Conference on Management, (pp. 617-623).

[5] SHARMA, D. A. (Dec 2018, Vol 6, Issue 12). Cryptocurrency: Evolution, Impacta and Future in India. GE International Journal of Management Research .

[6] Vora, G. (2015,6). Cryptocurrencies are disruptive Financial Innovations here. Modern Economy. , 816-832.

[7] C V Smalley https://www.thetaxadviser.com/newsletters/2017/apr/cryptocurrency-taxes.html

[8] Xing Li https://papers.ssrn.com/sol3/papers.cfm?abstract_id=2515233

Comparative Analysis of Facial Emotion Recognition Techniques

[1] Manisha M. Kasar, [2] S.H. Patil

[1] Department of Information Technology, Bharati Vidyapeeth Deemed to be University College of Engineering, Pune, India
[2] Department of Computer Engineering, Bharati Vidyapeeth Deemed to be University College of Engineering, Pune, India

Abstract:

Facial emotion is an essential way of exchanging information of personal emotions, detection of its implementations in human-computer interaction (HCI), safety control, monitoring, driver protection, fraud identification, etc. Facial emotions are more robust, flexible, and essential linguistic signs for a person to exchange information of their emotion and purpose throughout the communication. The aim of this study is to provide a summary of facial emotion recognition and their improvements across the past years. The paper describes the techniques used for face emotion classification and its comparative analysis of facial emotion recognition. Techniques for facial emotion classification can be categorized in two techniques. First type is depending on conventional image processing methods. Another type is depending on machine learning technique where features are classified through trained model. Classification is a task that requires the use of machine learning algorithms that learn how to assign a class label to examples from the problem domain. We study the primary movements and specify present limitation with the assumption. This study will give additional motivation for the frequently required high-performance and actual facial emotion recognition worked at database images.

Keywords:

Facial Emotion Recognition, image processing, Machine Learning, Emotion Classification

1. INTRODUCTION

Face emotion detection has the main idea of smart human-computer communication; it has a large approach framework. It is used in the areas of medical treatment, distance learning, gambling games, and everyone's safety [7]-[9]. In the area of artificial intelligence, the interaction between person and computer becoming effortless. The face emotion prediction is also applicable to the medical area. To notice the result of current antidepression, more correct medicine assessment may be made as per the regular information of suffers face emotions [6]. The approach of face emotion prediction in the educational field may validate the education process to keep a record of students' expression changes in teaching and give finer recommendations for educators to educate students in correspondence with their tendency. The feature extraction depicts taking out features that may be utilized for classification from given images or video sequences [6]. As per the category of input information, the current techniques of feature extraction are categorized into two classes: the first is formed on fixed images and the other is formed on a moving sequence [6]. The face emotion is multiple communication technique. Information is sent through a face contains sensation, feeling, generation, grade, perception, glamor, and near to additional substances as well [11]. Facial expressions in sign language are termed as non-manual parameters, and they are important to recognize the meaning of a sign language gesture. The expressions are happy, surprise, fear, anger, disgust, and sad these expressions are termed as basic/prototypic expressions. These emotions are predicated using the various stages of FER system. The Architecture of facial emotion recognition system is shown in figure 1 The Facial Emotion Recognition system includes the major stages such as face image pre-processing, Face Detection, feature extraction and classification.

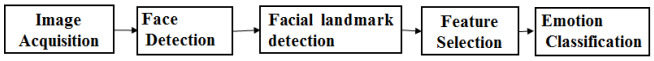

Fig. 1 Architecture of Facial Emotion Recognition System [2]

As shown in figure 1, first task of facial emotion recognition system is capture image by camera or video sequence or select image by database and this image is given for further stage of facial emotion recognition which is describe below:

- **Pre-processing**

Preprocessing is a process to remove unnecessary information and background noise, filtering and edge detection. There are some standard key edge detectors and preprocessing methods available including Sobel, Prewitt, Differences of Gaussian, Laplacian of Gaussian, Roberts, Kirsch and Canny Edge detector and Histogram equalization, logarithm transform (LOG), Gamma Intensity Correction (GIC) were used to pre-process facial expression images [3]. Now a days using deep learning we can pre-process images using filters to smooth or sharp the images.

 ISBN: 978-93-90214-20-4

- **Face Detection**

Face detection has the aim to search out whether the face is present in an available image or not. Face detection from the frontal face and partial frontal face, classifier will decide either the image is in the face or non-face category depends on knowledge accomplished from the image in training. A unique technique is viola Jones technique [4] is used to identify a face.

- **Face Landmark Detection**

Facial key point detection is a main process of face recognition and face expression recognition [5]. The maximum repeatedly utilize key points are regions of eyes, nose, lips, mouth, eyebrow and different another facial region [6]. Various current facial emotion recognition methods are studied here such as CNN [17], PCA [8], Gray Level Difference Method (GLDM) [9], LBP, 3D key point localization [10], 3D Point Distribution Model (PDM) method [11], CLM approach based on DRMF technique [10], Constrained Local Neural Field model [12], Fast corner detector method [13], etc. Utilizing this face key point analysis, we choose characteristics of face. Finally, we will apply expression categorization stage [7].

- **Feature Extraction**

It is process of identifying position [14] of face components like eyebrow, mouth, nose, eyes, lip, cheeks and others. The underlying features, typical methods of expression recognition using Gabor features include elastic map matching technology, Gabor wavelet network, Gabor feature Fisher classification, etc. Among them, BP neural network is one of the most widely used networks. It is simple in structure, easy to train, and has good self-learning ability and classification ability [14].

- **Feature classification**

Classification analysis is an important component of facial recognition, mainly used for finding the valuable data distribution and data models in the potential data. The data points within a cluster are more similar to each other than that in different clusters or class [1]. Using face key point analysis, we choose characteristics of face. Finally, we will apply expression categorization stage.

In this paper we are discussing different methods of facial emotion recognition which has been suggested by many researchers in various areas. In this paper section II gives details about earlier facial emotion recognition detection techniques. Section III gives details about Comparative Analysis of Facial emotion Detection Techniques and Section IV gives details about performance of facial emotion recognition and accuracy of methods and section V and VI gives details about conclusion and future scope.

2. STUDY OF EARLIER PROPOSED WORK

In this section we will discuss earlier proposed method by researchers. We will discuss traditional method and deep learning methods used for Face Expression recognition system. As we discuss in section 1 General architecture of FER system the first step is to detect the face in given input then it will go for key point extraction then next step comes here is feature extraction and feature classification. The methods proposed by some researchers are explain below.

2.1. CNN (Convolution Neural Network) and LBP (Local Binary Pattern)

The method proposed by Qintao Xu,Najing Zhao in 2020 [23] is using improved convolutional neural network model based on AlexNet model. A feature fusion algorithm based on EmotionNet and LBP was designed and named lbpcnn algorithm. Their experimental results prove that continuous convolution is better than monolayer convolution. And the feature fusion algorithm based on lbp-cnn can solve the image rotation problem to some extent. However, in actual scenes, face expression recognition is often interfered by complex background, uneven illumination and occlusion, etc. These problems are not yet resolve by the author for further improvement of the expression recognition algorithm. It can be better applied in complex scenes which still needs further research.

2.2 Convolutional neural network with 20 layers

The Method proposed by Erdem Canbalaban, Mehmet Önder Efe in 2019 [24] is using Convolutional neural network with 20 layers are used and different types of facial expressions are classified. In design process, they have faced different difficult problems and overcome each of them by applying required solution steps. Although the resolution of the sample images is quite low, from only 48×48 pixels, they managed to design a convolutional neural network which is capable of classifying seven different group effectively both offline testing and with real time data. Usage of well-designed Convolutional Neural Network and different data augmentation techniques increase the accuracy of the proposed method. To further improve the performance, they will apply different feature extraction methods with more powerful machine and increase the size of the images.

2.3 Deep Neural Network

The method proposed by Ali Mollahosseini1, David Chan, and Mohammad H. Mahoor in 2015[25] is using deep neural network architecture. Their network consists of two convolutional layers each followed by max pooling and then four Inception layers. The network is a single component architecture that takes registered facial images as the input and classifies them into either of the six basic or the neutral expressions. The results confirm the superiority of their network compared to several current methods in which engineered features and classifier parameters are usually tuned on a very few databases. Still there is issue in evaluation of cross database scenarios which is not yet resolved by the researchers.

2.4. Convolution Neural Network

The method proposed by Shekhar Singh and Fatma Nasoz in 2020 [26] is using CNNs, without requiring any pre-processing or feature extraction tasks. They illustrate

techniques to improve future accuracy in this area by using preprocessing, which includes face detection and illumination correction. Feature extraction is used to extract the most prominent parts of the face, including the jaw, mouth, eyes, nose, and eyebrows. They used a heuristic approach to find CNNs and will work on finding a more robust network in the future. They faced an over fitting issue due to 99.64% accuracy on the training dataset. We need to resolve this issue using various Optimization techniques of CNN.

2.5. Two-part convolutional neural network (CNN)

The method proposed by Ninad Mehendale in 2020 [27] is using CNN. The FERC is based on two-part convolutional neural network (CNN): The first part removes the background from the picture, and the second part concentrates on the facial feature vector extraction. In FERC model, expressional vector (EV) is used to find the five different types of regular facial expression. The two-level CNN works in series, and the last layer of perceptron adjusts the weights and exponent values with each iteration. The execution time was increasing with the number of layers, and it was not adding significant value to their study, hence not reported in the current manuscript. As a future scope of this study, researchers can try varying the number of layers for both CNN independently. Also, the vast amount of work can be done if each layer is fed with a different number of filters.

2.6. Deep learning approach

The method proposed by Shervin Minaee, Amirali Abdolrashidi in 2019 [28] was using Deep learning approach based on important parts of face, and achieves significant improvement. They also use a visualization technique which is able to find important face regions for detecting different emotions, based on the classifier's output. This proposed new framework for facial expression recognition using an attentional convolutional network using less than 10 layers to complete with much deeper network for emotion recognition. This system also focused on visualization method to highlights the salient regions of face images which are the most important parts in detecting facial expression. There seems to be missing a simple piece for attending to the important face regions for emotion detection.

2.7. Dual feature fusion Method

The method proposed by Awais Mahmood,Shariq Hussain ,Khalid Iqbal, and Wail S. Elkilani, in 2019 [29] was using dual feature fusion. Initially, the face portion is detected and extracted from input images using the Viola–Jones algorithm. For dual feature fusion, we first detect the facial landmark point on the face image and then the important local regions are located. Weber local descriptor (WLD) excitation and orientation image is also generated from the input images. In next step, DCT is used to select the high variance features from local regions along with excitation and orientation image of WLD. In order to improve the performance, both types of features are then fussed using the score-level fusion. Although WLD works well on the face images for the extraction of salient features, the variation of local intensity cannot effectively be represented by using the standard WLD because it neglects different orientations of the neighborhood pixel.

2.8. 2D landmark feature map (LFM)

The method proposed by Dong Yoon Choi, Byung Cheol Song in 2020 [30] was using 2D landmark feature map (LFM). The proposed 2D landmark feature map (LFM) is obtained by transforming conventional coordinate-based landmark information into 2D image information. LFM is designed to have an advantageous property independent of the intensity of facial expression change. Also, they propose an LFM-based emotion recognition method that is an integrated framework of convolutional neural network (CNN) and long short-term memory (LSTM). Experimental results show that the method achieves better accuracy in the well-known micro-expression datasets, i.e., SMIC and CASME II, respectively, which outperforms the conventional methods. It has not been taken into consideration that they recognize facial expressions of various intensity including FME.

2.9. Combining convolutional neural network with graph based convolutional neural network (GCN)

The method proposed by Xu Xu, Zhou Ruan, Lei Yang in 2020 [31] was using Combining convolutional neural network with graph based convolutional neural network (GCN). It was novel method for fully automatic facial expression recognition. A graph convolutional neural network is proposed for feature extraction and facial expression recognition classification. A new approach for FER that uses a geometric shape features from local face regions and GCNN is used for feature extraction. Experimental results showed that the better accuracy is obtained by the method. This study proposes a new FER idea and obtains better results. This study should generate more robust results which may be achieved by combining facial appearance features and geometric features.

2. 10. Landmark detector of DLib and SVM classifier

The method proposed by Hajar Chouhayebi,Jamal Riffi, Mohamed Adane Mahraz, Ali Yahyaouy, Hamid Tairi, Nawal Alioua in 2020 [32] was using landmark detector of DLib and SVM classifier. First, utilizing the face and landmark detector of DLib, the facial region and landmarks are detected in an input image. Second, based on distance, angle and triangle between some specified facial landmarks, GF are constructed. Finally, SVM is used for the classification of each feature vector to one of the basic facial expression. The experimental results show that using a fusion database can reach significant result. Still there need to work to minimize the incorrect recognition rate when the face is turned or partially covered by objects. To enrich the method by adding other factors like ethnic group,

age and gender and which play essential roles in emotional recognition and using deep learning-based methods.

The work done using existing techniques based on traditional methods and various CNN network are elaboratively discussed in this section. Together with this the issues and gaps of existing systems are also discussed here. The major issue in FER system to overcome, in actual scenes, face expression recognition is often interfered by complex background, uneven illumination and occlusion, etc. The training of CNN on noisy image data could cause an increase of misclassification error. One of the important issues in a FER task consists of dealing with the great variability of data, i.e. facial expressions can be affected by the level of expressiveness, race or personality. However, the major challenges in FER are to reduce computational time, accuracy rate and true prediction of emotions using good CNN architecture.

3. COMPARATIVE ANALYSIS

The experiments ate performed on various databases to extract points like fer_2013 [33], MultiPIE [34], MMI [35], CK+ [36], SFEW [37], FERC with Caltech faces [38], CMU [39] and NIST [40], JAFFE [41], FERG [42], MAHNOB-HCI [43], MEVIEW [44] and BUHMAP [45]

The fer_2013 [33] dataset consists of one training set and two test sets. Training set has 28,709 different 48×48-grayscale images in 7 facial expression categories and each test set has 3589 images. The Multi-PIE dataset [34] contains 3557 frontal and closed frontal face images with all 6 expressions and at illumination. MMI database [35] consists of images of high resolutions of 88 subjects and over 2900 videos of male and female. CK+ dataset [36] contains total 329 images including various expressions of each for varying resolutions 48×48 to 192× 192. Static face in the wild (SFEW) [37] dataset are 291 images from the available 1394 images in the database. FERC with Caltech faces [38], CMU [39] and NIST [40] was used more than 750K images. The JAFFE dataset [41] contains Japanese female face expression. There is total 213 images having 256×256-pixel resolutions. The FERG [42] database contains 55,767 annotated face images of six stylized characters. MAHNOB-HCI [43] was produced by sensing the faces and bio-signals generated while the subjects are watching the emotional stimulus contents. MEVIEW [44] dataset was produced by focusing on FME in wild conditions. Bogazizi University Head Motion Analysis Projection Database (BUHMAP-DB), that has 440 videos of 11 people playing 5 receptions on 8 gestures [45].

TABLE I. COMPARATIVE ANALYSIS OF FACIAL EXPRESSION RECOGNITION TECHNIQUES

Sr. No	Name of author and year	Dataset	Method used	Accuracy	Number emotion recognized
1	Qintao Xu, Najing Zhao, 2020	Fer_2013	CNN and LBP	65.58%	7
2	Erdem Canbalaban, Mehmet Önder Efe, 2019	Kaggle	CNN	61.8%	7
3	Ali Mollahosseini, David Chan, and Mohammad H. Mahoor, 2016	MultiPIE, MMI, CK+, FER2013.	SVM, Nearest Mean Classifier, Weighted Template Matching, and KNN	66.4%	7
4	Shekhar Singh, Fatma Nasoz, 2020	Fer_2013	CNN	61.7%	7
5	Ninad Mehendale, 2020	CK+, Caltech faces, CMU and NIST	CNN	78.65%	6
6	Shervin Minaee, Amirali Abdolrashidi, 2019	FER-2013, CK+, FERG, and JAFFE	Attentional CNN (ACNN)	70%	6
7	A. Mahmood, S. Hussain, Khalid Iqbal, and Wail S. Elkilani, 2019	MMI database, CK+ and static face in the wild (SFEW)	Weber local descriptor (WLD) and DCT	95.58%	6
8	Dong Yoon Choi, Byung Cheol Song, 2020	MAHNOB-HCI and MEVIEW	2D landmark feature map (LFM) and CNN	71%	5
9	Xu Xu, Zhou Ruan, Lei Yang, 2020	JAFFE, FER2013 and CK+	Graph Convolutional Neural Network (GCNN)	95.85%	6
10	H. Chouhayebi, J. Riffi, M. Adane Mahraz, A. Yahyaouy, H. Tairi, N. Alioua, 2020	Personal Database, BUHMAP and Fusion Database	Dlib face detector, SVM and HOG	88.5-%	4

The table I gives comparative analysis of various facial emotion recognition techniques. It includes various fields such as author name, Year of publication, Facial Emotion recognition method, Database names, accuracy and number of features extracted. The Method used field of table describes the method used for facial emotion recognition. The emotion recognition accuracy of different methods is from 65% to 96% and it is shown in figure 2. The number of face emotions extracted field describes the emotions recognized in that papers are 4,5,6,7 respectively. The CNN and LBP[23] using fer_2013 [35] dataset, CNN[24] using fer_2013 [33], SVM, Nearest Mean Classifier, Weighted Template Matching, and K-nearest neighbors [25] using MultiPIE [34], MMI [35], CK+ [36] datasets, CNN [26] Using fer_2013 [33], CNN [27] using extended Cohn–Kanade expression, Caltech faces [38], CMU [39] and NIST [40] datasets, attentional CNN [28] using FER-2013 [33], CK+ [36], FERG [42], and JAFFE [41] datasets, Weber local descriptor (WLD) [29] and DCT using MMI [35] and CK+ [36] datasets, 2D landmark feature map (LFM) and CNN [30] using MAHNOB-HCI [43], MEVIEW [44], Graph Convolutional Neural Network (GCNN) [31] using JAFFE [41], FER2013 [33] and CK+ [36] datasets, Dlib face detector, SVM and HOG [32] using BUHMAP [45] dataset, dataset achieves 65.58%, 61.8%, 66.4%, 61.7%, 78.65%, 70%, 95.58%,71%, 95.85% and 88.5%, accuracy respectively. As per the comparative analysis from Table I Weber local descriptor (WLD) [29] and DCT using MMI [35] and CK+ [36] datasets and Graph Convolutional Neural Network (GCNN) [31] using JAFFE [41], FER2013 [33] and CK+ [36] datasets achieve better accuracy as compare to other methods of Table I.

4. 4. PERFORMANCE COMPARISON

The performance comparison of this study is based on the Facial Emotion Recognition accuracy and expression count analysis on various databases. The Facial Emotion Recognition accuracy of various Emotion Recognition techniques is shown in figure 2. The X- axis indicates the accuracy of various Facial emotion Recognition techniques and y axis indicates the names of Facial Emotion Recognition methods and database used. The accuracy value of each method is evaluated from its own paper and different datasets are used in every paper which is shown in below figure.

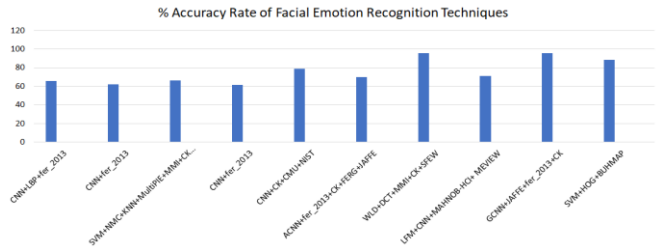

Figure 2. Accuracy Rate of Facial Emotion Recognition Techniques

The above figure 2 shows accuracy rate of Facial Emotion Recognition methods using various datasets. As Shown in figure, the Weber local descriptor (WLD) [29] and DCT method using MMI [35] and CK+ [36] datasets and Graph Convolutional Neural Network (GCNN) method [31] using JAFFE [41], FER2013 [33] and CK+ [36] datasets achieve better accuracy as compare to other methods shown in figure. The number of emotions recognized by method on face images using different techniques are describe in figure 3. Where the X-axis denotes the name of Facial Emotion Recognition method and database used, the Y-axis denotes the number emotions detected using Facial emotion Recognition method. The value of facial emotion recognized is considered from its own paper, most of the method detects 7 emotions using various datasets.

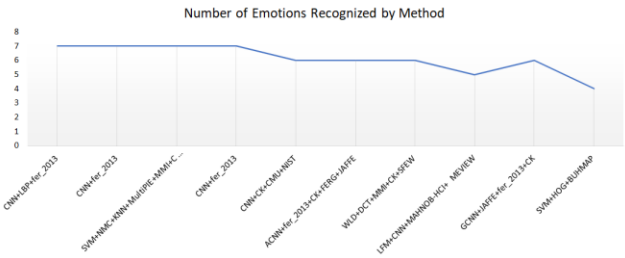

Figure 3. Number of Emotions Recognized by Method

The figure 3 shows Number of Face Emotion Recognized by various methods. The CNN and LBP[23], CNN[24], SVM, Nearest Mean Classifier, Weighted Template Matching, K-nearest neighbors [25], and CNN [26] recognizes all 7 emotions like fear, anger, Happy, Sad, Surprise, Disgust, Neutral. But, the methods CNN [27], attentional CNN [28], Weber local descriptor (WLD) [29] and DCT, 2D landmark feature map (LFM) and CNN [30], Graph Convolutional Neural Network (GCNN) [31], Dlib face detector and SVM and HOG [32] recognizes 6, 5, 4 emotions respectively. We compared figure 2 and figure 3, as per analysis we found the methods achieves less accuracy for more emotion extraction on large database images. Such as CNN and LBP[23], CNN[24], SVM, Nearest Mean Classifier, Weighted Template Matching, K-nearest neighbors [25] and CNN [26] these methods uses fer_2013 dataset for emotion extraction and other listed methods of Table 1 having more accuracy but they are extracting less emotions on small data size.

The methods discussed in section 2 have various limitations that have solved by many authors. Still, there are some issues in facial emotion recognition like face image gallery does not consider, various views of the face image have not considered and they had only worked on neutral images, Accuracy of the proposed system is weak, the effectiveness of predicting the facial emotion from large databases is poor. The key point detection process is performed manually. Inputted image having a composite background and different lighting situations may be additionally somewhat complicated in pinpointing or tracking. Face

emotions analysis turns to decline if the test image has a various illumination background as well as the training images. If lightning is not constant, the facial point may be analyzed incorrectly. Execution of partly occluded images that had not been taken in consideration. To control the issue of an unconstrained environmental problem, the facial emotion recognition using Convolution Neural network with modified structure of CNN using fer_2013 dataset. Which improves the facial emotion recognition effectiveness and accuracy.

5. 5. CONCLUSION

As per the above discussion the paper summarized the information evaluation of research equivalent to facial emotion recognition techniques. Facial emotion recognition an inspirational and prime section in biometric applications. The evaluation time, correctness and the presentation of the face detection methods under unconstrained lightning with different postures is a significant concern in the facial expression recognition system. Here, we consider unique designs, viewpoints, techniques, a dataset for training or testing images and presentation calculation of facial emotion recognition technique utilized in every research. Each author carries owned method for detecting a facial emotion from a face database several authors has tried to resolve the issues related to the previously suggested techniques still, and there are few profits and constraints in those analyzed methods. There is a necessity to implement a useful technology for facial emotion recognition that will decrease estimation time and improve effectiveness of prediction of emotions.

6. 6. FUTURE SCOPE

Our future work will establish on the facial emotion recognition which predicts emotions from the image using modified structure of CNN on fer_2013 dataset which consist 28,709 images. Which increase the efficiency of prediction facial emotions from face image.

REFERENCE

[1] S. Happy and A. Routray, “Automatic facial expression recognition using features of salient facial patches,” Affective Computing, IEEE Transactions on, volume 6, number 1, January 2015, pp. 1–12.

[2] Sunil Kumar, M.K.Bhuyan, and Biplab Ketan Chakraborty, “An Efficient Face Model for Facial Expression Recognition”, National Conference on Communication, Guwahati, India, 4-6, March, 2016, pp.1-6.

[3] W. Zheng, “Multi-view facial expression recognition based on group sparse reduced-rank regression,” IEEE Transactions on Affective Computing, volume 5, number 1, 2014, pp.71–85.

[4] J´er´emie Nicolle K´evin Bailly Vincent Rapp Mohamed Chetouani, “Locating Facial Landmarks with Binary Map Cross-Correlations”, IEEE International Conference on Image Processing, Melbourne, VIC, Australia, 15-18 Sept. 2013, pp.2978-2982.

[5] Dipankar Das, M. Moshiul Hoque, Jannatul Ferdousi Ara, Mirza A. F. M Rashidul Hasan, Yoshinori Kobayashi, and Yoshinori Kuno, “Automatic Face Parts Extraction and Facial Expression Recognition”, International Forum on Strategic Technology, Cox’s Bazar, Bangladesh, 21-23, October, 2014, pp. 128-131.

[6] Hongli Zhang, Alireza Jolfaei, And Mamoun Alazab, “A Face Emotion Recognition Method Using Convolutional Neural Network and Image Edge Computing”, Data-Enabled Intelligence for Digital Health, 28, October, 2019, pp. 159081- 159089

[7] E. Batbaatar, M. Li, and K. H. Ryu, “Semantic-emotion neural network for emotion recognition from text”, IEEE Access, vol. 7, 2019, pp. 111866-111878.

[8] Y. Zhang, L. Yan, B. Xie, X. Li, and J. Zhu, “Pupil localization algorithm combining convex area voting and model constraint," Pattern Recognition. Image Anal., vol. 27, no. 4, 2017, pp. 846-854.

[9] H. Meng, N. Bianchi-Berthouze, Y. Deng, J. Cheng, and J. P. Cosmas, “Time-delay neural network for continuous emotional dimension prediction from facial expression sequences,” IEEE Trans. Cybern., vol. 46, no. 4, Apr. 2016 pp. 916-929.

[10] Qirong Mao, Qiyu Rao, Yongbin Yu, and Ming Dong, “Hierarchical Bayesian Theme Models for Multipose Facial Expression Recognition”, IEEE Transactions on Multimedia, Volume 19, Issue 4, 15, November, 2016, pp. 861 – 873.

[11] I.Michael Revina, W.R. Sam Emmanuel “A Survey on Human Face Expression Recognition Techniques”, Journal of King Saud University Computer and Information Sciences, In press, corrected proof Available online, 5, September, 2018, pp. 1-10

[12] S.Anila & Dr. N.Devarajan, “Preprocessing Technique for Face Recognition Applications under Varying Illumination Conditions”, Global Journal of Computer Science and Technology Graphics & Vision, Volume 12, Issue 11, Version 1.0, 2012, pp. 12-18.

[13] Chengeta K., Viriri S., “Image Preprocessing Techniques for Facial Expression Recognition with Canny and Kirsch Edge Detectors”, Lecture Notes in Computer Science, vol 11684, Springer, 09, August, 2019, pp. 85-96.

[14] Divya Meena, Ravi Sharan, “An Approach to Face Detection and Recognition”, IEEE International Conference on Recent Advances and Innovations in Engineering. Jaipur, India, December 23-25, 2016, pp. 1-6.

[15] Celiktutan, Oya, Sezer Ulukaya, and Bülent Sankur, "A Comparative Study of Face Landmarking Techniques", EURASIP Journal on Image and Video Processing, 2013, pp.1-27.

[16] Humid Luann, Mohammed Ouanan, Brahim Aksasse, "Facial landmark localization: Past, present and future", 4th IEEE International Colloquium on Information Science and Technology, Tangier, Morocco, 24-26, October ,2016, pp. 487-493

[17] Naveen Kumar Gondhi Navleen Kour Sidra Effendi Keshav Kaushik, "An Efficient Algorithm for Facial Landmark Detection using Haar-Like Features coupled with Corner Detection following Anthropometric Constraints", International Conference on Telecommunication and Networks, Noida, India, 10-11, August, 2017, pp. 1-6.

[18] T. Patel, "A Survey on Facial Feature Extraction Techniques for Automatic Face Annotation," International Conference on Innovative Mechanisms for Industry Applications, Bangalore, India, 21-23 February,2017, pp. 224–228.

[19] Debaraj Rana, Sunita Dalai, Bhawna, Sujata Minz, N. Prasanna, Tapasri Tapasmita Sahu, "Comparative Analysis of Face Recognition using DCT, DWT and PCA for Rotated faces", International Journal of Scientific Research Engineering & Technology, Volume 3, Issue 5, August 2014, pp. 852-857.

[20] Priyanka Nair, Subha V, "Facial Expression Analysis for Distress Detection", International conference on Electronics, Communication and Aerospace Technology, Coimbatore, India, 29-31, March, 2018, pp. 1652-1655.

[21] S L Happy, and Aurobinda Routray, "Automatic Facial Expression Recognition Using Features of Salient Facial Patches", IEEE Transactions on Affective Computing, Volume 6, Issue 1, January, 2015, pp. 1-12.

[22] Panagiotis Perakis, Georgios Passalis, Theoharis Theoharis, "3D Facial Landmark Detection under Large Yaw and Expression Variations", IEEE Transactions on Pattern Analysis and Machine Intelligence, Volume: 35, Issue: 7, July, 2013, pp. 1552 – 1564.

[23] Q. Xu and N. Zhao, "A Facial Expression Recognition Algorithm based on CNN and LBP Feature," IEEE 4th Information Technology, Networking, Electronic and Automation Control Conference (ITNEC), Chongqing, China, 12-14, June, 2020, pp. 2304-2308.

[24] E. Canbalaban and M. Ö. Efe, "Facial Expression Classification Using Convolutional Neural Network and Real Time Application," International Conference on Computer Science and Engineering (UBMK), Samsun, Turkey, 11-15 September, 2019, pp. 23-27.

[25] A. Mollahosseini, D. Chan and M. H. Mahoor, "Going deeper in facial expression recognition using deep neural networks," IEEE Winter Conference on Applications of Computer Vision (WACV), Lake Placid, NY, USA, 7-10, March, 2016, pp. 1-10.

[26] S. Singh and F. Nasoz, "Facial Expression Recognition with Convolutional Neural Networks," Annual Computing and Communication Workshop and Conference (CCWC), Las Vegas, NV, USA, 2020, pp. 0324-0328.

[27] Mehendale, N., "Facial emotion recognition using convolutional neural networks (FERC)", Springer Nature Applied Science 2, 18, February, 2020, Article number: 446.

[28] Shervin Minaee, Amirali Abdolrashidi, "Deep-Emotion: Facial Expression Recognition Using Attentional Convolutional Network", Computer Vision and Pattern Recognition, 4, February, 2019,

[29] Awais Mahmood,Shariq Hussain ,Khalid Iqbal, and Wail S. Elkilani, "Recognition of Facial Expressions under Varying Conditions Using Dual- Feature Fusion", Mathematical Problems in Engineering, volume 2019, pp. 1-12.

[30] Dong Yoon Choi, Byung Cheol Song, "Facial Micro-Expression Recognition using Two-Dimensional Landmark Feature Maps", IEEE Access, Volume 8, 03, July, 2020, pp. 121549 – 121563.

[31] Xu Xu, Zhou Ruan, Lei Yang, "Facial Expression Recognition Based on Graph Neural Network", International Conference on Image, Vision and Computing, Beijing, China, 10-12, July, 2020, pp. 211-214.

[32] Hajar Chouhayebi,Jamal Riffi, Mohamed Adane Mahraz, Ali Yahyaouy, Hamid Tairi, Nawal Alioua, "Facial expression recognition based on geometric features", International Conference on Intelligent Systems and Computer Vision, Fez, Morocco, 9-11, June, 2020, pp. 1-6.

[33] I. J. Goodfellow et al., "Challenges in representation learning: A report on three machine learning contests," Neural Networks, vol. 64, pp. 59–63, 2015.

[34] R. Gross, I. Matthews, J. Cohn, T. Kanade, and S. Baker, "Multi-pie", IVC, 2010, pp.807 – 813, (2010).

[35] M. Pantic, M. Valstar, R. Rademaker, and L. Maat, "Webbased database for facial expression analysis," in Proceedings of the 2005 IEEE International Conference on Multimedia and Expo, p. 5, Amsterdam, Netherlands, July 2005.

[36] P. Lucey, J. F. Cohn, T. Kanade, J. Saragih, Z. Ambadar, and I. Matthews, "/e extended Cohn-Kanade dataset (CK+): a complete dataset for action unit and emotion-specified expression," IEEE Computer Society Conference on Computer Vision and Pattern Recognition Workshops (CVPRW), pp. 94–101, San Francisco, CA, USA, June 2010.

[37] A. Dhall, R. Goecke, S. Lucey, and T. Gedeon, "Static facial expression analysis in tough conditions: data, evaluation protocol and benchmark," IEEE International Conference on Computer Vision Workshops, pp. 2106–2112, Barcelona, Spain, November 2011.

[38] Caltech Faces (2020) http://www.vision.caltech.edu/html-files/archive.html, Accessed 05 Jan 2020

[39] The CMU multi-pie face database (2020) http://ww1.multip ie.org/, Accessed, 05 Jan 2020

[40] NIST mugshot identification database (2020) https ://www.nist. gov/itl/iad/image -group /resources/biome tricspecial-databases-and-software, Accessed 05 Jan 2020.
[41] The Japanese Female Facial Expression (JAFFE) Database, „„http://www.kasrl. org/jaffe.html", accessed on (2017).
[42] Aneja, Deepali, Alex Colburn, Gary Faigin, Linda Shapiro, and Barbara Mones", Modeling stylized character expressions via deep learning." In Asian Conference on Computer Vision, pp. 136-153. Springer, Cham, 2016.
[43] M. Soleymani, J. Lichtenauer, T. Pun, and M. Pantic, "A multimodal database for affect recognition and implicit tagging," IEEE Transactions on Affective Computing, vol. 3, no. 1, pp. 42-55, 2012.
[44] P. Husák, J. Cech, and J. Matas, "Spotting facial micro-expressions "in the wild"," In 22nd Computer Vision Winter Workshop (Retz). 2017.
[45] N. Sadek, N. Hikal, F. Zaki, "Intelligent Real-Time Facial Expression Recognition from Video Sequence based on Hybrid Feature Tracking Algorithms", 2017.

Energy Aware Load Balanced Multicast Routing in Wireless Sensor Networks

[1] Sreevidya R C, [2] Nagaraja G S

[1] BNM Institute of Technology, Bengaluru, India
[2] R V College of Engineering, Bengaluru, India

Abstract:

Wireless Sensor Network are unusual breed of wireless networks where the sensor nodes are primarily involved in sensing the tasks. Multicast routing refers to the routing scenario which has a single source node and multiple sink nodes. Energy awareness between the sensor nodes and balancing load between the cluster heads and cluster members is proposed in the paper. The life span of the network can be extended by proposed methodology. The data aggregated at the clusters and forwarding of data through the feed node helps in effective utilization of the available energy. The simulation experiment proves that the proposed model is more energy efficient where the nodes are aware of the available energy and balances the load at each node.

Keywords:

Wireless Sensor Network, Multicast routing, Energy aware, Load balancing

1. INTRODUCTION

In current era an efficient design of a Wireless Sensor Network (WSN)[1] has become a leading area of research. By applying signal processing approaches, the current conditions of the surrounding objects and environment of the sensor node can be assessed. Large numbers of sensor nodes have the ability to perform accurate sensing functionalities. WSN have wide applications in the field of imaging, weather monitoring, intrusion detection, tactical surveillance, monitoring ambient conditions such as movement, temperature, light, sound, disaster management, inventory control etc. The deployment of sensor nodes is done in both randomized fashion or it is manually planned. The main performance issue of WSN is its limited node energy supply. Energy awareness in WSN is not just confined in network layer, where energy efficient routing protocols are required, but, it is required in all the layers of WSN.

The OSI model has been predominantly used in WSN architecture. The architectural model discussed incorporates five main layers and three cross layers. Commonly in sensor network five layers includes physical, datalink , network, transport and application. The three cross planes included are power management, task management and mobility management. These layers of the WSN as shown in fig.1 are stated to accomplish the network and make the sensors coordinate in attempt to optimize the network's performance The main performance issue of WSN is its limited node energy supply. The current research in this area has extensively investigated the novel methods to eliminate energy consumption, and prolong the connectivity of the network. Energy awareness in WSN is not just confined in network layer, where energy efficient routing protocols are required, but, it is required in all the layers of WSN

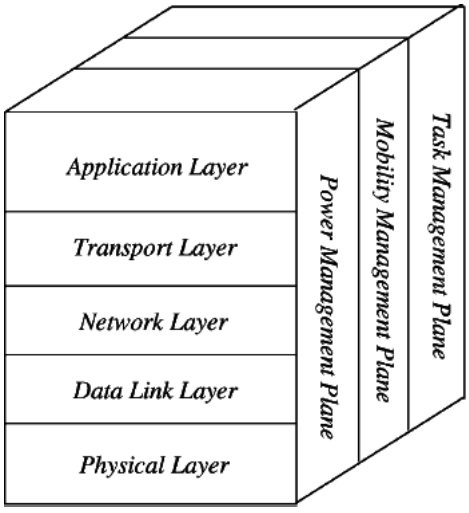

Fig 1: Layered approach

Sensors that are used in WSN are visual, infrared, Low sampling rate, thermal, radar, seismic, magnetic and acoustic sensors to track a wide range of environmental conditions. Sensor nodes will be used for continuous sensing, event identification, event detection, and local actuator control. Environmental, home, health, military, commercial areas are some of the applications in WSN.

2. MULTICAST ROUTING

The use of multicast is fascinating because it allows you to send the same report to multiple sink,, as seen in fig 2.
Incorporation of multicast will lead to reduction of usage of bandwidth in many of the applications listed: data duplication, tasks and commands to a particular group of sensors, queries to different sensors and so on. [6]

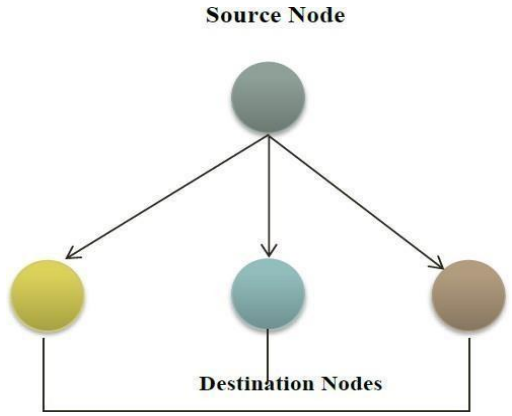

Fig 2: Multicast Routing Scenario

The notion of multicast is premised on the idea of a group. A group of receivers expresses their desire to receive a specific data stream.[2]. Different routing protocols exist where some use techniques like flooding, source based trees or shared tree algorithms. There are many scenarios in which it is necessary to send the same information to a group of sensor nodes when using multicast. Multicast routing can be classified into:

- Tree Based Routing Protocol
- Energy Based Routing Protocol
- Cluster Based Approach
- Steiner Based multicast routing protocols

Cluster based approach- The approach mainly helps in multicast communication.

In cluster Based Approach the energy efficiency is deployed in sensor networks randomly, where cluster head (CH) is in charge of each cluster. The cluster head coordinates with cluster members y receiving messages from other sensor nodes in the cluster and communicates with destination node. The sensor nodes communicate easily with each other and for long communication.

The members of cluster will communicate with each other straight forward without any error, but very long distance communication will involve CH messages. A round is a brief period of time during which clusters are sustained. An election phase and a data transfer phase make up a round. Following the election process, each cluster head is discovered. There is a chance that various node will act as a cluster head [3]. Most of the cluster will pull down the span time of its life but very few will be retained for large number of rounds. As a result of the effective distribution of nodes, the number of head elections is reduced, and the load on long-range transmissions is reduced.

3. RELATED WORK

Energy efficient and scalable routing is performed using multicast routing in Wireless Sensor Network. The structured view of nodes themselves organize into various groups, where each group has a leader. The node with leading energy factor processes and forwards to the sink. Abid Ali Minhas, et al projected the comparison of various routing protocols in perspective of energy efficiency. They compare tree based protocols and cluster based protocols [4].

Weiliang Li, Jianjun Hao work improves the throughput of the network and reduce the control overhead by using Tree-based multicast routing [5]. The multicast communication in wireless sensor networks happen between the sensor devices and several sink nodes. The multicast routing protocols in the Adhoc environment is discussed for load balancing. The protocol ensures high performance and robustness when the network load is increased. The packet delivery ratio is high and low latency with low control overhead is achieved. E.M Belding-Royer, C E Perkins have emphasized on distance vector routing using the multicast approach with dynamic movement of the hosts [6] [7].

The differences can cause changes in the links between any two stations, resulting in an unsustainable moving topological structure. By dynamically inspecting each node, each will be able to perform rerouting in order to forward messages. [8]. Juan A. Sanchez et al. projected GMR [9], A geographic multicast routing protocol. The protocol proposed the neighbor selection through cost approach. It estimates the efficiency by finding the packet delivery ratio and optimization of the tree. The localized algorithm [10] fabricates the multicast tree on the basis of spiral tree, and then considers multicast routing with duplicate routes. The method is quite dense which chooses the direct route with the most of diverted nodes. Qingfeng Huang et al. [11] disusses the concept of space and time complexity in forwarding of message.

4. ENERGY AWARENESS AND LOAD BALANCING

Since the nodes get operated with limited battery power sensor networks are power constrained. Some of the nodes die early due to limited battery and the communication between the nodes is disconnected. Awareness among the nodes should be present where the available energy in the node is utilized efficiently. The routing protocol should distribute the energy evenly over all the available nodes. The overall transmission and receiving power should be minimized. In the sensor network the nodes are constrained by limited energy for their operation. Due to this they have a very short lifetime. Each node consumes a certain amount of energy for transmission and reception of data. If the node consumes more energy the lifespan of the node decreases and leads to the disconnection from the network. The node which consumes more energy gets drained up ending in network disconnection when the communication fails at the end points. If the intermediate nodes suffer from energy constraints the network connection becomes sparser leading to network partitioning. So, each node in the sensor networks participating in the communication should be aware of the energy consumed in transmission and reception process. Each time the node receives an

acknowledgement for the available remaining energy. Based on this the node can stop the additional activities of participating in routing [12] and forwarding process of other nodes data. They participate in their own transmission process of data. The proposed methodology focuses on creating awareness among the nodes in the network through sending acknowledgements about the remaining energy and the number of neighboring nodes in the network. According to the recent works energy awareness in the sensor nodes could be presented in different ways. One such approach would be possible through clustering approach. The sensor nodes are divided into many different clusters and the energy is balanced through the cluster head selection process to extend the network lifetime. One of the best way to extend the network lifetime is through clustering approach which involves transmission of data to the base station through data aggregation and fusion techniques. In the process, the data aggregated and fused through proper techniques reduces the overall energy consumption. The nodes in the cluster are divided into high energy nodes and low energy nodes. The high energy nodes become the cluster heads and collect the data from the other nodes which are the cluster members. The low energy nodes sense the data in the close proximity range.

5. ENERGY MODEL

Any sending node will have four states which they belong to. It can be either in sleep state, idle state, transmit state or receive state. The overall energy can be measured as E.

$$E=IE - (SE + RE + TE) \quad (1)$$
$$=IE – (Sw\ ST + RwRT + TwTT)$$
$$=IE – (Sw(SL/R) + Rw(RL/R) + TwTT)$$

E-Total Energy IE- Initial Energy
R-Data Transfer Rate RT- Receiving Time TT- Ideal Time
Tw-Energy transmitted n watts ST-Sending time
RL- Length of the received packet

The data transmission among the nodes in the network has to be balanced efficiently. In the large scale network energy consumed to perform data transmission can be balanced by employing multihop communication between cluster heads. If the cluster heads are located far away from the base stations they consume more energy in data transmission due to single hop communication. The energy consumption linearly increases as the distance of the transmission increases. So, it is a good communication technique to enhance to multihop process between cluster head nodes so that considerable amount of energy consumption can be reduced. In the process of communication one of the cluster heads can be treated as a feed node where the aggregated data acts as the feed to the next cluster head. The message it carries with it is the available energy and the neighbor node details of its cluster. Based on the distance taken by the feed node to communicate the energy consumption ca be reduced and load balancing can be done in the network. In the process one of the cluster head is chosen as the feed node which can forward the data through. The feed node should have the maximum energy to forward the data and should be nearer to the cluster members.

$$Efeed=\frac{Dist\ (CH->FN)+ No.\ of\ Cluster\ members}{RE} \quad (2)$$

Efeed-Energy at the feed node
Dist(CH->FN)- Distance from cluster head to feed node
RE – Remaining energy

6. SIMULATION

Simulation of the proposed approach was performed on network simulator NS2[13]. Certain parameters were evaluated to observe the performance of the proposed methodology and was compared against the standard benchmark protocol LEACH**.**

Table 1: Simulation Parameter

Parameters	Values
Area of simulation	500X500
Basestation locations	(150,50), (100,100), (130,80)
Initial Energy	2J
Mobility Model	Random
Communication bandwidth	1Mbps
Time of each round	20s
Size of packet	500Bytes
Simulation time	2000s
Traffic Pattern	CBR

7. EXPERIMENTAL ANALYSIS

To evaluate the performance different topology scenarios were considered of varying number of nodes such as 20, 50, 80, and 100. Random point model was used for simulations with CBR traffic generated and multiple sinks. Sinks were placed at different points to analyse four metrics in the trusted environment.

The fig 3 indicates the graph specified for different nodes and the energy consumed at each round. The x-axis indicates the total number of nodes and the y-axis indicates the energy consumption in joules. The graph lines are specified in different colors. The green line indicates the values w.r.t the LEACH and the red line indicates the value of the proposed energy aware and load balanced method (EALB).

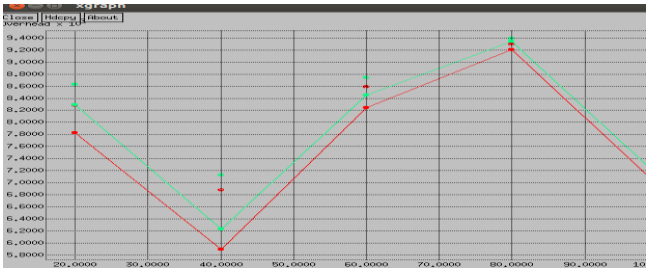

Fig. 3: Energy and Number of Nodes

 ISBN: 978-93-90214-20-4

The fig 4 indicates the graph specified for different nodes and the delay at each round. The x-axis indicates the total number of nodes and the y-axis indicates the delay in ms. The graph lines are specified in different colors. The green line indicates the values w.r.t the LEACH and the red line indicates the value of the proposed energy aware and load balanced method (EALB)

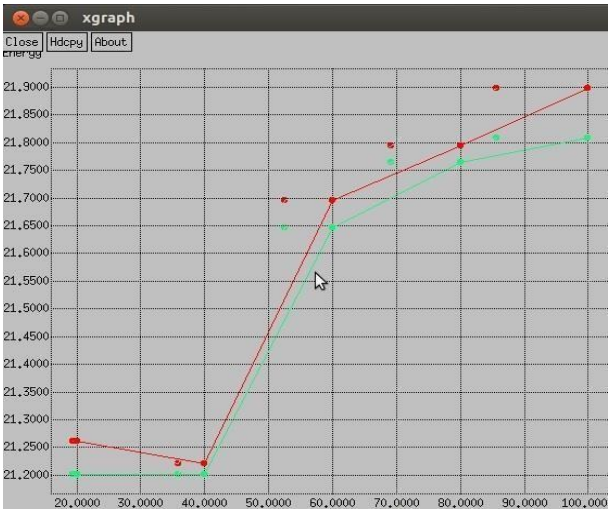

Fig.4: Delay and Number of Nodes

The fig 5 indicates the graph specified for different nodes and the routing overhead at each round. The x-axis indicates the total number of nodes and the y-axis indicates the delay in ms. The graph lines are specified in different colors. The green line indicates the values w.r.t the LEACH and the red line indicates the value of the proposed energy aware and load balanced method (EALB).

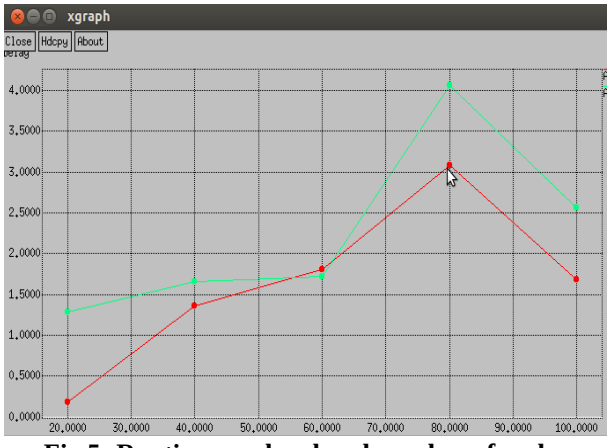

Fig.5: Routing overhead and number of nodes

8. CONCLUSION & FUTURE WORK

Wireless Sensor Network is used in environments where wired networks cannot be deployed and the wired setup is not possible. The WSNs have limited computation and communication resources with limited battery power. Clustering approach helps in data gathering from different nodes and routed further to multiple sinks or base stations. The data aggregation makes use of multi hop technique. The nodes
in the network are made energy aware and load balancing is done at the clusters which increase the lifetime of the network. In the future, energy efficient cooperative communication could be carried out for multicast routing.

REFERENCE

[1] W.Heinselman, A.Chandrakasan and H.Balakrishnan, Energy Efficient Communication Protocol for Wireless Microsensor Networks, Proceedings of the 33rd Hawaii International Conference on System Sciences (HICSS'00), January 2000.

[2] S.Lindsey, C.Raghavendra, PEGASIS: Power Efficient Gathering in Sensor Information Systems, IEEE Aerospace Conference Proceedings, 2002, vol.3, 9-16 pp. 1125-1130.

[3] A.Manjeshwar and D.P. Agarwal, TEEN: a routing protocol for enhanced efficiency in wireless sensor networks, In 1st International Workshop on parallel and Distributed Computing Issues in Wireless Networks and Mobile Computing, April 2001.

[4] Abid Ali Minhas, Fazl-e-Hadi, Danish Sattar, KashifMustaq and S. Ali Rizvi "Energy Efficient Multicast Routing Protocols for Wireless Sensor Networks" IEEE 2011.

[5] Weiliang Li and Jianjun Hao "Research on the Improvement of Multicast Ad Hoc On-demand Distance Vector in MANETS" IEEE Vol.1 2010.

[6] C W Wu and Y C Tay, "AMRIS: A Multicast Protocol for AdHoc Wireless Networks", In Proc. of the IEEE Military Communications Conference (MILCOM-99), Atlantic City, NJ, November 1999. 25–29.

[7] E M Belding-Royer and C E Perkins,"Multicast operation of the ad-hoc on-demand distance vector routing protocol", In Proc. Of ACM/IEEE MOBICOM'99, Seattle, WA, August 1999. 207– 218.

[8] J G Jetcheva, D B Johnson, "Adaptive Demand- Driven Multicast Routing in Multi-Hop Wireless Ad Hoc Networks", In Proc. of ACM MobiHoc'01, Long Beach, CA, October, 2001. 33–44.

[9] Heng Liu, Yan-tao Liu, Ting Yan, "Making On-demand Multicast Routing Protocol Aware of Energy in Wireless Sensor Networks" In Proc of IEEE, 2008.

[10] M.Gerla et al., "On-demand multicast routing protocol (ODMRP) for ad hoc networks". Internet draft, <draft-ietfmanet-odmrp-04.txt>, (2000)

[11] Juan A. Sanchez,Pedro M. Ruiz, and Ivan Stojmenovic, "GMR: Geographic Multicast Routing for Wireless Sensor Networks", IEEE Sensor, Mesh, and Ad Hoc Communications and Networks SECON, Sept. 25-28, 2006, Reston, Virginia, USA.

[12] Chen Y. "Research on multicast routing protocols in sensor networks" [MS. Thesis]. Changsha: Hunan University, 2005.

[13] YU Bin, SUN Bin, WEN Nuan, etc.NS2 And Network Simulation [M].Beijing:Posts & Telecom Press,2007.

Real-Time Face Detection and Recognition Based Attendance System Using Raspberry Pi

[1] Ajay Kumar, [2] Atul Kumar Yadav, [3] Kamini Verma, [4] Pooja Patel, [5] Shweta Tripathi

[1][2][3][4] B.Tech. Final Year, Department of Electronics Engineering, Dr. A.I.T.H. Kanpur, India
[5] Assistant Professor Electronics Engineering, Dr. A.I.T.H. Kanpur, India

Abstract:

Project is designed to detect objects in Real-time and Face Recognition in real-time. It has a record in the database of persons after face recognition as an attendance system. This is a prototype developed for attendance purpose which allows a person in an institute or organization. The idea of the system is that we design an embedded system by using Raspberry pi and Pi-cam for detection of people and recognition of individual and mark the attendance in database. We are using Python language for scripting and Open-CV for image processing in real-time video streaming.

Keywords:

OpenCV, Raspberry Pi, Haar cascade, face_recognition, CNN

1. INTRODUCTION

In this technologically advanced world, taking attendance manually is obsolete which is time taking for both teacher and student. Proxies can be applied easily in manual mode of attendance. By considering these cons of manual attendance, an Automatic attendance system is needed to be developed which takes attendance error-free and secure. Humans have unique faces. Our Attendance system is based on face recognition which recognizes the face and marks the attendance in the database by recognizing unique face ids. Raspberry pi 4 is chosen by us to make it available for all platforms and the pi camera module is also interfaced with the raspberry pi 4. This project uses the modified algorithm of Haar's Cascades proposed by Viola-Jones for face detection and uses LBP histograms for face detection and the face_recognition module based on deep learning is used for face recognition using training data. The System automatically updates attendance in the CSV file after recognizing faces.

2. BLOCK DIAGRAM

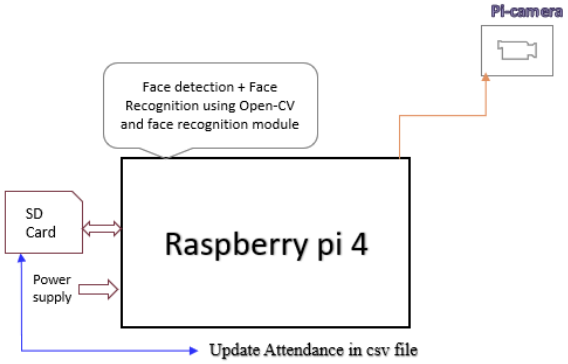

Figure 1 Block diagram of the proposed project

a). Raspberry Pi 4

Raspberry Pi 4 is a Linux based small single-board computer with a 1.5 GHz 64-bit quad-core ARM Cortex-A72 processor, Broadcom Video-Core VI 500 MHz graphics card, onboard Bluetooth, 802.11ac Wi-Fi, Ethernet, two USB 2.0 ports, two USB 3.0 ports,40 GPIO pins, 4GB Ram and a pair of micro 4k HDMI ports. It is widely used in many areas, such as for Robotics, weather monitoring, because of its low-cost device and open open-source. Raspbian operating system is used by us in raspberry pi.

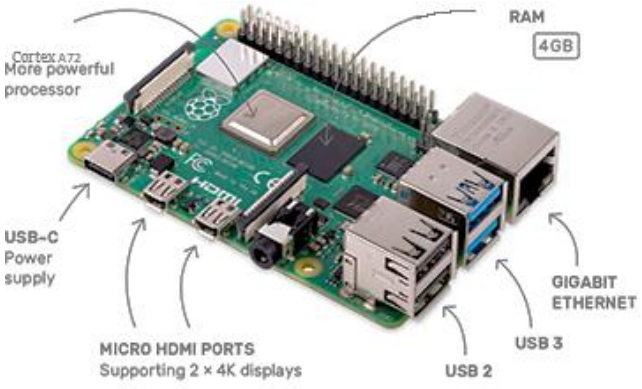

Figure 2 Raspberry pi 4

b). Pi Camera

In Raspberry Pi camera module of 5MP is used by us in this project. It can capture pictures in many formats and video in raw h.264 by using simple Linux commands-

```
sudo raspistill -o image.jpg      //image capture
sudo raspivid -o video.h.264      //video capture
```

 ISBN: 978-93-90214-20-4

c). SD Card
In Raspberry pi, there is no onboard ROM available so SD Card is used to storing the Operating system and other system files. SD cards vary according to their storage capacity. We are using a 32 GB SD card in this proposed project.

d). Power Supply
The 5V - 3 A Power Supply is needed for Raspberry pi to be operated. Type-C cable is used in the power supply.

3. SOFTWARE REQUIREMENT

There is a requirement of the following software- Raspbian Operating system, Open-CV, C-make, dlib, face_recognition, and NumPy library of Python Language. Installation of the Raspbian operating system is simple, firstly we will have to download the OS from the official site of the raspberry pi. Make it bootable in SD Card and mount the SD card into the raspberry pi.

a). Python language-
Python is an open-source interpreted programming language that is easy-to-read and powerful developed Guido van Rossum. We are using the latest version of Python in our Project Python 3.8, download python from the python official website and install it on our raspberry pi or we can use the terminal using the command – sudo apt-get install python3

b). Open-CV
To develop real-time computer vision applications, we can use OpenCV, which is a cross-platform library. Open-CV focuses on image processing, video processing, and analysis including features like face detection and object detection. Object Detection using Haar-cascade-based cascade classifiers is an effective object detection method. Haar cascade classifier is a machine learning-based approach where a cascade function is trained from a lot of positive and negative images. It is then used to detect objects in other images. Installation of Open-CV on a Raspberry Pi 4 takes more than 2 hours and the installation process is provided by the official site of Open-CV.
To install the library, install pip in the system after that follow the steps in the command prompt:
Step 1: pip install opencv-python
Step 2: pip install opencv-contrib-python

c). Haar-Cascade Classifier
Haar Cascade is a classifier that is used to detect the objects for which it is trained from the source. Training data is saved as an XML file. By superimposing the positive image over a set of negative images, Haar Cascade is trained. The training requires a high-speed processor or GPU and thousands of training images. We need a haar cascade frontal face recognizer to detect the face from our pi-camera.

d). Face_recognition module
This module recognizes and manipulates faces from the image by using Python or from the command line. This is the world's simplest face recognition library built with deep learning. This deep learning model has an accuracy of 99.38% on the Labeled Face. Firstly, this module will detect faces in images or videos then encode that faces and after that, it will perform face recognition on test images or real-time video streaming.

e). NumPy
NumPy is the package for scientific computing in Python written in C++ which provides a multidimensional array object other mathematical operation can be performed. In our project, we use this to convert images into the multidimensional array to perform operations like encodings
To install the library following pip command is used -pip install NumPy

4. APPROACH

There are four steps to make the proposed project ready to recognize face and take attendance automatically.
1. Creation of data set
2. Face Detection from the dataset
3. Encode the face data
4. Face Recognition
5. Mark Attendance

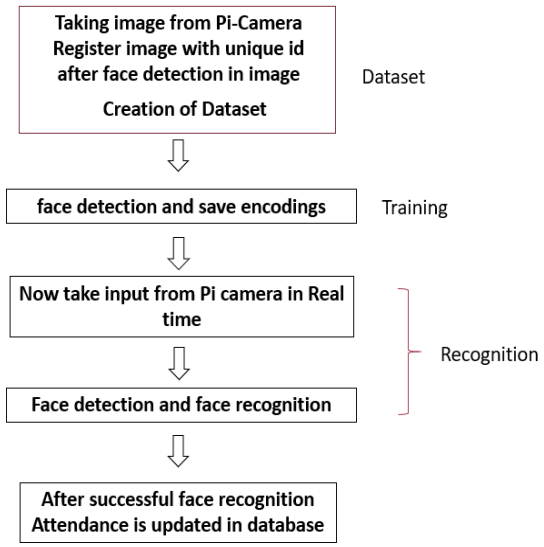

Figure 3 Flaw Chart

Firstly, we have to collect data images of each person and after that detect the face in the image by using Open-CV and face recognition module which encoded each face and save each encoding with face id to perform face recognition. After face recognition, our python script writes the attendance of that person in our database with time and date.

1. Creation of data set

Object Detection using Haar feature-based cascade classifiers is an effective object detection method proposed by Paul Viola and Michael Jones in their paper, "Rapid Object Detection using a Boosted Cascade of Simple Features" in 2001.

OpenCV already contains many pre-trained classifiers for face, eyes, smile, etc. Those XML files can be download from the haar cascades directory.

```
#Import all needed modules
import cv2
import os
camera = cv2.VideoCapture(0)
camera.set(3, 640) # set video width
camera.set(4, 480) # set video height
face_detector=cv2.CascadeClassifier('haarcascade_frontalfa
ce_default.xml')
# For each person, enter one numeric face id
face_id = input('\n enter user name ')
count = 0   # sampling face count

while(True):
   ret, img = camera.read()


          gray=cv2.cvtColor(img,cv2.COLOR_BGR2GRA
Y)
   faces = face_detector.detectMultiScale(gray, 1.3, 5)
   for (x,y,w,h) in faces:
      cv2.rectangle(img, (x,y), (x+w,y+h), (255,0,0), 2)
      count += 1
      # Save the captured image into the datasets folder
      cv2.imwrite("datasets/" + str(face_id) + '.' + str(count)
+ ".png", gray[y:y+h,x:x+w])
   cv2.imshow('image', img)
   k = cv2.waitKey(100) & 0xff
   if k == 27:
      break
   elif count >= 10: # Take face sample and stop video
       break
print("Exiting Program")
camera.release()
cv2.destroyAllWindows()
```

by using the above script, we store face images with their unique id or name of the person. As much as face data is collected in our dataset our model recognizes more people.

2. Face Detection from the dataset

Face Detection performed according to the Dataset with Open-CV and face_recognition module with few lines of python code. Face Detection python code using CNN

```
import face_recognition
image=face_recognition.load_image_file("test.jpg")
face_locations = face_recognition.face_locations(image,
model="cnn")
# face_locations is stored an array which is listing the co-
ordinates of each face.
```

3. Encode face-data

After face detection and we have to encode the faces and save encodings as training data. Encoding is done by the face_encodings function of the face recognition module.

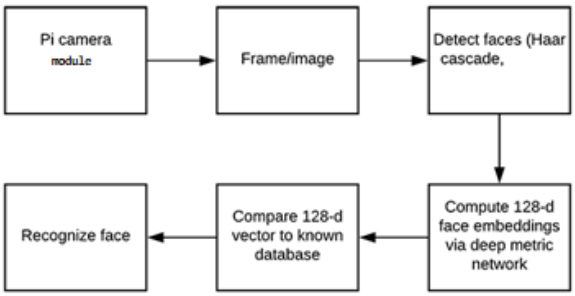

Figure 4 face encoding process

```
test_encoding=face_recognition.face_encodings(img)[0]
unknown_encoding=face_recognition.face_encodings(unkn
own_image)[0]
```

after that we have compare known face which is already in our database and we encode it already and unknown encodings of test image and if comparing result is less than 0.5 then faces are similar otherwise different faces.

4. Face recognition

```
import face_recognition
me=face_recognition.load_image_file("me.jpg")
my_encoding=face_recognition.face_encodings(me)[0]
# my_encoding now contains 'encoding' of facial features
that can be compared to other picture of a face
test=face_recognition.load_image_file("unknown.jpg")
test_encoding=face_recognition.face_encodings(test)[0]
#with compare_faces function we can match two face
encodings are of the same person
results=face_recognition.compare_faces([my_encoding],
test_encoding)
if results[0] == True:
print("Same face")
else:
print("Unknown face!")
```

5. Mark Attendance

If our model detects and recognizes faces that are from our database then our python script writes attendance in a CSV file with the face id attached to the faces, date, and time. Attendance is saved in SD Card which is mounted in Raspberry pi 4.

5. CONCLUSION

Our proposed project “Real-Time Face Detection and Recognition Based Attendance System Using Raspberry Pi”

detects faces in real-time video streaming and takes attendance in the database. This model saves time to take attendance and more secure than the conventional attendance system which takes more time also less secured because a proxy can be entertained. This machine learning model which is implemented in this project was chosen after a lot of research and accuracy of 99.38% on the Labeled Face of this deep learning-based face recognition module.

6. ACKNOWLEDGMENT

All the authors would like to thank Shweta Tripathi, Assistant Professor of Electronics Engineering, for technical support during this project.

7. FUTURE SCOPE

This project can be utilized for many applications such as security systems, facial lock systems, gender recognition, and criminal identification. Tracing a specific person is also done by this type of project. Another variant of this project can be used in home security and organizational security.

REFERENCE

[1] Viola, P., & Jones, M. (2001). Rapid object detection using a boosted cascade of simple features. In Computer Vision and Pattern Recognition, 2001. CVPR 2001. Proceedings of the 2001 IEEE Computer Society Conference on (Vol. 1, pp. I-511). IEEE.

[2] Priya Pasumarti, P.Purna Sekhar "Classroom Attendance Using Face Detection and Raspberry-Pi" International Research Journal of Engineering and Technology (IRJET).

[3] NirmalyaKar, MrinalKantiDebbarma, AshimSaha, and DwijenRudra Pal, "Implementation of Automated Attendance System using Face Recognition", International Journal of Computer and Communication Engineering, Vol. 1, No. 2, July 2012.

[4] Arjun Raj, Mahammed Shoheb, Arvind K, Chethan K S, "Face Recognition Based Smart Attendance System" ECE, PES University, Bangalore, INDIA

[5] Evta Indra, Muhammad Yasir, Andrian, Delima Sitanggang, Oloan Sihombing, Saut Parsoran Tamba "Design and Implementation of Student Attendance System Based on Face Recognition by Haar-Like Features Methods" Faculty of Technology and Computer Science Universitas Prima Indonesia, Medan, Indonesia *evtaindra@unprimdn.ac.id

[6] P. Lad and S. More, "Student Attendance System Using Iris Detection," no. 2, pp. 3293–3298, 2017.

[7] AparnaBehara, M.V.Raghunadh, "Real-time Face Recognition System for time and attendance applications", International Journal of Electrical, Electronic, and Data Communication, ISSN 2320-2084, Volume-1, Issue-4.

Automatic Covid-19 Assistance Smart Library

[1] Piyush Chaurasia, [2] Mona Savita, [3] Rahul, [4] Abhishek Singh, [5] Shweta Tripathi

[1][2][3][4][5] Department of Electronics Engineering, Dr. Ambedkar Institute of Technology for Handicapped, Kanpur, Uttar Pradesh, India

Abstract:

The covid-19 (coronavirus) has a deep impact on the lives of people around the world. Coronavirus spreads more rapidly when people are in close contact with each other. To contain the spread of coronavirus there some safety measures like maintaining social distancing, wearing masks, sanitization, etc. are very important. Therefore, we are making an Automatic covid-19 Assistance Smart library system in our college library. This smart library system helps the student, teachers, and staff to maintain social distancing and prevent them from the coronavirus disease.

This smart library system replaces the previous method of transaction of the books in the library. There is no need to do any paperwork all the information fetch by the smart card. Librarians can also send notice to the students regarding their dues and late fees through E-mail. Therefore, the whole management system will design using Arduino Microcontroller, Raspberry pi 3, and Temperature sensor. From this project, we want to provide a safe system to access the library.

Keywords:

Face mask detector, Smart library, Raspberry pi 3, Arduino Uno, Temperature sensor

1. INTRODUCTION

Wearing a mask and use of the sanitizer is necessary and helpful to contain the spread of coronavirus[1]. It is very important to wear a mask in public places, schools, colleges, etc. The use of technology has been increased in the covid-19 pandemic as it plays a vital role in doing the work of the school, colleges, offices, etc[2]. Most of the manual work is slowly shifted to digital technology. The traditional library system has a lot of handwritten work to do which is time taking process and the contamination of the coronavirus will also be there. The smart library system is useful to contain the spread of the coronavirus inside the library and it is also providing students a better way to do the transaction of the books in a very little time[3]. The system is also limiting the number of students allowed inside the library which helps maintain the social distancing. The use of the Raspberry pi 3 and Arduino breaks the traditional role of using the library and gives an easy and efficient way to use the library[4]. The main purpose of the Automatic Covid-19 Assistance Smart Library is to provide the services of the library without human intervention. To implement the Automatic Covid-19 Assistance Smart Library we are using the Raspberry pi 3 for the mask detection and temperature sensor at the entrance of the library[4], there is a temperature sensor and mask detector, if a person has a temperature within the set limit and wears a mask then only the gate will open otherwise it will not open. Before entering the library, the individual goes through the sanitization process**.** Inside the library, there is an ATM-like module based on an Arduino microcontroller interface with a four-button system, and each button is made for specific work like borrow, return, reissue, and account details. Each student has their unique QR code card which is to be scan after that student can access the library and do the transaction of the books[3]. All the data of the student are stored in the database and the system will send the message regarding transaction by email and Whatsapp API[5][6][7]. It provides a graphical user interface for the library administrator that eases the management of the library system[8]. Administrator can easily register students, books using a QR code.

2. RELATED WORK

A. Door safety system

In this system, we are using three modules which are described as:

1- Contactless temperature sensor: non-contact temperature sensor used to measure body temperature. For that purpose, we are using an infrared-based MLX90614 temperature sensor. This temperature sensor works on the principle of IR thermopile sensor and Stefan-Boltzmann law[9]. It converts the computation value into 17-bit "ADC that can be accessed using I2C communication protocol. Importing Adafrut_MLX90614 to read the temperature sensor"[12]. The temperature sensor measures the ambient temperature as well as object temperature.

Ambient temperature value varies from -40 to 125 degree Celsius

Object temperature value varies from -70 to 382 degree Celsius

2- For the implementation of face mask detection firstly, we have used the Haar Cascade file with mouth and eyes classifier. Haar Cascade classifier accepts the face with lips and eyes it shows not wears a mask and if it can not detect lips it shows person wear a mask whether or not he is wearing a mask[3] then we are using TensorFlow. It is divided into two phases.

Train face mask detection

Apply face mask detection
We load the face mask detection dataset from disk and train the face mask classifier using Keras and TensorFlow[10] which automatically detect whether a person is using a mask or not.
When face mask detection is trained, we load face mask classifier from disk and detect face in imagination stream and interact face region of interest and then we apply face mask classifier to each face ROI to determine mask or not mask then show result as shown in Figure 1.

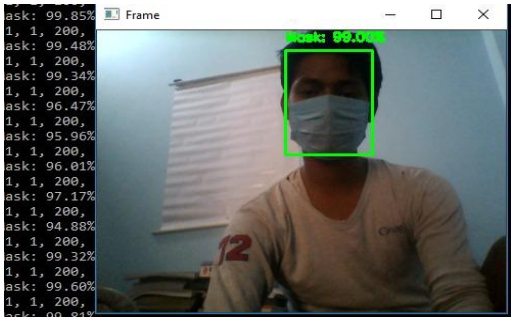

Figure 1. Mask detection

B. Library Management System

The smart library management system facilitates the ease of using a manual library system. Mostly the student search the book and fill up the all requirement in paper manually. But to avoid the manual system we are introducing a smart library system which works smartly. Like if the user wants to issue the book then he will not have to do anything manually like fill up the card and share the information with the librarian he will have to use a keypad for different purposes.
The user will go to the system counter and then he should identify himself by his identity card. To identify himself he must scan their identity card and then he will give a command to the system using a keypad.
Student can scan their smart card which has a QR code for the transaction of the books. QR code is scanned through the system camera, Pyzbar library of python and OpenCV library is used to read the QR code. We use the decode function to decode the data of the QR code and once the QR code is scanned all the details of the student will be shown on the LCD.

```
import cv2
from pyzbar.pyzbar import decode
cap = cv2.VideoCapture(0)
cap.set(3, 640)
cap.set(4, 480)
while True:
  success, img = cap.read()
  for barcode in decode(img):
      myData = barcode.data.decode('utf-8')
      print(myData)
      print('Scanned')
  cv2.imshow('Result', img)
```

Figure 2. QR code scan

1) Book Issue:

The user must be scan their id card until it detects and recognized their account. If the user is not a registered member then he can not access the library. After scanning the card the user can access their account There will be a 4×4 keypad, the user will press key one to issue the book after that the system will search in the database that how many books he has already issue if there will be a 3 book issued then it will deny the request. if there will be fewer than 3 books then the user will scan the QR code of the book and then the book will be added to his account after issued the book user gets the WhatsApp message and email which gives the details of their account transaction.

2) Book Return:

For Book returning process the user must be scan their id card and then there will be four options in which the Book return option was there. then the user will press key two for returning the book after that user should scan the QR code of the book and system will decode the QR code and it will search in the database if the data was found in the database then it will remove from their account and then print book returned. the user will get the Whatsapp message and email regarding their account transaction it will show in a message that the book has returned successfully.

3) Book Reissue:

If the user issues the book from the library, then he must be resued within a time limit. There are time limits to take the book if the book time limit will complete. The user should reissue the book if the user will not reissue the book within the time limit then he will be charged for late reissue of the book which is decided by the librarian. If the book time limit is exceeded then the user will get the message for reissue the book.
To reissue the book user must scan their id card and then it can access the keypad to reissue the book user will press key three and then scan the QR code of the book .then system will decode the QR code and update the issue date and provide a new issue date if the book was late then it counts the date and add to the penalty charge after this process the user will again get a message on their phone.

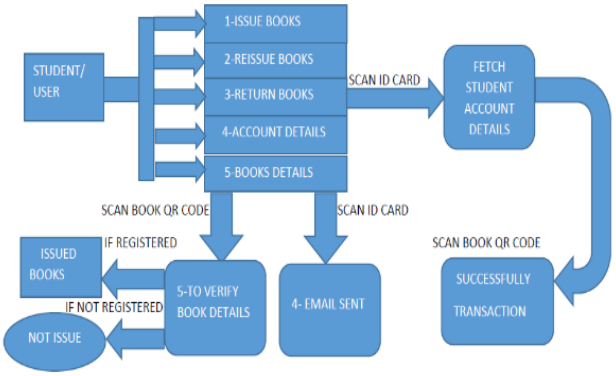

Figure 3. Block diagram of user module

3. HARDWARE IMPLEMENTATION

The smart library system is designed in such a way that before entering the library a person has to go through several processes which are made keeping in mind all the safety measures that should be followed to contain the spread of the coronavirus. Students are authorized to enter the library only when they are checked by the mask detector and temperature sensor at the entrance of the library. A mask detector of 5 MP camera Omni vision 0v5647 is used to detect the student whether the student wears a mask or not with an accuracy of 99%. Mask detector is designed on the raspberry pi 3 by the use of python language and tensor flow library is used to implement it[11].

Besides this the body temperature of the student will also be checked by the temperature sensor MLX90614 non-contact infrared temperature sensor is used to measure the temperature of the student. "Temperature sensor has a 1.2 to 2.6 µm sensitivity, extended InGaAs sensor, compact size 1.5" dia × 2.5", 2-stage thermo-electric cooling and 0.5,1.0 &2.0mm dia"[12]. TMP006 python library is used for the temperature sensor by using Raspberry pi 3. Both mask detector and temperature sensor are implemented by using the raspberry pi 3. If the student wears a mask and has a normal body temperature, then the gate will open, and the student is allowed to enter and at the same time, the sanitizer spray opens for the 5sec to sanitize the body of the student. Sanitizer spray is also operated by the Raspberry pi 3.

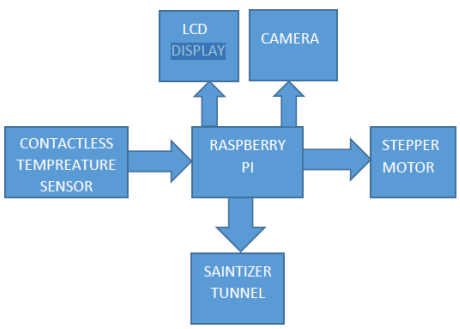

Figure 4. Block diagram of smart door safety system

The keypad relates to Arduino Uno by using the keypad.h library. The data is sent to the system from the Arduino Uno through the Bluetooth module.

For read and write of the data from the serial port, we establish the connection by pyserial module of python.

Code for establish the connection:
a = serial. Serial("COM4",9600)

Code for writing the data on port:
a.write (n.encode ())

Code for reading the data:
a.read line().decode("ASCII")

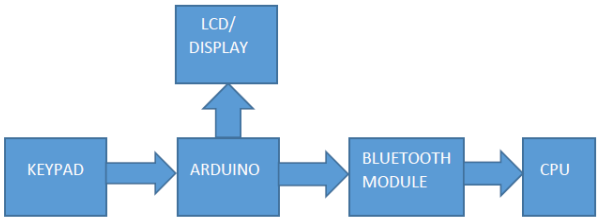

Figure 5. Block diagram of smart library management

4. SOFTWARE

Message – for sending messages by e-mail and WhatsApp.
By e-mail: we send the message by using smtplib library of python on the registered ID of the student[7].

```
import smtplib as s
def Mail(sender,password,receiver,massage):
    ob=s.SMTP("smtp.gmail.com",587)
    ob.starttls()
    print('Sending mail')
    ob.login(sender,password)
    ob.sendmail(sender,receiver,massage)
```

By WhatsApp: we send the message by using twilio.rest library of python using API[6].

```
from twilio.rest import Client

account_sid = '********'
auth_token = '**********'
client = Client(account_sid, auth_token)
message = client.messages.create(
                    from_='whatsapp:+14155238886',
body='Hi this whatsapp bot for automatic massaging in Smart-library-by Smart library project  ',
to=******)
```

A. Database management

for storing data and managing library work we use the mysql.server. To establish a connection with the MYSQL database we use mysql.connector library.

"import mysql.connector"

 ISBN: 978-93-90214-20-4

Connector = mysql.connector.connector(host = 'local host', user = 'root', password = "**********")

B. GUI for the library management

we develop GUI of the library management using the Tkinter library of python, PIL library for importing images. We use the Tkinter library for developing heading, entries, frame of the text area and the photo of the student is also on GUI. Fetching the data of the entries from the database and show the text field by SQL language.

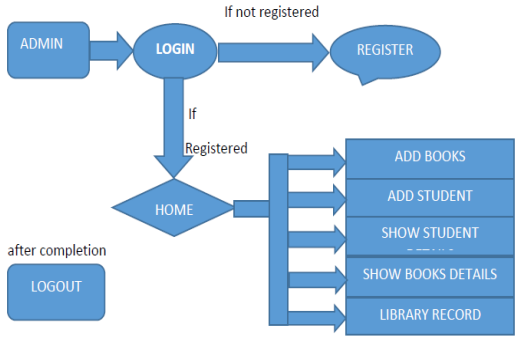

Figure 6. Block diagram of admin module

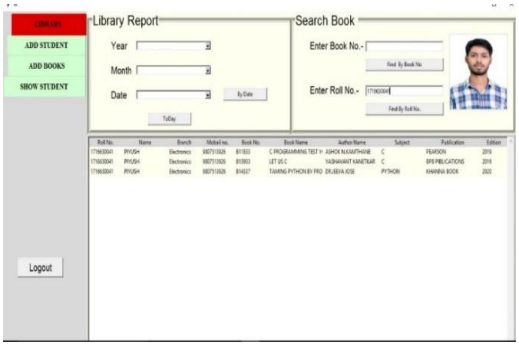

Figure 7. GUI window after issue book

5. CONCLUSION

The Automatic Covid-19 Assistance Smart Library can be made operational in the pandemic situation. Smart Library provides the students a self-transaction facility of books which avoids long queues at the counter. In this paper, we have taken a limited database of mask and unmasked faces to detect the mask of students, and future we can do the work with a large-scale database to detect more variable faces.

6. ACKNOWLEDGMENT

The authors would like to express their deep sense of gratitude to the Department of Electronics Engineering Dr. Ambedkar Institute of Technology for Handicapped, Kanpur, Uttar Pradesh.

REFERENCE

[1] G. Deore, R. Bodhula, V. Udpikar, and V. More, "Study of masked face detection approach in video analytics," in *2016 Conference on Advances in Signal Processing (CASP)*, 2016, pp. 196–200.

[2] V. C.-C. Cheng *et al.*, "The role of community-wide wearing of face mask for control of coronavirus disease 2019 (COVID-19) epidemic due to SARS-CoV-2," *J. Infect.*, vol. 81, no. 1, pp. 107–114, 2020.

[3] D. Bagal and P. Saindane, "Librany-A Face Recognition and QR Code Technology based Smart Library System," in *2019 International Conference on Communication and Electronics Systems (ICCES)*, 2019, pp. 253–258.

[4] N. Petrović and Đ. Kocić, "IoT-based System for COVID-19 Indoor Safety Monitoring," *Prepr. IcETRAN*, vol. 2020, pp. 1–6, 2020.

[5] E. Dynomant, M. Gorieu, H. Perrin, M. Denorme, F. Pichon, and A. Desfeux, "MEDOC: a Python wrapper to load MEDLINE into a local MySQL database," *arXiv Prepr. arXiv1710.06590*, 2017.

[6] S. Jain, S. Sharma, and R. Tomar, "Integration of Wit API with Python Coded Terminal Bot," in *Emerging Technologies in Data Mining and Information Security*, Springer, 2019, pp. 397–406.

[7] J. Goerzen, "Simple Message Transport Protocol," in *Foundations of Python Network Programming*, Springer, 2004, pp. 197–210.

[8] K. Yuvaraj, G. M. Oorappan, K. K. Megavarthini, M. C. Pravin, R. Adharsh, and M. A. Kumaran, "Design And Development Of An Application For Database Maintenance In Inventory Management System Using Tkinter And Sqlite Platform," in *IOP Conference Series: Materials Science and Engineering*, 2020, vol. 995, no. 1, p. 12012.

[9] S. Costanzo and A. Flores, "A Non-Contact Integrated Body-Ambient Temperature Sensors Platform to Contrast COVID-19," *Electronics*, vol. 9, no. 10, p. 1658, 2020.

[10] A. Das, M. W. Ansari, and R. Basak, "Covid-19 Face Mask Detection Using TensorFlow, Keras and OpenCV," in *2020 IEEE 17th India Council International Conference (INDICON)*, 2020, pp. 1–5.

[11] D. S. J. Kumaresan, S. Shameem, M. Priyadharshini, M. James, and R. L. Priya, "Real time object detection using Image Processing," *Eur. J. Mol. Clin. Med.*, vol. 7, no. 4, pp. 2403–2411, 2020.

[12] Adafrut_MLX90614 to read the temperature sensor. https://circuitdigest.com/microcontroller-projects/iot-based-contactless-body-temperature-monitoring-using-raspberry-pi-with-camera-and-email-alert#:~:text=MLX90614%20sensor%20converts%20the%20computational,calibration%20of%200.02%C2%B0C

Designing and Analysing A Petri Net Model of A Small Eatery In Times Of Covid

[1] Ridhi Bakshi, [2] Srishti Patel, [3] Sangita Kansal

[1][2][3] Delhi Technological University, Delhi, India

Abstract:

The notion of Petri Net, formerly developed by Carl Adam Petri, is useful for modeling and analyzing a system's behavior. Petri Net is a graphical tool, defined as a bipartite graph consisting of two types of nodes, places (conditions) and transitions (activities). In general, a discrete event dynamic system consists of activities that can model the system by consecutively listing its states; prior and after to the occurrence of these activities.

In this paper, a Petri Net model for a small eatery has been proposed, keeping in view the spread of the COVID-19 virus. Emphasis has been given to practicing social distancing and allowing a minimum number of people together at any stage. This model, which accounts for two service tables (which can be occupied by new customers subsequently) and one service provider (waiter) and their respective activities, has been interpreted as a dynamic system. Furthermore, the model's design has been validated structurally and behaviorally using techniques from Linear Algebra, transitive matrices, and transition vectors. The reachability tree has been made for drawing out more behavioral conclusions. Besides, inference of properties like cyclic/acyclic nature, conflict, concurrency, boundedness, conservativeness, safeness, liveness, and deadlock has been interpreted physically with the proposed model.

Keywords:

Petri Net (PN), Transition vectors, Eatery model, Structural Analysis, Behavioral Analysis

1. INTRODUCTION

One of the eminent mathematical graphical tools used for modeling discrete event dynamic systems is a *Petri Net* (PN); formally defined as a bipartite graph consisting of two types of nodes, the *places*, and the *transitions*. The *places* refer to a certain set of conditions that are to be satisfied and are denoted using a circle ○. The other set of nodes, or, the *transitions* are the events or activities that occur and lead to the change in the state of the system. These are denoted using a vertical line | or a rectangular bar. These places and transitions are connected via *directed edges* or *arcs*. Present in a system are some basic entities called *tokens* which get created and destroyed in the places (conditions) and can travel in a system under certain parameters that can change the state of the system. This shall be discussed in subsequent sections. The preliminaries of Petri Nets [5]-[7] have been discussed in Section II.

2. PETRI NETS: BASIC DEFINITONS AND RULES

A. Structure of Petri Net

A Petri Net structure is composed of four parts, written as a 4- tuple. It is represented as *PN= (P, T, I, O),* where *P* is the set of all places; *T* is the set of all transitions; *I* is the matrix that explains the association of input places and the transitions; and *O* is the matrix that explains the association of output places and the transitions. For a PN consisting of say, m-places and n- transitions where $P=\{p_1, p_2, \dots, p_m\}$ and $T=\{t_1, t_2, \dots, t_n\}$, matrices *I* and *O* can have the values a_{ij} which can take the value either 0 or 1 such that:

$a_{ij}=$ 1, p_i is an input (output) place for transition t_j. 0, p_i is not an input (output) place for transition t_j. *Remark:* The set of places and the set of transitions are disjoint; i.e., $P \cap T = \emptyset$. We sometimes refer to functions instead of matrices, where the *input function* can be defined as $I: T \to P^\infty$ and the *output function* is defined as $O: T \to P^\infty$ where *T r*epresents the set of transitions and P^∞ denotes the bag[1] of the places.

B. Marking of Petri Net

A *marking* of a Petri Net PN, at a certain given state *t* is the assignment of the tokens to the set of places. It is denoted by $M_t = \{M_1, M_2, \dots, M_m\}$ where M_i gives the number of tokens that are available at the place p_i at a certain state *t*. A marking *M* is a function defined from *P*, the set of all places to the non-negative integers i.e., $M: P \to Z^+$, where clearly, $M(p_i) = M_i$. The marking at initial state (at t=0) is called the *initial marking* $M_0: P \to Z^+$. A *marked Petri Net PN* w.r.t M_0 is a 5-tuple structure where *PN= (P, T, I, O,*M_0*).*

C. Transition enabling and firing

Any transition, say t_j in a system, is *enabled* and can *fire* with one or multiple input places; if the number of tokens in all the input places is at least equal to the multiplicity of all the input arcs for t_j of those places respectively. We also call this the *triggering* of t_j. When t_j in a system triggers, a token gets deleted from its input places and eventually gets created in the respective output places,

[1] A *bag* is a collection of elements from a certain predefined domain which allows multiple existence of elements, unlike that in sets. [6]

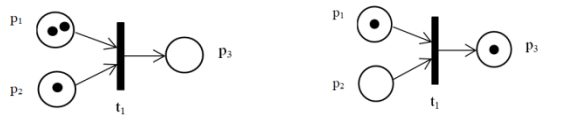

(a) (b)

Fig. 1 (a) Before firing of t_j. (b) After firing of t_j.

i.e., a transition *t* in a *marked Petri Net* having marking *M* gets enabled to fire, if for all $p_i \in P$*(i=1* to *m)*, $M(p_i) \geq \#(p_i, I(t_j))$.

3. TRANSITIVE MATRIX AND TRANSITION VECTORS

The *incidence matrix* (composite change matrix) [6] evaluated as *D=O-I*, is used in linear algebra techniques to understand the dynamic behavior of a system. However, the analysis of a Petri Net using this technique is meaningful only when the rank of *D* is full. The concept of the *transitive matrix* [4] gives better analytical results. The labeled place (transition)-transitive matrix is defined as $L_{BP} = I^t.D_t.O$, where D_t is the diagonal-transition matrix for T=$\{t_1, t_2, \ldots, t_n\}$ and *I*, *O* are the *input* and *output matrices* respectively. The entry in the i^{th} row and j^{th} column of labeled place transitive matrix ($L_{BP}[i,j] = t_k$) denotes a transitive relation from the input place p_i to the output place p_j by firing the transition t_k. L_{BP} fails to include all source/sink transitions and thus, limits the analysis to Petri Nets without source/sink transitions. The *transition vectors*, T_R and T_C, and results based on it, as suggested in [2], have been used to overcome this ambiguous situation. The i^{th}components of T_R and T_C give the set of input and output transitions of p_i, respectively. These components of the transition vectors are a finite linear combination of $t_k \in T$*(k=1, 2,…, n)* with positive integer coefficients.

4. A PETRI NET MODEL OF A SMALL EATERY

Given the spread of the COVID-19 virus, social distancing is the need of the hour. In this paper, designed and proposed is a small eatery model that is supposed to provide service to its customers while practicing social distancing and allowing a minimum number of people together at any possible stage. Thus, this proposed model of a small eatery that originally had four tables has revised the seating plan to provide service at two alternate tables while taking all necessary precautions against the virus and ensuring social distancing. Further, for the arrival of any new customer at the eatery, two separate waiting places have been marked, which shall eventually pave the way to the respective table (either first or second). The model has been designed such that the new customers cannot occupy the tables unless the previous customers who are seated on the tables eat and vacate. Also, the seated customer shall place the order once. It is assumed and supposed that the customer at the waiting place cannot shift to the other waiting place w.r.t the other table. Fig. 2 shows the Petri net structure of the proposed model where $P = \{p_1, p_2, p_3, p_4, p_5, p_6, p_7, p_8, p_9, p_{10}\}$ and $T = \{t_1, t_2, t_3, t_4, t_5, t_6, t_7\}$ are the places (conditions) and transitions (events) respectively.

The presence of a token at a place denotes the condition to be true; while the absence of a token means that the condition corresponding to a place is not true (or is not happening). A prior assumption for this hypothesis is that when the first two customers arrive, a token is created at the places p_1 and p_3 respectively, and another token is created at the place p_2 signifying the availability of the service provider (waiter).

Table 1. (a) Depiction of places (conditions) of the proposed model. (b) Depiction of transitions (activities) of the proposed model.

PLACES	CONDITIONS
p_1	Customer is seated at sanitized first table and is then ready to place the order.
p_2	The service provider (waiter) is free and can provide service to the customer at either table.
p_3	Customer is seated at sanitized second table and is then ready to place the order.
p_4	The customer at first table is waiting for the food to be served.
p_5	The order is finalized by the service provider (waiter).
p_6	The customer at second table is waiting for the food to be served.
p_7	The customer at first table eats and vacates the place.
p_8	The customer at second table eats and vacates the place.
p_9	A new customer has arrived to occupy the first table.
p_{10}	A new customer has arrived to occupy the second table.

(a)

TRANSITIONS	ACTIVITIES
t_1	The service provider (waiter) takes orders from the customer at first table.
t_2	The service provider (waiter) takes orders from the customer at second table.
t_3	The service provider (waiter) serves the order to the customer at first table.
t_4	The service provider (waiter) reports the order in the kitchen.
t_5	The service provider (waiter) serves the order to the customer at second table.
t_6	First Table is sanitized and a menu card is placed.
t_7	Second Table is sanitized and a menu card is placed.

(b)

 ISBN: 978-93-90214-20-4

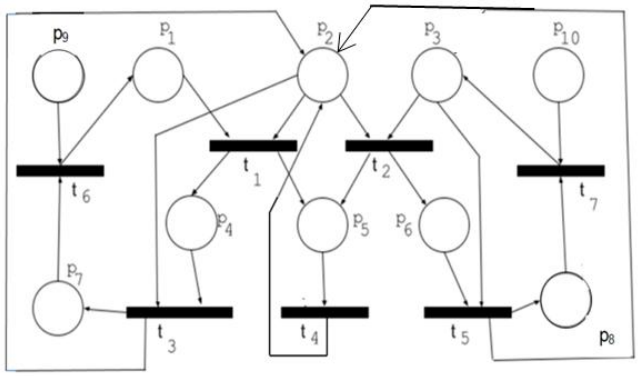

Fig .2 Petri Net graph of the proposed model.

Thereafter, whenever the new customer arrives, it is denoted in the model by the creation of a token at p_9 and p_{10} for the first and second table respectively.

5. ANALYSIS AND INTERPRETATION OF THE MODEL

A. Structural Analysis

- *Conservation Property [6]:* A Petri Net *PN= (P, T, I, O)* with an initial marking M_0 is said to be *conservative* if for all $M^+ \in R\ (PN,M_0)$,

$\sum_{p_i \in P} M^+(p_i) = \sum_{p_i \in P} M_0(p_i)$ *(1)*

where, the reachability set $R\ (PN,M_0)$ for a Petri Net *PN* with the initial marking M_0 is the smallest set of markings defined as:

1) $M^+ \in R\ (PN,M_0)$

2) If $M^+ \in R\ (PN,M_0)$ and M^{++} is immediately reachable from M^+, then $M^{++} \in R\ (PN,M_0)$.

Thus by conservation, we mean conservation of the tokens in place i.e., the token count for all the places at any state remains constant.

A Petri Net is *structurally conservative (partially)* [5] if there exists a positive (non-negative) vector w such that

$D.w=0$, where $w \geq 0$ *(2)*

In order to find the incidence matrix, *D*, we calculate the input matrix *I*, and the output matrix *O* for the proposed model in Fig. 2; as follows,

$$I = \begin{bmatrix} 1&1&0&0&0&0&0&0&0&0 \\ 0&1&1&0&0&0&0&0&0&0 \\ 0&1&0&1&0&0&0&0&0&0 \\ 0&0&0&0&1&0&0&0&0&0 \\ 0&1&0&0&0&1&0&0&0&0 \\ 0&0&0&0&0&0&1&0&1&0 \\ 0&0&0&0&0&0&0&1&0&1 \end{bmatrix}$$

$$O = \begin{bmatrix} 0&0&0&1&1&0&0&0&0&0 \\ 0&0&0&0&1&1&0&0&0&0 \\ 0&1&0&0&0&0&1&0&0&0 \\ 0&1&0&0&0&0&0&0&0&0 \\ 0&1&0&0&0&0&0&1&0&0 \\ 1&0&0&0&0&0&0&0&0&0 \\ 0&0&1&0&0&0&0&0&0&0 \end{bmatrix}$$

The incidence matrix $D=O-I$ is given by,

$$D = \begin{bmatrix} -1&-1&0&1&1&0&0&0&0&0 \\ 0&-1&-1&0&1&1&0&0&0&0 \\ 0&0&0&-1&0&0&1&0&0&0 \\ 0&1&0&0&-1&0&0&0&0&0 \\ 0&0&0&0&0&-1&0&1&0&0 \\ 1&0&0&0&0&0&-1&0&-1&0 \\ 0&0&1&0&0&0&0&-1&0&-1 \end{bmatrix}$$

System of equations for (2) is given by,

$-w_1 - w_2 + w_4 + w_5 = 0$

$-w_2 - w_3 + w_5 + w_6 = 0$

$-w_4 + w_7 = 0$

$w_2 - w_5 = 0$

$-w_6 + w_8 = 0$

$w_1 - w_7 - w_9 = 0$

$w_3 - w_8 - w_{10} = 0$

Solving these equations, we get a solution,

$$w = \begin{bmatrix} w_1 \\ w_2 \\ w_3 \\ w_4 \\ w_5 \\ w_6 \\ w_7 \\ w_8 \\ w_9 \\ w_{10} \end{bmatrix} = \begin{bmatrix} 1 \\ 2 \\ 3 \\ 1 \\ 2 \\ 3 \\ 1 \\ 3 \\ 0 \\ 0 \end{bmatrix}$$

The existence of a non-negative vector *w* such that $D.w=0$ implies that the Petri Net model is *partially conservative*. This suggests that the Petri Net might be conservative w.r.t some initial marking and might not be conservative w.r.t some other initial marking. Hence the token count may vary after certain stages. This is further elaborated in the proposed model in subsequent section.[2]

For studying properties like conflict, concurrency, self-loop, state machine, cyclic/acyclic nature [3], [5]-[7], we compute the transitive matrix [4] and transition vectors [2] for the proposed model.

The Labeled Place-Transitive matrix is given by,

$$L_{bp} = \begin{bmatrix} 0&0&0&t_1&t_1&0&0&0&0&0 \\ 0&t_3+t_5&0&t_1&t_1+t_2&t_2&t_3&t_5&0&0 \\ 0&0&0&0&t_2&t_2&0&0&0&0 \\ 0&t_3&0&0&0&0&t_3&0&0&0 \\ 0&t_4&0&0&0&0&0&0&0&0 \\ 0&t_5&0&0&0&0&0&t_5&0&0 \\ t_6&0&0&0&0&0&0&0&0&0 \\ 0&0&t_7&0&0&0&0&0&0&0 \\ t_6&0&0&0&0&0&0&0&0&0 \\ 0&0&t_7&0&0&0&0&0&0&0 \end{bmatrix}$$

The row-transition vector corresponding to the above labeled Place-Transitive matrix is given by,

$$T_R = [2t_6 \quad 2t_3 + t_4 + 2t_5 \quad 2t_7 \quad 2t_1 \quad 2t_1 + 2t_2 \quad 2t_2 \quad 2t_3 \quad 2t_5 \quad 0 \quad 0] \quad (3)$$

[2] Elaborate discussion on Page number 6.

and the column transition vector is given by,

$$T_C = [2t_1 \;\; 2t_1 + 2t_2 + 2t_3 + 2t_5 \;\; 2t_2 \;\; 2t_3 \;\; t_4 \;\; 2t_5 \;\; t_6 \;\; t_7 \;\; t_6 \;\; t_7]^t \quad (4)$$

- *Cyclic/acyclic nature:* A Petri Net is *acyclic* if T_R and (or) T_C has at least one zero component.[2]

The transition vector corresponding to our proposed model T_R has zero components at the ninth and tenth place; thus, the Petri Net model is *acyclic.* Also, a Petri Net is *acyclic* if and only if it has at least one source and (or) one sink place [2]. To understand the physical interpretation of the Petri Net's acyclic nature, let us suppose the Petri Net is not acyclic. Then there must exist a directed path $x_i \rightarrow x_j$, $\forall\, x_i, x_j \in$ P∪T. However, for $x_i = p_9$, there is no incoming arc; hence the directed path is not possible for p_9. Further, if p_9 and p_{10} would not have been source places, there would have been a cycle that would have repeated endlessly; hence the dynamics between the customer and the waiter would go on, without the possibility of the arrival of a new customer.
Moreover, it is inferred from [2] that the acyclic nature of Petri Net does not mean that it cannot contain a cycle. [2] provides an algorithm to find a directed cycle in a Petri Net from the concept of transition vectors. We can find a directed cycle $p_1t_1p_4t_3p_7t_6p_1$, in the proposed model. The same can be interpreted as the arrival of a customer at the first table; the service provider(waiter) taking his order; the customer waiting for food; the service provider(waiter) serving him; and finally, the customer eating and vacating the place, followed by the entry of a new customer.

- *Self-loop free:* A Petri Net is *self-loop free* if and only if the corresponding same components of T_R and T_C have no identical values/entries. [2]

The transition vectors that correspond to our proposed model show that the PN is self-loop free. From Fig. 3, it can be inferred that under any condition that happens to be accurate, it would not continue to occur an indefinite number of times. To support this, on the contradictory, let if possible, a self-loop exists at the place p_4 w.r.t the transition t_3. This self-loop can be interpreted as the customer waiting for the food, followed by being served; waiting for the food again; and the cycle repeats. Undoubtedly, this turns out to be an irrelevant situation making our assumption wrong. Thus, the proposed Petri Net model is self-loop free, and no condition/event shall occur indefinite number of times.

- *State Machine:* A Petri Net is said to be state machine if and only if all the components of T_R and T_C are respectively distinct. [2]

In the transition vector, T_R of the proposed model, the ninth and tenth component is identical, equal to zero. Hence the model is not a state machine which implies that it necessarily does not have one input and one output place for every transition i.e., more than one conditions can simultaneously hold true for an activity to occur. For e.g., from Fig. 4 it is evident that both p_1 and p_2 lead to the happening of t_1. Therefore, this shall give rise to either concurrency, or conflict, or both.

- *Conflict:* As it has been seen that the proposed Petri Net model is not a state machine, thus conflict may or may not arise.

A Petri Net is *conflict-free* if and only if every component of T_C has exactly one transition, or, in case any component has more than one transition, the same transitions set must appear in the corresponding component of T_R. [2]
In the proposed model, the column transition vector T_C has more than one transitions in the first component, and the corresponding entry of T_R is different, implying that there is a conflict between t_1 and t_2 .Thus, the Petri Net model is not conflict-free. All possible conflicts that can arise in the Petri Net model are between the transitions t_1, t_2, t_3, t_5. The preciseness of the conflicting transitions is mentioned in the *behavioral aspect of conflict*.[3]

- *Concurrency:* A Petri Net is said to be structurally concurrent if and only if at least one entry of the column transition vector T_C has coefficient 2 or greater than 2. [2]

Since the column transition vector T_C of the proposed model has coefficient 2 in the entries of its first, second, third, fourth and sixth components, the transitions in these components along with the remaining transitions form structurally possible concurrent transitions. All the possible concurrent transitions have been mentioned in Table 3[4] along with transitions showing behavioral concurrency[5].

B. Behavioral Analysis

There can be many possible scenarios for this Petri Net model to work, depending upon the customers (those being provided the service inside and those waiting outside) and the service provider at the eatery. We throw light on two possible scenarios for the proposed model.

Scenario 1: As per the first scenario, after the eatery is open to provide service at the initial stage, it has two customers seated on the sanitized first and second tables respectively, and the service provider is free to serve the two customers. In this scenario, it is assumed that no new customer has arrived at the eatery.

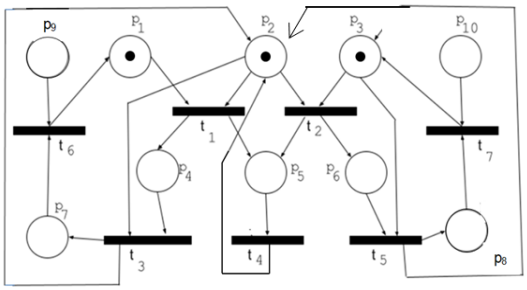

Fig. 3 Petri Net Structure of the proposed model depicting scenario 1 with the initial marking M_0.

[3] Elaborate discussion on Page number 6.
[4] On page number 7.
[5] Elaborate discussion on Page number 6.

The initial marking that depicts this scenario is M_0={1,1,1,0,0,0,0,0,0,0}. Fig. 3 depicts the Petri net model for the above-depicted scenario with the initial marking M_0 and the set of all reachable markings are mentioned in Table 4(a).[6]

Scenario 2: The second possible scenario says that, after the eatery is open to provide service, it has two customers at the initial stage, seated on the sanitized first and second table respectively, and the service provider (waiter) is free to serve the two customers. In this scenario, the arrival of new customer(s) is possible at the eatery; and it is assumed that two customers are respectively in the separate waiting places (p_9 and p_{10}) to occupy the first and second table respectively after the previously seated customers vacate the tables. The initial marking that depicts this scenario is G_0={1,1,1,0,0,0,0,0,1,1}. Fig. 4 depicts the Petri net model for the above-depicted scenario with the initial marking G_0. We shall now discuss these scenarios and further analyze the proposed Petri net model for the same.

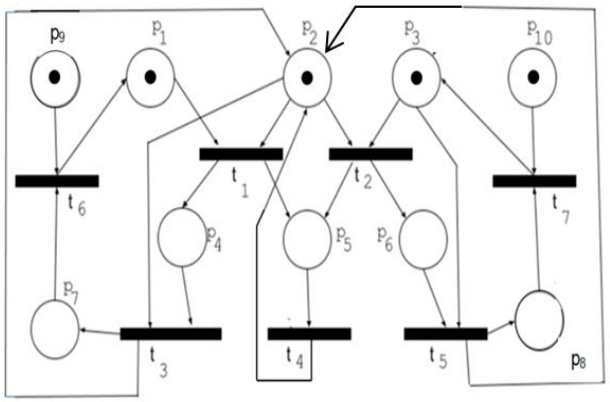

Fig. 4 Petri Net Structure of the proposed model depicting scenario 2 with the initial marking G_0.

One possibility in this scenario is that the service provider (waiter) initially visits the first table and takes the order, where after the order is reported to the kitchen, and the customer waits until the order gets prepared for serving. Then, he visits the second table and takes the order, which is further reported to the kitchen. Now, orders for both the tables have been placed, and the service provider is idle until the food gets prepared. When the service has been provided at both the tables, the customers eat and vacate the place. Continuing further, if Scenario 2 is taken into account, then the arrival of a new customer is possible for the first table and (or) the second table, and the process can repeat.

- *Reachability* [6],[8]: The reachability problem considers a marked Petri Net PN with an initial marking M_0 and a marking M_1 and aims at answering if M_1 is reachable from M_0, that is; whether M_1 belongs to the set *R (PN, M_0)*. The reachability tree or graph is an analytic tool for representing the reachability set of the Petri Net.

Suppose we construct a reachability tree[7] for the given Petri Net; in that case, we need to consider the marking of the Petri Net at that state as a node, and an arc would represent firing of transition from the initial marking to the subsequent set of new markings. Fig. 5 shows the *Reachability tree*[8] of the Petri Net model shown in Fig. 3. Additionally, refer to Fig. 6 in Appendix for the reachability tree[9] of the Petri Net model as shown in Fig. 4.

From Fig. 5, it can be perceived that several paths can be chosen for the functioning of the proposed model yielding dissimilar results.

In total, six different paths exist from the initial marking M_0 to the final marking M_{10}, which infers that both the customers have been served and have vacated the eatery, and no new customer has arrived (as per scenario 1). Table 2 highlights all the likely paths from the reachability tree in Fig. 5.

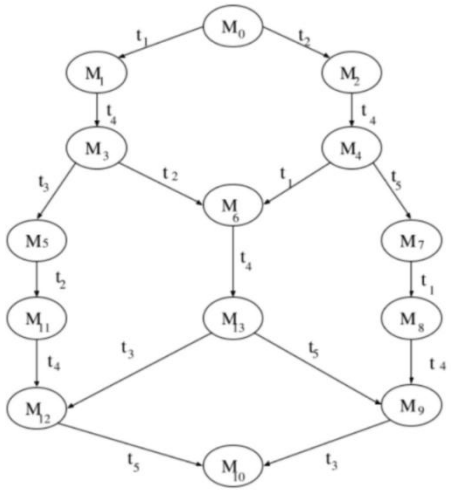

Fig. 5 Reachability Tree for the Petri Net Structure of the proposed model depicting scenario 1 and all possible markings due to various transitions firing.

Table 2. List of all possible paths

1.	M_0	M_1	M_3	M_5	M_{11}	M_{12}	M_{10}
2.	M_0	M_1	M_3	M_6	M_{13}	M_{12}	M_{10}
3.	M_0	M_1	M_3	M_6	M_{13}	M_9	M_{10}
4.	M_0	M_2	M_4	M_6	M_{13}	M_9	M_{10}
5.	M_0	M_2	M_4	M_6	M_{13}	M_{12}	M_{10}
6.	M_0	M_2	M_4	M_7	M_8	M_9	M_{10}

The above-mentioned six paths exhibit the possible order of activities w.r.t the occurrence of the required pre-conditions.

[6] Refer to Appendix.

[7] A Tree is a connected digraph without a directed cycle.

[8] Refer to Table 4(a) in Appendix for values of all markings.

[9] Refer to Table 4(b) in Appendix for value of all markings.

- *Safeness*[5]: A place p_i in a Petri Net structure with an initial marking M_0 is *safe* if for all markings M' that belong to the Petri Net's reachability set, $M'(p_i) \leq 1$ *i.e.* the total number of tokens at any state in a place after firing of a transition is either 1 or 0. A Petri Net is said to be *safe* if all the places in that Petri Net are *safe*.

Here, it can be inferred from the reachability tree in Fig. 5 and Fig. 6[10], that the proposed Petri Net model is *safe* for any marking reachable from M_0 (in case of the first scenario) and G_0 (in case of the second scenario). Since the tokens' presence at a place in this model justifies the happening of that particular activity, the number of tokens at any place should be either 0 or 1. An infinite number of tokens at any place or number of tokens other than 0 and 1 at any place does not have any physical meaning with respect to the proposed model. Therefore, the conditional nature of the proposed Petri Net model is validated through the *safeness* property.

- *Behavioral Conservation:* We have already shown in section V*(A)* that the model is partially conservative.

For scenario-1: It can be inferred from the Table 4(a)[11] that the model is conservative, having an initial marking M_0.

To relate this property with the proposed model, let us consider a state where we have two customers seated at the first and second table respectively, and a service provider (waiter). At any given instance, the possible states of the customers are either the following-

1) Arrival at the table and ready to place the order.
2) Waiting for the food after placing the order.
3) Eating the served food and eventually leaving.

Similarly, the possible states of the service provider (waiter) are either the following -

1) Free to attend the customers.
2) Confirm the order for serving the food.

It can be seen that the state of customers and service provider (waiter) cannot be mingled; that is, a customer cannot be waiting for food and leaving at the same instance. Hence the shuffling of tokens is happening between the three states of the customer and two states of the service provider. This physical nature of the model is validated by the conservative nature of the model with respect to the initial marking M_0.

For scenario-2: It can be inferred from the Table 4(b)[12] that the model is not conservative, as the token count remains constant for few markings but eventually varies from being five for some markings; to four; and to three, at various stages. The physical nature indicates that the tokens are shuffling between the states of two customers at both the tables respectively; the service provider; and the two customers at the waiting place (p_9, p_{10}). Up to this activity (before firing of t_6 and t_7), the token count is constant, but as soon as the customers of the first and second table vacate, and the waiting customers get seated, the token count represents shuffling between those two new customers and the service provider; instead of four customers (since another pair of new customers has not arrived), and the service provider.

- *Boundedness* [5]: It is apparent that conservativeness is a particular case of boundedness.

Hence, this model is structurally as well as behaviorally bounded. Further, the number of tokens at any place can be either 0 or 1. The reachability trees in Fig. 5, 6, and Tables 4(a), (b) imply that the Petri Net is not unbounded. Thus, the proposed Petri Net model, which exhibits safeness, is *1-bounded* i.e., *behaviorally bounded* for both the scenarios.

- *Deadlock* [5]: Deadlock in a Petri Net is a situation where a transition or a set of transitions is unable to fire.

For the first scenario, from Fig. 3, it can be seen that the reachability tree in Fig. 5 has one vertex *i.e.*, $M_{10,}$ which has no outgoing arc [1]. Hence, deadlock appears at M_{10} as no transition from $T= \{t_1, t_2, t_3, t_4, t_5, t_6, t_7\}$ can fire. This suggests that the customers at both tables have been served, and the customers have vacated the eatery. Then, the service provider (waiter) becomes idle with no arrival of a new customer. Similarly, for scenario-2 from Fig. 5, it can be seen that the reachability tree in Fig. 6 shows deadlock at the node M_0. This deadlock is the stage when the initial customers seated at both the tables have eaten and vacated; also, the customers who were waiting to be seated at these tables have eaten and vacated while the service provider (waiter) has served all four customers and is currently idle as no new customer has arrived after this. The deadlock will thus persist until the new customer arrives.

- *Liveness* [5]: A Petri net model is said to be live w.r.t an initial marking if it is possible to fire all the transitions at least once using some firing sequence for all the markings in the reachability set. If there exists a transition, say *t in T* such that *t* can never be fired, then *t* is *dead*.

For scenario-1 in the proposed model, t_6 and t_7 act as the dead transitions because it is assumed that no new customer arrives in this scenario. Hence, the proposed model does not exhibit liveness for the initial marking M_0. Now considering scenario -2, we have a situation where every transition can be fired, as there are new customers who can occupy the first and the second table. Thus, there is no transition that is dead, and hence, the Petri Net model with respect to the initial marking G_0 is live. The physical interpretation of liveness is that all the activities that are mentioned in the model will happen at least once.

- *Behavioral Conflict* [6]: Two transitions are said to show conflict when the activities are in parallel i.e., either of the possible transition can occur/fire, but both cannot simultaneously. Two transitions have a common input place and exhibit non-determinism.

[10] Refer to Appendix.
[11] Refer to Appendix.
[12] Refer to Appendix.

From section V(*A*) (Conflict), the conflicts can possibly exist between the transitions t_1, t_2, t_3 *and* t_5. The design of the model (the token placing) is such that t_1 and t_3 cannot be enabled simultaneously since tokens can only be at p_4 after firing of t_1 (similarly, t_2 and t_5 cannot be enabled simultaneously). Hence the only conflicts that would occur in the Petri Net model for both scenarios would be between t_1 and t_2, t_1 and t_5, t_2 and t_3, and t_3 and t_5. The physical interpretation of the conflict between t_1 and t_2 implies that when both customers at first and second table are ready to place the order, the service-provider (waiter) can only serve/attend one table at a time.

- *Behavioral Concurrency* [6]: Two transitions are concurrent if they are independent to each other i.e., where one transition occurs independently of the other, either it can fire before, after, or in parallel to another enabled transition.

Table 3 gives the structural and behavioral concurrency between the transitions.

For understanding concurrency between two transitions, say t_1 and t_7, tokens are available for places p_1, p_2, p_8, and p_{10} i.e., a customer has arrived at the first table and is ready to place the order. Also, the service provider (waiter) is available to provide service to the customer, and a customer at the second table has already been served, after which he leaves, allowing the arrival of the next customer.

Henceforth, the service provider (waiter) who is serving at the first table; and sanitization of the second table, along with the placing of a menu card on it are two independent activities that exhibit concurrency.

For understanding concurrency between t_1 and t_4 (not behaviorally concurrent), the tokens must be available at places p_1, p_2, and p_5, which is not possible as per the Petri Net's design (token placing). Also, if true, it would imply that the waiter is idle and is finalizing the order for some customer at the same instance, which is absurd. Thus t_1 and t_4 not being behaviorally concurrent, validate the physical interpretation.

Table 3. List of all possible concurrent transitions.

First Transition	*Second Transition*	*Structural Concurrency*	*Behavioral Concurrency*
t_1	t_4	Yes	No
t_1	t_6	Yes	No
t_1	t_7	Yes	Yes
t_2	t_4	Yes	No
t_2	t_6	Yes	Yes
t_2	t_7	Yes	No
t_3	t_4	Yes	No
t_3	t_6	Yes	No
t_3	t_7	Yes	Yes
t_5	t_4	Yes	No
t_5	t_6	Yes	Yes
t_5	t_7	Yes	No

6. CONCLUSION

In this paper, we have discussed and interpreted the structural and behavioral properties of the proposed model. The proposed small eatery model has been construed so that it can be suitably related to the actual restaurant scenarios. This paper can be a motivation towards designing and analyzing larger restaurant/eatery models..

REFERENCE

[1] Desel J. and Reisig W. Place/Transition Petri Nets. Lectures on Petri Nets I: Basic Models, Vol. 1491; pp. 122-173, 1998.

[2] Farooq Ahmad, Huang Hejiao and Wang Xiaolong. Analysis of Structure Properties of Petri Nets Using Transition Vectors, Information Technology Journal Vol. 7, No. 2; pp. 285-291, 2008.

[3] Heiner M., Gilbert D. and Donaldson R. Petri Nets for Systems and Synthetic Biology, In Formal Methods for Computational Systems Biology, Springer, Vol. 5016 of LCNS; pp. 215-264, 2008.

[4] Itoh Y., Miyazawa I., Liu JH. and Sekiguchi T. On Analysis of Petri Net Properties based on Transitive Matrix, Proc. of IEEE on IECON, pp: 973-978, 1999.

[5] Murata T. Petri Nets: Properties, Analysis and Applications, Proc. of IEEE, Vol. 77, No. 4; pp. 541-580, April 1989.

[6] Peterson JL. Petri Net Theory and Modeling of Systems, Prentice-Hall, 1981.

[7] Peterson JL. Petri Nets, Computing Surveys, Vol. 9, No. 3; pp. 223–252, September 1977.

[8]Rongming Zhu, Ya Zhang and Lan Yang. A class of generalized Petri Nets and its State Equation, Advances in Mechanical Engineerig, Vol. 9, No. 8; pp. 1–17, 2017.

Side Wall Etched Ridge Waveguide Bragg Grating for Bio-sensing Application

[1] Dhanyashree K C, [2] Naik Parrikar Vishwaraj, [3] Gurusiddappa R. Prashanth, [4] Chandrika T Nataraj

[1][4] Department of Electronics and Telecommunication Engineering, Siddaganga Institute of Technology, Tumkur, India
[2][3] Department of Electronics and communication Engineering, National Institute of Technology, Goa, India

Abstract:

The rapid advancement of fabricating optical de- vices at micro-scale has led to increase its use in bio-sensor applications. In this work we propose a less expensive and simple fabrication strategy device for bio-sensing application. We designed and analyzed Sidewall Etched Ridge Waveguide Bragg grating (SERWBG) using Eigen mode expansion (EME). The shift in Bragg's wavelength of the device is proportional to the variation in refractive index (RI) of the cover layer, which is a bio- element component. The core waveguide height of the structure is varied, to obtain the optimal sensitivity by considering fabrication tolerances. The higher sensitivity of 262 nm/Refractive index Unit(RIU) for 100 nm waveguide height has been achieved.

Keywords:

biosensor, integrated optics, resonance wavelength, Ridge waveguide, Sidewall etched Bragg grating

1. INTRODUCTION

The use of optical sensors has been widespread as they are nonconductive,immune to electromagnetic interference and have a minuscule footprint, making them a reliable choice in environment subject to noise. Since the last decade optical sensors have become a major class of bio-sensors as they allow real time and cost-effective detection while providing good sensitivity [1]. These properties have made them a promising alternative to the traditional methods of bio-molecular sensing and medical diagnostics.Optical bio-sensors can be broadly classified into two types, viz. labeled and label-free based sensors. In the labeled method, the target bio-molecules are labeled with fluorescence markers helps detect the presence of the required molecule. This process is more often than not, time consuming, requires labelling and trained personnel and are expensive. In the label-free method, these labels/markers are absent. the target molecule is made to attach to the surface by using a suitable bio-receptor. This causes a variation in effective RI of the device and hence the propagation charac- teristics of the incident optical signal. [1–4]. This change is quantified to obtain a label free detection. Several of these label free bio-sensors based on fiber Bragg gratings(FBGs), ring resonators, photonic crystals, interferometers, and surface plasmon resonance have been explored [5–11]. Bragg grating based label free Integrated waveguide optics based bio-sensors are dependent on detection of wavelength shift of the Bragg wavelength due to perturbation on the surface of the grat- ing.In addition, it also provides features such as high-scale integration, scaling capability, multiplexed sensing and lab- on-chip integration [12-14].The surface corrugated bio-sensors are being steadily replaced by sidewall Bragg gratings as they can control weak-coupling coefficient and achieve apodization, thereby reducing the undesirable side lobes. They also enjoy significant advantages over surface Bragg gratings, in the form of lower insertion loss and increased tolerance in the fabrication process [15-16].

In this work, we propose a compact RI sensor based on sidewall etched ridge waveguide Bragg grating.The ridge waveguide is considered because of the advantages like, it has strong optical light confinement and ease of fabrica-tion[17].The device is designed using Lumerical MODE Solu- tions and coupled mode theory. The designed sensor has shown high sensitivity and an almost linear response. In addition, the structure is compact and the design is compatible with standard CMOS fabrication processes.

2. THEORY AND DESIGN

Fig. 1 and Fig. 2 show the designed SERWBG schematic and cross-sectional diagrams respectively. It is a three layered device, middle one being the core layer, of RI,nf , with height h, width W and SERWBG has been achieved by periodically etched sides of width ΔW with the grating period Λ. The bottom one being the substrate layer,of silicon dioxide material, and the top one is the cover layer of RI, nc consists of bio-analyte sample.

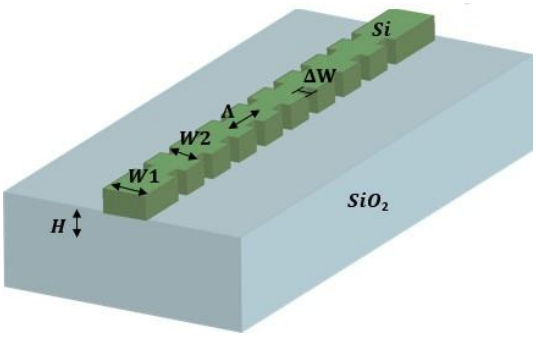

Fig. 1. Schematic diagram of the SERWBG

When the light propagates along the longitudinal direction, z of the grating, due to the sidewall etching of the waveguide,

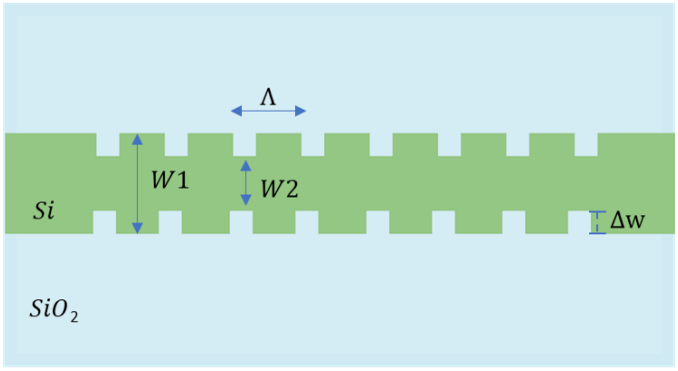

Fig. 2. Cross-sectional view

a particular wavelength, called Bragg wavelength, of light is reflected back and all other wavelengths are transmitted.
The cover layer RI corresponds to the bio-element sample. When the RI of the cover layers is varied, the effective RI of the grating changes. The change in effective RI leads to the shift in Bragg's wavelength. The theoretical study of the device has been done using Coupled mode theory. The Bragg wavelength is calculated using equation (1)

$$\lambda_B = 2n_{eff}\Lambda \quad (1)$$

where n_{eff} and Λ is the effective RI and pitch of the Bragg grating respectively
Bragg gratings are analysed by using coupled mode equations given in (2) and (3),

$$\frac{\partial a_{grat}}{\partial z} = -i\nu_c \exp(i\Delta\beta z) \quad (2)$$

$$\frac{\partial b_{grat}}{\partial z} = iK_c \exp(-i\Delta\beta z) \quad (3)$$

Where, a_{grat} and b_{grat} are the amplitudes of the forward and backward wave
$\Delta\beta$ is given by,

$$\Delta\beta = 2\beta - k \quad (4)$$

Where, β is the waveguide's propagation constant and $k = (2\pi)/\Lambda$. The coupling coefficient K_c, has been determined using (5),

$$K_c=(\frac{\pi k_0}{3})(\frac{n1^2-n2^2}{n2})(\frac{t}{t_g})[1+\frac{3(\lambda/t)}{2\pi(n2^2-n1^2)^{\wedge}1/2}+\frac{3(\lambda/t)^{\wedge}2}{4\pi^{\wedge}2(n2^2-n1^2)^1}] \quad (5)$$

The coupled mode equations are solved to obtain the expressions for forward and backward propagating wave,

$$a_{grat}(z) = \frac{-\Delta\beta\sinh(\alpha(z-L_g)) + i\alpha\cosh(\alpha(z-L_g))}{\Delta\beta\sinh(\alpha L_a) + i\alpha\cosh(\alpha L_a)}a(0) \quad (6)$$

$$b_{grat}(z) = \frac{K_c\sinh(\alpha(z-L_g))}{\Delta\beta\sinh(\alpha L_a) + i\alpha\cosh(\alpha L_a)}a(0) \quad (7)$$

$$\alpha = \sqrt{K_c^2 - (\frac{\Delta\beta}{2})^2} \quad (8)$$

The coefficients of reflection and transmission of the grating are calculated by using (9) and (10).

$$R = \left|\frac{b_{grat}(L_g)}{a(0)}\right|^2 \quad (9)$$

$$T = \left|\frac{a_{grat}(L_g)}{a(0)}\right|^2 \quad (10)$$

$$\frac{\Delta\lambda}{\lambda} = \wedge\frac{\Delta n_{eff}}{n_{eff}} \quad (11)$$

The sensitivity due to change in sample RI is defined as the ratio of change in the Bragg wavelength to the change in RI of the cover layer. Sensitivity is measured in terms of nm/RIU.

$$s = \frac{\Delta\lambda}{\Delta n_c} \quad (12)$$

TABLE I
Geometrical Parameters

Geometrical parameter	Value
Waveguide width	460 nm
Core RI	3.441
substrate RI	1.45
ΔW	40 nm
Duty Cycle	0.5

In this proposal, we have considered three different designs to enhance sensitivity. The waveguide height has been varied, they are denoted by Design A, B and C respectively and mentioned in Table II. The effect of reducing waveguide height also effects the effective RI and requires that the gratings period be recalculated We have done simulations for all the defined designs and results are shown.

TABLE II: Design parameters

Design	h	Λ	Grating Length
A	220 nm	320 nm	0.64 mm
B	150 nm	380 nm	0.76 mm
C	100 nm	480 nm	0.96 mm

3. RESULTS

The simulations have been done using Lumerical inc. tool. Fig.3 shows the mode profile diagram for the varying waveg- uide heights as shown in the table II of designs A, B and C. From the figure we could observe the light confinement towards the core is more in the case of 220 nm. The light spreading towards the surface of the waveguide is

more when the waveguide height decreased to 100 nm this leads to the more sensitivity because of the more part of the light propagates towards the outer surface of the waveguide.

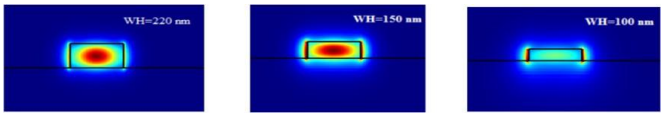

Fig. 3. Mode profile diagram for different waveguide height

Fig.4 shows the transmission and reflection spectra of SERWBG. The Fig.5 graphically represents the change in RI with reference to shift in Resonant wavelength of the cover layer, which is linearly proportional. From the Fig.6, we could observe the sensitivity for the Design C is greater than the other two designs.

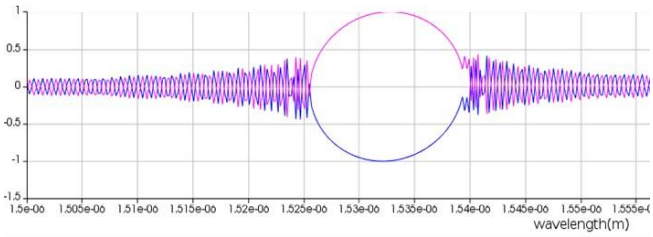

Fig. 4. Transmission and reflection spectra of SERWBG

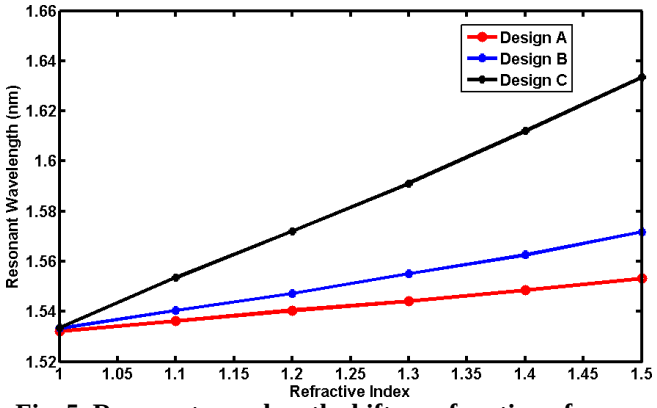

Fig. 5. Resonant wavelength shift as a function of cover layer RI

4. CONCLUSION

In this paper,we designed and proposed Sidewall Etched Ridge Waveguide Bragg Grating for Bio-sensing applications.

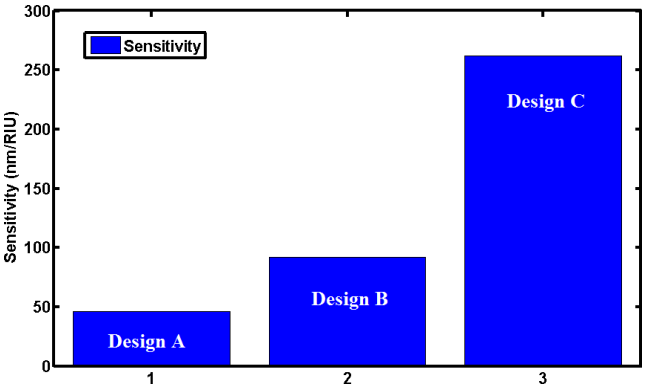

Fig. 6. Sensitivity representation of different Designs

We used Eigen Mode Expansion(EME) method for the design and analysis. The sidewall etched Bragg grating has advantage in fabrication compared to surface etched Bragg grating. We have considered three different designs based on the waveg- uide height and observed sensitivity for all the designs. We could achieve maximum sensitivity at 100 nm, which is 262 nm/RIU.

REFERENCE

[1] P. Damborsky´; J. Sˇvitel;J. Katrl´ık;Optical biosensors,Essays Biochem., vol. 60, no. 1, pp. 91–100, 2016.

[2] S. Balslev; M. Jorgensen; B. Bilenberg; K. B.Mogensen; D. Snakenborg; O. Geschke, et al.,Lab-on-a-chip with integrated optical transducers. Lab on a Chip, 2006, 6(2): 213–217.

[3] X. Fan; I. M. White; S. I. Shopova; H. Zhu; J. D. Suter; Y. Sun. Sensitive optical biosensors for unlabeled targets: A review. Anal. Chim. Acta, vol. 620, no. 1–2, pp. 8–26, 2008.

[4] S. Sahu; K. V. Kozadaev; G. Singh. Michelson interferometer based refractive index biosensor, Opt. InfoBase Conf. Pap., vol. 1, pp. 6–8, 2014.

[5] W. Yuan; H. P. Ho, C. L. Wong; S. K. Kong; C. Lin. Surface plasmon resonance biosensor incorporated in a michelson interferometer with enhanced sensitivity, IEEE Sens. J., vol. 7, no. 1, pp. 70–73, 2007.

[6] D. Irawan; T. Saktioto; J. Ali; P. YupapinDesign of Mach-Zehnder interferometer and ring resonator for biochemical sensing. Photonic Sensors, vol. 5, no. 1, pp. 12–18, 2015.

[7] X. Wang; C. K. MadsenHighly sensitive compact refractive index sensor based on phase-shifted sidewall Bragg gratings in slot waveguide. 2014.

[8] Y. Chen; H. MingReview of surface plasmon resonance and localized surface plasmon resonance sensor. Photonic Sensors, vol. 2, no. 1, pp. 37–49, 2012.

[9] S. Olyaee; S. Najafgholinezhad; H. AlipourBanaeiFour-channel label- free photonic crystal biosensor using nanocavity resonators. Photonic Sensors, vol. 3, no. 3, pp. 231–236, 2013.

[10] W. C. L. Hopman et alQuasi-one-dimensional photonic crystal as a compact building-block for refractometric optical sensors. IEEE J. Sel. Top. Quantum Electron., vol. 11, no. 1, pp. 11–15, 2005.
[11] L. M. LechugaBiosensors and Modern Biospecific Analytical Tech- niques. Vol. 44, edited by L. Gorton (Elsevier Science BV, Amsterdam, Netherlands, 2005)
[12] K. Zinoviev; L. G. Carrascosa; B. Sep; C. Dom; L. M. LechugaSilicon Photonic Biosensors for Lab-on-a-Chip Applications. vol. 2008, 2008.
[13] A. F. Gavela; D. G. Garc´ıa; J. C. Ramirez; L. M. LechugaLast advances in silicon-based Optical Biosensors. Sensors 2016,16(3),285.
[14] L. Zhu; Y. Huang; W. M. J. Green; A. YarivPolymeric multi-channel bandpass filters in phase-shifted Bragg waveguide gratings by direct electron beam writing. Opt. Express, vol. 12, no. 25, p. 6372, 2004.
[15] Naik Parrikar Vishwaraj; Chandrika T. N.; Ravi Prasad K. Jagannath; Prashanth G. R.; Srinivas T.Temperature Compensated Optical MEMS Multiparametric Sensor using Waveguide based Superstructure Bragg Grating. Current Optics and Photonics,vol 4, no 4,p.293-301.
[16] P. Prabhathan; V. M. Murukeshan; Z. Jing; P. V. RamanaCompact SOI nanowire refractive index sensor using phase shifted Bragg grating. Opt. Express, vol. 17, no. 17, p. 15330, 2009.
[17] Yuan P. Li, Charles H. Henry, Silicon Optical Bench Waveguide Tech- nology. Optical Fiber Telecommunications (Third Edition), Volume B 1997.

Laboratory Studies on Soil Characterization of Earth Slope Failure at Dessie South Wollo Ethiopia-A Case Study

[1] Belete Mulugeta, [2] Vijaykumar Nagappa, [3] Siraj Mulugeta Assefa, [4] Desalegn Gezahegn, [5] Abduselam Assen

[1][2][3][5] Wollo University, Kombolcha Institute of Technology, Ethiopia
[4] Wollo University, Dessie Campus, Ethiopia

Abstract:

In the densely populated highlands and almost all slope area of the country Ethiopia, where altitudes more than 1750m, increasing the number and size of landslides from past more than 30years is causing considerable damages and losses among the society and the government. Since from 1993 to present, about more than 300 people lives are lost, more than 200 houses damaged, more than 150km of roads are damaged. Landslide is one of the crucial hazard environmental constraints for the development viz urbanization and infrastructures of country Ethiopia. Besides it is observed that the slope failure is located on the sides of Dessie-Kombolcha road, which is the only access road connecting the two nearby cities. The detailed characterization of the soil mass will be carried out by using laboratory studies to back analysing the observed slope failure. The main objective of this detail investigation is to identify the causes of the slope failure in the area and provide appropriate remedial measures.

Keywords:

Soil, Failure, Landslides, Slope, Stability

1. INTRODUCTION

A slope is defined as a surface of which one end or side is at higher level than another; a rising or falling surface [1]. An earth slope is an un supported, inclined surface of a soil mass. The failure of a mass of soil located beneath a slope is called as slide [2]. It involves a downward and outward movement of the entire mass of soil that participates in the failure [3, 4]. The failure of an earth slope occurs due to the following reasons, Gravitational forces and forces due to flow of water or seepage of water in to the soil mass, disintegration of the of the soil mass structure and soil particles [5, 6]. The failure of earth slopes may occur slowly or suddenly [7]. Seepage or flow of water in soil is defined as the flow of a fluid or liquid, usually water, through a soil under a hydraulic gradient or slope [8, 9]. Shear strength of soil is the internal resistance per unit area that the soil can offer to resist failure and sliding along any plane inside it [10]. Knowledge of shear strength is required in solution of problems concerning the stability of soil masses and slope stability analysis [11]. Determining the design soil shear strength is one of the most important steps in the stability analyses of slopes [12, 13]. Typically, laboratory testing to determine soil shear strength is performed for cohesive soils while empirical correlations are utilized to assess the behavior and strength parameters for cohesion less soils [14]. Cohesive soils require a determination of whether or not undrained and or drained shear strength parameters are being investigated. The determination of which test to conduct depends on the identified failure mechanism and the sample location. The direct shear test is a cost effective and efficient test to quickly determine residual soil values [15, 16].

1.1. Types of Slope Failure

There are different types of slope failures such as,
1. Slope failure
2. Toe failure
3. Base failure

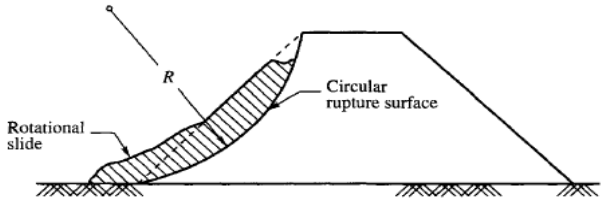

(a) Rotational slide

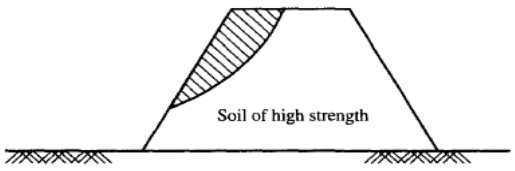

(b) Slope failure

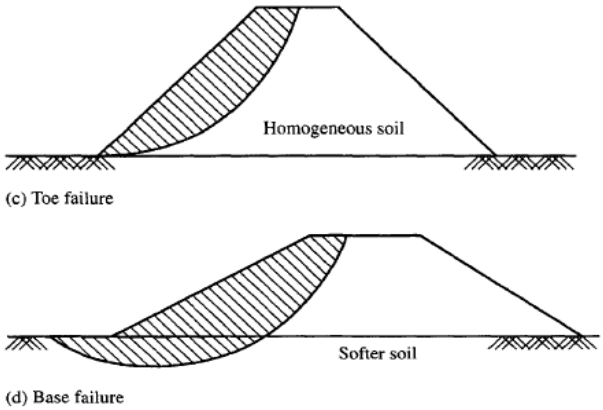

Fig. 1. Types of slope failure

Generally, slope failure of finite slopes is cohesive or cohesive-frictional soils tends to occur by rotation, the slip surface to the arc of a circle shown in figure 2.

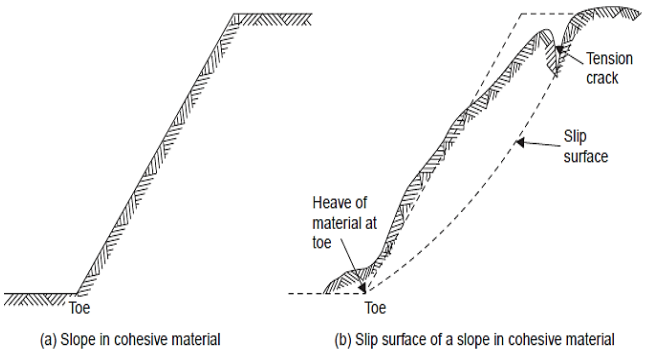

Fig. 2. Slope failure in cohesive soil

1.2. Landslides

The landslides are a serious hazardous problem in almost all parts of the world, because its causes economic and also social losses on government and public properties. The term landslide represents "the movement of a soil mass or rock [16]. Land sliding is either a natural disaster or it occurs as a result of human activities which disturb the soil or rock stability. This phenomenon differs according to their size and shape of the moving soil or rock mass, displacing mechanisms, velocity and other characteristics [17].

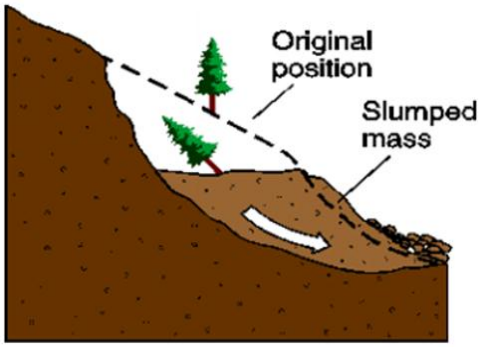

Fig.3. Landslides in earth slope

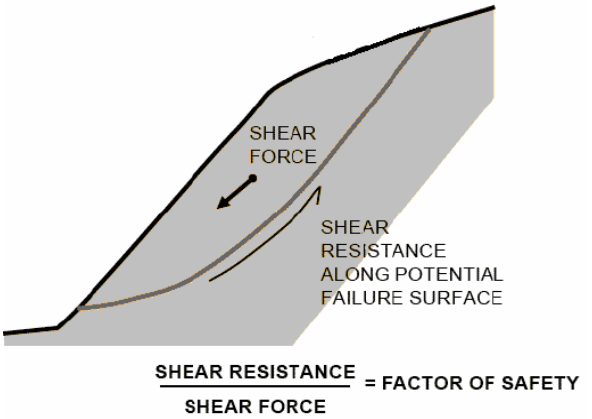

Fig. 4. Shear resistance v/s shear force during a landslide's movement

The landslides can occur on any part of the terrain given the right conditions of soil mass, moisture, and the slope angle [18]. It is a part of the natural process of the earth's surface geology, landslide serves to redistribute soil and sediments in a process that can be in abrupt collapses or in slow gradual slides [19]. Some features might be noticed before major landslides springs, seeps, or saturated ground in areas that have not typically been wet before, new cracks or unusual bulges in the ground, street pavements or sidewalks, trees, retaining walls or fences, offset fence lines, sunken or down-dropped road beds [20, 21]. Slopes with lower factor of safety means the potential of failing are higher than slopes with higher factor of safety [22, 23]. Therefore, slopes with higher factor of safety are safer than lower factor of safety as shown in figure 4 [24].

2. STATEMENT OF THE PROBLEM

The slope failure presented in this work has been observed around "Menberetsehay" on the way from Dessie to Kombolcha highway road. It was clear that the existing road width was obtained by cutting the adjacent steep ridge. However, the toe cut for the road way has triggered several shallow failures in that area. Apart from this during the construction of the road, the existing spring water with significant flow rate has been buried close to the toe part without providing any drainage system. The local communities are still believing the main causes to the failure are firstly the construction of the road in such loose soil mass and secondly the influence of the pore water pressure from the spring water trigger failure to the loose material. The movement covers almost half of the compound of Menberetsehay School and adjacent residence areas. The presence of several damaged class rooms, offices, nearby houses, trees clearly give witness to the presence of unstable movement of soil mass. Current active failures are reinitiated as a consequence of heavy rainfall. Some remedial measures like masonry retaining walls, piles were provided previously to reduce the slope movement. But, none of the adopted remedial measures were effective as observed during the site visit. The impact load of the

 ISBN: 978-93-90214-20-4

moving soil mass has also caused failure of the retaining wall. Currently, the transported soil mass has blocked full of the road width affecting the function of this important route public transportation as shown in figure 5 and large cracks in the soil have occurred as shown in figure 6.

Fig. 5. Failure of earth slope covered almost half of the existing Kombolcha to Dessie Road

Fig. 6. Large Tension cracks appeared in earth slope failure

3. METHODOLOGY

3.1.Laboratory Soil Testing required for Slope Failure Analysis

Specific information on laboratory testing, including standard tests performed and associated AASHTO methods. Geotechnical Guidelines for Sample Handling, testing and Data Reporting. Consolidated-undrained (C_U) and consolidation testing shall be conducted for each major cohesive soil layer in order to reliably characterize each layer's soil strength parameters.

1) Moisture Content
2) Particle Size Analysis and Soil Classification
3) Bulk unit weight and Dry unit weight by core cutter method or Sand replacement method
4) Atterberg Limits and Soil behaviour
   a) Plastic limit – plasticity index
   b) Liquid limit- Liquidity index
   c) Shrinkage Limit
5) Swelling test
6) Specific Gravity test
7) Compaction test
8) Permeability test
9) Unconfined compressive test
10) Direct shear test

4. RESULT AND DISCUSSION

There are from four soil samples have been collected from different places from test pits of different depths and laboratory studies have been conducted and the test results have been obtained as shown in table 1.

Table.1. Properties of Soil at Slope Failure

Test	Pit -1	Pit-2	Pit-3	Pit-4	Average Value
Bulk density (g/cm^3)	1.86	1.91	1.87	1.94	1.895
Maximum Dry density(g/cm^3)	1.38	1.51	1.43	1.55	1.467
OMC (%)	34.70	26.6	31.50	25.00	29.45
Liquid Limit (LL)	81.10	76.44	57.27	61.80	69.15
Plastic Limit (PL)	31.45	29.56	30.47	32.36	30.96
Plasticity Index (Ip)	49.7	46.9	26.8	29.4	38.20
Specific gravity (G)	2.38	2.31	2.38	2.55	2.405
Free swell	50	20	54.6	28.6	38.30
Permeability K (cm/s)	1.48E^{-5}	5.64E^{-8}	6.73E^{-6}	1.31E^{-7}	7.29E^{-5}
Cohesive C_u (kPa)	17.2	19.2	21.2	20.0	19.40
Angle of internal friction of the soil (φ ^{o})	18.4	25.8	17.7	23.4	21.32
Unit weight of soil γ (kN/m^3)	17	17.2	16.8	17	17
Gravel (%)	14.4	0	0	2.02	14.90
Coarse Sand (%)	4.28	0.13	8.29	3.75	4.112
Fine Sand (%)	17.31	2.56	38.10	9.20	16.792
Silt and Clay (%)	64.03	97.30	53.61	85.03	74.992

Table. 2. Identification of type of Soil at Slope failure site

Particle Size in mm	Soil Grade (%)	Test Pits			
		I	II	III	IV
80 - 4.75	Gravel	14.4	0	0	2.02
4.75 - 0.075	Sand	21.59	2.69	46.39	12.95
0.075 - 0.002 Less than 0.002 mm	Silt & Clay	64.03	97.30	53.61	85.03
Type of soil @ Test pits		c – ø soil	c – ø soil	c – ø soil	c – ø soil
Overall type of soil @ slope failure site		Black cotton soft soil mixed with sand particles			

The type of soil which is present in the slope failure site is black cotton soil mixed with sand particles as shown in table 2. Gibbs and Holtz in 1956 demonstrated that plasticity index of soil and liquid limit, W_L are very useful parameters for obtaining the characteristics swelling of most clays soil mixed with sand particles. The liquid limit & the swelling of clays soil both are depends on the amount of water absorbs the clay soil to its natural state. The relation between the plasticity index & swelling potential of clay soil are established as given in Table 3.

Table. 3. Relation between swelling potential and plasticity index, I_p

Plasticity Index Ip (%) Range	Swelling potential Range	Plasticity Index Ip of soil @ Test pit of Slope Failure		Swelling Potential	Swelling Potential Result
		Test Pit	*Ip (%)*		
0-15	Low	I	49.7	Very High	Very High
15-20	Medium	II	46.9	Very High	
25-30	High	III	26.8	High	
35 and above	Very High	IV	29.4	High	

Table. 4. Identification of plasticity nature of Soil based on the plasticity index of the Soil

Plasticity Index Ip Range	Plasticity nature of soil	Plasticity Index Ip of soil @ Test pit of Slope Failure		Description	Plasticity Index Ip Result
		Test Pit	*Ip (%)*		
0	Non-plastic	I	49.7	Very High plasticity	Very High plasticity
1-5	Slightly plastic	II	46.9	Very High plasticity	
5-10	Low plastic	III	26.8	High plastic	
10-20	Medium plastic	IV	29.4	High plastic	
20-40	High plastic				
Above 40	Very High plasticity				

Soil colloids particles are very minute and have a large surface per unit area of mass of soil. Colloids are also carrying the electrostatic +ve and -ve charges that are balanced by the adsorbed anions and cations. Therefore, there is a direct relationship between the swelling potential and colloidal content as shown in figure 7. For a given clay type of soil, the amount of swelling of soil will increases with the increase in amount of clay particles present in the soil. The clay mineral which is present the slope failure soil is identified as commercial illite or bentonite, this type of soil usual has more swelling and shrinkage characteristics as shown in table 5.

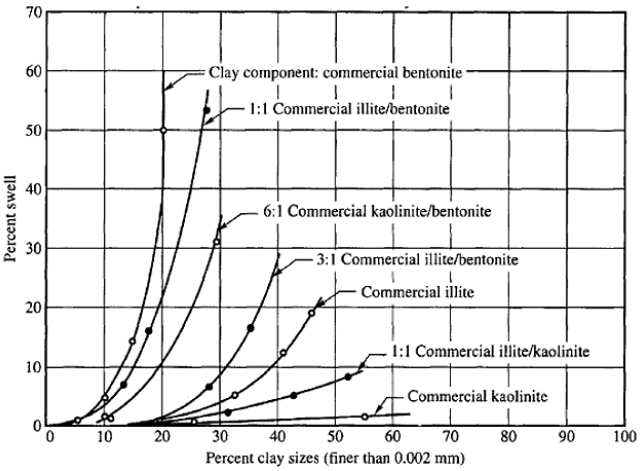

Fig. 7. Percent swell v/s Percent clay sizes

 ISBN: 978-93-90214-20-4

Table.5. Identification of clay mineral of soil

Test pit	Free swell	Percentage of clay size	Mineral present in soil
I	50	64.03	1:1 Commercial illite/ Bentonite
II	20	97.30	Commercial illite
III	54.6	53.61	1:1 Commercial illite/ Bentonite
IV	28.6	85.03	3:1 Commercial illite/ Bentonite

4.1. Major problems faced during the soil slope failure are as follows

a. Very low bearing capacity
b. High settlements (the rate of settlement is very slow and settlement may continue for several years)
c. Instability of deep excavations or Slopes
d. Deep seated slip failure
e. Lateral flow under surface loading leading to settlement
f. Large cracks appearance
g. More swelling potential

4.2. Causes of Earth Slope Failure

It is essential to understand the causes of slope failures, which are indicated in an analysis or which have developed in practice. These causes may be summarised simply as follows:

a) The slope is too high or too steep for materials of which it is composed.
b) The soil is too weak to sustain the slope at its present profile.
c) The pore water pressures are too high due to spring water, and thus adversely affect the soil strength.
d) Gravitational force
e) The slope is affected adversely by some external influence, for example applied loads from structures.
f) The factor of safety provided is very less at the road side
g) The present soil is not a natural soil; it is transported and deposited soil from the above hill slope area.
h) Due to presence of spring water at failure site, the water enters in the soil hence the shear strength soil will be less and expansion of soil taken place, since the slope is failed.

4.3. Earth Slope Failure Mechanism

Mechanism of Slope failure during the wet and hot dry days, the face of the slope become very desiccated and shrunken. The extent and depth of slope failure is depending on mainly the plasticity of the soil and its type of slope protection. During the rainstorm water or spring water, percolates in to the cracks or soil surface, the slope soil mass will starts swelling specially in case of more percentage of black cotton soil presence and saturated with reduction of its shear strength and increasing the voids ratio in the soil mass. Initially percolation of water takes place in the downward direction in the slope soil mass through the desiccation cacks. As the outer surface of the soil slope swells and saturated, parallelly the permeability of the surface soil slope increases with increase in rainfall intensity. Generally, when the shear strength of soil decreases due to saturation and swelling of the soil the shearing resistance of the soil is also decreases and the soil slope failure takes place. It is important to understand in soil mechanics the forces which are acting on the soil slope and which is the main driving force and the resisting force, which can prevent the slope failure. The factor of safety is the most important factor to prevent slope failure, it is the ratio of shearing resistance to the driving force.

5. CONCLUSION

From the above experimental demonstration, it is concluded that, the type soil present in the soil slope failure is identified as black cotton soft soil mixed with sand particles almost 75% of soil is silt and soft clay, therefore it is concluded that the swelling potential of the soil is very high. From plasticity index chart it is observed that the plasticity index Ip of the soil is very high, therefore large cracks are appeared on the surface the soil. The clay mineral which is present in the soil is identified as commercial illite/bentonite. The main causes of soil slope failure are identified as the presence of spring water in the soil slope, very low factor of safety, shear strength of soil is very low, the bulk density of the soil also very less and the presence of soil is huge amount of soil transported by storm water and deposited in slope many years before. The remedial measure provided and suggested a reinforced concrete cantilever retaining wall.

REFERENCE

[1] Abebe, B., Dramis, F., Fubelli, G., Umer, M., Asrat, A., Landslides in the Ethiopian highlands and the Rift margins. Journal of African Earth Sciences, 56, pp. 131-138, 2010.
[2] Alonso, E., Pinyol, N. M., Slope stability in slightly fissured clay stones and marls. Landslides, 10.1007/s10346-014-0526-5, pp.1-25, 2014.
[3] Ayalew, L., The effect of seasonal rainfall on landslides in the highlands of Ethiopia. Bull. Engineering and Geology and Environment, 58, pp. 9-19, 1998.
[4] Fubelli, G., Abebe, B., Dramis, F., Vinci, S., Geomorphological evolution and present-day processes in the Dessie Graben (Wollo, Ethiopia). Catena, 75, pp. 28-37, 2008.
[5] Helwany, S, Applied Soil Mechanics with ABAQUS Applications. John Wiley & Sons, Inc., Hoboken, New Jersey, 2007.
[6] N. C. Samtani, and C. S. Desai "Constitutive modeling and finite element analysis of slowly moving landslides using the hierarchical viscoplastic material model." Rep. to National Science Foundation. Dept. of Civil Engrg. and Engrg. Mech. University of Arizona, Tucson, Ariz, 1991.

[7] N. Samtani, C. S. Desai, and L. Vulliet, An interface model to describe viscoplastic behavior. International Journal for Numerical and Analytical Method in Geomechancis Vol XX, pp. 231-252, 1996.

[8] D. J. Varnes, Slope movement types and processes. In: Schuster, R.L., Krizek, R.J. (Eds.), Landslides-analysis and control. Transportation Research Board Special Report 176. National Academy of Sciences, Washington, DC, pp. 12–33, 1978.

[9] L. Vulliet and K. Hutter, Continuum model for natural slopes in slow movement. Geotechnique vol. XXXVIII, n. 2, pp. 199-217, 1988.

[10] L. Vulliet, and C. S. Desai, "Viscoplasticity and finite elements for landslide analysis."Proc. 11th Int. Cont: on Soil Mech. and Found. Engrg. International Society of Soil Mechanics and Foundation Engineering. Rio de Janeiro, Brazil, 1989.

[11] Burak AKBAS, Nejan HUVAJ. Probabilistic Slope Stability Analyses Using Limit Equilibrium and Finite Element Methods, Geotechnical Safety and Risk V T. Schweckendiek et al. (Eds.), pp 716-721, doi:10.3233/978-1-61499-580-7-716, 2015.

[12] A. Burman, S. P. Acharya, R. R. Sahay and D. Maity, A comparative study of slope stability analysis using traditional limit equilibrium method and finite element, Asian Journal of Civil Engineering, 16(4):467-492, 2015.

[13] Hamid Faiz, Ge Yong-gang Mehtab Alam, Hua Yan, and Izaz Ali1, Stability Analysis of Slopes Based on Limit Equilibrium and Finite Element Methods for Neelum Jhelum Hydropower Project, Pakistan- Case Study, American Journal of Engineering Research (AJER), 9(3): 134-147, 2020.

[14] N. I. Ismail, W. Z. Wan Yaacob and N. Ali, A Slope Stability Analysis at Hilly Areas of Kuala Lumpur Malaysia, International Journal of Engineering and Technology, 11(5): 310-315, doi: 10.7763/IJET. 2019.V11.1167, 2019.

[14] C. Jaeger, The Dynamics of the Slide, Rock Mechanics and Engineering Geology, Journal of the International Society for Rock Mechanics, 6 (4), pp 243-247, 1968.

[15] C. M. Lo, C. F. Lee, H. T. Chou, M. L. Lin, Landslide at Su-Hua Highway 115.9k triggered by Typhoon Megi in Taiwan, Landslides, pp 293–304, 2013.

[16] C. F. Lee, W. K. Huang, C. M. Huang, C. C. Chi, Deep-seated landslide mapping and geomorphic characteristic using high resolution DTM in northern Taiwan, In Workshop on World Landslide Forum, Springer, Cham, Switzerland, pp 767–777, 2017.

[17] C. M. Lo, C. F. Lee, J. Keck, Application of sky view factor technique to the interpretation and reactivation assessment of landslide activity. Environ. Earth Sci, pp 76, 375, 2017.

[18] C. Matthews, Z. Farook & P. R. Helm, Slope stability analysis – limit equilibrium or the finite element method? Technical Paper, Ground Engineering, pp 22-28, 2004.

[19] Pallavi Gupta, Anand Kumar Raghuwanshi and Saurabh Bhargava, Effect of Density and Moisture on the Slope Stability of Highway Embankment, International Journal of Engineering Sciences & Research Technology, 5(7), PP. 10-16, doi: 10.5281/zenodo.56885, 2016, July 2016.

[20] K. Pushpa, Dr. S. K. Prasad, Dr. P. Nanjundaswamy, Critical Analysis of Slope Stability Analysis Methods, International Journal of Engineering Research & Technology (IJERT), 5(7): 128-136, 2016.

[21] J. Peranić, V. Jagodnik, J. Arbanas, Rainfall infiltration and stability analysis of an unsaturated slope in residual soil from flysch rock mass, Proceedings of the XVII ECSMGE, Geotechnical Engineering foundation of the future, pp 1-8, doi:10.32075/17ECSMGE-2019-0906, 2019.

[22] N. Samtani, C. S. Desai and L. Vulliet, An interface model to describe viscoplastic behavior, International Journal for Numerical and Analytical Method in Geomechancis, pp 231-252, 1996.

[23] Vivek, Mandeep Multani, Pooja Rani Sinha and Rohit Tripathi, Slope Stability Analysis, International Journal of Core Engineering & Management (IJCEM), 2(3):121-146, 2015.

[24] R. Vineet, Desai, R. Maulik and Joshi, Slope Stability Evaluations by Limit Equilibrium and Finite Element Method, International Research Journal of Engineering and Technology (IRJET), 6(9): 756-751, 2019

Stress–Strain Behaviour of Bacterial Concrete Incorporated With Sugarcane Fibres

[1] Ms. P.Kala, [2] Mrs. N. Sivakami, [3] Dr. R. Angeline Prabhavathy, [4] Dr.Jessy Rooby

[1] Research scholar, Department of Civil Engineering, Hindustan Institute of Technology and Science, India
[2] Head of Department, Department of Civil Engineering, Government polytechnic college, Karaikudi, India
[3] Professor, Department of Civil Engineering, Hindustan Institute of Technology and Science, India
[4] Head of Department, Department of Civil Engineering, Hindustan Institute of Technology and Science, India

Abstract:

Bacterial concrete is one of the methods of rectifying the micro-cracks developed in the structural elements made of concrete. The gram-positive type bacteria Bacillus subtilis when acquainted with concrete produces calcite precipitation which heals the micro cracks in the concrete. Bacillus subtilis was used with a cell concentration of 10^6. The optimised percentage replacement of fine aggregates with sugarcane fibres of grain size less than 4.75 mm was 0.1 %. The effect of sugarcane fibres on the durability of bacterial concrete is presented in this paper.To study the Stress -Strain behaviour of Sugarcane based Bacterial concrete (SBC), appropriate analytic SS model is developed that resembles the experimental behaviour of the various samples such as Conventional Concrete (CC), Bacterial Concrete (BC) and SBC. This work mainly targets on utilizing the earlier models and offers a new SS model that can well represent the actual SS behaviour of SBC samples. After finding the SS behaviour of CC, BC and SBC specimens experimentally, equations are developed to characterise axial SS behaviour of CC, BC and SBC samples. From these mathematical equations, theoretical stress for CC, BC and SBC are calculated and compared with test values. The proposed equations have exposed good connection with test values authorizing the mathematical model developed.

Keywords:

Bacterial concrete, Stress-Strain curves, Saenz model, Bacillus Subtilis

1. INTRODUCTION

Concrete is generally used as a building material because it is readily available and cheap. The durability of concrete needs to be checked for many reasons namely the expansion of reinforcement bars, freezing and thawing effects, physical damage, chemical damage and crack formation.Formation of cracks is an inevitable quality of concrete structures. Crack formation in concrete structures is the reason for strength loss. They offer substances such as chlorides, carbon dioxide, oxygen and water to enter into it which leads to corrosion. Healing of cracks is necessary to strengthen the concrete structures and to increase the life span and to serve the purpose for which it is intended. Bacterial concrete is a new invention of crack healing in an environmentally friendly manner without human intervention. The cracks are sealed by biologically produced calcium precipitate. A gram positive, rod shaped with tough protective endospore, Bacillus subtilis is used. It can remain viable for decades. In this study, sugarcane fibres are used with bacterial concrete to enhance the biological process of bacteria. Sugarcane fibres increase crack control, ductility and reduce environmental pollution.

For many years, researchers have developed mathematical models for SS relationships to define the nature of concrete in compression. The SS model is a reliable tool to estimate the strength, elongation, contraction and shear behaviour of concrete structural members like beams, columns and slabs. The compressive SS behaviour of concrete is a noteworthy subject in the flexural analysis of RC beams and columns and for exploring the ductility of concrete. The quantity of energy absorbed can also be obtained by calculating the total area under the SS curve.

Figure 1 shows the SS curve of a ductile material. The stress and strain values obtained from the cylinder compressive strength test are plotted here. It is noted from the graph that, the curve does not follow any specific pattern.

Figure 2 shows the SS curve for cement paste and aggregates individually and it is a linear curve. But for concrete, the internal crack formation results in non-linearity of SS curve. After conducting cylinder compressive strength tests for various concrete samples such as CC, BC and SBC**.** the SS behaviour of each sample was analysed. A mathematical model is suggested to confirm the experimental values against the analytical values for CC, BC and SBC specimens.

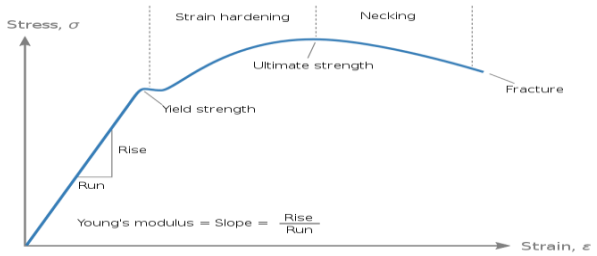

Figure 1 SS curve of a Ductile Material

 ISBN: 978-93-90214-20-4

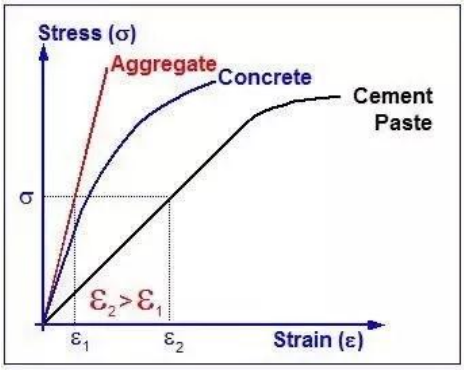

Figure 2 SS curve of cement and aggregates

1.1 Types of Stress and Strain

The types of stress are Normal stress, Shear stress or combination of both. In addition, they can be Uniaxial stress, Biaxial stress and Multi-axial stress. The forms of strain deformation are elongation, contraction, twisting and rotation.

1.2. Types of SS curves

If the stress and strain are calculated using original cross-section and gauge length, then they are designated as Engineering stress and Engineering strain. The curve drawn with these values is named as Engineering stress–strain curve shown in figure 3. If the stress and strain are derived from the reduced area at the time of failure of the specimen, then they are called True stress and True strain. This stage in the SS curve reveals its behaviour, which results in its mechanical properties. There are three stages in the SS curve, which are 1. Linear elastic region, 2. Strain hardening region and 3. Failure region. The area under the SS curve in Figure 4 is the Absorbed energy, which states the nature of ductility of the material.

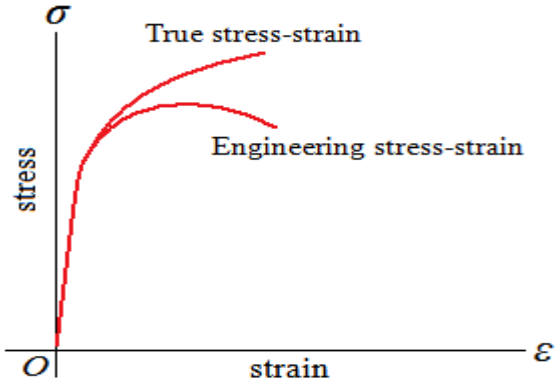

Figure 3 Engineering SSC and True SSC

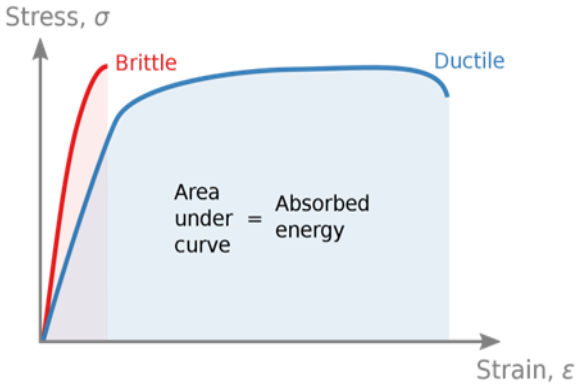

Figure 4 Area of Energy Absorption

2. METHODOLOGY

This paper mainly aims at developing the best aspects of earlier models and suggests a new SS model that denotes the SS behaviour of SBC. After attaining the SS behaviour of CC, BC and SBC experimentally, mathematical equations were developed to signify the axial SS behaviour of CC, BC and SBC mixes. From these equations, analytical stress for CC, BC and SBC were evaluated and compared with test values. The suggested equations have shown better correlation with experimental values, validating the mathematical model formed.

3. EXPERIMENTAL PROCEDURE

In this work, SS behaviour of CC, BC and SBC specimens of strength grade M25 were studied. Cylindrical specimens of size 150 mm diameter X 300 mm heights were cast. There were 3 cylinders made of CC, 3 cylinders of BC and 3 cylinders of SBC. The tests were carried out on each of these specimens. All specimens were subjected to an axial compression as per IS: 516 -1999 to analyse the stress–strain characteristics. The experimental set up was shown in figure 5.

Figure 5 Experimental Setup

 ISBN: 978-93-90214-20-4

4. MATHEMATICAL MODELLING FOR SS PERFORMANCE

Researchers have developed mathematical models for predicting the SS behaviour of concrete. Some models are stated below.

Table 1 Various Mathematical models

Models	Year	Curve Equation	Region	Remarks
Hognestad	1951	$f = f_0\left[2\frac{\varepsilon}{\varepsilon_0} - \left(\frac{\varepsilon}{\varepsilon_0}\right)^2\right]$	Ascending	
		$f = f_0\left[1 - 0.15\left(\frac{\varepsilon - \varepsilon_0}{\varepsilon_u - \varepsilon_0}\right)\right]$	Descending	
Desayi & Krishnan	1964	$f = \frac{E_0\varepsilon}{1 + (\varepsilon/\varepsilon_0)^2}$	Ascending and Descending	(E_0/E_s) Should be equal to 2
Saenz	1964	$f = \frac{E_0\varepsilon}{1 + (E_0/E_s - 2)((\varepsilon/\varepsilon_0) + (\varepsilon/\epsilon_0)^2}$		(E_0/E_s) Should be equal or greater than 2
Wang et al	1978	$f = f_0\left[\frac{A(\varepsilon/\varepsilon_0) + B(\varepsilon/\varepsilon_0)^2}{1 + C(\varepsilon/\varepsilon_0) + D(\varepsilon/\varepsilon_0)^2}\right]$	Ascending A=1.300501 B=-0.835818 C=-0.699498 D=0.1641812	Descending A=0.349777 B=-0.104963 C=-1.650222 D=0.895036
Carreira & Chu	1985	$f = \frac{A(\varepsilon/\varepsilon_0)f_0}{A - 1 + (\varepsilon/\varepsilon_0)^A}$	Ascending and Descending	$A = \frac{1}{1 - (E_s/E_o)}$
Thanoon	1997	$f = f_0\left[\frac{A(\varepsilon/\varepsilon_0)}{(\varepsilon/\varepsilon_0)^3 + B(\varepsilon/\varepsilon_0)^2 + C(\varepsilon/\epsilon_0) + D}\right]$	Ascending and Descending	For Plain Concrete A=1.10; B=-1.30; C=0.75; D=0.65

Table 2 Details of Notations

f	Stress Corresponding to the strain ε
f_o	Maximum Compressive Stress
ε_o	Strain Corresponding to maximum Stress
ε_u	Ultimate Strain
E_o	Initial Tangent Modulus at the Origin
E_s	Secant Modulus at the peak (f_0/ε_0)
A, B, C and D	Constants

4.1. Model for SS behaviour of SBC

Each model was checked with the observed SS values. The experimental data was correlated with Hognestad model, Wang et al model and modified Saenz 's model equations. The normalised stress and strain were calculated for each of the concrete samples. In Saenz's model equation, the constants A, B and C are identified in the ascending portion of the SS curve and D, E and F in the descending portion of the curve. The constants were found by applying the boundary conditions. There were four boundary conditions applied for the Saenz's model equation.

The Hognestad model was also checked with the experimental SS values. It was found that the experimental values were observed to be too different from the theoretical values for the elastic region and also for the failure region. In the middle region, the experimental and theoretical values were found to match.

In case of Wang et al model, the experimental values were in good correlation with theoretical values for the ascending portion and not for the descending portion.

The third trial was done with the Modified Saenz's equation. The equations for the both portions of theoretical SS curve are given below.

$y = \frac{Ax}{(1+Bx+Cx^2)}$ (Ascending portion of the SSC) (1)

$y = \frac{Dx}{(1+Ex+Fx^2)}$ (Descending portion of the SSC) (2)

Where y is the stress at any point; x is the corresponding strain at that point; similarly, the equations for ascending and descending portions of normalised SS curve are given below

$$f/f_0 = \frac{A\prime(\varepsilon/\varepsilon_0)}{(1+B\prime(\varepsilon/\varepsilon_0)+C\prime(\varepsilon/\varepsilon_0)^2)} \quad (3)$$

$$f/f_0 = \frac{D\prime(\varepsilon/\varepsilon_0)}{(1+E\prime(\varepsilon/\varepsilon_0)+F\prime(\varepsilon/\varepsilon_0)^2)} \quad (4)$$

The values of A', B', C', D', E' and F' were calculated by applying the boundary conditions. They are,

1. The ratio of SS ratio is zero at the origin; $(\varepsilon/\varepsilon_0) = 0$; $(f/f_0) = 0$
2. The strain ratio as well as the stress ratio at the peak is unity; $(\varepsilon/\varepsilon_0) = 1$; $(f/f_0) = 1$
3. The slope of the theoretical SS curve is zero; $(\varepsilon/\varepsilon_0) = 1$, $d(f/f_0)/d(\varepsilon/\varepsilon_0) = 0$
4. Record the Strain when $f/f_0 = 0.85$.

The values of A, B, C, D, E and F were calculated by using the equations given below. They are,

$A = A'(f_0/\varepsilon_0),\ B = B'(1/\varepsilon_0), C = C'(1/\varepsilon_0)^2$
$D = D'(f_0/\varepsilon_0),\ E = E'(1/\varepsilon_0), F = F'(1/\varepsilon_0)^2$

4.2 Formation of Theoretical Equations.

Table 3 Constants for ascending and descending portions of non-dimensional SSC

Sample	A'	B'	C'	D'	E'	F'
CC	3	1	1	0.126	-1.874	1
BC	0.35	-1.65	1	0.071	-1.929	1
SBC	0.65	-1.35	1	0.037	-1.963	1

Table 4 Peak Stress and its corresponding strain

CC		BC		SBC	
f_o	ε_o	f_o	ε_o	f_o	ε_o
20.09	0.00065	21.22	0.0006	25.46	0.000353

Table 5 Ascending and Descending Portions Constants for Theoretical SS Curve

Conventional Concrete					
A	**B**	**C**	**D**	**E**	**F**
92723.08	1538.46	2366863.91	3894.37	-2883.08	2366863.91
Bacterial Concrete					
A	**B**	**C**	**D**	**E**	**F**
12378.33	-2750.00	2777777.78	2511.03	-3215.00	2777777.78
Sugarcane Fibres Based Bacterial Concrete					
A	**B**	**C**	**D**	**E**	**F**
46881.02	-3824.36	8025102.52	2668.61	-5560.91	8025102.52

4.3. Assessment of Theoretical Stress using proposed Mathematical Equations

The Engineering SS, True SS and Normalised SS for CC,BC and SBC samples are tabulated in Tables 6,7 and 8 respectively. Figure 6 shows the SS curves of CC, BC and SBC. Theoretical stress have been found using proposed mathematical equations for CC, BC and SBC which are resulting from modified Saenz's model. After developing the equations for SS curves of CC, BC and SBC theoretical values of stress were calculated for each strain value and are tabulated in Tables 9,10 and 11 for CC , BC and SBC . Figure 7 shows the experimental and theoretical SS curves. Figure 8 shows the normalised experimental and theoretical SS curves.The theoretical SS curves were compared with experimental SS curves and found that, a good correlation was found with experimental SS curves for all samples of CC, BC and SBC.

4.4. Determination of Modulus of Elasticity, Secant Modulus and Initial Tangent Modulus

The static modulus of elasticity, E_c, the secant modulus (35–45% of the maximum stress) and initial tangent modulus (the slope of the tangent drawn at the origin of the SS curve) were determined from the stress–strain curve. Table 12 shows the modulus of elasticity of concrete, secant and initial tangent moduli for CC, BC and SBC samples.

Table 6 Engineering Stress and Strains and True Stress and Strains for CC Samples

CC SAMPLE						
Strain in mm	Stress in N/mm²	True Strain mm	True Stress N/mm²	Eff. Plastic strain mm	Normalised Strain mm	Normalised Stress N/mm²
0	0	0	0	0	0.00	0.00
0.00001	1.41	0.00001	1.41	0.00000	0.01	0.08
0.00004	2.83	0.00004	2.83	0.00003	0.06	0.15
0.00011	4.24	0.00011	4.24	0.00010	0.15	0.23
0.00011	5.66	0.00011	5.66	0.00011	0.16	0.31
0.00013	7.07	0.00013	7.07	0.00013	0.19	0.39
0.00017	8.49	0.00017	8.49	0.00016	0.23	0.46
0.00017	9.90	0.00017	9.90	0.00016	0.24	0.54
0.00022	11.32	0.00022	11.32	0.00021	0.31	0.62
0.00025	12.73	0.00025	12.74	0.00024	0.35	0.69
0.00029	13.58	0.00029	13.59	0.00028	0.40	0.74
0.00031	14.15	0.00031	14.15	0.00030	0.43	0.77
0.00032	16.98	0.00032	16.98	0.00031	0.45	0.93
0.00032	18.39	0.00032	18.40	0.00032	0.46	1.00
0.00033	18.96	0.00033	18.96	0.00032	0.46	1.03
0.00065	20.09	0.00065	20.10	0.00065	0.92	1.10
0.00071	18.32	0.00235	20.40	0.00235	1.00	1.00
0.00079	16.10	0.00290	18.40	0.00289	1.11	0.88
0.00085	14.32	0.00313	17.71	0.00312	1.20	0.78
0.00091	11.20	0.00330	15.60	0.00329	1.28	0.61

 ISBN: 978-93-90214-20-4

Table 7 Engineering Stress and Strains and True Stress and Strain for BC Samples

BC SAMPLES						
Strain in mm	Stress in N/mm²	True Strain mm	True Stress N/mm²	Eff. Plastic strain mm	Normalised Strain mm	Normalised Stress N/mm²
0	0	0	0	0	0.000	0.000
0.000027	1.41	0.000027	1.41	-0.000027	0.042	0.073
0.000053	2.83	0.000053	2.83	0.000000	0.083	0.146
0.000073	4.24	0.000073	4.24	0.000020	0.115	0.219
0.000093	5.66	0.000093	5.66	0.000040	0.146	0.291
0.000127	7.07	0.000127	7.07	0.000073	0.198	0.364
0.000153	8.49	0.000153	8.49	0.000100	0.240	0.437
0.000187	9.90	0.000187	9.90	0.000133	0.292	0.510
0.000233	11.32	0.000233	11.32	0.000180	0.365	0.583
0.000267	12.73	0.000267	12.74	0.000213	0.417	0.656
0.000320	14.15	0.000320	14.15	0.000267	0.500	0.728
0.000363	15.56	0.000363	15.57	0.000310	0.568	0.801
0.000413	16.98	0.000413	16.98	0.000360	0.646	0.874
0.000487	18.39	0.000487	18.40	0.000433	0.760	0.947
0.000533	19.81	0.000533	19.82	0.000480	0.833	1.020
0.000600	21.22	0.000600	21.23	0.000546	0.938	1.093
0.000640	19.42	0.000640	19.43	0.000586	1.000	1.000
0.000689	17.42	0.000689	17.43	0.000635	1.077	0.897
0.000701	15.33	0.000701	15.34	0.000647	1.095	0.789
0.000723	15.10	0.000723	15.11	0.000669	1.130	0.778

Table 8 Engineering Stress and Strains and True Stress and Strain for SBC Samples

SBC SAMPLES						
Strain in mm	Stress in N/mm²	True Strain mm	True Stress N/mm²	Eff. Plastic strain mm	Normalised Strain mm	Normalised Stress N/mm²
0	0	0	0.00	0	0.000	0.00
0.000080	1.41	0.00008	1.41	0.00000	0.226	0.06
0.000107	2.83	0.00011	2.83	0.00003	0.302	0.11
0.000133	4.24	0.00013	4.24	0.00005	0.377	0.17
0.000147	5.66	0.00015	5.66	0.00007	0.415	0.22
0.000167	7.07	0.00017	7.07	0.00009	0.472	0.28
0.000173	8.49	0.00017	8.49	0.00009	0.491	0.33
0.000197	9.90	0.00020	9.90	0.00012	0.557	0.39
0.000200	11.32	0.00020	11.32	0.00012	0.566	0.44
0.000200	12.73	0.00020	12.73	0.00012	0.566	0.50
0.000203	14.15	0.00020	14.15	0.00012	0.575	0.56
0.000213	15.56	0.00021	15.57	0.00013	0.604	0.61
0.000220	16.98	0.00022	16.98	0.00014	0.623	0.67
0.000220	18.39	0.00022	18.40	0.00014	0.623	0.72
0.000223	19.81	0.00022	19.81	0.00014	0.632	0.78
0.000237	21.22	0.00024	21.23	0.00016	0.670	0.83
0.000287	22.64	0.00029	22.64	0.00021	0.811	0.89
0.000347	24.90	0.00035	24.91	0.00027	0.981	0.98
0.000353	25.46	0.00035	25.47	0.00027	1.000	1.00
0.000458	23.10	0.00046	23.11	0.00038	1.296	0.91
0.000518	17.32	0.00052	17.33	0.00044	1.466	0.68
0.000558	15.30	0.00056	15.31	0.00048	1.579	0.60
0.000598	12.40	0.00060	12.41	0.00052	1.692	0.49
0.000638	10.10	0.00064	10.11	0.00056	1.806	0.40

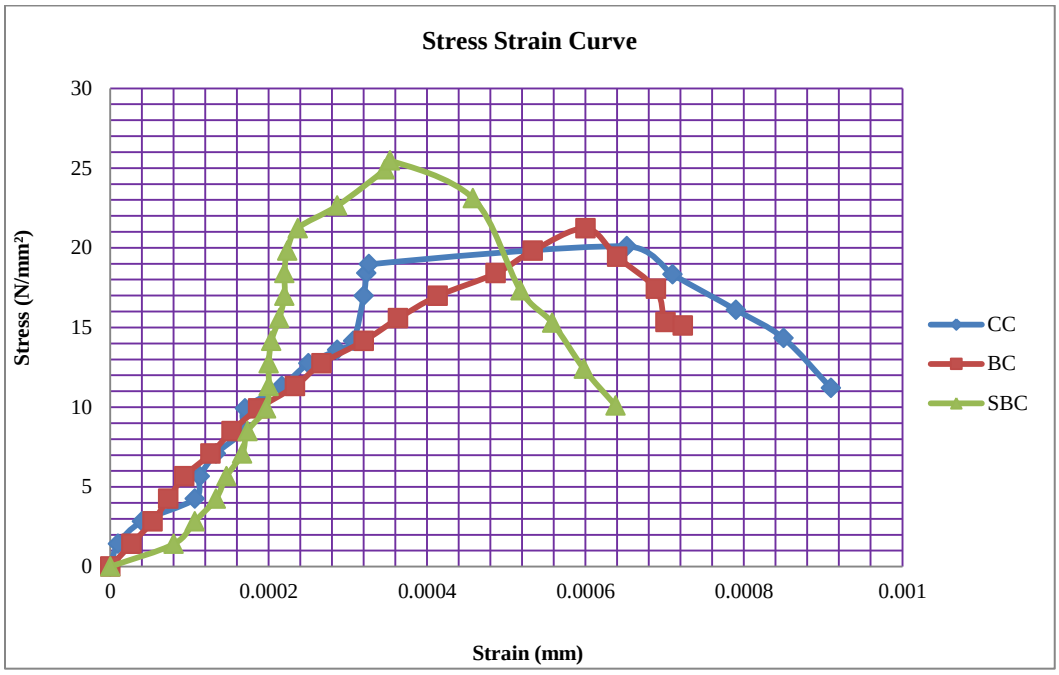

Figure 6 SS curve of CC, BC and SBC samples

Table 9 Experimental and Theoretical SS values for CC samples

CC SAMPLES					
Strain in mm	Experimental Stress N/mm²	Theoretical Stress N/mm²	Normalised Strain mm	Normalised Experimental Stress N/mm²	Normalised Theoretical Stress N/mm²
0	0	0.00	0.00	0.00	0.00
0.00001	1.41	0.91	0.02	0.07	0.05
0.00004	2.83	3.48	0.06	0.14	0.17
0.00011	4.24	8.30	0.16	0.21	0.41
0.00011	5.66	8.72	0.17	0.28	0.43
0.00013	7.07	9.91	0.20	0.35	0.49
0.00017	8.49	11.69	0.26	0.42	0.58
0.00017	9.90	11.85	0.26	0.49	0.59
0.00022	11.32	13.91	0.33	0.56	0.69
0.00025	12.73	15.13	0.38	0.63	0.75
0.00029	13.58	16.25	0.44	0.68	0.81
0.00031	14.15	16.78	0.47	0.70	0.84
0.00032	16.98	17.10	0.49	0.85	0.85
0.00032	18.39	17.18	0.50	0.92	0.86
0.00033	18.96	17.26	0.50	0.94	0.86
0.00065	20.09	20.09	1.00	1.00	1.00
0.00071	18.32	18.92	1.09	0.91	0.94
0.00079	16.10	15.42	1.21	0.80	0.77
0.00085	14.32	12.76	1.30	0.71	0.64
0.00091	11.20	10.53	1.40	0.56	0.52

Table 10 Experimental and Theoretical non-dimensional SS values for BC samples

BC SAMPLES					
Strain in mm	Experimental Stress N/mm²	Theoretical Stress N/mm²	Normalised Strain mm	Normalised Experimental Stress N/mm²	Normalised Theoretical Stress N/mm²
0	0	0.00	0.000	0.00	0.00
0.000027	1.41	0.36	0.042	0.07	0.02
0.000053	2.83	0.77	0.083	0.13	0.04
0.000073	4.24	1.12	0.115	0.20	0.05
0.000093	5.66	1.51	0.146	0.27	0.07
0.000127	7.07	2.25	0.198	0.33	0.11
0.000153	8.49	2.95	0.240	0.40	0.14
0.000187	9.90	3.96	0.292	0.47	0.19
0.000233	11.32	5.67	0.365	0.53	0.27
0.000267	12.73	7.11	0.417	0.60	0.34
0.000320	14.15	9.79	0.500	0.67	0.46
0.000363	15.56	12.24	0.568	0.73	0.58
0.000413	16.98	15.14	0.646	0.80	0.71
0.000487	18.39	18.85	0.760	0.87	0.89
0.000533	19.81	20.41	0.833	0.93	0.96
0.000600	21.22	21.22	0.938	1.00	1.00
0.000640	19.42	20.04	1.000	0.92	0.94
0.000689	17.42	16.71	1.077	0.82	0.79
0.000701	15.33	15.82	1.095	0.72	0.75
0.000723	15.10	14.23	1.130	0.71	0.67

Table 11 Experimental and Theoretical non-dimensional SS values for SBC samples

SBC SAMPLES					
Strain in mm	Experimental Stress N/mm²	Theoritical Stress N/mm²	Normalised Strain mm	Normalised Experimental Stress N/mm²	Normalised Theoritical Stress N/mm²
0	0	0.00	0.000	0.00	0.00
0.000080	1.41	5.03	0.226	0.06	0.20
0.000107	2.83	7.32	0.302	0.11	0.29
0.000133	4.24	9.88	0.377	0.17	0.39
0.000147	5.66	11.24	0.415	0.22	0.44
0.000167	7.07	13.34	0.472	0.28	0.52
0.000173	8.49	14.05	0.491	0.33	0.55
0.000197	9.90	16.52	0.557	0.39	0.65
0.000200	11.32	16.86	0.566	0.44	0.66
0.000200	12.73	16.86	0.566	0.50	0.66
0.000203	14.15	17.20	0.575	0.56	0.68
0.000213	15.56	18.21	0.604	0.61	0.72
0.000220	16.98	18.85	0.623	0.67	0.74
0.000220	18.39	18.85	0.623	0.72	0.74
0.000223	19.81	19.17	0.632	0.78	0.75
0.000237	21.22	20.38	0.670	0.83	0.80
0.000287	22.64	23.86	0.811	0.89	0.94
0.000347	24.90	25.45	0.981	0.98	1.00
0.000353	25.46	25.46	1.000	1.00	1.00
0.000458	23.10	22.20	1.296	0.91	0.87
0.000518	17.32	18.54	1.466	0.68	0.73
0.000558	15.30	17.47	1.579	0.60	0.69
0.000598	12.40	12.39	1.692	0.49	0.49
0.000638	10.10	9.68	1.806	0.40	0.38

Table 12 Modulus of Elasticity and Toughness

Sample ID	Elastic Modulus (GPa)	Toughness (MPa)
CC	29.31	264
BC	31.26	296
SBC	32.13	310

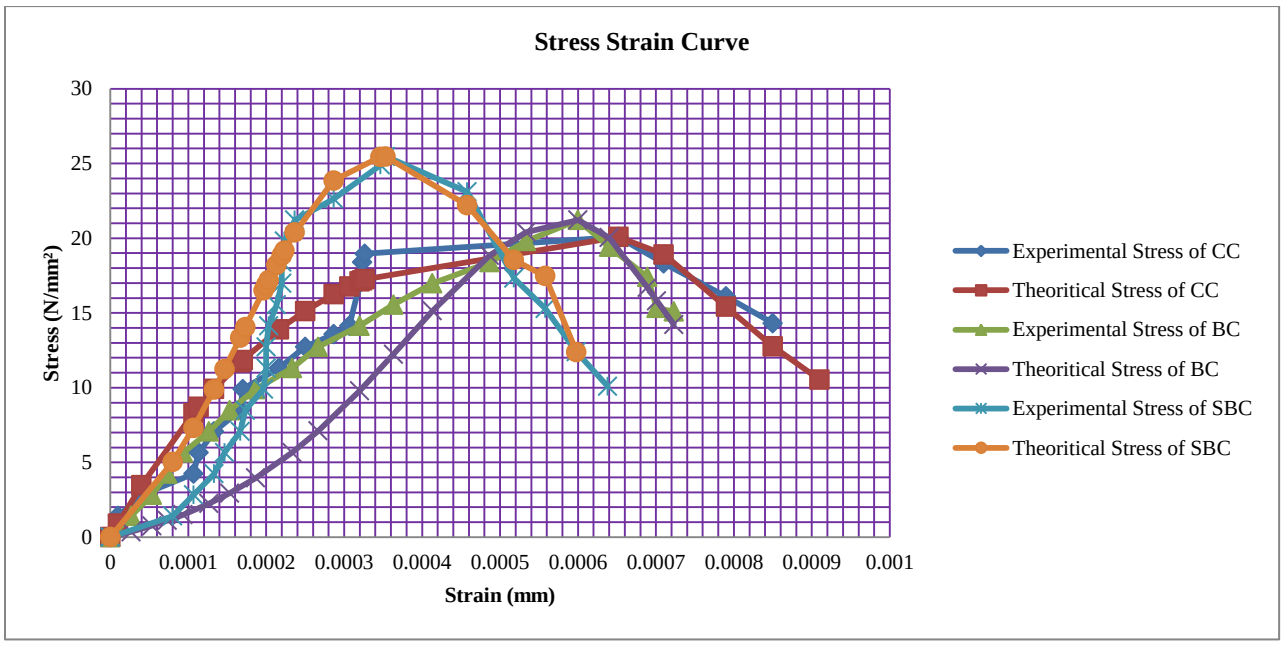

Figure 7 SS curves for various samples

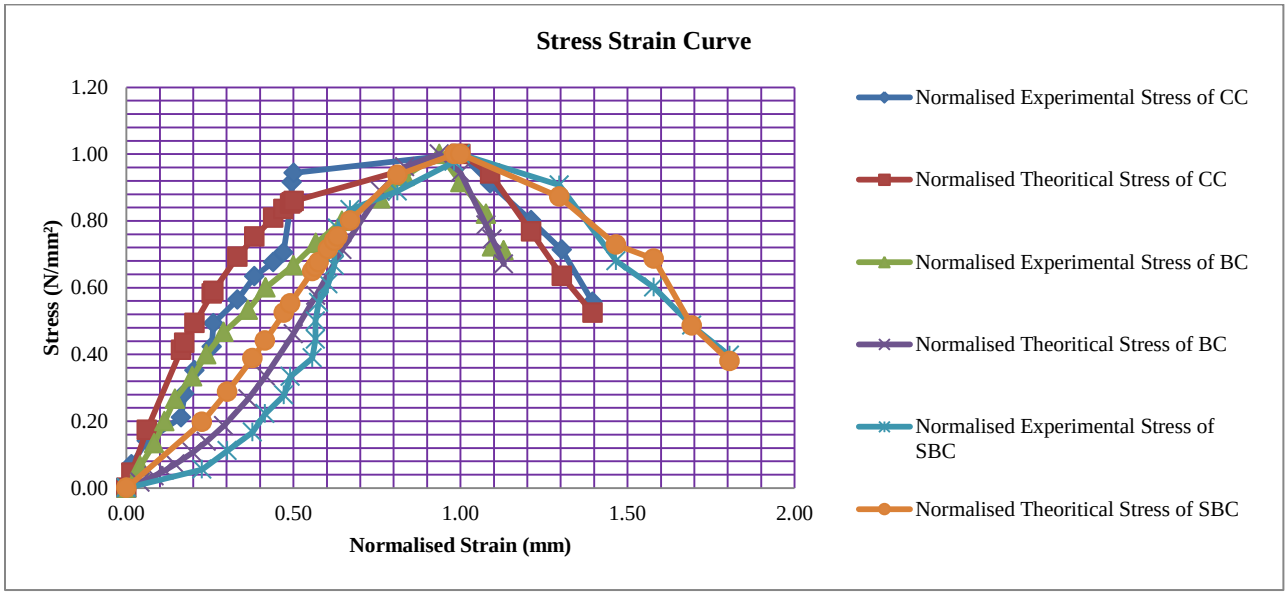

Figure 8 SS curves for various samples (Normalised values)

5. DISCUSSIONS

The Engineering stress and strain, True stress and strain and Normalised stress and strain were tabulated for the samples CC, BC and SBC in the tables 6, 7 and 8.. The stress–strain curves for the CC, BC and SBC were shown in Figure 6.

5.1 SS curves

Figure 6 denotes the SSC of M25 grade SBC. Replacement of small portion (0.1%) of aggregate with Sugarcane fibres in BC has influence on the SSC of concrete. The shape of the SS curve for all the samples were different from each

other. The Peak stress of SBC sample is 25.46 N/mm^2, of BC sample is 21.22 N/mm^2 and for CC sample is 20.09 N/mm^2. The corresponding strains are 0.000353 mm for SBC samples, 0.0006 mm for BC samples and 0.00065 mm CC samples. It is found that the peak stress is maximum for SBC samples.

5.2 Validation of suggested model

The comparative analysis graph of experimental and theoretical SS values was represented in figure 7. The SSC of BC and CC were having similar curve shapes. But the shape of SBC is different. The Normalised experimental and theoretical SS curves are shown in figure 8. The Normalised theoretical values of each sample were in good correlation with its Normalised experimental values. The SBC samples have revealed improved stress values for the same strain levels compared to that of CC and BC samples.

5.3 Modulus of Elasticity and Toughness

Toughness of M25 grade SBC mix has revealed an increase of 4 % and 17 % when compared to same grade of BC and CC mixes.

6. CONCLUSION

From the test results obtained throughout this study, the following conclusions can be made:

1. The SBC samples have shown better stress values for the same strain levels compared to that of CC and BC samples.
2. The strain at peak stress of CC is 0.00065 mm and for BC is 0.00060 mm. but the strain at peak stress for SBC is 0.000353 mm .
3. The Mathematical equations for the SS values of CC, BC and SBC samples have been suggested in the form of y = Ax/(1+Bx+Cx2), both for ascending and descending portions of the curves with different set of constants. The proposed equations have revealed that there is a good connection with test values.
4. The Saenz mathematical model was found to be best suited for analysis of the behaviour of SBC samples.
5. Toughness of SBC sample is increased by 4% when compared to BC and increased by 17% when compared to CC.

REFERENCE

[1] ACI Committee 363, "State-of-the-Art Report on High Strength Concrete," ACI Journal, vol. 81, no. 4, pp. 364-411, July-August, 1984.

[2] Attard, M. M. & Setunge, S. 1996. “SS relation-ship of confined and unconfined concrete.” ACI Materials Journal 93(5): 432-442.

[3] Carreira D, Chu K-H. “SS relationship for plain concrete in compression,” ACI Journal, No. 6, 82(1985)797-804.

[4] Hsu L S, Hsu C T T 1994 “Complete stress–strain behaviour of high strength concrete under compression.” Mag. Concr. Res. 46: 301–312.

[5] K. K. B. Dahl, "Uniaxial SS Curves for Normal and High Strength Concrete," ABK Report no. R282, Department of Structural Engineering, Technical University of Denmark, 1992.

[6] M. M. Attard and S. Setunge, "SS Relationship of Confined and Unconfined Concrete," ACI Materials Journal, vol. 93, no. 5, pp. 432-442, September-October, 1996.

[7] Madhu Karthik Murugesan Reddiar (2009) “SS Model Of Unconfined And Confined Concrete And Stress-Block Parameters,” A MS Thesis, Texas A&M University

[8] P. T. Wang, S. P. Shah, and A. E. Naaman, "SS Curves of Normal and Lightweight Concrete in Compression," ACI Materials Journal, vol. 75, no. 11, pp. 603- 611, November-December, 1978.

[9] Popovics, S. (1973). "A numerical approach to the complete SS curves of concrete." Cement and Concrete Research, 3(5), 583-599.

[10] Saenz LP. Discussion of Paper by Desai P, Krishnan S. “Equation for SS curve of concrete,” Journal of ACI, Proc., No. 9, 61(1964) 1229-35.

[11] Thorenfeldt, E., Tomaszewicz, A., and Jensen, J.J. (1987). "Mechanical properties of highstrength concrete and application in design." Proc. of the Symposium on Utilization of High-Strength Concrete, Tapir, Trondheim, Norway, 149-159.

[12] Tsai, W.T. (1988). "Uniaxial compression SS relation of concrete." J. Struct. Eng., 114(9), 2133-213

Mixed Mode Fracture Toughness for Asymmetric Four Point Bend Specimen of Jute/Glass Fiber Reinforced Epoxy Composite

[1] Vijay Kumar T N, [2] Dr.C M Sharanaprabhu, [3] Dr.Shashidhar K Kudari

[1] Department of Mechanical Engineering B.I.E.T, Davanagere, India
[2] Department of Mechanical Engineering, PESITM, Shivamogga, India
[3] Department of Mechanical Engineering, CVRCE, Hyderabad, India

Abstract:

The demand for hybrid composites for developing a new class of material is in great demand recently. Combination of natural and synthetic fibre yields better mechanical performance. In our work jute/glass reinforced epoxy composites are prepared by using hand layup process. Fracture toughness of the composites are determined for asymmetric four point bend (A4PB) mixed mode specimen. The specimens are fabricated and tested for different s/d ratios. From the experimental values it can be concluded that fracture toughness increases from s/d=0 to s/d=1.

Keywords:

Mixed mode, fracture toughness, Asymmetric, fiber reinforced

1. INTRODUCTION

Over the last decades, some of the testing methods used to determine fracture mechanics properties are compact shear (CS) Double edge notch shear (DENS) End notched flexure (ENF) end-loading shear tests (ELS) are commonly used. There were some drawbacks with these specimens like crack closure and beam specimen geometry. To overcome this asymmetric four point bend test was followed to overcome these disadvantages [1-3]. The fracture toughness of fiber reinforced composite specimens was determined by conducting a test called asymmetric four-point bending test which is basically a bending test specimens with rectangular shaped were prepared. In this test thickness and crack lengths are varied for specimens [4-9]. In many engineering applications to problems the cracks are not transverse to the maximum principal stress direction. Mixed-mode (combined modes I and II) condition exists at the tip of such cracks. Hence, analysis of mixed mode crack problems becomes important in structural related problems. Forecast of crack start and location with its propagation path under mixed-mode loading is desirable for prediction of life in engineering materials. Fiber reinforced polymer composites which are used for aerospace and automobile application comes under failure by mixed-mode loading [10-13]. Hence experimental investigation is necessary for bidirectional Fiber reinforced composites under mixed-mode loading. He and Hutchinson provided accurate results for the stress intensity factors for the asymmetric four-point bend specimen with an initial pre crack. A basic solution for an infinitely long specimen loaded by a constant shear force and a linear moment distribution provides the reference on which the finite geometry solution is based. This note was prompted by a comparison of existing numerical solutions for the crack specimen known as the asymmetric four-point specimen [14-15].

Experimentation

Jute/glass reinforced epoxy laminated composites are having their own applications towards aerospace and automobile and other areas. The present work has carried with the reinforcements like jute and E-Glass and matrix with epoxy resin (Lapox L12) at normal temperature and curing agent hardener (K6).All these products were procured with different suppliers. The bidirectional fibres jute with 210 gsm thickness of 0.87mm and E- Glass with 200gsm of 0.21mm thickness.

Fabrication:

The main purpose is to evaluate the fracture toughness of jute/glass hybrid composite material for two different ratios of thickness and variation of crack length with s/d ratios. For both the conditions of adding with and without of filler material flyash. For the preparation of specimen's common process hand layup technique is used. Layers of fiber mat are placed one above the other according to the calculation of required thickness.

Fracture mixed mode test: Mixed mode (I/II) fracture toughness test for reinforced hybrid polymer composite was conducted according to the guidelines provided by He and Hutchinson. Fracture tests were carried out on A4PB specimens with a thickness of 5.4 and 7.2 mm thickness (B/W=0.3 and 0.4) with pre crack of 5.4, 7.2, mm respectively for both the thickness with and without flyash filler material. Fig. 1 gives the details of major dimensions of the samples used in the tests and Fig. 2 shows mixed mode testing fixture for accepting all the mixed mode distances for A4PB specimens from pure Mode-I to pure

 ISBN: 978-93-90214-20-4

Mode-II. In this test method, a notched specimen was loaded in bending that has initial pre crack. Specimens prepared were loaded on a digital controlled Universal Testing Machine. The specimens were loaded on fixture which are designed and fabricated using mild steel to conduct the fracture test for Mode-I and Mode-II. The test was monitored and conducted at room temperature, as it is very difficult to find the first fracture point damage in laminated composites. In order to overcome this disadvantage, the maximum load that the specimen can sustain are recorded. Using these values of peak load, the fracture toughness KI and KII are calculated. The magnitudes of KI and KII are calculated by analytical formulations given in Eqns.

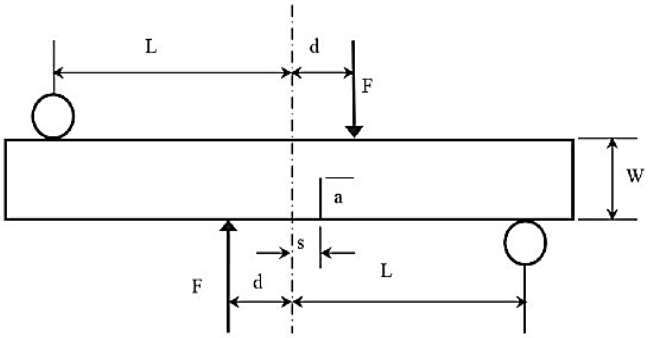

Figure 1: Specimen configuration used in the analyses W=18mm, d= 26mm, L=52mm, a=9mm

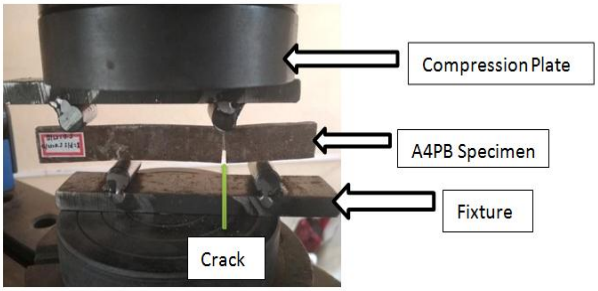

Figure 2: Arrangement of Asymmetric four point bend specimen in UTM

$$KI = \frac{6sQ\sqrt{Ma}}{W^2} F1\left(\frac{a}{W}\right) \quad (1)$$

$$KII = \frac{\left(\frac{a}{W}\right)^{\frac{3}{2}}}{w^2(1-W)^2} FII\left(\frac{a}{W}\right) \quad (2)$$

$$Q = \frac{P(L-d)}{(L+d)} \quad (3)$$

Results and Discussion

The nature of fracture toughness for hybrid reinforced polymer composite is analysed through the results obtained. The specimen loaded for the crack position for both with and without flyash conditions. The crack positions are marked by various s/d ratios with an increase by 0.2. Set of specimens were tested and an average peak load considered as that peak load of the specimen. These peak loads are used to calculate stress intensity factors (fracture toughness). Analytical values are calculated by using equations (1) (2) and (3).

Table 1: Average peak loads of B/W=0.3 a/W=0.3 a=5.4mm without flyash.

s/d Ratios	average peak load P(N)	K1 (MPa m1/2)	K11 (MPa m1/2)	Keff (MPa m1/2)
s/d=0	3300	0	11.36	11.36
s/d=0.2	3200	14.2	11.01	17.96
s/d=0.4	3000	27.56	10.67	29.55
s/d=0.6	2400	31.98	8.26	33.02
s/d=0.8	2200	39.06	7.55	39.78
s/d=1	2100	46.62	0	46.62

Table 2: Average peak loads of B/W=0.3 a/W =0.3 a=5.4mm with flyash.

s/d Ratios	average peak load P(N)	K1 (Mpa m1/2)	K11 (Mpa m1/2)	Keff (Mpa m1/2)
s/d=0	4170	0	20.52	20.52
s/d=0.2	3400	15.11	16.72	22.53
s/d=0.4	3100	28.65	14.76	32.22
s/d=0.6	2700	35.97	13.28	38.34
s/d=0.8	2400	42.64	11.79	44.23
s/d=1	2300	51.11	0	51.11

Table 3: Average peak loads of B/W=0.4 a/W=0.3 a=7.2mm without flyash.

s/d Ratios	average peak load P(N)	K1(Mpa m1/2)	K11 (Mpa m1/2)	Keff (Mpa m1/2)
s/d=0	5130	0	16.81	16.81
s/d=0.2	4200	24.23	13.6	29.37
s/d=0.4	3930	45.35	12.73	47.1
s/d=0.6	2940	50.89	9.52	51.77
s/d=0.8	2730	63.01	8.84	63.62
s/d=1	2340	67.51	0	67.51

Table 4: Average peak loads of B/W=0.4 a/W=0.3 a=7.2mm without flyash.

s/d Ratios	average peak load P(N)	K1(Mpa m1/2)	K11 (Mpa m1/2)	Keff (Mpa m1/2)
s/d=0	5560	0	18.01	18.01
s/d=0.2	4850	27.97	15.69	32.07
s/d=0.4	4200	48.47	13.6	50.34
s/d=0.6	3850	66.68	12.47	67.83
s/d=0.8	3300	69.24	9.71	69.91
s/d=1	2750	79.37	0	79.37

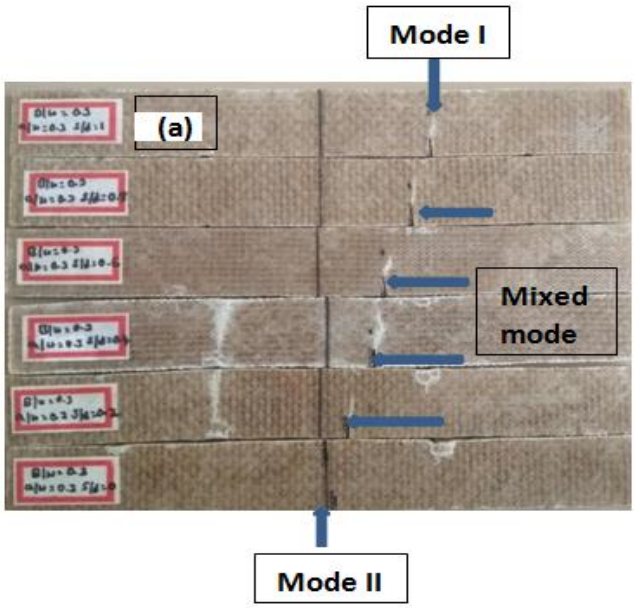

Fig 3: Fractured without flyash specimens of laminates

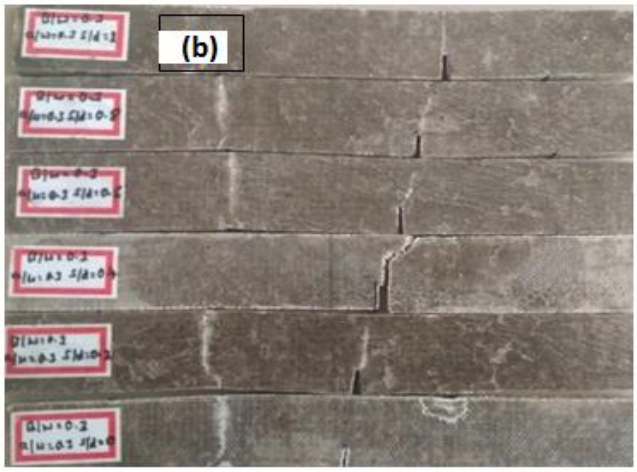

Fig 4: Fractured with flyash specimens of laminates at different loading positionat different loading position

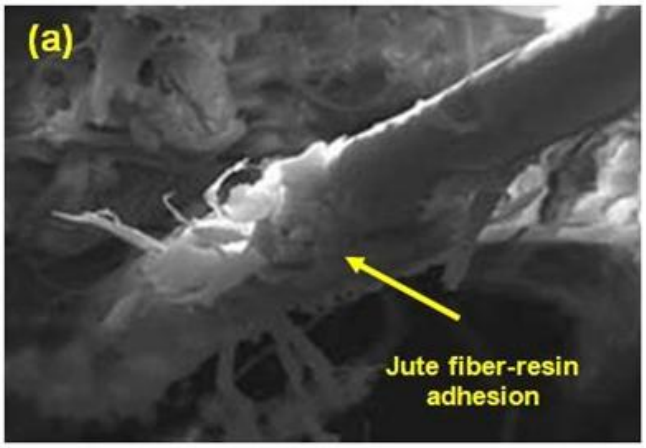

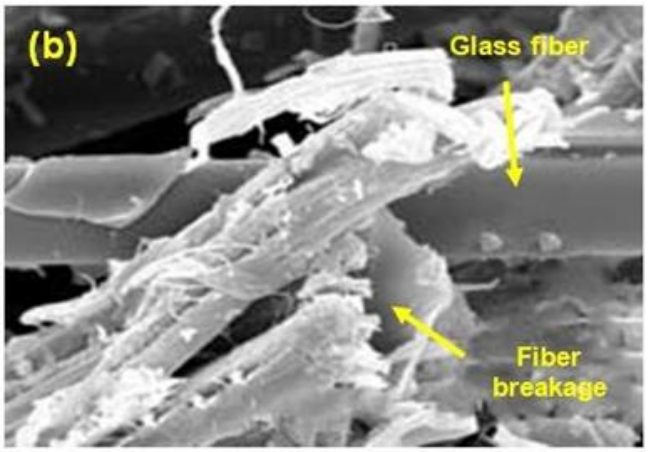

Fig 5: SEM images of jute fiber adhesion and fiber breakage

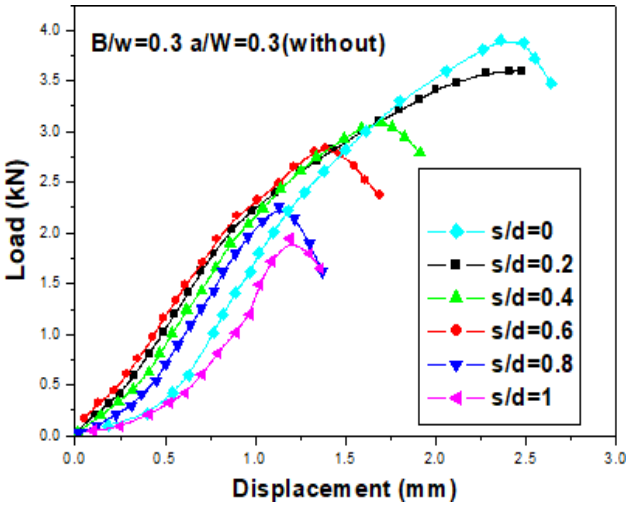

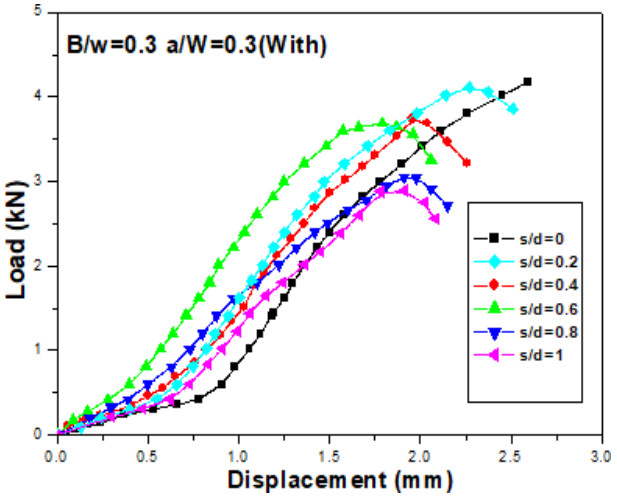

Fig 6: load v/s displacement graph for B/w=0.3 a/W=0.3 without and with flyash

Conclusins: from the experimental results of Keff for both without and with flyash we can conclude that with flyash filler material is giving better results in both the cases of a/W=0.5 and a/W=0.6 So from the data it is proved that by adding additive to the hybrid reinforced composite the properties like basically fracture toughness can be increased. And we can make use of this novelty of using flyash it is best suited for engineering applications.

REFERENCE

[1] Hiroshi Yoshihara "Mode II fracture mechanics properties of wood measured by the asymmetric four-point bending test using a single-edge-notched specimen" Engineering Fracture Mechanics 75 (2008) 4727–4739

[2] Hiroshi Yoshihara "Interlaminar shear strength of medium-density fibreboard obtained from asymmetrical four-point bending tests" construction and building materials 34 (2012) 11-15

[3] Abilash Desai C. M. Sharanaprabhu S. K. Kudari "Experimental Investigation on Critical Energy Release Rate for an Asymmetric Four Point Bending" Conference Paper · June 2018 Research gate.

[4] Abilash Desai C. M. Sharanaprabhu S. K. Kudari "Glass/epoxy fiber orientation effects on translaminar fracture toughness under Mixed mode(I/II) load using FPB specimen" Frattura ed Integrità Strutturale, 53 (2020) 426-433; DOI: 10.3221/IGF-ESIS.53.33

[5] Dragos Alexandra Apostol "Mixed-mode Testing for an Asymmetric Four-point Bending Configuration of Polyurethane Foams" Applied Mechanics and Materials Vol. 760 (2015) pp 239-244

[6] M.R.M. Aliha, M.R. Ayatollahi and B. Kharazi "Numerical and Experimental Investigations of Mixed Mode Fracture in Granite Using Four-Point-Bend Specimen" Fatigue and Fracture Lab., Department of Mechanical Engineering, Iran University of Science and Technology, Narmak, Tehran, 16846, Iran

[7] Xiaolong Dong , Hongwei Zhao, Lin Zhang Hongbing Cheng and Jing Gao "Geometry Effects in Four-Point Bending Test for Thin Sheet Studied by Finite Element Simulation" School of Mechanical Science and Engineering, Jilin University, Changchun 130025, China

[8] Dragos Alexandru Apostol, Dan Mihai Constantinescu, Liviu Marsavina and Emanoil Linul "Mixed-mode Testing for an Asymmetric Four-point Bending Configuration of Polyurethane Foams" Applied Mechanics and Materials Vol. 760 (2015) pp 239-244

[9] Dragos Alexandru apostol , Dan Mihai constantinescu , Liviu marşavina , Emanoil linul " particularities of the asymmetric four-point bending testing of polyurethane foams" U.P.B. Sci. Bull., Series D, Vol. 78, Iss. 2, 2016 ISSN 1454-2358

[10] S. K. Kudari, C. M. Sharanaprabhu "On the relationship between stress intensity factor (K) and minimum plastic zone radius (MPZR) for four point bend specimen under mixed mode loading" International Journal of Engineering, Science and Technology Vol. 2, No. 5, 2010, pp. 13-22

[11] M. Y. He J. W. Hutchinson "Asymmetric Four-Point Crack Specimen" Journal of Applied Mechanics Brief Notes

[12] S.M.J. Razavi, M.R.M. Aliha, F. Berto "Application of an average strain energy density criterion to obtain the mixed mode fracture load of granite rock tested with the cracked asymmetric fourpoint bend specimen" theoretical and applied fracture mechanics.

[13] A.R. Shahani, S.A. Tabatabaei "Effect of T-stress on the fracture of a four point bend specimen" Materials and Design 30 (2009) 2630–2635

[14] Cicilia Maria Erna Susanti, Tetsuya Nakao, Hiroshi Yoshihara "Examination of the Mode II fracture behaviour of wood with a short crack in an asymmetric four-point bending test" engineering fracture mechanics.

[15] Wakako Araki, Kentaro Nemoto, Tadaharu Adachi, Akihiko Yamaji "Fracture toughness for mixed mode I/II of epoxy resin" Available online 23 November 2004 Elsevier

Stabilization of Black Cotton Soil using Waste Shredded Tyre Chips and Powder with Fly Ash for Subgrade

[1] K.Nandini Chandravathi, [2] Dr.S.Krishna Rao, [3] Anil Podeti

[1] Assistant Professor, Civil Engineering Department, VBIT, Hyderabad, India
[2] Professor, Civil Engineering Department, VBIT, Hyderabad, India
[3] Assistant Professor, Civil Engineering Department, VBIT, Hyderabad, India

Abstract:

Pavement construction with Black cotton soils (BC soils) has been a challenge to the highway engineers. In BC soils water has got easy access into the pavement which saturates the sub grade soil and thus lowers its bearing capacity, ultimately resulting in heavy depressions and settlement and the softened sub grade has a tendency to up heave into the upper layers of the pavement, especially when the sub-base consists of stone soling with lot of voids. Black cotton soil having low bearing capacity and high swelling has to be improved by a variety of ground improvement techniques. From Tyre manufacturing industries more waste is being generated which is leading environmental pollution. . In this study, In order to improve shear strength and bearing capacity of the soil, fly ash, shredded tyre chips and tyre powder are used. In the present investigation, shredded rubber tyre powder from waste has been chosen as the reinforcement material at percentage of 10% and 8% and fly ash which is included into the soil at percentages of 12% and 15% by weight of soil. The investigation has been focused on the strength behaviour of soil reinforced with randomly included shredded rubber fibre. The samples were subjected to California bearing ratio and unconfined compression tests. The tests have clearly shown a significant improvement in the shear strength and bearing capacity parameters of the studied soil and also gave the comparison of usage between shredded tyre chips and tyre powder.

Keywords:

Sub grade, Flexible pavement, Tyre chips

1. INTRODUCTION

Properties of soil plays an important role in construction work, because we can change the material if it hasn't good quality, but it is very difficult to replace the soil. If the property of soil is not too good, because the transportation of soil and change of all existing soil is very difficult work. for such condition we use some admixture and material which improve some important property of soil. Method of using low cost material and admixture to improve the property of soil is called soil stabilization. BCS is the inorganic clay of compressibility medium to high. It is rich in montmorillonite mineral because of which it is weakest among all soils. Stabilization of soil improves the properties of soil and make it more stable. The major environmental issue worldwide is solid waste management. Scrap tyres are generated and accumulated in large volumes in India. By using scrap tyres we can reduce environmental problems to some extent. Along with this we are also using fly ash. In this study an attempt is made to improve properties of BCS.

2. OBJECTIVES OF THE STUDY:

The present study is taken up with the following objectives
1. To study the effect of varying percentage of shredded tyre chips and fly ash on properties of black cotton soil.
2. To investigate the combined effect of varying percentage of quantity of shredded tyre chips and fly ash at various percentages on soil.
3. To examine the variation of liquid limit, plastic limit, MDD, OMC, CBR black cotton soil with and without adding tyre chips and fly ash.

3. METHODOLOGY

Among all the soils BCS is occupying most of the places in India. But the problem is its properties are not suitable for construction. So in this study we are conducting investigations on BCS by adding additives and alternative material like tyre powder and tyre chips, and all the properties of soil are checked with different combinations, and comparing all the different combinations.

COMBINATION OF SAMPLES FOR EXPERIMENTAL STUDY: In this project we use 5 types of combinations to improve the properties of black cotton soil.

1. Normal soil (BCS)
2. Combination 1 (BCS + 15% Of Fly Ash +10% Of Tyre Powder)
3. Combination 2 (BCS + 12% Of Fly Ash +8 % Of Tyre Powder)
4. Combination 3 (BCS + 15% Of Fly Ash +10% Of Tyre Chips)

 ISBN: 978-93-90214-20-4

5. Combination 4 (BCS + 12% Of Fly Ash +8 % Of Tyre Chips)

4. EXPERIMENTAL RESULTS

a. PROPERTIES OF BLACK COTTON SOIL:

INDEX PROPERTIES:

Experiments	Test values
Grain size analysis	Well graded soil
Liquid limit	40%
Plastic limit	18.03%
Plasticity index	21.97%
IS classifications	CI
Free swell index	35.3%
Compaction test	OMC=14% & MDD=1.62 g/cc
Permeability test	3.73*10^-3 cm/sec

ENGINEERING PROPERTIES:

Experiments	Test values
California bearing ratio test	1.15 %
Unconfined compressive strength test	0.553 kg/cm^2
Cohesion values	0.276 kg/cm^2

ANALYSIS WITH DIFFERENT COMBINATIONS

Experiment	Normal soil	BCS + 15% Of Fly Ash +10% Of **Tyre Powder**	BCS + 12% Of Fly Ash +8 % Of **Tyre Powder**	Experiment	Normal soil	BCS + 15% Of Fly Ash +10% Of **Tyre chips**	BCS + 12% Of Fly Ash +8 % **Of Tyre chips**
Compaction	OMC=14% MDD=1.62	MDD=1.59 gm/cc OMC=15 %	MDD=1.60 gm/cc OMC=15%	Compaction	OMC=14 % MDD=1.62	MDD=1.56gm/cc OMC=15%	MDD=1.58gm/cc OMC=14%
CBR	2.5mm=1.15% 5mm=1.4%	2.5mm=5.3% 5mm=5.1 %	2.5mm=15.4 % 5mm=13.0%	CBR	2.5mm=1.15% 5mm=1.4 %	At 2.5mm =5.7% At 5mm =5.55%	At 2.5 mm =14.0% At 5mm =12.8%
UCS	Qu=0.553 kg/cm^2 C=0.276kg/cm^2	Qu=2.35 kg/cm^2 C=1.17kg/cm^2	Qu=8.10 kg/cm^2 C=4.05 kg/cm^2	UCS	Qu=0.553 kg/cm^2 C=0.276kg/cm^2	Qu=3.64 kg/cm^2 C=1.82kg/cm^2	Qu=8.2kg/cm^2 C=4.1kg/cm^2

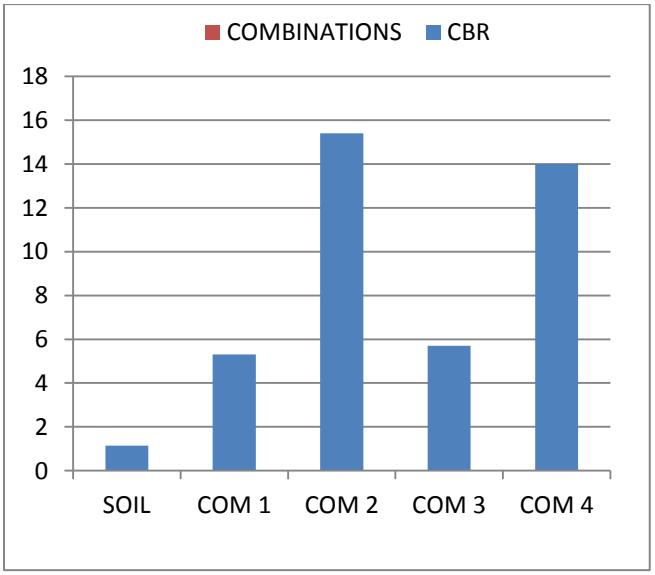

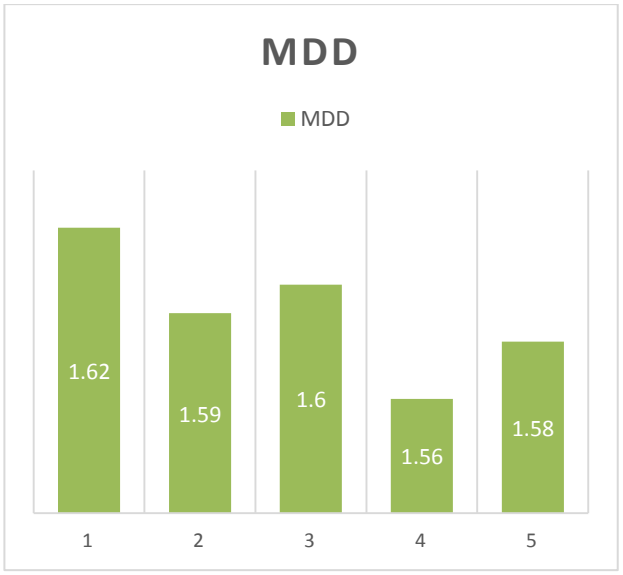

 ISBN: 978-93-90214-20-4

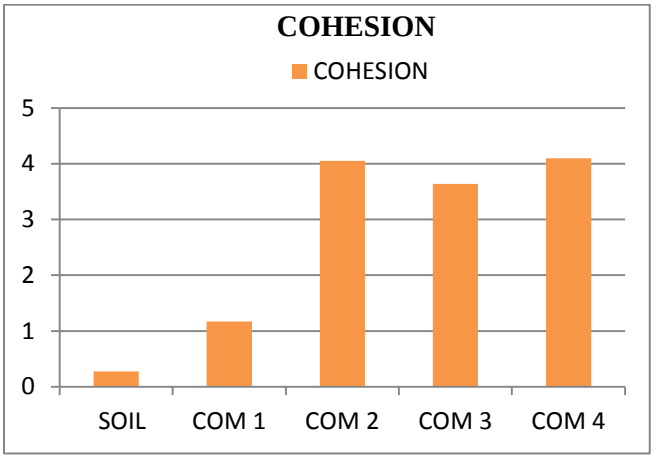

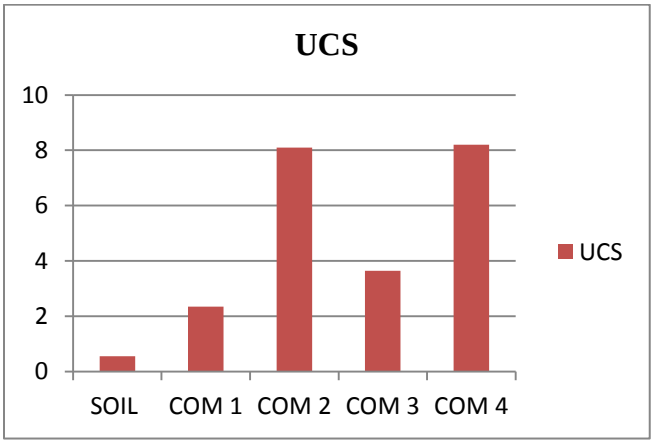

5. CONCLUSIONS

1. The study shows that as the % of shredded tyres increases, the MDD of soil decreases due to addition of light weight material.
2. Finally the black cotton soil properties are improved by adding of tyre chips and fly ash.
3. We tried improvement in CBR and unconfined compressive strength to the black cotton soil.
4. According to MORTH specification For subgrade of pavement CBR value must be >10%,we got the CBR value is 15.4% The % of shredded tyre chips, powder and fly ash increases ,the CBR ,UCS and Cohesion values are decreased. so addition of shredded tyre is restricted to 10 % only. So, we can use this black cotton soil for subgrade in pavements

REFERENCE

[1] Yilmaz, A. and Degirmenci, N. (2009). Possibility of using waste tire rubber and fly ash with Portland cement as construction materials. Waste Management, 29 (5) 1541-1546

[2] Ayothiraman,R., Abilash Kumar Meena.,. Improvement of subgrade soil with shredded waste tyre chips. Proceedings of Indian Geotechincal Conference kochi, Paper no H –003. 2011, pp.365–368.

[3] Ayothiraman,R., Abilash Kumar Meena.,. Improvement of subgrade soil with shredded waste tyre chips. Proceedings of Indian Geotechincal Conference kochi, Paper no H –003. 2011, pp.365–368

[4] GhatgeSandeepHambirao1,Dr.P.G.Rakaraddi, Soil Stabilization Using Waste Shredded Rubber Tyre Chips, e-ISSN: 2278-1684,p-ISSN: 2320-334X, Volume 11, Issue 1 Ver. V (Feb. 2014)

A Brief Overview of Artificial Intelligence in the field of Medical and Healthcare

[1] Rishabh Rawat, [2] Rohan Praksh, [3] Dr. Yasha Hasija

[1][2] B.Tech., Delhi Technological University, India
[3] Associate Professor, Delhi Technological University, India

Abstract:

Artificial Intelligence is the branch of computer science and engineering which is redefining the task which requires human intelligence. The field of AI is rapid and fast growing. Artificial Intelligence (AI) is powered by the availability of large datasets, new deep learning algorithms, and substantial advances in computing power. The programs can be conveniently used for collection of radiology data (X-ray / CT scan / MRI scan) from images that are usually visually noticeable, potentially enhancing the prognostic & diagnostic value extracted from the image dataset. AI is even fueling the debate of whether or not it will replace human radiologists in the future. In this review, we will first briefly look at what AI is, how it has developed over time, and where is it being used in the field of healthcare.

Keywords:

Artificial Intelligence, Medical, Healthcare

1. QUICK OVERVIEW IF ARTIFICIAL INTELLIGENCE IN HEALTH CARE

1.1 What is AI and what are its benefits?

AI is the branch of engineering and computer science which tries to engineer intelligence into machines to solve complex problems that would otherwise require human cognitive function. The four main benefits that Artificial Intelligence brings is that –

In the heart of Artificial Intelligence comes Machine Learning. The machine may use several probabilistic models and neural networks, which would provide a framework for Learning and Understanding. This has emerged as one of the principal theoretical ways for re-engineering machines that would learn itself from the data that it acquires through experiences.[1]

In the 1950s, AI was introduced and had an influence on different areas, gamming finance and marketing. In the area of healthcare, however, the greatest influence of AI has been. Artificial intelligence will contribute an additional 15.7 trillion to the world economy by 2030, according to the latest PwC report, with a 26 percent boost to local economies, and the biggest impact will be in the area of healthcare.[2]

1.2 Reasons behind the growth in healthcare

The three major reasons behind the growth of AI in healthcare industry is String Availability of medical data now[3]–[5]: We generate abundant of medical data on daily basic. Data from smartphones, smart-watches, and medical records are easily available.

Introduction and development of complex algorithm[6]–[8]: With the availability of huge higher dimensional data, AI systems requires an faster and efficient algorithms to process. It is difficult for machines to process and analyze data of these dimension. But this problem became simpler when Deep learning and neural Network were introduced.

Increase in commercially available computational power has been a major reason behind the growth of AI. Neural network and deep learning models requires huge computational power[9]. Because of new research and development powerful GPUs are commercially available at affordable cost[10], [11].

1.3 Motivation

Medical literature extensively discusses the advantages of Artificial Intelligence. [12]. AI uses a sophisticated algorithm to learn from the vast volume of healthcare data. AI models can learn and correct themselves, based on the feedback, in order to increase its accuracy. It can also assist human doctors and physicians by providing them the

 ISBN: 978-93-90214-20-4

medical information from various online & offline sources to ensure proper care of the patient[13]. AI can also help in reducing various therapeutic and diagnostic errors that occurs in clinics. AI can also extract relevant patient's information in real time by taking various smart devices into account, such as smartphone, smart bands, smart watches, wearable bio sensors etc, which are connected to cloud based services[14].

More and more Startups in the Health domain have started to use AI in their business.

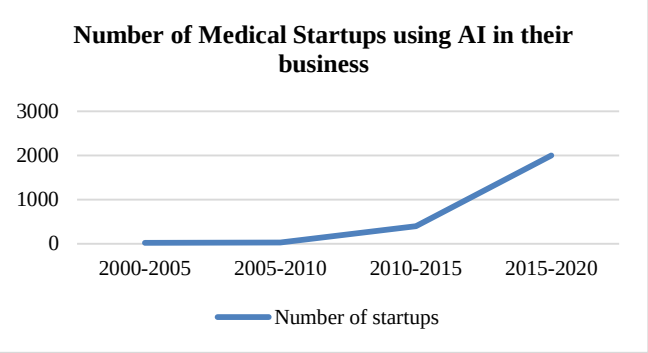

Fig 1: The graph shows number of Medical startups from the year of 2000 to 2020.

2. DEVELOPMENT OF ARTIFICIAL INTELLIGENCE

2.1 Early Rule Based Systems

Simple rule-based systems demonstrated potential for effective diagnosis and treatment of disease in the 1970s, but because these systems were not better than humans and also did not had proper well defined integration with commercial clinical workflow, resulted in poor adaptation of these systems[15].

2.2 Expert systems – The very First Demonstration of AI

The first successful demonstration of Artificial Intelligence was expert systems in the 1980s. The dominant technology for the stimulation of artificial intelligence was expert systems back in the 1980s, which was even widely adopted commercially in that and later times. "It was based on a simple principle of "if-else," like "if it's hot, get an ice cream".

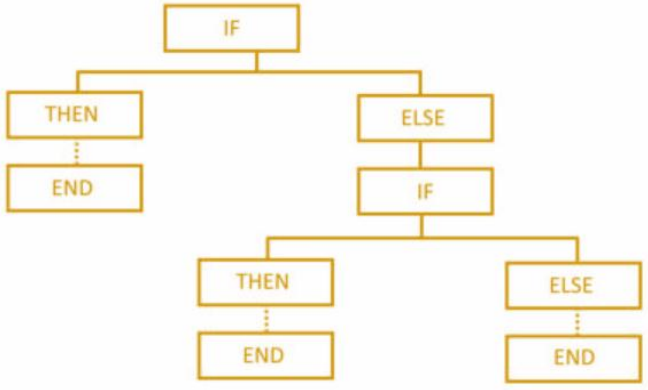

In the field of healthcare, they were welcomed to be used as the assistance in decision support for some decades. Some are still being used. Many of these 'rule-based systems' are still in use today since these guidelines are refined today by Electronic Health Record (EHR) with their systems.

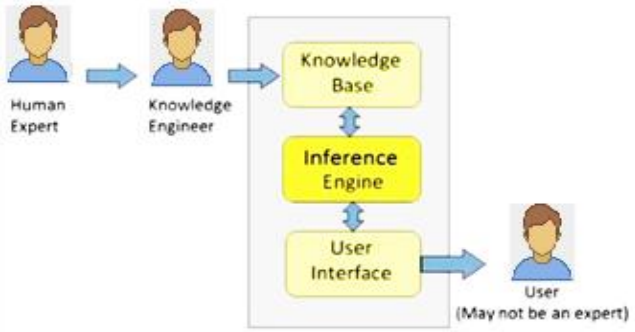

Fig2: a pictorial representation of how expert systems are made [16]

These expert systems worked on the simple decision tree logic. Generally, human experts and knowledge engineers are used to laying down the rules for these systems in order to predict the outcome. But the problem comes when we have thousands of attributes in data. In those cases, rules begin to conflict and time-consuming. Another problem was that if there is any update in knowledge, then the whole logic/decision tree changes, ie. A small change or update insignificance of attributes results in completely different decision rules.

2.3 Age of Deep Learning and Machine Learning

The main problem with the Expert systems was it was not robust with the new Electronic Health Record (EHR). With the rapid advancement in commercially available computing power and complex algorithm, more reliable systems have been developed.

In health care, machine learning is used in personal medicine, predicting the treatment protocol and the likelihood of patient success[17]. This precision in medicine application/prediction comes under a supervised learning approach, in which training data's outcome is known. The neural network is more complex form of AI and is widely used for machine learning. Since the 1960s, the idea of the neural network has existed and is now well known in healthcare research[18]. This has been used for numerous categorical purposes, such as predicting whether or not a specific illness is contracted by the patient. It uses features or variables or dataset attributes as its inputs. It works much like how our brain's neurons operate, but the comparison to the functions of the brain is comparatively week-long. The neural network is also very capable of mimicking the cognitive actions of humans.

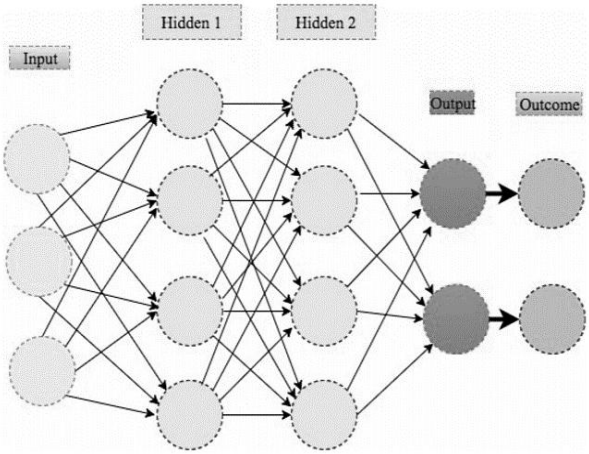

Deep learning is advanced form of neural network. It can be described as a neural network with several hidden layers or variables to predict the outcome. These layers are also called hidden layers. One may use tens or thousands of hidden layers in such models; this would dramatically increase the precision but requires huge computational power in the training phase. Today's graphical processing units and cloud architecture make it easy for researchers to work on it, and the computational power is increasing every day. Deep learning is another common applications in radiology feild(CT/x-ray/PET/MRI scans).

Potential cancerous lesions, early predictions, and detections are being used and are also a hot research area for most researchers[19]. Deep learning is being used extensively in radiology because of its complex data, where even human physicians have high chances of errors[12], [20][21]. The graph below shows a simple comparison of the overall performance of Artificial Intelligence VS Human radiologist.[22]

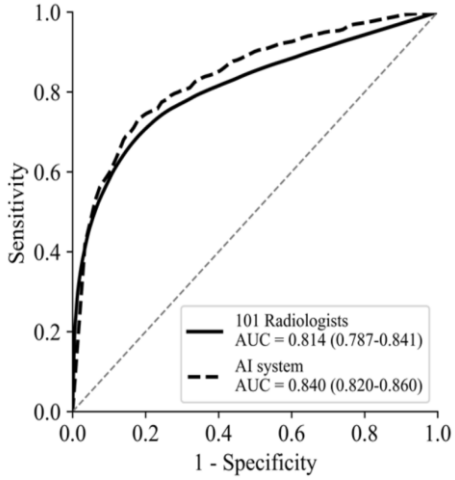

Fig Overall performance of AI vs. 101 Radiologists[22]

For the recognition of speech, extracting digital data and records from physical notes or records can also be done using deep learning is often increasingly used. Unlike a probabilistic or statistical model, each internal layer and variables of the model has absolutely no meaning to the human researcher. Which makes model difficult to comprehend.

3. APPLICATIONS OF ARTIFICIAL INTELLIGENCE IN THE FIELD OF HEALTH CARE

We can broadly differentiate the use of AI in Healthcare industry into six domains

- Drug discovery and Manufacturing
- Disease identification and manufacturing
- Personalised medicine treatment
- Medical Imaging
- Personalised Medical Treatment
- Smart Health Records

3.1 Personalized Medicine

The term personalized medicine was first introduced in 1999, a short article that described SNP (Single Nucleotide Polymorphism) as a link to track genetic disease[23]. The aim behind this is to find the possibility for a drug design to target the patient's genetic and molecular makeup[24]. This approach is based on scientific advances in understanding how the unique human profile of cells and genes makes cell susceptible to certain diseases. The research gave a the idea that this knowledge can be used in the field of personalized and precision medicine for individuals and can also be used to predict the patient's disease faster, based on its genetic makeup.

For reference, BRAF (humans genome) that is responsible for the creation of B-Raf protein in human and is involved in transmitting signals within cells to control cell proliferation which have been shown to mutate into cancer[25]. In 2011, a drug named vemurafenib, a B-Raf protein inhibitors, & a BRAF V600E mutation trial companion were recommended for the treatment of menstrual melanoma. Vemurafenib is effective for treating individuals who are being screened for V600E_BRAF mutation cancer. Around 60 percent of melanoma infected people have a this mutation and about 90 percent of melanoma infected individuals have BRAF mutation.[26]

Advances in advanced testing, advanced biomedical research of data and technologies, such as DNA sequencing, photographic contracts, and wireless health monitoring devices, have created the need for researchers to develop strategies for analyzing, compiling, and translating large amounts of data. Although various mathematical approaches are designed to embrace the 'big data' generated

by these experiments, experience with the use of AI techniques suggests that they may be particularly useful[27]. In addition, the use of a wide range of biomedical technology in research studies has shown that people vary widely in genetic, chemical, physical, expression, and behavioral levels, especially in terms of disease processes and treatment response. This suggests that sometimes there is a need to tailor, or 'customize,' the medication into sharp and often distinct traits for individual patients. Given the importance of data research to reveal the right policies and strategies for personalized medicine[28]. This is where AI comes in and can deliver major advantages in tackling the crucial obstacles that health care professionals face when it comes to big data-speed, scale, diversity, and validity. In fact, almost 80 per cent of respondents in the recent Oracle Health Sciences survey suggested that they expect AI and ML to enhance individual care predictions and recommendations[29].

The advantages are clear. With the strength of AI and machine learning capabilities, pharmaceutical firms can obtain, store and interpret vast data sets faster than handmade processes. This allows them to carry out testing more rapidly, based on genetic variation in patients' considerable resources, and to create tailored therapies more quickly. It also provides a good picture of how small, unique groups of patients with shared characteristics respond to medication so that they can measure the costs and doses of care they can provide to individuals.

3.2 Smart Health

With the ever-growing world population, the general appointment of patients and doctors is no longer valid. Therefore, Smart health care is very important. Smart health care can be used at all levels, from monitoring children's temperature to tracking various medical implications in the elders[30]. Some of the common sensors used for measuring blood pressure, electrocardiogram (ECG), blood glucose, temperature, oxygen saturation, electromyogram, gyroscope, and heart rate, generate huge data store in databases for further analysis. It was estimated that such sensors create more than 2.5 million terabytes of data in a single day. The data are analyzed to provide feedback and prescription to the patients[31]. These healthcare services, which are provided by using wearable devices, fall into Mobile health systems[32]. Mobile health systems are needed, in particular where health clinics are needed, where hospitals are situated away from individuals and groups, or where Medicare is comparatively inexpensive[33]. Neural Language Processing and Machine Learning can create automatic retrieval information assistance across multiple data sources and provide diagnostic methods[32]. Data collection using smart sensor nodes as wearable devices or inside the body of the patient is the first stage. Furthermore, this access points are associated to login sites or gateways or to portable devices. Connected applications communicate with patients and medical personnel at home, in the office or elsewhere. Mobile health systems and wearables such as wearable biosensors, fitness watches works in collaboration with cloud services for data storage. Applications like these are available and provide great flexibility, draw the attention of patients and reduce the cost of health care[34]. Since it has four major features, Includes coherent phrases, visual aids, welcoming controls, and instant contact networks, these apps are rich in offering a great forum for patients. After the processing of data, Data should be preprocessed before submitting it to some Machine Learning Algorithm. Data preprocessing allows to disinfect, format, and arrange the raw data. The Cardiovascular Disease database based experiment focused on 200 patients. Various Machine learning algorithms, such as KNN, SVM, Naive Bayes Model are used and algorithm’s precision, sensitivity and specificity are measured which are used to identify patients[35].

The outcome of different Machine Learning algorithms on the same set of data sets allows to determine which model can produce a meaningful result and the best rating in term of accuracy, sensitivity and specificity. With the rise of innovations in the area of artificial intelligence, Mobile health systems integrate with these technologies to help people monitor their health-related data, and this will also assists in various diagnostic and disease prediction of the patients[36].

3.3 Disease Prediction

Evolution is inevitable and unexpected. Infectious, fast-growing disease-causing viruses and bacteria can cause a great burden of illness and death. In addition to substantial developments in the diagnosis, care and prevention of infectious diseases, the advent of emerging diseases continues to be a significant problem for people around the globe[37], This problems highlighting the need for improved action to tackle them. A recent example is the SARS COVID19, which was first identified in Wuhan, China, it later on matured and spread to become a global pandemic. With the rise of broad data in the scientific and healthcare domain, reliable interpretation of diagnostic data favors early identification, patient treatment and community services[38]. However, the precision of the study is reduced where the consistency of the medical data is insufficient. Different areas also have different features of particular regional pathogens, which can decrease the prognosis of outbreaks of disease. The graph below shows the accuracy of various ML algorithms such as CNN, RNN, Naïve Byes, decision tree and neural for the to prediction of diseases such as Coronavirus and Hypertension.[39]

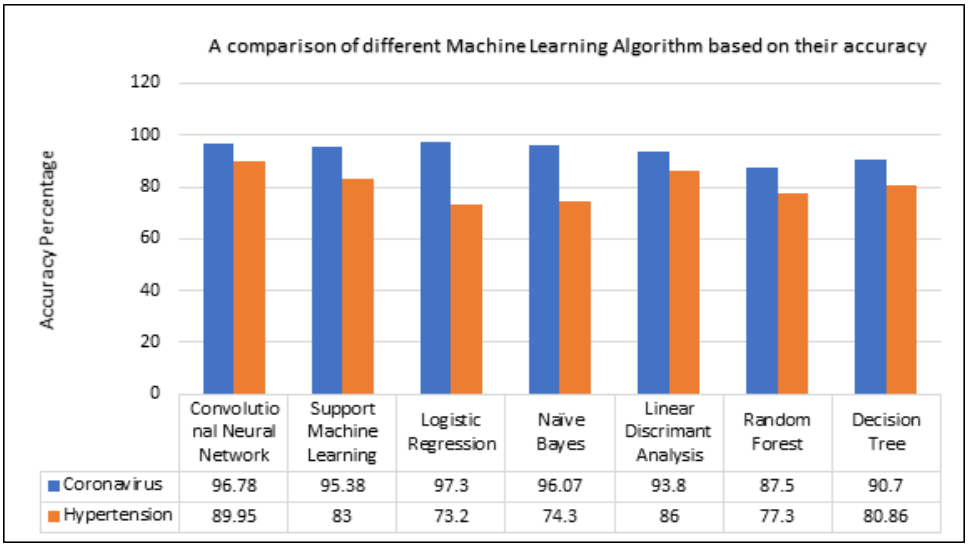

M. Chen proposes a new algorithm for predicting CNN disease risk using a systematic and informal algorithm hospital details. They have made prediction models for diabetes, cerebral palsy, and heart disease. Prediction is based on structured data. The prediction models are based on different ML algorithms and models such as the KNN, random forest etc. The decision tree algorithm's result is better than Naïve Bayes and the KNN algorithm.[40] He also created a CNN based model that predicts the level of risk of developing Cerebral Infarction. The accuracy of the disease prediction models reaches up to 94.8%. This paper used structured as well as unstructured data in training and testing the model.

REFERENCE

[1] Z. Ghahramani, "Probabilistic machine learning and artificial intelligence," *Nature*. 2015, doi: 10.1038/nature14541.

[2] Deloitte, "No Title," 2018. www2.deloitte.com/content/dam/insights/us/articles/4780_State-of-AI-in-the-enterprise/AICognitiveSurvey2018_Infographic.pdf.

[3] J. P. Cohen, P. Morrison, L. Dao, K. Roth, T. Q. Duong, and M. Ghassemi, "Covid-19 image data collection: Prospective predictions are the future," *arXiv Prepr. arXiv2006.11988*, 2020.

[4] T. Barrett *et al.*, "NCBI GEO: Archive for functional genomics data sets - Update," *Nucleic Acids Res.*, 2013, doi: 10.1093/nar/gks1193.

[5] T. Barrett *et al.*, "NCBI GEO: archive for high-throughput functional genomic data," *Nucleic Acids Res.*, vol. 37, no. Database, pp. D885–D890, Jan. 2009, doi: 10.1093/nar/gkn764.

[6] S. Pouyanfar *et al.*, "A survey on deep learning: Algorithms, techniques, and applications," *ACM Computing Surveys*. 2018, doi: 10.1145/3234150.

[7] L. Liu *et al.*, "Deep Learning for Generic Object Detection: A Survey," *Int. J. Comput. Vis.*, vol. 128, no. 2, pp. 261–318, Feb. 2020, doi: 10.1007/s11263-019-01247-4.

[8] A. Shrestha and A. Mahmood, "Review of deep learning algorithms and architectures," *IEEE Access*. 2019, doi: 10.1109/ACCESS.2019.2912200.

[9] T. Ridnik, H. Lawen, A. Noy, E. Ben Baruch, G. Sharir, and I. Friedman, "TResNet: High Performance GPU-Dedicated Architecture," *arXiv*, Mar. 2020, [Online]. Available: http://arxiv.org/abs/2003.13630.

[10] B. R. Boswell, M. Y. Siu, J. H. Choquette, J. M. Alben, and S. Oberman, "Generalized acceleration of matrix multiply accumulate operations." Google Patents, 2019.

[11] C. Gao, D. Neil, E. Ceolini, S.-C. Liu, and T. Delbruck, "DeltaRNN," in *Proceedings of the 2018 ACM/SIGDA International Symposium on Field-Programmable Gate Arrays*, Feb. 2018, pp. 21–30, doi: 10.1145/3174243.3174261.

[12] S. E. Dilsizian and E. L. Siegel, "Artificial intelligence in medicine and cardiac imaging: Harnessing big data and advanced computing to provide personalized medical diagnosis and treatment," *Curr. Cardiol. Rep.*, 2014, doi: 10.1007/s11886-013-0441-8.

[13] Pearson. Tony, "IBM Watson -- How to replicate Watson hardware and systems design for your own use in your basement (Inside System Storage)," *IBM- Blog*. 2011.

[14] H. Shin *et al.*, "Electrodiagnosis support system for localizing neural injury in an upper limb," *J. Am. Med. Informatics Assoc.*, vol. 17, no. 3, pp. 345–347, May 2010, doi: 10.1136/jamia.2009.001594.

[15] J. Bush, "How AI Is Taking the Scut Work Out of Health Care.," *Harvard Bus. Rev. Digit. Artic.*, 2018.

[16] A. Team, "No Title," 2020. .

[17] S.-I. Lee *et al.*, "A machine learning approach to integrate big data for precision medicine in acute myeloid leukemia," *Nat. Commun.*, vol. 9, no. 1, p. 42, Dec. 2018, doi: 10.1038/s41467-017-02465-5.

[18] M. Sordo, "Introduction to Neural Networks in Healthcare," *Knowl. Manag. Med. care*, 2002.

[19] R. Fakoor, F. Ladhak, A. Nazi, and M. Huber, "Using deep learning to enhance cancer diagnosis and classification," *Proc. ICML Work. Role Mach. Learn. Transform. Healthc.*, 2013.

[20] V. L. Patel *et al.*, "The coming of age of artificial intelligence in medicine," *Artif. Intell. Med.*, 2009, doi: 10.1016/j.artmed.2008.07.017.

[21] C. S. Lee, P. G. Nagy, S. J. Weaver, and D. E. Newman-Toker, "Cognitive and system factors contributing to diagnostic errors in radiology," *American Journal of Roentgenology*. 2013, doi: 10.2214/AJR.12.10375.

[22] A. Rodriguez-Ruiz *et al.*, "Stand-Alone Artificial Intelligence for Breast Cancer Detection in Mammography: Comparison With 101 Radiologists," *JNCI J. Natl. Cancer Inst.*, vol. 111, no. 9, pp. 916–922, Sep. 2019, doi: 10.1093/jnci/djy222.

[23] R. E. ASHCROFT, "Adam Hedgecoe, The Politics of Personalised Medicine: Pharmacogenetics in the Clinic , Cambridge University Press, Cambridge, 2004, 208 pp., hbk $75.00, ISBN 0 521 84177 1, pbk $32.99, ISBN 0 521 60265 3.," *Ageing Soc.*, vol. 26, no. 1, pp. 154–156, Jan. 2006, doi: 10.1017/S0144686X05224649.

[24] T. Feiler, K. Gaitskell, T. Maughan, and J. Hordern, "Personalised Medicine: The Promise, the Hype and the Pitfalls," *New Bioeth.*, vol. 23, no. 1, pp. 1–12, Jan. 2017, doi: 10.1080/20502877.2017.1314895.

[25] H. Davies *et al.*, "Mutations of the BRAF gene in human cancer," *Nature*, vol. 417, no. 6892, pp. 949–954, Jun. 2002, doi: 10.1038/nature00766.

[26] P. B. Chapman *et al.*, "Improved Survival with Vemurafenib in Melanoma with BRAF V600E Mutation," *N. Engl. J. Med.*, vol. 364, no. 26, pp. 2507–2516, Jun. 2011, doi: 10.1056/NEJMoa1103782.

[27] M. E. Vidal, K. M. Endris, S. Jozashoori, F. Karim, and G. Palma, "Semantic data integration of big biomedical data for supporting personalised medicine," in *Studies in Computational Intelligence*, 2019.

[28] S. Armstrong, "Data, data everywhere: the challenges of personalised medicine," *BMJ*, p. j4546, Oct. 2017, doi: 10.1136/bmj.j4546.

[29] M. Falzarano and G. Pinto Zipp, "Seeking consensus through the use of the Delphi technique in health sciences research.," *J. Allied Health*, vol. 42, no. 2, pp. 99–105, 2013.

[30] M. M. Baig and H. Gholamhosseini, "Smart health monitoring systems: An overview of design and modeling," *J. Med. Syst.*, 2013, doi: 10.1007/s10916-012-9898-z.

[31] M. S. Jassas, A. A. Qasem, and Q. H. Mahmoud, "A smart system connecting e-health sensors and the cloud," 2015, doi: 10.1109/CCECE.2015.7129362.

[32] M. Haghi, K. Thurow, and R. Stoll, "Wearable Devices in Medical Internet of Things: Scientific Research and Commercially Available Devices," *Healthc. Inform. Res.*, vol. 23, no. 1, p. 4, 2017, doi: 10.4258/hir.2017.23.1.4.

[33] A. B. Labrique, L. Vasudevan, E. Kochi, R. Fabricant, and G. Mehl, "Mhealth innovations as health system strengthening tools: 12 common applications and a visual framework," *Glob. Heal. Sci. Pract.*, 2013, doi: 10.9745/GHSP-D-13-00031.

[34] B. Martínez-Pérez, I. De La Torre-Díez, and M. López-Coronado, "Mobile health applications for the most prevalent conditions by the world health organization: Review and analysis," *Journal of Medical Internet Research*. 2013, doi: 10.2196/jmir.2600.

[35] K. Naseer Qureshi, S. Din, G. Jeon, and F. Piccialli, "An accurate and dynamic predictive model for a smart M-Health system using machine learning," *Inf. Sci. (Ny).*, vol. 538, pp. 486–502, Oct. 2020, doi: 10.1016/j.ins.2020.06.025.

[36] W. Nilsen *et al.*, "Advancing the science of mHealth," *J. Health Commun.*, 2012, doi: 10.1080/10810730.2012.677394.

[37] D. Dahiwade, G. Patle, and E. Meshram, "Designing disease prediction model using machine learning approach," 2019, doi: 10.1109/ICCMC.2019.8819782.

[38] Y. Mohamadou, A. Halidou, and P. T. Kapen, "A review of mathematical modeling, artificial intelligence and datasets used in the study, prediction and management of COVID-19," *Appl. Intell.*, vol. 50, no. 11, pp. 3913–3925, Nov. 2020, doi: 10.1007/s10489-020-01770-9.

[39] C. Krittanawong, A. S. Bomback, U. Baber, S. Bangalore, F. H. Messerli, and W. H. Wilson Tang, "Future Direction for Using Artificial Intelligence to Predict and Manage Hypertension," *Current Hypertension Reports*. 2018, doi: 10.1007/s11906-018-0875-x.

[40] M. Chen, Y. Hao, K. Hwang, L. Wang, and L. Wang, "Disease Prediction by Machine Learning Over Big Data From Healthcare Communities," *IEEE Access*, vol. 5, pp. 8869–8879, 2017, doi: 10.1109/ACCESS.2017.2694446.

Single Cell RNA Sequencing Data Analysis: An Overview

[1] Dolcy Rao, [2] Kuldeep Singh Naga, [3] Dr. Yasha Hasija

[1][2][3] Delhi Technological University, India

Abstract:

The single-cell RNA-sequencing data analysis technique is a new technique. It has provided us with the dissection in the single-cell resolution of gene expression, which in turn reshapes a large number of transcriptomic studies. Various scRNA-seq protocols, procedures, and tools have been developed, all having their own functionalities, advantages, and drawbacks. Due to some reasons, like biological factors and technical constraints, the scRNA-seq data is even more complicated and contains more noise than the bulk RNA-seq dataset. And due to all these reasons, high computational challenges are expected to occur. In this paper, all the steps involved in the whole process of scRNA-seq data analysis are summarized. The scRNA-seq analysis majorly has two parts; the pre-processing part and the downstream analysis part. In this paper, the whole data analysis protocol is summarized stepwise.

Keywords:

RNA Sequencing, Single cell data, Normalization, Visualization

1. INTRODUCTION

Traditionally, we have been using bulk cell data analysis techniques for studying diseases, tissues, etc. of any organism. As we assume that if cells are from the same tissue, they are homogenous and hence we tend to skip some crucial cell-cell variability. But in single-cell data analysis, we consider the fact that while all cells in our bodies share broadly similar genotypes, each expresses a distinct transcriptome. The conventional bulk-cell sequence can only provide the typical cellular expression signal. In 2009, the first article discussing the single-cell analysis based on next-generation sequencing was published. Since then, there has been an explosion in the single-cell data analysis field. In this paper, all the steps involved in the single-cell data analysis are briefly summarised.

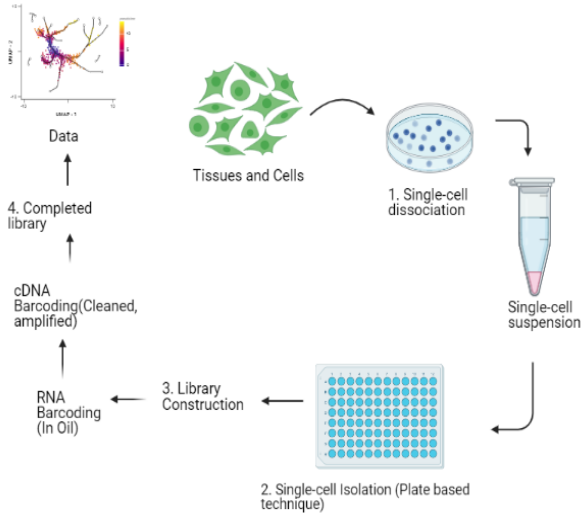

Figure 1: Single-Cell library preparation

2. PRE-PROCESSING

Studies are aimed to be done even more precisely with scRNA-seq data analysis techniques. There are some protocols through single-cell isolation and hence library preparation is done. Based on the protocol used for the library construction Unique Molecular Identifiers (UMIs) may or may not be used. And based on this processing of the raw data is performed to obtain molecular count matrices and/or read counts. Read quality control (QC) is carried out by raw data processing pipelines. Hence obtained read or count matrices have the barcode number x transcript number dimension.

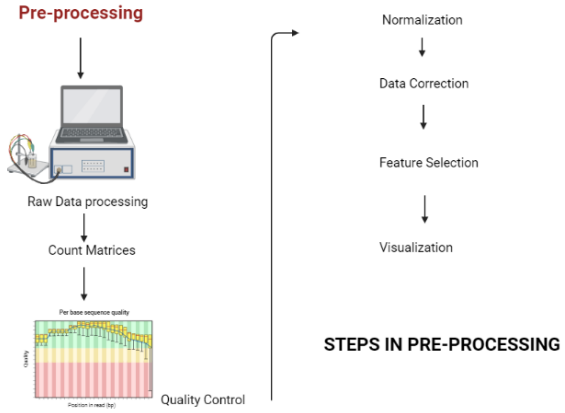

Quality control

Before we get on to the data analysis step, we have to confirm that all barcodes or more precisely cellular barcode data conform to viable cells. We consider three QC covariant for this step, precisely, the number of genes per barcode, the fraction of counts from mitochondrial genes per barcode, and count depth (the number of counts per

barcode)[1][2]. Outlier barcodes can correspond to, some cells we refer to as dying cells are the cells whose membranes are broken and doublets could also be there. These barcodes are filtered out by thresholding. We use thresholds with High-count depth for filtering out the probable doublets. There are three QC covariates and considering only one of them can lead to misrepresentation of cellular signals. Raw count matrices generally consist of over 20,000 genes. After filtration, this number is reduced significantly. To make sure that the data quality is adequate for downstream analysis, the quality control approach is carried out.

Normalization

Every count in a count matrix indicates the successful capture and sequencing of a molecule of cellular mRNA. Due to the variability underlying these stages, counting depths for identical cells can vary widely. Therefore, when gene expression, based on count data, is compared between cells, any difference may have emerged directly due to sampling effects. Normalization overcomes this problem by, for example, scaling count data to obtain correct relative abundances of gene expression between cells[3]. Count depth scaling, also known as "counts per million" or CPM normalization[4], is the most frequently used normalization procedure[5].

Data correction and integration

Undesired variability can still be there even after performing normalization. Further technical and biological covariates are individually targeted in data correction steps such as batch effects, dropouts, or cell cycle effects can also be there. Data correction is not often corrected for these covariates. The decision of which covariates to be taken under consideration will instead focus on the intended downstream process.

Regressing Out Biological Effects

Biological covariate correction aims to identify specific biological signals of concern[6]. The most frequently used correction method for biological covariates of data is the removal of the transcriptome effects of the cell cycle[7]. A simple linear regression of the cell cycle score is used to correct the data. Secondly, in context, it is important to comprehend biological signals. Unintentionally, the correction of one process may cover another signal. Finally, it was argued that cell size variation is usually due to the transcriptomic effect.

Batch Effects And Data Integration

When cells are treated in different groups, it can lead to batch effects. The effect arises on various steps: between cells treated in different groups but in the same experiment, the dataset used in the different experiments but from the same laboratory, or the ones from different laboratories. Correcting batch effects for the same experiments is known as a batch correction, whereas data integration is the integration of data from various experiments[8]. Linear and no linear methods are used for batch correction, data integration, respectively[9].

Expression Recovery

The dataset of single-cell transcriptome contains various noises[10][11]. Dropout is one of the common aspects of noise that need to be corrected. This is corrected by replacing the zero values with necessary expression values. This step has seemed to enhance the estimation of the gene-gene correlation[12].

Feature Selection, Dimensionality Reduction and Visualization

Even after performing all the filtering steps in the Quality Control step and filtering out the zero count gene, the dataset can still have more than 15,000 dimensions[13]. So as to scale down the computational load while downstream analysis step[14], to reduce the noise, and to visualize the data, we go for the dimensionality reduction step.

Feature Selection and Dimensionality reduction

So as to begin with, the initial step for this is feature selection. In this step only ‘informative” genes are kept, highly variable genes are used for the same. Based on the experiment approximately 1000-5000 genes can be selected for downstream analysis[15].

Further reduction in the single-cell expression matrix is done by using dimensionality reduction algorithms. The two main purposes for which dimensionality reduction is performed are visualization and summarization[16].

The most often used methods for this are Principal component analysis and diffusion maps. Principal component analysis can be called PCA, which is a linear approach for reducing dimensions.

Visualization

Generally, non-linear dimensionality reduction methods are used for visualization purposes. The most often used method in scRNA-seq visualization is the t-distributed stochastic neighbor embedding. The dimensions of t-SNE rely on local comparisons, to the detriment of the global system[17]. A partition-based graph abstraction is an alternative to traditional cell-level visualization[18].

3. DOWNSTREAM ANALYSIS

Following pre-processing, we use approaches called downstream analysis to obtain biological perspectives and explain the biological mechanism. Downstream analysis can be performed either at the cellular or the gene level. Cellular level analysis usually centres around: clusters and trajectories. The methods of cluster analysis try to describe the variation in the data based on cell classification into groups. Data is considered as a summary of a dynamic process in the analysis of trajectory. Trajectory analysis techniques look into this fundamental procedure.

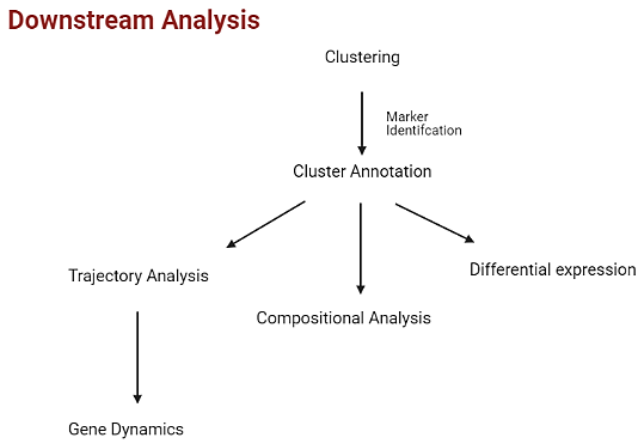

Cluster analysis

Clustering

On the basis of similarity of gene expression profiles, clusters are obtained by grouping cells. Clusters allow the identity of member cells to be inferred by us[19]. Clustering cell methods can predominantly be classified into two groups on the basis of whether previous knowledge is used. If a collection of familiar markers the techniques make use in clustering are based on previous knowledge. On the other hand, for again recognition of cell types with scRNA-seq data, unsupervised clustering techniques can be used[20].

Cluster annotation

The first step in cluster annotation is to find the marker genes of each and every cluster. These genes are the attributes of the clusters and are used to annotate clusters with the label. The identity of cells in the cluster is represented by this label. Finding cell identity/type of cell is a fundamental step for further inspection in the data processing procedure of scRNA-seq assessment, and there are two methods for identification of cell identity, for example, the cell-based and cluster-based annotation. To identify cell identities, the resemblance in cell-based data and reference cell databases are considered for cell-based strategy[21]. This can be done by multiple techniques such as Garnett, scrap, and CHETAH. Cluster-based techniques carry out the identification of cell type with the help of differentially expressed marker genes at the level of pre-computed clusters(Tabula Muris Consortium *et al*,2018).

Compositional analysis

The compositional nature of RNA-seq data is an important property that can not be ignored for all next-generation sequencing abundance data. Treating RNA-seq as compositional data opens up a new data analysis point of view, which removes normalization[23].

In contexts of cell compositional structure, we can analyze clustered information at the cell level. Analysis of compositional data depends on the percentage of cells that belong to each and every cell-identity group. Due to illnesses, these percentages can be changed. For determination of changes in the composition of single-cell data needs adequate cell numbers to strongly evaluate the percentages of the cell-identity group, and enough sample to analyze the anticipated background difference in the composition of the cell-identity cluster[24].

Trajectory analysis

Trajectory Inference

A discrete classification system like clustering can not sufficiently describe cellular diversity. Methods of trajectory inference explain single-cell information as a continuous mechanism[25]. By finding paths, this process is re-constructed Cellular space that minimizes transcriptional changes between adjacent cells. A pseudo-time variable describes the arrangement of cells along those paths. Trajectory Inference techniques should be decided on the basis of the complexity of the anticipated expected trajectory. When there is an integrated dimensionality reduction step, TI methods are used on decreased data or to corrected data[26]. Since a lot of biological processes occur at the same time inside cells, regression may be useful.

Gene expression dynamics

The trajectory is characterized by genes that vary smoothly through pseudo-time and can be used to recognize the basic biological process[27]. In addition, it is expected that this group of trajectory-linked genes will have genes that regulate the modelling process. These genes explain the underlying relationship between potential drug targets and the activation of biological processes.

Metastable states

Thick regions along a trajectory show preferential transcriptomic states, assuming that unbiased sampling of cells was performed[28]. When the trajectory is considered as a temporary procedure, the thick areas depict metastable states.

Cell-level analysis unification

By displaying single-cell groups as nodes and trajectories[29] in between groups as sides, both the static and dynamic nature of the data can be depicted.

Gene-level analysis

Molecular signals in the data are directly investigated by interpretation of gene set and regulatory gene network inference, differential expression testing. These methods use heterogeneity as a context in which order to discover significantly.

Differential expression testing

Genes that are differentially expressed between different cell groups, analysis of differential expression for them is very helpful. Genes which are differentially expressed are vital for analyzing the biological dissimilarity between the two compared situations. gene expression should be understood. In differential expression calling, the technical variability, dropouts, and huge size of sample single-cell RNA-seq data increase difficulties[30]. In addition, numerous feasible cell states can persist within a cell population, leading to gene expression multimodality in

cells. For DE testing, uncorrected, measured data should be used. Use limma and MAST for the Differential Expression test.

Analysis of gene set

Methods used for analysis at the gene-level usually result in a long list of candidate genes that are hard to explain[31]. Enhancement in the interpretation of these findings can be done by clustering the genes into sets constructed on shared attributes, and testing whether these attributes are excessively represented in the list of candidate genes Information regarding gene sets could be found in selected labeled databases for different applications. We typically group to explain DE outcomes genes that are based on participation in common biological procedures.

Gene regulatory networks

To identify the regulatory interactions of the genes gene regulatory network (GRN) are used. Genes don't work separately, so a gene's level of expression is determined by a complex interplay of regulatory interactions with other genes and small molecules.ScRNA-seq data network inference may give useful gene association comes up with the biologically significant perception that can not be found by bulk RNA-seq population-level[32] data. But because of the scRNA-seq technical noise and dissimilar cell subpopulations or states, the focus should be kept on the reconstruction of the network

REFERENCE

[1] T. Ilicic *et al.*, "Classification of low quality cells from single-cell RNA-seq data," *Genome Biol.*, vol. 17, no. 1, p. 29, Dec. 2016, doi: 10.1186/s13059-016-0888-1.

[2] J. A. Griffiths, A. Scialdone, and J. C. Marioni, "Using single-cell genomics to understand developmental processes and cell fate decisions," *Mol. Syst. Biol.*, vol. 14, no. 4, Apr. 2018, doi: 10.15252/msb.20178046.

[3] B. Vieth, C. Ziegenhain, S. Parekh, W. Enard, and I. Hellmann, "powsimR: power analysis for bulk and single cell RNA-seq experiments," *Bioinformatics*, vol. 33, no. 21, pp. 3486–3488, Nov. 2017, doi: 10.1093/bioinformatics/btx435.

[4] M. B. Cole *et al.*, "Performance Assessment and Selection of Normalization Procedures for Single-Cell RNA-Seq," *Cell Syst.*, vol. 8, no. 4, pp. 315-328.e8, Apr. 2019, doi: 10.1016/j.cels.2019.03.010.

[5] C. A. Vallejos, D. Risso, A. Scialdone, S. Dudoit, and J. C. Marioni, "Normalizing single-cell RNA sequencing data: challenges and opportunities," *Nat. Methods*, vol. 14, no. 6, pp. 565–571, Jun. 2017, doi: 10.1038/nmeth.4292.

[6] F. Buettner *et al.*, "Computational analysis of cell-to-cell heterogeneity in single-cell RNA-sequencing data reveals hidden subpopulations of cells," *Nat. Biotechnol.*, vol. 33, no. 2, pp. 155–160, Feb. 2015, doi: 10.1038/nbt.3102.

[7] E. Z. Macosko *et al.*, "Highly Parallel Genome-wide Expression Profiling of Individual Cells Using Nanoliter Droplets," *Cell*, vol. 161, no. 5, pp. 1202–1214, May 2015, doi: 10.1016/j.cell.2015.05.002.

[8] H. M. Kang *et al.*, "Multiplexed droplet single-cell RNA-sequencing using natural genetic variation," *Nat. Biotechnol.*, vol. 36, no. 1, pp. 89–94, Jan. 2018, doi: 10.1038/nbt.4042.

[9] W. E. Johnson, C. Li, and A. Rabinovic, "Adjusting batch effects in microarray expression data using empirical Bayes methods," *Biostatistics*, vol. 8, no. 1, pp. 118–127, Jan. 2007, doi: 10.1093/biostatistics/kxj037.

[10] D. Grün, L. Kester, and A. van Oudenaarden, "Validation of noise models for single-cell transcriptomics," *Nat. Methods*, vol. 11, no. 6, pp. 637–640, Jun. 2014, doi: 10.1038/nmeth.2930.

[11] P. V Kharchenko, L. Silberstein, and D. T. Scadden, "Bayesian approach to single-cell differential expression analysis," *Nat. Methods*, vol. 11, no. 7, pp. 740–742, Jul. 2014, doi: 10.1038/nmeth.2967.

[12] W. V. Li and J. J. Li, "An accurate and robust imputation method scImpute for single-cell RNA-seq data," *Nat. Commun.*, vol. 9, no. 1, p. 997, Dec. 2018, doi: 10.1038/s41467-018-03405-7.

[13] G. Heimberg, R. Bhatnagar, H. El-Samad, and M. Thomson, "Low Dimensionality in Gene Expression Data Enables the Accurate Extraction of Transcriptional Programs from Shallow Sequencing," *Cell Syst.*, vol. 2, no. 4, pp. 239–250, Apr. 2016, doi: 10.1016/j.cels.2016.04.001.

[14] P. Brennecke *et al.*, "Accounting for technical noise in single-cell RNA-seq experiments," *Nat. Methods*, vol. 10, no. 11, pp. 1093–1095, Nov. 2013, doi: 10.1038/nmeth.2645.

[15] R. R. Coifman *et al.*, "Geometric diffusions as a tool for harmonic analysis and structure definition of data: Diffusion maps," *Proc. Natl. Acad. Sci.*, vol. 102, no. 21, pp. 7426–7431, May 2005, doi: 10.1073/pnas.0500334102.

[16] N. C. Chung and J. D. Storey, "Statistical significance of variables driving systematic variation in high-dimensional data," *Bioinformatics*, vol. 31, no. 4, pp. 545–554, Feb. 2015, doi: 10.1093/bioinformatics/btu674.

[17] M. D. Luecken and F. J. Theis, "Current best practices in single-cell RNA-seq analysis: a tutorial," *Mol. Syst. Biol.*, vol. 15, no. 6, Jun. 2019, doi: 10.15252/msb.20188746.

[18] E. Becht *et al.*, "Dimensionality reduction for visualizing single-cell data using UMAP," *Nat. Biotechnol.*, vol. 37, no. 1, pp. 38–44, Jan. 2019, doi: 10.1038/nbt.4314.

[19] J. H. Levine *et al.*, "Data-Driven Phenotypic Dissection of AML Reveals Progenitor-like Cells that

Correlate with Prognosis," *Cell*, vol. 162, no. 1, pp. 184–197, Jul. 2015, doi: 10.1016/j.cell.2015.05.047.

[20] A. Wagner, A. Regev, and N. Yosef, "Revealing the vectors of cellular identity with single-cell genomics," *Nat. Biotechnol.*, vol. 34, no. 11, pp. 1145–1160, Nov. 2016, doi: 10.1038/nbt.3711.

[21] A. Saunders *et al.*, "Molecular Diversity and Specializations among the Cells of the Adult Mouse Brain," *Cell*, vol. 174, no. 4, pp. 1015-1030.e16, Aug. 2018, doi: 10.1016/j.cell.2018.07.028.

[22] "Single-cell transcriptomics of 20 mouse organs creates a Tabula Muris," *Nature*, vol. 562, no. 7727, pp. 367–372, Oct. 2018, doi: 10.1038/s41586-018-0590-4.

[23] A. L. Haber *et al.*, "A single-cell survey of the small intestinal epithelium," *Nature*, vol. 551, no. 7680, pp. 333–339, Nov. 2017, doi: 10.1038/nature24489.

[24] G. B. Gloor, J. M. Macklaim, V. Pawlowsky-Glahn, and J. J. Egozcue, "Microbiome Datasets Are Compositional: And This Is Not Optional," *Front. Microbiol.*, vol. 8, Nov. 2017, doi: 10.3389/fmicb.2017.02224.

[25] A. Tanay and A. Regev, "Scaling single-cell genomics from phenomenology to mechanism," *Nature*, vol. 541, no. 7637, pp. 331–338, Jan. 2017, doi: 10.1038/nature21350.

[26] G. La Manno *et al.*, "RNA velocity of single cells," *Nature*, vol. 560, no. 7719, pp. 494–498, Aug. 2018, doi: 10.1038/s41586-018-0414-6.

[27] L. Haghverdi, M. Büttner, F. A. Wolf, F. Buettner, and F. J. Theis, "Diffusion pseudotime robustly reconstructs lineage branching," *Nat. Methods*, vol. 13, no. 10, pp. 845–848, Oct. 2016, doi: 10.1038/nmeth.3971.

[28] L. Haghverdi, A. T. L. Lun, M. D. Morgan, and J. C. Marioni, "Batch effects in single-cell RNA-sequencing data are corrected by matching mutual nearest neighbors," *Nat. Biotechnol.*, vol. 36, no. 5, pp. 421–427, May 2018, doi: 10.1038/nbt.4091.

[29] W. Saelens, R. Cannoodt, H. Todorov, and Y. Saeys, "A comparison of single-cell trajectory inference methods," *Nat. Biotechnol.*, vol. 37, no. 5, pp. 547–554, May 2019, doi: 10.1038/s41587-019-0071-9.

[30] S. C. Hicks, F. W. Townes, M. Teng, and R. A. Irizarry, "Missing data and technical variability in single-cell RNA-sequencing experiments," *Biostatistics*, vol. 19, no. 4, pp. 562–578, Oct. 2018, doi: 10.1093/biostatistics/kxx053.

[31] A. Liberzon, A. Subramanian, R. Pinchback, H. Thorvaldsdottir, P. Tamayo, and J. P. Mesirov, "Molecular signatures database (MSigDB) 3.0," *Bioinformatics*, vol. 27, no. 12, pp. 1739–1740, Jun. 2011, doi: 10.1093/bioinformatics/btr260.

[32] S. Chen and J. C. Mar, "Evaluating methods of inferring gene regulatory networks highlights their lack of performance for single cell gene expression data," *BMC Bioinformatics*, vol. 19, no. 1, p. 232, Dec. 2018, doi: 10.1186/s12859-018-2217-z.

Novel Technologies to Combat Pandemics in Future

[1] S Vanitha, [2] Konda Rama Krishna

[1][2] Department of Biochemistry, Bhavan's Vivekananda College of Science, Humanities and Commerce, Secunderabad, Telangana, India

Abstract:

World wide spread of a new disease is Pandemic. Growth rate of a pandemic disease depends on its spreading rate and time. On account of present pandemic, majority of nations are affected, that has taken away life of many people. During this crisis, WHO has announced guidelines like wearing masks, regular sanitization and physical distancing to contain the spread and to stay safe and healthy. Affected nations have implemented lockdown as temporary measure. So, proper futuristic plans and approach is necessary to address the reoccurrence or emergence of new diseases effectively. Use of advanced, appropriate tools and technology at right situation can provide a solution to handle this sort of outbreaks in future. Artificial Intelligence helps in monitoring, planning and executing in compiling and analyzing the data of infected patients. Telemedicine can help the elderly people to communicate to their physician for counselling regarding their health status. Employing robotics and visual biometrics can prevent human-human as well as human-surface contact. Autonomous vehicles and drones could provide assistance, monitor and detect the infected or suspected patients to contain the disease. It can be understood that, implementation of these technologies can play a prominent and promising role in facing the challenges to be posed by pandemics in future.

Keywords:

Artificial intelligence, Drones, Pandemic, Robotics, Telemedicine

1. INTRODUCTION

An epidemic disease spreading across the international borders covering a wide area and affecting population in large can be defined as Pandemic [1], [2]. Pandemic disease cast out the immunity among population, causative agent like a virus or bacteria and pathogenesis of the disease. All epidemic diseases cannot be pandemic, because they may occur annually due to seasonal variations affecting the population. Similarly, a disease that is widespread or kills people but not infectious cannot be pandemic. As in the case of cancer, it is neither contagious nor infectious disease but causes many deaths worldwide [3]. In 2009, a six-phase classification for a novel virus transmission to infection was described by WHO (World Health Organization). But in February 2020, WHO declared that there is no official classification for a pandemic [4]. It might be due to the fact that, it discussed about the infection of the virus without including its virulence, severity and its mortality [5]. Centers for Disease Control and Prevention (CDC) of United states in 2014, introduced Pandemic Intervals Framework similar to WHO's pandemic phase [6]. This framework includes two pre-pandemic and four post-pandemic intervals. The two pre-pandemic intervals are Investigation and Recognition. The four post-pandemic intervals are Initiation, acceleration, deceleration and preparation.

Earlier history verbalizes that; data pertaining to Case Fatality Rate (CFR) may indicate the severity of a pandemic disease [7]. With CFR as only one parameter it may not be sufficient to assess the severity of a pandemic and its response due to several drawbacks [8]. To overcome this, in 2014, Centers for Disease Control and Prevention introduced Pandemic Severity Assessment Framework (PSAF) which is analogous to Pandemic Severity Index framed in 2007 [6]. It measures CFR that can be used to predict not only the severity but also evolution of pandemic. As per PSAF, outbreak of a disease severity can be measured based on infected persons severity of illness clinically and transmission among the people [9].

These two dimensions are characterized by measuring virulence using genetic markers and deaths to hospitalization ratio to calculate clinical severity, whereas R_0 – basic reproduction number and serial interval or using immunity to assess the mode of transmission. Each dimension is measured using a metric system. Guidelines given by PSAF can be used to assess the past pandemics using the metrics defined for each measure.

2. CONCERNS ABOUT PANDEMICS IN FUTURE

A. Antibiotic resistance

One of the major concerns among the health care professionals is that, there are possibilities for the re-emergence of few pathogenic diseases which were under control earlier. One of the main reasons could be organisms attaining resistant to antibiotics. Multidrug resistant tuberculosis, bacterial infections caused by *Staphylococcus aureus*, *Serratia marcescens* and *Enterococcus* has developed resistance to antibiotics. Organisms resistant to antibiotics are an important factor for HAI- Healthcare Associated Infections (Nosocomial). In recent years, healthy individual's acquiring strains of MRSA has raised a concern.

B. Viral hemorrhagic fevers

These are highly contagious and deadly diseases caused by Ebola virus, Lassa fever, Rift valley fever, Marburg disease

and Bolivian hemorrhagic fever are predicted to become pandemic in future theoretically. Their spread might be slow but with the infected vector, transmission in close contacts can cause serious illness and death. It becomes mandatory for the carriers that are vectors to be quarantined under the guidance and support of medical professionals to avoid the spread of the pathogen. So, it becomes essential for epidemiologist to continuously monitor these contagious diseases due to their potentiality to undergo genetic mutations at a rapid rate to become lethal after a stage.

C. Impact on Global Economy

1. Global Health Risk Framework in 2016 estimated, a $6 trillion effect in global economy due to the pandemic diseases. And also, $4.5 billion is been spent annually in prevention and response initiatives to decline the threat posed by pandemics. COVID-19 pandemic has found to have profound influence on world economy for the following years to come with huge drops in GDP and unemployment among the different groups in the population.

3. HOW TO CONTROL AN OUTBREAK

Outbreak of a pandemic disease can be controlled using two important strategies. It includes containment and mitigation. Fig. 1 shows the early stage of a pandemic outbreak control that is by containment.

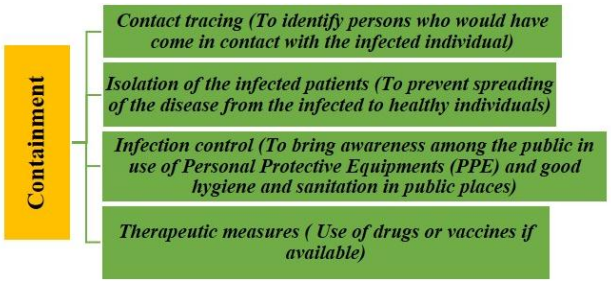

Fig. 1 Strategy one to control Pandemic- Containment

There may be situations where containing the disease spread may become unmanageable, so the next strategy is mitigation. Fig.2 shows the strategy to control the pandemic by mitigation.

Fig.2 Strategy two to control Pandemic- Mitigation

Mitigation goals are to lessen the cases, so that it can reduce the burden of frontline healthcare systems and also the health of population in general [10], [11]. During this time easy, continuous supply and access to PPE (Personal Protective Equipment), count of bed number to increase to meet the demand when in emergency [12]. If control measures are not followed strictly there are many chances for resurgence of disease. Sometimes, to control the outbreak both the strategies can be implemented [13].

The main aim in controlling the outbreak due to an infectious disease is by slowing or reducing the epidemic peak by making the curve to flatten gradually. During this crucial period enough time may be given for the scientist to look into the discovery of a potential drug candidate or for a vaccine. It also gives a brief relaxation for the frontline workers especially the doctors, nurses or midwives involved. Non pharmaceutical interventions may take up an upper hand in outbreak management. It includes washing or cleaning of hands with soaps or sanitizers, covering the face with an appropriate mask, quarantine themselves for a stipulated period of time, regular sanitization of public areas and most importantly social distancing. It is a measure among the community to decrease large gatherings in places like educational institutions, commercial entertainments and many more [10], [11].

Recent pandemic has resulted in a new strategy to control the outbreak called as suppression. It is a type of non-pharmaceutical interventions that is implementation of strict social distancing where the distance is more than one meter, suspected or confirmed cases to remain at home. Its aim is to reverse the situation, but it can have an impact on the economy of a country [14]. As per WHO recommendations, preparing the affected nations with pandemic is to implement necessary measures to control the transmission and mortality rates during this COVID-19 in terms of PHSM (Physical Health and Social measures). These measures include

i) Preventive measures at workplaces:

Personal protection like hand hygiene by washing the hands regularly with soap at least for 20 seconds or using alcohol-based hand sanitizer, making availability of respiratory equipment during emergency. Other standard measures include standard appropriate measures in offices or work places like installation of thermal scanners, encouraging work from home, use of teleworking, shifts to the staffs based on the need also can be implemented to reduce overcrowding and maintain hygiene and sanitization in the work place by use of disinfectants to clean the area regularly. Use of PPE- Personal Protective Equipment like medical mask while moving outside [15], [16].

ii) Environmental measures:

Social or physical distancing minimum of one meter is to be followed among a community or within a containment zone or within a population in general. Suspected cases and persons who had contact with infected persons by isolating themselves is a measure to avoid its further spread. In this context, WHO recommends that all the suspected cases and testing positive subjects should be identified, isolated with proper care and importantly identifying their contacts by tracing them and quarantining with precaution to break the

chain [17]. Physical distancing in crowded public places where there is limited ventilation like markets, cinemas, night clubs, restaurants, schools, mass gatherings like places of worship or any sporting events etc., should be strictly restricted to prevent the spread of the infection [18].

iii) Shutdown or Lockdown:

In a larger scale, other measures include implementation of restriction towards travelling within the country or abroad, shutdown of business and schools, avoiding mass gatherings. These measures are referred to as "shutdown" or "lockdown". Shutdown or lockdown implementation can be adjusted, retained or continued based on the evidence in its spread. These public health and social measures are not permanent, it depends on critical factors like food security, economy, number of cases and mortality rates. But use of protective measures like personal hygiene, wearing medical masks should be continued.

Pandemic situations created at any period has kept one community in demand always, they are the frontline workers. They are the backbone for an effective healthy community and play a critical role in providing good health solutions during difficult situations. Community health care workers with a good training and support like doctors, nurse, mid wives, paramedics and local pharmacists play a major role by providing essential services during any health crisis. They play a key role in managing, advising, caring, treating and preventing the occurrence of many types of communicable and non-communicable diseases. Availability of a strong, committed and quality health care workers are indispensable during the outbreak of a contagious disease.

Health care professionals play an important role during critical conditions especially in outbreak situations to provide safe and healthy environment. During the outbreak of SARS (Severe Acute Respiratory Syndrome) and MERS (Middle East Respiratory Syndrome), the health care providers were under unbelievable stress like chance of acquiring infections, denunciation, undermanned, suspicious, continuous exhaustive support was mandatory during pre and post pandemic situations. These factors have drastically affected them mentally and physically and they were under continuous stress. Under these circumstances' frontline workers with less experience on handling infectious diseases are under more psychological imbalance and are stressed in handling the situation. The suffering faced by the frontline workers during the earlier outbreak, has continued and it seems to continue in future also if proper guidelines, supporting systems for both physical and mental stamina, improvisation in easy mode of interaction between frontline workers and patients should be addressed by implementing the available latest technology. As contagious diseases can spread quickly, understanding, reacting quickly, handling new equipment's without being infected among unexperienced people are few tasks in front of them.

Risk management, protecting and precautionary measures among the frontline workers are to be addressed at the earliest to keep such sort of pandemic situations mitigated. The different problems faced by the frontline workers are

1. Exhaustion of job due to continuous flow of patients with infection, people with co morbidities for regular check-ups, emergency to be attended for patients with other health issues.
2. Shortage of workers, equipment, beds, PPE etc., to protect themselves and also the incoming patients as the number of infections has escalated.
3. Decision making during emergency, triage decisions like first sorting the patients whether they are symptomatic or asymptomatic and finalizing the treatment immediately to increase the number of survivors, second sorting the patients based on their condition whether they need emergency or not and third distribution of funds for its best utilization to provide sustainable solutions at the earliest.
4. Expansion in working hours has reduced their time to be spent with families and fellow mates, no proper rest and food has resulted in a psychological stress among the frontline workers.
5. Stigma of acquiring the infections and falling a prey to the infection and carrying it to others.
6. As the survival rate of patients decreases due to infection it causes a distrust about their potential and efficiency in handling the situations, they lose their mental stamina.
7. Use of their personal protective equipment like wearing gloves, gowns, mask, shield to protect themselves continuously has created a situation of no water and food consumption to avoid use of washrooms, marks and scars on face due to continuous use, wearing the shield or goggles reduces their power to view the containers with medicine, name of the tablets, etc.

Over all, it becomes mandatory to take care of them to optimize their services when needed. In the fight against corona virus, health care workers are playing a pioneer role and also at a high risk of getting infected. As most of the nations has a shortage of health care providers and if they themselves are quarantined, it could lead to a disastrous situation. So, in order to reduce the physical contact of health care workers with the infected patients, tools of technology such as artificial intelligence, telemedicine, robots and autonomous vehicles play a very important role as they help in communicating with the patients, providing food and medication to them. Along with this there are also some precautions need to be taken by every individual such as physical distancing, mask protection, maintaining hygiene inside home and surroundings as well which might lower the risk of getting affected with the virus.

4. MEASURES AND PLANS TO BE EXECUTED

In this era of advanced technology, it is very important to take the benefits of technology to treat and prevent the spread of the disease. The best example is the use of Infrared thermometers (Thermometer guns), which prevents the contact with the patients, telemedicine, artificial intelligence, robots, drones etc.

I. Telemedicine

It is a term coined in 1970, which means, "healing at a distance" where its main aim is to use information and computer technology (ICT) tools to enhance patients need and give better care and medical support. Presently, WHO has revised its definition as, a supporting system to the health care workers to use computer technology with exchange of important information to diagnose, treat and prevent the disease or any infection, to pursue a focused research and evaluate the results, knowledge about updated treatment strategies for new diseases whose final aim is to improve in medical community to tackle any crisis in future [19], [20].

Telemedicine or telehealth can be a best way to cut down one-on-one interactions between the patients and health care worker, reducing their chances of getting infected during the treatment of infectious diseases. In countries like USA, UK and China, telemedicine has already been adopted to tackle COVID-19. Of the $8 billion set apart in USA response to this pandemic, $500 million has been exclusively marked for Telehealth. Also there has been a conceptual frame work designed for telemedicine implementation to fight against COVID-19 [21].

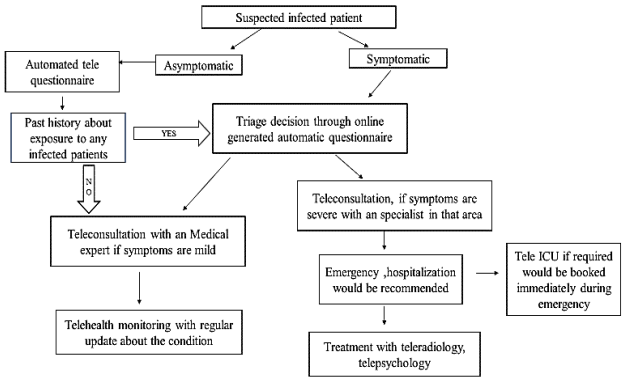

Fig. 3 Flowchart for Telemedicine

Telemedicine is in its genesis in India, which has to grow and will be adopted by frontline workers and patients in future years, with rules and regulations when followed strongly will nurture its growth to face the upcoming epidemics. Fig.3 explains about the basic procedure to practice telemedicine. To provide sufficient health care, medical workers must be able to integrate technology with tools available. Collecting the data and transmitting either by voice, images, pictures along with appropriate standards in clinical formats, procedures, any specific policies for sustainable care. Medical practitioners must be also aware of the chances of misusing it by unauthorized persons and must be able to detect it immediately. So, proper guidelines must be framed to make it easy, safe and quick solution to the patients especially to the people located in remote places.

Implementation of telemedicine should follow few strategies like

i. Mode of communication -Video (video via chats, using skype/online platform), Audio (Via phone, VOIP-voice over IP technology, etc.), Texting (chat based -using smartphones, mobiles, internet based or normal messaging using WhatsApp, Hangouts, Facebook) and Asynchronous (Fax/ email etc.).

ii. Time of interaction or exchange of information

iii. Reason for teleconsultation

iv. Interaction between whom

a. RMP (Registered Medical Practitioner) to his/her patient

b. RMP to a caregiver

c. RMP- RMP

Telemedicine in India is under strict planning and has prescribed seven important elements to be kept in place if anywhere / anybody wants to follow telemedicine consultation. They are

1. Context- Telemedicine to be followed should be relevant and adequate to meet the required context. Judging professionally, necessary mode for transfer of information availability on both sides and to decide whether there is a need for early diagnosis in person.
2. Identification of RMP and Patients – Proper information about RMP in terms of professional experience, specialization, registration number etc., and also personal details of patient is mandatory. It includes their name, age, sex, government issued identity card and their registration number generated during login for teleconsultation. Knowing each other is important during teleconsultation.
3. Mode of communication – There are three modes like audio, texting or video. Consultation completely is dependent on patient's convenience and available facility.
4. Consent – Taking a consent from a patient is of two types either explicit or implied. If it is explicit consent is acceptance given by the patient to start with telehealth consultation, it should be in message or voice message which has to be recorded by RMP. In the case of implied which means taking in-person consultation.
5. Type of consultation – It includes two types; one is first consult where the interaction is for the first time / or after a gap of few months or year / meeting for another ailment. Second consult is Follow-up consult where the patient is updating his/her condition within six months.
6. Patient evaluation – Before starting the consultation, RMP should procure proper documents pertaining to

the patient from past records to present condition. All the information has to be documented. Based on the history and present clinical condition, it is up to the RMP to decide what must be followed either to start with consultation or in-person treatment. Educating their patients, examination or recommending for a second opinion can be implemented.

7. Patient management –Education in planning a diet, importance of yoga and physical exercise, possible ways to avoid smoking, consumption of alcohol and tobacco. Regular counseling of the patients to increase positive attitude to mitigate the condition. Finally, prescribing effective medicines by strictly following the guidelines as categorized below

List O: Basic drugs like drugs available at all medical counters.

List A: Medicines prescribed during first consult provided they undertake follow up.

List B: Patients who are taking follow up consult along with in-person consult.

Prohibited List: Telemedicine RMP are not supposed to prescribe drugs that are prohibited [22].

This practice of telemedicine has a lot of benefits during the treatment of these infectious diseases such as

- It will prevent emergency rooms from being over-crowded.
- It will limit exposure among health care workers to infected individuals.
- It will also cut down use of masks, gowns and gloves for markers by keeping patients at home.
- With simple telemedicine enabled devices, even lay persons can perform basic examinations wherever they are and when need they can share the data to health care providers for detailed analysis.
- Remote and under-developed regions are primary areas where digital health can show its potential and this can prove hugely beneficial for rural health infrastructure, if cases shift from cities to villages.

The biggest challenge to overcome is, a lack of regulatory framework to authorize, integrate and reimburse telemedicine services, including in emergency and outbreak situations in most of the nations. In all such nations, the Covid-19 pandemic is a call to adopt the necessary regulatory frameworks for supporting wide adoption of telemedicine.

II. Artificial Intelligence

Artificial intelligence (AI) is a virtual technology trying to imitate human intelligence using information technology or machine language to solve issues. Earlier AI was used in playing games, recognition of language, retrieving images and so on. Advanced technology in machine language has enhanced the approach of AI in handling complex issues as how humans think and are one step ahead to take fast, accurate and reliable and acceptable results and economical to mankind. With the present scenario where the pandemic crisis has proven havoc to the society, it becomes apprehensive of how this latest technology can support and give logical solutions. Questions to be answered include how these high computational algorithms will be able to analyze, interpret and compile the data from past history with real time data information.

AI has been superior in present COVID-19 pandemic, where the health care providers are able to replace traditional thoughts and decision making based on the inputs given by machine learning (ML) process which is a subset of AI. They are able to handle huge dataset to give more reliable data in the diagnosis of a disease, identification of a lead candidate, variation to treat patients based on their conditions and attainable outcomes [23]. WHO and CDC are together able to observe the massive data being available on internet with easy access by real time Artificial Intelligence. Data are stored and can be retrieved from online platforms like social media, review and research articles, reports from hospitals, data of travel etc. Role of various organization enriched with knowledge of AI can pool this information and collaboratively work with other autonomous institutions to come up with plans, criteria, strategies of how to face the future in case of reappearance of another outbreak [24], [25]. Creating a new model system of AI in an awake to knock down the emergence of any epidemic is by predicting, preventing, probing and pausing the outbreak. Table I represents the various models and applications of AI developed by different countries

Table I: Few applications of AI in earlier and recent outbreak

Application	Type of AI	Efficiency and its use	Reference number
Warning Outbreak	Blue Dot – An AI driven algorithm (Florida)	Detected outbreak of Zika virus in Florida	[26]
Outbreak of COVID	-	9 days before WHO released its statement alerting the people on the emergence of corona virus	[27]
To analyze blood samples To predict survival rates of people infected with COVID-19	XG Boost ML based prognostic model HUST and Tingji Hospital in Wuhan	Accuracy was 90%	[28]

 ISBN: 978-93-90214-20-4

Differentiating pneumonia caused due to COVID-19 or due to other ailments within seconds	AI diagnostic tool which analyzes patients CT scan of chest (Wuhan, China)	Radiologist were relieved, improved diagnosis at early stages, isolating and treating infected patients was helpful in controlling this pandemic	[29]
Model to detect COVID-19 positive cases	COVID-Net a machine learning process to detect cases using X ray images of chest	Faster approach to treat the emergency patients	[30]
SARS-CoV-2 features	Google's DeepMind	Protein structure prediction of the virus	[31]
Scan crowded areas for COVID-19 individuals	AI based computer-based camera (China)	Early detection of positive cases in crowded places can contain the spread	[32]
Predict the occurrence of flu due to seasonal variation	Flu sense- surveillance platform	Contactless surveillance to check the outbreak of either COVID or SARS	[33]
Healthcare workers were assisted in contactless support to patients	AI powered autonomous service robots and humanoid robots (Wuhan, China)	To supply foods and medicine to patients	[34]

Artificial intelligence (AI) is transforming our lifestyle intending to mimic human intelligence by a computer/machine in solving various issues. Initially, AI was designed to overcome simpler problems like winning a chess game, language recognition, image retrieval, among others. With the technological advancements, AI is getting increasingly sophisticated at doing what humans do, but more efficiently, rapidly, and at a lower cost in solving complex problems.

Artificial intelligence (AI) is transforming our lifestyle intending to mimic human intelligence by a computer/machine in solving various issues. Initially, AI was designed to overcome simpler problems like winning a chess game, language recognition, image retrieval, among others. With the technological advancements, AI is getting increasingly sophisticated at doing what humans do, but more efficiently, rapidly, and at a lower cost in solving complex problems.

Artificial intelligence (AI) is transforming our lifestyle intending to mimic human intelligence by a computer/machine in solving various issues. Initially, AI was designed to overcome simpler problems like winning a chess game, language recognition, image retrieval, among others. With the technological advancements, AI is getting increasingly sophisticated at doing what humans do, but more efficiently, rapidly, and at a lower cost in solving complex problems.

Artificial intelligence (AI) is transforming our lifestyle intending to mimic human intelligence by a computer/machine in solving various issues. Initially, AI was designed to overcome simpler problems like winning a chess game, language recognition, image retrieval, among others. With the technological advancements, AI is getting increasingly sophisticated at doing what humans do, but more efficiently, rapidly, and at a lower cost in solving complex problems.

I in healthcare provides an upper hand undoubtedly over traditional analytics and clinical decision-making techniques. Machine learning (ML) algorithms, a subset of AI, can detect patterns from huge complex datasets to become more precise and accurate as they interact with training data, allowing humans to gain unprecedented insights into early detection of diseases, drug discovery, diagnostics, healthcare processes, treatment variability, and patient outcomes.

AI4 COVID-19, is an artificial intelligence screening tool to diagnose the respiratory diseases and differentiate sounds caused by COVID-19 patients from other coughs using a simple smartphone app. Patients are supposed to cough three times and the data transferred to cloud storage and received within two minutes to understand the condition [35]. It's a new era of implementing technology a culmination of science and machine language which can have pros and cons at initial stages. AI has started to venture during the present outbreak and has been successful in certain countries and the results obtained seems to be promising that future tools would be equaling human intelligence and can handle the outbreak in future.

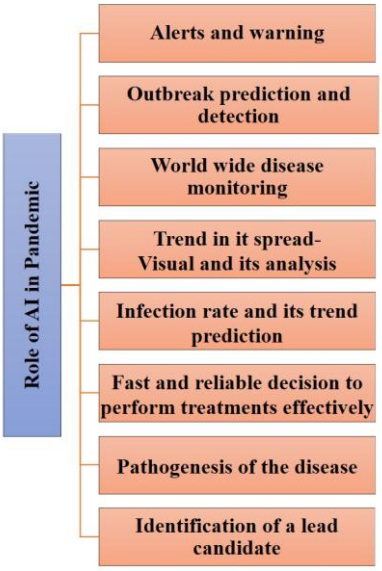

Fig. 4 Role of Artificial Intelligence in Pandemic

Internet of Things (IoT) in epidemiology and health care monitoring is an emerging field omnipresent with latest technologies. Outbreaks at regular intervals across the world requires interlinked mechanisms to combat them with web-based tools to assess the outbreak at its earliest stage. But availability and use of technology-based analysis is still not successfully reached either the healthcare workers or to the society [36].

Using deep learning and AI powered drug repurposing with the big data available it can become cost effective, quicker and can maximize the efforts in advanced drug trials and rather reduce the failures. With the development in CADD (Computer Aided Drug Designing) and using virtual screening by experimenting with an array of docking of candidate drugs it can help in designing anti-viral drugs to treat and increase the survival rate [37].

Fig. 4 explains about the role played by AI in various areas. Applications of AI during the present pandemic – COVID-19

1. Infection at its early-stage, Detection and diagnosis: It helps the patients and healthcare workers to be alert, decide treatment protocols quickly, devise and implement new treatment strategies using powerful programs available from AI. Using images obtained from scanning results like MRI (Magnetic Resonance Imaging) and CT (Computed tomography) to diagnose the disease stages [38], [39].
2. Treatment monitoring: Neural networks helps in identifying suspected individuals, status of its spreading capabilities with daily reports, recapture the images and follow up with steps in treatment and prognosis of the disease [40]-[42].
3. Reports on Mortality cases: Using AI with the data collected from various place of outbreaks, it can be understood about the type of spread like is it community or noncommunity-based spread, identify the red zones, its role in co-morbidity cases, geographical location and its impact can help us to plan to avoid the outbreak again.
4. Supporting the frontline workers: AI can break the stigma among them of getting infected, reduce their stress by giving time to rest and relax, with digital decision making it can be relief for patient and healthcare workers to see the decline in death rates [46]-[53].
5. Designing of vaccines or drugs: With no possible treatment, researchers are looking forward to use the AI based methods to test, treat and design, deliver and develop possible lead compounds on a real-time basis [40,41]. The efficacy of drug, ADMET (Absorption, distribution, metabolism, excretion, toxicity) can be experimented virtually and it reduces clinical trials with better dose response in short time. [43]-[45]
6. Containment of the present and future epidemics: With increase in neural networks, machine language, AI based technology can access the big data and could possibly replace the difficulties faced during this COVID-19 pandemic [54].

None the less, outbreaks that may happen in future should be managed and tackled smartly with advent of latest technologies. So, each individual should be responsible in any field to understand, update, learn, co-operate and break the chain of these outbreaks in future. It can be declared that, in future preventing these epidemics with AI will play a prominent and promising role as we are witnessing its significant role in present scenario.

III. Robotics

Robotic technology involves in crafting a robot artfully, fabricating with sensory inputs, automatic action and execution developed with computer programs to follow the command, respond wisely, collection and processing the information without intervention of human. Outbreak of this pandemic has led to a unique chance to give a kick start in the development of medical robots. To create contactless monitoring, treating infected patients, disinfecting hospitals and places frequently visited by people. The need for creating advanced and potential robots to face the future pandemics can be a game changer.

From the time Covid 19 outbreak, robots of various sizes, design and applications were into the supply chains to support the frontline workers in and out of hospitals, support patients and doctors, to clean surfaces regularly, to watch and guard the public places, and so on. They help in public and private sectors to run their business without any struggle. Fig 5 briefs about the advantages of using robots in a hospital, public places or in a residence.

Robot are of different types based on their design and application,

a) Delivery robots – robots designed like a cart supplies commodities and food at their doorsteps to patients those who are quarantined to protect themselves from delivery boys.

b) Autonomous robots- A robot with two large ultraviolet light radiating vertical tubes that rotates surrounding the room and disinfecting. A UVD robot, designed by a Danish consortium kills microorganisms using UV light. It works autonomously by moving through risk areas disinfecting, protects frontline workers and supporting staffs.
c) Social robots- gives company to people in isolation, accompanying and balancing the psychology of patients those who are staying alone indoors for a long time.
d) Telepresence robots- robots that carry a screen or a monitor on wheels trying to connect the isolated infected patient with their family members and also elders staying alone.
e) Medical robots- Cylindrical robots that rolls through intensive care units to take temperature, to measure blood pressure, monitor oxygen saturation levels for patients under ventilation and record the data.
f) Disinfection robots- drones that sprays disinfectants at public places, in containment areas,
g) Prototype robots- collects oropharyngeal swabs from suspected individuals avoiding the intervention of healthcare workers and specialized drones like quadcopter drones that transports collected samples to laboratories.
Every disastrous outbreak of an epidemic or pandemic that occurred earlier was stuffed with lessons that were taught and also to learn how to overcome them. But continuation in further research and setting up of start-ups for improving the wide applications of robots to face the future disastrous situation are dimming maybe due to insufficient funding, its importance still not recognized, but the momentum in its research should be addressed at the earliest [55]-[57].

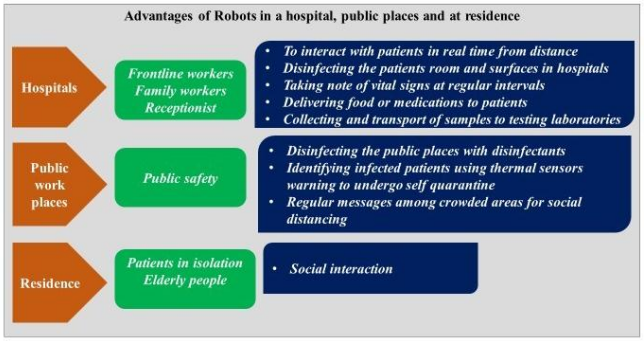

Fig. 5 Advantages of Robots (Hospital, Public places and Residence)

IV. Biometric Systems

Biometrics are used to identify individuals which works on the principle of machine learning and artificial intelligence technologies and algorithms. Identification of an individual using biometrics is based on their physiological and behavioural characteristics. Physiological identification includes finger print, iris recognition, face recognition, palm veins etc whereas behavioural identification is based on the individuals' keystroke, voice, typing rhythm and signature. In the present scenario, biometrics has found to play a key role in early detection of a disease using symptoms, screening the patient's temperature and in monitoring the public for their safety. The impact of Covid-19 has forced the contactless technologies to recognize individuals by scanning their iris and face to contain the spread of the disease.
With advancement in the development of available biometrics, face recognition and surveillance are upgraded to screen the individuals who are not wearing face masks. But the challenge that has to be addressed is, recognition of an individual when face is partially covered with their masks. Hand-held portable Biometric devices that can detect the changes in body temperature are installed near entrances for public security, transportation, hospitals and highly populated common places. These biometrics are contactless technologies. But biometrics identification based on fingerprint or face or iris recognition are contact-only sensing technology are of concern about safety and control during this pandemic. This has forced the government to strictly terminate the use of contact only based biometric systems.
As the demand for the biometrics has increased, facilitating in the fund investment for the development of advanced contactless biometric software and algorithm systems in assisting global efforts which would be in support to healthcare professionals. It can provide protection at national and international borders and for the safety of general public also [58].

V. Autonomous Vehicles and Drones

One of the promising Fourth Industrial Revolution in technology is Drones. They are playing a key role in fight against Covid-19 indirectly by assisting the healthcare takers, municipal agencies and other government officials by involving in activities like
1. Monitoring body temperature: Deploying special drones attached with thermal scanners to monitor the body temperatures among the people in a crowded area [59].
2. Medical supplies for those staying in remote areas and for the transport of collected samples from infected or suspected patients from collected area to their respective laboratories [60], [61].
3. Emergency need for food supplies and delivery during lockdown to make a contact free delivery system.
4. Surveillance done aerially with drones is to implement successful shutdown and maintenance of social distancing, Survey and mapping the red and green zones based on the rate of infection as a precautionary measure [62], [63].
5. Spraying the disinfectants- Drones are earmarked to spray disinfectants regularly by dividing the areas into different geographical locations for faster and effective sanitization [64], [65].
6. Warning by special drones carrying police sirens requesting people to stay indoors and to disperse the crowd in public areas and broadcasting the information by creating awareness on Covid-19 to the public.
Use of drones during the pandemic has advantages like it has reduced the human-to-human contact in preventing the

spread of the infection especially among the healthcare professionals. They have increased the safety and security of the public by supporting the available man power. When compared to local transportation, the speed of drones is designed to help them to reach their destinations quickly and easily so that, they can reach the remote areas which are in immediate need.

5. CONCLUSION

Covid-19 pandemic has triggered the moment of precautionary and preventive needle in a direction towards development of science and technology to focus on combating the outbreak. The efforts must be to channelize and prepare an effective road map to funnel all the tools and technologies to fight against the present and future outbreaks if any. As a support, WHO Academy regularly develops different user-friendly apps giving guidelines to public, it also provides guidance and different medical tools that are available and provides appropriate training for healthcare workers.

Use of modern technology and effective communication using internet, smart phones are transforming and restructuring individuals in their communication skills, looking out for an effective interchange of information and refine their thoughts and lives. These sophisticated technologies have a great impact in addressing current and future global issues in health sector.

Access, Quality, Integrity and low cost are some of the issues encountered by health care professionals in economically underdeveloped and also in developed countries. Facilities of telemedicine are able to provide solutions but with complexity in approaching it still persists. Even though, the technological profiles of few underprivileged families are able to meet the basic necessities for telemedicine but the available infrastructure facilities, hospital providers and experienced personals are negligible. AI development requires continuously updated software's and hardware's which might be cost effective, unemployment as they can carry out works repetitively and these machines work effectively for which they are programmed for.

Scientific researchers and innovators are keen in developing drones with varied utilities during this pandemic. Presently, use of drones or unmanned aircrafts is under the control of Ministry of Civil Aviation but wider deployment and barrier free approvals should be addressed. Design, development of drones should be provided with protocols like having a unique identification number or authorized or acknowledged number specialized for its use, it should be traceable, intention to use during crisis under controlled permitted government agencies and must be time bound that is only during pandemic condition.

Advantages and disadvantages are always a part of new inventions, but as humans we should be responsible to look for positive sides of invention and create a safe, secure and healthy place for the society to live in. Development and implementation of novel technologies for human welfare to fight against pandemics depends on a thin line between safety and destruction. So strong rules and regulations must be framed to implement these technologies successfully.

Acknowledgments

The authors would like to thank the Management, Principal and Department of Biochemistry of Bhavan's Vivekananda College of Science, Humanities and Commerce, Sainikpuri, Secunderabad for encouraging us in successfully completing this article.

REFERENCE

[1] Last JM, Editor. A Dictionary of epidemiology, 4th Edition, New York: Oxford University Press, 2001.

[2] Porta Miquel, Dictionary of Epidemiology, Oxford University Press; p. 179, 2008.

[3] A M Dumar, Swine Flu: What you Need to Know. Wild side press LLC p.17, 2009.

[4] "WHO says it no longer uses "pandemic" category, but virus still emergency". Reuters, February 2020.

[5] Der Spiegel, "A whole industry is waiting for an epidemic", July 2009.

[6] Holloway, Rachel, Rasmussen, Sonja A, Zaza, Stephanie, Cox, Nancy J, Jernigan, Daniel B, "Updated preparedness and Response Framework for Influenza Pandemics". Morbidity and Mortality Weekly Report. Center for Surveillance, Epidemiology and Laboratory services, Centers for Disease Control and Prevention, 63 (RR-6) pp 1-18. September 2014.

[7] Interim Pre-Pandemic Planning guidance: Community Strategy for Pandemic Influenza Mitigation in the United states, centers for Disease Control and Prevention, February 2007.

[8] Reed, Carrie, Biggerstaff, Matthew, Finelli, Lyn, Koonin, Lisa M, Beauvais, Denise, Uzicanin, Amra, Plummer, Andrew, Bresee, Joe, Redd, Stephen C, Jernigan, Daniel B, "Novel framework for assessing epidemiologic effects of influenza epidemics and pandemics". Emerging Infectious Diseases, 19 (1): 85-91, 2013.

[9] Qualls, Noreen; Levitt, Alexandra; Kanade, Neha; Wright-Jegede, Narue; Dopson, Stephanie; Biggerstaff, Matthew; Reed, Carrie; Uzicanin, Amra, "Community Mitigation Guidelines to prevent Pandemic Influenza-United States 2017", Morbidity and Mortality Weekly Report. Center for Surveillance, Epidemiology and Laboratory Services, Centers for Disease Control and Prevention. 66(RR-1), pp 1-34, 2017.

[10] Anderson RM, Heesterbeek H, Klinkenberg D, Hollingsworth TD, "How will country- based mitigation measures influence the course of the COVID-19 epidemic?" The Lancet. 395 (10228): 931-934, March 2020.

[11] "Community Mitigation Guidelines to Prevent Pandemic Influenza-United States, Recommendations and Reports. Centers for Disease Control and Prevention. 66 (1), April, 2017.

[12] Barclay, Eliza; Scott, Dylan; Animashaun, "The US doesn't just need to flatten the curve. It needs to raise the line". Vox. April, 2020.
[13] Baird Robert P, "What it means to contain and mitigate the Coronavirus", The New Yorker. March 2020.
[14] Imperial College, "Impact of non-pharmaceutical interventions (NPIs) to reduce COVID-19 mortality and healthcare demand, Covid -19 Response team, March, 2020.
[15] Advice on the use of masks in the context of COVID-19- https://www.who.int/publications-detail/advice-on-the-use-of-masks-in-the-community-during-home-care-and-in-healthcare-settings-in-the-context-of-the-novel-coronavirus-(2019-ncov)-outbreak.
[16] Getting your workplace ready for COVID-19 https://www.who.int/docs/default-urce/coronaviruse/advice-for-workplace-clean-19-03-2020.pdf.
[17] Considerations in the investigation of cases and clusters of COVID-19. https://www.who.int/who-documents-detail/considerations-in-the-investigation-of-cases-and-clusters-of-covid-19
[18] Key planning recommendations for Mass Gatherings in the context of the current COVID-19 outbreak https://web-prod.who.int/publications-detail/key-planning-recommendations-for-mass-gatherings-in-the-context-of-the-current-covid-19-outbreak
[19] WHO. A health telematics policy in support of WHO's Health-For-All strategy for global health development: report of the WHO group consultation on health telematics, 11–16 December, Geneva, 1997. Geneva, World Health Organization, 1998.
[20] Craig J, Patterson V. Introduction to the practice of telemedicine. Journal of Telemedicine and Telecare, 11(1):3–9, 2005.
[21] https://pubmed.ncbi.nlm.nih.gov/32238336/
[22] Telemedicine Practice Guidelines Enabling Registered Medical Practitioners to Provide Healthcare Using Telemedicine, BOARD OF GOVERNORS In supersession of the Medical Council of India, This constitutes Appendix 5 of the Indian Medical Council (Professional Conduct, Etiquette and Ethics Regulation, 2002], March 2020, https://www.mohfw.gov.in/pdf/Telemedicine.pdf
[23] Jiang F, Jiang Y, Zhi H, et al. Artificial intelligence in Healthcare: past, present and future. Stroke Vasc Neurol. 2:230-234, 2017.
[24] Hamet P, Tremblay J, Artificial intelligence in Medicine. Metabolism. 69: S36-S40, 2017.
[25] Wallis C. How artificial intelligence will change medicine. Nature. 576: S48-S48, 2019.
[26] Bogoch II, Brady OJ, Kramer MUG, et, al. Anticipating the International spread of Zika virus from Brazil. Lancet. 387:335-336, 2016.
[27] Niller E, An AI Epidemiologist Sent the First Warnings of the Coronavirus WIRED, 2020. https://www.wired.com/story/ai-epidemiologist-wuhan-public-health-warnings.
[28] Yan L, Zhang HT, Xiao Y, et al, Prediction of critically in patients with severe COVID-19 infection using three clinical features: a machine learning-based prognostic model with clinical data in Wuhan. Med Rxiv preprint. 2020.
[29] Chen J, Wu L, Zhang J et al, Deep learning-based model for detecting 2019 novel coronavirus pneumonia on high-resolution computed tomography: a prospective study. Med Rxiv preprint, 2020.
[30] Wang L, Wong A, COVID-Net: a tailored deep convolutional neural network design for detection of COVID-19 cases from chest radiology images, 2003.
[31] Jumper J, Tunyasuvunnakool K, Kohli P, Hassabis D, The Alpha Fold Team. Computational predictions of protein structures associated with COVID-19. DeepMind website, 2020. https://deepmind.com/research/open-source/computational-predictions-of-protein-structures-associated-with-COVID-19
[32] Chun A, Coronavirus: China's investment in AI is paying in a big way. South China Morning post:2020, 2020. https://www.scmp.com/comment/opinion/article/3075553/time-coronavirus-chinas-investment-ai-paying-big-way.
[33] Hossain FA, Lover AA, Corey GA, Reich NC, Rahman T, FluSense: a contactless syndromic surveillance platform for influenza-like illness in hospital waiting areas. Proceedings of the ACM on Interactive, Mobile, Wearable and Ubiquitous technologies, 2020.
[34] Hornyak T, What America can learn from China's use of robots and telemedicine to combat the coronavirus [Internet]. CNBC, 2020. https://www.cnbc.com/2020/03/18/how-china-is-using-robots-and-telemedicine-to-combat-the-coronavirus.html
[35] Ali Imran, Iryana Posokhova, Haneya N, Qureshi, Usama Masood, Sajid Riaz, Kamran Ali, Charles N John, Iftikhar Hussain, Muhammad Nabeel, AI4COVID-19:AI enabled preliminary diagnosis for COVID-19 from cough samples via an app. Informatics in Medicine Unlocked: 1-27, 2020.
[36] E Christaki, New technologies in predicting, preventing and controlling emerging infectious diseases. Virulence, 6(6), pp 558-565, 2015.
[37] Sweta Mohanty, Md Harun AI Rashid, Mayank Mridul, Chandanan Mohanty, Swati Swayamsiddha, Application of Artificial Intelligence in COVID-19 drug repurposing. Diabetes & Metabolic Syndrome: Clinical Research & Reviews. 14:1027-1031, 2020.
[38] Ai T, Yang Z, Hou H, Zhan C, Chen C, Lv W, Tao Q, Sun Z, Xia L. Correlation of chest CT and RT-PCR testing in coronavirus disease 2019 (COVID-19) in China: A report of 1014 cases. Radiology 2020. https://doi.org/10.1148/radiol.2020200642.
[39] Luo H, Tang QL, Shang YX, Liang SB, Yang M, Robinson N, Liu JP. Can Chinese medicine be used for prevention of coronavirus disease 2019 (COVID-19)? A review of historical classics, research evidence and

current prevention pro-grams, 2020. Chin J Integr Med 2020.https://doi.org/10.1007/s11655-020-3192-6.

[40] Haleem A, Vaishya R, Javaid M, Khan IH. Artificial Intelligence (AI) applications in orthopedics: an innovative technology to embrace. J Clin Orthop Trauma, 2019.https://doi.org/10.1016/j.jcot.2019.06.012.

[41] Biswas K, Sen P. Space-time dependence of coronavirus (COVID-19) outbreak. Ar Xiv preprint Ar Xiv:2003.03149. 2020.

[42] Stebbing J, Phelan A, Griffin I, Tucker C, Oechsle O, Smith D, Richardson P. COVID-19: combining antiviral and anti-inflammatory treatments. Lancet Infect Dis, 2020.

[43] Sohrabi C, AlsafiZ, O'Neill N, Khan M, Kerwan A, Al-Jabir A, Iosifidis C, Agha R. World Health Organization declares global emergency: a review of the 2019 novel coronavirus (COVID-19). Int J Surg 2020.

[44] Chen S, Yang J, Yang W, Wang C, BE Arnighausen T. COVID-19 control in China during mass population movements at New Year. Lancet 2020. https://doi.org/10.1016/S0140-6736(20)30421-9.

[45] Bobdey S, Ray S. Going viraleCOVID-19 impact assessment: a perspective beyond clinical practice. J Mar Med Soc ;22(1):9, 2020.

[46] Gozes O, Frid-Adar M, Greenspan H, Browning PD, Zhang H, Ji W, Bernheim A, Siegel E. Rapid ai development cycle for the Coronavirus (COVID-19) pandemic: initial results for automated detection &patient monitoring using deep learning CT image analysis. Ar Xiv preprint arXiv:2003.05037. 2020.

[47] Pirouz B, Shaffiee Haghshenas S, Shaffiee Haghshenas S, Piro P. Investigating a serious challenge in the sustainable development process: analysis of confirmed cases of COVID-19 (new type of coronavirus) through a binary classification using artificial intelligence and regression analysis. Sustainability 2020 Jan;12(6):2427, 2020.

[48] Ting DS, Carin L, Dzau V, Wong TY. Digital technology and COVID-19. Nat Med 2020.

[49] Wan KH, Huang SS, Young A, Lam DS. Precautionary measures needed for ophthalmologists during pandemic of the coronavirus disease 2019 (COVID-19). Acta Ophthal mol 2020.

[50] Li L, Qin L, Xu Z, Yin Y, Wang X, Kong B, Bai J, Lu Y, Fang Z, Song Q, Cao K. Artificial intelligence distinguishes COVID-19 from community-acquired pneumonia on chest CT. Radiology 2020.

[51] Smeulders AW, Van Ginneken AM. An analysis of pathology knowledge and decision making for the development of artificial intelligence-based consul-ting systems. Anal Quant Cytol Histol ;11(3), 1989.

[52] Gupta R, Misra A. Contentious issues and evolving concepts in the clinical presentation and management of patients with COVID-19 infection with reference to use of therapeutic and other drugs used in Co-morbid diseases (Hypertension, diabetes etc.). Diabetes, Metab Syndrome: Clin Res Rev 2020; 14 (3), 2020.

[53] Gupta R, Ghosh A, Singh AK, Misra A. Clinical considerations for patients with diabetes in times of COVID-19 epidemic. Diabetes & Metabolic Syndrome. Clin Res Rev 2020;14(3), 2020.

[54] Raju Vaishya, Mohd Javaid, Ibrahim Haleem Khan, Abid Haleem, Artificial intelligence (AI) applications for COVID-19 pandemic. Diabetes & metabolic Syndrome: Clinical Research & Reviews.14:337-339, 2020.

[55] Robin R Murphy, Justin Adams, Vignesh Babu Manjunath Gandudi, Center for Robots Assisted Search and Rescue, Robots are playing many roles in the Corona virus crisis- and offering lessons for future disasters, 2020.

[56] Erico Guizzo, Corona Virus Pandemic: A Call to Action for the Robotics Community, IEEE Spectrum, 2020.

[57] Matt Simon, Science. The Covid-19 Pandemic Is a Crisis That Robots Were Built For, 2020. https://www.wired.com/story/covid-19-pandemic-robots/

[58] Stuart Carlaw, Impact on biometrics of Covid-19, Biometric Technology Today, Vol (4) pp 8-9, 2020. PMCID: PMC 7173828. https://www.ncbi.nlm.nih.gov/pmc/about/covid-19/

[59] Alnoor Peermohamed and Raghu Krishnan, Cities employ drones to keep services up, Economic times, 2020.

[60] Garima Bora, "Covid-19: In the times of touch me not environment, drones are the new best friends", The Economic Times, 2020.

[61] Prachi Verma and Rica Bhattacharya, 'IIts are helping India win the COVID battle, The Economic Times, 2020.

[62] Tushar Tere, 'Drones to keep eye on lockdown violators', The Economic Times, 2020.

[63] Rahul Tripathi, Covid-19 lockdown: Authorities rely on drone eye to maintain vigil, The Economic Times,2020.

[64] Y V Phani Raj, Karimnagar to have drone solution for Covid-19, Telangana Today, 2020.

[65] Tarun Nair, 'Ajith Kumar-mentored "Team Daksha" Uses Drones to sanitize Public Places Amid Pandemic, Republic World, 2020.

A Novel Sensible Health Observation System

[1] Abinaya. R, [2] Lakshmi Priya. R, [3] Linga Suvetha.S, [4] Kanthimathi.M

[1][2][3] Student, Department of Computer Science and Engineering, National Engineering College, Kovilpatti, India
[4] Assistant Professor, Department of Computer Science and Engineering, National Engineering College, Kovilpatti, India

Abstract:

The Internet of Things provides higher medical facilities in health-care systems. It's a invasive, easy technology that permits everything to be connected and allows effective communication between the connected "things". IOT helps connect the individuals by neatly empowering their health and wealth through wearable gadgets. The projected system communicates via network-connected devices and appears at the patient's health and records their medical data. This system is going to be active for twenty four hours and provides medical care to the patients even inside the areas with no hospitals in their regions by connecting over the net. The system acquires data regarding their health standing via wearable devices that record their pulse and temperature. The obtained values are transferred to the cloud for straightforward access. The patient history are going to be hold on within the webserver, and therefore the doctor will access the data whenever required from any corner of the globe.

Keywords:

Internet of things, thingspeak, sensible health, Arduino Uno, pulse device, heart rate

1. INTRODUCTION

The use of good devices and mobile technologies` in health has caused a big impact on the planet. Health specialists endlessly benefit of those technologies, therefore generating a substantial improvement in health care . Likewise, Most of the standard users square measure being served from the advantages of the E-Health (health care supported by ICT) to boost for facilitate and assist their health. in keeping with the planet Health Organization,the highest getable customary of health could be a basic right for every and each individual. As this genuinely evokes US, we have a tendency to commit to propose a completely unique system that puts forward in good patient health observation system that uses sensors to trace very important patient parameters and uses the net to update the doctors to assist just in case of any problems at the earliest preventing death rates.

Patient Health observation mistreatment IoT could be a growing technology to modify the monitor of patients (e.g. within the home), which can increase the access in health care and reduce supply prices. This considerably improves the individual's quality of life. It permits patients to require care of their independence, stop complications, and minimize personal prices.

This system facilitates these goals by delivering care right to the house. Also, patients and their members of the family feel comfort knowing that they're being monitored and supported if a tangle arises. Pulse and sign ar the 2 most important indicators for human health. Rate is that the per-minute quantity of heartbeats unremarkably known as the heartbeat rate. To live the heartbeat rate, a rise among the blood flow volume are going to be used by conniving the pulses. IoT primarily good health observation systems aim to focus on the quality style and implementation patterns of intelligent IoT based intelligent health observation devices for patients. During this system, a tool is intended to live very important values like pulse and vital sign, directly moving patient health. The temperature detector and therefore the pulse detector on the device monitor connected information from the patient's tip analyzed with the Arduino UNO. These analysis results ar transferred to the "Smart Health" interface, created with the factor speak cloud network, that provides a platform to quickly collect and analyze information from the sensors connected through the net. the information is displayed on the webserver. once the patient's very important parameters reach vital levels, associate audible-visual alert is distributed to the patient and members of the family via factor speak. The device's primary purpose is to extend the probabilities of survival by providing medical help to the patient among the primary few hours just in case of attainable attack.

2. EXISTING SYSTEM

In the existing system, the folks within the rural areas or the underdeveloped countries face the shortage of treatment and health care services in time. basically the old patients face the barriers of often attending the clinic or to possess the extended keep within the hospitals a number of the inveterately unwell or sick patients undergoes the tough lifetime of carrying the wired device when and ineffective to maneuver and simple walk with the wires on their body all time. additionally thereto traveling is one in every of the burdens. therefore our project is cost-efficient and reduces all the barriers that the patients face it saves time and adaptability.

3. METHODOLOGY

A. Problem Description

Now a day's patients face problematic state of affairs because of specific reason for heart issues and attacks, that is due to the nonbeing of fine medical maintenance to

patients at the required time. Thus, the system uses Temperature and Heartbeat device for following the patient's health. The device is connected to the Arduino to follow the patient health and wireless fidelity affiliation to transfer the information to the webserver. Doctors and patient relatives will see their patient health condition whenever required from the corner of the planet.

B. Objective

In this project, a wireless patient observation system is developed that enables patients to be mobile in their social areas. The developed system ceaselessly measures the patient's pulse and temperature and provides observation and trailing through an internet server. The device's primary purpose is to form provision that they get medical care as shortly as doable.

C. System Architecture

The planned system of IoT primarily based heath watching system consists of Arduino microcontroller that is that the brain of the project. Arduino collects real time information of patient's health from pulse detector that measures heartbeat in minutes or pace (beats per minute). A digital temperature detector connected to Arduino measures temperature of the patient's body. A generic ESP8266 IoT module is connect with Arduino UNO, it's to blame for connecting the machine to net and additionally for causation health information to a IoT server (Thingspeak) for storing and watching. this is often helpful for a attention skilled for active watching of a patient on website.

Fig.1 shows the basic architectural design of the smart health monitoring system.

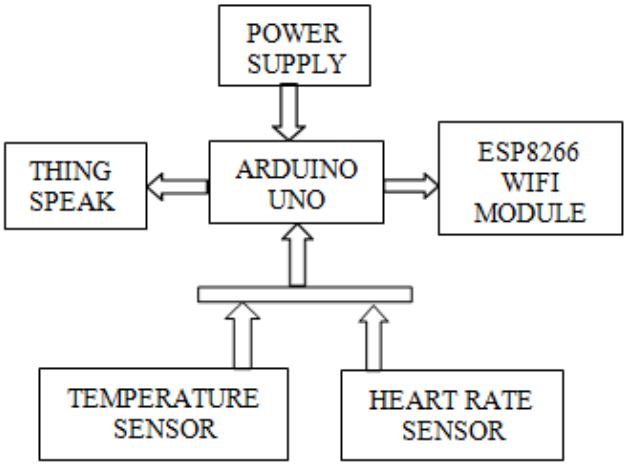

Fig.1 System Architecture

Arduino UNO

Arduino Uno could be a microcontroller board that is predicated on the ATmega328P (datasheet). It contains everything that must support the microcontroller. Connect the Arduino UNO to a pc with a USB cable or power it with a AC-to-DC adapter or battery to induce started.

Fig.2 Arduino UNO

Heartbeat Sensor

The heart rate is detected by the reflection of lightweight that is emitted by the inexperienced light- emitting diode on the APDS-9008 light device. Fig.3 shows the front and back sides of the heartbeat device.

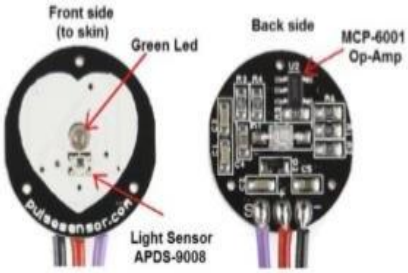

Fig.3 Pulse Sensor front and back sides

LM35 Temperature Sensor

In LM35 Temperature detector, the output voltage varies, supported by the temperature around it. Fig.4 shows the Pin Configuration of LM35 Temperature detector.

Fig.4 LM35 Temperature Sensor

ESP8266 Module

Fig.5 shows the ESP8266 Module that may be a terribly user friendly and cheap device to supply net property to your comes. The module will work each as AN Access purpose (can produce hotspot) and as a station (can connect with Wi-Fi), thence it will simply fetch information and transfer it to the net creating net of Things as simple as attainable.

 ISBN: 978-93-90214-20-4

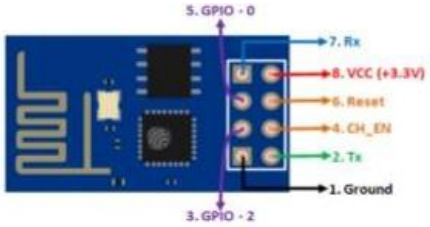

Fig.5 ESP8266 WiFi Module

Thingspeak

As in Fig.6, ThingSpeak is an IoT analytics platform service that enables you to combine, visualize and analyse live knowledge streams within the cloud. ThingSpeak provides instant visualizations of information denoted by your devices to ThingSpeak. With the flexibility to execute MATLAB® code in ThingSpeak you'll be able to perform on-line analysis and process of the info because it comes in. ThingSpeak is usually used for prototyping and proof of thought IoT systems that need analytics.

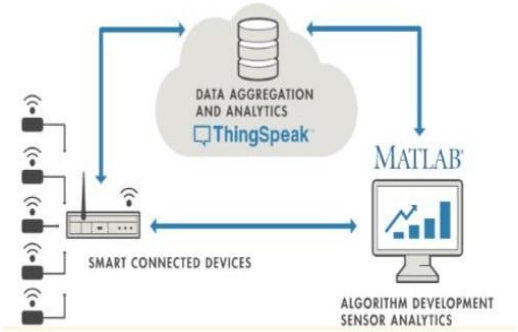

Fig.6 Thingspeak Network

ThingSpeak provides a superb tool for IoT primarily based comes. victimization the ThingSpeak website, we are able to monitor the detected values and management the system over the net, victimization the Thingspeak Channels and webpages provided by ThingSpeak. ThingSpeak Collects the knowledge from the sensors, Analyses and Visualizes the knowledge, and acts by triggering a reaction. the subsequent square measure the steps for channel creation in Thingspeak.

Step 1: First of all, We Create an Account on ThingSpeak.com, then Sign In and click on Get Started.

Step 2: Now go to the 'Channels' menu and click on New Channel option on the same page for further process.

Step 3: Now, we saw a form for creating the channel, fill in the Name and Description as per our choice. Then fill 'Pulse Rate', 'Temperature' in Field 1, Field 2 labels, and tick the Fields' checkboxes. Finally, Save the Channel. Now our new channel has been created. Fig.7 shows the channel creation.

Step 4:- We will see two charts and two gauges, as shown below. Note that the Write API key will use this key in our code.

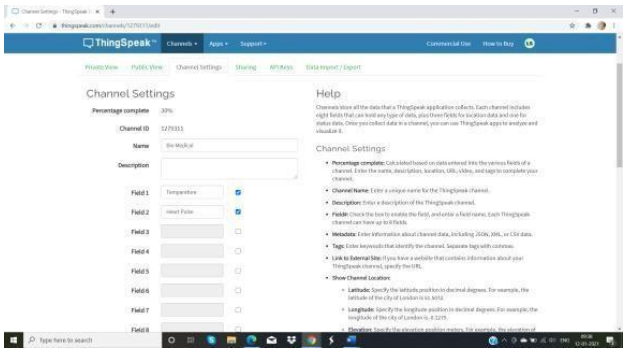

Fig.7 Channel creation

4. IMPLEMENTATION

A. Circuit Diagram

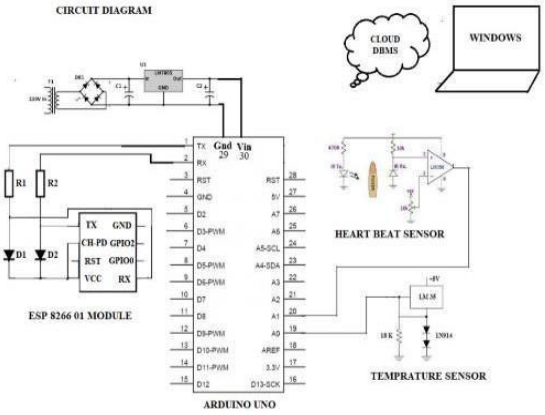

Fig.8 Circuit Diagram

The Arduino is liable for grouping, displaying and causing the information to ESP8266.

The whole circuit may be high-powered by using USB or via "Vin" pin (9V-12V). The ESP8266 module could be a microcontroller board with RAM, ROM, clock, communication protocols, and I/O pins a bit like the other microcontrollers and wishes to be programmed to create it practical. Arduino collects and sends patient's information to the ESP8266 Module. It'll connect with its selected server that's programmed to that and passes it. Measurement of vital sign will reveal heaps regarding the patient's health, and a aid skilled will determine abnormalities in a very patient's health.

Connect Pulse Sensor output pin to A1 of Arduino and other two pins to VCC & GND.

Connect LM35 Temperature Sensor output pin to A0 of Arduino and other two pins to VCC & GND.

The RX pin of ESP8266 works in 3.3V and will not communicate with the Arduino when we connect it directly with the Arduino.

The 5V into 3.3V. This can be done by connecting 2.2K & 1K resistor

The RX pin in the ESP8266 is connected with the pin 10 of Arduino through the resistors.

Connect the TX pin with the ESP8266 to the pin 1 of the Arduino.

 ISBN: 978-93-90214-20-4

B. Experimental Setup

The system is implemented by using the combination of hardware components and web server. All the hardware requirements are assembled in the working phase. The proposed system is demonstrated in Fig.9.

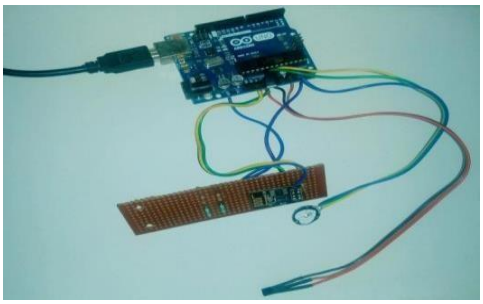

Fig.9 Smart heath monitoring system

IOT patient monitoring has two sensors. The temperature sensor and the Heartbeat sensor. This project is useful since the doctor can monitor patient health parameters by visiting a Thing Speak website. Now the doctor or family members will monitor or track the patient's health through the Android apps. To operate an IOT based health monitoring system project, we need a WiFi connection.

The microcontroller or the Arduino board connects with the WiFi network using a WiFi module.This project will work with a working WiFi network. So we create a WiFi zone using a WiFi module, or you can even create a WiFi zone using Hotspot on our mobile phone. The Microcontroller continuously reads input from these two senses. Then this values sends to the cloud by sending this data to a particular URL/IP address. Then, sending data to IP is repeated after a specific interval of time. For example, we have sent data every 30 seconds in this project.

In this project, we will send the LM35 temperature sensor data and heart rate sensor data to ThingSpeak using the ESP8266. ThingSpeak is an IOT platform that lets us store the data in the cloud and develop the Internet of things (IOT) applications.

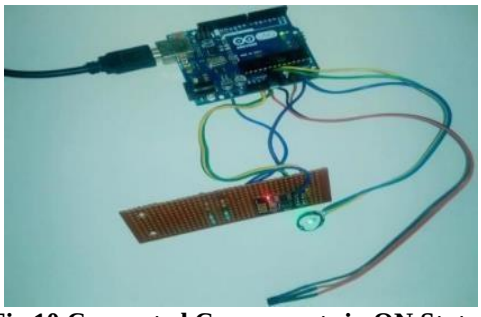

Fig.10 Connected Components in ON Status

C. Thingspeak Setup

To create a channel on thingspeak 1st, move to ThingSpeak.com and click on on “Get Started for Free”. Then the sign-up kind can return up enter the data needed and check in for thingspeak. After that, click on “New Channel” to make a channel to store the data. Fig.11 shows the data concerning the new channel. After that, move to the API keys section in thingspeak and duplicate that write API key and embody this API key in our code.

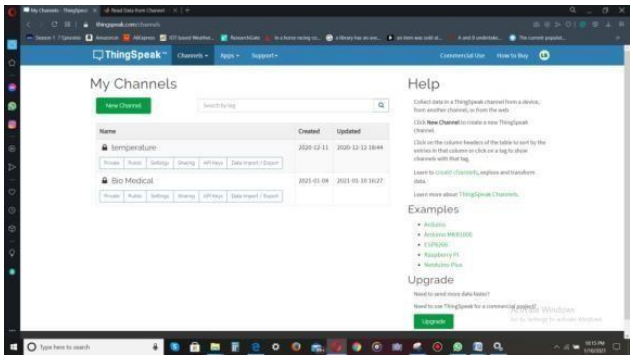

Fig.11 Smart Health Monitoring Channel

5. RESULT

The user prototype is depicted in Fig.12, where the system is tested with one user. It shows that one user's hand is attached with body temperature sensor (LM35), Heart rate sensor and the data displayed in the webserver.

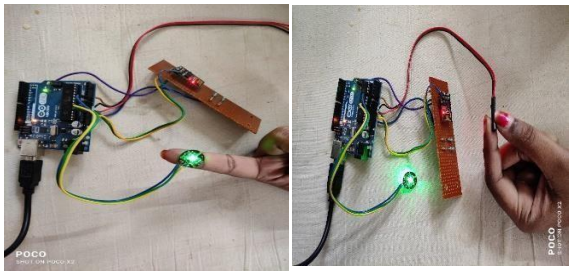

Fig.12 Prototype

After connecting the circuit and uploading the code in Arduino IDE software, the following graph shown in Fig.13 is generated in Thingspeak dashboard.

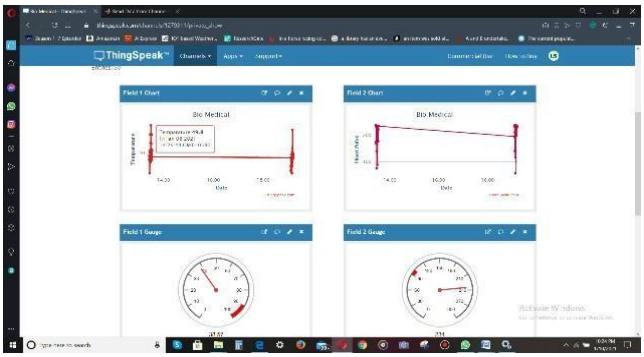

Fig.13 Temperature and heart rate sensor chart

After uploading and running the Arduino code, It should be connected with our WiFi and begin sending data to thingspeak about every 30 seconds. If any sudden changes happen in temperature values, the temperature widget which

is shown in Fig.14, should be alert by turning on a red colour.

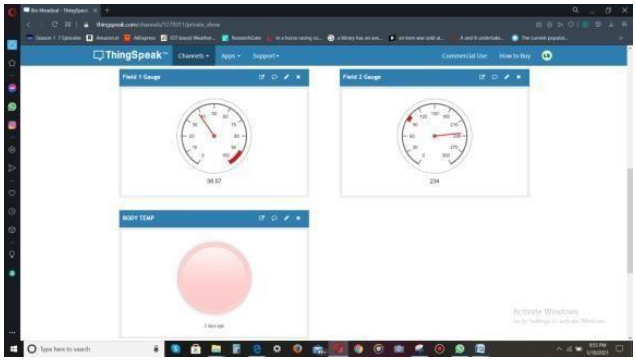

Fig.14 Temperature Widget

6. CONCLUSION AND FUTURE DEVELOPMENT

A. Conclusion

The health monitoring can be positively used in emergencies as it can be daily monitored, recorded and stored as a database. Patient health parameter data is held over the cloud. It is more advantage than maintaining the records on printed papers kept in the files. This device is used monitored and keep track of changes in the patient's health parameters over the period. So doctors can reference these changes or the history of the patient while suggesting the treatment or the medicines to the patient. Hospital stays and visit for daily routine are minimized due to remote monitoring system.

B. Future Development

We shall add GPS module in IOT patient observation system by using the Arduino Uno and WiFi module project. This GPS module can verify the position or the place of the patient by using the line of longitude and latitude values received. Then it'll send this location to the cloud webserver, that's the IOT by using the WiFi module. Then doctors will verify the patient's position just in case they need to require some preventive action.

REFERENCE

[1]A. Sparsh, T.L. Chiew. Remote health monitoring using mobile phones and web services Telemedicine and e-Health Journal, 16 (5) (2010), pp. 603-607.

[2]C.Min, G. Sergio, L. Victor, Z. Qian, L. MingA 2G-RFID-based E-healthcare system February IEEE Wireless Communication (2010), pp. 37-43 .

[3]S.M. HossainPatient status monitoring for smart home healthcare IEEE international conference on multimedia and expo workshop, ICMEN), Seattle (2016) .

[4]M. Andrea, R.P. Mario, F. Emanuele, L. Sauro, P. Filippo, C. Sara, S. Lorenzo, C. Annalis a, R. Luca, B. Riccardo, P. Loreto, O. Gianni, M.R. GianA smart sensing architecture for domestic monitoring: Methodological approach and experimental validation MDPI Sensors, 18 (7) (2018), pp. 1-22 .

[5]F. Muhammad, F. Iram, L. Sungyoung, L. Young-KooDaily life activity tracking application for smart homes using android smartphone 14th international conference on advanced communication technology, ICACT) (2012) .

[6]M. S. D. Gupta, V. Patchava, and V. Menezes. Healthcare based on iot using raspberry pi. In 2015 International Conference on Green Computing and Internet of Things (ICGCIoT), pages 796–799, Oct 2015.

[7]P. Gupta, D. Agrawal, J. Chhabra, and P. K. Dhir. Iot based smart healthcare kit. In 2016 International Conference on Computational Techniques in Information and Communication Technologies (ICCTICT), pages 237– 242, March 2016.

[8]N. V. Lopes, F. Pinto, P. Furtado, and J. Silva. Iot architecture proposal for disabled people. In 2014 IEEE 10th International Conference on Wireless and Mobile Computing, Networking and Communications (WiMob), pages 152–158, Oct 2014.

[9]R. Nagavelli and C. V. Guru Rao. Degree of disease possibility (ddp): A mining based statistical measuring approach for disease prediction in health care data min- ing. In International Conference on Recent Advances and Innovations in Engineering (ICRAIE2014), pages 1–6, May 2014.

[10]I. Chiuchisan, H. N. Costin, and O. Geman. Adopting the internet of things technologies in health care systems. In 2014 International Conference and Exposition on Electrical and Power Engineering (EPE), pages 532– 535, Oct 2014.

Recognition for Lateral Faces using Neural Networks

[1] Dr.M.Aruna Safali, [2] Rajitha Laxmi.Ch, [3] Y.Lavanya, [4] Bhagyasri Pavuluri

[1] Associate Professor, Dept of IT, NRI Institute of Technology
[2][4] Assistant Professor, Dept of ECE, RamaChandra College of Engineering, Chennai, Tamil Nadu, India
[3] Associate Professor, Dept of ECE, RamaChandra College of Engineering, Chennai, Tamil Nadu, India

Abstract:

Face recognition is most difficult and complicated technique. Recognition of lateral faces is very difficult compare with normal face recognition. Pattern recognition is mostly used in this system to recognise the lateral face patterns (LFP). Neural network is used to find the patterns and lateral face recognition can be done by this technique. After the many researches face recognition becomes difficulty for the various techniques based on their parameters. In this paper, the amalgamative lateral face recognition(ALFR) which is merged with machine learning and neural network features can be done by using synthetic dataset consists of 200 lateral faces. Performance shows the improved results of proposed technique.

Keywords:

lateral face patterns (LFP), neural networks (NN), face recognition

1. INTRODUCTION

Pattern recognition (PR) is a cutting edge machine learning issue with various applications in a vast field, including lateral face recognition (LFR), Character recognition (CR), Speech recognition (SR). The field of example acknowledgment is still especially in it is outset, in spite of the fact that as of late a portion of the boundaries that hampered such mechanized LFR has been lifted because of advances in PC equipment giving machines prepared to do the quicker and progressively complex calculation. FR is the most tedious task for the human brain. It is ordinarily utilized in applications, for example, human-machine interfaces and programmed access control frameworks. FR includes contrasting a picture and a database of put away faces so as to distinguish the person in that information picture. The related errand of face discovery has direct pertinence to confront acknowledgment since pictures must be broken down and faces distinguished before they can be perceived. Identifying faces in a picture can likewise center the computational assets of the face acknowledgment framework, streamlining the frameworks speed and execution. Face identification includes isolating picture windows into two classes; one containing faces (targets), and one containing the foundation (clutter). It is troublesome in light of the fact that despite the fact that shared characteristics exist between faces, they can differ significantly as far as age, skin shading and expression on faces.

LFR is an intriguing and effective use of Pattern acknowledgment and picture investigation. Facial pictures are basic for savvy vision-based human-PC association. Face preparing depends on the way that the data about a client's personality can be removed from the pictures and the PCs can act likewise. Face recognition has numerous applications, extending from diversion, Information security, and Biometrics [1]. Various strategies have been proposed to identify faces in a solitary picture. To construct completely mechanized frameworks, strong and effective face identification calculations are required. The face is identified once an individual's face comes into a view [2]. When a face is recognized, the face locale is edited from the picture to be utilized as "Test" into the information to check for potential matches. The face picture is preprocessed for variables, for example, picture size and enlightenment and to identify specific highlights. The information from the picture is then coordinated against the learning. The coordinating calculation will create a likeness measure for the match of the test face into the information.

An Amalgamative face recognition (AFR) strategy where nearby highlights are given as the contribution to the neural system. To start with, the face locale is separated from the picture by applying different pre-preparing exercises. The technique for finding the face district is known as face confinement. The neighborhood highlights, for example, eyes and mouth are removed from the face district. The separation between the eyeballs and the separation between the mouth endpoints are determined to utilize the distance computation algorithm. At that point the separation esteems between the left eye and the left mouth endpoint, the correct eye and the correct mouth endpoint, the left eye and the correct mouth endpoint, the correct eye, and the left mouth endpoint are determined. These qualities are given as contributions to the neural system.

 ISBN: 978-93-90214-20-4

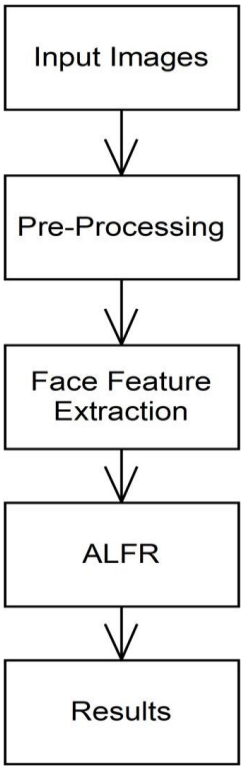

Figure: 1.1 System Architecture

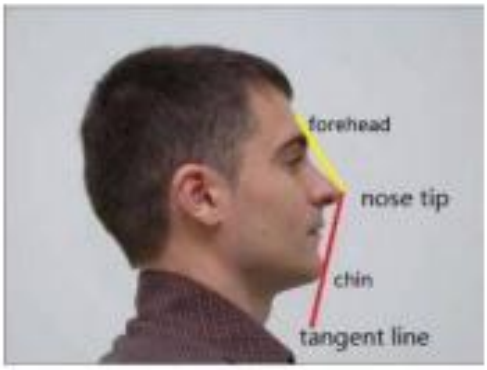

Figure: 2.1 Sample Lateral Face

2. METHODOLOGIES

In this chapter, various methodologies are discussed.

Feature Based Lateral Face Recognition (FBLFR)

The **FBLFR** method performs on human face. Input image can be in different face orientation where transformation of feature space is learned and applied on face for feature extraction. Objective is human's various face features like left eye, right eye, nose, mouth are to be extracted. Viola - Jones Skin detection method is best for feature extraction. In multiview face recognition as shown in Figure 3 and 4, face image pass as an input then local feature of face to be extracted. In result it develops mirror image of any best side of human face as 2D mug shown in Figure 3.1.

Figure: 3.1 Sample Lateral Faces

Figure: 3.2 Sample Lateral Faces

Figure: 3.3 Sample Lateral Faces

3.2 ROI Face Detection & Alignment

It involves the only region of the face from datasets and target sample. These pictures can have human body segment like the neck, bind, fabric, top or whatever other things that aren't required for acknowledgment. Utilizing viola-jones face identification system creators remove just face area. Viola-jones face identification system has three indispensable advances: I) include extraction, ii) boosting iii) multi-scale discovery. Distinguished face district may have a minor cross face as of typical human behavior. It conceals any hint of failure district as an element vector for further examination.

3.3 Face Features Vector Generation

Target images may have other background objects too, so using viola-jones face detection technique proposed method extract available faces from target image scene. At the end of this phase all faces are extracted and store it properly for future verification operation. In normal environment human face may not be straight always, so in recognition method

position of face feature landmark is changed, and as a result it gives less matching value so face recognition might be unsuccessful. For solution of this issue, we can rotate whole face by calculating distance from X and Y axis of both eyes.
y = left eye from Y axis − right eye from Y axis
x = left eye from X axis – right eye from X axis
Rotation angle = arctan (y/x)
Using above equation we have rotate whole face to prepare it straight then send for further steps. End of this step all faces are extracted and store it in form of feature vector for feature extraction.

3.4 Integrated Deep Model for Face Detection and Landmark Localization from ''In the Wild'' Images

In recent years the face detection and landmark localization are two main factors in facial analysis applications. Many of the issues are solved to detect the face recognition which increases the precision of face detection [20]. This reference proposed the novel method the Integrated Deep Model (IDM) and adopted the two traditional deep learning techniques such as Faster R-CNN and a stacked hourglass which improves the face detection precision and accurate landmark localization. The optimization function is integrated with the proposed system which increases the accuracy and reduces the false positive rate which is 63%. The IDM technique uses the Annotated Faces In-The-Wild, Annotated Facial Landmarks in The Wild and Face Detection Dataset and Benchmark face detection test sets and shows a high level of recall and precision when compared with various existing methods. The dataset used in this system is 300-W test sets which are focused on localization accuracy with original bounding boxes. The increase with our proposed system is 0.005% maximum with facial landmarks which border the face.

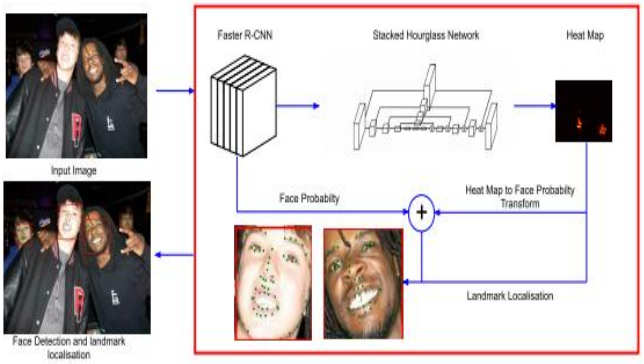

Figure: 3.6 Steps to process the IDM

Deep Learning Face Attributes in the Wild

Face attributes prediction is the most complicated issue to find the various complex face variations. In this system, they have shown the two categories such as LNet and ANet are the finely trimmed combined with tags and these are previously trained. For the face localization, LNet is the pre-trained traditional massive item and the other ANet is used to predict the attributes [21]. The proposed system provides not only accuracy but also the facts based on face learning. This will increase the face localization (LNet) and attribute prediction (ANet) with different pre-training techniques. The fine-tuned filters are used to get the image-level attribute tags and reply to the maps over all the images. This will also explain the high-level hidden neurons of ANet automatically which finds the semantic items after training with massive face findings.

Method	Dataset	Description	Result
Distribution Based	MIT test set	Two sets of high and low resolution gray scale images with multiple faces	81.9%
Neural Network	CMU test set	130 gray scale images	90.3%
Naive Bayes	CMU profile face test set	208 gray scale images	93.2%
Kullback relative Information	Kodak dataset	Faces of multiple size, pose and under varying.	98.0%

3. EXPERIMENTS

This is the synthetic dataset which consists of various lateral faces that can be used for training and then the input is given to system for face detection of lateral faces. These experiments are done by using the java programming language. There are 3 parameters are shown in the bases of performance such as sensitivity, specificity and accuracy.

Figure: 6 Dataset image

 ISBN: 978-93-90214-20-4

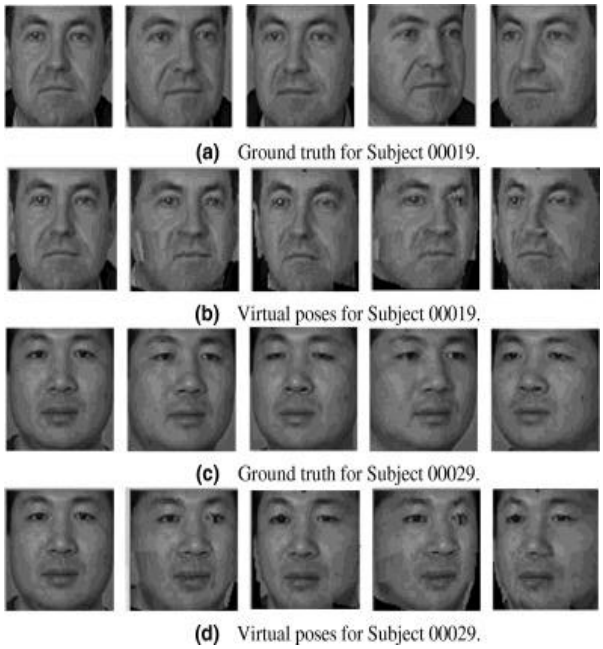

Figure: 7 Dataset image

Performance Evolution

By utilizing the performance measures namely False Positive Rate, False Negative Rate, Sensitivity, Specificity and Accuracy, the performance of the system is estimated. The basic count values such as True Positive (TP), True Negative (TN), False Positive (FP) and False Negative (FN) are used by these measures.

False Positive Rate (FPR)

The percentage of cases where an image was classified to normal images, but in fact it did not.

$$FPR = \frac{FP}{FP + TN}$$

False Negative Rate (FNR)

The percentage of cases where an image was classified to abnormal images, but in fact it did.

$$FNR = \frac{FN}{FN + TN}$$

Sensitivity

The proportion of actual positives which are correctly identified is the measure of the sensitivity. It relates to the ability of the test to identify positive results.

$$Sesitivity = \frac{No.of\ TP}{No.of\ TP + No.of\ TN}$$

Specificity

The proportion of negatives which are correctly identified is the measure of the specificity. It relates to the ability of the test to identify negative results.

$$Specificity = \frac{No.of\ TN}{No.of\ TN + No.of\ FP}$$

The following steps are utilized by the ALFR system

1.) **Initialize the lateral face0 images from the datasets.**
2.) **Pre-processing the samples.**
3.) **Training the samples.**
4.) **Start matching the sample images.**
5.) **Calculate the sensitivity**
6.) **Specificity and Accuracy.**
7.) **Show results**
8.) **Stop**

	Accuracy	Sensitivity	Specificity
ALFR	**89%**	**86%**	**89%**

Table: 1 Performance of Integrated system in terms of Accuracy

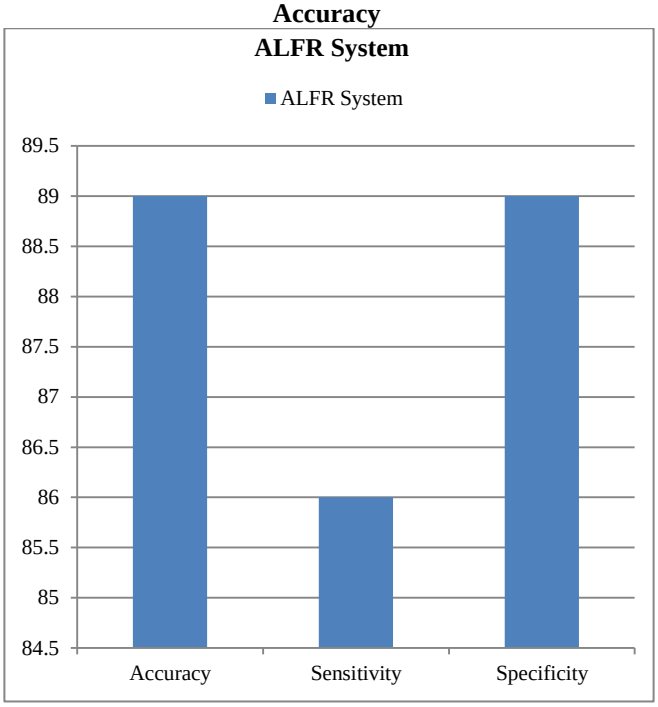

Figure: 11 Show the performance of Integrated System

4. CONCLUSION

In this paper, the proposed system focuses on improving the accuracy, sensitivity and specificity for the lateral faces. It is very needed for every face recognition according to the lateral faces. Recognition of lateral faces is mostly difficult to get the accurate result. But the proposed system works according to the input lateral face image.

REFERENCE

1. X. Zhang, Y. Gao "Face recognition across pose: A review" Pattern Recognition 42(11) (November 2009) 2876–2896
2. T. Ahonen, A. Hadid, M. Pietik¨ainen. "Face recognition with local binary patterns" In Proc. of ECCV, 2004
3. B. Babenko, P. Doll´ar, Z. Tu, S. Belongie "Simultaneous learning and alignment: Multi-instance and multi-pose

learning" In Workshop on Faces in 'Real-Life' Images: Detection, Alignment, and Recognition, 2008
4.A.F.Abate,M.Nappi,D.Riccio,G.Sabatino "2D and 3D face recognition: a survey" Pattern Recognition Lett.28(14)(2007) 1885– 1906
5. U. Kurmi, D. Agrawal. Study of Different Face Recognition Algorithms and Challenges. International Journal of Engineering Research (ISSN:2319-6890)(online),2347-5013(print) Volume No.3, Issue No.2, pp : 112-115 01 Feb. 2014
6.D.Jiang,Y.Hu,S.Yan,L.Zhang,H.Zhang,W.Gao, Efficient 3D reconstruction for face recognition, Pattern Recognition 38(6)(2005)787–798
7. A. Maghraby, M. Abdalla, "Hybrid Face Detection System using Combination of Viola - Jones Method and Skin Detection" International Journal of Computer Applications (0975 – 8887) Volume 71– No.6, May 2013
8.C.D.CastilloandD.W.Jacobs,Using stereo matching for 2-D face recognition across pose,in:ProceedingsoftheIEEEConferenceonCVPR,2007,pp.1–8
9. V.Blanz,T.Vetter,Facerecognition based on fitting a 3D morphable model, IEEE Trans.PatternAnal.Mach.Intell.25(9)(2003) 1063–1074
10.A.S.Georghiades,P.N.Belhumeur,D.J.Kriegman,Fromfewtomany: illumination cone models for face recognition undervariable lighting and pose, IEEE Trans.PatternAnal.Mach.Intell.23(6)(2001)643–660
11. K.W.Bowyer,C.Kyong,P.Flynn, A survey of approaches and challenges in 3D and multi-modal 3D + 2D face recognition , Comput.VisionImageUnderstanding 101 (1)(2006)1–15
12. Pantic, M., Valstar, M., Rademaker, R., Maat, L.: Web-based database for facial expression analysis. In: IEEE Int. Conf. on Multimedia and Expo, IEEE (2005) 317–321
13. V.Blanz,T.Vetter, Face recognition based on fittinga 3D morphablemodel, IEEE Trans.Pattern Anal.Mach.Intell.25(9) (2003)1063–1074
14. Aghajanian J. and Prince S., "Face Pose Estimation in Uncontrolled Environments," International Conference on Computer Vision, available at: http://www.bmva.org/bmvc/2009/ Papers/Paper256/Abstract256.pdf, last visited 2009
15. C. Moujahdi, S. Ghouzali. Inter-Communication Classification for Multi-View Face Recognition. The International Arab Journal of Information Technology, Vol. 11, No. 4, July 2014
16. Zhaoxiang Zhang, Chao Wang and Yunhong Wang, "Video-Based Face Recognition: State of the Art".
17. V. Kr¨ueger and S. Zhou.,"Exemplar-based face recognition from video.", In Proc. European Conf. on Computer Vision, volume 4, pp: 732-746.
18. Masi et al., "Learning Pose-Aware Models for Pose-Invariant Face Recognition in the Wild," in IEEE Transactions on Pattern Analysis and Machine Intelligence, vol. 41, no. 2, pp. 379-393, 1 Feb. 2019.
19. J. Zhao, J. Han and L. Shao, "Unconstrained Face Recognition Using a Set-to-Set Distance Measure on Deep Learned Features," in IEEE Transactions on Circuits and Systems for Video Technology, vol. 28, no. 10, pp. 2679-2689, Oct. 2018.
20. G. Storey, A. Bouridane and R. Jiang, "Integrated Deep Model for Face Detection and Landmark Localization From "In The Wild" Images," in IEEE Access, vol. 6, pp. 74442-74452, 2018.
21. Z. Liu, P. Luo, X. Wang and X. Tang, "Deep Learning Face Attributes in the Wild," 2015 IEEE International Conference on Computer Vision (ICCV), Santiago, 2015, pp. 3730-3738.

A Review on Data level Approaches to address the Class Imbalance Problem

[1] Kamlesh Upadhyay, [2] Prabhjot kaur, [3] SVAV Prasad

[1][3] Lingayas Vidyapeeth, Faridabad, India
[2] Maharaja Surajmal Institute of Technology, GGSIP University, New Delhi, India

Abstract:

Effective data mining shows an important role in current situation of huge data sets. Classification is a best tool to find patters from data. There are variety of classification models that are proposed by our researchers over the time to accomplish this task. However, various traditional classification models are available which efficiently work to detect those classes which have comparable instances. But in case of data having skewed class distribution, the standard classification models do not work properly because they show biasness towards the majority patterns. So, in case of applications which look for rare cases where we need minority class, it is not helpful and doesn't give genuine performance of the classifier. Among various proposed solutions for class imbalance problem, Data level technique (undersampling, oversampling and Hybrid) is quite easy and effective, which allow us to remove or add data within classes or to do both to balance the data. In this review paper, below an insight of Data level technique is presented to overcome the class imbalance problem (CIP).

Keywords:

Standard classifiers, Data Mining, Machine Learning, Class Imbalance problem, Classification, Oversampling, Undersampling, Hybrid, Ensemble

1. INTRODUCTION

In Data mining we find a set of usable data from a set of large data set in space. It means this is the process of analyzing patterns of data in large batches of data from database [1]. The extracted data related information is suitable for studying the statistical and basic characteristics of actual row data and to defining a differential and comprehensive structure for data pull out for the future analysis for new cases and unknow cases[2]. However, the data pattern that is being extracted by data mining is affected by various factors. Factors included dimension data and large size of data, unstructured data, also noise in data and data with missing attribute, redundant data, duplicate and about imbalanced data set. Hence this creates the need to design some advanced and perfect models for data analysis. The Machine Learning domain in AI offers varies advanced leaning models for varies problems. Classification model is one of the popular ML models is used for class imbalance. It is a significant data analysis model that offers to create an advance and predictive learning model that will learn the pattern to the given set of data pattern (known as training set). These models are identified the inter-relationship about data attributes values and respective target variable values [3]. Some well-known and popular classification algorithms are termed as (K-NN) K-Nearest Neighbour, Artificial Neural Network (ANN), Naïve Bayes and Decision Tree (DT) and next is Support Vector Machine (SVM) [4] [5] etc. Although, the performance of above learning algorithms (and some other as well) totally depending upon the pattern available in the data in database. This inspires the researchers to further investigate the happening to be with class imbalance problem (CIP). In-fact the class imbalance Problem occurs due to skewed distribution of data set presence among different classes in a dataspace, that is commonly known as imbalanced data. This is very first explained by author Japkowicz [6] in details in his work. Although Standard classification algorithms (SCA) lead to produce inappropriate results when they are directly working with the imbalanced dataset because they directly shows biasness for majority class instances because traditional data classifiers always assume that the data distribution used for testing and training the model is same and hence wrongly classifying the minority class patterns over majority class. Another notable issue with standard classification algorithm (SCA) is their wrong assumption that error for different classes have the exactly same classification cost, but usually minority class is related with a misclassification cost that is higher. Thus, the issue should be well handled for CIP for creating an effective classification model. Hence, to deal with this problem, we have many solutions are proposed by the research scholars year by year. On very high level all the available solutions are divided in three base categories: first is - Data level solutions [7], second one is Algorithmic Solutions and third one is Ensemble learning based solutions [8] [9]. In all the above described categories, the first category - data level solutions are relatively popular because of its quite easy implementation, feasibility, execution, high accuracy and proficiency. In the current review paper on CIP, an overall understanding into the Data level techniques has been presented with an brief emphasis on their working technique, logic and principle.

The paper is divided in the following category. Section 2 contains, very brief overview on available solutions for handling the class imbalance problem (CIP) is described. In section 3 explained a brief survey on first category- Data level methods considered in this study and in last section which is 4th section is presented with conclusions.

2. REVIEW ON SOLUTION TO CLASS IMBALANCE PROBLEM

Existing solution for Class imbalance problem (CIP) has been presented in this section. Below Figure 1 represents a graphical diagram for the solution to (CIP)class imbalance problem.

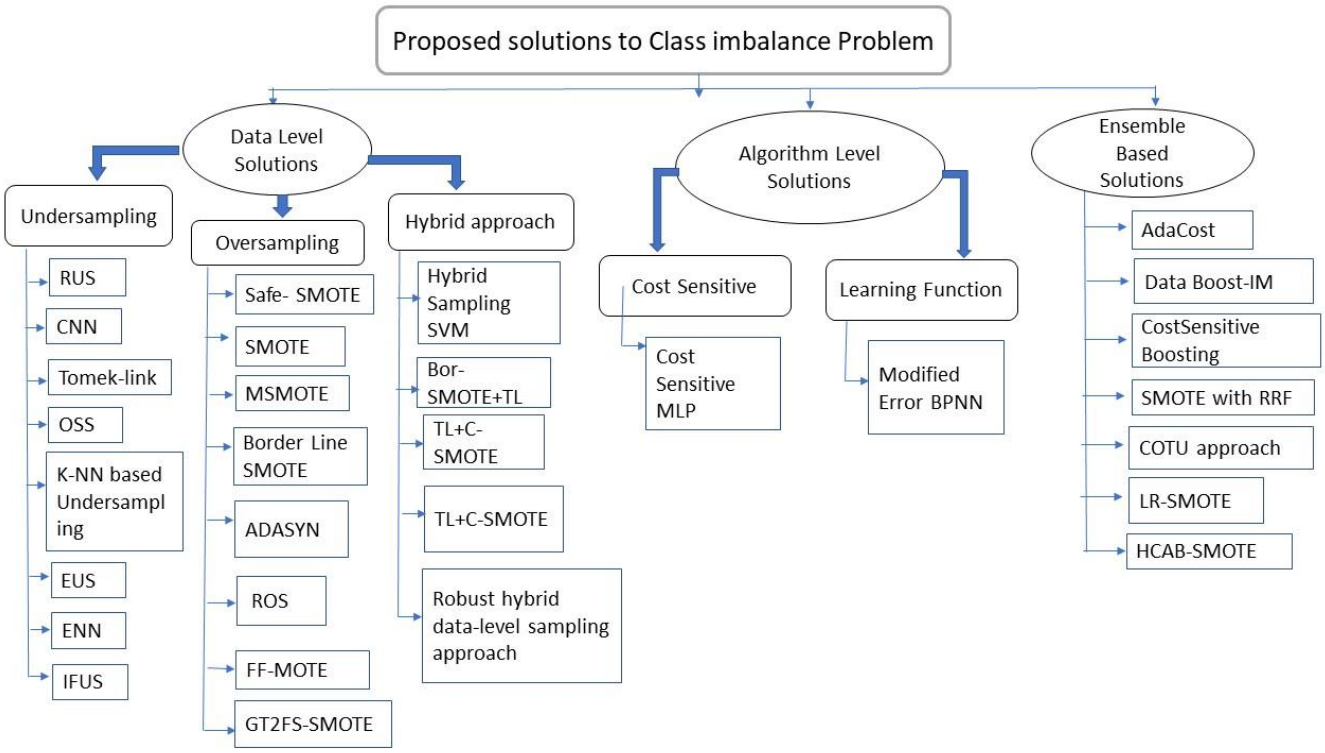

Fig. 1. Class Imbalance Problem- Types of available Solutions

As shown in Fig. 1, Data level technique has three common approaches, specifically undersampling, oversampling, and Hybrid (combination of oversampling and undersampling) and all three categories are quite effective in different kind of problem conditions as per effectiveness. The underdamping techniques are very effective when we talk about the datasets with lower proportion of class imbalance whereas in case of higher ration of data imbalance can be tackled very well by oversampling. while doing oversampling, size of the available training dataset supposed to increase, due to duplication of patterns, that creates an overfitting and high learning time. In reverse, undersampling techniques are more useful in cases when we need to handle large data set that are imbalanced with less calculation time as in this technique; we reduce the size of dataset. Whereas hybrid approach is the combination of both underdamping and oversampling techniques and it is used when we don't have pattern to increase or decrease the dataset directly.

In case of data-level approaches, the real data got changed either by removing or by generating the instances to balance the dataset. Considering this fact, the best research strategy is to think about developing such machine learning algorithms, which can deal with the CIP efficiently with the original data that is available with us without any modification. Such techniques are known as algorithm level techniques. Unlike data level techniques, the working area of these approaches is the internal structure of the algorithm. Under this category, either the traditional classification techniques are modified, or new techniques are developed to avoid the sensitivity/biasness of the algorithm towards the majority class [8].

In the Ensemble learning technique solutions, the probability of classifier that is weak is enhanced by the help of assembling an existing set of varied classifiers to generate a strong outcome to keep high-performance [9]. Boosting and bagging are two popular ensemble approaches. The Boosting algorithms [12] focus on problematic instances that can be classify without any differentiating in their existing classes. The most common and known boosting algorithm is AdaBoost [20], that builds iteratively an ensemble of existing/new models. As per explained by Prof. Zhou Zhi-Hua [13], the data boosting algorithms are very useful and efficient, and able to perform

in the classification in existing imbalanced datasets, because of the minority instances over majority instance are possible to be misclassified, and therefore, they are having weights higher in the following data cycle. Though, Mikel G. et al. [14] considered that the combination of data sampling methods can decrease the additional costs of automatically finding the optimal distribution of representative classes, samples and it also reduce the biasness of a specific learning algorithm. Among all these methods, we are having SMOTEBoost, RUSBoost, and DataBoost-IM.
Bagging constructs N classifiers on N different datasets [15]. Where Each dataset of N classifiers is known as bag; it is found by random sampling with data replacement. Now in imbalanced datasets, In a bag majority instances count will be high. Collecting the instances is the main factor can be apply to bagging. The common bagging algorithms are overbagging, Under aging and underoverbagging.

3. SURVEY ON DATA-LEVEL HYBRID TECHNIQUES

Data level techniques are those wherein the data is pre-processed before classifying the data using traditional classifiers. The main aim of the data level techniques is to rebalance the data before classification. The root cause of the class imbalance problem is imbalanced data-sets i.e. one class has more number of instances than other and the result of smaller class is influenced by the bigger class. Moreover, the risk factor is directly proportional to the imbalance ratio i.e. as the data set become more imbalance the impact of majority class is more on the results of minority class. Data level techniques are further classified into undersampling, oversampling and hybrid approach. Fig. 2 shows the techniques proposed by the researchers under data-level categories and Table-1 lists the detailed description.

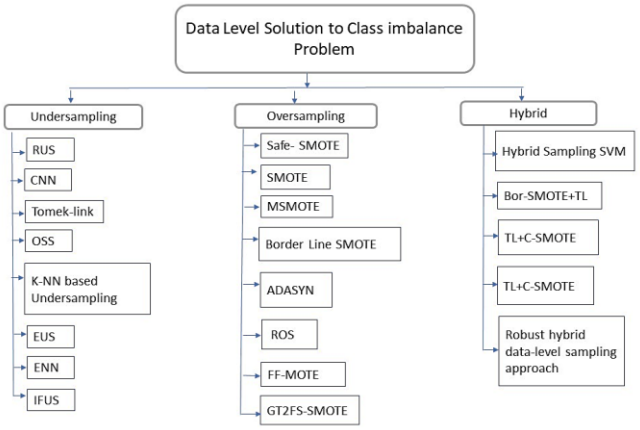

Fig. 2. List of Data-level techniques for Solutions to class Imbalance problem

3.1 Data-level technique using Undersampling

Undersampling allow us to eliminate data from majority class for balance the data. RUS (Random undersampling) is the basic undersampling approach which allows us to randomly delete the data to balance the data-set. Table-1 lists the description of techniques based upon undersampling approach.

TABLE I. Description of data- level undersampling techniques

Purposed Technique	Tools and Procedure	Highlight /Contributions	Authors/Published year
OSS [25]	it is specific with noisy borderline and redundant data, explained (OSS) here one side selection is taken to produce a steady majority class subset post removal the borderline and noisy pattern	Explains noisy and borderline and safe redundant patterns	Kubat and Matwin-1997
IRUS [26]	Its Inverse Random and a Undersampling (IRUS) technique dependent on the previous probability, p of the minority class. And in the order of p^2 the Majority class patterns are selected.	Produced high (TRP) during training.	Tahir et al.-2012
Redundancy-driven-modified Tomek-link [18]	Proposed collective removal of outlier, noisy and redundant patterns and provide elimination and detection for majority class with smallest contribution in valuation of correct class labels.	K-NN classifier performance are improved with it.	Devi et al.-2017
ENN [11]	It Uses ENN rule to identify insignificant pattern of majority class for 3-NN classification rule the ENN rule is explained as the prototype selection method.	Detects the error-prone or error- contributing majority class patterns.	Laurikkala-2019
EUS [27]	in this method majority classes are undersampled multiple times to produced a set of results and then its evaluated through a fitness function.	Accomplishes higher accuracy when there is highly imbalanced datasets	Garcia et al.-2009
K-NN sampling [28]	Working K-NN strategy is used for undersampling technique where each NN is defined by a distance function. Also including RUS. Pattern are noticed based on majority pattern over distance of minority, where K is specific to problem.	K-NN approximation with the minority as well as majority NNs.	Zhang et al.-2003

CSMOUTE [29]	Explained Synthetic Minority Undersampling (SMUTE) by including two utmost nearest majority instances to the synthetic undersampling.	Better result for classifier with complicated decision boundary and for example MLP and SVM.	Koziarski-2020
Fast-CBUS [30]	The Fast Cluster based undersampling is predicted that clusters of minority set and then generate K-clusters by taking into consideration equivalent majority patterns over - the minority outlines in every cluster. Each generated cluster is used as to train a classifier after that at last final labels of data patterns are found with the help of inverse intra cluster distance post weighting the data set.	Pareto frontier (efficiency) better in terms of computational cost and performance measures	Ofek et al.-2017

3.2 Oversampling

In Oversampling test data is increasing for minority class with the help of method first either randomly by replicating the existing test data or by generating data synthetically using a technique to improve the imbalance. ROS (Random oversampling) is the basic oversampling techniques which using random approach to re-create the synthetic data within minority class to balance the data. SMOTE is the most popular technique which increases the size of minority class by using interpolation method. In Table 2, we discussed the oversampling techniques.

TABLE 2. Description of various Oversampling techniques

Purposed Technique	Tools and Procedure	Highlight /Contributions	Authors/Published Year
ROS [31]	In this method the MI instances are increased randomly by replicating the minority instances to balance the original data-set . The main disadvantage of ROS method is that it can increase the possibility of over fitting, as it is replicating the same instances.	Its first technique to increase the data randomly using oversampling.	A. Fernandez et al-2004
SMOTE[10]	In this technique, data instances are synthetically generated in the minority class rather than replacement. In this method, oversampling is done by considering all the minority class data and new data is generated by using interpolation method	It is more stable that ROS, it is the first technique to generate data synthetically.	N. V. Chawla et al-2002
CBO[32]	Cluster based oversampling is provided to deal with the class imbalance within class. It uses k-means clustering technique to detect random cluster and calculate the cluster center by the mean of feature vector	In this technique the class is divided into cluster and then cluster are compared with other by finding the euclidean distance and then allocated to the class having minimum Euclidean distance	H. He and E. A. Garcia-2004
ADASYN[33]	Adaptive Synthetic Sampling He et al. proposed a very simple and effective method to generate synthetic instances. It uses K-nearest neighbor method to select the dense region in the dataset and generate instances within the dense region	It is a synthetic oversampling method, sometime more effective than SMOTE, its used KNN method.	He et al-2008
MSMOTE[34]	Modified SMOTE – it consider two thing first distribution of minority class samples, and second eliminates noise samples by excepting mediation. The mixture of MSMOTE and AdaBoost are used at several highly and considerable imbalanced data sets.	The comparable results show that the calculational performance of MSMOTE is far better than SMOTEBoost the minority class and F-values both are improved	Shengguo Hu,Yanfeng Liang,Ying He-2009

FF-MOTE [35]	Fuzzy C means algorithum is used to cluster the data to smaller and bigger class of imbalance data Then, the technique, FF-SMOTE, is applied on the smaller class and generate the synthetic data points and balance the data.	On this data is firstly pre-processed with help of FF-smote and then classified with the help of traditional classifier.	Prabhjot Kaur and Anjana Gosain-2019
GT2FS-SMOTE [36]	This is An Intelligent Oversampling Approach which is Based Upon General Type-2 Fuzzy Sets to Detect Web Spam-GT2FS-SMOTE is an intelligent oversampling method When compare to SMOTE, that is used to balance the data distribution before classification. It produces more accurate result to SMOTE and as simple as SMOTE.	Its is similar to SMOTE in terms of computational complexity but more effective, another advantage of GT2FS-SMOTE is- it reduces the chances of selecting noisy data.	Prabhjot Kaur and Anjana Gosain-2020

3.3 Hybrid approach

All those techniques that uses both oversampling as well as undersampling approach to improve the imbalance ratio (IR) before classification process comes under the Hybrid approaches.

TABLE III. Description of various Hybrid Data level Techniques

Purposed Technique	Tools and Procedure	Highlight /Contributions	Authors/Published Year
SVM_MTD[37]	In this technique majority classes are over instances where as minority classes can be under instance, It uses Gaussian-Fuzzy-membership function and α-cut for oversampling and uses mega-trend-Diffusion-membership function to generate new instances for minority class	To enhance the classification accuracy, it transforms the data attribute dimensions from 2-dimentional space to higher-dimension space by using classification associated information.	Li Der-Chiang, Chiao-Wen Liu and Susan C. Hu-2010
SMOTE_RSB[38]	This study proposed new hybrid approach by combining undersampling and oversampling. It combined SMOTE with a technique based upon rough sets	In this technique the quality of new synthetic data generated is controlled by using rough set theory.	Ramentol Enislay et al-2012
HybridDA[39]	The LRSMOTE algorithm used traditional SMOTE. The described method based on 2 step filtering firstly it uses SVM and k-means to reduce noise in data set that come from original sources, and then changes the formula generated by the new sample. Further it uses SMOTE technique to generate data form sample or Neighbour sample.	They used grid search for selecting the optimized values of misclassification cost, gamma and kernel type .	Akbani and al-Rifaie -2016
Robust hybrid data-level sampling approach (RHDLSA) [40]	This technique used multiple phases to solve the problem, in first phase its find out and remove the noise in data post that it detects majority and minority clusters by applying K-based fuzzy cluster method. In second step majority and minority cluster balancing are done. Further it used α-cut in majority class to reduce the size of data. And post that uses SMOTE to generate synthetic data and finally when all redundant data removed it uses Decision tree to balance the data.	DKFCM (Kaur et al. 2013, 2011) clustering method is being used here for separate data in majority and minority cluster and removing the noise.	Prabhjot Kaur and Anjana Gosain-2020

4. CONCLUSIONS

Class imbalance problem is a critical problem, now a days, when we have to detect rare cases from the database. In this paper, Data level techniques to handle class imbalance are reviewed. Data level methods balances the data set before classification. Major advantage of data level approaches are that we can use existing classification algorithms to classify the data.

REFERENCE

[1] T. Hastie, R. Tibshirani, J. Friedman, "The Elements of Statistical Learning: Data Mining, Inference, and Prediction", Springer; 2nd ed. 2009.

[2] U. Fayyad, G. Piatetsky-Shapiro, P. Smyth, "From Data Mining to Knowledge Discovery in Databases", American Association for Artificial Intelligence, vol. 17, no. 3, pp. 37-54, 1996.

[3] E. Alpaydin, "Introduction to Machine Learning", 2nd ed., MIT press, Cambridge, MA. U.S.A. ISBN: 978-81-4160-9, 2010.

[4] A. T. Oladipupo, "Types of machine learning algorithms", INTECH Open Access Publisher, 2010.

[5] S. B. Kotsiantis, "Supervised Machine Learning: A Review of Classification Techniques", Informatica, vol. 31, pp. 249-268, 2007.

[6] N. Japckwicz, "Learning from Imbalanced datasets: A comparison of various strategies", In. proceedings of AAAI 2000, 2000.

[7] G. H. Nguyen, A. Bouzerdoum S. Phung, "Learning pattern classification tasks with imbalanced data sets", In P. Yin (Eds.), Pattern recognition, pp. 193-208, 2009.

[8] H. Garcia, E. A. He, "Learning from Imbalanced Data", IEEE Transactions on Knowledge And Data Engineering, vol. 21, no. 9, pp. 1263-1284, 2009.

[9] G. Mustafa, Z. D. Niu, A. Yousif, J. Tarus, "Solving the Class Imbalance Problems using RUSMultiBoost Ensemble", 10th Iberian Conference on Information Systems and Technologies, pp. 1-6, 2015.

[10] N. V. Chawla et al., "SMOTE: Synthetic Minority Over-sampling Technique", Journal of artificial Intelligence Research, Vol. 16, pp. 321-357, 2002.

[11] Aouatef Mahani and Ahmed Riad Baba Ali (December 9th 2019). Classification Problem in Imbalanced Datasets, Recent Trends in Computational Intelligence, Ali Sadollah and Tilendra Shishir Sinha, IntechOpen, DOI: 10.5772/intechopen.89603. Available from: https://www.intechopen.com/books/recent-trends-in-computational-intelligence/classification-problem-in-imbalanced-datasets

[12] Schapire RE. The strength of weak learnability. Machine Learning. 1990;52: 197-227. DOI: 10.1007/BF00116037

[13] Zhou ZH. Ensemble Methods:Foundations and Algorithms. 1st ed.Florida: Chapman and Hall/CRC; 2012. 236 p. DOI: doi.org/10.1201/b12207

[14] Galar M, Fernández A, BarrenecheaE, Bustince H, Herrera F. A review onensembles for the class imbalance problem: Bagging, boosting and hybridbased approaches. IEEE Transactions onSystems, Man, and Cybernetics, Part C: Applications and Reviews. 2012;424:463-484. DOI: 10.1109/TSMCC.2011.2161285

[15] Breiman L. Bagging predictors.Machine Learning. 1996;242:123-140.DOI: 10.1023/A:1018054314350

[16] Wang S, Yao X. Diversity analysis on imbalanced data sets by using ensemble models. In: IEEE Symposium Series on Computational Intelligence and Data Mining (CIDM 2009); 30 March-2 April 2009; Nashville, TN,USA; 2009. pp. 324-331

[17] Barandela R, Valdovinos R, Sánchez R. New applications of ensembles of classifiers. Pattern Analysis and Applications. 2003;63:245-256. DOI:10.1007/s10044-003-0192-z

[18] D. Devi, S. K. Biswas, B. Purkayastha, "Redundancy-driven modified Tomek-link based undersampling: A solution to class imbalance". Pattern Recognition Letters, vol. 93, pp. 3–12, 2017.

[19] C. Drummond and R. C. Holte, "C4.5, class imbalance, and cost sensitivity: Why under-sampling beats over-sampling," in Proc. Int. Conf.Mach. Learn. Workshop Learn. From Imbalanced Data Sets II, 2003, pp. 1–8

[20] Y. Freund and R. Schapire, "Experiments with a new boosting algorithm,"in Proc. 13th Int. Conf. Mach. Learn., 1996, pp. 148–156.

[21] G. Weiss, K. McCarthy, and B.Zabar, "Cost-sensitive learning vs. sampling: Which is best for handling unbalanced classes with unequal errorcosts?" in Proc. Int. Conf. Data Mining, 2007, pp. 35–41.

[22] Y. Sun, M. S. Kamel, A. K. C. Wong, and Y. Wang, "Cost-sensitiveboosting for classification of imbalanced data," Pattern Recognit., vol. 40, no. 12, pp. 3358–3378, Dec. 2007.

[23] N. V. Chawla, D. A. Cieslak, L. O. Hall, and A. Joshi, "Automatically countering imbalance and its empirical relationship to cost," Data Mining Knowl. Discov., vol. 17, no. 2, pp. 225–252, Oct. 2008.

[24] Turney PD. Cost-sensitive classification: Empirical evaluation of a hybrid genetic decision tree induction algorithm. Artificial Intelligence Research. 1995;2:369-409. DOI: 10.1613/jair.120

[25] M. Kubat, S. Matwin, "Addressing the Curse of Imbalanced Training Sets: One Sided Selection", In Proceedings of the Fourteenth International Conference on Machine Learning, pp.179–186, 1997.

[26] M. A. Tahir, J. Kittler, F. Yan, "Inverse random under sampling for class imbalance problem and its application to multi-label classification", Instance Recognition, vol. 45, pp. 3738-3750, 2012

[27] S. Garcia, F. Herrera, "Evolutionary Under-Sampling for Classification with Imbalanced Data Sets: Proposals and Taxonomy", Evoloutionay Computation, vol. 17, no. 3, pp. 275-306, 2009.

[28] J. Zhang, I. Mani, "kNN approach to unbalanced data distributions: A case study involving information extraction", In Proceedings of the ICML'2003, 2003.

[29] M. Koziarski, "CSMOUTE: Combined Synthetic Oversampling and Undersampling Technique for Imbalanced Data Classification", Machine Learning, Cornell Univeristy, 2020 (Pre-print)

[30] N. Ofek, L. Rokach, R. Stern, A. Shabtai, "Fast-CBUS: A fast clustering-based undersampling method

for addressing the class imbalance problem", Neurocomputing, vol. 243, pp. 88-102, 2017.

[31] A. Fernandez et al., "Analysing the classification of imbalanced data-sets with multiple classes: Binarization techniques and adhoc approaches", Knowledge Based Systems, Vol. 42, pp. 97-110, April 2013.

[32] H. He and E. A. Garcia, "Learning from imbalanced data", IEEE Transactions on knowledge and data engineering, Vol. 21, No. 9, pp. 1263-1284, 2009.

[33] He Haibo et al., "ADASYN: Adaptive synthetic sampling approach for imbalanced learning", In Proceedings of IEEE International Joint Conference on Neural Network, 2008, IEEE.

[34] Shengguo Hu,Yanfeng Liang,Ying He, "MSMOTE: Improving Classification Performance When Training Data is Imbalanced, 2009 Second International Workshop on Computer Science and Engineering

[35] Prabhjot Kaur, Anjana Gosain, "FF-SMOTE: A Metaheuristic Approach to CombatClass Imbalance in Binary Classification"ISSN: 0883-9514 (Print) 1087-6545 (Online) Journal homepage: https://www.tandfonline.com/loi/uaai20

[36] Prabhjot Kaur,Anjana Gosain, "GT2FS-SMOTE: An Intelligent Oversampling Approach Based Upon General Type-2 Fuzzy Sets to Detect Web Spam", Arabian Journal for Science and Engineering https://doi.org/10.1007/s13369-020-04995-5

[37] Li Der-Chiang, Chiao-Wen Liu and Susan C. Hu, "A learning method for the class imbalance problem with medical data sets", Computers in biology and medicine, Vol. 40, No.5, pp. 509-518, 2010.

[38] Ramentol Enislay et al., "SMOTE-RSB*: a hybrid preprocessing approach based on oversampling and undersampling for high imbalanced data-sets using SMOTE and rough sets theory", Knowledge and information systems, Vol. 33, No. 2, pp. 245-265, 2012.

[39] Al-Rifaie, Mohammad Majid and Haya Abdullah Alhakbani, "Handling class imbalance in direct marketing dataset using a hybrid data and algorithmic level solutions", In Proceedings of SAI Computing Conference (SAI), 2016, IEEE.

[40] Prabhjot Kaur, Anjana Gosain, "Robust hybrid data-level sampling approach to handle imbalanced data during classification", Soft Computing (2020) 24:15715–15732 https://doi.org/10.1007/s00500-020-04901-z

Performance Investigation of Next Generation-Passive Optical Network Employing Hybrid Wavelength Division Multiplexing-Optical Time Division Multiplexing

[1] Parveen Kumar, [2] Ajay Kumar

[1] Research Scholar, IK Gujral Punjab Technical University, Kapurthala, India
[2] Department of Electronics and Communication Engineering, Beant College of Engineering and Technology, Gurdaspur, India

Abstract:

Over the last few years, hybrid information transmission systems have been considered as a feasible technological solution to meet the high-bandwidth demands of future generation communication links. In this paper, we propose a hybrid wavelength division multiplexed (WDM)-optical time division multiplexed (OTDM)-based next generation-passive optical network (NG-PON) for future high-speed access networks. 40 Gbit/s information with 4 optical line terminals has been transmitted to different number of optical network units i.e. 64, 128, and 256 using passive optical power splitter. The proposed system performance has been investigated using Q Factor, bit error rate, signal to noise ratio, received power and eye diagrams of the received signal as the performance metrics. Also, the system performance is compared for PIN and APD photo detector to find the optimal system performance. Further, we have also compared the performance of different electrical filters at the receiver to optimize the link performance.

Keywords:

NG-PON; WDM; OTDM; propagation length; electrical filter

1. INTRODUCTION

The ever rising surge in the demand of information services offered by the Internet has led to the requirement of high channel bandwidth for the end terminal users which has affected the access networks. For meeting the high bandwidth requirements, optical fibre communication is regarded as the most viable information transmission infrastructure for access networks [1, 2]. The access networks which employ optical fibre trunk lines are referred as optical access networks and can be classified into two categories: active optical network (AON) employing active network components and passive optical network (PON) employing passive network components. PON performs notably better than AON in terms of quality of signal transmission, power requirements, and cost of implementation [3]. The PON architecture consists of an optical line terminal (OLT) unit at the services provider terminal which is connected to several optical network units (ONU) at the end user terminal through an optical distribution network (ODN) between them. The data streams from the OLT is transmitted to several ONUs and vice-versa through a 1: N optical splitter at the ODN where N is the number of end terminal users. This allows the ONUs to share the same medium of information transmission and thus minimizes the cost of implementation of access network due to sharing of hardware and equipment [4]. Conventional PON architectures employ optical time division multiplexing (OTDM) technique to transmit multiple data streams over the same wavelength channel at different specific time slots. But due to low information transmission rates and high power losses, OTDM-based PON architectures were unable to meet the demands of next-generation access networks. Wavelength division multiplexing (WDM)-based PON architectures provided a better technological solution to implement next-generation access networks by transmitting independent data streams over different wavelength carriers, thus enhancing the information transmission rates of the network. Although WDM increases the information rates of the PON system, but it has a limitation of serving only a limited number of end terminal users. The Full Service Access Network (FSAN) group has proposed the hybridization of WDM and OTDM technologies for the commercial implementation of next generation-passive optical networks (NG-PON). The proposed hybrid WDM-OTDM-based PON architecture explores the benefit of multiple wavelength channels offered by WDM technique and additional number of end terminal users per wavelength channel by OTDM technique [5, 6].

In the year 2011, S.H. Oh et al. proposed a WDM-PON architecture employing tunable external cavity laser for transmitting independent 2.5 Gbit/s data streams over 20 km of standard single mode fibre (SSMF) [7]. In the year

2014, R. Goyal et al. proposed a hybrid WDM-OTDM PON architecture with 5 Gbit/s transmission rate and 128 ONUs [8]. The authors compared the performance of erbium doped fibre amplifier, RAMAN amplifier and semiconductor optical amplifier in the proposed system in the presence of inter-symbol interference and channel crosstalk. The authors reported reliable 5 Gbit/s transmission at 80 km for 128 ONUs with good performance. In the year 2014, K.P Kaur et al. reported a 40 Gbit/s downstream PON transmission up to 100 km fibre length using WDM architecture [9]. In the year 2017, A. Kaur reported a hybrid WDM-OTDM PON architecture where 25 Gbit/s downstream data and 10 Gbit/s upstream data is transmitted up to a propagation length of 60 km with good BER performance of the system [10]. In the year 2019, M. Kumari et al. reported an OTDM architecture-based PON system where 20 Gbit/s information was transmitted in upstream and downstream direction up to a maximum fibre length of 80 km with good signal reception [11].

The performance of optical transmission systems is dependent on a number of network components including choice of photo detectors at the receiver, which covert the incoming optical signal to electrical signal and electrical filter, which removes unwanted noise frequencies from the received information signal [12]. In the proposed work, we have reported a hybrid WDM-OTDM-based PON system where 4 OLT transmit net 40 Gbit/s information in the downstream direction and the proposed system performance is evaluated for different number of ONUs i.e. 64, 128, and 256. The proposed PON performance is also compared for PIN and APD photo detector at the receiver. We have also evaluated the proposed PON performance for different electrical filters at the ONU for finding the optimal link transmission performance. Remainder of the paper is organized as follows: the proposed hybrid WDM-OTDM-based PON system architecture is discussed in Section 2. The simulation results of the numerical evaluation of the proposed PON and the conclusions are presented in Section 3 and Section 4 respectively.

2. PROPOSED HYBRID WDM-OTDM-BASED PON ARCHITECTURE

Fig. 1 presents the schematic architecture of the proposed hybrid WDM-OTDM-based PON system, modelled and investigated over Optisystem simulation tool.

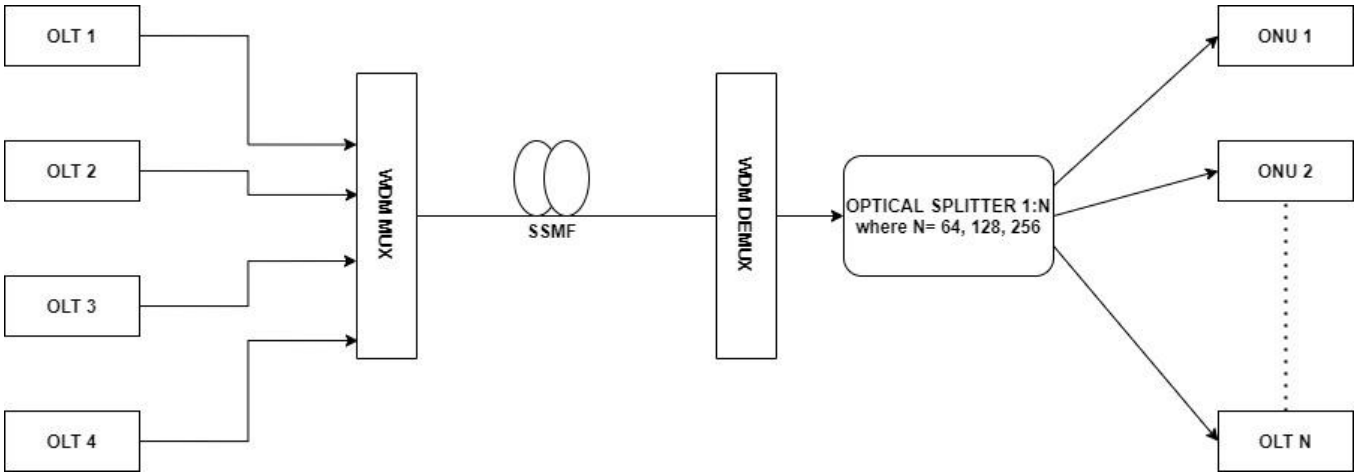

Fig. 1 Schematic architecture of the proposed hybrid WDM-OTDM-based PON

The proposed PON system involves downstream data transmission from 4 independent OLTs to different number of ONUs i.e. 64, 128, and 256 through a SSMF to achieve a net transmission rate of 40 Gbit/s. Further, the system performance in evaluated for propagation length of optical fibre varying from 100 – 150 km. For each OLT, 4 independent 2.5 Gbit/s data streams are OTDM to generate 10 Gbit/s data per OLT. In each OLT, a pseudo random bit sequence generator generates 2.5 Gbit/s binary information which is encoded to return-to-zero (RZ) electrical pulses using a RZ line encoder. This signal is then modulated over 10 dBm optical laser signal from a laser diode using a Mach-Zehnder modulation having 25 dB extinction ratio. 4 distinct 2.5 Gbit/s RZ-encoded data streams are OTDM to generate 10 Gbit/s data per OLT. 4 different wavelengths are used for each OLT i.e. 1547.60 nm, 1548.40 nm, 1549.20 nm, and 1550 nm with 0.8 nm (100 GHz) channel spacing. 10 Gbit/s data from each OLT are multiplexed using WDM multiplexer (MUX) having a bandwidth of 10 GHz to realize 40 Gbit/s data transmission in the downstream direction through a SSMF with 0.2 dB/km attenuation. The SSMF has a dispersion coefficient of 16.75 ps/nm/km with a dispersion slope of 0.075 ps/nm^2/km and a polarisation mode dispersion coefficient of 0.05 ps/$\sqrt{km}$. At the receiver side, independent wavelength channels are separated using WDM de-multiplexer (DEMUX) and the data is then transmitted to different number of ONUs using passive optical splitters. At each ONU, the data signal is retrieved using a photo detector followed by a square root device and an electrical filter. The quality of the received

signal is evaluated using bit error rate (BER) analyser. Fig. 2 (a) and (b) presents the optical spectrum of the transmitted signal after WDM MUX and the received signal after WDM DEMUX.

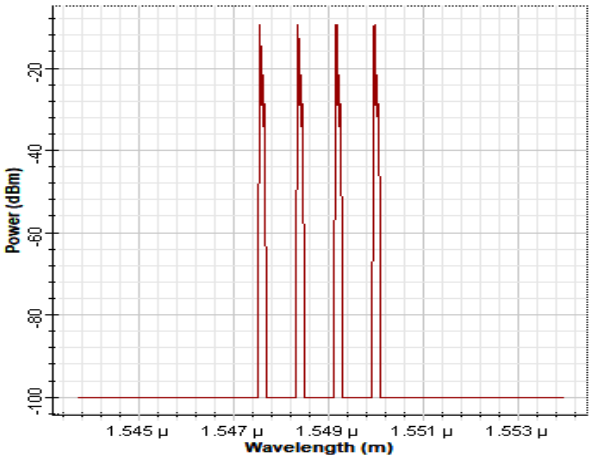

(a)

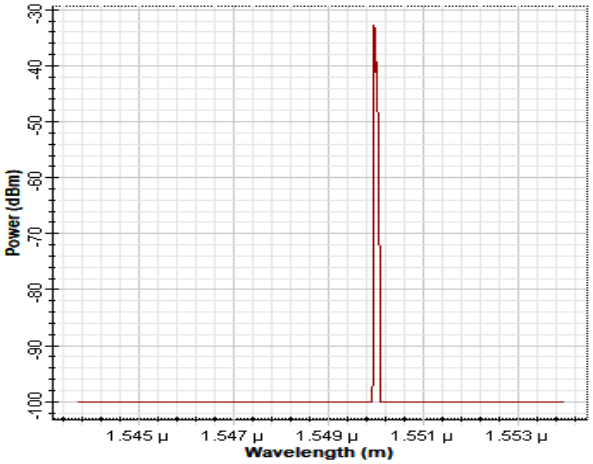

(b)

Fig. 2 Optical spectrum of (a) transmitted signal after WDM MUX (b) received signal after WDM DEMUX

3. RESULTS

In this work, the performance of the proposed hybrid WDM-OTDM-based PON system has been investigation over increasing propagation length of the optical fibre for different number of ONUs using Quality Factor (Q Factor), BER, signal to noise ratio (SNR), and received power as the evaluation metrics as discussed in Fig. 3. Fig. 3 (a) shows that the Q Factor of the received signal is 14.80, 11.53, and 8.79 dB for 64 ONUs; 14.56, 11.03, and 8.13 dB for 128 ONUs; and 13.96, 10.20, and 7.37 dB for 256 ONUs at a propagation length of 100, 125, and 150 km respectively. Fig. 3 (b) shows that the BER of the received signal is -49.20, -30.41, and -18.19 for 64 ONUs; -47.68, -27.94, and -15.76 for 128 ONUs; and -43.98, -24.11, and -13.16 for 256 ONUs at a propagation length of 100, 125, and 150 km respectively. Fig. 3 (c) shows that the SNR of the received signal is 53.94, 48.30, and 42.13 dB for 64 ONUs; 50.60, 44.68, and 38.80 dB for 128 ONUs; and 47.10, 40.82, and 33.68 dB for 256 ONUs at a propagation length of 100, 125, and 150 km respectively. Fig. 3 (d) shows that the received power is -46.05, -51.69, and -57.86 dBm for 64 ONUs; -49.39, -55.31, and -61.91 dBm for 128 ONUs; and -52.89, -59.17, and -66.31 dBm for 256 ONUs at a propagation length of 100, 125, and 150 km respectively. A degradation in the received signal quality is observed with increasing propagation length of the fibre which is due to increasing losses due to signal attenuation and nonlinear effects. The results in Fig. 3 demonstrates reliable 40 Gbit/s data transmission up to a propagation length of 150 km with good performance. Table 1 presents the clear eye diagrams of the received signals for different ONUs with increasing propagation length in the proposed PON system.

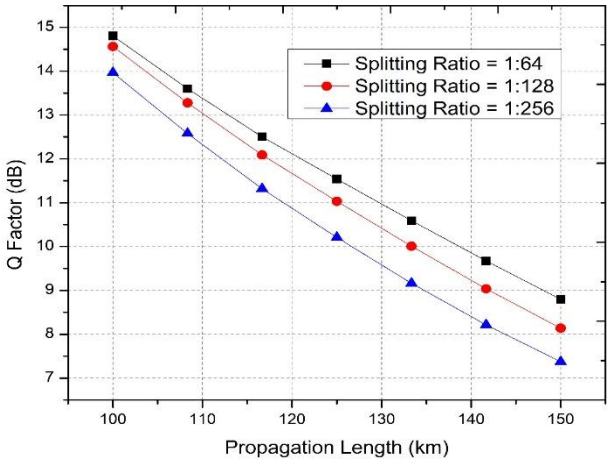

(a)

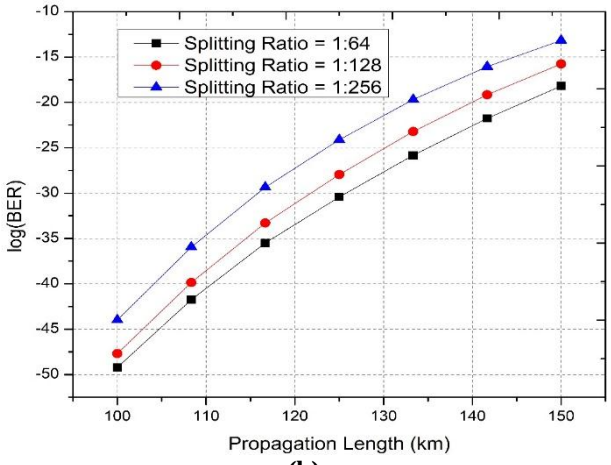

(b)

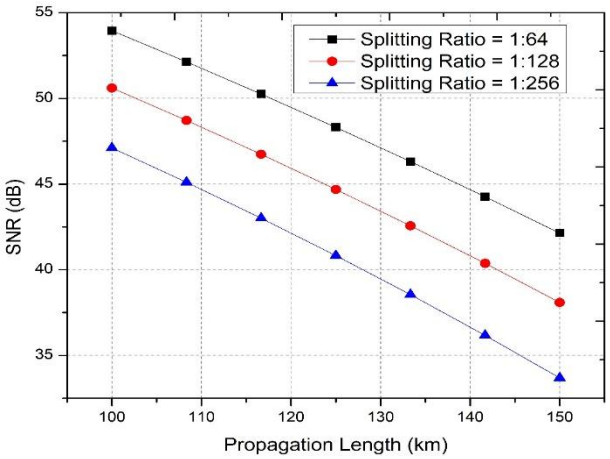

(c)

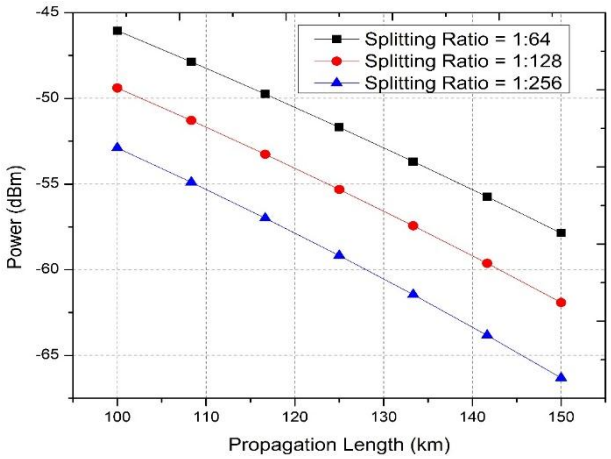

(d)

Fig. 3 (a) Q Factor (b) log(BER) (c) SNR (d) Power v/s Propagation Length (km) for different ONUs

Table 1 Eye diagrams for different number of ONUs with increasing propagation length

Propagation Length	64 ONUs	128 ONUs	256 ONUs
100 km	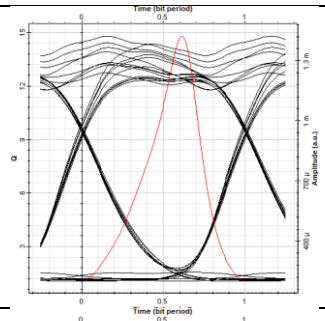	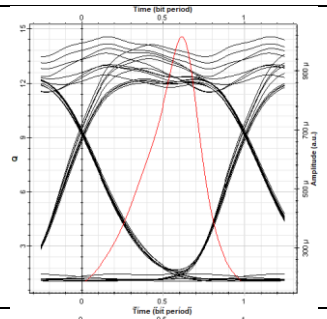	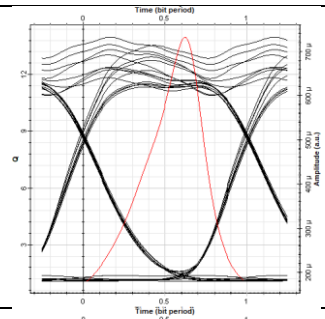
125 km	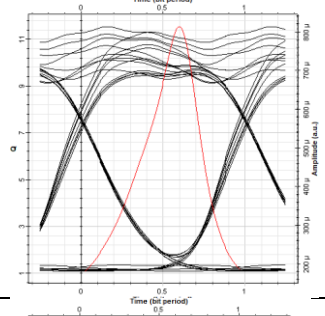	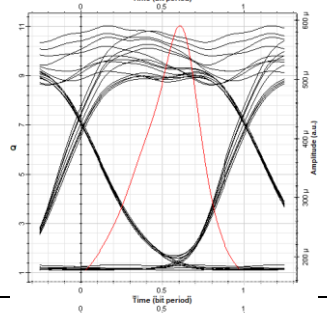	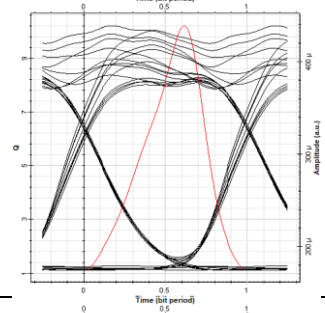
150 km	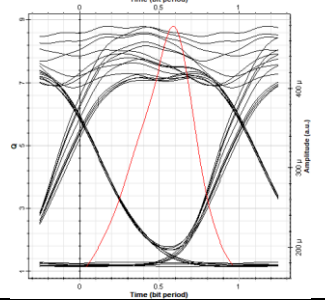	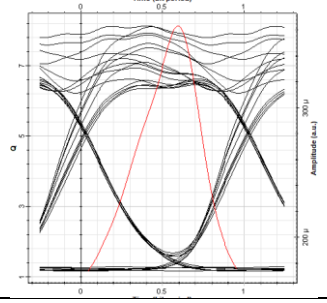	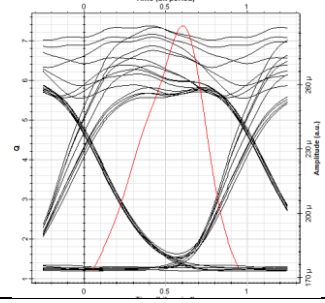

Fig. 4 shows the performance comparison of PIN and APD in the proposed PON system with increasing propagation length of optical fibre in terms of Q Factor and BER of the received signal. The results show that the Q Factor is 14.54, 11.26, and 8.48 dB for PIN and 14.80, 11.53, and 8.79 dB for APD at a propagation length of 100, 125, and 150 km respectively. Similarly, the BER is -49.20, -30.41, and -18.19 for PIN and -47.56, -29.04, and -17.01 for APD at a propagation length of 100, 125, and 150 km respectively. The results show that APD performs better than PIN in the

proposed PON system and is a better choice of realizing long-haul transmission PON. Table 2 compares the eye diagrams of the received signal for PIN and APD with increasing propagation length of optical fibre in the proposed PON system.

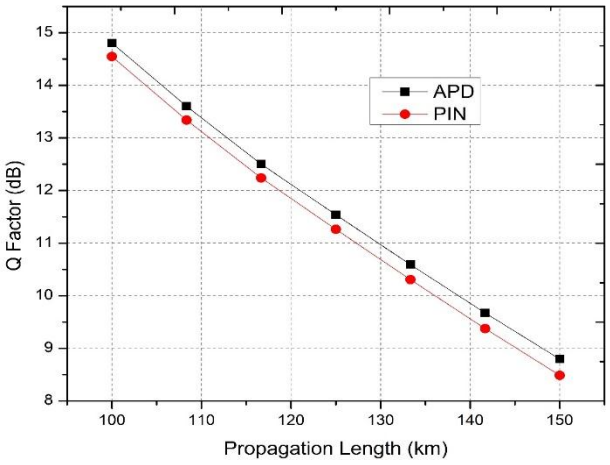

(a)

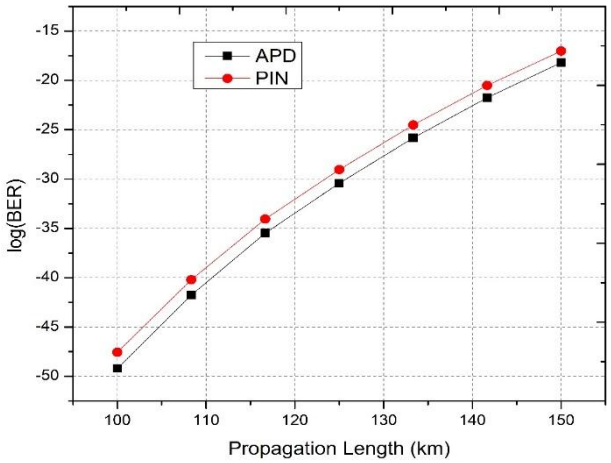

(b) Fig. 4 (a) Q Factor (b) log(BER) v/s Propagation Length (km) for PIN and APD at the receiver

Table 2 Eye diagrams for PIN and APD at the receiver with increasing propagation length

Propagation Length	PIN	APD
100 km	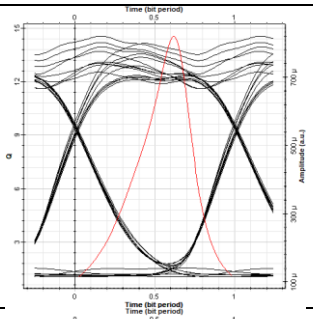	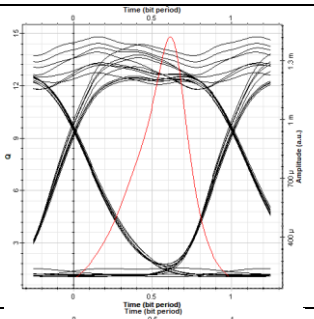
125 km	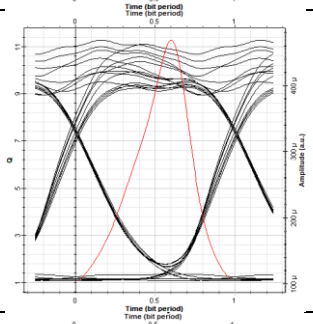	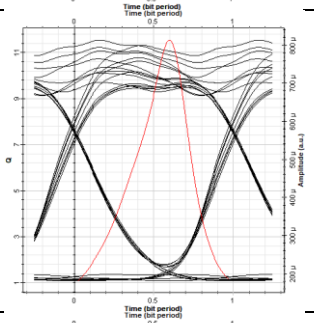
150 km	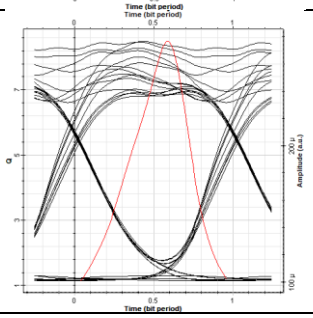	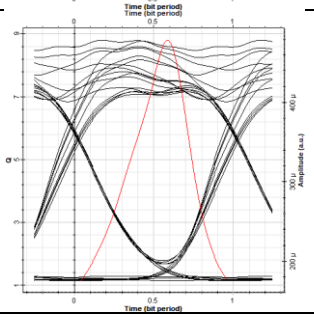

 ISBN: 978-93-90214-20-4

In this work, we have also compared the performance of different electrical filters at the ONUs in the proposed hybrid WDM-OTDM-based PON system as shown in Fig. 5. The results show that the best performance in terms of Q Factor of the received signal is demonstrated by Chebyshev filter which signifies enhanced propagation length performance in the proposed system. Fig. 6 shows the eye diagrams of the received signal at 150 km in the proposed system for different electrical filter at the ONU.

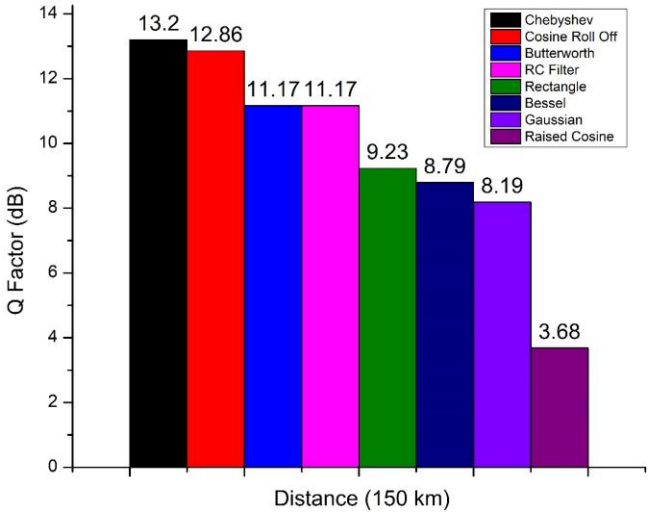

Fig. 5 Performance comparison of different electrical filters at the ONU

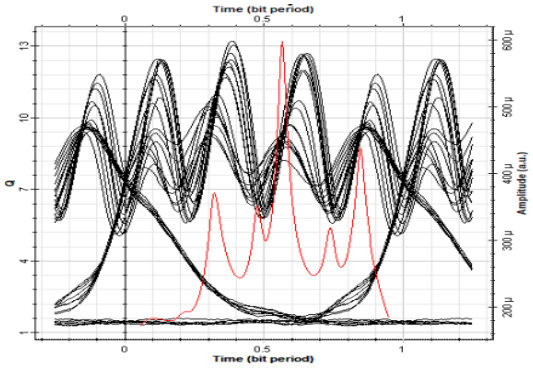

(a)

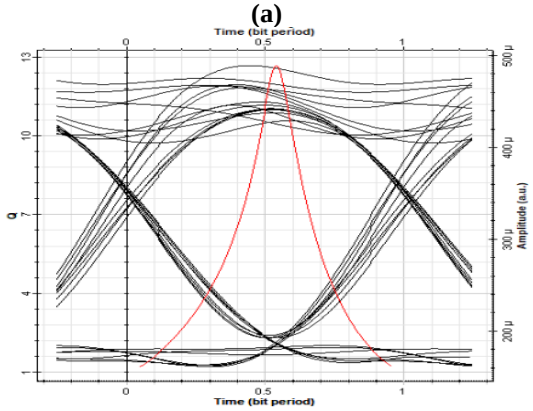

(b)

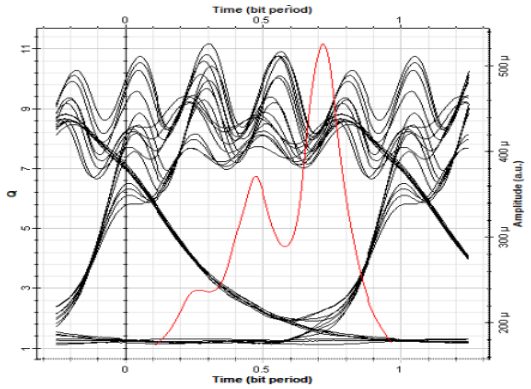

(c)

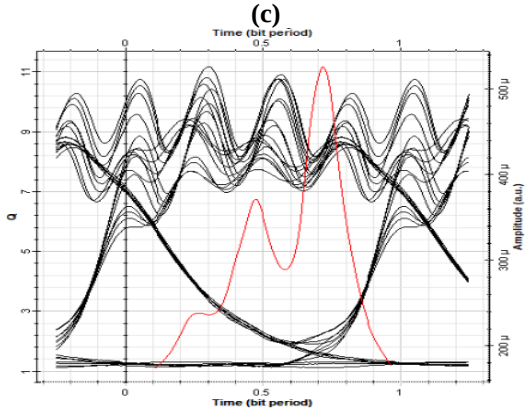

(d)

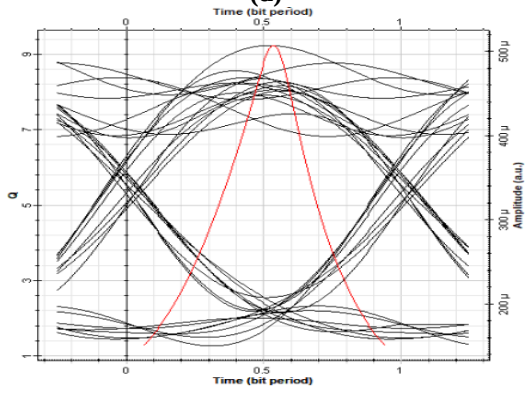

(e)

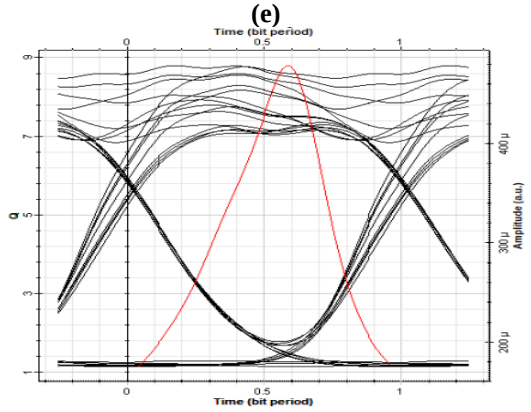

(f)

 ISBN: 978-93-90214-20-4

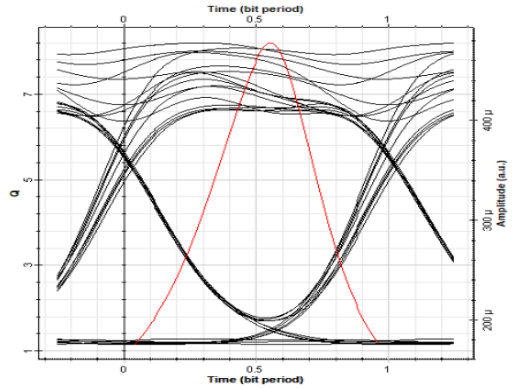

(g)

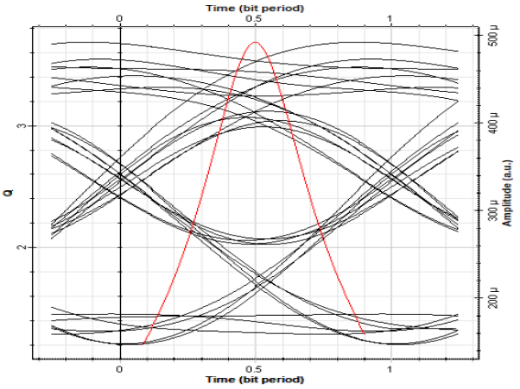

(h)

Fig. 6 Eye diagram of the received signal at 150 km link distance for (a) Chebyshev Filter (b) Cosine Roll Off Filter (c) Butterworh Filter (d) RC Filter (e) Rectangle Filter (f) Bessel Filter (g) Gaussian Filter (h) Raised Cosine Filter

We have also reported the performance comparison of the proposed hybrid WDM-OTDM-based PON system with existing works in the literature (Table 3) and the results show that the proposed system performs better as compared to the previously published literature.

Table 3 Performance comparison of the proposed hybrid WDM-OTDM-based PON system with existing literature

Reference, Authors	Journal	Technique	Bit rate	Propagation Length
Ref [7] S.H. Oh et al.	IEEE Journal on Selected Topics in Quantum Electronics	WDM-PON	2.5 Gbit/s	20 km
Ref [9] K.P. Kaur et al.	Optik, Elsevier	WDM-PON	40 Gbit/s	100 km
Ref [11] M. Kumari et al.	Journal of Optical Communications	OTDM-PON	20 Gbit/s	80 km
Proposed work	-	Hybrid WDM-OTDM PON	40 Gbit/s	150 km

4. CONCLUSIONS

In this work, a hybrid WDM-OTDM-based NG-PON system has been proposed and investigated for different number of ONUs at the receiver terminal. It can be seen from the reported results that as the propagation length of the optical fibre increases, the quality of the received signal degrades. The proposed PON system demonstrates reliable 40 Gbit/s data transmission up to a propagation length of 150 km with acceptable performance. Also, the performance of PIN and APD photo detectors at the ONU has been compared and from the results it can be concluded that APD performs better in terms of received signal quality. The proposed PON system has further been investigated for different electrical filters at the receiver and the results show that Chebyshev filter demonstrates the highest Q Factor of the received signal and is a suitable candidate for realizing long-haul PON systems.

REFERENCE

[1] K. Iwatsuki and J.-I. Kani, "Applications and technical issues of wavelength-division multiplexing passive optical networks with colorless optical network units," Journal of Optical Communications and Networking, vol. 1, no. 4, pp. C17–C24, 2009.

[2] M. E. Abdalla, S. M. Idrus, and A. B. Mohammad, "Hybrid TDM-WDM 10G-PON for high scalability next generation PON," in Proceedings of the IEEE 8th Conference on Industrial Electronics and Applications (ICIEA '13), pp. 1448–1450, June 2013.

[3] Y. Cao and C. Gan, "A scalable hybrid WDM/OCDMA-PON based on wavelength-locked RSOA technology," Optik, vol. 123, no. 2, pp. 176–180, 2012.

[4] H. Bai and Y. Wang, "Tunable wavelength converters based switching structure for WDM-TDM hybrid PON," Optik, vol. 124, no. 22, pp. 5388–5390, 2013.

[5] A. O. Aldhaibani, S. Yaakob, R. Q. Shaddad, S. M. Idrus, M. Z. Abdul Kadir, and A. B. Mohammad, "2.5

Gb/s hybrid WDM/TDMPON using radio over fiber technique," Optik, vol. 124, no. 18, pp. 3678–3681, 2013.

[6] A. M. Khan, J. Zhang, Y. Zhao, G. Gao, S. Chen, and D. Wang, "Simple and spectrally-efficient design of high capacity hybrid WDM/TDM-PON with improved receiver sensitivity," The Journal of China Universities of Posts and Telecommunications, vol. 20, no. 3, pp. 114–120, 2013.

[7] S. H. Oh et al., "Tunable External Cavity Laser by Hybrid Integration of a Superluminescent Diode and a Polymer Bragg Reflector," in IEEE Journal of Selected Topics in Quantum Electronics, vol. 17, no. 6, pp. 1534-1541, Nov.-Dec. 2011.

[8] R. Goyal, R.S. Kaler, "Investigation on polarization dependent bidirectional hybrid (WDM/TDM) utilizing QAM modulation with different amplifiers," Optoelectronics and Advanced Materials, Vol. 8, No. 7-8, pp. 631-634, 2014.

[9] K. P. Kaur, R. Randhawa, R.S. Kaler, "Performance analysis of WDM-PON architecture using different receiver filters," Optik, Vol. 125, no. 17, pp. 4742-4744, 2014.

[10] A. Kaur, B. Kaur, K. Singh, "Design and performance analysis of bidirectional TWDM-PON employing QAM-OFDM for downstream and re-modulation for upstream," Optik, Vol. 134, pp. 287-294, 2017.

[11] M. Kumari, R. Sharma and A. Sheetal, "Comparative Analysis of High Speed 20/20 Gbps OTDM-PON, WDM-PON and TWDM-PON for Long-Reach NG-PON2," Journal of Optical Communications, published online, ahead of print, 2019. https://doi.org/10.1515/joc-2019-0005

[12] S. Park, Y. Choi, S. P. Jung, K. Y. Cho, Y. Takushima, and Y. C. Chung, "HybridWDM/TDMA-PON using self-homodyne and differential coding," IEEE Photonics Technology Letters, vol. 21, no. 7, pp. 465–467, 2009.

112 Gbit/s Next Generation-Passive Optical Network Transmission System Using Polarisation Multiplexed-Quadrature Phase-Shift Keyed Modulation with Coherent Detection

[1] Parveen Kumar, [2] Ajay Kumar

[1] Research Scholar, IK Gujral Punjab Technical University, Kapurthala, India
[2] Department of Electronics and Communication Engineering, Beant College of Engineering and Technology, Gurdaspur, India

Abstract:

Over the last few years, hybrid information transmission systems have been considered as a feasible technological solution to meet the high-bandwidth demands of future generation communication links. In this paper, we propose a hybrid wavelength division multiplexed (WDM)-optical time division multiplexed (OTDM)-based next generation-passive optical network (NG-PON) for future high-speed access networks. 40 Gbit/s information with 4 optical line terminals has been transmitted to different number of optical network units i.e. 64, 128, and 256 using passive optical power splitter. The proposed system performance has been investigated using Q Factor, bit error rate, signal to noise ratio, received power and eye diagrams of the received signal as the performance metrics. Also, the system performance is compared for PIN and APD photo detector to find the optimal system performance. Further, we have also compared the performance of different electrical filters at the receiver to optimize the link performance.

Keywords:

NG-PON 2; PM-QPSK; coherent detection; digital signal processing; propagation length

1. INTRODUCTION

Passive optical network (PON) technology is contemplated as a promising solution for future generation broadband access networks in the scenario of fibre to the home (FTTH) services. Its many merits include high-speed internet availability, high quality transmission capability for triple play services for voice, data, and video signals, point-to-multipoint (P2MP) architecture, and cost-effectiveness [1]. The Institute of Electrical and Electronics Engineers (IEEE) and International Telecommunication Union (ITU) have proposed several PON standards over the past few decades. The PON architectures proposed by IEEE and ITU can be broadly classified into two groups. The first group consists of asynchronous transfer mode PON (ATM PON), broadband PON (BPON), and gigabit PON (GPON) and the second group consists of Ethernet PON (EPON). The GPON standard requirements were standardized by Full Service Access Network (FSAN) group which was ratified as ITU-T G.984 standard and is practically implemented in Middle East, North America, Europe, and Australia [2]. The EPON standard requirements were defined by IEEE 802.3 and is implemented in Asia [3]. The PON architecture consists of an optical line terminal (OLT) connected to several optical network unit (ONU) terminals through an optical distribution network (ODN) [4]. The OLT is located at the central office (CO) premises and is connected to several ONUs through passive optical splitters making PON a P2MP architecture.

The PON technology is divided into 3 generations: deployed PON, next-generation passive optical network stage 1 (NG-PON 1) and next-generation passive optical network stage 2 (NG-PON 2). The deployed PON employs time division multiple access (TDMA) technology and has downstream transmission rate of 1 Gbit/s for EPON and 2.4 Gbit/s for GPON. The data transmission rate for both EPON and GPON standards was increased to 10 Gbit/s in NG-PON 1 [5]. However, NG-PON 1 was unable to meet high channel bandwidth requirements and quality of service requirements for future access networks. The research community is focussed on developing newer standards and architectures for NG-PON 2 for dealing with future high bandwidth requirements of the end users and service providers. Four key technologies that have been proposed to provide 40 Gbit/s downstream data transmission and 10 Gbit/s upstream data transmission are wavelength division multiplexed (WDM) PON, optical time division multiplexed (OTDM) PON, optical code division multiplexed access (OCDMA) PON, and orthogonal frequency division multiplexed (OFDM) PON [6, 7]. In the year 2017, Y-M Zhang et al. reported a 10 Gbit/s downstream data transmission up to a propagation length of 16 km in a NG-PON 2 system employing reconfigurable WDM technique using low-cost directly modulated lasers

[8]. In the year 2019, M. Kumari et al. reported a 20 Gbit/s downstream transmission and 20 Gbit/s upstream transmission over an 80 km standard single mode fibre (SSMF) by employing OTDM technique [9]. A. Kumar et al. reported the modelling of a hybrid WDM-OTDM-based PON system and compared the performance of different modulation formats [10]. The authors reported feasible 10 Gbit/s transmission along 96 km bidirectional optical fibre for 96 end terminal users with good signal quality of the received signal. In the year 2020, H. Mrabet reported a novel OCDMA-PON architecture employing 2-dimensional hybrid coding [11]. The authors reported reliable 40 Gbit/s data transmission in downstream direction up to a maximum propagation length of 142 km. In the year 2020, Y. Shao et al. reported the experimental demonstration of 32-quadrature amplitude modulation (QAM)-based OFDM-PON architecture using which 5 Gbit/s information is transmitted over 42 km of SSMF [12].

Although the proposed technologies increase the data transmission rates in NG-PON 2, but the challenges including minimizing the deployment cost, increasing the data transmission rate and capacity, extending propagation length and minimizing power consumption still persists and is needed to be further investigated. This research work proposes a novel polarisation multiplexing-based NG-PON 2 architecture using quadrature phase-shift keyed signals. Further to improve the transmission performance, coherent detection and digital signal processing (DSP) algorithms at the receiver are also proposed. Rest of the article is organized as: the schematic of the proposed NG-PON 2 system is discussed in Section 2. The system investigation results are discussed in Section 3. Section 4 concludes this research article.

2. SYSTEM ARCHITECTURE

Fig. 1 shows the schematic architecture of the proposed polarisation multiplexed-quadrature phase-shift keyed (PM-QPSK) modulation-based NG-PON 2 system which is modelled over Optisystem simulation tool.

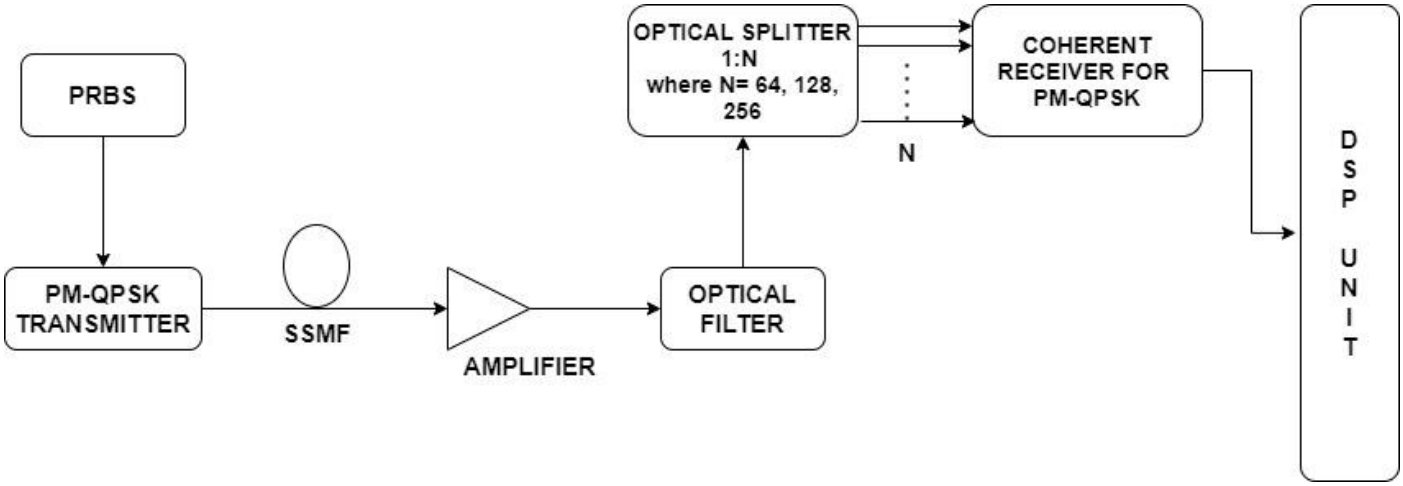

Fig. 1 Proposed NG-PON 2 schematic architecture employing PM-QPSK signal

The pseudo-random bit sequence (PRBS) generator generates 112 Gbit/s binary data and directs it to PM-QPSK transmitter section (Fig. 2). At the PM-QPSK transmitter, binary data bits from PRBS is serial-to-parallel (S/P) converted and directed to upper and lower QPSK modulator sections. Fig. 3 shows the internal schematic of QPSK modulator. Each QPSK modulator section is modulated using a distinct polarised beam from a continuous wave (CW) laser and a polarisation splitter. In QPSK modulator, the function of QPSK sequence generator is to group 2-bits as a symbol. The bits are divided into even and odd bits and transmitted to upper and lower M-ary pulse generator, which generates electrical pulse based on incoming bits. The electrical pulses drive the RF plates of the dual-electrode Mach Zehnder Modulator (MZM). There is a 90^0 phase shift between upper and lower arm for providing in-phase (I) and quadrature (Q) modulation. Both the I and Q modulated signals are combined using cross coupler and directed towards polarisation combiner. The 112 Gbit/s PM-QPSK signal is then directed towards SSMF having 0.2 dB/km attenuation coefficient, 16.75 ps/nm/km dispersion coefficient, 0.075 ps/nm^2/km dispersion slope, and 0.05 ps/$\sqrt{km}$ polarisation mode dispersion coefficient.

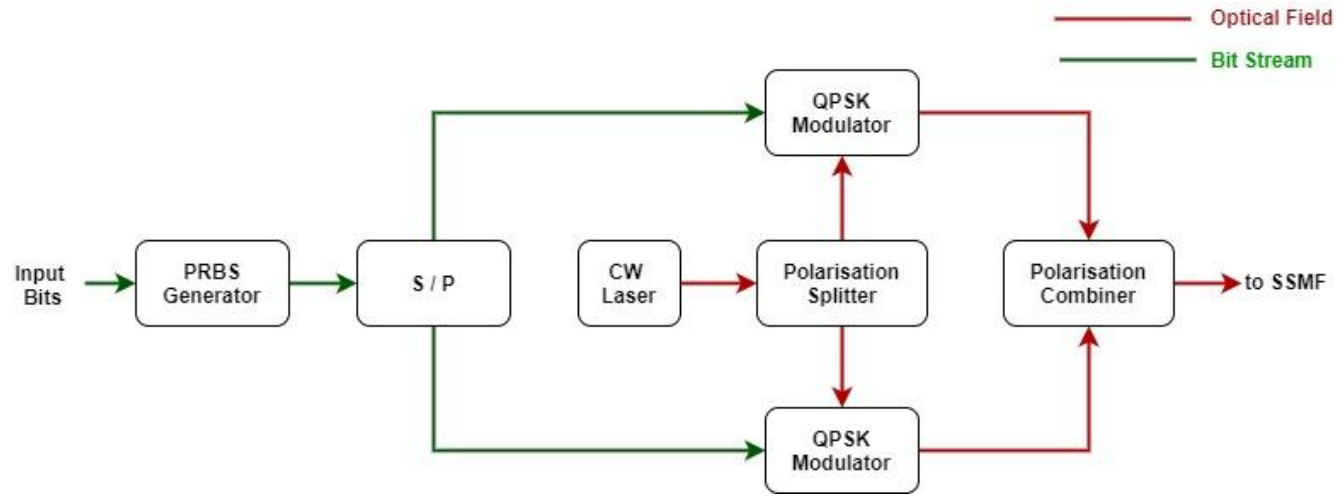

Fig. 2 PM-QPSK transmitter schematic

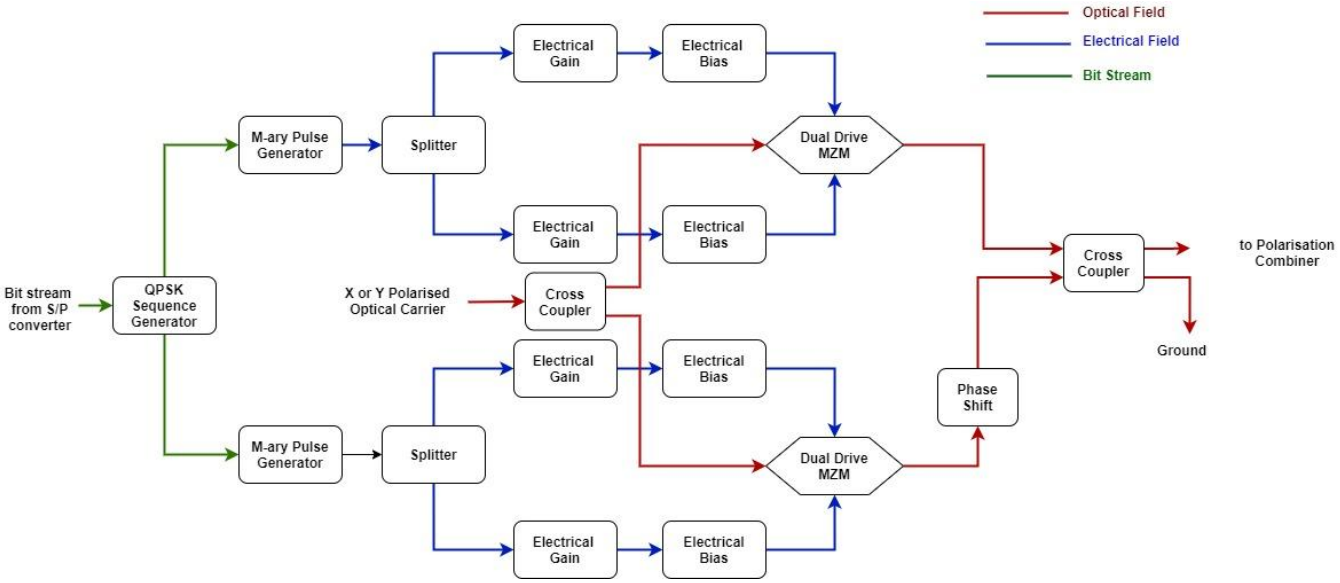

Fig. 3 Internal QPSK modulator schematic

The received data signal is amplified using an optical amplifier with a gain of 20 dB and a noise figure of 4 dB. A Gaussian filter with 60 GHz bandwidth is employed at the receiver unit. The optical splitter splits the incoming optical signal to different number of ONUs. At each ONU, the information is retrieved using PM-QPSK coherent receiver (Fig. 4) followed by a DSP unit. At the PM-QPSK receiver, the input optical signal is polarisation split and mixed with corresponding signals from local oscillator. The 90^0 optical hybrid converts phase information to optical intensity, which is converted to electrical signal using balanced detectors (BD) and electrical amplifiers (EA). The DSP unit (Fig. 5) performs key algorithms including filtering, nonlinear and dispersion compensation and quadrature imbalance (QI) compensation, adaptive equalization, frequency offset estimation (FOE) and carrier phase estimation (CPE). The data bits are retrieved using a decision making circuit followed by a QPSK sequence decoder and parallel-to-serial (P/S) converter.

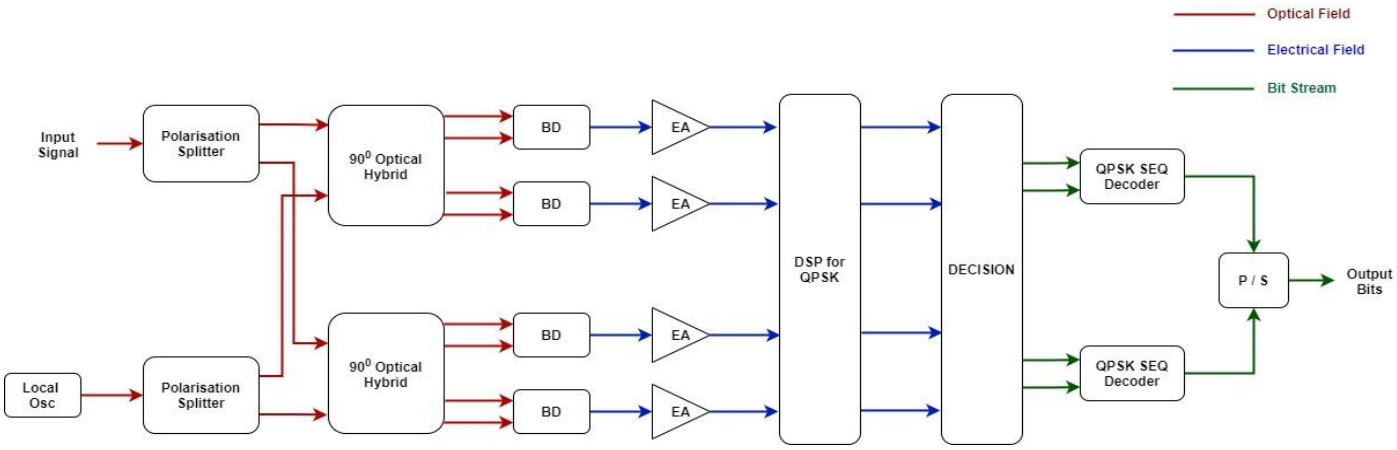

Fig. 4 PM-QPSK receiver schematic

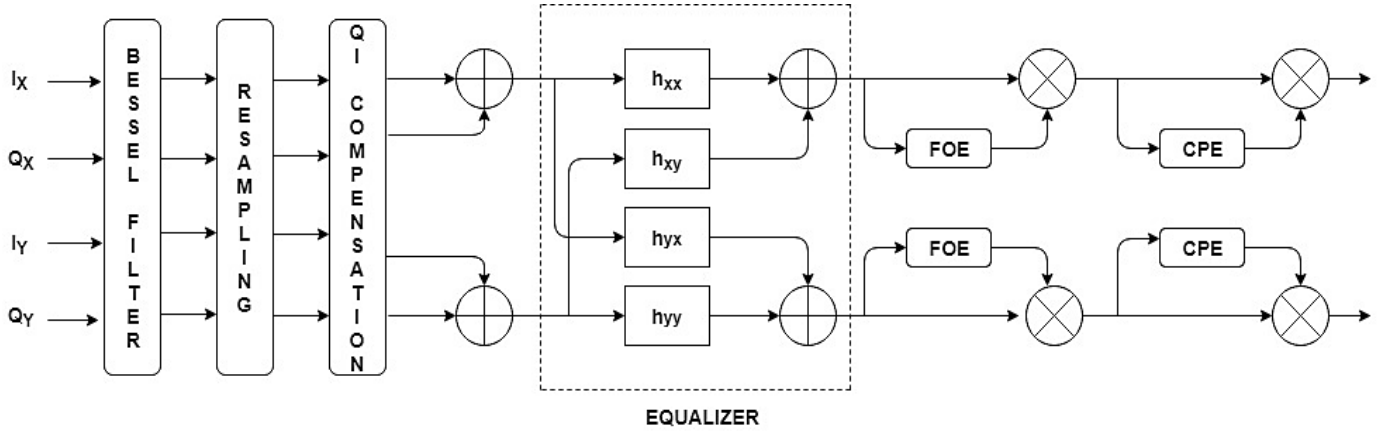

Fig. 5 DSP unit schematic

3. RESULTS

The proposed PM-QPSK-based NG-PON 2 transmission system is investigated for increasing propagation length of fibre for different number of ONUs using bit error rate (BER), received power, and constellation graphs as the performance evaluation metrics. The results in Fig. 6 (a) show that the BER is -4.81, -2.91, -1.83, and -0.83 for 64 ONUs, -3.38, -2.46, -1.49, and -0.40 for 128 ONUs, and -2.78, -1.87, -0.78, and -0.37 for 256 ONUs at a propagation length of 180, 190, 200, and 210 km respectively. The results in Fig. 6 (b) show that the received power is -38.21, -40.01, -41.70, and -43.24 dBm for 64 ONUs, -41.22, -43.02, -44.71, and -46.25 dBm for 128 ONUs, and -44.23, -46.03, -47.72, and -49.26 dBm for 256 ONUs at a propagation length of 180, 190, 200, and 210 km respectively. The results show that with increasing propagation length, the quality of received signal deteriorates due to increasing nonlinear losses and signal attenuation. The maximum achievable propagation length with acceptable BER of 3.8×10^{-3} (FEC Limit [13]) is 185 km for 256 ONUs. Table 1 shows the constellation graphs of the received signal with increasing propagation length for different number of ONUs. Fig. 7 shows the performance improvement of the received signal by using the proposed DSP unit in the NG-PON 2 system.

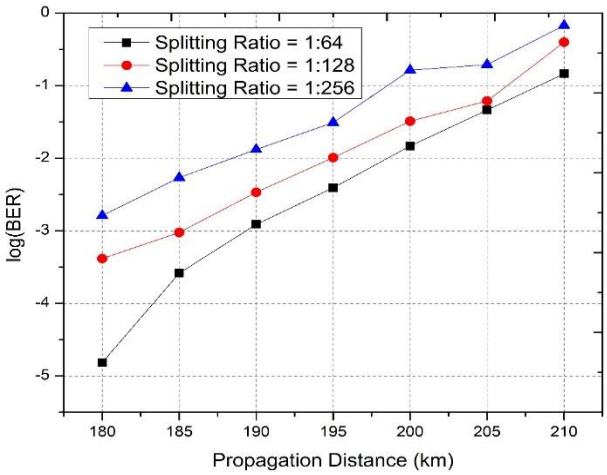

(a)

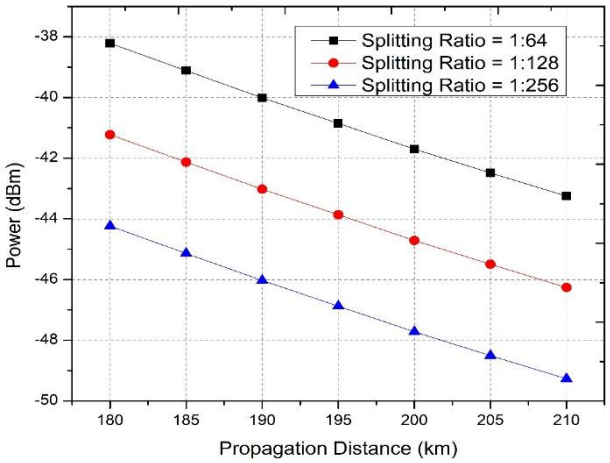

(b)

Fig 6 (a) BER (b) Received power v/s increasing Propagation Length for different number of ONUs

Table 1 Constellation graphs for different number of ONUs with increasing propagation length

Propagation Length	64 ONUs	128 ONUs	256 ONUs
180 km	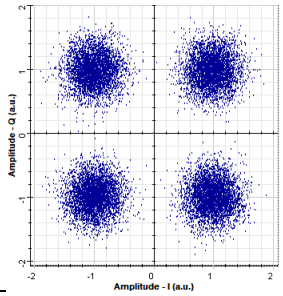	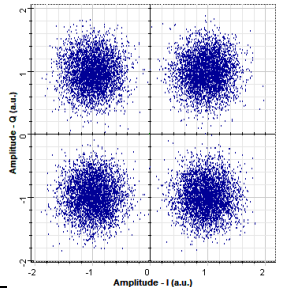	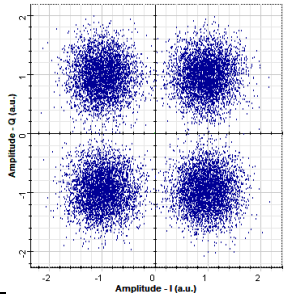
190 km	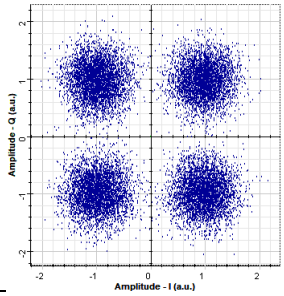	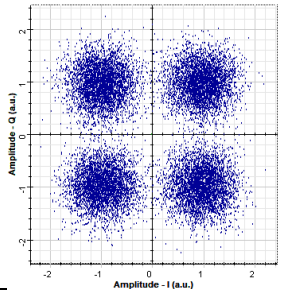	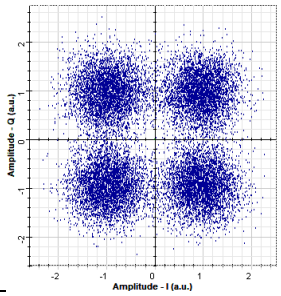
200 km	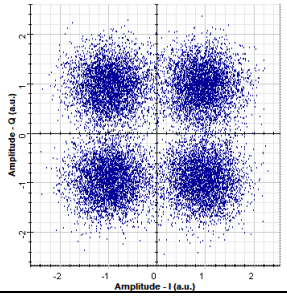	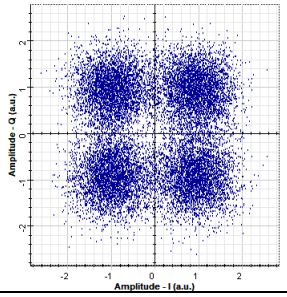	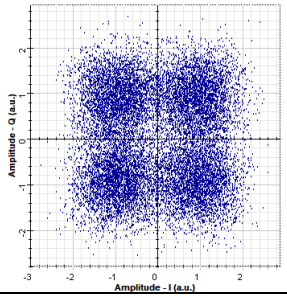

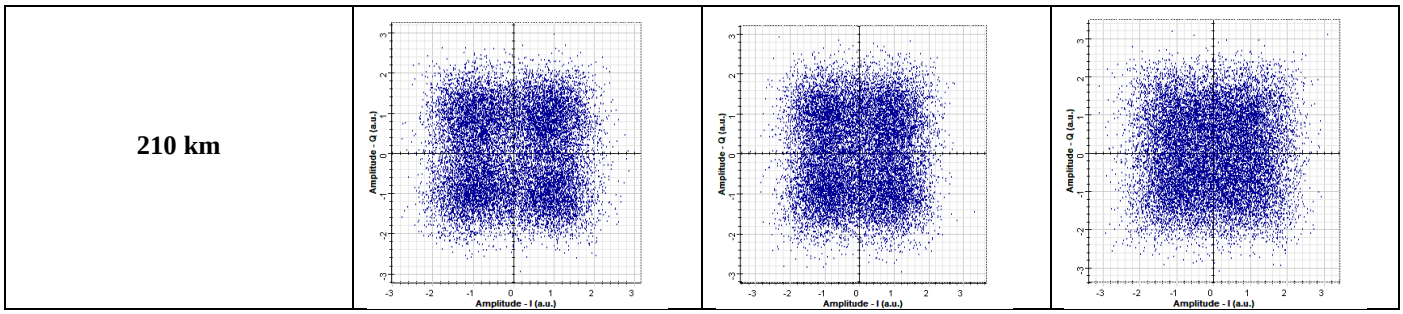

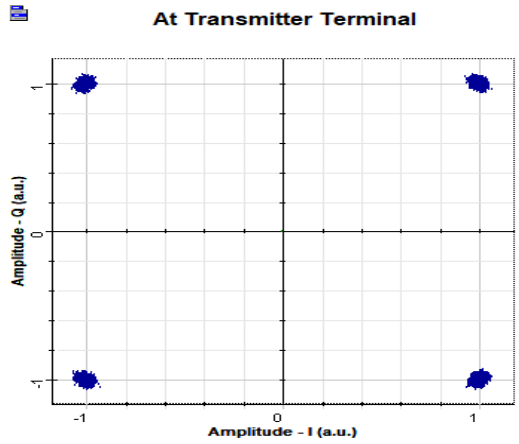

(a)

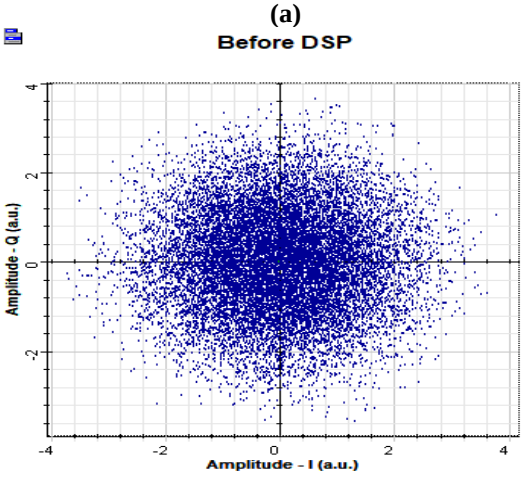

(b)

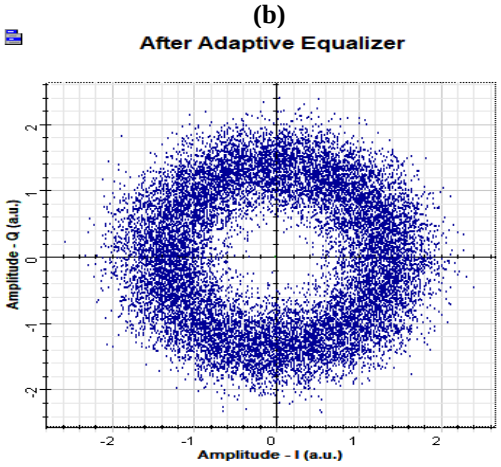

(c)

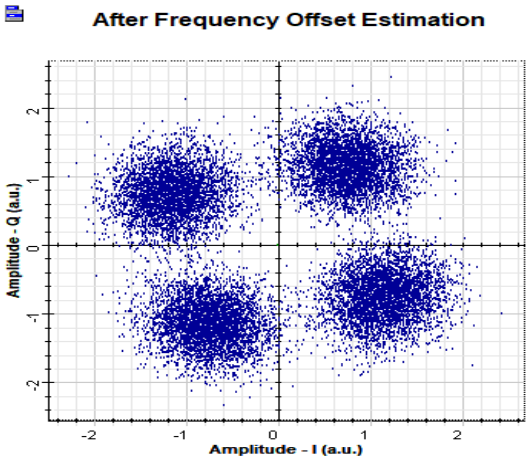

(d)

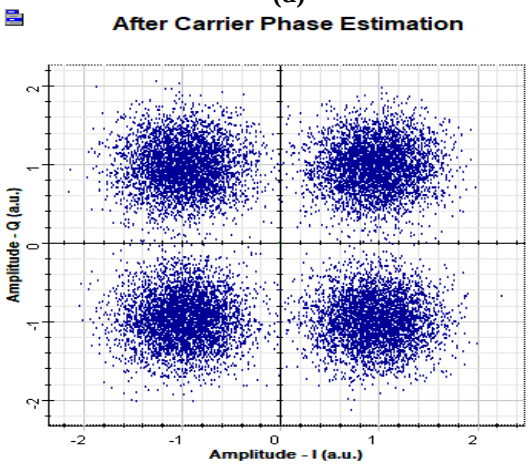

(e)

Fig 7. Improved performance of the NG-PON 2 system in terms of constellation graphs of the received signal using the DSP unit at the receiver

Further we have analysed the received sensitivity of the proposed NG-PON 2 system for different number of ONUs in Fig. 8. The results presented show that for all three cases, the received power required to achieve an acceptable BER is -45 dBm. Also, we have compared the transmission performance of the proposed NG-PON 2 system with existing literature (Table 2) and the comparison shows that the proposed system exhibits superior performance in terms of propagation length and transmission bit rate.

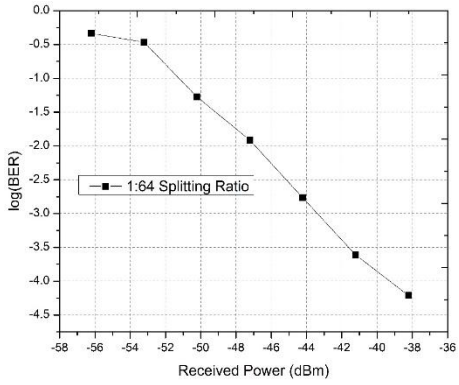

(a)

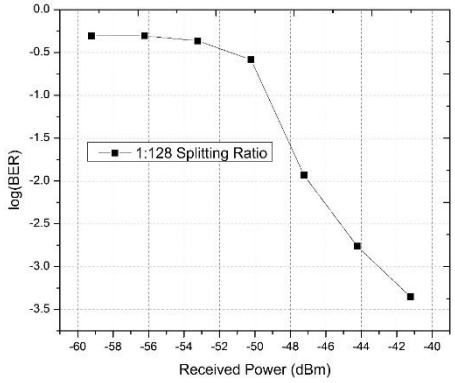

(b)

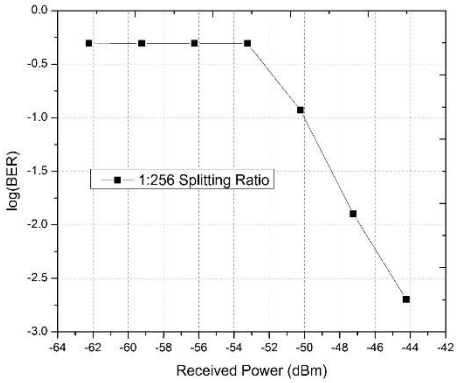

(c)

Fig 8 Receiver sensitivity plots for (a) 64 (b) 128 (c) 256 ONUs

Table 2 Performance comparison of the proposed PM-QPSK-based NG-PON 2 system with existing literature

Reference, Authors	Journal	Technique	Propagation Length	Bit rate
Ref [8] Y-M Zhang et al.	Optoelectronics Letters, Springer	WDM-PON	16 km	10 Gbit/s
Ref [9] M. Kumari et al.	Journal of Optical Communications, DeGruyter	OTDM-PON	80 km	20 Gbit/s
Ref [10] A. Kumar et al.	Journal of Optical Communications, DeGruyter	Hybrid WDM-OTDM-PON	96 km	10 Gbit/s
Ref [11] H. Mrabet	Applied Sciences, MDPI	OCDMA-PON	142 km	40 Gbit/s
Ref [12] Y. Shao et al.	Journal of European Optical Society-Rapid Publications	OFDM-PON	42 km	5 Gbit/s
Proposed work	-	PM-QPSK-based NG-PON 2 with coherent receiver and DSP	185 km	112 Gbit/s

4. CONCLUSION

The present work discusses the numerical investigation of a PM-QPSK-based NG-PON 2 system employing coherent detection and DSP at the receiver for improved performance. 112 Gbit/s information has been transmitted in the downstream direction for different number of ONUs. From the results presented, it can be concluded that the maximum achievable propagation length of the proposed NG-PON 2 system with acceptable BER is 185 km. Also, the system demonstrates significant improvement in terms of received signal quality by deploying proposed DSP unit. The receiver sensitivity of the proposed system is also evaluated and is calculated to be -45 dBm for all three configurations of the system. The proposed NG-PON 2 performance is also compared with existing literature and the comparison shows that the proposed system performs better in terms of propagation length and bit transmission rate. The proposed NG-PON 2 system can be exploited for future high channel bandwidth applications in 5^{th} generation communication networks.

Acknowledgement- The authors are thankful to IK Gujral Punjab Technical University, Kapurthala for providing necessary technical assistance and software to accomplish this work

REFERENCE

[1] A. Ragheb and H. Fathallah, "Candidate modulation schemes for next generation-passive optical networks (NG-PONs)," in *High Capacity Optical Networks and Enabling Technologies (HONET), 2012 9th International Conference on*, 2012, pp. 226-231.

[2] J. J. V. Olmos, J. Sugawa, H. Ikeda, and K. Sakamoto, "GPON and 10G-EPON coexisting systems and filtering issues at the OLT," in *OptoeElectronics and Communications Conference (OECC), 2011 16th*, 2011, pp. 828-829.

[3] D. Van Veen, D. Suvakovic, L. Man Fai, H. Krimmel, A. J. de Lind van Wijngaarden, J. Galaro, J. Dungee, B. Farah, S. Corteselli, B. Weeber, R. Tebbe, D. Eckard, J. Smith, J. Bouchard, J. Kotch, and P. Vetter, "Demonstration of a symmetrical 10/10 Gbit/s XG-PON2 system," in *Optical Fiber Communication Conference and Exposition (OFC/NFOEC), 2011 and the National Fiber Optic Engineers Conference*, 2011, pp. 1-3.

[4] B. Skubic, J. Chen, J. Ahmed, L. Wosinska, and B. Mukherjee, "A comparison of dynamic bandwidth allocation for EPON, GPON, and next-generation TDM PON," *Communications Magazine, IEEE*, vol. 47, pp. S40-S48, 2009.

[5] C. Ling, S. Dahlfort, and D. Hood, "Evolution of PON: 10G-PON and WDM-PON," in *Communications and Photonics Conference and Exhibition (ACP), 2010 Asia*, 2010, pp. 709-711.

[6] N. Cvijetic, Q. Dayou, and H. Junqiang, "100 Gb/s optical access based on optical orthogonal frequency-division multiplexing," *Communications Magazine, IEEE*, vol. 48, pp. 70-77, 2010.

[7] Y. Luo, X. Zhou, F. Effenberger, X. Yan, G. Peng, Y. Qian, and Y. Ma, "Time-and wavelength-division multiplexed passive optical network (TWDM-PON) for next-generation PON stage 2 (NG-PON2)," *Journal of Lightwave Technology*, vol. 31, pp. 587-593, 2013.

[8] Y-M. Zhang, Y. Liu, Z-K. Zhang *et al.* "Reconfigurable WDM-PON empowered by a low-cost 8-channel directly modulated laser module," *Optoelectron. Lett.* Vol. 13, pp. 423–426 (2017).

[9] M. Kumari, R. Sharma and A. Sheetal, "Comparative Analysis of High Speed 20/20 Gbps OTDM-PON, WDM-PON and TWDM-PON for Long-Reach NG-PON2," Journal of Optical Communications, published online, ahead of print, 2019. https://doi.org/10.1515/joc-2019-0005

[10] A. Kumar and R. Randhawa,. "An Improved Hybrid WDM/TDM PON Model with Enhanced Performance Using Different Modulation Formats of WDM Transmitter" Journal of Optical Communications, published online, ahead of print, 2018. https://doi.org/10.1515/joc-2018-0154

[11] Mrabet, Hichem "A Performance Analysis of a Hybrid OCDMA-PON Configuration Based on IM/DD Fast-OFDM Technique for Access Network," *Appl. Sci.* Vol. 10, Issue. 21, Article No-7690 (2020).

[12] Y. Shao, Y. Long, A. Wang, A. *et al.* "Research on optical 32QAM-OFDM-PON access scheme with different numbers of sub-carriers using DMT modulation," *J. Eur. Opt. Soc.-Rapid Publ.* Vol. 16, Article No-10 (2020).

[13] M. Singh, J. Malhotra, M.S. Mani Rajan, V. Dhasarathan, M. H. Aly, "Performance evaluation of 6.4 Tbps dual polarization quadrature phase shift keying Nyquist-WDM superchannel FSO transmission link: Impact of weather conditions," Alexandria Engineering Journal, vol. 59, no. 2, pp.977-986, 2020.

Live Streaming Robot for Military Environment

[1] K.Harsha Vardha, [2] K.Sai Bhargav, [3] V.Sai Nikhilesh, [4] B.Alekya, [5] Dasi.Swathi, [6] S.Ganga Silpika

[1][2][3][4][6] Dept of ECE, VR Siddhartha college of EngineeringAndhra Pradesh, India
[5] Dept of ECE, PVP Siddhartha Institute of Technology Andhra Pradesh, India

Abstract:

This paper presents the design of a surveillance robot for military application. The military robot has the ability to detect objects by using a PIR sensor and an ultrasonic sensor which can measure the distance from the object. When it detects an object it alerts the people by a buzzer sound. This robot is used to detect the objects and also gives the live streaming by using open cv technology. By using this technology face recognition and motion tracking and hitting the target are done and the robot can be controlled from the web page wirelessly. When the object or person is detected the laser light is focused on the person by giving the command. We can control it manually from the keyboard and we will use the raspberry pi camera to capture the images.

Keywords:

Raspberry pi, Raspberry pi camera, PIR sensor

1. INTRODUCTION

Nowadays, surveillance robot plays a very important role in military application. It can give continuous live streaming Video from the boarder's camera is fixed On the top of the robot so it can give video streaming. The camera can rotate in various directions like left, right, forward, reverse, and Stop commands are available to control it. We can control the camera using a servo motor to change its direction. This type of robot gives information about the situations in the borders. This type of robot can also use in various applications like medical, and industrial application where security is needed by using this robot we can reduce the harms causing to humans can give continuous live video streaming and also gives the security as only the authorized persons can access this video streaming webpage .in this system user will be able to view and operate the robot even if persons are faraway and the user will have to log in with IP address that means better protection is provided and no one will not be able to control and view this video. In this project the robot can control wirelessly from the webpage & the webpage is security-based it has the user id and password to log in and view the video streaming. The robot is continuously watching and sending the video to the authorized person [1][2].

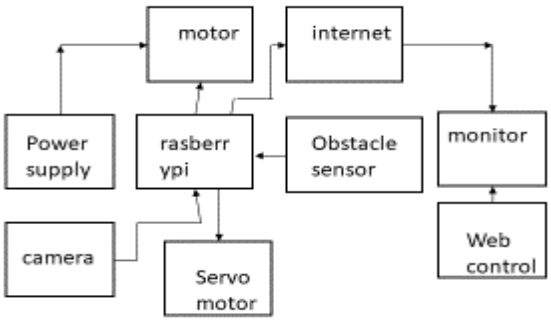

Figure:1 Block diagram of the live streaming robot

2. HARDWARE

2.1 Raspberry pi model B:

we used third generation Raspberry pi 3 . This powerful, low cost and small size single board computer can be used for many applications .It is most powerful processor and it is 10 times faster than previous generation. It has 40 pins it has many ports to connect various devices like camera, USB port etc[3][4].

Specifications:

Clock frequency: 1.2GHZ
Processor operating voltage: 3.3v
Raw voltage input: 5v, 2A power source
Operating temp: -40 to +85 degree
Video o/p: HDMI
USB: 2.0(four sockets)
Flash memory: 16G bytes SSD memory card
Internal ram: 1G bytes DDR2
Wireless connectivity: BCM43143
Ethernet: 10/100 Ethernet
Maximum total current drawn from all I/O Pins: 54mA
current through each I/O pin: 16mA

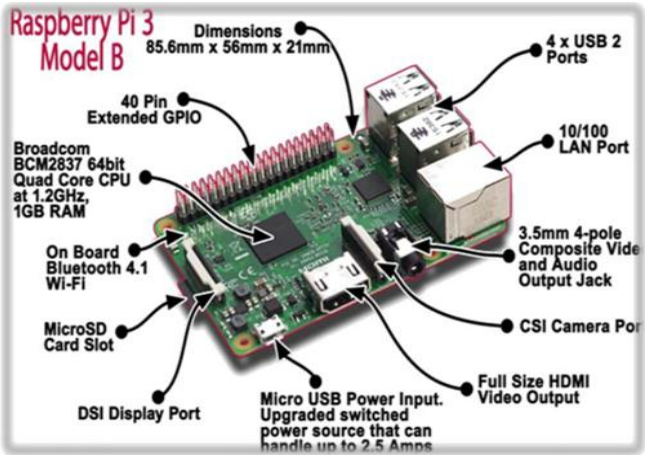

Figure 2: Raspberry pi 3 model B

2.2 ultrasonic sensor:

The purpose of ultrasonic sensor is for taking the measurements in different environments. The ultrasonic sensor plays an important role in robotics & their automation. It can detect the object and gives the distance between the sensor and object .Ultrasonic sensor has 4 pins they are Vcc, trigger, echo, Gnd and range is 2cm-80cm.

Figure 3: ultrasonic sensor

2.3 Raspberry pi camera

In this webcam c170 is used it has video capture upto 1024*768 pixels and photos upto 5mega pixels, video calling (640*480 pixels)

2.4 servo motor:

In this , the servo motor purpose is used to rotate the camera in its maximum limit of 180 degrees for the purpose of camera auto focus. Camera is fixed to servo motor by giving the commands the camera is rotate with the help of servo motor .servo motor has 3 pins positive, negative, control wire. Servo motor is control by pwm which is provided by the control wires[8].

Figure 4: Raspberry pi camera

Figure 5: servo motor

2.5 DC motor:

The purpose of dc motor is used to drive the robot. The motor speed is depends on the wheel diameter &Rpm(rotations per minute). The operating voltage is 4.5 to 9v and loaded current is 250mA, rated voltage is 6v.

Figure 6: DC motor

2.6 PIR Sensor:

For the detection of the humans who are present in the field will be possible by using the PIR sensor.it can detect the humans between 5m to 12meters range. In this project we use the buzzer to indicate the result of PIR sensor if the person is detected by the pir sensor the buzzer will gives the sound[5].

Figure7 :PIR Sensor

2.7 L293D Motor Drive:

L293D driver allows motor to drive on different direction.L293D motor driver is 16 pin IC by using this control the two sets of dc motors simultaneously in any direction two sets of dc motor can control with single IC.

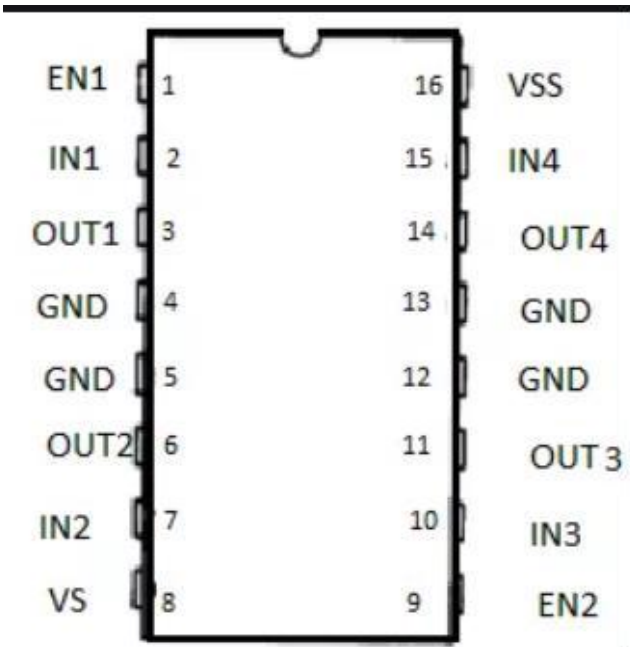

Figure 8:7 L293D Motor Drive

3. IMPLEMENTATION

Stage 1:In this stage connect all the components such as raspberry pi, camera, PIR sensor, ultrasonic sensor,

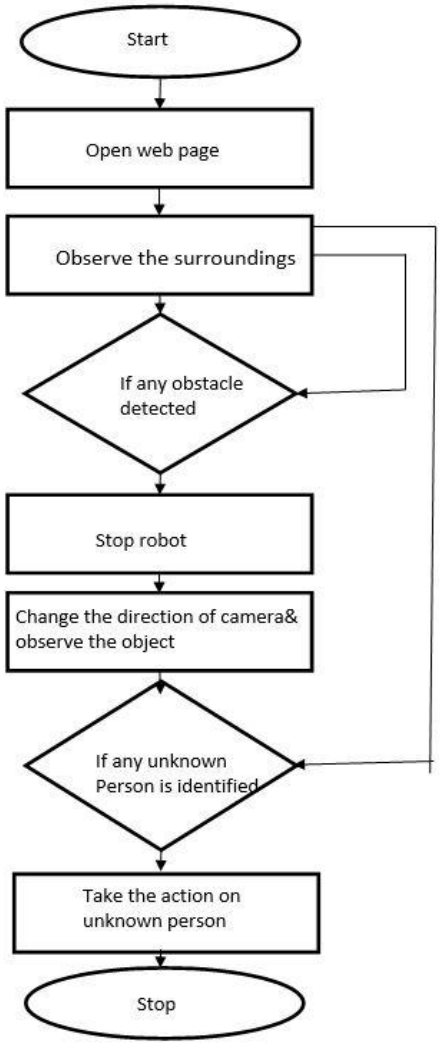

FLOW CHART

Test each and every component by giving the power supply to the kit.

Stage 2: Installation of software

The advanced IP scanner is used for scanning, monitoring and managing IP address space for a network& it is an essential tool in networking that enables users to scan IP addresses to obtain the information about devices in a network. This includes information on the status of IP to DNS, DNS to IP, DNS status connected switch ports& status. It gives information about in which port of raspberry pi connected &IP address of that port.

The VNC viewer software is installed on the computer&It is a graphical desktop sharing system that uses the remote frame buffer protocol (RFB) to remotely control another computer which is raspberry pi nothing but single board computer.

The VNC viewer is the program that represents the screen data originating from server, receives the updates from it& controls it by informing the server by collected local input with the help of these two software's and camera is

mounted on the servo motor to get the live video streaming[6][7].

4. DEVELOPMENT OF WEB PAGE

The very essential part is to build a webpage which is giving the live video streaming of the field. The robot can be controlled by giving the commands such as forward, reverse, left, right& stop which are built in the web page.
The camera can be controlled for giving the live streaming by the servo motor .the servo motor rotates 180 degree phase shift to cover all the directions of the field. The 4 motors are connected to the robot 2 motors are on front side and another 2 motors on the back side of robot these are controlled by motor driver L293D to drive the robot
The main requirement of the project is to provide the security .the security to this project is given with the user id and password. If the authorized person is required to control the robot, firstly the person has to login into the webpage &the login credentials are only shared with that person only to avoid the loss of misuse of the information.

5. RESULT

After the complete setup is made, then go to see the live video streaming of surroundings & according to giving the commands to the robot through webpage.Then identifying of the person is done by using the PIR sensor & ultrasonic sensor the buzzer connected to the robot circuit will be activated and gives sound.

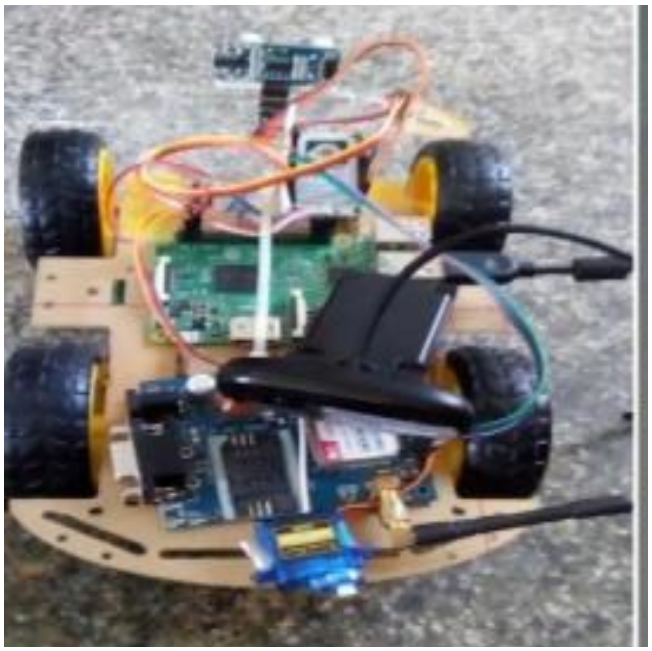

Figure 9 :Complete setup of Robot

If the unknown person is identified then the authorized person will give the commands to the robot to focus the laserlight on the unknown person to cause effect[8][9][10].

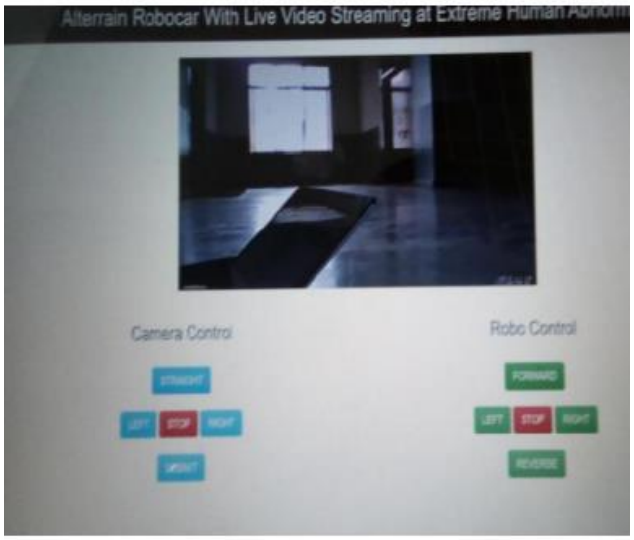

Figure 10: Developed Web page

The main aim of webpage creation is to control the robot in various directions.

6. CONCLUSION

In this paper we developed a live video streaming military robot which is very useful to our country to protect from enemies by avoiding the loss of our military man power. It provides the real time conditioning based information and controls the robot in various directions by giving the command.

REFERENCE

[1] Minal S. Ghute, KanchanP.Kamble ,MridulKorde "Design of Military Surveillance Robot"2018 First International Conference on Secure Cyber Computing and Communication (ICSCCC) December 15-17,Jalandhar

[2] Miss. SalunkheDisha M1, Miss. JagtapAshwini U1, Miss. GhodekarDarshana R1,Asst. Prof. Shelke Poonam V2 "Wireless Multifunctional Robot for Military Applications." International Research Journal of Engineering and Technology (IRJET) e-ISSN: 2395-0056 pISSN: 2395-0072 Volume: 05 Issue: 03 | Mar-2018

[3] SweetaDeshmukh, Priyadarshini, Mamta,MadhuraDeshmukh, Dr.Md.Bakhar"IOT Based Surveillance Robot." International Journal of Innovative Research in Computer and Communication Engineering Vol.5, Special Issue 4, June 2017.

[4] Vanitha, M., M. Selvalakshmi, and R. Selvarasu. "Monitoring and controlling of mobile robot via internet through Raspberry Pi board."Science Technology Engineering and Management (ICONSTEM,Second International Conference on 30-31 march IEEE 2016.

[5] Saravana Kumar K , Priscilla P, Germiya K Jose , Balagopal G "Human Detection Robot using PIR

Sensors" International Journal of Science, Engineering echnology Research (IJSETR)Volume 4, Issue 3, March 2015 "PDCA12-70 data sheet," Opto Speed SA, Mezzovico, Switzerland.

[6] Sundaram, Aditya, et al. "Remote Surveillance Robot System{A Robust Frame-work Using Cloud." Nanoelectronic and Information Systems(iNIS), 2015 IEEE International Symposium on. IEEE2015.

[7] KetanDumbre, SnehalGaneshkar, AjinkyaDhekne, "Robotic Vehicle Control using Internet via Webpage and Keyboard", International Journal of Computer Applications(0975-8887), Volume 114-No.17,March 2015.

[8] M. Priyanka and V. Raja ramanan, "Unmanned Aerial Vehicle for Video Surveillance Using Raspberry Pi", International Journal of Innovativee search in Science, Engineering andTechnology, Volume 3, SpeciaMarch 2014.

[9] M. MdAthiq UR Raza Ahamed, WajidAhamed, "A Domestic Robot for Security Systems by Video Surveillance using ZigbeeTechnology",International Journal of Scientific Engineering and Technology, Volume 2Issue 5,pp:448- 453,(ISSN:2277-1581), 1 May 2013.

[10] Pavan.C, D B.Sivakumar "Wi-Fi ROBOT FOR VIDEO MONITORING &SURVEILLANCE SYSTEM" International Journal of Scientific & Engineering Research Volume 3, Issue 8, August-2012 ISSN 2229-5518

Structural, Functional Characterization of NS5 Protein of Kyasanur Forest Disease (KFD) Virus and It's Interaction Studies with Existing and Novel Drugs by Molecular Docking Approach

[1] Sharanappa Achappa, [2] S.V. Desai

[1][2] Department of Biotechnology, KLE Technological University, Hubballi, India

Abstract:

Kyasanur forest disease Virus (KFDV) a highly pathogenic virus belongs to the flaviviridae family, genus flavivirus, causes an haemorrhagic disease in human beings. Kyasanur Forest Disease (KFD) was recognized first as a febrile illness in Kyasanur Forest of Shimoga district, Karnataka state, India in 1957 [1]. KFD is a zoonotic disease transmitted by the bite of infected ticks. The natural cycles involve infection of a non- human vertebrate host (mammal or bird), transmitted by Haemaphysalis ticks. Thus this virus was named Kyasanur Forest Disease Virus (KFDV) [2]. The black-faced langur (*Presbytis entellus*) and red-faced bonnet (*Macaca radiate*) are the typical monkeys that acquire the virus [1]. It is noteworthy that in recent years KFDV broke the geographical localization and spread out to newer areas which are often separated by several kilometres from the endemic regions from Shimoga to other states of India [3]. The reservoir of KFDV is present in the forest which makes it difficult for controlling the emergence of the disease. Therefore, it needs an interdisciplinary approach on KFD and understanding their vectors and epidemiology. As the current vaccination strategy is barely successful, unavailability of effective anti-viral raises the possibility for novel therapeutic approaches against KFD. In view of this, the present research work is outlined to provide the best possible approach by use of Bioinformatics tools to understanding molecular mechanism of proteins and their structural aspects provides the opportunity to address the issue related to the development of novel therapeutic drugs against KFD. This research work aims to understand structural and functional characterization of NS5 protein of KFD, developing of new drugs by using docking tools and also understanding the mechanism of ligand protein interaction.

Keywords:

NS5 Protein, KFD, Virus, Molecular Docking, Novel Drugs

1. INTRODUCTION

KFDV is a member of the *Flaviviridae* virus family, with no current viral order [4]. Three genera are associated with this family: *Hepacivirus*, *Pestivirus* and *Flavivirus*. The *Flavivirus* genus is divided into three different groups: Tick-Borne (TB), Mosquito-Borne (MB) and No Known Vector (NKV) groups. The TB viruses are divided into two sub-groups: Mammalian (M-TB) and Seabird (S-TB). Kadam Virus, Meaban Virus and Saumarez Reef Virus are placed within the sub-group of S-TB. M-TB includes: Langat Virus (LGV), Powassan Virus (POWV), Tick-Borne Encephalitis Virus (TBEV) and it contains the KFDV, Omsk Hemorrhagic Fever Virus (OHFV) and Alkhurma Hemorrhagic Fever Virus (AHFV), which are of interest to this study [5].

In 1957 an epizootic (an epidemic in animal populations) [6] event occurred within a population of monkeys, in a localized region of southwest India. This area is the Kyasanur Forest of Shimoga district, Karnataka state, India [1]. Thus this virus was named Kyasanur Forest Disease Virus (KFDV) [2]. The typical monkeys that acquire the virus are the black-faced langur (*Presbytis entellus*) and red-faced bonnet (*Macaca radiate*) [1]. Shortly after the outbreak, the first human cases were observed. Epizootics continued throughout the Shimoga district almost every year since the first KFDV discovery in 1957.

Clinical symptoms of KFD can be seen in two stages, *i.e.* it has a biphasic course of illness. After the incubation period of approximately 3-8 days, "flu-like" symptoms develop. This is called a febrile or "with fever period" and symptoms include: fever, headache, vomiting, severe back and extremity pain and prostration. The febrile period can last for one to two weeks and convalescence may begin ending the infection [1,7,8]. Some patients suffer the second phase illness course and may succumb to severe ailments such as: meningoencephalitis, conjunctival inflammation, bradycardia, hemorrhagic fevermanifestations (hemorrhagic pneumonitis, gastrointestinal bleeding), coma and possibly death [5,9]. Morphologically, Flaviviruses are quite complex in the structure. When the virus is a mature infectious particle, it is characterized as a dense icosahedral nucleocapsid (~35-50 nm) that houses the single-stranded (ss) RNA genome of positive-sensed polarity and is surrounded by a lipid bilayer envelope carrying two surface proteins.

Flaviviruses have a positive-stranded RNA genome of about 10-11 kb in length. Translation of the genome creates a long polyprotein that is then co and post-translationally cleaved into 10 proteins by cellular and viral proteases. The 5' end of the genome encodes for three structural proteins and seven non-structural proteins follow to the 3' end. The polyprotein is organized in the following way: C-prM-E-NS1-NS2A-NS2B-NS3-NS4A-NS4B-NS5,

Virus entry occurs by receptor-mediated endocytosis, and the acidic pH in the endosome induces structural alterations in E that lead to membrane fusion and the release of the nucleocapsid into the cytoplasm. After uncoating, the plus-stranded RNA genome is translated to initiate virus replication. Virus assembly occurs in the endoplasmic reticulum (ER) and leads to the formation of immature (prM-containing) particles that are transported through the exocytic pathway. There is evidence that the acidic pH in the trans-Golgi network (TGN) causes an irreversible conformational change in the prM–E complex that is required for the maturation cleavage by cellular furin or a related protease, Mature infectious particles are released by exocytosis.

2. METHODOLOGY

Sequence Analysis: BLAST[10] was performed to identify the percentage similarity between different proteins using the sequence of NS5 obtained from Uniprot database database . The Phylogenetic Analysis was carried out using CLUSTAL Omega tool [11] by performing multiple sequence analysis. Protein property analysis was carried out using ProtParam[12] and subcellular localization of target protein was predicted using CELLO v.2.5[13].

Structure Analysis: The 3D structure of NS5 was predicted by homology modeling using I-Tasser structure prediction program[14] and active site was also predicted by I-Tasser server. Structural evaluation and stereo chemical analyses were performed using ProSA-web server [15] and z-score was obtained. This score give authenticity about quality of model generated in the study. The final structure obtained was analyzed by Ramachandran plot using PROCHECK [16] for stero chemical analysis.

Virtual Screening and docking: The dug like compound for this virtual screening were obtained from Zinc database[17].Drug like compound similar to **5-nitrocytidine 5'-(tetrahydrogen triphosphate) (NSC)** of 50 compounds were screened using igemDock software.The results from this screening were computed and top ten compounds were selected and were subjected for docking analyses using igem dock[18].

3. RESULTS AND DISCUSSION:

NS5 protein sequence was retrieved from UniProt database with UniProt ID of D7RF80.1. Extracted sequence was subjected sequence analysis to extract homologous sequence by using BLASTp by using SwissProt as a database search and by keeping all other algorithm parameter as default value. It is found that Tick-borne encephalitis virus (strain HYPR), Langat virus (strain TP21), Louping ill virus (UniProt ID – Q01299, P29837 and P22338 respectively) was most similar with e value of 0.0 and percent identity of 88%. WEST NILE VIRUS (P06935), DENGUE VIRUS 1(P17763) with e-value of 7e-158 and 2e-152 with percentage identity of 67%. Highly similar proteins from BLASTp analysis was considered for performing phylogenetic analysis by using CLUSTAL Omega tool. Phylogenetic analysis for the NS5 protein is as shown in fig 1.

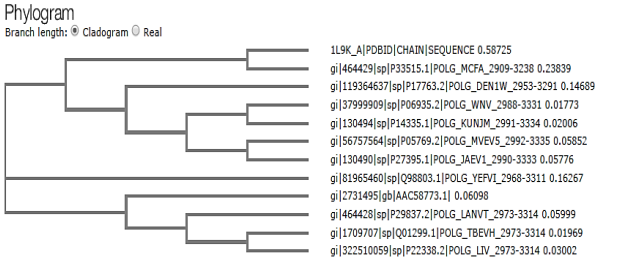

Fig 1:Phylogram of NS5 protein showing phylogenetic relationship.

Phylogram showed that KFD NS5 protein was closely related to Langat virus (P29837), Thick born Encephalitis (Q01299) and Louping ill virus (P22338), whereas other flavivirus seems to be divergent from above mentioned.

ProtParam tool was used for the analysis of protein physical and chemical parameters. The results of ProtParam were as follows, molecular weight (9494.8), theoretical PI (6.79), hydropathicity (-0.481) and instability index (27.13-shows the protein is stable)

Subcellular localization of the NS5 proteins was analyzed by using cello v2.5 and results are shown in fig 2.

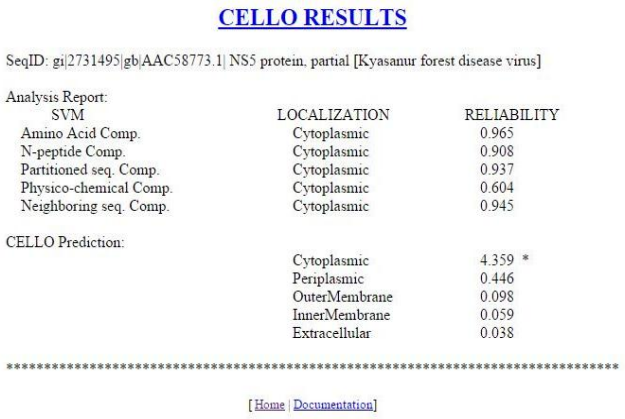

CELLO RESULTS

SeqID: gi|2731495|gb|AAC58773.1| NS5 protein, partial [Kyasanur forest disease virus]

Analysis Report:

SVM	LOCALIZATION	RELIABILITY
Amino Acid Comp.	Cytoplasmic	0.965
N-peptide Comp.	Cytoplasmic	0.908
Partitioned seq. Comp.	Cytoplasmic	0.937
Physico-chemical Comp.	Cytoplasmic	0.604
Neighboring seq. Comp.	Cytoplasmic	0.945

CELLO Prediction:

	Cytoplasmic	4.359 *
	Periplasmic	0.446
	OuterMembrane	0.098
	InnerMembrane	0.059
	Extracellular	0.038

****

[Home | Documentation]

Fig 2: Cello results for NS5 protein

From the result predicted from cello v.2.5, the subcellular localization of NS5 is in cytoplasmic with reliability score of 4.359.

3D structure of NS5 protein was determined by I-Tasser server and the model predicted was shown in fig 3.:

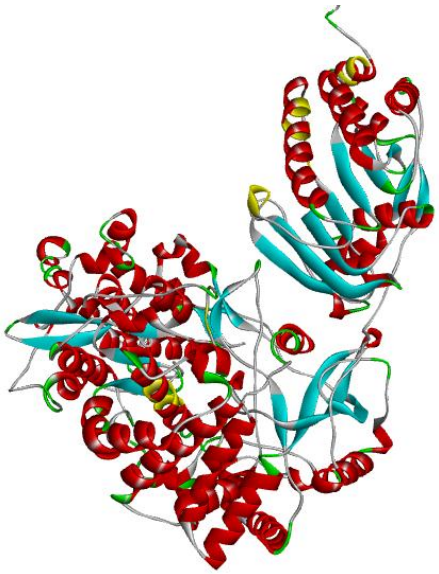

Fig 3: Structure of Model 1 obtained from I-Tasser

For NS5 protein three models were generated. The confidence level of Model1 was 2.00. The confidence of each model is quantitatively measured by C-score and is calculated based on the significance of threading template alignments. C-score of a higher value signifies a model with a higher confidence and vice-versa. PDB Templates used by I-Tasser for determining the model are 4k6ma, 5tfra and 6qsna.

Structural evaluation and stereo chemical analyses for NS5 protein was carried out using ProSA web and the result was shown in fig 4.

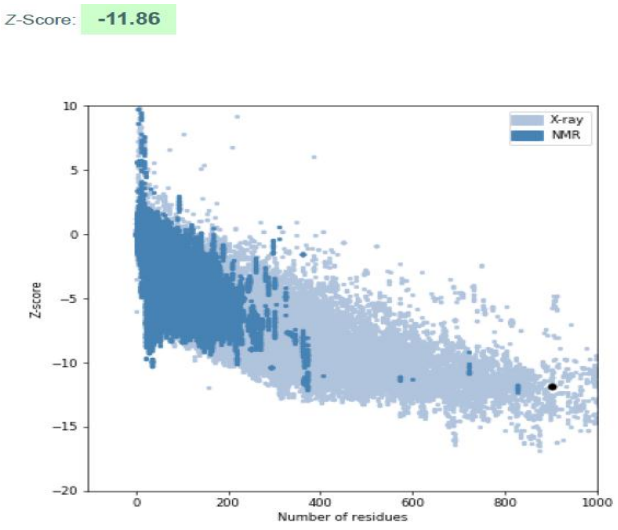

Fig 4: Prosaweb result for NS5

The *z*-score indicates overall model quality. Its value is displayed in a plot that contains the *z*-scores of all experimentally determined protein chains in current PDB. The z-score of -11.86 for NS5 protein falls within the range of experimentally determined structures available in PDB as shown in fig 4.Local model quality is shown in fig 5.

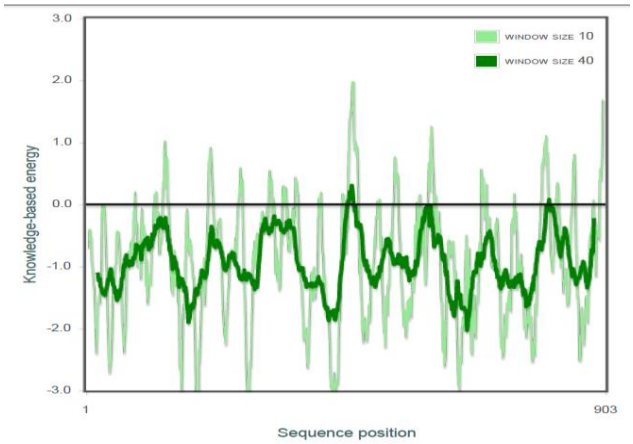

Fig 5:Prosaweb local model quality for NS5

This plot shows local model quality by plotting energies as a function of amino acid sequence position. Amino acid with positive energy indicates faulty amino acid.

Quality and reliability assessment for the NS5 protein was carried out using ProCheck as shown in fig 6.

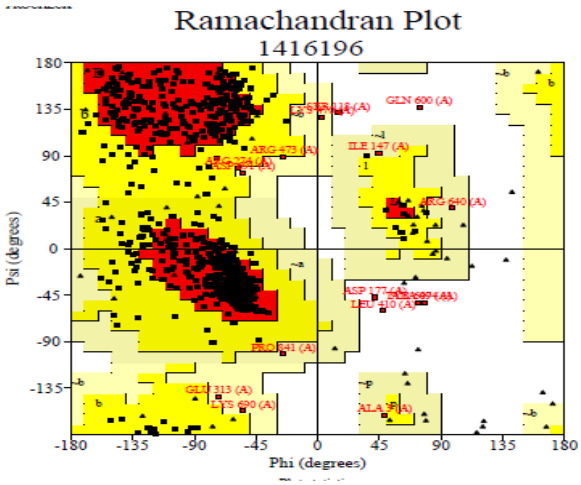

Fig 6: Ramchandran plot for NS5 protein

In the Ramachandran plot above red color refers to "no steric hindrance", yellow color refers to "some steric constraints "and whitecolour represents "forbidden zone". It can be observed in the figure that most of the residues are in red region and the percentage of residues in most favored regions is 97% and only 0.8% of residues are in disallowed regions which classify our protein as stable and chemically realistic.

Virtual screening was carried out by downloading compounds similar to N5C from Zinc database in the mol2 format. This mol2 file contained 50 molecules similar to 5-Nitrocytidine 5'-(Tetrahydrogen Triphosphate) (N5C), which were screened using Igem dock and from the results computed, top fifteen compounds with their scores are

tabulated in table no.1 and fig 7 and 8 shows the interaction of drug with NS5 protein.

Table No.1: Shows ligand with docking score by igemdock

Sr.No.	Zinc Id No	Igem dock score
1	Zinc 8216074	**-169.51**
2	Zinc8216134	**-136.7**
3	Zinc12495027	**-128.57**
4	Zinc12495268	**-140.08**
5	Zinc12495280	**-152.27**
6	Zinc 12495285	**-160.47**
7	Zinc12660526	**-133.19**
8	Zinc13431045	**-130.71**
9	Zinc12431047	**-138.53**
10	Zinc13431048	**-133.93**
11	Zinc13431049	**-136.8**
12	Zinc13431050	**-157.59**
13	Zinc13431052	**-137.19**
14	Zinc13431055	**-138.78**
15	Zinc13431057	**-127.86**

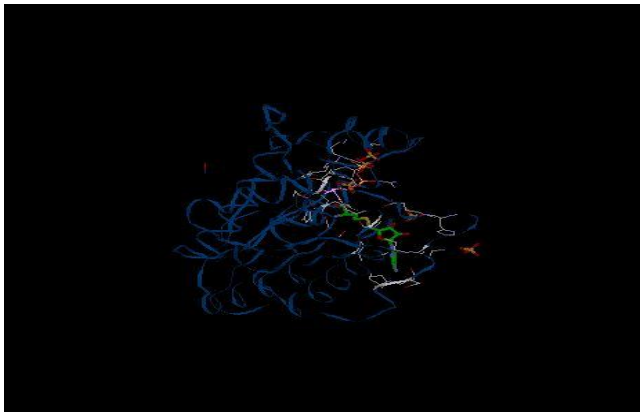

Fig 7. Interaction of Zinc 8216074 with NS5 protein

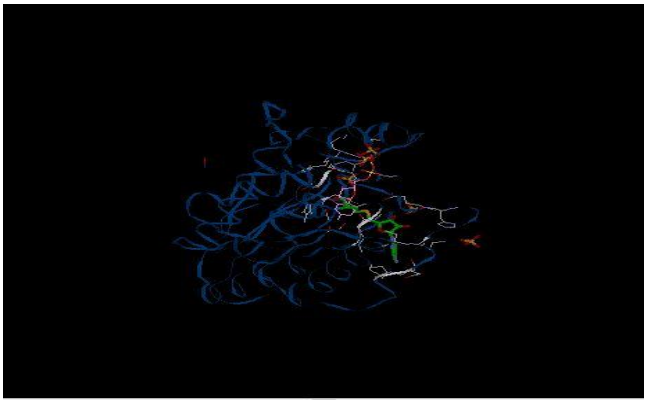

Fig8. Interaction of Zinc8216134 with NS5 protein

4. CONCLUSION

Kyasanur Forest disease containssevenproteins but here we are focusing on NS5, which is required for the viral entry and establishment of infection. Firstly we retrieved sequences of NS5 protein from UniProt database. BLASTp and Phylogenetic analysis showed that other types of Kyasanur Forest disease as well as some of the different type of Flavivirusare closely related and appears to be obtained from same ancestor. Protein were then submitted to Protpram tool to obtain the instability index and grand average of hydropathicity(GRAVY).The instability index classifies whether the protein is stable or instable. The instability index obtained for NS5 is 27.13 ,which classifies the proteins to be stable. Cello v.2.5 software was used to obtain a sub cellular localization of the proteins. Results obtained from Cello v.2.5 show that NS5 protein is localized in cellular localization is in cytoplasmic and involved in the entry of virus to the host cell. Homology modeling, to obtain the 3D structure of protein the sequences were submitted to I-Tasser. Many models were generated based on the C-value we decided model1 to be selected for NS5 protein. To check the quality of model and for Structural evaluation and stereo chemical analyses, protein structure was submitted to Prosa-Web. Quality of model is decided on the Z score obtained for a model. Z-score obtained for NS5 was 11.86. Based on these values, quality of our model was good. Ramachandran plot was obtained to check stero-chemical hindrance and model with 97% of amino acid fall in favoured region. Virtual screening was carried out to screen the compounds that appropriately dock with target sites. Top 15 compounds was docked with NS5 protein by using igem dock tool.

REFERENCE

[1] Pattnaik, P. (2006). "Kyasanur forest disease: an epidemiological view in India." Rev Med Virol 16(3): 151-65.

[2] Dandawate, C. N., G. B. Desai, et al. (1994). "Field evaluation of formalin inactivated Kyasanur forest disease virus tissue culture vaccine in three districts of Karnataka state." Indian J Med Res 99: 152-8.

[3] Ajesh K., Nagaraja B., Sreejith K. (2017). Kyasanur forest disease virus breaking the endemic barrier: an investigation into ecological effects on disease emergence and future outlook. Zoonoses Public Health 64, e73–e80. 10.1111/zph.12349.

[4] Fauquet, C. M., M. A. Mayo, et al. (2005). Virus Taxonomy. San Diego, USA, London, UK, Elsevier Inc.

[5] Howley, P. M. and D. M. Knipe (2007). Fields' Virology, Lippincott Williams & Wilkins.

[6] Artsob, H. and R. Lindsay (2008). "Arboviruses." Elsevier Inc. International Encyclopedia of Public Health One(First Edition): 219-226.

[7] Goodman, J. L., D. T. Dennis, et al. (2005). Tick-Borne Diseases of Humans, ASM Press.

[8] Grard, G., G. Moureau, et al. (2007). "Genetic characterization of tick-borne flaviviruses: New insights into evolution, pathogenetic determinants and taxonomy." Virology 361(1): 80-92.

[9] Adhikari Prabha, M. R., Prabhu, M. G., Raghuveer, C. V.,Bai, M.,& Mala, M. A. (1993). Clinical study of

100 cases of Kyasanur Forest disease with clinicopathological correlation. *Indian Journal of Medical Sciences*, *47*, 124–130.

[10] Altschul SF, Gish W, Miller W, Myers EW, Lipman DJ: Basic local alignment search tool. *Journal of molecular biology* 1990, 215(3):403-410.

[11] Larkin MA, Blackshields G, Brown NP, Chenna R, McGettigan PA, McWilliam H, Valentin F, Wallace IM, Wilm A, Lopez R *et al*: Clustal W and Clustal X version 2.0. *Bioinformatics* 2007, 23(21):2947-2948.

[12] Gasteiger E. HC, Gattiker A., Duvaud S., Wilkins M.R., Appel R.D., Bairoch A.;(In) John M. Walker (ed):: Protein Identification and Analysis Tools on the ExPASy Server;. *The Proteomics Protocols Handbook, Human Press* 2005:571-606.

[13] Yu CS, Lin CJ, Hwang JK: Predicting subcellular localization of proteins for Gram-negative bacteria by support vector machines based on n-peptide compositions. *Protein science : a publication of the Protein Society* 2004, 13(5):1402-1406.\

[14] Zhang Y: I-TASSER server for protein 3D structure prediction. *BMC bioinformatics* 2008, 9:40.

[15] Wiederstein M, Sippl MJ: ProSA-web: interactive web service for the recognition of errors in threedimensional structures of proteins. *Nucleic acids research* 2007, 35(Web Server issue):W407-410.

[16] Morris AL, MacArthur MW, Hutchinson EG, Thornton JM: Stereochemical quality of protein structure coordinates. *Proteins* 1992, 12(4):345-364.

[17] Irwin JJ, Shoichet BK: ZINC--a free database of commercially available compounds for virtual screening. *Journal of chemical information and modeling* 2005, 45(1):177-182.

[18] Macindoe G, Mavridis L, Venkatraman V, Devignes MD, Ritchie DW: HexServer: an FFT-based protein docking server powered by graphics processors. *Nucleic acids research* 2010, 38(Web Server issue):W445-449.

[19] Sadanandane C., Elango A., Marja N., Sasidharan P. V., Raju K. H. K., Jambulingam P. (2017). An outbreak of Kyasanur forest disease in the Wayanad and Malappuram districts of Kerala, India. Ticks Tick Borne Dis. 8, 25–30. 10.1016/j.ttbdis.2016.09.010.

[20] Patil D., Yadav P., Shete A., Nuchina J., Meti R., Bhattad D., et al. . (2017). Occupational exposure of cashew nut workers to Kyasanur forest disease at Goa, India. Int. J. Infect. Dis. 61, 67–69. 10.1016/j.ijid.2017.06.004.

[21] Pai S., HN H. K. (2017). Epidemiological trends in Kyasanur Forest Disease in Karnataka State, South India. J. Pharm. Pract. Commun. Med. 3, 103–107. 10.5530/jppcm.2017.3.24.

[22] Roy, P. R. P., Maiti, D., Goel, M. K., and Rasania, S. (2017). Kyasanur Forest Disease: an emerging tropical disease in India. *J. Res. Med. Dental Sci.* 2, 1–4. doi: 10.5455/jrmds.2014221.

[23] Muraleedharan, M. (2016). Kyasanur Forest Disease (KFD): rare disease of zoonotic origin. *J. Nepal Health Res. Counc.* 14, 214–218.

[24] Mourya, D. T., & Yadav, P. D. (2016). Recent scenario of emergence of Kyasanur Forest disease in India and public health importance. Current Tropical Medicine Reports, 3, 7–13.

[25] Chandran P., Thavody J., Lilabi M., Bina T., Kanan S. (2016). An outbreak of Kyasanur Forest Disease in Kerala: a clinico epidemiological study. Indian J. For. Commun. Med.3, 272–275. 10.18231/2394-6776.2016.0010.

[26] Cook, B. W., Ranadheera, C., Nikiforuk, A. M., Cutts, T. A., Kobasa, D., and Theriault, S. S. (2016). Limited effects of Type I interferons on Kyasanur Forest Disease Virus in cell culture. *PLoS Negl. Trop. Dis.* 10:e0004871. doi: 10.1371/journal.pntd.0004871.

[27] Rodríguez-Mallon, A. (2016). Developing anti-tick vaccines. *Methods Mol. Biol.* 1404, 243–259. doi: 10.1007/978-1-4939-3389-1_17.

[28] Murhekar, M. V., Kasabi, G. S., Mehendale, S. M., Mourya, D. T., Yadav, P. D., & Tandale, B. V. (2015). On the transmission pattern of Kyasanur Forest disease (KFD) in India. *Infectious Diseases of Poverty*, *4*, 37. doi: 10.1186/s40249-015-0066-9.

[29] John, J. K., Kattoor, J. J., Nair, A. R., Bharathan, A. P., Valsala, R., and Sadanandan, G. V. (2014). Kyasanur Forest disease: a status update. *Adv. Anim. Veter. Sci.* 2, 329–336. doi: 10.14737/journal.aavs/2014/2.6.329.336.

[30] Sprong, H., Trentelman, J., Seemann, I., Grubhoffer, L., Rego, R. O., Hajdušek, O., et al. (2014). ANTIDotE: anti-tick vaccines to prevent tick-borne diseases in Europe. *Parasit. Vectors* 7:77. doi: 10.1186/1756-3305-7-77.

[31] Dodd K. A., Bird B. H., Khristova M. L., Albariño C. G., Carroll S. A., Comer J. A., et al. . (2011). Ancient ancestry of KFDV and AHFV revealed by complete genome analyses of viruses isolated from ticks and mammalian hosts. PLoS Negl. Trop. Dis.5:e1352. 10.1371/journal.pntd.0001352.

[32] Kasabi G. S., Murhekar M. V., Sandhya V. K., Raghunandan R., Kiran S. K., Channabasappa G. H., et al. . (2013a). Coverage and effectiveness of Kyasanur forest disease (KFD) vaccine in Karnataka, South India, 2005–10.

[33] Kasabi G. S., Murhekar M. V., Yadav P. D., Raghunandan R., Kiran S. K., Sandhya V. K., et al. . (2013b). Kyasanur forest disease, India, 2011–2012. Emer. Infect. Dis. 19, 278–281.

[34] Mourya, D. T., Yadav, P. D., Sandhya, V. K., & Reddy, S. (2013). Spread of Kyasanur Forest disease, Bandipur Tiger reserve, India, 2012–2013. Emerging Infectious Diseases, 19, 1540–1541.

In - silico Analysis of Gut Microbiota and Its Influence on Insulin Secretion

[1] Sharanappa Achappa, [2] Varsha.Lambi, [3] L.R.Patil, [4] Anil R. Shet

[1][2][3][4] Department of Biotechnology, KLE Technological University, Hubballi, India

Abstract:

Gut microbes are the microorganisms including bacteria, archaea and fungi that live in the digestive tracts. Gut microbes play a key role in digestion, extraction, synthesis and absorption of many nutrients and metabolites including bile acids, amino acids, vitamins and short chain fatty acids. These microbes have a crucial immune function against pathogenic bacteria colonization by inhibiting their growth. Gut microbiota varies between individuals, these variations are due to the enterotypes of BMI and external factors such as lifestyle, exercise frequency, ethnicity and dietary and cultural habits. The variations among the gut microbiota affect the host's health. The interactions between the gut microbes and the host insulin secretion are studied. The proteins and the receptors responsible for the insulin secretion influenced by the gut microbes are identified and the identified proteins are free fatty acid receptors(FFAR1, FFAR2, FFAR3, FFAR4), Glucagon like peptide(GLP-1), Glucagon like peptide receptor(GLP1R) and Glucose like transporters (GLUT1, GLUT2, GLUT3). The structure analysis of the proteins was done using ProSA-Web, Pro-Check and the physical and chemical properties were analyzed using Prot-Param. The interactions of the proteins are analyzed. Summarized here is the role of gut microbiota in the host insulin secretion which leads to glucose homeostasis in the host.

Keywords:

Gut microbes, SCFAs, Free fatty acid receptors, glucagon like peptide, glucose like transporters

1. INTRODUCTION

Gut microbes are present in different parts of the gastrointestinal tract but the colon alone has 70% of all the microbes in the human body 20 microbiota are strictly anaerobes. There are many bacterial file among them the dominant microbiota includes Prevotella, Bacteroides, Ruminococcus colonization of the human gut with microbes begins immediately at birth however after one year of age the intestinal microbiota of children start at resemble like young adult besides the the mother microbiota composition including bile acids, vitamins and SCFA[4].

Humans do not have the enzymes that break down the complex carbohydrates therefore first these complex carbohydrates are permitted to short chain
fatty acids[7]. The bacterial species like bacteroidetes and firmicutes breakdown these complex carbohydrates [5],the most abundantly produced SCFA are acetate, propionate and butyrate in the ratio 40:40:20 to 75:15:10[1].

The SCFAs provide energy to colonocytes [1], act as signaling molecules, and act as substrate [9] for gluconeogenesis and lipogenesis.

The main objective in our study is to see how short chain fatty acid acts produced by gut microbiota acts as signaling molecules in insulin secretion .The gut microbiota and host glucose are in symbiotic relationship [3].The protein that we have confined are free fatty acid receptors (FFAR1, FFAR2, FFAR3, FFAR4) [8], Glucagon like peptide (GLP-1) [2], Glucagon like peptide receptor (GLP1R) and Glucose like transporters (GLUT1, GLUT2, GLUT3*).* The structural and functional characteristics of their proteins were done using Prot-Param, a tool for computation of various physical and chemical properties of proteins. Followed by SOPMA for predicting secondary structure, SWISS Model server for homology modeling of protein , Robetta for 3D structure analysis , Protein Structure analysis and to check the structure for any potential errors was done using ProSA web, protein ligand binding site was identified using COACH-D,

2. MATERIALS AND METHODS:

Sequence Analysis: BLASTp [10] was performed to identify the percentage similarity between different proteins using the sequences of FFAR1, FFAR2, FFAR3, FFAR4, GLP-1, GLP1R, GLUT1, GLUT2, GLUT3 obtained from Uniprot database. The Phylogenetic Analysis was carried out using CLUSTAL Omega tool [11] by performing multiple sequence analysis. Protein property analysis was carried out using Prot-Param [12].

Structure Analysis: The 3D structure of FFAR1, FFAR2, FFAR3, FFAR4, GLP-1, GLP1R, GLUT1, GLUT2, GLUT3 was predicted by homology modeling using the Robetta structure prediction program [17]. Structural evaluation and stereo chemical analyses were performed using ProSA-web server [13] and z-score was obtained. This score gives authenticity about the quality of the model generated in the study. The final structure obtained was analyzed for stereo chemical analysis by Ramachandran plot using PROCHECK [14]. COACH-D was performed to predict protein ligand binding site [15].

Virtual Screening and docking: iGEMDOCK was used for post-screening analysis; *i*GEMDOCK provides

 ISBN: 978-93-90214-20-4

biological insights by deriving the pharmacological interactions from screening compounds without relying on the experimental data of active compounds. The pharmacological interactions represent conserved interacting residues, which often form binding pockets with specific physico-chemical properties, to play the essential functions of a target protein. Our experimental results show that the pharmacological interactions derived by *i*GEMDOCK are often hot spots involving in the biological functions. In addition, *i*GEMDOCK provides the visualizations of the protein-compound interaction profiles and the hierarchical clustering dendrogram of the compounds for post-screening analysis [16].

3. RESULTS & DISCUSSION:

The proteins were retrieved from Uniprot-KB. The UniprotKB IDs of the proteins FFAR1 (300) is O14842, FFAR2 (330aa) is O15552, FFAR3 (346aa) is O14843, FFAR4 (361aa) is Q5NUL3, GLP-1 (463aa) is P01275, GLP1R (180aa) is P43220, GLUT1 (492aa) is P11166, GLUT2 (524aa) is P11168, GLUT3 (496aa) is P11169.

The Robetta server provides automated tools for protein structure prediction and analysis. For structure prediction, sequences submitted to the server are parsed into putative domains and structural models are generated. For comparative modeling, the confidence corresponds to the agreement in structure between the partial threaded models from the top alignment of each independent alignment method, with confidence of 1 being a good model and 0 being bad. From the results obtained to us we can infer that FFAR1, FFAR2, GLUT1, GLUT2 and GLP1R have the confidence value near to 1 of 0.80, 0.74, 0.89, 0.83 and 0.65 respectively, indicates good models and GLP-1 has the confidence score of 0.17 indicating not so good model. Fig 1 shows the structure of different proteins and receptors predicted by Robetta server.

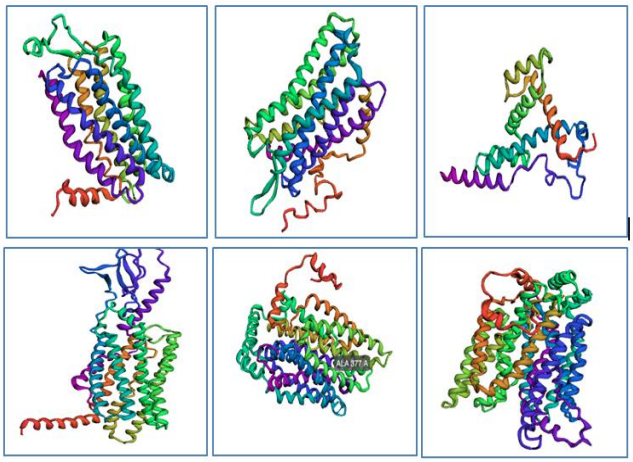

Fig.1. 3D structure predicted by Robetta; a. Structure of FFAR1, b.FFAR2, c.GLP-1. d.GLP1R, e. GLUT1, f. GLUT2.

In order to analyze predicted 3D structure of proteins, ProSA-Web analysis was performed to check the quality of predicted structure. The *z*-score indicates overall model quality. Its value was displayed in a plot that contains the *z*-scores of all experimentally determined protein chains in current PDB. It can be used to check whether the *z*-score of the input structure is within the range of scores typically found for native proteins of similar size. Fig 2 shows z-score of different predicted structures and also indicates that the predicted 3D structures are in-line with experimentally determined structure. This indicates the goodness of the predicted model.

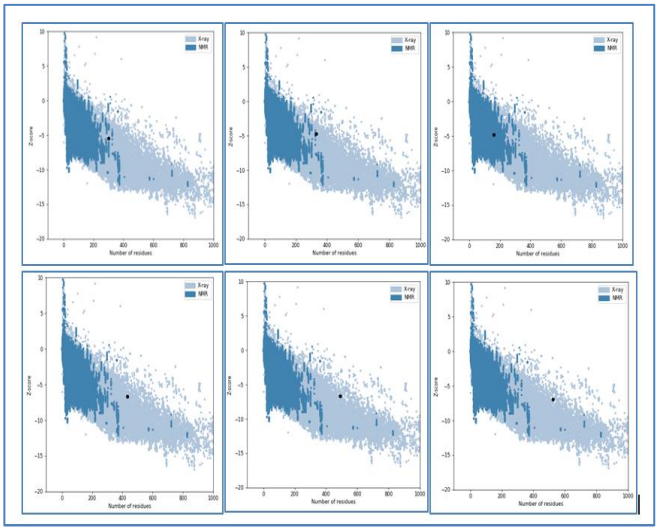

Fig.2. Z-score of 3D structure predicted by Robetta; a. Structure of FFAR1, b.FFAR2, c.GLP- 1. d.GLP1R, e. GLUT1, f. GLUT2.

ProtParam tool was used to compute various physical and chemical parameters for a given protein stored in Swiss-Prot or TrEMBLor for a user entered protein sequence. The computed parameters include the molecular weight, theoretical pI, amino acid composition, atomic composition, extinction coefficient, estimated half-life, instability index, aliphatic index and grand average of hydropathicity (GRAVY)

Table 3.1: Physicochemical Properties of protein obtained from Prot Param.

Protein name	FFAR1	FFAR2	GLP-1	GLP1R	GLUT1	GLUT2
No. of amino acid	300	330	180	440	492	524
Molecular weight	31457.08	37143.78	3298.66	50812.02	54083.78	57489.53
Theoretical PI	9.63	9.50	5.53	8.25	8.93	8.09
Instability index	29.01	48.02	17.69	42.16	36.57	36.57
Aliphatic index	111.67	116.64	71.67	97.27	108.94	107.19
gravy	0.644	0.490	-2.30	0.154	0.534	0.554

 ISBN: 978-93-90214-20-4

In the Ramachandran plot above red color refers to “no steric hindrance”, green color refers to “some steric constraints" and white color represents “forbidden zone”. It can be observed in the fig 3 that most of the residues of all the proteins are in red region and the % of residues in most favored regions for FFAR1 is 93.4%, FFAR2 is 90.3%,, GLP-1 is 91.1%, GLP1R is 95.1%, GLUT1 is 96.9% , GLUT2 is 95.2% and the residues in disallowed regions are FFAR1 is 0.8%, FFAR2 is 0.3%, GLP-1 is 0.7%, GLP1R is 0.0%, GLUT1 is 0.2%, GLUT2 is 0.0% which classify the 3D structure determined by Robetta are stable, chemically realistic and allows conformational changes in native form.

Ligand binding sites for the predicted protein were determined by using COACH-D server. COACH-D server predicts different binding sites with tentative ligands based on the homologous protein templates from PDB database. Predicted binding sites are represented by c-score, which indicates the quality of the binding site. C-score near to 1 indicates the good model. Fig 4, shows binding sites of different proteins with their highest c-score value. The c-score of FFAR1 is 0.16, FFAR2 is 0.13, GLP1 is 0.03, GLUT1 is 0.11 and GLUT2 is 0.16.

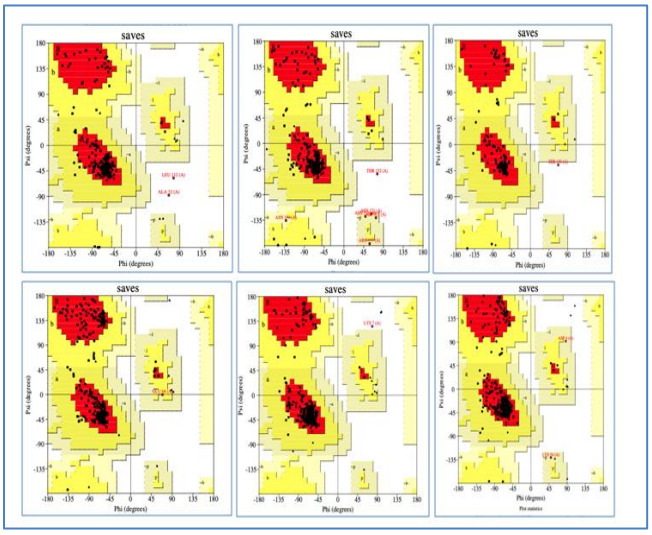

Fig.3. Ramachandran plot predicted by Pro-Check for proteins predicted by Robetta; a. Structure of FFAR1, b.FFAR2, c.GLP-1. d.GLP1R, e. GLUT1, f. GLUT2.

COACH-D was used for prediction of protein-ligand binding site prediction for which we give input as amino acid sequence as input or 3-D structure of a query protein. The output of the COACH-D is a protein structure with its binding site in ball and stick model and a tabular column with the c-score to check the reliability of the products, The c-score or the confidence score is in the range of [0, 1] and also the docking energies of the complex structures are listed under the ‘Energy’ and the ‘Energy’ columns.

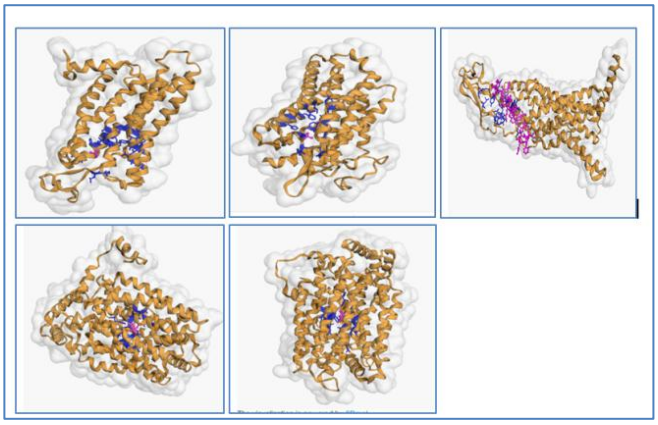

Fig.4. Ligand binding site prediction by COACH-D server for proteins predicted by Robetta; a. Structure of FFAR1, b.FFAR2, c.GLP- 1. d.GLUT1, e. GLUT2.

Molecular docking of predicted proteins was performed with their natural ligands (molecules) by using igemdock. Energy value with interaction analysis was done to check the amino acids of proteins involved in binding to their natural ligands.

FFAR1 protein was docked with acetate, butyrate, and propionate by using igemdock. The energy value for acetate, butyrate and propionate was -44.09, -53.53 and -48.43 respectively. Amino acids involved in binding with ligands were Leucine, Aspartate, Histidine, Tryptophan at 151, 152, 153, and 150 positions respectively. Fig No.5 shows the binding of acetate, butyrate and propionate to FFAR1.

FFAR2 protein was docked with acetate, butyrate, and propionate by using igemdock. The energy value for acetate, butyrate and propionate was -45.13, -52.81 and -48.93 respectively. Amino acids involved in binding with ligands were Serine, Arginine, Tyrosine, Tyrosine, and Phenylalanine at 104, 107, 108, 199, and 202 positions respectively. Fig No. 5 shows the binding of acetate, butyrate and propionate to FFAR2.

GLUT1 protein was docked with glucose by using igemdock. The energy value for glucose was -76.23. Amino acids involved in binding with ligands were Glutamine, Tyrosine, Tryptophan, Asparagine, Asparagine, Phenylalanine, and Tryptophan at 283, 292, 388, 411, 415, 26, and 412 positions respectively.

Fig No.5 shows the binding of glucose to GLUT1.

GLUT2 protein was docked with glucose by using igemdock. The energy value for glucose was -71.04. Amino acids involved in binding with ligands were Aspartate, Lysine, Aspartate, Glutamate, Arginine, Tyrosine, Aspartate, Valine at 4, 271, 272, 3, 264, 266, 268, 269, positions respectively. Fig No.5 shows the binding of glucose to GLUT2.

 ISBN: 978-93-90214-20-4

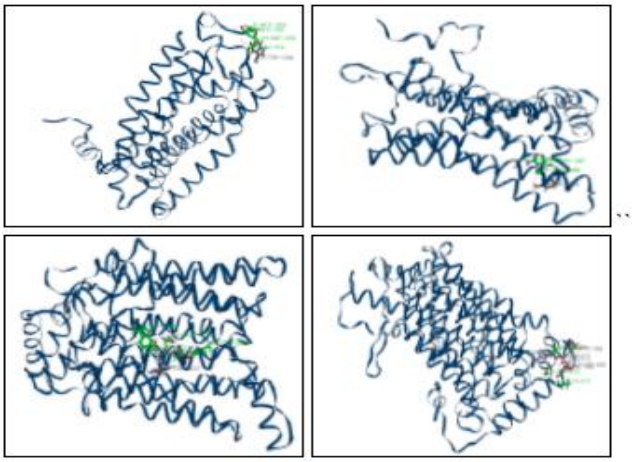

Fig.5. Binding of proteins with natural ligands. a. Binding of acetate, butyrate and propionate with FFAR1. b. Binding of acetate, butyrate and propionate with FFAR2. c. Binding of GLUT1 with glucose. d. Binding of GLUT2 with glucose

4. CONCLUSION:

Short chain fatty acids (Acetate, Butyrate, Propionate) acting as signaling molecules for insulin secretion is our consideration for this study. In this process we have identified a set of proteins (FFAR1, FFAR2, GLP-1, GLP1R, GLUT1, GLUT2) that we have analyzed using different computational tools. Similar organisms having these proteins were retrieved from the BLAST which showed maximum similarity with respect to our proteins. The FASTA sequences of these proteins were retrieved and submitted to different computational tools for analysis. Tertiary structure was determined through Robetta server. The quality of the 3D structure determined by Robetta server was estimated using ProSa-web and Procheck. Results from these tools showed the quality of the 3D structure showed in line with the available structures in PDB. Molecular docking of the proteins with natural ligands were performed to study the molecular interaction using igem dock.

REFERENCE

[1] Rosa Krajmalnik-Brown, PhD , Zehra-Esra Ilhan , Dae-Wook Kang, PhD , and John K DiBaise, MD (2012), Effects of Gut Microbes on Nutrient Absorption and Energy Regulation, Nutritional clinical practise; 27(2): 201-214.

[2] John A. Williams(2014), GLP-1 (Version 1.0), Pancreapedia: Exocrine Pancreas Knowledge Base.

[3] Fernando F. Anhê, Nicole G. Barra, and Jonathan D. Schertzer(2019), Glucose alters the symbiotic relationships between gut microbiota and host physiology, Endocrinology and Metabolism; 318: E111–E116.

[4] Inna Sekirov, Shannon L. Russell, L. Caetano M. Antunes, And B. Brett Finlay(2010), Gut Microbiota in Health and Disease, 90: 859–904

[5] Harry J. Flint, Karen p. Scott, Sylvia H. Duncan, petra Louis1 and evelyne Forano(2012), Microbial degradation of complex carbohydrates in the gut ; Gut Microbes, 3:4, 289-306.

[6] Prashant Nadkarni , Oleg G. Chepurny, George G. Holz, Regulation of Glucose Homeostasis by GLP-1, Progress in Molecular Biology and Translational Science; 121: 23-65.

[7] Jin He , Peiwen Zhang, Linyuan Shen , Lili Niu, Ya Tan , Lei Chen, Ye Zhao , Lin Bai, Xiaoxia Hao, Xuewei Li, Shunhua Zhang , and Li Zhu(2020), Short-Chain Fatty Acids and Their Association with Signalling Pathways in Inflammation, Glucose and Lipid Metabolism, International Journal of Molecular Science; 21:6356.

[8] Alyce M. Martin, Emily W. Sun, Geraint B. Rogers, and Damien J. Keating(2019), The Influence of the Gut Microbiome on Host Metabolism Through the Regulation of Gut Hormone Release, Frontiers in Physiology;10: 428**.**

[9] William W.L. Hsiao, PhDa, Christine Metz, PhDb, Davinder P. Singh, BAb, and Jesse Roth, MDb(2008), The Microbes of the Intestine: An Introduction to Their Metabolic and Signaling Capabilities, Endocrinology and Metabolism; 37(4): 857- 871.

[10] Altschul SF, Gish W, Miller W, Myers EW, Lipman DJ: Basic local alignment search tool. *Journal of molecular biology* 1990, 215(3):403-410.

[11] Larkin MA, Blackshields G, Brown NP, Chenna R, McGettigan PA, McWilliam H, Valentin F, Wallace IM, Wilm A, Lopez R *et al*: Clustal W and Clustal X version 2.0. *Bioinformatics* 2007, 23(21):2947-2948.

[12] Gasteiger E. HC, Gattiker A., Duvaud S., Wilkins M.R., Appel R.D., Bairoch A.;(In) John M. Walker (ed):: Protein Identification and Analysis Tools on the ExPASy Server;. *The Proteomics Protocols Handbook, Human Press* 2005:571-606.

[13] Wiederstein M, Sippl MJ: ProSA-web: interactive web service for the recognition of errors in three dimensional structures of proteins. *Nucleic acids research* 2007, 35(Web Server issue):W407-410.

[14] Morris AL, MacArthur MW, Hutchinson EG, Thornton JM: Stereochemical quality of protein structure coordinates. *Proteins* 1992, 12(4):345-364.

[15] Q Wu, Z Peng, Y Zhang, J Yang, *COACH-D: improved protein-ligand binding site prediction with refined ligand-binding poses through molecular docking*, **Nucleic Acids Research**, 46: W438–W442 (2018).

[16] Macindoe G, Mavridis L, Venkatraman V, Devignes MD, Ritchie DW: HexServer: an FFT-based protein docking server powered by graphics processors. *Nucleic acids research* 2010, 38(Web Server issue):W445-449.

[17] Jianyi Yang, Ivan Anishchenko, Hahnbeom Park, Zhenling Peng, Sergey Ovchinnikov, and David Baker. Improved protein structure prediction using predicted interresidue orientations. (2020) PNAS 117 (3) 1496-1503

Study on Causes of Cracks in Buildings and Its Preventive Measures

[1] N. Sarubala, [2] Dr. N. Nagarajan

[1] PG Scholar, Department of Civil Engineering, Annamalai University, Annamalai Nagar, Tamilnadu, India
[2] Associate Professor, Department of Civil Engineering, Annamalai University, Annamalai Nagar, Tamilnadu, India

Abstract:

Cracking in structures is a difficult puzzle for engineers and are often required to look into their causes and to carry out suitable repairs and remedial measures in effective manner. Proper understanding of various causes of cracking, its behavior, characteristics are very important and it will be helpful to notify whether cracks are structural or non-structural. Structural cracks are those which are due to incorrect design, faulty construction or overloading and these may endanger the safety of a building. Non-structural cracks which are due to moisture changes, thermal variations, elastic deformation, creep, chemical reaction, foundation movement and settlement of soil, vegetation, etc...Identification of such cracks in a correct time and adopting preventive measures are essential. Cracking may also leads to severe collapse of structure. Different repairing material and techniques are there for different forms of cracks. In this paper, we will study about the causes of cracks in buildings and to provide suitable repairing techniques and preventive measures.

Keywords:

Cracking, Preventive Measures, Repairing Techniques, Materials

1. INTRODUCTION

A building component develops cracks whenever stress in the component exceeds its strength. According to IS: 456-2000, the surface width of crack should not exceed 0.3mm in members where cracking is not harmful and does not have any serious adverse effects upon the preservation of reinforcing steel, nor upon the durability of the structures. In the members where cracking in tensile zone is harmful either because they are exposed to moisture or in contact of soil or ground water, an upper limit of 0.2mm is suggested for maximum width of crack. For particularly aggressive environment such as the severe category, the assessed surface width of crack should not in generally exceed 0.1mm. A commonly known classification of cracks, based on their width is (a) thin less than 1mm in width, (b) medium 1 to 2 mm in width and (c) wide more than 2mm in width. Cracks may be of uniform width throughout or may be narrow at one end, gradually widening at the other, cracks may be straight, toothed, stepped, map pattern or random and may be vertical, horizontal or diagonal. Occurrence of closely spaced fine cracks at surface of a material is sometimes called crazing. Internal stresses in building components could be compressive, tensile or shear. Most of the building materials that are subject to cracking namely masonry, concrete, mortar, etc., are weak in tension and shear in a number, are able to cause cracking. The aim of this project is to study the causes, preventions, repairs of cracks in the buildings. In this study an attempt is made to bring the collective information of various possible reasons for damages due to cracks and their prevention of the same using appropriate method.

2. CAUSE OF CRACKS

A. Permeability of concrete

Low permeability is a key factor to concrete durability. The permeability of cement paste is a function of water-cement ratio given good quality materials, satisfactory proportioning and good construction practice; the permeability of the concrete is a direct function of the porosity and interconnection of pores of the cement paste.

B. Thermal movement

Ambient temperature changes and loss of heat of hydration in portion of structure at different rate lead to temperature variations and subsequent thermal movement. The thermal movement in a component depends on a number of factors such as temperature variations, dimensions, coefficient of thermal expansion and some other physical properties of materials

C. Creep movement

Radial and slow time dependent deformation of concrete structure under sustained loads is known as creep. It may generate excessive stress and lead to the crack development. Creep increases with increase in water and cement content, water cement ratio and temperature.

D. Corrosion of reinforcement

Corrosion will produce iron oxide and hydroxide on steel bar surface, consequently its volume increases. This increase in volume causes high radial bursting stresses around reinforcing bars and result in local radial cracks. These splitting cracks results in the formation of longitudinal cracks parallel to the bar.

E. Moisture movement

Most of the building materials with pores in their structure in the form of inter-molecular space expand on absorbing moisture and shrink on drying.These movements are cyclic in nature and are caused by increase or decrease in inter pore pressure with moisture changes. Shrinkage can be of plastic or dry. Factors that cause cement or mortar to experience shrinkage include excessive water, and cement quantity; rich cement mixtures suffer greater shrinkage.

F. Improper structural design

Several problems can occur due to incorrect structural design, detailing, and specifications.Errors that may occur at this stage include inadequate thickness, insufficient reinforcement, incorrect geometry, improper utilization of materials, and incorrect detailing.

G. Movement due to chemical

The concrete may crack as a result of expansive reactions between aggregate, which contains active silica, and alkaline derived from cement hydration. The alkali silica reaction results in the formation of swelling gel. This tends to draw water from other portions of concrete. Consequently, local expansion occurs and results in cracks in the structure.

H. Foundation movement and settlement of soil

Shear cracks in buildings occurs when there is large differential settlement of foundation either due to unequal bearing pressure under different parts of the structure or due to bearing pressure on soil being in excess of safe bearing strength of the soil or due to low factor of safety in the design of foundation.

3. METHODS OF TESTING

A. Nondestructive testing system

To assess the quality of concrete in its damaged state without any disturbance of surrounding concrete

B. Partially destructive testing system

To assess the quality of concrete in its damaged state with partial disturbance surrounding concrete.

C. Destructive testing system

To assess the quality of concrete with complete disturbance of concrete (loaded up to failure)

4. METHODS OF CRACK REPAIR

A. Epoxy injection

It is one of the basic methods to repair the crack in which epoxy resins is used to inject the crack that are narrow as 0.05mm. This repair method may get damage due to leakages and silt contamination damage. To overcome this damage, Skillful execution and tactics is required to execute this method.

B. Routing and Sealing

It is a very simple method to repair remedial cracks but not the structural cracks. Joint sealant material is used to fill and seal the crack surface. While sealing the joint it is important to take care of the width to depth aspect ratio to give enough room left for the movement.

C. Stitching the Cracks

This is one of the long lasting methods in which entry and exit points are made across the cracked surface then U-shaped metallic staples are then passed through the holes and anchored with the help of grout or an epoxy based system.

D. Drilling and Plugging

It is one of the cost effective method to repair vertical cracks. Key is formed in the cracks by drilling it vertically and grout is passing down in it which will prevent leakages and the consequence loss of soil from the walls.

5. RESULT AND DISCUSSION

A. Beam (Reinforcement Corrosion)

Fig. 1 Cracks due to Corrosion of Reinforcement

Causes

Increase of moisture of air into the concrete cause's corrosion of reinforcement and results in volume expansion of steel bars, consequently causing cracks and spalling of concrete cover.

Remedy

Remove the concrete at the spalled areas to expose the corroded steel bars. Scrape and clean the steel bars using by air compressor to remove the rust. Apply two coat of anti-rust paint to the steel bars. Before patching the area, apply a bonding against the affected surface to ensure proper adhesion. Patch up the hacked area using polymer modified mortar.

B. Beam (Improper Structural Design)

Fig. 2 Cracks due to Improper Structural Design

Causes
Cracks in concrete beam due to corrosion or insufficient concrete cover
Remedy
The crack portion should be gently cleaned of all loose materials, fill the crack portion by pressure grouting. The material such grouting can be epoxy or cement with suitable admixture.

C. Staircase

Fig. 3 Cracks due to Improper Specification

Causes
Fine materials take surface area and required more water formix, the use of excessive fine material i.e. silt, clay, and dust in aggregate concrete
Remedy
Apply slight cut on the edges in straight line provide neat joint. Make the surface damp 24hours before application of new plaster, if the reinforcement is corroded, the polymer coat is apply on the corroded area then the surface area is plastered.

D. Roof

Fig. 4 Cracks due to Improper Structural Design

Causes
Cracks due to insufficient concrete cover.
Remedy
Remove the concrete at the spalled areas to expose the corroded steel bars. Scrape and clean the steel bars using by air compressor to remove the rust. Apply two coat of anti-rust paint to the steel bats. Before patching the area, apply a bonding against to the affected surface to ensure proper adhesion. Patch up the hacked area using polymer modified mortar.

E. Wall (shrinkage cracks)

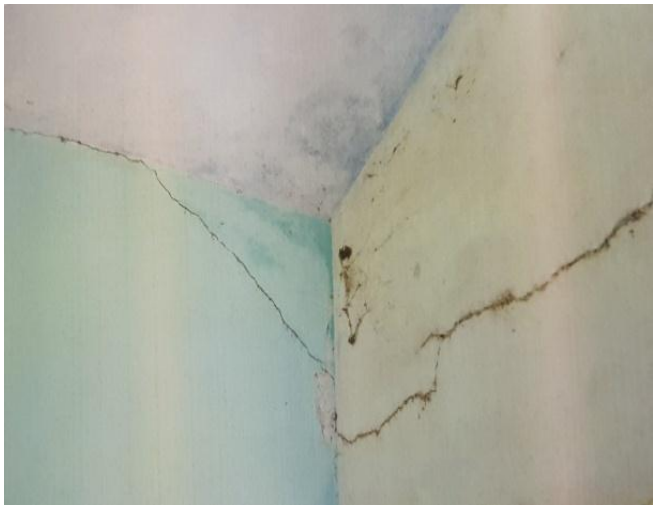

Fig. 5 Cracks due to Creep Movement

Causes
Shrinkage in concrete depends on number of factors such as cement and water ratio, excessive fine material, use of admixtures, compression of cement, temperature, humidity and curing, etc.
Remedy
The first and most important step of repair is to prepare the surface to be repaired by cleaning it from loose particles, laitance, dirt, grease, and paint which interfere with the

 ISBN: 978-93-90214-20-4

bonding. This can be done by wire brushing, grinding, sand blasting, water blasting, etc. The plastic shrinkage crack has hardened can be repaired by brushing cement grout into the crack. This should be done as soon as possible after the concrete has hardened. Injecting low viscosity polymers are preferable though not necessary.

F. Wall (seepage cracks)

Fig. 6. Cracks due to Moisture Movement

Causes

Building materials with pores in their structure in the form of intermolecular space expands on absorbing moisture and shrink on drying. These movements are cyclic nature and are caused due to temperature.

Remedy

Defective plaster should be removed and the edges should be slight cut in square or rectangle shape to provide a neat joint, clean the surface with wire brush and wash it. Wet the surface 24 hours before application of cement mortar, cracked portion should be filled with cement mortar, keep the surface wet at least for 3 days. When surface is dry, finish it according to adjoining area on the wall.

G. Parapet

Fig. 7 Crack due to Corrosion of Reinforcement

Causes

Cracks due to corrosion along the reinforcement

Remedy

The crack portion should be widen gently and be cleaned of all loose materials and vegetation. Fill the crack portion by pressure grouting. The material for such grouting can be epoxy or cement.

6. CONCLUSION

This field of study and the collection of data in the case studies have been assembled to help engineers and contractors build more safety.

It involves examination of their causes is the first step to prevention of failure and also shows failure in RCC building ranges from spalling to deterioration due to various factors like dampness, corrosion, cracks, salinity, water leakage etc. and these are studied and discussed the way of analyzing the failure with sources using visual observation followed by recommendation for it.

It should be carefully noted that the engineers bear a legal responsibility for any negligence or acts of commission that result either direct or indirect failure.

REFERENCE

[1] M.S. Shetty, "Concrete Technology- Theory and Practice", S. Chand and Company Ltd, New Delhi, 2005.

[2] B.L. Gupta and Amit Gupta, "Maintenance and Repair of Civil Structures", Standard Publishers & Distributors, Delhi.

[3] B. Vidivelli, "Rehabilitation of Concrete Structures", Standard Publishers & Distributors, Delhi.

[4] "Control of Cracking in Concrete Structures", Report of ACI Committee 224. ACI journal, 1972.

[5] "Cracking in Buildings", British Research Establishment Digest – 75.

[6] IS: 3414-1968 "Design and installation of joints in buildings", Indian Standard Institution.

[7] IS: 456-2000 "Code of Practice for plain and reinforced concrete (third revision)", Indian Standard Institution.

[8] IS: 383-1970 "Specification for coarse and fine aggregates from natural sources for concrete (second revision)", Indian Standard Institution.

[9] Jai Krishna & Jain (OP), "Plain and reinforced concrete", 1968, Vol. 11, Chand and Bros, Roorkee.

[10] M.L.Gambhir "Concrete Technology", 2005, 3rd Edition, the McGraw-Hill Companies, New Delhi.

Impact Assessment of Civilization on Pond System in and Around Chidambaram Town, Cuddalore District, Tamilnadu

[1] N. Sarubala, [2] Dr. S. Sivaprakasam

[1] PG Scholar, Department of Civil Engineering, Annamalai University, Annamalai Nagar, Tamilnadu, India
[2] Associate Professor, Department of Civil Engineering, Annamalai University, Annamalai Nagar, Tamilnadu, India

Abstract:

A lake or pond is the water body which holds certain volume of water generally in all seasons of the year. Urban town areas are confronting a water emergency because of loss of watershed, expanding contamination levels, disintegrating water balance, infringement, unlawful developments, and encroachments. Recovery and revival of water bodies in urban town communities is particularly significant from a general wellbeing viewpoint as they give different environment benefits that are needed to oversee microclimate, biodiversity and supplement cycling. Due to impact of civilization and anthropogenic activities, the pond system in the Chidambaram town area was shrunk more and some pond system get vanished. The aim of this study is to assess the shrunk and vanished water bodies and to suggest some measures for restoration of pond systems. The assessment is done with the help of Google Earth pro by comparing historical images of the pond system.

Keywords:

Water Bodies, Anthropogenic activities, Shrunk, Encroachment

1. INTRODUCTION

Water is the most prime factor for sustenance of life. It exists in different forms such as rainfall, river water, ground water, ponds and lakes etc. In urban areas water bodies play an important role as a source of drinking water, absorption of flood water and a conduit for ground water recharge. The increasing urban sprawl in proportion to population growth posed severe pressure on urban and rural lakes by asking them non potable, impairing their absorption capacity, deteriorating water quality, disturbing aquatic biodiversity and finally resulting in the water body vanishing. When a surface water bodies is formed, it develops a "Water Economy," a balance of some kind in its inflow/ out flow "budget". This involves several key factors first the inflow. Surface water bodies receive their water from precipitation, from ground flow (via run off, rivers and the lakes and from ground water seeping in), (Jeanne K Hanson, 2007). (Thulborn's study) improved the adjustment factor to predict the effect of urbanization on the flood frequency curve. (Miller) proved that the relative increase in peak flows and reduction in flood duration and response time of a catchment is greatest at low level of urbanization. In this study the assessment of shrinkage of water bodies is done by using Google Earth Pro and purpose of this is mainly because the water is one of the basic needs which is required by all living beings.

A. Objective

This study has attempted the following objectives to assess the current situation of water bodies in and around Chidambaram town due to civilization:

- To found out the shrunk and abandoned water bodies.
- To suggest the suitable measures for restoration and renovation of water bodies that are shrunk to a larger extent.

2. STUDY AREA

Chidambaram is a town and municipality in Cuddalore district in the Indian state of Tamilnadu. It is the headquarters of the Chidambaram taluk. It covers an area of 4.8 square kilometer. It is located at 11.30˚ N to 79.48˚ E. The topography is almost plain with forests around the town, with no major geological formation. There are no notable mineral resources available in and around the town. The soil types are alluvial and red that are conductive for crops like paddy, pulses, and chili peppers. Chidambaram receives and area of 10mm annually which is lesser than the state average of 1008mm. After 45 years, on December 4 Friday 2020, there was a downpour of 340mm in a day.

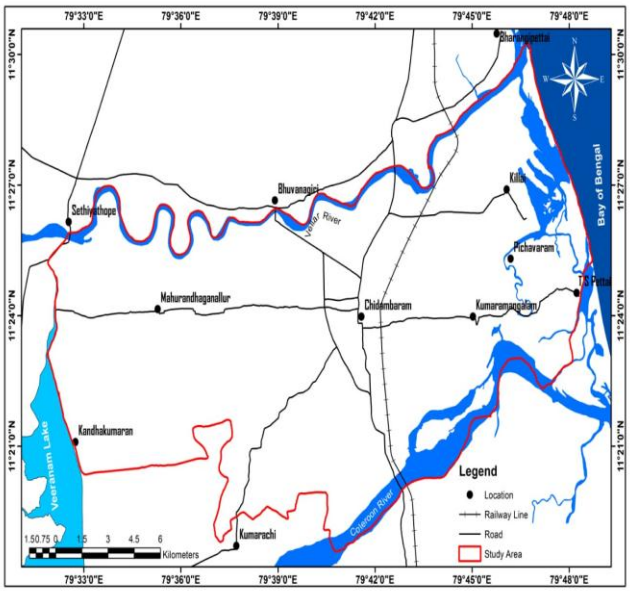

Fig. 1 Study area map

3. METHODOLOGY

The current status of pond photos and Historical images have been used for various years to denote the shrinkage of the pond system and also to delineating the current encroachment area Using Google Earth pro. Google earth pro also refers to geographic browser that accesses satellite and aerial imagery, topography, ocean bathymetry and other geographic data over the internet to represent the earth. GPS is used to reach the exact location of the ponds in easier manner. Also the field investigation was conducted in Chidambaram Municipality.

4. RESULTS AND DISCUSSION

The ancient town of Chidambaram is blessed with a large number of ponds and temple tanks and is around 100 acres with a rough storage capacity of 50 crore litres. All these tanks have traditionally been major sources of water with a rich history, carrying religious significance. However these ponds have been subjected to siltation, pollution and encroachment.

II- List of ponds located in the study area

S.No.	Name of Ponds	Latitude/Longitude
1	SippiKulam	11˚23'42"/ 79˚41'38"
2	KumaranKulam	11˚23'52"/ 79˚42'02"
3	ThatchanKulam	11˚23'34"/ 79˚41'20"
4	Palamankulam	11˚23'50"/ 79˚42'09"
5	Veeranarkulam	11˚24'12"/ 79˚42'02"
6	Periyannakulam	11˚24'24"/ 79˚41'30"
7	Koori kulam	11˚24'45"/ 79˚41'17"
8	Vannankulam	11˚24'31"/ 79˚41'03"
9	ElamaiKulam	11˚23'52"/ 79˚41'21"
10	AnnaimaduguKulam	11˚24'32"/ 79˚41'06"
11	EswaranKulam	11˚24'41"/ 79˚41'04"
12	AyeeKulam	11˚23'30"/ 79˚41'44"
13	SivapriyaiKulam	11˚24'22"/ 79˚41'37"
14	GnanapragasamKulam	11˚23'33"/ 79˚41'53"
15	NagacherryKulam	11˚24'01"/ 79˚40'54"
16	OmaKulam	11˚24'31"/ 79˚41'03"

A. Abandoned ponds

Field investigation was conducted in Chidambaram Municipality to assess the status of pond covering totally 16 No. of ponds in study area. In which three ponds namely SippiKulam, KumaranKulam, PalamanKulam were transformed to other forms of land use. It was considerably encroached by Houses, Small traders, Temple, Roads, and others. This is mainly because of urbanization and anthropogenic activities. The major reason behind this is high population density.

B. Shrunken ponds

VeeranarKulam, PeriyannaKulam, Koori Kulam, ThatchanKulam, VannanKulam totally five ponds were in degraded state. This is mainly because of improper maintenance, pollutions like dumping garbage's, flowing of sewage into pond instead of entering the STP for its treatment, edges of the pond were encroached by the disadvantaged group hutments and poor landless people have been using it for keeping their cattle, storing fodder, growing vegetables and making cow dung cakes.

C. Relatively good ponds

ElamaiKulam, AnnaimeduKulam, EswaranKulam, AyeeKulam were relatively good. During summer season there were not much water in the site. There were no signs of encroachment and dumping of garbage but So much of algae and weed growth were seen. One pond named ElamaiKulam border was broken due to heavy rainfall and the area were pond located is severely affected by flood. The above listed ponds don't have any proper footstair. Activities like bathing, washing, watering the animals were assessed in the site.

D. Good status ponds

SivapriyaiKulam, GnanapragasamKulam, NagacherryKulam, OmaKulam were in good condition. These ponds were cleaned, bunds were strengthened, desiltation also done and boundaries of ponds were fenced by district administration in August 2019. At present fences were damaged by animals, and people's ill activities. By comparing the other ponds, the pollution effect were less. Some of the ponds had been leased for fish culture purpose. Fish culture is an activity, involves regular stocking, fertilization, feeding, protection from predators and taking care of the environment.

Fig.1 Current status of Abandoned Ponds

II- Present status of ponds

No. of ponds	Present status of pond	Activities in Pond	Needs of Pond
3	Transformed	➢ Hutments for landless poor people ➢ Small traders ➢ Apartments ➢ Houses ➢ Open defecation	No Activities
5	Shrunken	➢ Garbage filling ➢ Sewage inflow ➢ Keeping their cattle ➢ Making cow dung ➢ Storing fodder ➢ Unwanted tress at the sides (P.juliflora)	➢ Fodder collection ➢ Grazing for cattle ➢ Fuel wood collection
4	Relatively Good	➢ Algae and weed growth ➢ Not much water during summer	➢ Human activities like bathing, washing, watering the animals, and so on...
4	Good	➢ No encroachment ➢ Lesser amount of pollution and weed growth	➢ Fish culture ➢ Irrigation purpose ➢ Reduce flooding during rainy days

E. Historical Images of ponds Using Google Earth Explorer:

Historical images is the collection of aerial images which were collected over multiple dates. The below images which shows the shrunk of pond area to a larger extent.

Fig. 2 Aerial Imagery of Abandoned Ponds

5. CONCLUSION

It has been clearly known that the pond system in the urban areas were affected more due to population growth, civilization, anthropogenic activities. From the study we come to knew that four ponds were abandoned and eight ponds were shrink to a larger extent. Pond system mainly affected by anthropogenic activities like dumping garbage, encroachment, sewage flow into water without treatment, open defecation. The past historical images of the pond and current status photograph of pond were clearly showed the impact of civilization over pond system. The selected study area is also a flood prone area. To overcome the above mentioned problems and to renovate the pond system following suggestions and precautions should be done.

- Install the STPs inside the city is one of the way to prevent the sewage flow into water bodies.

- Conducting various awareness drives like painting walls of keeping water bodies clean and to maintain properly.
- Each and every year desiltation process should be done before onset monsoon season. Deepening and maintaining the area extent of pond will capture the excess storage of water and percolate it underground.
- Proper law should be implemented for the removal of encroachments and to protect the catchment area.
- Constructing water harvesting structure within the water bodies.
- Plantation of saplings along the bund.
- Fencing the boundary of the pond properly.

REFERENCE

[1] DevanandaBeura 'Depletion of Water Bodies Due To Urbanization and Its Management', Volume 3 IERJ, E-ISSN No: 2454-9916, Issue: 6, June 2017

[2] Manoj.p. et al 'Rejuvenation of water bodies by adopting rainwater harvesting and groundwater recharging practices in catchment area', Sengupta, M. and Dalwani, R. (Editors). 2008, Proceedings of Taal2007: The 12World Lake Conference: 766-776

[3] Ningrui Du .J, HenkOttens and Richard Sliuzas (2008) - Spatial impact of urban expansion on surface water bodies- A case study of Wuhan, China, Journal of Landscape and Urban Planning 94 (2010) 175–185, Elsevier

[4] ParidhiRustogi et al 'Revival and Rejuvenation Strategy of Water Bodies in a Metropolitan City: A Case Study of Najafgarh Lake, Delhi, INDIA', ISSN: 2320-5407, Int. J. Adv. Res. 5(2), 189-195, January 2017

[5] Ramachandraiah .C and Sheela Prasad, Impact of Urban Growth on Water Bodies: The Case of Hyderabad, EABER PAPER NO. 6, (September 2004.)

Study on Properties of Fly Ash Metakaolin Geopolymer Concrete

[1] R. Sharath Kumar, [2] Dr. K. Karthikeyan

[1] PG Scholar, Department of Civil Engineering, Annamalai University, Annamalai Nagar, Tamilnadu, India
[2] Associate Professor, Department of Civil Engineering, Annamalai University, Annamalai Nagar, Tamilnadu, India

Abstract:

Fly ash and Metakaolin, as source material, to produce geopolymer under Steam curing at 60^0C for 24 hours. In geopolymer, Fly ash and metakaolin acted as binder and NaOH and $NaSiO_3$ were alkaline activators and Napthalene based Superplasticizer is used. The mix was designed for molarity of 8M, 10M, 12M and 14M at an alkaline ratio of 2.5. Five different mix compositions such as 100% Fly ash, 75% Fly ash with 25% Metakaolin, 50% Fly ash with 50% Metakaolin, 25% Fly ash with 75% Metakaolin and 100% Metakaolin. The compressive strength of the mixes was determined at 3, 7 and 28 days. The test results show that geopolymer mortar made with 75% Metakaolin and 25% Fly ash for 12M resulted higher compressive strength. Further, the geopolymer study was extended from mortar to concrete. From compressive strength of mortar, the mix composition of concrete is determined as 75% Metakaolin and 25% Fly ash. The properties such as Compressive strength, Tensile strength and modulus of elasticity were evaluated at the age of 7 days. The mix achieved good improvement in strength.

Keywords:

Geopolymer, Metakaolin, Fly ash

1. INTRODUCTION

Concrete is one of the most widely used construction material.It is usually associated with Portland cement as the main component for concrete. Utilization of concrete as a major construction material is a worldwide phenomenon and the concrete industry is the largest user of natural resources in the world. The demand for concrete as construction material is on increase. Massive use of concrete is driving the massive global production of cement, estimated as about 2.8 billion tons.

The climate change due to global warming is one of the greatest environmental issues has become a major concern. Global warming is caused by emission of greenhouse gases, such as CO_2 to the atmosphere by human activities. Among the greenhouse gases, CO_2 contributes 65% of the global warming. Associated with this is the inevitable carbon-di-oxide emission of about 7% of the total global production. The production of one ton of cement emits one ton of CO_2 into the atmosphere. Geo Polymer Concrete is one of the green alternatives of the Portland Cement Concrete. Geo Polymer synthesized from materials of geological origin or by-product materials such as fly ash that are rich in silicon and aluminium.

Geo Polymers are a relatively new group of materials which were developed by Joseph Davidovits in 1970's become the better alternative binder. The Geo Polymer also reduces the CO_2 emission to the atmosphere caused by cement industries about 80%.

A. Geopolymer

The geopolymer technology was first introduced by Davidovits in 1978. His work considerably shows that the adoption of the geopolymer technology could reduce the CO_2 emission caused due to cement industries. Geopolymer are members of the family of inorganic polymers. The chemical composition of the geopolymermaterial is similar to natural zeolitic materials, but the microstructure is amorphous. Any material that contains mostly Silicon(Si) and Aluminium(Al) in amorphous form is a possible source material for the manufacture of geopolymer. Metakaolin or calcined Kaolin, low calcium ASTM class F Fly Ash, natural Al-Si minerals, combination of calcined minerals and non-calcined minerals, combination of fly ash and metakaolin, combination of granulated blast furnace slag and metakaolin have been studied as source materials.

B. Geopolymerisation Process

The source material silicon and aluminium to react with oxygen is termed as polymerization.

Three types of polymer network:

- Poly sialate (-Si-O-Al-O-)
- Poly sialate-siloxo(-Si-O-Al-O-Si-O-)
- Poly sialatedisoloxo(-Si-O-Al-O-Si-O-Si-O)

C. OBJECTIVES OF THE STUDY

- To evaluate the Strength Properties of High Calcium Fly ash Geopolymer mortar which is extended to Concrete with partial replacement of Metakaolin Blend under Steam Curing.

2. MATERIALS AND METHODS

A. Materials

The materials used for making blended material based Geopolymer concrete specimens are Fly ash, Metakaolin,

Coarse aggregates, Fine aggregates, alkaline liquids and Water.

B. Fly ash

Fly ash is a fine powder which is a byproduct from burning pulverized coal in electric generation power plants. Fly ash is a pozzolan, a substance containing aluminous and siliceous material that forms cement in the presence of water. When mixed with lime and water it forms a compound similar to Portland cement. Class C Fly ash can be a cost-effective substitute for Portland cement in some markets.Fly ash is also known as "Pulverised fuel ash" in the United Kingdom. It is one of the coal combustion products, composed of the fine particles that are driven out of the boiler with flue gases.

In modern coal-fired power plants, Fly ash is generally captured by electrostatic precipitators or other particle filtration equipment before the flue gases reach the chimneys. Depending upon the source and makeup of the coal being burned, the component of Fly ash vary considerably. Fly ash generally includes substantial amounts of Silicon dioxide(SiO_2), Aluminium Oxide(Al_2O_3) and Calcium Oxide(CaO). Two classes of fly ash are defined, they are Class C fly ash and Class F fly ash. The Chief difference between these classes is the amount of calcium, silica, alumina, and iron content in the ash. The chemical properties of the Fly ash are largely influenced by the chemical content of the coal burned. Class C Fly ash is used in this work and it is obtained from Neyveli Thermal Power Plant. Class C Fly ash having pozzolonic properties, also has some self-cementing properties.

In the presence of water, Class C Fly ash hardens and gets stronger over time. It generally contains more than 20% lime (CaO). Unlike Class F, Self-cementing Class C fly ash does not require an activator. Alkali and sulphate contents are generally higher in Class C fly ashes.

Fig. 1 Fly ash

C. Metakaolin

Metakaolinis adehydroxylatedform of the clay mineral kaolinite. Stone that are rich in kaolinite are known as china clay or kaolin, traditionally used in the manufacture ofporcelain. The particle size of metakaolin is smaller thancementparticles, but not as fine assilica fume.

Kaolin is mined and crushed, it is separated from sand, refined to remove impurities and stored in store. kaolin is fed into rotary kiln to produce metakaolin is obtained from the calcinations of kaolinite clays at temperatures in the range of 650^0C - 800^0C,high enough to allow for loss of hydroxyls but below temperatures that cause the formation of a vitreous phase and crystallization of other phases such as mullite.

Metakaolin is very fine and highly reactive, gives fresh concrete a creamy, non-sticky texture that makes finishing easier. Metakaoline appears as a whitish haze on concrete, is caused when calcium hydroxide reacts with carbon dioxide in the atmosphere.The quality and reactivity of metakaolin is strongly dependent of the characteristics of the raw material used.

Metakaolin can be produced from a variety of primary and secondary sources containing kaolinite:

- High purity kaolin deposits
- Kaolinite deposits or tropical soils of lower purity
- Paper sludge waste (if containing kaolinite)
- Oil sand tailings (if containing kaolinite)

Fig.2 Metakaolin

D. Sodium Hydroxide:

A combination of Sodium silicate and Sodium Hydroxide solution are chosen as an alkaline liquid. The sodium Hydroxide (NaOH) in flakes or pellet from with 97% to 98% purity was also purchased from a local supplier in bulk. The NaOH solids were dissolved in water to make the solution. The mass of NaOH solids in a solution varied depending on the concentration of the solution expressed in terms of Molarity (M).

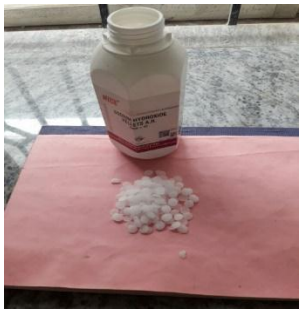

FIG. 3 Sodium Hydroxide

E. Sodium Silicate:

The Sodium Silicate Solution (Na_2O = 13.7%, SiO_2 = 29.4%, and Water = 55.9% by mass) was purchased from a local Supplier in bulk. These are available in aqueous

solution and in solid form.The pure compositions are colorless or white. The commercial samples are often greenish or blue as shown in Fig 4.

Fig. 4 Sodium Silicate solution

F. Fine Aggregate:

River sand, (Grading Zone-II conforming to IS: 383-1987) was used as fine aggregates in the experimental investigation. In the present work locally available sand was collected. The properties of the sand were studied in accordance with IS: 383 and the results are given in Table 1. The Specific gravity of sand was found in the laboratory by using Pycnometer and the other accessories the test was done on the sample thrice the average of which reported the result as 2.55 Kg/m^3. The Fineness modulus was determined in the laboratory by Sieve analysis method. Hence the Fineness modulus of this locally available Sand is 2.6.

G. Coarse Aggregates:

Two sizes of Coarse aggregates were used in this project i.e. 12 mm graded aggregate as per IS: 383, and 6mm graded aggregate as per IS: 383 was used.The Specific gravity (G) of coarse aggregate usually called coarse aggregate is the ratio of the weight in air of the given volume of dry coarse aggregate at a stated temperature to the weight in air of an equal volume of distilled water at a stated temperature.

Local aggregates, comprising 12mm and 6mm coarse aggregates in saturated surface dry condition, were used. The coarse aggregates were crushed granite type of aggregates. The Specific gravity of Coarse aggregate was found in laboratory by Pycnometer and other accessories the test was done on the sample thrice the average of which reported the result as 2.6 Kg/m^3.

H. Superplasticizer:

It is known as high range water reducers.These are chemical admixtures used where well-dispersed particle suspension is required.The plasticizer used are Naphthalene based super plasticizer. Their addition to concrete or mortar allows the reduction of the water, not affecting the Workability of the Concrete.

Fig. 5Superplasticizer

I. Physical and Chemical properties of materials:

Table I Physical properties of materials

Materials/ Properties	Appearance	Specific Gravity Kg/m^3	Bulk Density Kg/m^3	Particle Size	Fineness Modulus
Fly ash	Dark Grey	2.15	-	-	-
Metakaolin	Creamish ivory powder	2.56	-	2-3 micron	-
Fine Aggregate (Zone II)	-	2.55	1791.1	-	2.6

Table II Chemical composition of Fly ash, Metakaolin

Chemical Compositions	**Fly ash**	**Metakaolin**
SiO_2	63.11%	52.22%
Al_2O_3	19.58%	40.35%
Fe_2O_3	5.03%	2.13%
MgO	0.24%	0.79%
CaO	17.13%	0.21%
Na_2O	0.29%	0.59%
K_2O	0.84%	0.61%
LOI	1.55%	1.8%
TiO_2	-	1.0%

3. MIX PROPORTION

A. Mix proportion of Mortar cube:

Based on the limited part research on geopolymer pastes available as the true and the experience grained during the preliminary experimental work the following mix combinations were considered for Fly ash – Metakaolin based Geopolymer Mortar. Various Source materials mixes selected for Mortar cubes are Fly ash 100%, 75% Fly ash with 25% Metakaolin, 50% Fly ash with 50% Metakaolin, 25% Fly ash with 75% Metakaolin, 100% Metakaolin. Ratio of Sodium Silicate Solution to Sodium Hydroxide Solution by mass was 2.5.

Molarity of Sodium Hydroxide (NaOH) solution is chosen as 8M, 10M, 12M, and 14M throughout the experimental study. Ratio of activator solution to binder, by mass is in the range of 0.5 for all types of Mix ratios. Based on these above ratios, the mix proportions in Table 3 were tabulated.

Table III Mix proportion of Fly ash- MetakaolinGeopolymer Mortar

S.No	Materials	Mass(Kg/m^3)				
		FA	$F_{75}M_{25}$	$F_{50}M_{50}$	$F_{25}M_{75}$	M
1	Fly ash	568.35	426.26	284.17	142.08	-
	Metakaolin	-	142.08	284.17	426.26	568.35
2	Sodium Silicate Solution	202.95	202.95	202.95	202.95	202.95
3	Sodium Hydroxide Solution	81.18	81.18	81.18	81.18	81.18
4	Fine Aggregate	1705.05	1705.05	1705.05	1705.05	1705.05

A. Mix Proportions of GPC

Source material mixes selected are 25% Fly ash with 75% Metakaolin. Ratio of Sodium Silicate to Sodium Hydroxide solution by mass was 2.5. Molarity of Sodium Hydroxide (NaOH) solution is chosen as 8M, 10M, 12Mand 14M throughout the experimental study. Ratio of Activator solution to binder by mass is in the range of 0.5.The density of Geopolymer concrete is 2400 Kg/m^3. The total aggregate content was taken as 75% in the mix. In which, 70% coarse aggregate and 30% fine aggregate were used. In case of coarse aggregate, 6mm and 12mm aggregate were used. Extra water is provided as the calculations based on liquid binder ratio. The mix proportion values tabulated on the Table IVS were based on these ratios.

Table IV Mix proportion of Fly ash-MetakaolinGeopolymer Concrete

S.No	Materials	Mass(Kg/m^3)
		$F_{25}M_{75}$
1	Fly ash	100
	Metakaolin	300
2	Sodium Silicate Solution	142.85
3	Sodium Hydroxide Solution	57.14
4	Fine Aggregate	540
5	Coarse Aggregate	1260

4. RESULTS AND DISCUSSIONS

A. General

This chapter presents the results of mechanical properties of bi-blended material based geopolymer mortar, at curing mode of steam temperature. Also presents the results of bi-blended geopolymer concrete.

B. Compressive Strength of Mortar Cube

The Mortar Cube of Size 70.6 x 70.6 x 70.6mm was casted with alkaline ratio of 2.5. The casted cube was kept under Steam Curing for 24 hours at 60^o C. Then the casted cubes were kept under room temperature up to the date of testing. Then it is tested in Compression testing Machine. The Compressive Strength of 3, 7 and 28 days were mentioned in tables below for all Molarities.

Table V Compressive Strength of Geo polymer mortar for 8M

Molarity	Metakaolin Replacement (%)	Compressive Strength (N/mm^2)		
		3 Days	7 Days	28 Days
8 M	0	0.8	3.01	3.64
	25	4.9	5.09	6.2
	50	5.7	8.88	10.92
	75	14.0	14.9	18.62
	100	6.2	7.6	9.42

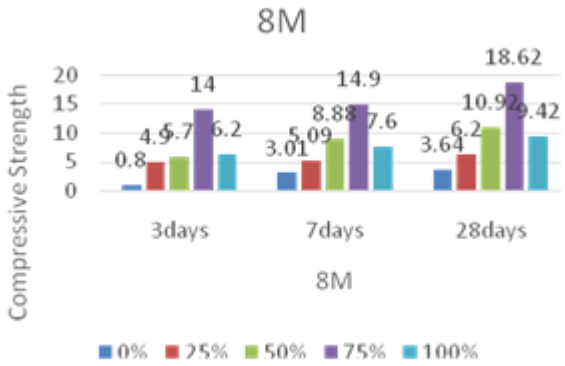

Fig. 6 Compressive Strength of Geo polymer mortar for 8M

Table VI Compressive Strength of Geopolymer Mortar for 10M

Molarity	Metakaolin Replacement (%)	Compressive Strength (N/mm^2)		
		3 Days	7 Days	28 Days
10 M	0	1.4	3.0	3.81
	25	3.67	4.26	5.36
	50	4.39	5.79	7.17
	75	14.2	14.73	18.41
	100	10.2	11.5	14.72

 ISBN: 978-93-90214-20-4

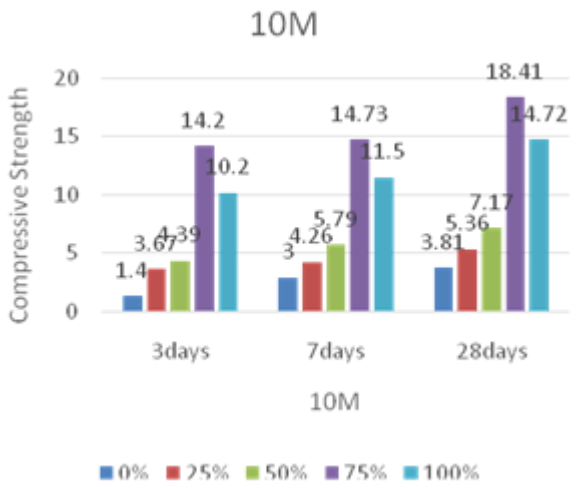

Fig. 7 Compressive Strength of Geo polymer mortar for 10M

Table VII Compressive Strength of Geopolymer mortar for 12M

Molarity	Metakaolin Replacement (%)	Compressive Strength (N/mm^2)		
		3 Days	7 Days	28 Days
12 M	0	2.61	3.28	4.0
	25	2.53	5.64	7.05
	50	3.17	4.64	5.75
	75	15.64	18.6	23.25
	100	10.3	14.01	17.51

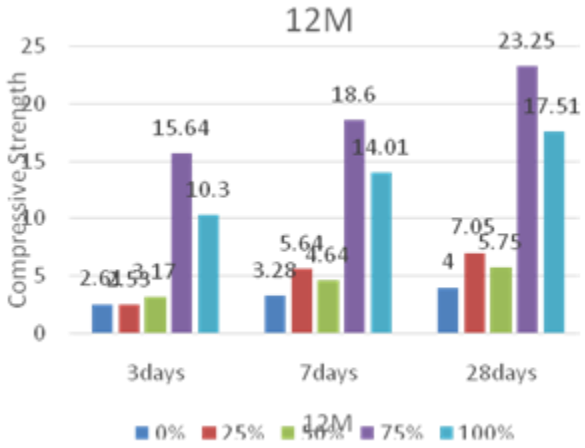

Fig. 8 Compressive Strength of Geo polymer mortar for 12M

Table VIII Compressive Strength of Geopolymer mortar for 14M

Molarity	Metakaolin Replacement (%)	Compressive Strength (N/mm^2)		
		3 Days	7 Days	28 Days
	0	2.23	2.81	3.51
14 M	25	3.08	3.73	4.7
	50	8.28	11.74	14.08
	75	15.56	16.74	21.09
	100	13.8	15.23	18.27

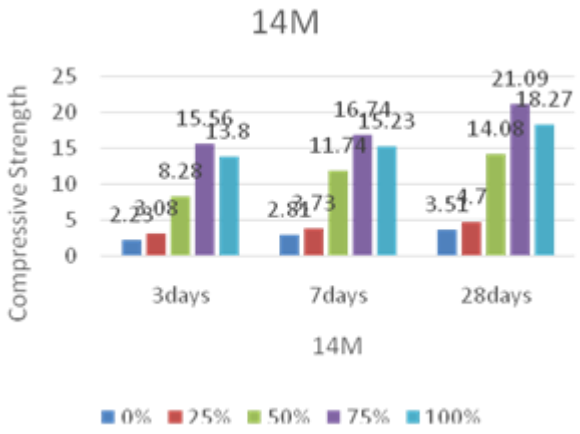

Fig. 9 Compressive Strength of Geo polymer mortar for 14M

C. Compressive Strength of concrete cube

Table IX Compressive strength of Fly ash – Metakaolin GPC

S.No	Molarities	Mixing Combination	Size of Cube	Load at Failure(KN)	Compressive Strength (N/mm^2)
					7 days
1	8M	Fly Ash-25% Metakaolin-75%	150 x 150 x 150mm	330.5	14.69
2	10M			374.6	16.65
3	12M			429.7	19.10
4	14M			613.4	27.26

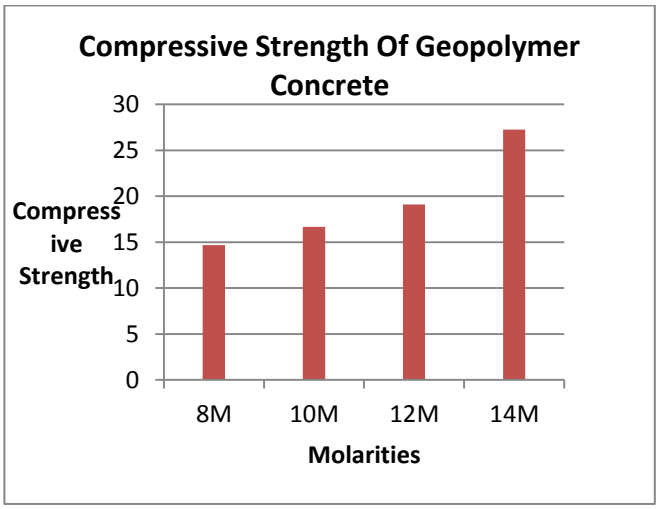

Fig. 10 Compressive Strength of Geo polymer Concrete

 ISBN: 978-93-90214-20-4

The Compressive Strength of Fly ash- Metakaolin based geopolymer concrete is shown in Table 9.25% of Flyash and 75% of metakaolin are used as a binder material.

D. Split Tensile Strength test

Table X Split tensile strength of Fly ash – Metakaolin GPC

S.No	Molarities	Mixing Combination	Size of Cylinder	Load at Failure (KN)	Split Tensile Strength (N/mm^2)
					7 days
1	8M	Fly Ash-25% Metakaolin -75%	L = 300mm D = 150mm	76.0	1.075
2	10M			96.0	1.358
3	12M			110.5	1.563
4	14M			111.0	1.570

The split tensile strength of Fly ash- Metakaolin based geopolymer concrete was determined by using 150mm diameter and 300mm height cylinders. The test results of7dayssplit tensile strength of geopolymer concrete are shown in TableX.

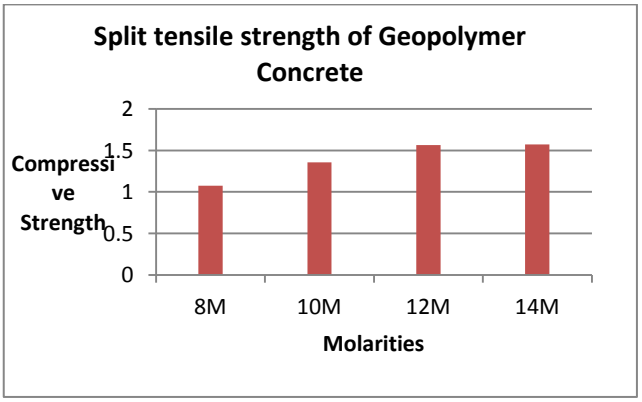

Fig. 11 Split tensile Strength of Geo polymer Concrete

E. Flexural Strength Test

Table XI Flexural strength of Fly ash – Metakaolin GPC

S.No	Molarities	Mixing Combination	Size of beam	Breaking Load (KN)	Breaking Value 'a' In mm	Modulus of Rupture (N/mm^2)
						7 days
1	8M	Fly Ash-25% Metakaolin-75%	500 x 100 x 100 mm	8.23	125	3.08
2	10M			7.90	150	3.16
3	12M			8.58	141	3.43
4	14M			8.62	178	3.44

The flexural strength of ambient and steam cured geopolymer concrete was determined by using 500x100x100mm beams. The test results of flexural strength of Fly ash- Metakaolingeopolymer concrete is shown in the Table XI.

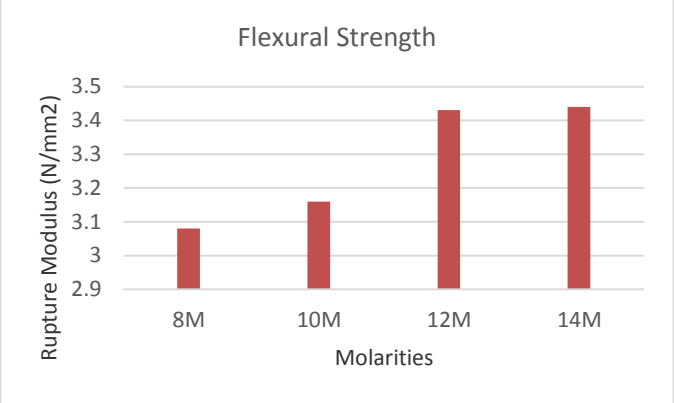

Fig. 12 Flexural Strength of Geo polymer Concrete

5. CONCLUSION

The Experimental study on Mechanical properties of Steam cured High calcium Fly ash with Metakaolin Blend has the following Conclusions:

1. Geopolymer Mortar made with 25% of Fly ash and 75% of Metakaolin gives higher Compressive strength than other mix Combinations at the age of 3,7 and 28 days.
2. GeopolymerMortar made with 25% of Fly ash and 75 % of Metakaolin gives higher compressive strength for Sodium Hydroxide Concentration of 8M, 10M, 12M and 14M with an alkaline ratio of 2.5.
3. Then, the extended work ofHigh calcium Fly ash and metakaolin based geopolymer concrete also shows a promising result in Compression, tension, Flexural and for the same proportion such as 25 % of Fly ash and 75 % of Metakaolin at an early age under Steam Curing.
4. The above promising strength results states that the Fly ash with a Metakaolin Blend could be used a source material for the Geopolymer.

REFERENCE

[1] Arioz.O., Tuncan.M.,Arioz.E., Kilinc.K.,"Geopolymer a new generation Construction Material"

[2] Bhosale.M.A., Shinden.N. (2012) " Geopolymer Concrete by Using Fly Ash in Construction" Vol 1, Issue – 3, pp no: 25-30

[3] ChunchuBala Rama Krishna, Rama Krishna.M (2015) "An Experimental Study on Geo-Polymer Concrete with Fly Ash and Metakaolin as Source Materials" Vol 2, Issue no – 12, pp.no: 1110-1117.

[4] Daniel L.Y. Kong a, Jay G. Sanjayan A, and KwesiSagoe-Crentsil (2007) "Comparative performance of geopolymers made with metakaolin

and fly ash after exposure to elevated temperatures" Vol 37, pp no: 1583-1589.

[5] GokhanGorhan, RidvanAslaner, and Osman Sinik (2016) " The effect of curing on the properties of Metakaolin and Fly ash based Geopolymer paste" Vol 97 pp no : 329 - 335

[6] Haiyan Zhang, VenkateshKodur, Shu Liang Qi, Liang Cao, Bo wu (2014) " Development of Metakaolin – Fly ash based geopolymer for fire resistance applications" Vol 55, pp no : 38 - 45

[7] Kamarudin.H., Mustafa Al Bakri.A.M., Binhussain.M., Ruzaidi.C.M.,Luqman.M., Heah.C.Y., Liew.Y.M. (2011) "Preliminary Study on Effect of NaOH Concentration on Early AgeCompressive Strength of Kaolin-Based Green Cement" Vol 10, pp no: 18-24.

[8] Muthuanand.M.,Dhanalakshmi.G., "Metakaolin based Geopolymer Concrete" pp no: 9-12.

[9] Ping Duan,Chunjie Yan, and Wei Zhou (2015) "Influence of partial replacement of fly ash by metakaolin on mechanical properties and microstructure of fly ash geopolymer paste exposed to sulfate attack"pp no: 1-44.

[10] RohitZende., Mamatha., A "Study on Fly ash and GGBS Based Geopolymer concrete under Ambient Curing" Vol 2, Issue-7, pp no: 3082-3087.

Design of a New Solar Rooftop System with Different PV Module Sizes

[1] Y.B.T.Sundari, [2] Y.David Solomon Raju, [3] Ch.Sumalatha

[1] Assistant Professor, ECE Department, Holy Mary Institute of Technology and Science, Hyderabad, India
[2] Associate Professor, ECE Department, Holy Mary Institute of Technology and Science, Engineering and Technology, Hyderabad, India
[3] Assistant Professor, ECE Department, Shadan Women's College of Engineering and Technology, Hyderabad, India

Abstract:

Day by day, solar energy conversion technologies are increasing everywhere. Installation and commissioning of the Solar PV systems are generally expensive. It is challenging to increase load capacity immediately. The load can increase by adding the PV modules and with sufficient inverter capacity. In solar rooftop systems for domestic appliances, 250Wp (60 cells) size modules and 315Wp (72 cells) modules are used. Nevertheless, sometimes people will need minor load extension. With the same size of the module, the installation cost will be increased, and space for installation will also increase. Simultaneously, with the high rating modules, there will be a chance of wastage of power due to fewer loads necessary. A new solar rooftop system is developed in this work, containing solar PV modules of different sizes, which converts solar energy into electricity. The proposed system will support less load requirement with low cost and less space for installation. For long-life operation with high performance, this new model system depends upon proper maintenance. For this, 1.2Kw load with four of 315Wp modules are connected to the 300watts load with two of 150Wp modules, resulting in better performance. This real-time application of the new model design can reduce the cost, and it can be fitted on the same structure used for the 300Wp modules. So it can be used when in need of increasing the load at low cost and quickly.

Keywords:

PV system; Sizes of modules; Wp; loads

1. INTRODUCTION

Energy development is the field of activities focused on obtaining sources of energy from natural resources. These activities include the production of conventional, alternative and renewable sources of energy. Non-renewable resources are significantly depleted by human use, whereas renewable resources are produced by ongoing processes that can sustain indefinite human exploitation.[1].

Solar energy is radiant light and heat from the Sun that is harnessed using a range of ever-evolving technologies such as solar heating, photovoltaic's, solar thermal energy, solar architecture, molten salt power plants and artificial photosynthesis. It is an essential source of renewable energy. Its technologies are broadly characterized as passive solar and active solar depending on how they capture and distribute solar energy or convert it into solar power. Active solar techniques include photovoltaic systems, concentrated solar power and solar water heating to harness the energy.

Passive solar techniques include orienting a building to the Sun, selecting materials with favourable thermal mass or light-dispersing properties, and designing spaces that naturally circulate air.

Solar power systems in India is a fast developing industry. The country's solar installed capacity reached 25.21 GW as of 31 December 2018. The Indian government had an initial target of20 GW capacity for 2022, which was achieved four years ahead of schedule. At the end of 2018, worldwide solar PV power is expected to exceed 500 GW, capable of producing roughly 2.8 % of the worldwide electricity demand. The EU's share in 2017 is about 26% of the worldwide installed capacity and can provide about 4.5 % of its electricity demand.[5]. So this system is mainly focused on reducing the cost and to increase the load of the roof top solar PV system in emergency load requirement conditions and also observed that two different types of rating (sizes) of solar PV modules can be used in Solar PV installation. .For this 1.2Kw load with four of 315Wp modules are connected to the 300watts load with two of 150Wp modules and the results are shown the better performance. This real time application of new model design can reduce the cost and it can be fitted on the same structure that used for the 300Wp modules. So it can be used when in need of increasing the load at low cost and quickly.

2. LITERATURE REVIEW

The site survey, rooftop and modules:

Site Survey: Shading on solar thermal collectors reduces performance by an amount proportional to shading level. However, PV arrays are much more sensitive to shading.[1][2].

Depending on the shading magnitude and location, the reduction in output can be disproportionately higher than the percentage of array area shaded. Even a 10% shading can cause the loss of most of the output in the worst cases.

For this reason, installers must carefully assess the shading potential at an installation site and be prepared to adjust the array position and orientation to minimize shading. Preferably, arrays should be installed in a location with no shading at any time. However, site constraints may make this difficult to achieve, especially during winter, early morning, and late afternoon, when the low Sun casts long shadows from far away objects. At a minimum, arrays should have an unobstructed solar window from 9 AM to 3 PM (solar time), as shown in Fig. 1. throughout the summer, when the Sun is highest in the sky and the majority of solar radiation is available. Also the array circuit design and module choice (for cell circuit configuration) can minimize the effect of unavoidable shading.

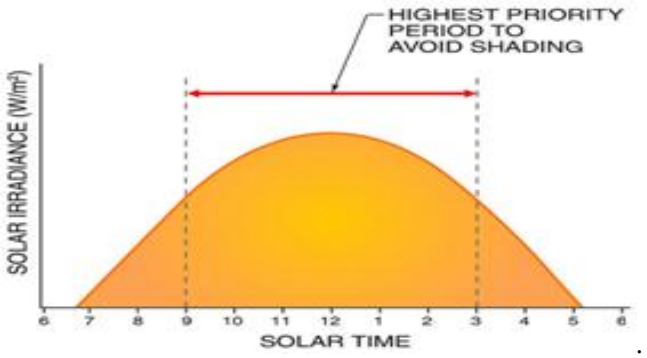

Fig.1: Shading priority.

The Solar Pathfinder consists of a latitude-specific sun path diagram covered by a transparent dome. The dome reflects the entire sky and horizon on its surface, indicating the position and extent of shading obstructions. The sun path diagram can be seen through the dome, illustrating the solar window. The Solar Pathfinder is placed at a proposed array location and elevation. It is levelled and oriented to the true south with the built-in compass and bubble level. (The compass reading may require adjustment for magnetic declination.) Looking straight down from above, the user observes reflections from the sky and surroundings superimposed on the sun path diagram, which indicates shading obstructions.

AC Load	Quantity		Power Rating (W)		Average Daily Use (hrs/day)		Average Daily Energy Use (Wh/day)
Incandescent Lighting	6	x	60	x	6	=	2160
Refrigerator	1	x	475	x	12	=	5700
Microwave	1	x	1200	x	0.5	=	600
Toaster	1	x	1200	x	0.15	=	180
Dishwasher	1	x	1500	x	0.5	=	750
Furnace Fan	1	x	500	x	2	=	1000
TV	1	x	130	x	3.5	=	455
VCR	1	x	40	x	0.75	=	30
Ceiling Fans	3	x	50		6		900

Fig. 2: Example of load analysis

The installer may need to conduct a detailed electrical load analysis, as shown in Fig. 2 example, especially for systems that will include batteries. The analysis should include a list of each load and its estimated or measured peak power demand, average daily time of use, and total energy consumed. Sometimes reasonable estimates of power consumption can be determined from equipment nameplate ratings, but measurements give the most accurate information. Special measurements may be required, such as in-rush current draw or power quality factors.[3][5].

Rooftop: Signs of deterioration differ for various types of roofing. For conventional asphalt shingles, deterioration includes brittleness, cracking, loss of granular coating, warping, or curling up from the shingle edges. Asphalt shingles generally are the least expensive but have the shortest life of all roof coverings, particularly in hot climates. The thickness of the roof decking and covering dictates the appropriate length of fasteners needed to install the array. The thickness can usually be determined by looking under the eave drip edge or flashing along an edge of the roof.[4],[7].

Modules and wattage: Mono-crystalline, Poly-crystalline, String ribbon solar cells, thin-film solar panels, Building-integrated photovoltaic modules [12]. The 36 cells modules are also called the 12volts module system. Its Wattage is 150wp. The 60 cells modules are also called a 20volts module system. Its Wattage is 250wp. The 72 cells modules are also called the 24volts module system. Its Wattage is 315wp.

3. CASE STUDY

There are many problems in Solar PV Installation like site survey, due to shading effect, due to soil, selection of the solar panels, maintenance, cost and civil foundation.

(i) **Problems in sites:**

- Photovoltaic (PV) modules are being increasingly used in large as well as small scale installation. The PV panels' performance is affected by the shading effect due to trees, passing clouds, neighbouring buildings and any other.
- The land is vital in any typical solar installation. The general rule of thumb is that for every 1KW of solar panels needed, the area required is approximately 100 square feet. This means that for a 1MW solar PV power plant, the area required is about 2.5 acres or 100,000 square feet.
- The civil foundation for solar PV system plants' structure will be primarily based on solar conditions at the site and the soil. When the soil does not support the solar PV installer based on the soil conditions, the following foundations are used for the solar PV system installation.
  1. Ramming foundation
  2. Pile foundation
  3. Regular civil foundation

(ii) Climate problems with solar panels: Solar panel converts sunshine into power. So if the panels are covered with snow, they cannot produce electricity. Snow generally is not heavy enough to cause structural issues with your

panels, and since most panels are tilted at an angle, the snow will slide off.

Solar panels generally required very little maintenance since there are no moving parts. A few times a year, the panel should be inspected for any dirt or debris that may collect on them.

(ii) Problems in Sizes of PV modules: Along with all the above problems, the following problems are also will be considered

The most typical modules used for residential installations module are 65 inches by 39 inches, while the common size for commercial applications is 77 inches by 39 inches. But the problems are

- If less Load requirement is there in a residential or commercial application. People should add the same size of the panel or module, but there was a chance of the wasting of power due to the large size of the panel or module usage, and also it will occupy more place
- The large size module cost will increase with the rating of power in watts.

To overcome all the above problems with better maintenance, this present new model proposed Solar Rooftop system will support emergency load requirement conditions compared with the previous Solar Rooftop system. So this new model solar PV system is installed with different modules, 72 cells (315wp), and 36 cells with 36 cells (150wp) and the load analysis shown better performance.

PROPOSED SOLUTION: SCENARIOS AND ASSUMPTIONS

PROPOSED SOLUTION: SCENARIOS AND ASSUMPTIONS
PROPOSED SOLUTION: SCENARIOS AND ASSUMPTIONS
PROPOSED SOLUTION: SCENARIOS AND ASSUMPTIONS

4. PROPOSED SYSTEM

This system is mainly focused on reducing the cost and to increase the load of the roof top solar PV system in emergency load requirement conditions and also observed that two different types of rating (sizes) of solar PV modules can be used in Solar PV installation. .For this 1.2Kw load with four of 315Wp modules are connected to the 300watts load with two of 150Wp modules and the results are shown the better performance. This real time application of new model design can reduce the cost and it can be fitted on the same structure that used for the 300Wp modules. So it can be used when in need of increasing the load at low cost and quickly.

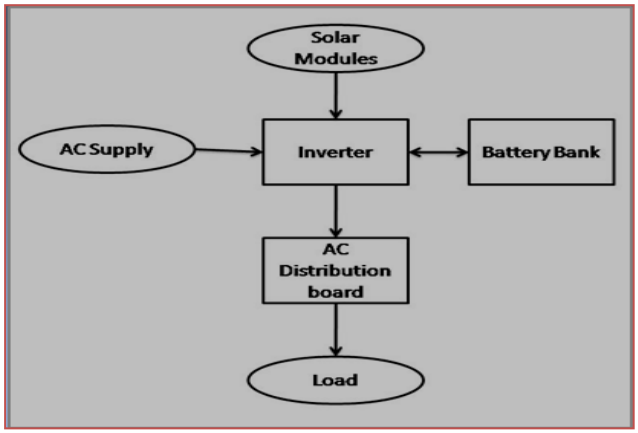

Fig. 3: Block diagram of proposed system

Sizing of the system: The following Fig. 4 describes the connection of New model Solar System with different sizes of 72 cells(315 wp) of four PV modules connected with 36 cells(150wp) of two PV Modules on the Flat Rooftop**.**

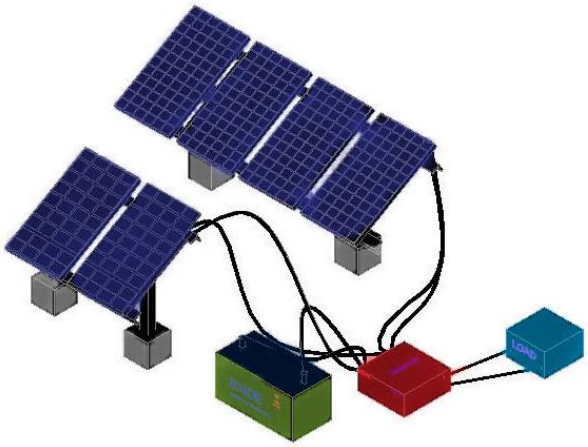

Fig. 4: New model Solar PV System with different sizes of PV modules

Table 1: Requirement of Load

Appliance	Number	Wattage	Working Hours	Energy (kWh/day)
Lights	1	60	6	0.36
Fans	4	80	6	1.92
Computer	1	200	4	0.8
Printer	1	220	2	0.44
Other load	1	276	5	1.38
Total		1050		4.8

Evaluating Proposed Solution: The following are the steps to required to calculate the sizing of the flat roof top PV system

a) Surveying the site

b) Calculating the amount of energy needed

c) Sizing the solar system

 ISBN: 978-93-90214-20-4

(1) System size
(2) Module size
d) Inverter size

a) Surveying the site:
The site survey establishes the suitability of the rooftop for installing solar PV system. But things to watch out for include

- *Space available – 1 kW of panels would require*

100-130(about 12m2) of shade-free roof area

- Orientation – A south-facing roof is ideal for those in the northern hemisphere
- Module Size according to load requirement

b) **Calculating the amount of energy needed:** The amount of energy needed is determined based on the load that needs to be supported. The load can be calculated as

- Total energy requirement/day (Wh) = Wattage of appliance*No. of appliances*Hours of working
- This should be divided by 1,000 to be converted into kWh/day.

c) Sizing the solar system:
(1) System size: This load requires 4.8 kWh/day.
Adding a 30% safety margin to this, and assuming the insulation to be 4kWh/m2/day,

System size = (Energy Requirement*1.3) /insulation level
= 4.8*1.3/4 = 1.56 or 1560Wp.

(**2) Module size:** Calculated the panel requirement for this system size by taking large size of module 315Wp Modules at 36V.
No. of panels = System size/Panel Rating= 1050/315 = 4.95
Therefore the system requires 5 panels of 315Wp at 36V.
*For this 300Wp is needed so the two 150Wp modules are connected to existing solar Flat roof top plant which consists four modules of 315Wp in this system and reaches the system requirement

d) Inverter size: We use a 30% safety margin when calculating the inverter size.
Required Inverter size = Total Wattage of all appliances*(1+30%)
Therefore, required inverter size = 1050 * (1+30%) = 1365 W
The inverter size is greater than the required solar panel capacity (1560Wp), eliminating the inverter's risk of throttling the panel's output.
Civil foundation and Mechanical installation: The site survey first determines the type of mounting structure to be installed by checking the type of rooftop. This new model system installed on the flat rooftop is a flat concrete roof so for this, the double pole-mounted structure is used
In a double pole-mounted structure, we put two C-channels on the roof with the help of concrete. This is called a pedestal then we connect vertical and horizontal L-channels to hold the modules in place. We call this GI structure.

Advantages of this system: Increasing the load capacity with low cost by using the two 150Wp instead of one 315Wp.Future expansion is easy compared to other rooftop systems. The connections can be changed between two strings whenever we want. By changing the inverter the capacity, this system can be connected to more load also

5. RESULTS

I-V Characteristics of load analysis:
Observations of the load (fans, light bulb, computer, printer) analysis in different timings per day. The I-V characteristics of table form and graph show n in below figures

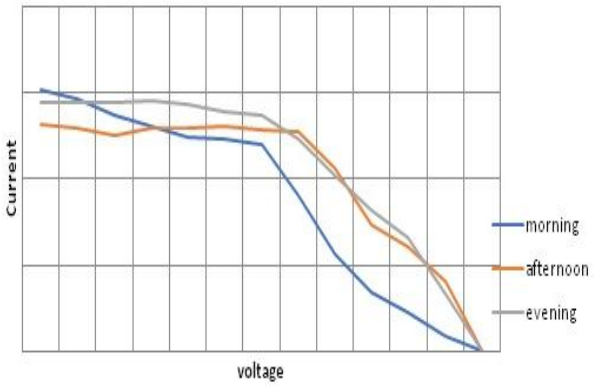

Fig. 5*: *I-V Curves

6. CONCLUSION

In solar rooftop systems for domestic appliances 250Wp (60 cells) size modules and 315Wp (72 cell) modules are used. But sometimes the people will need less load extension, then with the same size of module installation cost will be increased and space for installation will also increase and at the same time with the high rating modules there will be a chance of wastage of power due to fewer loads necessary. So this proposed system will support in less load requirement with low cost and less space for installation. For long life operation with the high performance this new model system depends upon the proper maintenance.
This proposed system may applicable for heavy load requirement also by increasing the capacity of the inverter; everyone can implement this system for their domestic appliances easily and quickly. So hope that in future the whole domestic appliances can run only on the solar PV system with low cost and high performance.

S.NO	One day								
	Morning			Afternoon			Evening		
	Voltage (V)	Current (A)	Power (W)	Voltage (V)	Current (A)	Power (W)	Voltage (V)	Current (A)	Power (W)
1	29.9	50.6	1512.94	25.6	51.3	1313.28	28.6	50.3	1438.58
2	30.3	48.2	1460.46	26.3	49.3	1296.59	29.5	49	1445.5
3	31	44	1364	27.5	45.6	1254	31.2	46.3	1444.56
4	31.8	41	1303.8	32.5	39.9	1296.75	31.5	46.1	1452.15
5	32.3	38.4	1240.32	32.8	39.5	1295.6	31.6	45.3	1431.48
6	32.7	37.5	1226.25	33.7	38.7	1304.19	32.5	42.8	1391
7	32.8	36.6	1200.48	34.2	37.5	1282.5	33.4	41.01	1369.734
8	33.7	26.8	903.16	34.9	36.5	1273.85	34.9	35.2	1228.48
9	34.5	16.2	558.9	35.4	29.9	1058.46	35.6	28.5	1014.6
10	35	9.8	343	35.5	20.5	727.75	35.8	22.9	819.82
11	35.6	6.3	224.28	35.9	16.9	606.71	36	18.4	662.4
12	36.3	2.4	87.12	36.1	11.2	404.32	36.05	9.15	329.8575
13	36.05	0.01	0.3605	36.4	0.02	0.728	36.2	0.04	1.448

Table 2: I-V characteristics for an entire day

ACKNOWLEDGMENT

This work is supported by Dr. A.Vijaya Sarada Reddy, Secretary of Holy Mary Group of Institutions in Hyderabad .& Nalanda Educational Society in Guntur, Vice Chair person of Andhra Pradesh School Education, Regulatory and Monitoring Commission and Head of Skill development center of NES, Guntur.

REFERENCE

[1] S Charan Teja, Pradeep Kumar Yemula "Energy management of grid connected rooftop solar system with battery storage", International Conference on Innovative Smart Grid Technologies - Asia (ISGT-Asia) ISSN: 2378-8542

[2] Yehia Abdelrehim Anwar ; Mohamed Abdul Raouf Shafei ; Doaa Khalil Ibrahim" "An economic analysis of rooftop solar power plant and energy auditing for commercial building in Egypt "International Conference on 2017 Saudi Arabia Smart Grid (SASG)

[3] J Sreedevi ; N Ashwin ; M Naini Raju "A study on grid connected PV system" IEEE International Conference 2016 National Power Systems Conference (NPSC)

[4] R. Ramakumar ; H.J. Allison ; W.L. Hughes "Solar energy conversion and storage systems for the future" IEEE Transactions on Power Apparatus and Systems (Volume: 94 , Issue: 6 , Nov. 1975)

[5] E. L. Ralph, "Large scale solar electric power generation", Solar Energy Journal, vol. 14, pp. 11-20, 1972.

[6] W. L. Hughes, C. M. Summers, H. J. Allison, "An energy system for the future", IEEE Transactions on Industrial Electronics, pp. 08-111, May 1963.

[7] State wise installed solar power capacity", (PDF) Ministry of New and Renewable Energy Govt. of India. 1 March 2016, March 2016.

[8] B. K. Perera, P. Ciufo, S. Perera, "Point of Common Coupling (PCC) voltage control of a grid-connected solar Photovoltaic (PV) system", 39th Annual Conference of the IEEE Industrial Electronics Society (IECON 2013), pp. 7475-7480, 2013.

[9] T. Schott, A. Mermoud, B. Wittmer, "Analysis of PV Grid Installations Performance Comparing Measured Data to Simulation Results to Identify Problems in Operation and Monitoring", 31st Eur. Photovolt. Sol. Energy Conf. Exhib., pp. 2265-2270, Nov. 2015.

[10] K. Sangeetha Sizing of Solar rooftop installation International Journal of Engineering Research & Technology (IJERT) IJERT ISSN: 2278-0181 Issue 6, June – 2014

[11] Eti Choudhary , Deepti Aggarwal. Installation of civil foundation for solar rooftop Indian Journal of Science and Technology, DOI: 10.17485/ijst/2016/v9i30/99169, August 2016 . ISSN (Print) : 0974-6846 ISSN (Online) : 0974-5645

[12] http://www.trinasolar.com/us/product/duomax72/duomax-peg14.

Systematic Review of Recent Handover Techniques Femtocell and Microcell in LTE-A

[1] Atul B.Wani, [2] Dr.Anupama A.Deshpande, [3] Dr. S.H.Patil

[1] Research Scholar
[2] Professor, JJTU, India
[3] Professor, BVDU, Pune, India

Abstract:

The growing need for wireless networks calls concerning the appropriate of heterogeneous networks to sufficient client necessities. Mobility administration is rated one of the relevant factors to before-mentioned networks. The handover is a unity of the foremost characteristics of mobility management concerning the long term evolution of advanced (LTE-A) framework, which relies simply upon the hard hand over Femtocell suggests an economically appealing strategy to enhance quality, coverage, and performance in the present organization. The cellular organization operators need to alter the existing single-level macrocell organization to offer the types of the assistance of femtocells to its clients. In this article, we offer a review of handover techniques on femtocell deployment. Various aspects of femtocell networks in a different domain are talked about. Femtocell can be a dominant alternative to redirect and take out a significant the part of the transfer from the Macro Base Station. For a specific area inside a macrocell practically a microcell, the designated recurrence collection is not identical to the adjacent territory. This paper present the review of various handover mechanisms introduced for communication between LTE-A components such as Femtocell and Microcell. The outcome of this paper to discover the challenges of recent handover methods.

Keywords:

Handover, HetNet, LTE-Advanced, Femtocell, eNB, HeNB, power consumption, performance evaluation, simulation

1. INTRODUCTION

The progression in LTE network topology becomes radio link appearance and range fertility as the fifth-generation (5G) networks develop to HetNets. Identity of the foremost purposes for the use of HetNets is the improvement into space and the development of such coverage of the LTE framework [1]. Tiny cells, for illustration, picocells, are granted at the macrocell barriers to develop perhaps weak coverage that happens for various purposes, for example, track trouble and fading. Picocells are more given inside the macrocell coverage, in hotspots, to improve a lot of transactions offloading from more general blocks on more modest things [2]. Later on 5G networks, techniques, for example, handover including cell reselection remain becoming many mind boggling because of the thick deployment of various sorts of blocks containing the effects concerning mobility execution within big further little groups in diverse environmental circumstances. Because of the fixed suspension, and subsequently, unarbitrary determined specification, the appearance regarding various materials achieved go for great possible abasement if versatility heartiness moreover handover problems occur not analyzed during HetNets connected through macro-only network situations [3].

While mobility into the wireless network influences the handover order including the chance to make radio connection downfall and obstacles, the computed difficulty is that effect about mobility toward the connection feature; for instance, connection modification through associate moreover information delivery. Seamless including powerful mobility, into expanding on handover points while HetNets, signifies becoming glanced at toward LTE-Advanced unto reduce obstacles including packet loss through handover [4]. Mobility enrichment shown during this examination has migrated designed based upon the versatility effects discussed in the 3GPP special article [5]. This article exhibited the consequences of discontinuous reception (DRX) deep series toward the handover through diverse motion speeds furthermore outstanding consequences proved that a comprehensive sleeping the session, while the user equipment (UE) directs off each transceiver circuit, makes combined extra radio connection defeats in more precious velocities. Figure 1 shows the general architecture of LTE network that consist of various components such as small cells, Wi-Fi, Macro Base Station (BS), Mobile User Equipment (MUE), etc. The small cells commonly called as Femtocell as well.

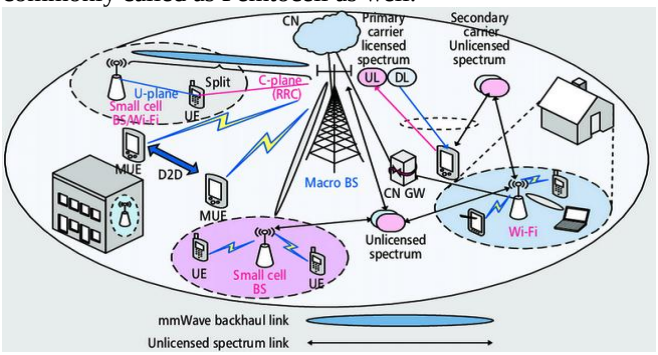

Figure 1. General architecture of LTE-A

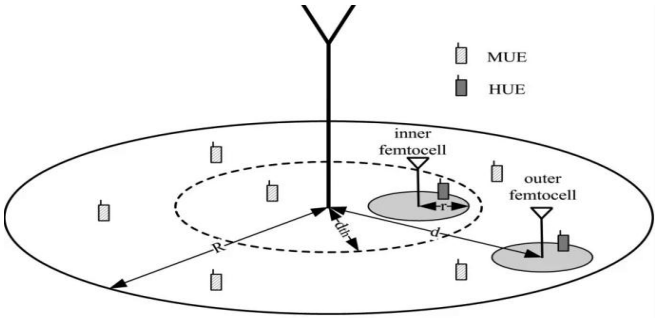

Figure 2. Illustration of structure of femtocell and macrocell

The figure 2 further illustrated the structure of LTE-A macrocell which consist of several femtocells or small cells. The main challenge of such networks is related to handover mechanism among femtocell and macrocell components. In the next section, we present a recent paper literature review based on handover techniques on femtocell and microcell in LTE. In section III presents the comparative table base on exiting methods and performance matrix. Finally, we discussed the conclusion and future work.

2. HANDOVER MECHANISM

In [6] the author proposed the bandwidth restriction including admission authority policy based upon traffic provisions concerning several QoS correlated management. The session aware load balancing furthermore the context-aware handover procedure were prepared, that supports the bandwidth limitation for many traffic conditions and teaches also, users up to operate out the handover up to distribute traffic stock consistently all completed the network. This load balancing tool provided further end-users for connect with the WiFi network while practicing the WiMAX including a delicious handover into support QoS/QoE. In [7] the author presented a congestion charge tool for the 3GPP LTE-A networks, which remains regarded while NGN. Certainly, this interworking connecting being radio access modifications are improved inside the MIH protocol, which promotes coordination among congestion controller mechanism furthermore mobility management. Their congestion control device was combined within the VHO period to forestall including encouraging excess state also was performed by the 3GPP LTE-equipment moreover the MIH IS, which implies the vital material into this complete construction. In [8] the author suggested the prediction tool on into contraction the handover breakdown rate also ping-pong handover rate, within withdraw that delay progressing moreover trying eNB beside moreover complete data, they recommended remarkably outspoken specifications to predict and 3GPP Release 8, that UE past Information reported through eNB UE account information, decreasing this handover crash rate furthermore ping-pong handover valuation with doing aforementioned account data similar Region-Domain, Time-Domain including Time At Trigger. In [9] the author has performed the accomplishment estimation regarding the advanced LTE HO problem-solving operations also, Time-To-Trigger (TTT) parameters estimation into duplicate the character concerning SON. Because the relevant HO parameter perspective is essential for adequate network administrations, different amounts of Hysreresisa3 additionally Time To Trigger have been estimated to recognize the most suitable optimal handover significations estimation. This intended HO calculative operation with modernized significations context prepared to change precise network achievements in the duration of bigger throughput moreover reducing precise network obstruction. The aforementioned summary simply examines the entirety of Oneself Organizing Network characteristics referring are the Self Optimizing.

In [10] author proposed various handover plans for Fella LTE networks. In this investigation, they mathematically analyzed the got SINR by little cells become part in decoupling, regarding a contrivance going in decoupling provinces of those little cells, in different cell resistance situations. Simulation outcomes determine the signalling impression of Man in handovers, developed uplink SINR, reduced power consumption of contraptions in both single tiny cell, and various small cell situations.

In [11] the author presented a proposal, specifically, NCA up to streamline support allocation through handover during highway situations. Highway handover situation, wherever in, a blocked destination hub, during times of resource blocks (RB), points over every package trouble case. To improve supply allocation through handover determinations, they perform the Network Coding Approach (NCA) founded on Coordinated Different spot.

In [12] the author introduced an adjusted grimy article coding method up to decrease the significant influence from inter-cell resistance. To decrease the consequence of resistance, specific user feedback quantizes CSI to the second station, including suddenly relevant proceeding was taken on a spread signal.

In [13] the author has proposed a frequency allocation schemes forward with resistance management toward macro-femtocell also miniature femtocell organization founded LTE-A network. During this method, the network remains separated into different groups. Each bunch is distributed among a macrocell about individual microcells. Femtocells were conveyed within a macrocell or a microcell to increase cellular coverage. Under this method, three provinces simultaneously including interior including obvious divisions occur granted for personal macrocell moreover microcell through frequency distributed [14].

In [15] the author has presented an advanced handover strategy, in the duration of continuing critical significant, moreover connecting within the improved UE trajectory furthermore the HeNB cell locating. Every polynomial role does utilized to anticipate these scheduled UE location while the cosine purpose accompanying with range is utilized for the selection of a suitable destination cell. The structure algorithm was assessed and abruptly related to the

performed operation founded on the handover product, the quantity of signaling measures, packet deferral ratio, packet distress ratio, moreover structure throughput.

In [16] proposed a prediction handover algorithm for the handover performance in the femtocell network by using two kinds of handover problem-solving operations which are approved Reference Signal Received Power or Reference Signal Received Quality (RSRQ) A2-A4-RSRQ handover procedures. This investigation was implemented in phases of the character of handovers, the representation of irrelevant handovers, moreover user the continued use throughput. The main operator of user throughput degeneration is also dissolved.

In [17] author proposed an improved handover operations remain to reduce the number of redundant handovers in LTE-A systems as well as decreasing the production of destination femtocells including calls checking possibility throughout the handover.

In [18] author presented Intra-LTE Handover and determined that the optimal framework of Handover parameters can reduce handover frustrations all completed the handover period in changing mobility requirements. This advanced plot estimated the Handover optimization model based on the different UE speed and handover device within LTE to meet the special prerequisites in error-prone conditions. The error model is organized and reductions are examined utilizing track source.

In [19] the author investigated the utilization of intensity messages toward overcoming false handovers. They introduced a graph-based structure that utilizations signal intensity report forwards the transferable approach of the UE to perform more useful handover settlements. This structure affects that specific signal frequency through the UE from all eNBs in its approach imply prepared a priori during all-time occurrences and produces a baseline connecting to getting the smallest product of handovers that can be reached. The frameworks appropriated the specific signal determination during the prevailing time occurrence exclusive moreover measures the signal features toward ultimate time occurrences.

In [20] author presented the Q-learning method on the degree of most effective use of a resource is utilized into the increase that appearance from handover significant, for instance, handover margin (HOM) including the time to trigger (TTT) and assessed during the duration from complete framework delay, a common product concerning handover and framework throughput toward understanding into giving long term evolution (LTE) discovery seamless including secure handover commencing with the whole-cell when over the subsequent, grasping this optimization is founded on Q-learning approach referring produces a smallest average estimate of handover per user furthermore further has the highest throughput.

In [21] paper author has elaborated the femtocell (FC) system forward with its difficulties. They examine on explaining the significance of femtocells and their development conditions. As well, the technological tests allowed in the femtocell network were described in that paper.

In [22] Received signal intensity is practiced as the basic pattern and examined. Received Power turns as the building block for constructing conceivable handover crosswise heterogeneous Radio Access Innovations. This advanced procedure suggested an upward handover based on different signal intensities. Enhanced Weighted Sum Technique is incorporated for Handover decision making. Several measures were also used.

In [23] the author presented an address of the frequency expenses and the power waste those consequences of the delivery regarding the handover-related frequency in a Long Term Evolution (LTE) wireless mobile network. They examine significant supplements from these distinguishing conveying signal information across a particular wireless interface, including their influence proceeding power loss both about the eNB and at the User Equipment (UE) through handover (HO). A measured by the quantity investigation remains performed practicing structure status simulations. They recognize that, inside the HO cycle, the greatest contributor to air-interface signaling expenses is the frequency of the determination record by the UE. This uplink (UL) transmission faces various channel derangement, because of intervention and communication spectrum, during appropriate block volumes.

In [24] the proposed algorithm is founded on the Reference Signal Received Power (RSRP), Reference Signal Received Quality (RSRQ), including remarkable User Equipment (UE) specifications similar changing control also that place interior the femtocell appropriated as HO resolution rules. The impulse after this intended algorithm was to decide the numerous recognized target femtocell amongst several contestants further into reducing the involved HO in femtocell based cellular interfaces.

In [25] author distinguished proposed concerning wireless in HetNets. The beginning is similar to the signal also the other thing is linked upon data transmission; i.e., handover furthermore links measure adaptation. This has happened indicated that the two cycles were changed by the user mobility level and such achievement depreciates near block boundaries. The target was to streamline the user offloading through picocells be conditional on their measured velocities with the goal that comprehensive framework production remains maximized. The network-driven explication and interaction among groups that deliver seamless handover was represented.

In [26] author proposed the deep reinforcement learning (DRL) founded method for determining these formed nonconvex difficulties of reducing estimate cost in times of absolute suspension. Nevertheless, real-world systems manage to produce a huge amount from users including MEC servers requiring vast quantities of various actions, were assessing the sequence concerning every achievable action displays useless. Accordingly, prevailing DRL systems may be complicated or even impracticable to immediately refer to this recommended standard. Based on

the recursive dissolution of the performance range possible to respectively position, they offered a DRL-based algorithm toward common server variety, collaborative offloading, furthermore handover toward a multi-access point wireless system.

In [27] the author discussed the optimization of the handover procedure to reduce the problems that take place during the handover of the vehicle, especially with higher speeds. The idea was to design a cross-layer between the transport layers including the data link layer of the rules within an algorithm. Consequently, the recommended design can accommodate a vehicle activity and handover scheme to decrease the suspension time.

In [28] author proposed an effective detachment validation handover design through integrating SDN means Software Defined Network moreover AMACs imply Aggregated Message Authentication Codes procedures within the 5G-V2X system into overcome handover signaling above and delivery obstruction throughout the validation.

In [29] author proposed the two tiers micro femtocell based independent ultra-dense wireless mobile network operation, where femtocell distribution demands position interior the microcell found proceeding user frequency. The femtocells design associations according to the adjacency including the special collection of every combination was conducted using a lump of weighted bulk meat. Dedicated frequency associations were completed during micro furthermore femtocell users though the greatest producer of each femtocell group allots meters to its companion femtocells found on auction competition. Agilent EXG vector signal dynamo N5172B, EXA vector sign examiner 9010A and Agilent signal studio software was practiced for the innovative scheme of production evaluation of the recommended material.

In [30] presented an appearance during sustained, including target unconventional human toward robot handovers practicing real-time robotic perception, and administration. They strive concerning universal eligibility beside a general design producer, and attached hold collection operation, and by practicing a particular gripper-mounted RGB-D camera, therefore negative relying on surface sensors. The robot is managed via visual servoing into some target regarding attention. Placing great importance on security, they work on two understanding more complex structure human anatomy character segmentation including control finger segmentation. Pixels that happen believed up to relate to the individual remain separated of competitor hold shows, consequently guaranteeing that this robot carefully accumulates the target outdoors conflicting by the human companion.

3. COMPARATIVE STUDY

	Year of Methodology	Performance Metrics	Simulation Tool
Comparative Study	**Comparative Study**	**Comparative Study**	**Comparative Study**
The comparative table of analysis of literature methods are following	The comparative table of analysis of literature methods are following	The comparative table of analysis of literature methods are following	The comparative table of analysis of literature methods are following

R. No.	Year	Methodology	Performance Metrics	Simulation Tool
7	2015	In proposed congestion controller in 3GPP LTE-A networks. Their system includes of three stages: congestion obstruction, congestion discovery, and congestion announcement. Moreover, it is connected with the vertical handover process, when making the handover resolution, as well as the variety of the destination network.	An increase in the signalization rate of only 3% connected to when the excess command is turned off. Also, simulation outcomes give a high level of possible resource management and a low package drop rate.	The the congestion control system was investigated within a simulation examination utilizing a MATLAB accomplice.
8	2015	3GPP Release 8, the UE History Information reported by eNB UE history report, overcoming the handover crash rate and ping-pong handover rate by practicing the account data like Region-Domain, Time-Domain, and Time To Trigger.	In the simulation including two alternate designs, the recommended approach explicated more reliable execution of handover failure rate and ping-pong handover rate	They practiced a system-level simulation of LTE networks based on Matlab. Associated with the established scheme with Time UE visited message
10	2016	Handover schemes for Due to incorporation (DUDe) LTE networks. Aside from this, they have mathematically explained the obtained SINR by small cells practiced component in decoupling, concerning a thing running in decoupling fields of these little cells, in various cell resistance situation	DUDe in handovers, enhanced uplink SINR, reduced power consumption of materials in both single little cell and various small cell situations	They have used MATLAB based LTE system simulator.

12	2016	Modified Dirty paper coding (MDPC) has been introduced to alleviate Inter-cell Interference. To overcome the consequence of interference, every user feedback quantizes CSI to the base station and then proper precoding is performed on the transferred signal.	They associate the sum rate of the Modified Dirty Paper Coding and Zero-Forcing technique. Simulation outcomes explain that the sum rate of Modified dirty journal coding is 23% higher than the Zero-Forcing procedure.	
14	2017	Handover method offered compared to the two-tier long term evolution advanced (LTE-A) network by applying two methods, the effective administration prediction system and the distance within the modern user equipment (UE) region and the HeNB place	The transmission measure product, the package delay ratio, and the container loss ratio and accessions operation throughput.	
17	2017	The author has introduced an improved handover algorithm that decreases the number of additional handovers in LTE-A networks as well as decreasing the number of target femtocells and calls blocking possibility throughout handover.	The advanced algorithm defeats of decreasing the abundance of handovers and the ratio of T-HeNB in the operation.	Visual Studio environment with C#
19	2018	They introduced a graph-based structure that uses signal power learning along the mobile trajectory of the UE to make more reliable handover arrangements. The signal intensity data for reducing deceptive handovers.	It is shown that this advanced algorithm significantly decreases the number of handovers while still keeping good signal features for information throughout the trajectory of the UE.	simulation of real-world data
23	2019	A simulation analysis is performed for the signaling charge and the power consumption throughout HO in an LTE network when multiple cell dimensions, UE speed, offset, and TTT states are applied.	As a consequence, uplink signaling retransmissions are triggered causing more powerful signaling charge and consequently more expensive power consumption, this being especially damaging to battery-powered devices	
27	2020	In this proposed designed cross-layer between the transport layer and the data link layer of the protocol through an algorithm.	This system adapted a vehicle speed and handover method to decrease the delay time. The result certainly confirms that the optimal scheme can complete the least delay time of HO in any estimation of carrier speed.	
29	2020	The two-tier micro-femtocell based heterogeneous ultra-dense cellular network policy, where femtocell allocation requires location inside the microcell based on user frequency	This policy network reduces power transmission by 23%–41%, increases signal-to-interference-plus-noise ratio by 12%–39%, and frightful efficiency by 10%–37% than the current competing heterogeneous cellular network operations.	Agilent EXG vector signal generator N5172B, EXA vector signal analyzer 9010A, and Agilent signal studio software
30	2021	Object-Independent Human-to-Robot Handovers Using Real-Time Robotic Vision	In experiments including 13 objects, the robot was competent to favorably take the an object from the peoples in 81.9% of the tests.	singular gripper-mounted RGB-D camera,

4. RESEARCH GAPS

1. Sustainability, cost-viability, well-sent designs, and the capacity to maintain high data rate wireless communications for HetNets to maintain WiFiWiMAX combination in a HetNet condition. Nevertheless, the compelling utilization of those two additions from the end-users' point-of-see.
2. Seamless handover when UE transfers is one of the main problems in LTE-A. To develop more extra several parameters if the eNB supports obtaining a more expert parameter via more excellent simulation.
3. To increase the overall dimensions of the cellular network, little cells, for illustration, Femtocells are immediately meaning communicated in the LTE-Advanced system and are determined to be a suitable resolution to bandwidth restriction and coverage problems.
4. The handover methodology transforms out to be added sensitive especially over high mobility speed, and for real-time administrations. For Long Term Evolution Advanced (LTE-A) based 5G system is to increase the cell volume and cell coverage of indoor users.
5. Wireless gadgets to enhance infirmed voice and data reception within the macrocell. To lead by using the various ways, (for example microcell, hotspots, and so on), the femtocell is a significantly less costly option that can be installed by the end consumer.
6. Handover management is one of the main constituents describing the viability of various wireless network discovery. Because of the special features of a femtocell, an additional handover occurs more habitually.
7. A mobile hub that is connected to its base station surrenders its connection while connected mobility creates a vacillation of signal features for building handover decisions, which can create false handovers in a high eNB deployment.
8. With the evolution of cellular networks, many standards have appeared, to satisfy the growing need for ubiquitous, top notch voice, data, and multimedia administrations. Moreover benefits even at the cell-edges and indoor provinces where the necessity for the cellular administrations is rarely the less. In spite of the fact that there is a growing prerequisite for higher data rate administrations can be as handover delay or signal misfortune that leads to throughput degrading and may cut the communication.
9. The deployment of many femtocells performs the effect of decreasing the number of additional users' handovers provocation of great significance. Femtocells obtain a more powerful data rate and increase the coverage area in cellular networks. Expanding an immense number of femtocells produces about the further progressive introduction of a HO system.

5. CONCLUSION & FUTURE WORK:

Femtocell is an encouraging discovery for the caustic edge wireless network. At the instant, the implementation of femtocell change allows specific problems, for instance, latency problems, due to the backhaul associate via the internet, which is very essential for delay-touchy multimedia management, handover warning, and multimedia stream routing to maintain mobility. This paper introduced the systematic review of late handover techniques femtocell and microcell in LTE. Because of its essential points, related to help, fast, affection, and play, and so on, femtocell influences the mobile researchers to hunt for large deployment if the interference problems can be managed appropriately. It is apparently seen that practicing the macro femtocell including diminutive femtocell collection based LTE-A network, power transmission and track accident can be transformed to not as significant as that of a macro femtocell based LTE-A system. For future, we suggest design of multi-objective LTE-A handover mechanism among femtocell and microcell systems with goal of reducing the latency, delay, and data loss.

REFERENCE

[1]. Zhang, H., et al. (2015). 5G wireless network: MyNET and SONAC. IEEE Network, 29, 14–23.

[2]. Wang, P., et al. (2015). QoS-aware cell association in 5G heterogeneous networks with massive MIMO. IEEE Network, 29, 76–82.

[3]. Ge, X., et al. (2014). 5G wireless backhaul networks: Challenges and research advances. IEEE Network, 28, 6–11.

[4]. TR 136 912, LTE; feasibility study for further advancements for E-UTRA (LTE-Advanced), 3GPP (2017).

[5]. TR 36.839, Technical specification group radio access network; evolved universal terrestrial radio access (E-UTRA); mobility enhancements in heterogeneous networks, 3GPP (2012).

[6]. A. Sarma, S. Chakraborty and S. Nandi, "Deciding Handover Points Based on Context-Aware Load Balancing in a WiFi-WiMAX Heterogeneous Network Environment," in IEEE Transactions on Vehicular Technology, vol. 65, no. 1, pp. 348-357, Jan. 2016, doi: 10.1109/TVT.2015.2394371.

[7]. H. Mzoughi, F. Zarai, M. S. Obaidat and L. Kamoun, "3GPP LTE-Advanced Congestion Control Based on MIH Protocol," in IEEE Systems Journal, vol. 11, no. 4, pp. 2345-2355, Dec. 2017, doi: 10.1109/JSYST.2015.2407373.

[8]. Y. Wang, J. Chang and G. Huang, "A Handover Prediction Mechanism Based on LTE-A UE History Information," 2015 18th International Conference on Network-Based Information Systems, Taipei, 2015, pp. 167-172, doi: 10.1109/NBiS.2015.29.

[9]. I. N. Md Isa, M. D. Baba, R. Ab Rahman and A. L. Yusof, "Self-organizing network based handover mechanism for LTE networks," 2015 International

Conference on Computer, Communications, and Control Technology (I4CT), Kuching, 2015, pp. 11-15, doi: 10.1109/I4CT.2015.7219527.

[10]. M. K. Giluka, M. S. A. Khan, G. M. Krishna, T. A. Atif, V. Sathya and B. R. Tamma, "On handovers in Uplink/Downlink decoupled LTE HetNets," 2016 IEEE Wireless Communications and Networking Conference Workshops (WCNCW), Doha, 2016, pp. 315-320, doi: 10.1109/WCNCW.2016.7552718.

[11]. I. Jouli, K. Hassine and M. Frikha, "Optimizing Bandwidth Capacity during Soft Handover in LTE-A System: Network Coding Based Approach," 2016 Global Summit on Computer & Information Technology (GSCIT), Sousse, 2016, pp. 97-101, doi: 10.1109/GSCIT.2016.13.

[12]. K. Chikte and Rajesh A, "Performance analysis of an improved CSI feedback technique for LTE-A system with Femtocell Interference," 2016 IEEE International Conference on Engineering and Technology (ICETECH), Coimbatore, 2016, pp. 1055-1058, doi: 10.1109/ICETECH.2016.7569411.

[13]. A. Mukherjee, D. De and P. Deb, "Interference management in macro-femtocell and micro-femtocell cluster-based long-term evaluation-advanced green mobile network," in IET Communications, vol. 10, no. 5, pp. 468-478, 24 3 2016, doi: 10.1049/iet-com.2015.0982.

[14]. D. Pant, V. Kumar, P. Dhuliya and T. Lal, "Performance analysis of femtocell in macro-cellular environment," 2016 2nd International Conference on Advances in Computing, Communication, & Automation (ICACCA) (Fall), Bareilly, 2016, pp. 1-4, doi: 10.1109/ICACCAF.2016.7748984.

[15]. Ahmad, Rami; Sundararajan, Elankovan A.; Othman, Nor E.; Ismail, Mahamod (2017). An efficient handover decision in heterogeneous LTE-A networks under the assistance of users' profile. Telecommunication Systems, (), –. doi:10.1007/s11235-017-0374-4

[16]. Amirrudin, Nurul 'Ain; Ariffin, Sharifah Hafizah Syed; Abd. Malik, Nik Noordini Nik; Ghazali, Nurzal Effiyana (2017). Analysis of Handover Performance in LTE Femtocells Network. Wireless Personal Communications.

[17]. Omitola, Olusegun O.; Srivastava, Viranjay M. (2017). An Enhanced Handover Algorithm in LTE-Advanced Network. Wireless Personal Communications.

[18]. H. S. Suma, R. Mathew and C. P. Prabodh, "Analysis of Intra-LTE Handover in an Error Prone Environment," 2018 International Conference on Inventive Research in Computing Applications (ICIRCA), Coimbatore, 2018, pp. 504-508, doi: 10.1109/ICIRCA.2018.8597405.

[19]. S. Biswas, S. Chakraborty and A. Gupta, "Reducing Spurious Handovers in Dense LTE Networks based on Signal Strength Look-ahead," 2018 14th International Conference on Wireless and Mobile Computing, Networking and Communications (WiMob), Limassol, 2018, pp. 1-8, doi: 10.1109/WiMOB.2018.8589147.

[20]. M. Adel, M. S. Darweesh, H. Mostafa, H. Kamal and M. El-Ghoneimy, "Optimization of Handover Problem Using Q-learning for LTE Network," 2018 30th International Conference on Microelectronics (ICM), Sousse, Tunisia, 2018, pp. 188-191, doi: 10.1109/ICM.2018.8704001.

[21]. P. Sambanthan and T. Muthu, "Role of Femtocell Networks beyond 4G," 2018 IEEE International Conference on System, Computation, Automation and Networking (ICSCA), Pondicherry, 2018, pp. 1-5, doi: 10.1109/ICSCAN.2018.8541156.

[22]. Preethi, G. A.; Gauthamarayathirumal, P.; Chandrasekar, C. (2019). Vertical Handover Analysis Using Modified MADM Method in LTE. Mobile Networks and Applications.

[23]. M. Tayyab, G. P. Koudouridis, X. Gelabert and R. Jäntti, "Signaling Overhead and Power Consumption during Handover in LTE," 2019 IEEE Wireless Communications and Networking Conference (WCNC), Marrakesh, Morocco, 2019, pp. 1-6, doi: 10.1109/WCNC.2019.8885459.

[24]. M. Mandour, F. Gebali, A. D. Elbayoumy, G. M. Abdel Hamid and A. Abdelaziz, "Handover Optimization and User Mobility Prediction in LTE Femtocells Network," 2019 IEEE International Conference on Consumer Electronics (ICCE), Las Vegas, NV, USA, 2019, pp. 1-6, doi: 10.1109/ICCE.2019.8662064.

[25]. Khwandah, Sinan A.; Cosmas, John P.; Lazaridis, Pavlos I.; Glover, Ian A.; Zaharis, Zaharias D.; Prasad, Neeli R. (2019). Energy Efficient Mobility Enhancement in LTE Pico–Macro HetNet Systems. Wireless Personal Communications, (), –. doi:10.1007/s11277-019-06623-4

[26]. T. M. Ho and K. -K. Nguyen, "Joint Server Selection, Cooperative Offloading and Handover in Multi-access Edge Computing Wireless Network: A Deep Reinforcement Learning Approach," in IEEE Transactions on Mobile Computing, doi: 10.1109/TMC.2020.3043736.

[27]. H. E. I. Jubara, "An efficient handover procedure in vehicular communication," 2020 2nd International Conference on Computer and Information Sciences (ICCIS), Sakaka, Saudi Arabia, 2020, pp. 1-5, doi: 10.1109/ICCIS49240.2020.9257665.

[28]. G. Li and C. Lai, "Platoon Handover Authentication in 5G-V2X : IEEE CNS 20 Poster," 2020 IEEE Conference on Communications and Network Security (CNS), Avignon, France, 2020, pp. 1-2, doi: 10.1109/CNS48642.2020.9162271.

[29]. A. Mukherjee, P. Deb, D. De and M. S. Obaidat, "WmA-MiFN: A Weighted Majority and Auction Game Based Green Ultra-Dense Micro-Femtocell Network System," in IEEE Systems Journal, vol. 14, no. 1, pp. 353-362, March 2020, doi: 10.1109/JSYST.2019.2911977.

[30]. P. Rosenberger et al., "Object-Independent Human-to-Robot Handovers Using Real Time Robotic Vision," in IEEE Robotics and Automation Letters, vol. 6, no. 1, pp. 17-23, Jan. 2021, doi: 10.1109/LRA.2020.3026970.

Comparative Analysis of Drift Detection Techniques used in Ensemble Classification Approach

[1] Rucha Chetan Samant, [2] Dr. Suhas H. Patil

[1] PhD Scholar, Department Of Computer Engineering, Bharati Vidyapeeth Deemed to be university, College of Engineering, Pune, India
[2] Professor, Department Of Computer Engineering, Bharati Vidyapeeth Deemed to be university, College of Engineering, Pune, India

Abstract:

In this era of fast developing world, most of the applications are producing large volumes of continuous and vivid dimensional data. In these applications like IOT sensors, social media applications, online advertisements, communication gateways are producing non ending information at a rate of millions of records per day, call as data stream. The large volume, high generation speed and change in information are main three features of this data stream.

Traditional Data analysis techniques are not capable of handling data stream processing. Data classification is major task in data analysis and in case of stream data classification it becomes more tedious. The data stream classification has major challenge of dealing with drift. There are many approached developed to deal with drift in data stream. Here comparative study of main drift detection approaches is done which are basically used in various ensemble based classification.

Keywords:

Concept Drift, Data Streams, Drift Detector, Ensemble based classifier

1. INTRODUCTION

The progression in LTE network topology becomes radio link appearance and range fertility as the fifth-generation (5G) networks develop to HetNets. Identity of the foremost purposes for the use of HetNets is the improvement into space and the development of such coverage of the LTE framework [1]. Tiny cells, for illustration, picocells, are granted at the macrocell barriers to develop perhaps weak coverage that happens for various purposes, for example, track trouble and fading. Picocells are more given inside the macrocell coverage, in hotspots, to improve a lot of transactions offloading from more general blocks on more modest things [2]. Later on 5G networks, techniques, for example, handover including cell reselection remain becoming many mind boggling because of the thick deployment of various sorts of blocks containing the effects concerning mobility execution within big further little groups in diverse environmental circumstances. Because of the fixed suspension, and subsequently, unarbitrary determined specification, the appearance regarding various materials achieved go for great possible abasement if versatility heartiness moreover handover problems occur not analyzed during HetNets connected through macro-only network situations [3].

While mobility into the wireless network influences the handover order including the chance to make radio connection downfall and obstacles, the computed difficulty is that effect about mobility toward the connection feature; for instance, connection modification through associate moreover information delivery. Seamless including powerful mobility, into expanding on handover points while HetNets, signifies becoming glanced at toward LTE-Advanced unto reduce obstacles including packet loss through handover [4]. Mobility enrichment shown during this examination has migrated designed based upon the versatility effects discussed in the 3GPP special article [5]. This article exhibited the consequences of discontinuous reception (DRX) deep series toward the handover through diverse motion speeds furthermore outstanding consequences proved that a comprehensive sleeping the session, while the user equipment (UE) directs off each transceiver circuit, makes combined extra radio connection defeats in more precious velocities. Figure 1 shows the general architecture of LTE network that consist of various components such as small cells, Wi-Fi, Macro Base Station (BS), Mobile User Equipment (MUE), etc. The small cells commonly called as Femtocell as well.

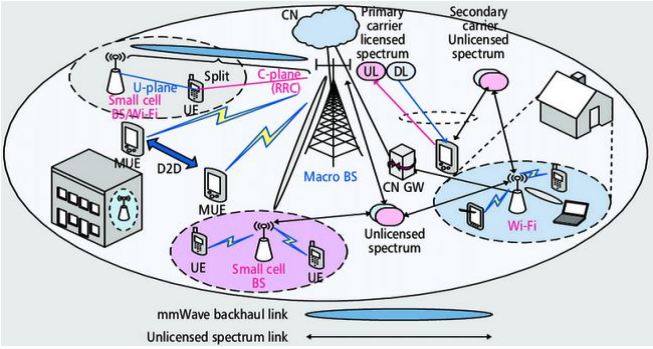

Figure 1. General architecture of LTE-A

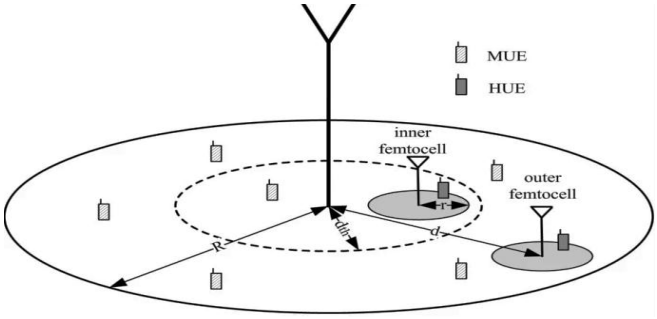

Figure 2. Illustration of structure of femtocell and macrocell

The figure 2 further illustrated the structure of LTE-A macrocell which consist of several femtocells or small cells. The main challenge of such networks is related to handover mechanism among femtocell and macrocell components. In the next section, we present a recent paper literature review based on handover techniques on femtocell and microcell in LTE. In section III presents the comparative table base on exiting methods and performance matrix. Finally, we discussed the conclusion and future work.

2. HANDOVER MECHANISM

In [6] the author proposed the bandwidth restriction including admission authority policy based upon traffic provisions concerning several QoS correlated management. The session aware load balancing furthermore the context-aware handover procedure were prepared, that supports the bandwidth limitation for many traffic conditions and teaches also, users up to operate out the handover up to distribute traffic stock consistently all completed the network. This load balancing tool provided further end-users for connect with the WiFi network while practicing the WiMAX including a delicious handover into support QoS/QoE. In [7] the author presented a congestion charge tool for the 3GPP LTE-A networks, which remains regarded while NGN. Certainly, this interworking connecting being radio access modifications are improved inside the MIH protocol, which promotes coordination among congestion controller mechanism furthermore mobility management. Their congestion control device was combined within the VHO period to forestall including encouraging excess state also was performed by the 3GPP LTE-equipment moreover the MIH IS, which implies the vital material into this complete construction. In [8] the author suggested the prediction tool on into contraction the handover breakdown rate also ping-pong handover rate, within withdraw that delay progressing moreover trying eNB beside moreover complete data, they recommended remarkably outspoken specifications to predict and 3GPP Release 8, that UE past Information reported through eNB UE account information, decreasing this handover crash rate furthermore ping-pong handover valuation with doing aforementioned account data similar Region-Domain, Time-Domain including Time At Trigger. In [9] the author has performed the accomplishment estimation regarding the advanced LTE HO problem-solving operations also, Time-To-Trigger (TTT) parameters estimation into duplicate the character concerning SON. Because the relevant HO parameter perspective is essential for adequate network administrations, different amounts of Hysreresisa3 additionally Time To Trigger have been estimated to recognize the most suitable optimal handover significations estimation. This intended HO calculative operation with modernized significations context prepared to change precise network achievements in the duration of bigger throughput moreover reducing precise network obstruction. The aforementioned summary simply examines the entirety of Oneself Organizing Network characteristics referring are the Self Optimizing.

In [10] author proposed various handover plans for Fella LTE networks. In this investigation, they mathematically analyzed the got SINR by little cells become part in decoupling, regarding a contrivance going in decoupling provinces of those little cells, in different cell resistance situations. Simulation outcomes determine the signalling impression of Man in handovers, developed uplink SINR, reduced power consumption of contraptions in both single tiny cell, and various small cell situations.

In [11] the author presented a proposal, specifically, NCA up to streamline support allocation through handover during highway situations. Highway handover situation, wherever in, a blocked destination hub, during times of resource blocks (RB), points over every package trouble case. To improve supply allocation through handover determinations, they perform the Network Coding Approach (NCA) founded on Coordinated Different spot.

In [12] the author introduced an adjusted grimy article coding method up to decrease the significant influence from inter-cell resistance. To decrease the consequence of resistance, specific user feedback quantizes CSI to the second station, including suddenly relevant proceeding was taken on a spread signal.

In [13] the author has proposed a frequency allocation schemes forward with resistance management toward macro-femtocell also miniature femtocell organization founded LTE-A network. During this method, the network remains separated into different groups. Each bunch is distributed among a macrocell about individual microcells.

Femtocells were conveyed within a macrocell or a microcell to increase cellular coverage. Under this method, three provinces simultaneously including interior including obvious divisions occur granted for personal macrocell moreover microcell through frequency distributed [14].

In [15] the author has presented an advanced handover strategy, in the duration of continuing critical significant, moreover connecting within the improved UE trajectory furthermore the HeNB cell locating. Every polynomial role does utilized to anticipate these scheduled UE location while the cosine purpose accompanying with range is utilized for the selection of a suitable destination cell. The structure algorithm was assessed and abruptly related to the performed operation founded on the handover product, the quantity of signaling measures, packet deferral ratio, packet distress ratio, moreover structure throughput.

In [16] proposed a prediction handover algorithm for the handover performance in the femtocell network by using two kinds of handover problem-solving operations which are approved Reference Signal Received Power or Reference Signal Received Quality (RSRQ) A2-A4-RSRQ handover procedures. This investigation was implemented in phases of the character of handovers, the representation of irrelevant handovers, moreover user the continued use throughput. The main operator of user throughput degeneration is also dissolved.

In [17] author proposed an improved handover operations remain to reduce the number of redundant handovers in LTE-A systems as well as decreasing the production of destination femtocells including calls checking possibility throughout the handover.

In [18] author presented Intra-LTE Handover and determined that the optimal framework of Handover parameters can reduce handover frustrations all completed the handover period in changing mobility requirements. This advanced plot estimated the Handover optimization model based on the different UE speed and handover device within LTE to meet the special prerequisites in error-prone conditions. The error model is organized and reductions are examined utilizing track source.

In [19] the author investigated the utilization of intensity messages toward overcoming false handovers. They introduced a graph-based structure that utilizations signal intensity report forwards the transferable approach of the UE to perform more useful handover settlements. This structure affects that specific signal frequency through the UE from all eNBs in its approach imply prepared a priori during all-time occurrences and produces a baseline connecting to getting the smallest product of handovers that can be reached. The frameworks appropriated the specific signal determination during the prevailing time occurrence exclusive moreover measures the signal features toward ultimate time occurrences.

In [20] author presented the Q-learning method on the degree of most effective use of a resource is utilized into the increase that appearance from handover significant, for instance, handover margin (HOM) including the time to trigger (TTT) and assessed during the duration from complete framework delay, a common product concerning handover and framework throughput toward understanding into giving long term evolution (LTE) discovery seamless including secure handover commencing with the whole-cell when over the subsequent, grasping this optimization is founded on Q-learning approach referring produces a smallest average estimate of handover per user furthermore further has the highest throughput.

In [21] paper author has elaborated the femtocell (FC) system forward with its difficulties. They examine on explaining the significance of femtocells and their development conditions. As well, the technological tests allowed in the femtocell network were described in that paper.

In [22] Received signal intensity is practiced as the basic pattern and examined. Received Power turns as the building block for constructing conceivable handover crosswise heterogeneous Radio Access Innovations. This advanced procedure suggested an upward handover based on different signal intensities. Enhanced Weighted Sum Technique is incorporated for Handover decision making. Several measures were also used.

In [23] the author presented an address of the frequency expenses and the power waste those consequences of the delivery regarding the handover-related frequency in a Long Term Evolution (LTE) wireless mobile network. They examine significant supplements from these distinguishing conveying signal information across a particular wireless interface, including their influence proceeding power loss both about the eNB and at the User Equipment (UE) through handover (HO). A measured by the quantity investigation remains performed practicing structure status simulations. They recognize that, inside the HO cycle, the greatest contributor to air-interface signaling expenses is the frequency of the determination record by the UE. This uplink (UL) transmission faces various channel derangement, because of intervention and communication spectrum, during appropriate block volumes.

In [24] the proposed algorithm is founded on the Reference Signal Received Power (RSRP), Reference Signal Received Quality (RSRQ), including remarkable User Equipment (UE) specifications similar changing control also that place interior the femtocell appropriated as HO resolution rules. The impulse after this intended algorithm was to decide the numerous recognized target femtocell amongst several contestants further into reducing the involved HO in femtocell based cellular interfaces.

In [25] author distinguished proposed concerning wireless in HetNets. The beginning is similar to the signal also the other thing is linked upon data transmission; i.e., handover furthermore links measure adaptation. This has happened indicated that the two cycles were changed by the user mobility level and such achievement depreciates near block boundaries. The target was to streamline the user offloading through picocells be conditional on their measured velocities with the goal that comprehensive framework

production remains maximized. The network-driven explication and interaction among groups that deliver seamless handover was represented.

In [26] author proposed the deep reinforcement learning (DRL) founded method for determining these formed nonconvex difficulties of reducing estimate cost in times of absolute suspension. Nevertheless, real-world systems manage to produce a huge amount from users including MEC servers requiring vast quantities of various actions, were assessing the sequence concerning every achievable action displays useless. Accordingly, prevailing DRL systems may be complicated or even impracticable to immediately refer to this recommended standard. Based on the recursive dissolution of the performance range possible to respectively position, they offered a DRL-based algorithm toward common server variety, collaborative offloading, furthermore handover toward a multi-access point wireless system.

In [27] the author discussed the optimization of the handover procedure to reduce the problems that take place during the handover of the vehicle, especially with higher speeds. The idea was to design a cross-layer between the transport layers including the data link layer of the rules within an algorithm. Consequently, the recommended design can accommodate a vehicle activity and handover scheme to decrease the suspension time.

In [28] author proposed an effective detachment validation handover design through integrating SDN means Software Defined Network moreover AMACs imply Aggregated Message Authentication Codes procedures within the 5G-V2X system into overcome handover signaling above and delivery obstruction throughout the validation.

In [29] author proposed the two tiers micro femtocell based independent ultra-dense wireless mobile network operation, where femtocell distribution demands position interior the microcell found proceeding user frequency. The femtocells design associations according to the adjacency including the special collection of every combination was conducted using a lump of weighted bulk meat. Dedicated frequency associations were completed during micro furthermore femtocell users though the greatest producer of each femtocell group allots meters to its companion femtocells found on auction competition. Agilent EXG vector signal dynamo N5172B, EXA vector sign examiner 9010A and Agilent signal studio software was practiced for the innovative scheme of production evaluation of the recommended material.

In [30] presented an appearance during sustained, including target unconventional human toward robot handovers practicing real-time robotic perception, and administration. They strive concerning universal eligibility beside a general design producer, and attached hold collection operation, and by practicing a particular gripper-mounted RGB-D camera, therefore negative relying on surface sensors. The robot is managed via visual servoing into some target regarding attention. Placing great importance on security, they work on two understanding more complex structure human anatomy character segmentation including control finger segmentation. Pixels that happen believed up to relate to the individual remain separated of competitor hold shows, consequently guaranteeing that this robot carefully accumulates the target outdoors conflicting by the human companion.

3. COMPARATIVE STUDY

	Year of Methodology	Performance Metrics	Simulation Tool
Comparative Study	**Comparative Study**	**Comparative Study**	**Comparative Study**
The comparative table of analysis of literature methods are following	The comparative table of analysis of literature methods are following	The comparative table of analysis of literature methods are following	The comparative table of analysis of literature methods are following

R. No.	Year	Methodology	Performance Metrics	Simulation Tool
7	2015	In proposed congestion controller in 3GPP LTE-A networks. Their system includes of three stages: congestion obstruction, congestion discovery, and congestion announcement. Moreover, it is connected with the vertical handover process, when making the handover resolution, as well as the variety of the destination network.	An increase in the signalization rate of only 3% connected to when the excess command is turned off. Also, simulation outcomes give a high level of possible resource management and a low package drop rate.	The the congestion control system was investigated within a simulation examination utilizing a MATLAB accomplice.
8	2015	3GPP Release 8, the UE History Information reported by eNB UE history report, overcoming the handover crash rate and ping-pong handover rate by practicing the account data like Region-Domain, Time-Domain, and Time To Trigger.	In the simulation including two alternate designs, the recommended approach explicated more reliable execution of handover failure rate and ping-pong handover rate	They practiced a system-level simulation of LTE networks based on Matlab. Associated with the established scheme with Time UE visited message

10	2016	Handover schemes for Due to incorporation (DUDe) LTE networks. Aside from this, they have mathematically explained the obtained SINR by small cells practiced component in decoupling, concerning a thing running in decoupling fields of these little cells, in various cell resistance situation	DUDe in handovers, enhanced uplink SINR, reduced power consumption of materials in both single little cell and various small cell situations	They have used MATLAB based LTE system simulator.
12	2016	Modified Dirty paper coding (MDPC) has been introduced to alleviate Inter-cell Interference. To overcome the consequence of interference, every user feedback quantizes CSI to the base station and then proper precoding is performed on the transferred signal.	They associate the sum rate of the Modified Dirty Paper Coding and Zero-Forcing technique. Simulation outcomes explain that the sum rate of Modified dirty journal coding is 23% higher than the Zero-Forcing procedure.	
14	2017	Handover method offered compared to the two-tier long term evolution advanced (LTE-A) network by applying two methods, the effective administration prediction system and the distance within the modern user equipment (UE) region and the HeNB place	The transmission measure product, the package delay ratio, and the container loss ratio and accessions operation throughput.	
17	2017	The author has introduced an improved handover algorithm that decreases the number of additional handovers in LTE-A networks as well as decreasing the number of target femtocells and calls blocking possibility throughout handover.	The advanced algorithm defeats of decreasing the abundance of handovers and the ratio of T-HeNB in the operation.	Visual Studio environment with C#
19	2018	They introduced a graph-based structure that uses signal power learning along the mobile trajectory of the UE to make more reliable handover arrangements. The signal intensity data for reducing deceptive handovers.	It is shown that this advanced algorithm significantly decreases the number of handovers while still keeping good signal features for information throughout the trajectory of the UE.	simulation of real-world data
23	2019	A simulation analysis is performed for the signaling charge and the power consumption throughout HO in an LTE network when multiple cell dimensions, UE speed, offset, and TTT states are applied.	As a consequence, uplink signaling retransmissions are triggered causing more powerful signaling charge and consequently more expensive power consumption, this being especially damaging to battery-powered devices	
27	2020	In this proposed designed cross-layer between the transport layer and the data link layer of the protocol through an algorithm.	This system adapted a vehicle speed and handover method to decrease the delay time. The result certainly confirms that the optimal scheme can complete the least delay time of HO in any estimation of carrier speed.	
29	2020	The two-tier micro-femtocell based heterogeneous ultra-dense cellular network policy, where femtocell allocation requires location inside the microcell based on user frequency	This policy network reduces power transmission by 23%–41%, increases signal-to-interference-plus-noise ratio by 12%–39%, and frightful efficiency by 10%–37% than the current competing heterogeneous cellular network operations.	Agilent EXG vector signal generator N5172B, EXA vector signal analyzer 9010A, and Agilent signal studio software

30	2021	Object-Independent Human-to-Robot Handovers Using Real-Time Robotic Vision	In experiments including 13 objects, the robot was competent to favorably take the an object from the peoples in 81.9% of the tests.	singular gripper-mounted RGB-D camera,

4. RESEARCH GAPS

1. Sustainability, cost-viability, well-sent designs, and the capacity to maintain high data rate wireless communications for HetNets to maintain WiFiWiMAX combination in a HetNet condition. Nevertheless, the compelling utilization of those two additions from the end-users' point-of-see.
2. Seamless handover when UE transfers is one of the main problems in LTE-A. To develop more extra several parameters if the eNB supports obtaining a more expert parameter via more excellent simulation.
3. To increase the overall dimensions of the cellular network, little cells, for illustration, Femtocells are immediately meaning communicated in the LTE-Advanced system and are determined to be a suitable resolution to bandwidth restriction and coverage problems.
4. The handover methodology transforms out to be added sensitive especially over high mobility speed, and for real-time administrations. For Long Term Evolution Advanced (LTE-A) based 5G system is to increase the cell volume and cell coverage of indoor users.
5. Wireless gadgets to enhance infirmed voice and data reception within the macrocell. To lead by using the various ways, (for example microcell, hotspots, and so on), the femtocell is a significantly less costly option that can be installed by the end consumer.
6. Handover management is one of the main constituents describing the viability of various wireless network discovery. Because of the special features of a femtocell, an additional handover occurs more habitually.
7. A mobile hub that is connected to its base station surrenders its connection while connected mobility creates a vacillation of signal features for building handover decisions, which can create false handovers in a high eNB deployment.
8. With the evolution of cellular networks, many standards have appeared, to satisfy the growing need for ubiquitous, top notch voice, data, and multimedia administrations. Moreover benefits even at the cell-edges and indoor provinces where the necessity for the cellular administrations is rarely the less. In spite of the fact that there is a growing prerequisite for higher data rate administrations can be as handover delay or signal misfortune that leads to throughput degrading and may cut the communication.
9. The deployment of many femtocells performs the effect of decreasing the number of additional users' handovers provocation of great significance. Femtocells obtain a more powerful data rate and increase the coverage area in cellular networks. Expanding an immense number of femtocells produces about the further progressive introduction of a HO system.

5. CONCLUSION & FUTURE WORK:

Femtocell is an encouraging discovery for the caustic edge wireless network. At the instant, the implementation of femtocell change allows specific problems, for instance, latency problems, due to the backhaul associate via the internet, which is very essential for delay-touchy multimedia management, handover warning, and multimedia stream routing to maintain mobility. This paper introduced the systematic review of late handover techniques femtocell and microcell in LTE. Because of its essential points, related to help, fast, affection, and play, and so on, femtocell influences the mobile researchers to hunt for large deployment if the interference problems can be managed appropriately. It is apparently seen that practicing the macro femtocell including diminutive femtocell collection based LTE-A network, power transmission and track accident can be transformed to not as significant as that of a macro femtocell based LTE-A system. For future, we suggest design of multi-objective LTE-A handover mechanism among femtocell and microcell systems with goal of reducing the latency, delay, and data loss.

REFERENCE

[1] Jicheng Shan, Hang Zhang, Weike Liu, and Qingbao Liu. “Online Active Learning Ensemble Framework for Drifted Data Streams”, in Proc. IEEE Transactions On Neural Networks And Learning Systems, pp. 1 – 13, 2018.

[2] Radin Hamidi Rada, Maryam Amir Haeria, “Hybrid Forest: A Concept Drift Aware Data Stream Mining Algorithm”, 10 Feb 2019.

[3] Alejandro Ortiz-Díaz, F. Roberto Bayer, F. Baldo, A. Verdecia-Cabrera, L. María Palomino Mariño and I. Frías-Blanco, "Fast Adaptive Stacking of Ensembles Adaptation for Supporting Active Learning. a Real Case Application," 2018 14th International Conference on Natural Computation, Fuzzy Systems and Knowledge Discovery (ICNC-FSKD), Huangshan,

China, 2018, pp. 732-738, doi: 10.1109/FSKD.2018.8686851.

[4] Joao Roberto ,Maria do Carno, "An iterative boosting-based ensemble for streaming data classification", in The Journal Science Direct Information Fusion pp. 1-18, 2018

[5] R. S. M. de Barros, S. G. T. de Carvalho Santos, P. M. G. Júnior, "A boosting-like online learning ensemble," in *Proc. IEEE IJCNN*, pp. 1871–1878, Jul. 2016.

[6] https://www.researchgate.net/publication/220907178_Learning_from_Time-Changing_Data_with_Adaptive_Windowing

[7] Gama J., Medas P., Castillo G., Rodrigues P. (2004) Learning with Drift Detection. In: Bazzan A.L.C., Labidi S. (eds) Advances in Artificial Intelligence – SBIA 2004. SBIA 2004. Lecture Notes in Computer Science, vol 3171. Springer, Berlin, Heidelberg. https://doi.org/10.1007/978-3-540-28645-5_29

[8] Manuel Baena-Garc´ıa1 , Jos´e del Campo-Avila ´ 1 , Ra´ul Fidalgo1 , Albert Bifet2 , Ricard Gavald`a2 , and Rafael Morales-Bueno1 "Early Drift Detection Method", https://www.researchgate.net/publication/245999704_Early_Drift_Detection_Method.

[9] N. C. Oza and S. Russell, "Online bagging and boosting," in Artificial Intelligence and Statistics. Morgan Kaufmann, 2001, pp. 105–112.

[10] S. G. T. C. Santos, P. M. Gonc¸alves, Jr., G. D. S. Silva, and R. S. M. Barros, "Speeding up recovery from concept drifts," in Machine Learning and Knowledge Discovery in Databases, ser. LNCS. Springer, 2014, vol. 8726, pp. 179–194.

[11] Dua, D. and Karra Taniskidou, E. ,"UCI Machine Learning Repository" [http://archive.ics.uci.edu/ml]. Irvine, CA: University of California, School of Information and Computer Science. 2017.

[12] https://github.com/vlosing/driftDatasets

An Experimental approach for strengthening High Performance Concrete with hybrid Fibers: Steel and Polypropylene

[1] N.V.N.Prabath, [2] Dr.P.Ramadoss

[1] Research Scholar, Pondicherry Engineering College, Pondicherry, India
[2] Professor, Pondicherry Engineering College, Pondicherry, India

Abstract:

Due to extended use of concrete structures in military applications and runways, concrete structures are subjected to heavy/impact loads that vary both in velocity and intensity. Addition of fibers helps concrete overcome its shortcomings such as low durability, high shrinkage and less resistance to impact loading. The addition of fibers in high performance concrete (HPC) can overcome its shortcomings such as low durability, high shrinkage and less resistance and also improve the brittle behavior and the energy absorption capacity. In this study, we focused to develop the strengthening of HPC using steel and Polypropylene fibers. Moreover, an increase in volume fractions of both steel and polypropylene fibers leads to an increase in the compressive, splitting tensile and flexural strengths of concrete. The experimental results showed that the use of hybrid fibers with 1% in HPC concrete has improved the strength of the concrete when compared to HSC and single fibers with HPC.

Keywords:

high performance concrete, steel and Polypropylene fibers, HSC, concrete

1. INTRODUCTION

The large-scale use of concrete in construction is mainly due to its various advantages, which include high mechanical strength, easy production, and molding, with relatively low cost [1].Fibers may be incorporated into the concrete in the form of fabrics and textiles, or randomly dispersed in the matrix. Nevertheless, the use of dispersed fibers has been more evident for economic reasons [2]. The combination of using lightweight aggregates together with reinforcing fibers has been introduced in order to improve the material and mechanical characteristics of the lightweight concrete in [3] both fresh and hardened state and has led to the development of the fiber reinforced lightweight concrete whose application has been reported in several experimental and real case studies [4]. Over decades, in an attempt to overcome the inherent drawbacks of plain concrete, fibers are introduced into the concrete mix, commonly known as fiber reinforced concrete to enhance the mechanical properties of concrete, especially for its tensile and post-cracking behavior [5]. For example, High Strength Concrete (HSC) specimens using steel, carbon, polyethylene and polypropylene, steel fibers in the hardened state have improved the flexural strength and ductility performance and reduced the crack width [6, 7]. Hybridization of fibers is normally done by blending two types of fibers in concrete which mostly results in improved mechanical properties of concrete [8]. Therefore utilization of silica fume together with Fly ash produces an interesting alternative and can be termed as high strength and high-performance concrete [9]. Also, flexural behavior is increased to some extent. It also possesses the ability to reduce plastic shrinkage in concrete [10].

The choice of w/cm will be eliminated from the concrete specification [11]. The judicious selection and use of chemical admixtures will continue to enhance the durability of concrete [12]. Moreover, the synergetic effect of hybrid fiber on the flexural properties of concrete and the corresponding fiber reinforcing mechanism were analyzed and discussed [13]. Finally, based on a new comprehensive fiber reinforcing index, analytical equations were developed to predict the flexural loads, deflections and toughness of HFRC with varying hybrid fiber parameters [14].In order, to prove the performance of the high-strength concrete [15] reinforced with steel and polypropylene fibers, it is necessary more research because of several chemical and physical transformations of the paste and aggregates, which results in changes in the concrete's mechanical performance and durability [16]. Our suggested fibers are composites with higher ductility and strain hardening behavior have been developed in previous studies.

The rest of the paper is structured as follows: Following to this introduction section, section 2 reviews the recent existing literatures; section 3 presents the experimental investigation and also depicts the testing procedure of the investigation. Section 4 illustrates the result of the experimental and simulation modeling. Finally, the conclusion part concludes the section with future scope.

2. LITERATURE REVIEW

In 2019 Z.H. Mohebi et al. [17], Fibers are added to concrete mixture by 0.15%, 0.30% and 0.45% volume

fraction of concrete. Failure deflections of splice specimens made of fiber reinforced concrete are 20% higher than that of plain concrete specimens on average. Results indicate that existing prediction equations for bond strength are acceptable and even yield more accurate values when polypropylene fibers are added to concrete mixtures. In 2018 De AlencarMonteiro, V. M. et al. [18], has been suggested the addition of polypropylene, hooked-end and hybrid fibers was effective in improving the post-peak strength of the composites, even though the use of steel fibers promoted higher values of flexural residual stress due to its geometrical and material properties. The flexural toughness of FRC beams with polypropylene 1%, polyolefin 1% and hybrid-1% (PP–PO) was evaluated from the area under the load–deflection curve and compared with control specimens (CS) (without fibers). The flexural strength and ductility were higher for FRC beam specimens reinforced with hybrid fibers by Sakthivel, P. B et al. 2019 [19]. The flexural toughness (FT) at beam defection, L/150 (L=span length) and flexural toughness ratio (FTR) were found to be higher for FRC-hybrid PP–PO beam specimens than the specimens reinforced with PP and PO and control specimens. Upon a simplified spring model, the effects of fiber reinforcement at different loading stages were further discussed by Huang, L et al. 2019 [20]. Hybrid fibers could exert obvious positive influences on the bond strength, due to the synergetic effects in inhibiting the propagation of cracks at multi-scale and multi-stages. Finally, an analytical model was proposed to estimate the ultimate bond strength, in which the effects of fiber reinforcement, stirrup confinement and geometrical shape of the deformed bar were taken into consideration.

Nowadays, with progress in the cement industry provides, it has become possible to produce cement type I with strength classes of 32.5, 42.5, and 52.5 MPa. On the one hand, the microstructure of cement has changed and modified by NS, MS, and polymers, therefore, it is very important to determine the optimal percentage of each additive for those CSCs by Fatemeh ZAHIRI et al.2019 [21]. Results indicated the sensitivity of each CSC can be different on the NS or MS in compressive strength of concrete. Experimental and analytical work was carried out to investigate the behavior of GFRP reinforcement versus traditional steel reinforcement in self-compacting concrete columns under eccentric loads by Hassan, A et al. 2019 [22]. The GFRP-reinforced columns have lower carrying capacities than the steel-reinforced columns, with a difference of ~24%. The analytical results show good agreement with the experimental results for steel-reinforced columns, whereas the GFRP-reinforced columns report a noteworthy contrast. The composites were tested under three-point monotonic and cyclic flexural loads. Pullout tests were performed to study the fiber-matrix interaction. It was observed that the sisal fiber could provide the same level of residual strength as the polypropylene fiber, as long as the equivalence of the dosages of the fibers is taken into account by Castoldi, R. et al. 2019 [23]. The composites were classified according to fib Model Code 2010 based on parameters obtained from flexural tests.

The ANN configuration consists of the input layer with three nodes, a single hidden layer of ten nodes of the output layer with five nodes by Awolusi, T. F et al.2019 [24]. The ANN training was done by splitting the experimental data into the training and testing set. The divergence of the RMSE between the output and target values of the test set was monitored and used as a criterion to stop training. The purpose of the present study was to investigate the effects of fibers on the performance of self-compacting concrete (SCC) by Mashhadban, H et al. 2016 [25]. Then this experimental data was used to train the feed-forward artificial neural network type. Finally, the trained ANN (artificial neural network) and PSOA (particle swarm optimization algorithm) are used to generate a polynomial model for predicting SCC properties. The obtained results showed that the mechanical properties can be significantly improved by fiber reinforcement and workability of the SCC decreases with increasing fiber content.

3. BENEFITS OF SELECTED FIBERS

- When steel fibers are added to mortar, Portland cement concrete or refractory concrete.
- Flexural strength of the composite is increased from 25% to 100% - depending on the proportion of fibers added and the mix design and also increasing the initial first crack strength.
- Steel fibers are relatively short and closely spaced as compared with continuous reinforcing bars of wires.
- It's added to concrete in low volume dosages (often less than 1%), and have been shown to be effective in reducing plastic shrinkage cracking. Its increased stability and cohesion of the fresh concrete is that the time required to develop stiffness is greatly reduced.

3.1. Strengthening HPC and HSC with fibers: A proposed methodology

Generally, the construction strength and durability is very important in recent times. The main challenges which affects the construction area is heavy wind and water scarcity; to avoid these issues the proposed methodology introduced a new method. In this methodology, we focused to develop strengthening concrete using HPC, HSC, synthetic fibers and hybrid fibers. In this evaluation process, three different structures are used, i.e. cube, cylinder, and prism along with fiber properties. The fibers act as an eco-friendly nature, nonabrasive, high specific strength, and fairly good mechanical properties. The specimens are cast and cured for 28 days before testing. The specimens are loaded and find the structural properties of all the specimens.

3.2 Experimental Program

(a) Materials, mixtures and specimens Preparation

In the experimental investigation examines the effects of adding steel fibers, polypropylene fibers and hybrid fibers

with different ratios on HPC and HSC concretes. The fibers which are utilized in this examination are steel fibers (0, 0.5, 1, and 1.5%) and polypropylene fibers (0.25, 0.5, and 1%). An adequate number of cubes, cylinders, and prisms are thrown and these specimens are investigated for 28 days. Here, the mechanical properties, for example, compressive strength, tensile strength, and flexural strength are examined dependent on these three curing days. The mix proportions of HPC and HSC are depicted in table 1.

Table 1: Basic concrete mix design

Mix design	*w/c ratio*	*C (kg)*	*Silica fume*	*Water (kg)*	*C.A (kg)*	*F.A (kg)*	*Super plasticizer (%)*	*Fiber content*	
								Steel (%)	*Polypropylene (%)*
HSC	0.38	460, 589	0	175, 165	1168, 1102	618, 589	1.75, 2.75	0	0
HPC	0.38	392, 502	68, 88	175, 165	1168, 1102	618, 589	1.75, 2.75	0.5-1.5	0.25-1

All the experiments that are embraced to decide the characteristics of materials are completed according to the system given by significant Indian standards. In this examination, the M60 and M75 grade of concrete was utilized for the whole investigation. The material used in this investigation consists of Ordinary Portland Cement (OPC), coarse aggregate, fine aggregate and super plasticizer. The fiber properties of steel and polypropylene are shown in table 2. The materials such as coarse aggregate, fine aggregate, sand, cement, water, fibers, and super plasticizer were used in this investigation. A total of 34 specimens are prepared (2 sets of specimens) by varying properties.

The mix design quantities of HSC are 0.38 in water cement ratio; cement is varied by 460 and 589 kg. The fine aggregate is used by mass of the content as 618 and 589 kg and the coarse aggregate as 1168 and 1102 kg. The super plasticizer is added by 1.75% and 2.75% in HSC. The mixing quantities of HPC and HFHPC for cement, fine aggregate, coarse aggregate, water, silica fume, super plasticizer are 392 kg and 502 kg; 618 kg and 589 kg, 1168 and 1102 kg, 175 and 165 kg, 1.75% and 2.75 kg. The fiber percentages which are used in HPC are 0.5%, 1%, nd 1.5% in steel fibers and also 0.25%, 0.5%, 1% in polypropylene fiber and the water cement ratio is 0.38 and 0.28. The mechanical properties of FRC are mainly dependent upon fiber parameter, fiber content, matrix strength, and fiber matrix interaction.

Table 2: Properties of Fiber

Fiber	*Length (mm)*	*Diameter (mm)*	*Aspect ratio*	*Tensile strength (Mpa)*	*Modulus of elasticity (Gpa)*	*Specific weight (kg/m3)*
Steel Fiber	60	0.75	80	1100	200	7850
Polypropylene fiber	20	0.034	0.5	551	2800	9.1

Testing Methods

Compressive Strength (CS): Compressive strength tests were directed on standard cubes of dimension *150* x *150* x *150 mm*. The specimens were put away in molds for 24 h. Subsequent to de-moulded cubes are kept in ordinary water for relieving; the compressive strength was tried after the end of particular curing periods.

Split Tensile Strength (STS): STS was led on *200* x *100 mm* cylindrical test specimen to assess the tensile capacity given by concrete as per explicit standards.

Flexural Strength (FS): FS test was led on prisms of measurements *500mm* x *100mm* x *100mm* for three curing days utilizing the flexural test machine and the outcomes were tabulated.

Table 1: Description of the specimen used in this study

S. No.	Specimen Name	Concrete mix	Description of specimen
1	S1	HSC	High Strength Concrete
2	S2	HPC	High Performance Concrete
3	HP1	HPSFRC0.5	High Performance Steel Reinforced Concrete SF-0.5, 1, 1.5%
4	HP2	HPSFRC1	
5	HP3	HPSFRC1.5	
6	HP4	HPPFRC0.25	High Performance Polypropylene Reinforced Concrete SF-0.25, 0.5, 1%
7	HP5	HPPFRC0.5	
8	HP6	HPPFRC1	
9	HP7	HPHFRC1	HPSF0.5PF0.25
10	HP8	HPHFRC2	HPSF0.5PF0.5
11	HP9	HPHFRC3	HPSF0.5PF1
12	HP10	HPHFRC4	HPSF1PF0.25

 ISBN: 978-93-90214-20-4

13	HP11	HPHFRC5	HPSF1PF0.5
14	HP12	HPHFRC6	HPSF1PF1
15	HP13	HPHFRC7	HPSF1.5PF0.25
16	HP14	HPHFRC8	HPSF1.5PF0.5
17	HP15	HPHFRC9	HPSF1.5PF1

(b) Sample preparation and testing procedure

An effort has been made in this research to investigate the effects of different fiber parameters, which can vary simultaneously, on the mechanical properties of concrete with different strengths. All aggregates were added to the mixer and mixed for few revolutions to ensure the absorption of water by the aggregates and then the cement was mixed in a dry state for few minutes. A proper mix of concrete is essential for the strength of the concrete. Before the concreting, all the mix materials were weighed and kept for concreting as per design mix proportions. Premixed super plasticizer with water was added to the aggregates and mixed for three minutes, followed by a rest of three minutes, then mixed again for two minutes. The mixer was stopped and the concrete mixture was cast in different molds according to the specimen sizes. For fiber reinforced concrete, fibers were added to the concrete after the preparation of the concrete mixture and mixed for five minutes to allow well dispersion of the fibers in the concrete. The experimental setup and the testing procedure are shown in figure 1 (a), (b) and (c).

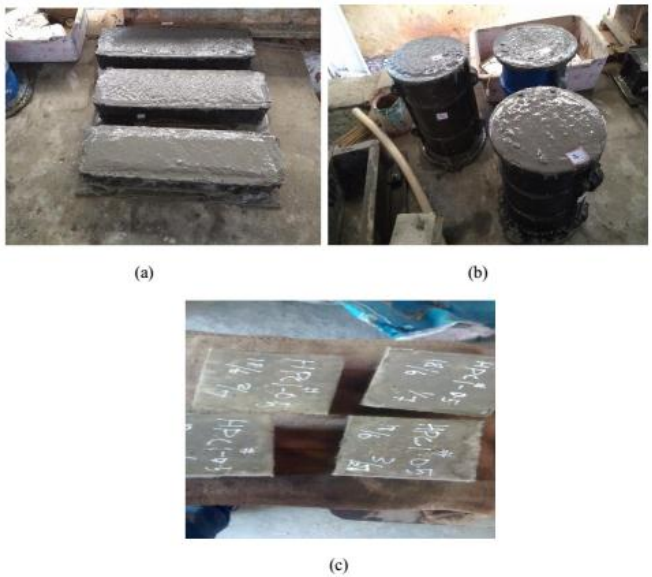

Fig.1: Experimental setup: (a) casting cubes (b) casting cylinders (c) prism

(c) Casting and curing

Casting of specimens was done by batching of materials, preparation of moulds and placing of concrete in the moulds. During the placing of fresh concrete into mould, proper cares were taken to remove entrapped air by using a table vibrator to attain maximum strength. After leveling the fresh concrete in the mould, it was allowed to dry for 24 hrs. Curing is an important process to prevent the concrete specimens from losing their moisture while they are gaining their required strength. All concrete specimens were cured in water at room temperature for 28 days. After curing, concrete specimens were removed from the curing tank and air dried to conduct tests on hardened concrete. Three specimens were cast for each type of the test and for each mix. The compressive strength, flexural strength and split tensile strength specimens were tested after 28 days. The strengths of the three specimens were computed and presented in the results.

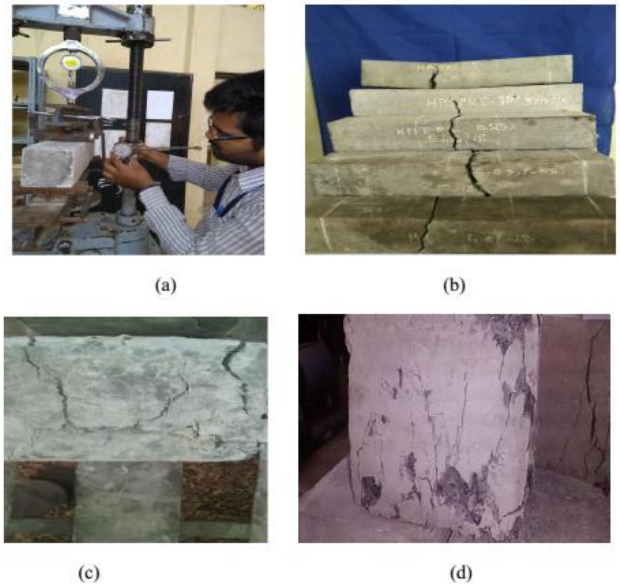

Fig. 2: Testing Procedure (a) test setup (b) after loading cube, (c) cylinder and (c) prism

3.3 Predicting the Experimentation by Simulation Modeling

To validate these experimental parameters we propose a simulation modeling i.e. Artificial Neural Network (ANN). ANN is intended to simulate the behavior of biological systems composed of "neurons". Typically, an artificial neural network has anywhere from dozens to millions of artificial neurons called units arranged in a series of three layers: (i) Input layer (ii) Hidden layer (iii) Output layer. It is physical cellular systems, which can acquire, store and utilize experiential knowledge. When a neural network is fed with input data in the input layer, the values are forwarded to one or more nodes in the next layer. These nodes perform calculations on the values they receive, and forward the results to one or more nodes in the next layer, which repeat the process. Figure 3 shows the sample structure of ANN which is obtained in the simulation process.

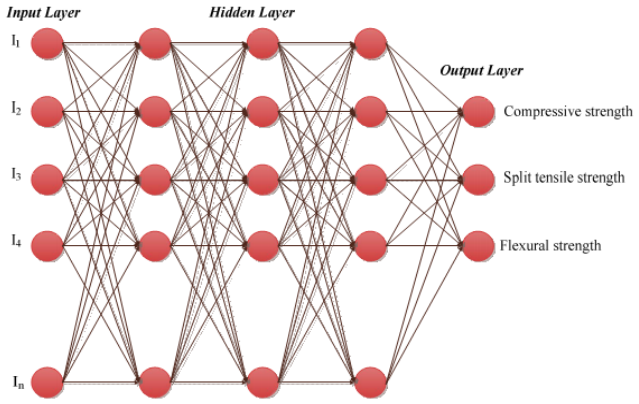

Fig. 3: ANN basic structure

3.3.1 Steps of ANN:

(i) The neural network is designed to validate the strengthening parameters with the input parameters such as cement, water, fine aggregate, coarse aggregate, silica fume, super plasticizer, two ratios of water/cement. These input parameters are taken as in the form of $I_i = [I_1, I_2, I_3 \ldots\ldots\ldots I_n]$. The ANN default structure and the proposed work which is implemented in MATLAB are modeled in below figure. Here, I_i represents the input layer; $[I_1, I_2, I_3 \ldots\ldots\ldots I_n]$ are the above presented input parameters.

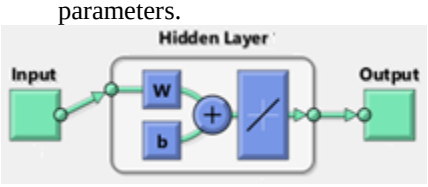

(a) Default ANN structure

(ii) The input layer weight α_i and the hidden layer weights β_{ij} are initialized in this layer. The basic and activation function of the ANN structure is evaluated by using the equation (1).

$$HL_b = \sum_{j=1}^{N} HL_A \times \beta_{ij} \qquad HL_A = \sum_{x=1}^{l} \frac{1}{1+exp(-I_i)} \quad (1)$$

Where HL_b symbolizes the basis function; HL_a symbolizes the activation function, and N refers to the number of data.

(iii) The final structure of the NN is the output layer which is connected by the hidden layer and neurons. In this work we have predicted the output in this layer as compressive strength, split tensile strength, and flexural strength.

$$O = \sum_{x=1}^{l} \alpha_{(optimal)\,j} \frac{1}{1+exp\left(-\sum_{j=1}^{N} I_i \times \beta_{ij}\right)_{optimsl}} \quad (2)$$

(iv) The validation of this proposed simulation modeling reduced the experimentation time and the output layer obtains the results as nearly equal to the experimental result.

4. RESULTS AND DISCUSSION

In this result section discussed the results of experimental investigation i.e. strengthening HSC and HPC concrete by fibers. After that, the experimental study is validated using a soft computing technique that is implemented in the working platform of MATLAB software version 2016a with 4GB RAM and i5 processor. The predicted results are compared with experimental and existing approaches with the help of graphs, charts, and tables.

4.1 Experimental Results

(i) Compressive strength:

Compressive strength is one of the most important properties of concrete and influences many other describable properties of the hardened concrete. The mean compressive strength required at a specific age, usually 28 days, determines the nominal water-cement ratio of the mix. Generally, cubes are used for determining the compressive strength in concrete. In the present investigation for M60 grade concrete mix proportion is obtained as per IS 10262: 2009 method. Several specimens are prepared without adding fibers (4 specimens), and it is noticed that mixes are stiff with poor workability. In order to improve workability of the concrete, experimental specimens are prepared to fix the dosage of fibers. For fiber mixed specimens, the separate fibers are added for 12 specimens and totally 18 specimens were prepared with hybrid fibers. In general, the strength of concrete at 7 days is only 60–65% of design strength depending on external conditions. Concrete gain its strength with time after casting. The rate of gain of concrete compressive strength in higher during the first 28 days of casting and then it slows down. The compressive strength gained by concrete after 28 days with respect to the grade of concrete is shown in table 3.

Table 3: Experimental results for investigated specimens: Type I: w/c: 0.38

Specimens	Compressive strength (Mpa)	Split tensile strength (Mpa)	Flexural strength (Mpa)
HSC	68.85	5.49	6.99
HPC	75.05	5.75	8.12
HPSFRC0.5	77.85	6.26	9.14
HPSFRC1	82.5	6.48	9.60
HPSFRC1.5	88.65	7.51	10.35
HPPFRC0.25	75.95	5.84	8.54

HPPFRC0.5	77.65	5.97	8.64
HPPFRC1	79.4	6.25	8.87
HPHFRC1	78.55	6.45	9.25
HPHFRC2	79.68	6.93	9.38
HPHFRC3	82.54	7.13	9.69
HPHFRC4	83.75	7.16	9.94
HPHFRC5	85.5	7.48	10.25
HPHFRC6	86.85	7.89	10.39
HPHFRC7	90.05	8.1	10.47
HPHFRC8	92.25	8.69	10.58
HPHFRC9	93.9	9.37	10.79

Table 3: Experimental results for investigated specimens: Type II: w/c: 0.28

Specimens	Compressive strength (Mpa)	Split tensile strength (Mpa)	Flexural strength (Mpa)
HSC	83.4	6.41	7.28
HPC	87.3	6.795	8.61
HPSFRC0.5	88.15	7.2	10.41
HPSFRC1	92.1	7.96	11.26
HPSFRC1.5	98.7	8.69	12.8
HPPFRC0.25	87.9	6.84	9.06
HPPFRC0.5	90.2	7.19	9.51
HPPFRC1	92.6	7.69	9.89
HPHFRC1	89.15	7.9	10.68
HPHFRC2	90.2	8.31	11.02
HPHFRC3	93.7	8.97	11.36
HPHFRC4	94.2	8.7	11.87
HPHFRC5	96.8	9.1	12.43
HPHFRC6	98.05	9.8	12.89
HPHFRC7	99.8	9.2	13.34
HPHFRC8	101.3	9.91	13.49
HPHFRC9	102.65	10.42	13.82

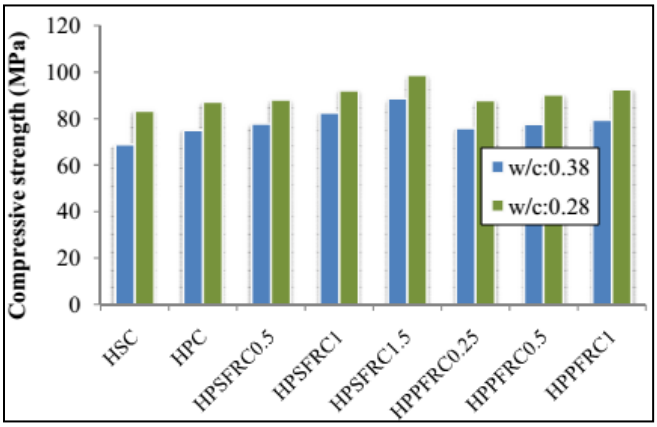

(a)

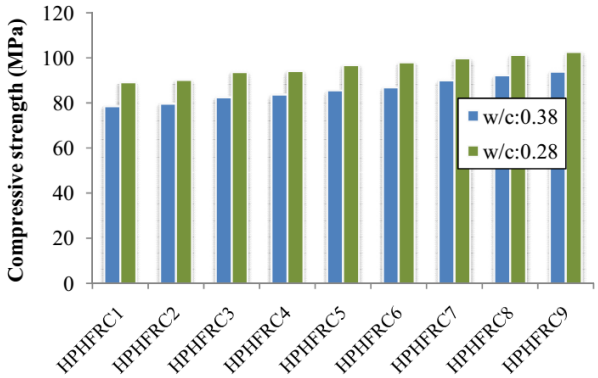

(b)

Fig.5: Experimental results for Compressive strength (a) separate specimens (b) hybrid specimens

Table 3 & 4 shows that the compressive strength for 28 days curing specimens. The compressive strength of HSC specimen is 68.85 Mpafor 0.38 w/c and 83.4 Mpa in 0.28 w/c. The strength of HPC can be increased up to 75.05 in 0.38 w/c and 87.3 in 0.28 w/c. If the sisal fibers and polypropylene fibers are added separately with the percentage of 0.5%, 1% and 1.5%, 0.25%, 0.5% and 1% in HPC, the compressive strength has been increased for both w/c ratios. Moreover, the addition of hybrid fibers i.e. different percentages of steel and polypropylene fibers increases the strength of the concrete and reduces the crack propagation. Hybrid fibers are found to have synergetic effects on the flexural behavior of concrete for all the fiber types. An increase in the volume fractions for both steel and polypropylene fibers leads to an increase in the properties of concrete. The hybridization with the combination of straight steel and polypropylene fibers exhibits the most obvious synergy. The failure of specimens without fibers or only with polypropylene fibers is in a brittle manner with neat fracture surfaces, while that of specimens with steel fibers is ductile. The comparison between mechanical properties of high strength fiber reinforced concrete has been presented. The above said compressive strength results are visualized in figure 5.

(b) Split Tensile Strength:

The tensile strength will affect the cracking behavior, stiffness, damping action, durability of concrete, based on the split strength the behavior of concrete under shear loads are determined. The tensile strength is determined either by direct tensile tests or by indirect tensile tests such as split cylinder tests. In split tensile test cylinders after 28 days were removed from the curing tank and was left to dry for 24 hours after that cylinder is placed in CTM for testing. The load is applied until the cracks were in the cylinder specimen.

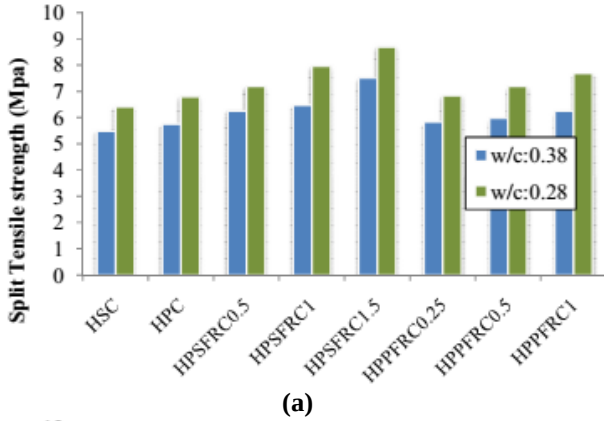

(a)

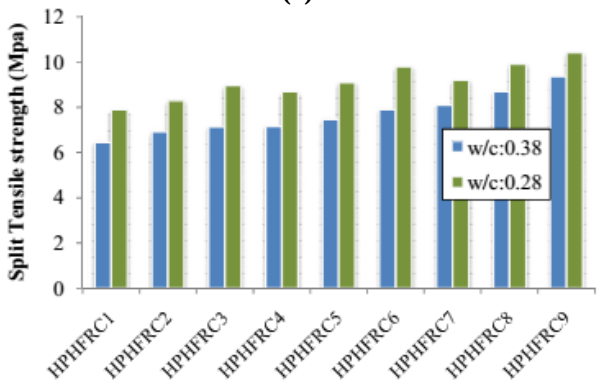

(b)

Fig. 6: Experimental results for split tensile strength (a) Specimens with separate fiber (b) specimens with hybrid fibers

The split tensile strength of HPC increases with increase in percentage of fiber percentages. Table 3, 4 and figure 6 shows the result of split tensile strength which occurs in all the specimens for both w/c ratios. The tensile strength of concrete is much lower than the compressive strength, largely because of the ease with which cracks can propagate under tensile loads. Although tensile strength is usually not considered directly in design (normally assumed equal to zero), its value is still needed because cracking in concrete tends to be of tensile behavior. High-strength concrete is, therefore, more brittle and stiffer than normal-strength concrete. Here, HSC for first type of w/c is 5.49 Mpa, and the second type of w/c achieves 6.41 Mpa in HSC specimens. For the comparison of HSC and HPC specimens, HSC requires more strength; that means HPC attains higher strength than HSC. In addition, the strength of HPC has been added because of including fibers. Specimens with separate fibers attains more value than HPC i.e. 6.26, 6.48, 7.51 in HPSFRC and 5.84, 5.97, 6.25 Mpa in HPPFRC for 0.38 w/c. Similarly, the w/c 0.28 requires the same type of result. Specifically, the hybrid specimens reach higher strength than these types of specimens. Hybrid specimen combines the fiber percentage of steel and polypropylene. The maximum split tensile strength achieves 9.37 in 0.38 w/c, and also 10.42 in 0.28 w/c. The split tensile strength increased value can be shown in figure 6 for varying w/c ratios.

(c) Flexural strength:

HPC exceeds the properties and constructability of normal concrete. Normal and special materials are used to make these specially designed concretes that must meet a combination of performance requirements. High-performance concrete almost always has a higher strength than normal concrete. High-strength concrete has been successfully mixed in transit mixers and central mixers; however, many of these concretes tend to be sticky and cause build-up in these mixers. The flexural strength is expressed as Modulus of Rupture (MR) in psi (MPa). It is also known as bend strength, or fracture strength. Flexural strength is a mechanical limitation for brittle material such as concrete which is defined as a material's capacity to defend against bend or twist under load. Flexural strength is the measure of the tensile strength of concrete. The data required to calculate flexural strength are measured by experimentation, with square samples of the material placed under load in a single point testing setup.

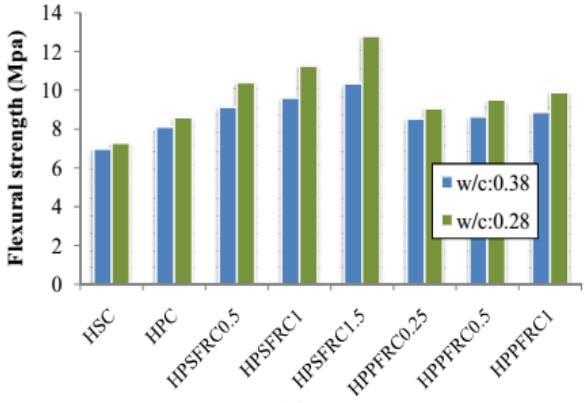

(a)

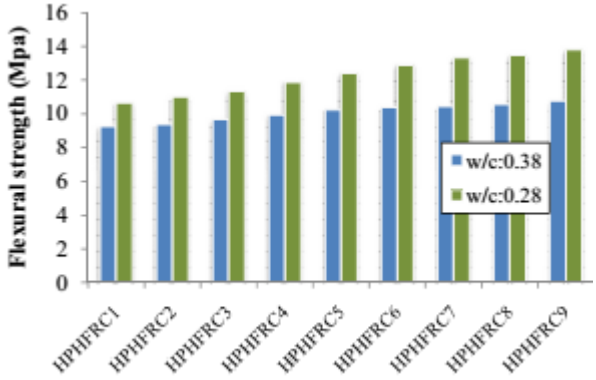

(b)

Fig.7: Experimental results for flexural strength (a) Specimens with separate fiber (b) specimens with hybrid fibers

The flexural strength of various mixes at 28 days curing is given in Table 3 and 4. The flexural strength of mixes at 28 days was found to be in the range of 6.9 MPa-13.9MPa in

0.38 w/c and 7.28 Mpa to 10.8 Mpa in 0.28 w/c. The variation in flexural strength of the HSC mix and HPC mixes was significant. It was seen there was significant increase in flexural strength with age for all the mixes. In prism, the hybrid specimen performs the flexural range of 0.38 w/c is 9.25, 9.38, 9.69, 9.94, 10.25, 10.39, 10.47, 10.58, and 10.78 Mpa. For 0.28 w/c; the maximum flexural strength reaches HPFRC 9 as 13.82 Mpa, in this specimen the sisal fiber is taken as 1% and polypropylene fiber as 1%. If the fiber increases, the value of flexural strength also increased.

4.3 Simulation Results

Table 5: Simulation results for Type I: w/c -0.38

Specimens	*Compressive strength (Mpa)*	*Split tensile strength (Mpa)*	*Flexural strength (Mpa)*
HSC	66.32	5.54	7.25
HPC	74.15	5.9	8.35
HPSFRC0.5	78.32	6.35	9.35
HPSFRC1	81.41	6.78	9.84
HPSFRC1.5	89.05	8.03	10.05
HPPFRC0.25	74.66	5.98	8.94
HPPFRC0.5	78.69	6.05	8.99
HPPFRC1	78.58	6.33	9.04
HPHFRC1	79.66	6.54	9.41
HPHFRC2	80.14	6.84	9.47
HPHFRC3	81.45	7.19	10.05
HPHFRC4	84.33	7.25	10.12
HPHFRC5	85.62	7.58	10.40
HPHFRC6	87.14	7.19	10.56
HPHFRC7	91.02	8.35	10.90
HPHFRC8	91.47	8.57	11.06
HPHFRC9	94	9.56	11.36

Table 6: Simulation results for Type II: w/c -0.28

Specimens	*Compressive strength (Mpa)*	*Split tensile strength (Mpa)*	*Flexural strength (Mpa)*
HSC	84.15	6.02	7.36
HPC	88.36	6.85	8.71
HPSFRC0.5	90.15	7.35	10.96
HPSFRC1	93.25	7.15	12.14
HPSFRC1.5	99.47	9.26	13.14
HPPFRC0.25	85.14	7.41	10.48
HPPFRC0.5	90.14	7.08	10.45
HPPFRC1	93.16	7.77	10.69
HPHFRC1	91.25	7.51	11.05
HPHFRC2	91.74	8.45	11.69
HPHFRC3	94.74	9.25	12.06
HPHFRC4	95.36	8.9	12.98
HPHFRC5	97.18	8.74	13.08
HPHFRC6	99.58	9.71	13.74
HPHFRC7	100.36	9.34	14.39
HPHFRC8	102.22	9.14	13.47
HPHFRC9	105.47	10.65	14.06

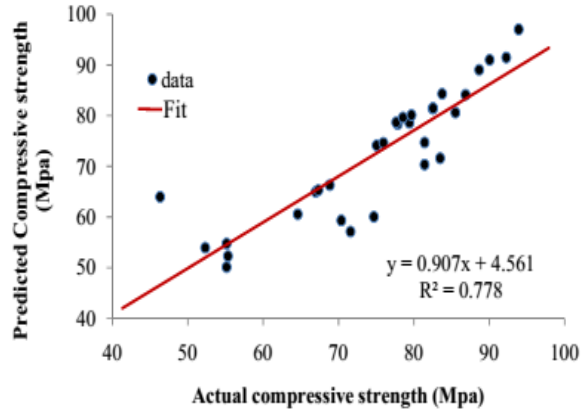

(a)

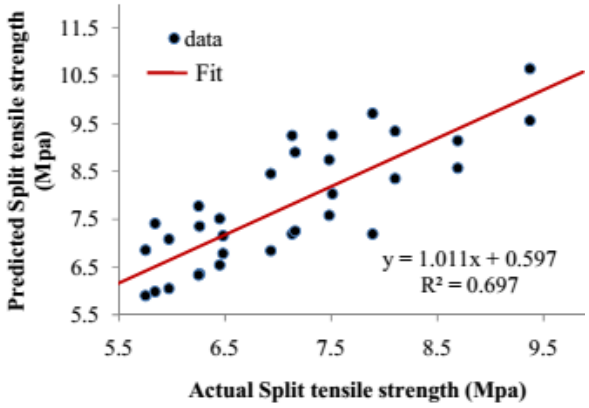

(b)

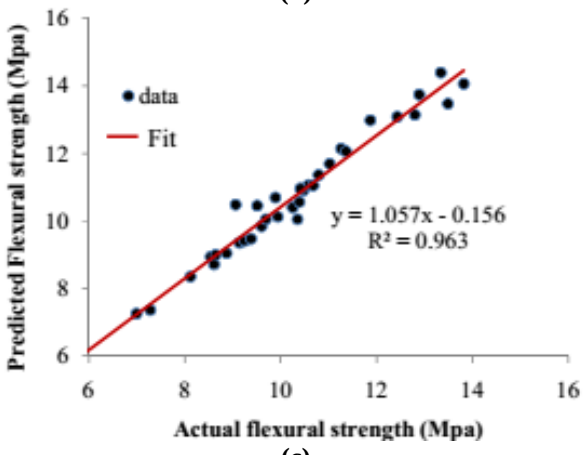

(c)

Fig. 8: Correlation analysis (a) Compressive strength (b) split tensile strength (c) Flexural strength

Table 5, and 6 show the validation results which is achieved in our investigation procedure. In tables, the result of compressive strength split tensile strength and flexural

strength are shown for proposed ANN. This table compares the proposed model into existing techniques (ANN) which depicted for 28 curing days and two w/c ratios. The prediction result predicts the results optimally in proposed ANN model compared to experimental results. The prediction procedure is however easy when no need to make expensive and computational time of mechanical properties. In simulation modeling, the prediction result can be validated by using correlation analysis. A figure 8 shows that the difference of predicted and experimental values, the linear line shows the difference of these values. When compared to experimental values, the predicted result achieves nearly equal. The error value gets reduced in proposed simulation modeling.

5. CONCLUSION

In the proposed research focused to develop the strengthening of high performance concrete using fibers. Two different fibers are used to strengthen the concrete; here hybrid fibers are used to enhance the structures. Three different types of specimens are investigated (cubes, cylinders, and prisms) to find out the compressive strength, split tensile strength, and flexural strength. In this experimental investigation, two types of w/c ratios are used such as 0.38 and 0.28. Totally 34 specimens are examined with varying two fiber percentage. The results of the test are taken by curing specimens for 28 days. The test result showed that the use of hybrid fibers with high percentages is one of the effective and economical methods to improve structural parameters of high performance concrete. Specimens with steel fibers and polypropylene have the highest compressive and splitting tensile strengths, and flexural strengths for two w/c ratios. The maximum compressive strength attains in hybrid specimens HPFRC9 are 93.9 and 102.65 Mpa, split tensile strength is 9.37, and 10.42 Mpa, and flexural strength is 10.79 and 13.82 in both type I and type II w/c ratios (0.38 and 0.28). The validation results of these experimental results are optimally predicted using ANN. ANN gives optimal result which obtains nearly equal to experimental result and it has minimum error. The hybrid fibers work in perfect mix and get enhancements in mechanical performance. The optimization system can improve the effectiveness of the model just as diminishing the computational expenses. For the future study on our research paper, the durability tests on the concrete can be determined for the same above considered materials or for the different materials. The strength properties of the same materials for the different grade of concrete or for higher curing period can be considered.

REFERENCE

[1] Li, B., Chi, Y., Xu, L., Shi, Y. and Li, C., 2018. Experimental investigation on the flexural behavior of steel-polypropylene hybrid fiber reinforced concrete. Construction and Building Materials, 191, pp.80-94.

[2] Meda, A., Rinaldi, Z., Spagnuolo, S., De Rivaz, B. and Giamundo, N., 2019. Hybrid precast tunnel segments in fiber reinforced concrete with glass fiber reinforced bars. Tunnelling and Underground Space Technology, 86, pp.100-112.

[3] Yoddumrong, P., Rodsin, K. and Katawaethwarag, S., 2018, April. Experimental study on compressive behavior of low and normal strength concrete confined by low-cost glass fiber reinforced polymers (GFRP). In 2018 Third International Conference on Engineering Science and Innovative Technology (ESIT) (pp. 1-4). IEEE.

[4] Lee, J.H., 2017. Influence of concrete strength combined with fiber content in the residual flexural strengths of fiber reinforced concrete. Composite Structures, 168, pp.216-225.

[5] Khan, M. and Ali, M., 2018. Effect of super plasticizer on the properties of medium strength concrete prepared with coconut fiber. Construction and Building Materials, 182, pp.703-715.

[6] Abbass, W., Khan, M.I. and Mourad, S., 2018. Evaluation of mechanical properties of steel fiber reinforced concrete with different strengths of concrete. Construction and Building Materials, 168, pp.556-569.

[7] Subbulakshmi, Dr. B. Vidivelli , and K. Nivetha,StrengthBehaviour of High Performance Concrete using Fibres and Industrial by Products,Journal of Engineering Research & Technology,Vol.3(8),pp.1219-1224.

[8] Erdal, H.I., Karakurt, O. and Namli, E., 2013. High performance concrete compressive strength forecasting using ensemble models based on discrete wavelet transform. Engineering Applications of Artificial Intelligence, 26(4), pp.1246-1254.

[9] Mínguez, J., González, D.C. and Vicente, M.A., 2018. Fiber geometrical parameters of fiber-reinforced high strength concrete and their influence on the residual post-peak flexural tensile strength. Construction and Building Materials, 168, pp.906-922.

[10] Bi, Y.Z., Zhang, D.L. and Hu, J.H., 2012. Application of modified polypropylene (crude) fibers concrete to strengthen the support structures in deep mine roadway. Journal of Coal Science and Engineering (China), 18(4), pp.379-384.

[11] Younis, K.H., Ahmed, F.S. and Najim, K.B., 2018, September. Effect of Recycled-Steel Fibers on Compressive Strength and Shrinkage Behavior of Self-Compacting Concrete. In 2018 11th International Conference on Developments in eSystems Engineering (DeSE) (pp. 268-272). IEEE.

[12] Guo, R., Bi, Z. and Wang, F., 2016, August. Influence of different mixing methods on the axial compressive strength of basalt fiber recycled concrete. In 2016 3rd International Conference on

Informative and Cybernetics for Computational Social Systems (ICCSS) (pp. 368-371). IEEE.

[13] Alzyoud, S. and Ziadat, A., Effect of fibers on concrete fresh, mechanical and transport properties. In 2018 Advances in Science and Engineering Technology International Conferences (ASET) (pp. 1-5). IEEE.

[14] Abbass, W., Khan, M.I. and Mourad, S., 2018. Evaluation of mechanical properties of steel fiber reinforced concrete with different strengths of concrete. Construction and Building Materials, 168, pp.556-569.

[15] Khan, M. and Ali, M., 2018. Effect of super plasticizer on the properties of medium strength concrete prepared with coconut fiber. Construction and Building Materials, 182, pp.703-715.

[16] Abdalla, J.A., Hawileh, R. and Al-Tamimi, A., 2011, April. Prediction of FRP-concrete ultimate bond strength using Artificial Neural Network. In 2011 Fourth International Conference on Modeling, Simulation and Applied Optimization (pp. 1-4). IEEE.

[17] Mohebi, Z.H., Bahnamiri, A.B. and Dehestani, M., 2019. Effect of polypropylene fibers on bond performance of reinforcing bars in high strength concrete. Construction and Building Materials, 215, pp.401-409.

[18] deAlencarMonteiro, V.M., Lima, L.R. and de Andrade Silva, F., 2018. On the mechanical behavior of polypropylene, steel and hybrid fiber reinforced self-consolidating concrete. Construction and Building Materials, 188, pp.280-291.

[19] Rahman, N.A., Hassan, A., Yahya, R., Lafia-Araga, R.A. and Hornsby, P.R., 2012. Polypropylene/glass fiber/nanoclay hybrid composites: morphological, thermal, dynamic mechanical and impact behaviors. Journal of Reinforced Plastics and Composites, 31(18), pp.1247-1257.

[20] Huang, L., Xu, L., Chi, Y., Deng, F. and Zhang, A., 2019. Bond strength of deformed bar embedded in steel-polypropylene hybrid fiber reinforced concrete. Construction and Building Materials, 218, pp.176-192.

[21] Zahiri, F. and Eskandari-Naddaf, H., Optimizing the compressive strength of concrete containing micro-silica, nano-silica, and polypropylene fibers using extreme vertices mixture design. Frontiers of Structural and Civil Engineering, pp.1-10.

[22] Hassan, A., Khairallah, F., Mamdouh, H. and Kamal, M., 2019. Structural behaviour of self-compacting concrete columns reinforced by steel and glass fibre-reinforced polymer rebars under eccentric loads. *Engineering Structures*, *188*, pp.717-728.

[23] de Souza Castoldi, R., de Souza, L.M.S. and de Andrade Silva, F., 2019. Comparative study on the mechanical behavior and durability of polypropylene and sisal fiber reinforced concretes. Construction and Building Materials, 211, pp.617-628.

[24] Awolusi, T.F., Oke, O.L., Akinkurolere, O.O., Sojobi, A.O. and Aluko, O.G., 2019. Performance comparison of neural network training algorithms in the modeling properties of steel fiber reinforced concrete. Heliyon, 5(1), p.e01115.

[25] Mashhadban, H., Kutanaei, S.S. and Sayarinejad, M.A., 2016. Prediction and modeling of mechanical properties in fiber reinforced self-compacting concrete using particle swarm optimization algorithm and artificial neural network. Construction and Building Materials, 119, pp.277-287.

Application of Splines for Approximation

[1] Kallur V Vijayakumar, [2] A.S. Hariprasad, [3] H. T. Rathod

[1] Assistant Professor, Department of Mathematics, BMSIT&M. Bengaluru, India
[2] Professor & Head, Department of Mathematics, RRCE, Bengaluru, India
[3] Former Professor, Department of Mathematics, Central College, Bengaluru, India

Abstract:

We consider the application of splines to function and integral function approximations, where the integral function refers to the indefinite integral whose lower limit is a constant and upper limit is a variable or function of a variable. Integral function approximation are very useful, one simple and immediate application refers to the construction of a table of integral for example the table of logarithms, normal distribution etc, other applications are possible in the evaluation of multiple integrals over triangular and tetrahedral regions to name a few.

Keywords:

Splines, Approximation

1. INTRODUCTION

A qauartic spline that interpolates the first derivatives of the given function at the knots and the second derivatives between them is discussed. A feasible algorithm for the determination of the quartic spline for the second derivative parameter λ =0, 1/2, 1 is presented. We consider the application of quartic splines to function and integral function approximations, where the integral function refers to the indefinite integral whose lower limit is a constant and upper limit is a variable or function of a variable. Integral function approximation are very useful in the construction of a table of integral, for example the table of logarithms, normal distribution etc, other applications are possible in the evaluation of multiple integrals over triangular and tetrahedral regions. In this paper, we limit ourselves to simple application that is when the upper limit is a variable. A method based on spline integration to approximate the integral function is presented and compared the performance of quartic spline with standard cubic splines with the aid of graphs by using MATLAB programming.

2. SPLINES & QUARTIC SPLINE INTERPOLANT

The spline is a flexible strip used to produce a smooth curve through a designated set of points. In computer graphics the term spline curve refers any composite curve forms with polynomial sections satisfying specified continuity conditions at the boundary of the pieces. A spline function is a function that consists of polynomial pieces joined together with certain smoothness conditions. A simple example is the polygonal function (or spline of degree 1), whose pieces are linear polynomials joined together to achieve continuity, as in figure below. The points $t_0, t_1, t_2, \ldots\ldots, t_n$ at which the function changes its character are turned knots in the theory of splines. Thus, the spline function shown in below figure has eight knots.

Figure First-degree spline function

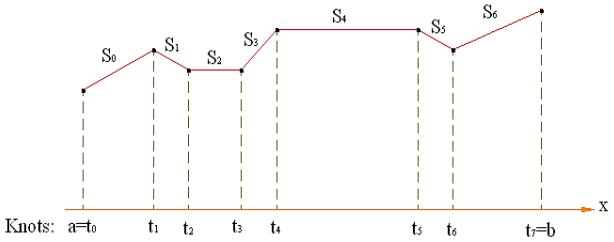

Such a function appears complicated when defined in explicit terms. So we write

$$S(x) = \begin{cases} S_0(x) & x \in [t_0, t_1] \\ S_1(x) & x \in [t_1, t_2] \\ & \vdots \\ & \vdots \\ S_{n-1}(x) & x \in [t_{n-1}, t_n] \end{cases}$$

Where $S_i(x) = a_i x + b_i$ because each piece of $S(x)$ is a linear polynomial. Such a function $S(x)$ is piecewise linear.

Spline of degree k

A function S is called a spline of degree k if:

1. The domain of S is an interval [a, b].
2. $S, S', S'', \ldots., S^{(k-1)}$ are all continuous functions on [a, b].
3. There are points t_i(called knots of S) such that $a = t_0 < t_1 < t_2 < \ldots\ldots, < t_n = b$ and S is a polynomial of degree at most k on each subinterval $[t_i, t_{i+1}]$.

Higher degree splines are used whenever more smoothness is needed in the approximating function. From the definition of a spline function of degree k, we see that such a function will be continuous and have continuous derivatives $S', S'', \ldots. S^{k-1}$. If we want the approximating spline to have a continuous mth derivative, a spline of degree atleast $m + 1$ is selected. Consider a situation in which knots $t_0 < t_1 < t_2 < \ldots\ldots, < t_n$ have been prescribed. Suppose that piecewise polynomial of degree m is to be defined with

 ISBN: 978-93-90214-20-4

its pieces are joined at the knots in such a way that the resulting spline S has m continuous derivatives. At a typical interior knot t, we have the following circumstances. To the left of t, $S(x) = p(x)$; to the right of t, $S(x) = q(x)$, where p and q are mth degree polynomials. The continuity of mth derivatrive S^mimplies the continuity of the lower order derivatives $S^{m-1}, S^{m-2}, \ldots . S', S$. Therefor, at the knot t,

$$\lim_{x \to t^-} S^{(k)}(x) = \lim_{x \to t^+} S^{(k)}(x) \qquad (0 \le k \le m)$$

From which we conclude that $\lim_{x \to t^-} p^{(k)}(x) = \lim_{x \to t^+} q^{(k)}(x) \qquad (0 \le k \le m)$

Since p and q are polynomials their derivatives of all orders are continuous and so the above equation is same as

$$p^{(k)}(t) = q^{(k)}(t) \qquad (0 \le k \le m)$$

This condition forces p and q to be the same polynomial because by Taylor's theorem,

$$p(x) = \sum_{k=0}^{m} \frac{1}{k!} p^{(k)}(t)(x-t)^k = \sum_{k=0}^{m} \frac{1}{k!} q^{(k)}(t)(x-t)^k = q(x)$$

This argument can be applied at each of the interior knots $t_0, t_1, t_2, \ldots \ldots t_{n-1}, t_n$ see that S is a simply one polynomial throughout the entire interval. Thus we need a piecewise polynomial of degree $m+1$ with at most m continuous derivatives in order to have a spline function that is not just a single polynomial throughout the entire interval. We need to keep in mind that the ordinary polynomials do not serve well in the curve fitting.

3. QUARTIC SPLINE INTERPOLANT

Let *f* be a function defined on the interval [a,b] and let the knots $\{x_i\}_{i=0}^{N+1}$ $a = x_0 < x_1 < x_2 < \ldots\ldots < x_N < x_{N+1} = b$ be the (*N*+1) distinct points. Note that x_i 's divide [a, b] into *N*+1 subintervals. A function *S* is said to be a quartic spline on the interval [a, b], if S, S', S'' *and* S''' are continuous in [a, b] and S is a polynomial of degree ≤ 4 in each knot interval $[x_{i-1}, x_i]$. We now consider a standard form of quartic spline interpolant.

Given the real numbers $f_i'(i = 0,1,2, \ldots . N+1)$, $f''_{i+\lambda}(i = 0,1,2, \ldots . N), f_0$ *and* f_{N+1}, then there exists a unique quartic spline function S (*x*) such that

(1) On each subinterval $[x_i, x_{i+1}], i = 0, 1, 2, \ldots, N$, S(*x*) coincides with the quartic polynomial $S(x) = S_i(u) = a_i + b_i u + c_i u^2 + d_i u^3 + e_i u^4$, $u = \frac{x - x_i}{h}, h = x_{j+1} - x_j, 0 \le u \le 1.$ (1.2.1)

(2) S, S' *and* S''satisfy the interpolatory conditions $S'(x_i) = S_i' = f_i', i = 0.1.2 \ldots . N+1$

$s''(x_i + \lambda h) = s''_{i+\lambda} = f''_{i+\lambda},\ i = 0, 1, 2 \ldots . N$, $s(x_0) = s_0 = f_0,\ s(x_{N+1}) = s_{N+1} = f_{N+1}$

when ever $0 \le \lambda \le 1, \lambda \ne \frac{3 \pm \sqrt{3}}{6}$ and N is even if $\lambda = \frac{1}{2}$.

APPLICATIONS

Function Approximations

Let us consider the integral representation $\int_a^x f'(t)dt = f(x) - f(a),\ if\ f(t) = \int f'(t)dt$

Clearly *f*(*a*) is arbitrary and if *f*(*a*) = 0, we can write $f(x) = \int_a^x f'(t)dt \quad with\ f(t) = \int f'(t)dt$

Example 1: Let $f'(t) = \frac{1}{t}$ then $\int_1^x \frac{dt}{t} = f(x)$ since $f(t) = \int f'(t)dt = \int \frac{dt}{t} \quad and\ f(1) = 0$

Example 2: Let $f'(t) = \frac{1}{t+1}$ then $\int_1^x \frac{dt}{t+1} = f(x) - f(1)$where $f(t) = \int f'(t)dt = \int \frac{dt}{t+1} = \log(t+1) \quad and\ f(1) = log2.$

The above subtle points must be noted while applying the quartic spline algorithm to numerical integration. Thus quartic spline approximation for $F(x) = f(x) - f(a)$, with $f(t) = \int f'(t)dt$ is suggested for the application. Suitable caution must be taken while programming.

Now consider the Runge Function as an example $f(x) = \frac{1}{1+25\,x^2}, x \epsilon [-1,1]$

and find approximation of this by quartic spline.

Let $F(x) = \int_{-1}^x f'(t)dt = \frac{1}{1+25\,x^2} - \frac{1}{26} = f(x) - \frac{1}{26}, x \epsilon [-1,1]$

we observe that $F(-1) = F(1) = 0 \quad and\ F'(x) = f'(x),\ F''(x) = f''(x)$

Hence, the application of the quartic spline theory proposed in the previous section computes the sequence $\{F(x_i)\}_{i=1}^{N}$, assuming $F(x_0)$and $F(x_{N+2})$ as known values. Thus to obtain the approximations to Runge's function $\{f(x_i)\}_{i=0}^{N+2}$, we have to use the functional relation $f(x) = F(x) + \frac{1}{26}$. We have discussed this for the cases λ=0, 0.5, 1 through MATLAB.

4. ERROR PLOTS FOR CUBIC AND QUARTIC SPLINES

We have also displayed error plots for standard cubic splines (natural clamped and not a knot splines) and superposed these plots by quartic splines for λ=0, 1/2 and 1. We find that the performance of quartic splines is superior compared with the standard cubic splines.

5. CONCLUSIONS

We have discussed the function approximation, integral function approximation using quartic spline interpolant. Performance of the proposed quartic spline is compared with the standard cubic splines (natural, clamped and not a knot splines).

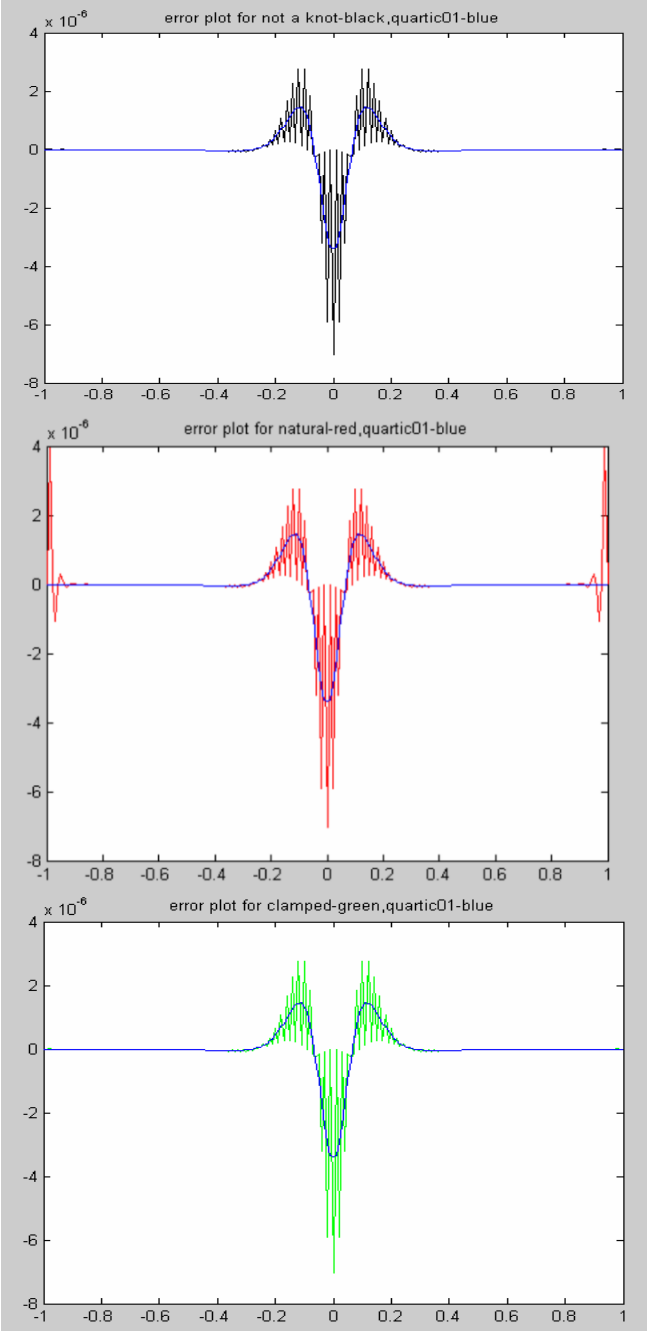

REFERENCE

[1] Arshad Khan, Islam Khan and Tariq Aziz, A survey on parametric spline function approximation, Applied Mathematics and Computational, 171, 983 – 1003 (2005).

[2] De Boor C., On uniform approximation by splines, J. Approx. Theory I, 219–235, (1968).

[3] De Boor C., Practical Guide to Splines, Springer – Verlag, Berlin, New York (1978).

[4] Herriot, J. G. and Reinsch, C. H., Algorithm 507, procedures for Quintic Natural Splines Interpolation ACM Transactions on Mathematical Software, 2(3), 281- 289 (1976).

[5] Hossein Behforooz G,. A new approach to spline functions, Applied Numerical Mathematics, 13(4), 271-276(1993).

[6] Joshi, T. C and Saxena, R. B: on quartic Spline interpolation, Ganita 33, 97 -111(1982).

[7] Micula C., Sanda Micula, Hand Book of Splines, Kluwer Academic Publishers (1999).

[8] Phythian, J. E and Williams R: Direct cubic spline approximations to integrals with applications in nautical, International Journal for Numerical Methods in Engineering, 23, 305 – 315 (1986).

[9] Prasad J. and Verma, A. K., Lacunary interpolation by quintic splines, SIAM. Journal of Numerical Analysis, 16(6), 1075 – 1079 (1979).

[10] Sallam S., W. Ameen Numerical solution of general nth-order differential equations via splines Applied Numerical Mathematics, 6(3), 1990, 225-238.

[11] Sommariva A. and M. Vianello, Gauss-Green Cubature over spline curvilinear polygons, Applied Mathematics and Computation 183(2), 1098 - 1107 (2006)

[12] Stroud A.H and D. Secrist, Gaussian Quadrature Formulas, Prentice hall, Englewood Clifs , New jersey, 1966.

[13] Tarazi El, M. N and Sallam, S: On quartic splines with application to quadrature, computing 38, pp 355-361 (1987).

Economic Crimes a Great Threat to Nation with Special Focus to Banking, and Cyber Related Economic Crimes

Arun Kumar Jain

Research Scholar, Manipal University, Jaipur, India

Abstract:

Bank fraud is the use of potentially illegal means to obtain money, assets, or other property owned or held by a financial institution, or to obtain money from depositors by fraudulently posing as a bank or other financial institution.

Some of the above crimes are also covered FEMA. This process creates a channel to hide the original or true nature of the funds. Money laundering is the process of converting the nature from black money to white money with the objective of hiding its source and enabling it to be used later in a legal form.

Keywords:

Economic Crimes, Cyber, Banking, Threat, Crimes, Economic

1. INTRODUCTION

Bank is a financial institution which is treated as a very strong support system to the financial system of a country in which place a key role in economic and financial development of a nation.

Bank performs the duty as intermediary in rooting the funds from surplus units to deficit units to the fully and optimum utilization of funds.

The nation which have efficient banking system has a significant positive external benefits which increase the economic transaction in general.

In the recent error there is a big transformation in banking system from the traditional ways of manual intervention to automation and system based/computer based banking system.

The level of growth of a nation depends on the quality of the financial institutions and banking system.

The term finance in our words can be understood as equivalent to money and the word system in the term financial system employees a set of complexities and interconnected institutions agents practices market transactions liabilities and claims in the economy.

Reliance Market can be understood as a market in which financial assets are generated or transferred or destroyed.

Bank plays a vital role in the movement of currency Alia the physical currency notes were transferred through manual intervention and now it can be transferred through banking channels easily and Bank plays a key role in movement of currency also.

It contains market for government securities corporate securities foreign exchange derivatives short term finance or money market and capital market sector and its portfolio.

Financial system service in the form of services that are important in a modern economy.

Banking system facilitates trade and market and hence specialization and production.

Indian financial system can be divided into two groups one is organized sector and another is unorganized sector.

Financial system is also divided for distributed in two users of financial services and providers.

Financial institutions sell their services to household businesses and government and public stakeholders they are the uses of financial services.

2. ORGANIZED INDIAN FINANCIAL SYSTEM

The system comprises of an effective network of banks and other financial and investment institutions and range of financial instruments. They can together function in various development capital and money markets for the nation short term funds are mainly provided by the commercial and cooperative banking structure.

The organized financial system consists of these systems banking system cooperative system developed banking system that is public and private money markets financial companies.

3. UNORGANIZED FINANCIAL SYSTEM

Unorganized financial system consists of less controlled money lenders lending pawnbrokers landlords extra in this form the financial system is not directly controlled by the RBI.

There are other investment agencies companies and chit funds which are also not regulated by RBI or government in a systematic manner.

However there also controlled by rules and regulations and are therefore within the Ambit of the monetary authorities

as the World bank is an organisation for receiving storing providing money and other financial mechanism to different stakeholders with the economy and assisting them in deploying these funds in productive activities the state of bank in financial sector could be described as a classical example of financial repression until the beginning of 1990 era.

Banking system in India is performed in two ways private sector banking and public sector banking there are so many banks which has been nationalized and there are so many banks which are working in an private manner the controls of RBI are applicable to all of them but the ownership position is different in private sector and public sector banks.

By virtue of increasing competition day by day, as you think that there are two sides of every coin one is positive science and second is negative side so when we look up on the positive aspect of banking increasing channel then we see the economic growth and very dynamic approaches for the betterment of our society in the form of economic assistance.

In the tough competitive environment the risk of economic crimes is increasing day by day in the form of frauds socio-economic crimes and other manners.

Although the competition is a sign of growth and progress this importance has also being understood by the reserve Bank of India when it was observed that competition is expected by the private sector banks and other liberal entities branches of foreign banks also.

Before some competitive diversification of ownership is also selected by public sector banks and private sector banks the new sector that is private sector has energized and increase the level of growth in Indian banking sector as a whole and a new technology is now in the form new products are being introduced continuously and new business practices have become common.

Now we would analyze the types of economic crimes which are faced by banking industry the reasons the impact and the analysis and the people behind in the cause behind and the motive behind search crimes will be described in the brief.

Because of the technological development and rapid growth and changes in business scenario recently the activities of banking sector and its growth since nationalization have given reforms by the government of India during the last 50 years has impacted Indian economy.

In developing countries the bank plays a very major role and it has acquired some new dimensions.

In 21st century the actual and expected contribution of banking sector in the market is very important towards the development of national economy probably India may be the first country in the developing economy of the world which has taken such initiatives in merging technology with its development initiatives at all levels.

The challenge of development is to improve the quality of life especially in the poor world's countries a better quality of life generally calls for hiring in comes but it involves more much more it encompasses essence in themselves better education high standards of health and nutrition less poverty and a clean environment more equality of opportunity greater individual freedom richer cultural life.

After the independence the banking did not remained in the passive role of money keeping money lender only but also became active participant in the economic growth of a nation with the establishment and incorporation of reserve Bank of India as the central bank in 1934 and national eyes Asian of the State Bank of India in 1955 these two banks were given a defined role for the development of the nation by Central Government of India.

After sometime it was felt by the government that the role of RBI and SBI are not sufficient to deal with the needs of this country hens some bold decisions taken and in 1969 in 1984 3 and 6 major private banks were nationalized.

This action of nationalization of private banks into a nationalized bank played a vital role for the banks in place of their traditional commercial rule that was assigned to them in their place of incorporation through nationalization the European banking system received the finite indianised characteristics and became a permanent tool of Indian financial system.

Banking system is the engine to drive the economy of India to achieve the goal of welfare state as well as the cope with the international developments in 20th century recently it has Cyber crime is a term used to broadly described criminal activity in which computers or computer networks are a tool, a target or a place of criminal activity and include everything from electronic cracking to denial of service attacks. It is also used to include traditional crimes in which computer or networks are used to enable the illicit activity.

4. INTRODUCTION:

Information technology and internet worldwide has been inevitable in every activity of mankind. Like any other technology it has also it’s pro and cons for the economies of the world as far as its economic aspects are concerned. We are witnessing daily the cyber crime or computer backed assisted and generated crime in the economy of world at every place of the globe as computers are every place of the globe so the reach of the cyber criminals are also at every place and corner of the world.

Cyber crime includes the crime which are committing by the highly skilled professionals of the modern technology and computer knowledge along with the other disciplinary knowledge off finance management, law and communication which makes them culprits of the perpetrators highly dangerous and equipped in the crime commitment in a manner that cannot be supervised me, investigated or controlled by traditional police, administration and the skill of the traditional policing system as these perpetrators are very much skilled, slid, dynamic, and professional cum intelligent in learning the new development in the technology which our traditional law and order responsible police is certainly not.

The traditional police and its staff with tools of knowledge and skill with qualification along with the diversified duties in the traditional crimes are helpless to curb such super criminals.

A cyber mob attack refers to a large group which tries online to shame or threaten a target. In this type of crime, collectively trolled to an individual with the hope of publicly punishing such individual and if it has an economic object then it is converted into cyber economic crime.

Cyber stalking means a course of conduct with the object to kill or harass or intend to kill or injure a target so that the target should suffer fear and extreme emotional distress. One example we can quote that a freelance journalist was targeted of cyber stalking from a man and it is very common in the developed countries like US and Europe.

In the cyber economic crimes, computer is used as a tool and it is not a target for a perpetrator. The perpetrator of old traditional crimes like pick picketers, thrives, robbers etc. have acquired technical expertise and going tech savvy using computer for online economic crime instead of offline crimes.

5. CONCLUSION

Crimes takes place due to weakness in systems. Fraudsters target weakness in banks.

Weakness in one bank affect the whole industry. Some of the measure to control these crime are:-

1. Improve searches with technology.
2. We should have regular cross communication and meetings.
3. We should use engineering and engineers to find loop holes in systems.
4. Banks and all other companies should follow a proper system of every work.
5. Regular training and other motivational program should be organized.

The best approach is to start with a multi-factor authentication/multi-layered security structure. This multi-layered approach from a software perspective, combined with old-fashioned out-of-band phone calls to the customer to confirm a questionable transaction, can cut the institution's headaches and the business' fraud losses.

Reconcilement of banking accounts and transactions on a daily basis -- either at end of day or at least at the beginning. This will help catch any transactions you didn't make, and the sooner you bring it to your bank's attention, the better chance to retrieve the money, with the bank doing a recall or reversal of the transaction. The longer you wait, the less likely it is that you'll see that money recovered.

Independent assessment of the vulnerability of your business to cybercrime and data leakage • Propose a response to security breaches and cybercrime attacks • Investigate incidents of cyber attacks and data leakages and identify the root causes (such as who was involved, who it happened to and how to ensure it does not happen again)

Fraud awareness programs should be organized.

REFERENCE

[1] https://www.bankinfosecurity.com/5-tips-to-reduce-banking-fraud-a-2534

[2] https://legal.thomsonreuters.com/en/insights/white-papers/combating-money-laundering-five-ways-to-help.

[3] https://www.pwc.com/cz/en/bankovnictvi/assets/pdf/pwc-forensic-capability-brochure.pdf

A Study on Predictive Maintenance Analytics Approach using Deep Learning Algorithms for Fault Detection in Smart Manufacturing

[1] Shaila Mary J, [2] Dr. Ajitha S

[1] Assistant Professor, Mount Carmel College, Bengaluru, India
[2] Associate Professor, Ramaiah Institute of Technology, Bengaluru, India

Abstract:

The latest developments in the Internet of Things (IoT) are giving rise to the growth of interconnected devices, facilitating numerous usage of smart applications in every sector, particularly manufacturing industry. These enormous number of IoT devices produces a large volume of data that require smart big data analysis and processing methods, such as Deep Learning (DL). Remarkably, the DL algorithms combined with Predictive Maintenance (PdM) approach, when applied in the Industrial Internet of Things (IIoT), can enable several applications such as smart assembling, smart manufacturing, efficient networking, machine fault detection and thereby predicting and managing the downtime of machine assets. In this paper, we present the key possibilities of Deep Learning in Industrial Internet of Things (IIoT). Firstly, we review different DL techniques, such as convolutional neural networks, auto-encoders, and recurrent neural networks and their usage in fault detection in manufacturing industries. Then we reviewed and outlined a comparative study on deep learning models for machine fault detection. Also, we identify some research challenges concerning the effective design and appropriate implementation of PdM framework in IIoT for machine fault detection.

Keywords:

Auto-encoders, Convolutional Neural Networks, Deep Learning, Industrial Internet of Things, Recurrent Neural Networks, Smart industries

1. INTRODUCTION

In recent years, with the trend of smart manufacturing, industry has augmented attention on artificial intelligence and machine learning techniques due to their ability of creating automated models that handle the big amount of data collected, which is growing exponentially. Industries are under continuous pressure – to increase product quality, improve factory efficacy, stay competitive, and boost security to remain sustainable and profitable. The visualization of Industry 4.0, otherwise known as the fourth industrial revolution, is the amalgamation of smart computing and network technologies in production and manufacturing industries for the purposes of automation, reliability, and efficient productivity, implicating the development of an Industrial Internet of Things (IIoT).

The term Industrial AI (Artificial Intelligence) is gaining more prominence and emerging as a key changer in today's world. It is defined as **"AI relating to the physical operations and systems of an industrial enterprise".** "AI-driven systems can automate and reinvent fundamental industrial processes e.g., from product development and manufacturing to supply-chain and field operations" [1]. In Industrial AI market report the focus of this report is on IIoT (Industrial Internet of Things) where Artificial Intelligence predominantly is performed on IoT-type data sources of industrial enterprises on machine components (e.g., bearings, pumps, conveyers, turbines, motors) PLCs / Industrial PCs / Gateways / Controllers, industrial assets in the field (e.g., pipelines), robots, containers, trucks, ships in logistics, warehouses and many more [1]. Deep learning is being extensively used for data analytics in IoT applications. The role of deep learning models in analyzing highly complex heterogeneous IoT data is remarkable though it poses several challenges it has given much impetus to the researchers to investigate in the use case of fault detection in smart manufacturing [2].

2. INDUSTRIAL INTERNET OF THINGS (IIoT)

The industrial internet of things (IIoT) refers to the usage of the internet of things (IoT) devices and sensors in manufacturing industries. IIoT embraces technologies like machine learning, big data analytics, PLC (Programmable logic controller) and SCADA (Supervisory control and Data acquisition). It also implements automation technology for self-diagnosis of machines. [3]. IIoT also focuses on machine-to-machine (M2M) communication, big data, and machine learning that allows industries and enterprises to have better productivity and efficiency in their operations by reducing the downtime of machine assets.

A. IIoT and Big data

Smart factory requires smart data and it is evident that the data generated due to massive deployment of sensors and IoT devices in industrial machines gives rise to big data. The following set of challenges for smart factory are identified as follows [4]:

- ***Data Management and Lifecycle*** – the challenge is to effectively manage heterogeneity and integration of data generated and collected from various sources
- ***Data processing architecture*** – the challenge is to ensure data processing in real time that is architectures have to be scalable and elastic, also whether processing to be done on premises or in the cloud
- ***Data analytics*** – the challenge is to provide advanced algorithms for the multi perspective semantic representation across different data sets in smart manufacturing to develop predictive and prescriptive analytics for automated machine configurations without human intervention
- ***Data protection and security*** – the challenge is ensure the privacy of sensitive industrial data and protection against cyber-attacks, access control and data integrity
- ***Data Visualization*** –the challenge is to present data in natural language interaction interfaces

B. DL techniques in IIoT

Deep Learning is a subset of Machine Learning. The typical aspect of Deep Learning is the accurateness and efficacy of the model, when trained with large amount of data. Deep Learning systems can match and even exceed the intellectual powers of the human brain. It is extensively accredited that choosing the correct DL framework for the specific applications becomes a difficult task for many research investigators, developers and scientists. Deep learning in the field of equipment maintenance and fault diagnosis is still in the experimental stage, for the manufacturing industry sector, IoT and cyber-physical systems (CPS) are the fundamental elements towards smart manufacturing. (Industry 4.0). Given that high-accuracy smart systems is critical in such applications, it directly leads to increased efficiency and productivity, along with decreased maintenance overheads and operation expenses. Consequently, DL can play a vital role in the area of fault diagnosis [5].

3. PREDICTIVE MAINTENANCE ANALYTICS IN INDUSTRY 4.0

Predictive maintenance refer to a set of procedures to precisely monitor the **current condition** of devices or any type of equipment, using either **local** or **cloud analytics applications** to predict impending device failure by using **real-time analytics** and **supervised or unsupervised deep learning models.**

PdM 4.0 is a paradigm shift which is all about predicting future failures in machine assets and then prescribing the most effective preventive measure by applying advanced big data analytic techniques about mechanical condition, usage history, environment, maintenance schedule of a machine asset. A predictive maintenance (PdM) policy uses deep learning methods to determine the health condition of machine so as to preemptively perform maintenance to defer adverse machine performance.

Maintenance strategies are designed to avoid and decrease the rate of machine failures and the expenses associated. Failures can be defined as any change or anomaly in the system causing an unsatisfactory level of performance. The impact of failure in a critical machine is a tremendous risk to the downtime costs and, it in turn becomes bottleneck in production operations. Machine failure can be triggered by normal degradation due to continuous usage and accidental failure [6].

Predictive maintenance applies deep learning models and big data analytical methods to proactively predict an impending machine failure, it then delivers the resulting statistics and suggests maintenance schedules to the IT departments to take immediate action. Figure 1 gives the general classification of maintenance approaches implemented commonly in machine industries.

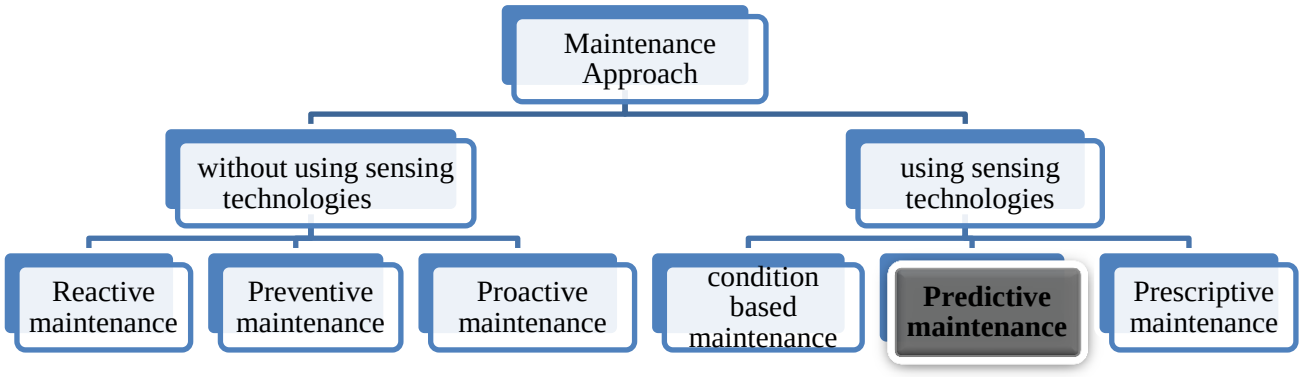

Figure 1 - General classification of Maintenance approach/strategies

4. IV TAXONOMY OF DEEP LEARNING MODELS FOR FAULT DETECTION

The application of traditional ML techniques on large datasets exposes few vulnerabilities of these models, such as the inability to deal with the high dimensionality of the data feature space, and changing data aggregation. Alternatively, DL refers to techniques for learning high-level features from data in a hierarchical manner using

weighted layer architectures. Four main groups of DL architectures commonly used are [7]:

- AutoEncoders (AE)
- Convolutional Neural Networks (CNN)
- Deep Belief Networks (DBN)
- Recurrent Neural Networks (RNN)

In the above background, we carried out a study on categories of DL models used particularly for machine fault detection and is presented in Table 1.

Table 1: Summary of deep learning models for fault detection

Model & its variants	Learning Model	Typical Input Data	Characteristics	Limitations	Machine/ Equipment
AE [8 - 12] Sparse AE Denoising AE Contractive AE Stacked AE Deep AE	Unsupervised	Heterogeneous multivariate complex data sets	Commonly used in image denoising, feature extraction and dimensionality reduction	Constrained to data that is similar to its training data	Chemical Industrial process/machine pump/wind turbine/elevator systems
CNN [13 - 17] 1DCNN IFCNN FDCCNN	Supervised	Image, sound, multivariate sensor signals	Widely used in computer vision – suitable for machine fault detection by extracting features of 2D image data, accuracy rate is high with fixed environment	Not suitable for detecting faults of objects in dynamic real time environment Requires large training datasets	Electric Motor/bearing/ wind turbine/gear/compressor/petrochemical pump/semiconductor
DBN [18 - 22]	Supervised, Unsupervised	Heterogeneous multivariate data sets	Strong ability to extract features High recognition of fault rates	Not suitable for small test data sets, involves high computational costs	Aircraft rolling bearing/Railway Wagon Wheel set/transformer/photovoltaic array/gas regulator
RNN [23- 27]	Supervised	Heterogeneous multivariate time series sequential data	Commonly used in identifying faults characterized by long term temporal dependencies	Not suitable for long sequences of data, computationally slow	Underwater Robots/Railway track circuit/Electrical Gas generator

5. V PREDICTIVE MAINTENANCE FRAMEWORKS IN SMART MANUFACTURING

In this study, we reviewed few PdM frameworks implemented in smart manufacturing which has been outlined in table 1, though there are features and limitations in each of the framework there is no common process flow for the PdM framework due to product and data heterogeneity. So there is a need for developing PdM framework in smart manufacturing which can be generalized and could lead to a paradigm shift - Maintenance as a Service/Software (MaaS) where machines can “self-diagnose” or “auto correct” and schedule maintenance resulting in entirely programmed maintenance workflow. This could lead to more research avenues where maintenance policies implemented in production industries can be fully automated without human intervention.

Table 2: Summary of some existing predictive maintenance frameworks in smart manufacturing

Predictive Maintenance Framework	Features/Advantages	Data Analytics Algorithms Used	Limitations
Prophesy[28]	The platform facilitates integration of various analytics algorithms and methods to predict and forecast with parameters such as RUL.(Remaining Useful Life)	1. RNN (Recurrent Neural Network) 2. LSTM (Long Short Term Memory)	Not generic but specific that is product based
iSTEP[29]	A robust model for feature filtering, feature ranking and down sampling.	1. RF (Random Forest) 2. LR (Linear Regression) 3. SVM (Support Vector Machine) 4. GBT (Gradient Boosting Tree)	Evaluation of different down-sampling ratios for the non-failure class needs to be addressed and more complex self-tuning strategies have to be developed.
REDTag[30]	Used to early predict the breakages of shipped packages by remote monitoring.	1. GBT (Gradient Boosting Tree) 2. SVM (Support Vector Machine) 3. LR (Linear Regression)	Dynamic self-tuning approaches in the predictive patterns from the assimilated data is not investigated.
PdM 4.0[31]	A functional system that allows the implementation of intelligent PdM.	1. .ANN (Artificial Neural Network) 2. DT(Decision Tree) 3. SVM 4. K-NN(K – Nearest Neighbor) 5. PCA(Principal Component Analysis) 6. CNN(Convolution Neural Network) 7. AE(Auto Encoder) 8. DBN(Deep Belief Network)	Fusing multi-source data, identification/prediction accuracy, optimizing maintenance scheduling challenges are not met No clear standards for PdM defined and large dataset adds on to the scalability problem, data visualization and class imbalance issues.
Predictive Maintenance Framework for Conveyor Motors Using Dual Time-Series Imaging and CNN[32]	Accurate predictive maintenance flags for conveyor motors are classified.	1. ANN(Artificial Neural Network) 2. CNN(Convolution Neural Network 3. DBN(Deep Belief Network) 4. RNN(Recurrent Neural Network) 5. SAE(Sparse Auto Encoder)	Diverse data types are not included such as non-linear time series input. Also over fitting issues and dimensionality problems
FIWARE[33]	Is a data driven open source platform for predictive maintenance.	1. RNN (Recurrent Neural Network) 2. HMM (Hidden Markov Model) 3. LSTM (Long Short Term Memory)	Optimal predictive maintenance schedule plan needs to be developed.
PROGRAMS – PROGnostics based Reliability Analysis for Maintenance Scheduling[34]	An combination of long and short term prediction in a multi-stage predictive maintenance framework.	1. ANN (Artificial Neural Network) 2. Data driven Algorithms	Needs huge computational and simulation time

6. CONCLUSION

In this study, we have noted that there is a requirement for real time data sets and large training data for generating accurate results, then the issues of big data analytics such as high dimensionality, feature extraction, imbalance data, and heterogeneity so on needs to be addressed. Also there is no generic PdM framework with deep learning models to be applied for machine fault detection in smart manufacturing. Research has to be focused on developing more robust specific deep learning models for fault detection of equipment to make Maintenance as a Service (MaaS) a reality.

REFERENCE

[1] Misha Rykov, Knud Lasse Lueth, Padraig Scully, Eugenio Pasqua, "Industrial AI Market Report 2019-2025" – published in www.iot-analytics.com, 2019.

[2] Tausifa Jan Saleem, Mohammad Ahsan Chishti (2019) "Deep Learning for Internet of Things Data Analytics." Procedia Computer Science 163(2019): 381-390.

[3] Karmakar, Avish & Dey, Naiwrita & Baral, Tapadyuti & Chowdhury, Manojeet & Rehan, Md. (2019)," Industrial Internet of Things: A Review 1-6." 10.1109/OPTRONIX.2019.8862436.

[4] https://www.bdva.eu/node/1002, A Discussion Paper on Big Data challenges for BDVA and EFFRA Research & Innovation roadmaps alignment, version 1, 2018.

[5] M. Mohammadi, A. Al-Fuqaha, S. Sorour and M. Guizani, "Deep Learning for IoT Big Data and Streaming Analytics: A Survey," in *IEEE Communications Surveys & Tutorials*, vol. 20, no. 4, pp. 2923-2960, Fourthquarter 2018, doi: 10.1109/COMST.2018.2844341.

[6] Lee, C. & Cao, Yi & Ng, Kam K.H.. (2017). Big Data Analytics for Predictive Maintenance Strategies. 10.4018/978-1-5225-0956-1.ch004.

[7] A. Essien and C. Giannetti, "A Deep Learning Model for Smart Manufacturing Using Convolutional LSTM Neural Network Autoencoders," in *IEEE Transactions on Industrial Informatics*, vol. 16, no. 9, pp. 6069-6078, Sept. 2020, doi: 10.1109/TII.2020.2967556.

[8] H. Ren, Y. Chai, J. Qu, K. Zhang and Q. Tang, "An Intelligent Fault Detection Method Based on Sparse Auto-Encoder for Industrial Process Systems: A Case Study on Tennessee Eastman Process Chemical System," *2018 10th International Conference on Intelligent Human-Machine Systems and Cybernetics (IHMSC)*, Hangzhou, China, 2018, pp. 190-193, doi: 10.1109/IHMSC.2018.00051.

[9] J. Fan, W. Wang and H. Zhang, "AutoEncoder based high-dimensional data fault detection system," *2017 IEEE 15th International Conference on Industrial Informatics (INDIN)*, Emden, Germany, 2017, pp. 1001-1006, doi: 10.1109/INDIN.2017.8104910.

[10] T. H. Dwiputranto, N. A. Setiawan and T. B. Aji, "Machinery equipment early fault detection using Artificial Neural Network based Autoencoder," *2017 3rd International Conference on Science and Technology - Computer (ICST)*, Yogyakarta, Indonesia, 2017, pp. 66-69, doi: 10.1109/ICSTC.2017.8011854.

[11] X. Wu, G. Jiang, X. Wang, P. Xie and X. Li, "A Multi-Level-Denoising Autoencoder Approach for Wind Turbine Fault Detection," in *IEEE Access*, vol. 7, pp. 59376-59387, 2019, doi: 10.1109/ACCESS.2019.2914731.

[12] Mishra, K., Krogerus, T., & Huhtala, K. (2019). Deep Autoencoder Feature Extraction for Fault Detection of Elevator Systems. *ESANN*.

[13] D. Choi, J. Han, S. Park and S. Hong, "Comparative Study of CNN and RNN for Motor fault Diagnosis Using Deep Learning," *2020 IEEE 7th International Conference on Industrial Engineering and Applications (ICIEA)*, Bangkok, Thailand, 2020, pp. 693-696, doi: 10.1109/ICIEA49774.2020.9102072.

[14] Jiao, Jinyang & Zhao, Ming & Lin, Jing & Liang, Kaixuan. (2020). A comprehensive review on convolutional neural network in machine fault diagnosis.

[15] J. He, J. Wang, L. Dai, J. Zhang and J. Bao, "An Adaptive Interval Forecast CNN Model for Fault Detection Method," *2019 IEEE 15th International Conference on Automation Science and Engineering (CASE)*, Vancouver, BC, Canada, 2019, pp. 602-607, doi: 10.1109/COASE.2019.8843086.

[16] K. B. Lee, S. Cheon and C. O. Kim, "A Convolutional Neural Network for Fault Classification and Diagnosis in Semiconductor Manufacturing Processes," in *IEEE Transactions on Semiconductor Manufacturing*, vol. 30, no. 2, pp. 135-142, May 2017, doi: 10.1109/TSM.2017.2676245.

[17] Kolar, D., Lisjak, D., Pająk, M., & Pavković, D. (2020). Fault Diagnosis of Rotary Machines Using Deep Convolutional Neural Network with Wide Three Axis Vibration Signal Input. Sensors, 20(14), 4017. doi:10.3390/s20144017

[18] T. Yang and S. Huang, "Fault Diagnosis Based on Improved Deep Belief Network," *2017 5th International Conference on Enterprise Systems (ES)*, Beijing, China, 2017, pp. 305-310, doi: 10.1109/ES.2017.57.

[19] C. Tao, X. Wang, F. Gao and M. Wang, "Fault diagnosis of photovoltaic array based on deep belief network optimized by genetic algorithm," in *Chinese Journal of Electrical Engineering*, vol. 6, no. 3, pp. 106-114, Sept. 2020, doi: 10.23919/CJEE.2020.000024.

[20] Y. Liang, Y. Xu, X. Wan, Y. Li, N. Liu and G. Zhang, "Dissolved gas analysis of transformer oil based on Deep Belief Networks," *2018 12th International Conference on the Properties and Applications of*

Dielectric Materials (ICPADM), Xi'an, China, 2018, pp. 825-828, doi: 10.1109/ICPADM.2018.8401156.

[21] A. Yun, W. Yahui and L. Yuexiao, "Research on gas pressure regulator fault diagnosis based on deep confidence network (DBN) theory," *2017 Chinese Automation Congress (CAC)*, Jinan, China, 2017, pp. 3821-3825, doi: 10.1109/CAC.2017.8243446.

[22] H. Wang, H. Li, Y. Li and Y. Duan, "Railway Wagon Wheelset Fault Diagnosis Method Based on DBN," *2020 Global Reliability and Prognostics and Health Management (PHM-Shanghai)*, Shanghai, China, 2020, pp. 1-6, doi: 10.1109/PHM-Shanghai49105.2020.9280980.

[23] S. Zhang, S. Zhang, B. Wang and T. G. Habetler, "Deep Learning Algorithms for Bearing Fault Diagnostics—A Comprehensive Review," in *IEEE Access*, vol. 8, pp. 29857-29881, 2020, doi: 10.1109/ACCESS.2020.2972859.

[24] J. Wang, G. Wu, Y. Sun, L. Wan and D. Jiang, "Fault diagnosis of Underwater Robots based on recurrent neural network," *2009 IEEE International Conference on Robotics and Biomimetics (ROBIO)*, Guilin, China, 2009, pp. 2497-2502, doi: 10.1109/ROBIO.2009.5420479.

[25] T. de Bruin, K. Verbert and R. Babuška, "Railway Track Circuit Fault Diagnosis Using Recurrent Neural Networks," in *IEEE Transactions on Neural Networks and Learning Systems*, vol. 28, no. 3, pp. 523-533, March 2017, doi: 10.1109/TNNLS.2016.2551940.

[26] M. Alrifaey, W. H. Lim and C. K. Ang, "A Novel Deep Learning Framework Based RNN-SAE for Fault Detection of Electrical Gas Generator," in *IEEE Access*, vol. 9, pp. 21433-21442, 2021, doi: 10.1109/ACCESS.2021.3055427.

[27] Y. Huang, C. Chen and C. Huang, "Motor Fault Detection and Feature Extraction Using RNN-Based Variational Autoencoder," in *IEEE Access*, vol. 7, pp. 139086-139096, 2019, doi: 10.1109/ACCESS.2019.2940769.

[28] Ioannis T Christou, Nikos Kefalakis, Andreas Zalonis, John Soldatos, Raimund Brochler (2020) "End to End Industrial IoT Platform for Actionable Predictive Maintenance." IFAC PapersOnline 53-3(2020) 173 - 178.

[29] Daniele Apiletti, Claudia Barberis, Tania Cerquitelli, Alberto Macii, Enrico Macii, Massimo Poncino, and Francesco Ventura "iSTEP, an integrated Self-Tuning Engine for Predictive maintenance in Industry 4.0" (2018) IEEE International Conference on Parallel & Distributed Processing with Applications, Ubiquitous Computing & Communications, Big Data & Cloud Computing, Social Computing & Networking, Sustainable Computing Communications DOI 10.1109/BDCloud.2018.00136.

[30] Stefano Proto , Evelina Di Corso , Daniele Apiletti , Luca Cagliero , Tania Cerquitelli, Giovanni Malnati, And Davide Mazzucchi (2020) "REDTag: A Predictive Maintenance Framework for Parcel Delivery Services", IEEE Access – Multidisciplinary Open Access Journal, Digital Object Identifier 10.1109/ACCESS.2020.2966568.

[31] Yongyi Ran, Xin Zhou, Pengfeng Lin, Yonggang Wen, Ruilong Deng, Nanyang (2020) "A Survey of Predictive Maintenance: Systems, Purposes and Approaches", IEEE COMMUNICATIONS SURVEYS & TUTORIALS, VOL. XX, NO. XX, NOV. 2019.

[32] Kahiomba Sonia Kiangala, Zenghui Wang, (Member, IEEE) "An Effective Predictive Maintenance Framework for Conveyor Motors Using Dual Time-Series Imaging and Convolutional Neural Network in an Industry 4.0 Environment", IEEE Access, Digital Object Identifier 10.1109/ACCESS.2020.3006788.

[33] Go Muan Sang, Lai Xu, Paul de Vrieze, Yuewei Bai, "Towards Predictive Maintenance for Flexible Manufacturing Using FIWARE", S. Dupuy-Chessa and H. A. Proper (Eds.): CAiSE 2020 Workshops, LNBIP 382, pp. 17–28, 2020. https://doi.org/10.1007/978-3-030-49165-9_2.

[34] P. Aivaliotis, K. Georgoulias, R. Ricatto, M. Surico, "Predictive maintenance framework: Implementation of local and cloud processing for multi-stage prediction of CNC machines' health".

Road Safety Audit: A Case-study on NH-16

[1] Chitti Babu Kapuganti, [2] Sai Srinivas Nalam, [3] Manoj Kumar Reddy Lomada

[1] Assistant Professor, GITAM School of Architecture, GITAM (Deemed to be University), Visakhapatnam, India
[2] B. Tech Student, Department of Civil Engineering, GITAM (Deemed to be University), Visakhapatnam, India
[3] Master of Science student, Construction Mgmt & Surveying, Heriot–Watt University, Edinburgh, UK

Abstract:

The Indian road network is around 5.5 million kilometers, of which 80% covers traveler movement. In the present situation, road accidents are often as human death occurs for every four minutes. In India majority of the road accident fatalities are in the age group 18 to 55 years. It is mandatory to check the safety of roads for accident reduction and prevention. A road safety audit is a tool for the enhancement of road safety and to recognize potentially dangerous areas and recommends remedial safety measures. This research conducts road safety audit for the stretch of 2.5 kilometers on NH-16 from Maddilapalem junction to Hanumantavaka junction. This stretch covers five conflict points and has moderate traffic during daytime. This paper presents a statistical relationship between the number of accidents, type of vehicle, and nature of accident for 2017, 2018, and 2019 accident data. A detailed analysis is carried out based on potholes, pavement unevenness, fatigue cracking. This study suggests necessary measures for reducing accidents and crash severity.

Keywords:

Accidents, Road Safety, Road Safety Measures

1. INTRODUCTION

Road Safety Audit (R.S.A.) is a sophisticated method for upgrading road safety, identifying the most likely accidental dangerous areas, and suggesting compensatory measures to provide new roads. R.S.A. can identify aspects of engineering interventions that could give rise to road safety problems and suggest modifications that could improve road safety. [1]-[2]

R.S.A. benefits include minimizes the risk of high severity crashes that may differ from design deficiencies in a road project; minimizes the need for network and physical remedial works caused by road safety deficiencies at various projects, including construction; reduces the whole life cost of the project; Improves awareness and improvements in the safe design process. [3]-[5]

R.S.A. is an essential aspect of quality assurance applied to the implementation of a road project. It assesses a road's operation, focusing on road safety as it affects a road project's users by considering all potential users. R.S.A. has a safety benefit of a 10-60% reduction in total crashes.

NH-16 is a major highway connecting four states in the country with the highest coverage in Andhra Pradesh. This investigation evaluates the safety audit aspect of NH-16 from Hanumanthawaka junction to Maddilapalem junction.

The origin point has the collision of the localized transport, inter City vehicle movement, the flow of heavy vehicles, interstate transport, and cement transport lorries for the other districts in the state.

This stretch consists of Hanumanthawaka junction, Venkojipalem Petrol Bunk, Hanuman Temple, M.V.P. Double Road, Isukathota junction, Automotive junction, and Maddilapalem junction as shown in the Figure 1. Venkojipalem Petrol Bunk, Isukathota junction, and Maddilapalem junction are the most crucial junctions identified in the study.

Figure 1: Google map of the selected stretch

The contribution of this study is three-fold. First and foremost, we develop a statistical relationship between accident rates and various factors causing accidents for identifying accident-prone zones in the selected stretch. Secondly, we review road geometrics and traffic conditions of the road stretch with potholes, pavement unevenness, and fatigue cracking. Finally, our study suggests necessary measures for reducing accidents and crash severity.

2. ACCIDENT DATA

Road Accidental data of years 2017, 2018, 2019 collected from the first information report (F.I.R.) from the selected stretch's local police stations

This study considers seven classes of vehicles such as Heavy Goods Motor Vehicles (HGMV), Heavy Passenger

Motor Vehicles (HPMV), Light Motor Vehicles (LMV), Light Motor Vehicles Non-Transport (LMV-NT), Light Motor Vehicles - Transport (LMV-Tr), Motorcycle with Gear (MCWG) and Motorcycle without Gear (MCWOG).
This analysis considers road accident fatalities as fatal and non-fatal and the nature of collision as head-on collision, rear-end collision, and side collision.

Table 1: Number of Accidents

Year	Fatal	Non-Fatal	Total
2017	16	66	82
2018	14	64	78
2019	16	53	69

Table 2: Number of Accidents based on class of vehicle

Class of Vehicle	2017	2018	2019
HGMV	11	9	3
HPMV	7	7	9
LMV	12	23	18
LMV-NT	16	20	8
LMV-TR	17	6	12
MCWG	8	8	6
MCWOG	11	5	13

Table 3: Number of accidents according to class of vehicle and fatality

Class of Vehicle	Fatal	Non-Fatal
HGMV	7	16
HPMV	6	17
LMV	3	50
LMV-NT	7	37
LMV-TR	11	24
MCWG	4	18
MCWOG	8	21

Table 4: Number of accidents according to class of vehicle and Nature of collision

Class of Vehicle	Head-on collision	Rear-end collision	Side collision
HGMV	13	7	3
HPMV	15	8	-
LMV	19	19	15
LMV-NT	23	16	5
LMV-TR	17	14	4
MCWG	10	5	7
MCWOG	10	6	13
Total	107	75	47

Table 5: Year wise accidents at each Location

Location	2017	2018	2019
Hanumanthawaka Junction	2	8	3
Venkojipalem Petrol Bunk	16	6	16
Hanuman Temple, Venkojipalem	6	4	13
MVP Double Road	10	20	4
Isukathota Jn. NH-16	16	20	13
Automotive Jn. NH-16	12	16	5
Maddilapalem, NH-16	20	4	15

Major accidents are fatal accidents that occur for the involvement of heavy vehicles. As per the test analysis concerning accident data, the number of accidents increased due to negligible and rashness of the driver, over-speed at junction areas.
The number of fatal and non-fatal accidents in above mentioned years is given in Table 1. In the year 2017, total accidents are 82, and in the year 2019, total accidents are 69, which indicates the rate of accidents has reduced. 20% of accidents are fatal, and 80% of accidents are non-fatal.

Table 6: Number of Accidents at locations according to fatality

Location	Fatal	Non-Fatal
Hanumanthawaka Junction	2	11
Venkojipalem Petrol Bunk	13	25
Hanuman Temple, Venkojipalem	5	18
MVP Double Road	4	30
Isukathota Jn. NH-16	10	39
Automotive Jn. NH-16	4	29
Maddilapalem, NH-16	8	31

Number of accidents based on the vehicle class according to year have given in the Table 2. In 2018, LMV accidents are as high as 23. Number of accidents according to class of vehicle and fatality are given in Table 3. LMV non-fatal accidents observed in the considered stretch are 50. LMV-NT non-fatal accidents in considered stretch are 37. Number of accidents according to class of vehicle and nature of collision is given in Table 4. In the considered stretch, 47% of accidents are head-on collision, 33% of accidents are rear-end collision and remaining 21% are side collision accidents.
Number of fatal and non-fatal accidents at each location have presented in Table 6. At Venkojipalem Petrol Bunk, the number of fatal accidents is 13 and at Isukathota Jn. NH-16, the number of non-fatal accidents are 39 observed. Fatal accidents majorly observed at Venkojipalem Petrol Bunk, Isukathota Jn. NH-16 and Maddilapalem, NH-16. Non-fatal accidents observed mostly at Isukathota Jn. NH-16, MVP Double Road and Automotive Jn. NH-16.
Number of accidents at each location according to class of vehicle and fatality are shown in Table 7. In the selected stretch, Highest number of non-fatal accidents occurred at Maddilapalem, NH-16 due to LMV.

3. INVESTIGATION AND GENERAL OBSERVATIONS

A. Potholes

A pothole is a structural defect on a road surface. At times of heavy rainfall, water may stagnate in the subsurface of the road [6]. The stagnated water may weaken the subsurface of the pavement and then fatigues and breaks the poorly supported asphalt surface within the affected area. These affected areas form potholes on the asphalt pavement. Potholes lead to pavement unevenness the damage to tires, wheels, and vehicle suspensions is liable to occur. Potholes

are three types: small potholes (25x200mm), Medium potholes (25-50x500mm), large potholes (>50x500mm). The remedy of potholes is to remove the debris and rocks and clean the surface with pneumatic air pressure and fill it with fine aggregates and finally, asphalt pavement should be sequentially up to the road surface. List of potholes observed on the selected stretch is given in Table 8.

Figure 2: Potholes on the road surface

Table 7: Number of accidents at location according to class of vehicle and fatality

Type of Activity	HGMV		HPMV		LMV		LMV-NT		LMV-TR		MCWG		MCWOG	
Type of fatality	Fatal	Non-Fatal	Fatal	Non-Fatal	Fatal	Non-Fatal	Fatal	Non-Fatal	Fatal	Non-Fatal	Fatal	Non-Fatal	Fatal	Non-Fatal
Hanumanthawaka junction														
2017										2				
2018		2				2		2			1		1	
2019				1		1		1						
Venkojipalem Petrol Bunk														
2017	2			4	1			2	2			2	1	2
2018			1		1	2		2						
2019	1	1	1			3	1		1	5		1	1	1
Hanuman Temple Venkojipalem														
2017		1				2				1	1		1	
2018		1		1		1		1						
2019			2	4			1					3		3
MVP Double Road														
2017		1		1		4				2		1		1
2018	2	2	2	2		5		5				2		
2019						4								
Isukathota Jn. NH-16														
2017	1	2						4	1	2	1	2	1	2
2018		2		1	1	4	1	3	2	4		1		1
2019	1			1		2		2	1	1		1		4
Automotive Jn. NH-16														
2017		1				2		4	2	1				2
2018						6		5				3		2
2019								1	2	1				1
Maddilapalem, NH-16														
2017		3		2		3	2	4		4		1		1
2018						1		1			1		1	
2019						8	2			1		1	2	1

Table 8: Type and location of potholes

Latitude & longitude	Problem
(17.734922, 83.319544)	Medium Potholes
(17.735748, 83.319648)	Medium Potholes
(17.736235, 83.321002)	Large Potholes
(17.736274, 83.321222)	Large Potholes
(17.739701, 83.325434)	Medium Potholes
(17.740532, 83.327011)	Medium Potholes
(17.741461, 83.32753)	Large Potholes
(17.743237, 83.328234)	Medium Potholes
(17.743317, 83.328322)	Large Potholes
(17.743456, 83.328316)	Medium Potholes

 ISBN: 978-93-90214-20-4

(17.743759, 83.327901)	Large Potholes
(17.744789, 83.328548)	Small Potholes
(17.746567, 83.328785)	Large Potholes
(17.746997, 83.32916)	Medium Potholes
(17.747295, 83.330343)	Medium Potholes
(17.747379, 83.330404)	Small Potholes
(17.74771, 83.331124)	Small Potholes
(17.748015, 83.33174)	Small Potholes
(17.749027, 83.331876)	Medium Potholes
(17.753484, 83.332346)	Small Potholes

B. Fatigue cracks

Fatigue cracks are typical pavement distress that shows a weakened soil structure beneath the failed asphalt layer [7]. They are longitudinal and interconnecting cracks in the hot mix asphalt layer due to repeated application of wheel loads, generating tensile stress that eventually creates cracks at bottom surfaces. Fatigue cracks observed in the selected stretch is given in the Table 9.

As fatigue cracks indicate loss of subgrade support, the remedy is to remove the cracked area, replace the inferior subgrade surface with the fresh subgrade, compact well and lay semi-dense bitumen concrete. Figure 3 shows the fatigue crack on the road surface.

Table 9: Location of Fatigue cracks on the selected stretch

Latitude & Longitude	Problem
(17.736243, 83.321019)	Fatigue cracks
(17.736314, 83.32127)	Fatigue cracks
(17.736315, 83.321282)	Fatigue cracks
(17.736526, 83.321376)	Fatigue cracks
(17.73702, 83.322194)	Fatigue cracks
(17.739701, 83.325434)	Fatigue cracks
(17.739702, 83.325381)	Fatigue cracks
(17.740532, 83.327011)	Fatigue cracks
(17.741958, 83.327764)	Fatigue cracks
(17.74272, 83.328102)	Fatigue cracks
(17.744789, 83.328548)	Fatigue cracks
(17.746567, 83.328785)	Fatigue cracks
(17.746997, 83.32916)	Fatigue cracks
(17.747056, 83.330092)	Fatigue cracks
(17.747132, 83.333615)	Fatigue cracks
(17.747168, 83.329799)	Fatigue cracks

Figure 3: Fatigue cracks on road surface

Figure 4: Erased road markings on the road surface

Figure 5: Erased road markings on the road surface

Figure 6: Pavement Unevenness at junction

Table 10: Location of unclear markings on the selected stretch

Latitude & Longitude	PROBLEM
(17.73624, 83.321466)	No clear Pedestrian crossings
(17.736931, 83.322164)	No clear Pedestrian crossings
(17.738561, 83.32334)	No clear Road markings
(17.740473, 83.326886)	No clear Road markings
(17.740936, 83.327496)	No clear Pedestrian crossings
(17.746567, 83.328785)	No clear Road markings
(17.746656, 83.328199)	No clear Pedestrian crossings
(17.74684, 83.328665)	No clear Road markings
(17.747219, 83.330201)	No clear Pedestrian crossings

TABLE 11: Location of pavement

Latitude & Longitude	Problem
(17.744668, 83.328111)	Pavement unevenness
(17.749027, 83.331876)	Pavement unevenness
(17.748015, 83.33174)	Pavement unevenness
(17.747675, 83.33171)	Pavement unevenness
(17.747379, 83.330404)	Pavement unevenness
(17.738572, 83.323787)	Pavement unevenness
(17.739796, 83.325779)	Pavement unevenness

C. Road marking

Clear road markings give directions to the road user and control the behavior of the vehicles [8]. Inadequate road markings raise the irregular movement of vehicles at junctions that are prone to road accidents. Erased road markings on the road surface are shown in the Figure 4 and Figure 5. Location of unclear road markings are shown in Table 10.

To avoid erasing road markings, they have to rehabilitate for every five years by using hot thermoplastic road applied paints at the surfaces, and it is to be applied at a heat of 200°C to make the coating surface harder upon cool down.

D. Pavement unevenness

Pavement unevenness is type of pavement failure due to improper compaction of fill, subgrade, and pavement layers. Pavement unevenness causes inconvenience to road user and damages vehicle. It effects speed, safety, riding comfort, vehicle condition, fuel consumption and operating costs [9].

The remedy to pavement unevenness is to remove uneven pavement and compact subgrade fully and then lay new surface matching the older surface. List of locations with pavement unevenness are given in Table 11. Pavement unevenness on the road surface is shown in the Figure 6.

4. CONCLUSION

Based on the Road Safety Audit for the stretch of NH-16, the following points need to consider the betterment of road conditions and minimizing the accidents and crash severity.

- Fatal accidents happened in the selected stretch are about 20%, and non-fatal accidents are about 80%.
- In the three years 2017, 2018 and 2019, number of accidents are in decremental manner which indicates there is improvement in the roads.
- Accidents due to LMV class of vehicles are more compared to other classes of vehicles.
- Head on collision accidents due to LMV-NT are more compared to other classes of the vehicles.
- Potholes, Fatigue cracks and Erased road markings mentioned in the locations must repair for road user comfort.

Execute regular repairs and periodical maintenances can reduce the number of accidents. Conducting safety awareness programs for road users may reduce crash severity of accidents.

REFERENCE

[1] Awsarmal, P., et al. Case Study for Road Safety Audit of Aurangabad City, vol. 170, 2020. doi:10.1051/e3sconf/202017006008.

[2] IRC:SP:84-2014, Indian Road Congress, (2014)

[3] Theofilatos, Athanasios, and George Yannis. "A review of the effect of traffic and weather characteristics on road safety." Accident Analysis & Prevention 72 (2014): 244-256.

[4] Wu, Yina, Mohamed Abdel-Aty, and Jaeyoung Lee. "Crash risk analysis during fog conditions using real-time traffic data." Accident Analysis & Prevention 114 (2018): 4-11.

[5] Gargoum, Suliman A., and Karim El-Basyouny. "Exploring the association between speed and safety: A path analysis approach." Accident Analysis & Prevention 93 (2016): 32-40.

[6] Setyarini, Niluh Putu Shinta Eka, and Leksmono Suryo Putranto. "Cipali Toll Road Safety Audit." In IOP Conference Series: Materials Science and Engineering, vol. 852, no. 1, p. 012001. IOP Publishing, 2020.

[7] Chatterjee, Sudipa, Partha Sarathi Bandyopadhyaya, and Sudeshna Mitra. "Identifying Critical Safety Issues on Two-Lane National Highways in India–A Case Study from NH 117 and NH 60." Transportation research procedia 48 (2020): 3908-3923.

[8] Dhankute, Ayush, and Manoranjan Parida. "Risk Analysis for a Four-Lane Rural Highway Based on Safety Audit." In Recent Advances in Traffic Engineering, pp. 599-618. Springer, Singapore, 2020.

[9] Liu, Pengfei, Visaagan Ravee, Dawei Wang, and Markus Oeser. "Study of the influence of pavement unevenness on the mechanical response of asphalt pavement by means of the finite element method." Journal of Traffic and Transportation Engineering (English Edition) 5, no. 3 (2018): 169-180.

Least Mean Fourth Based Weighted Median Filters For Image Restoration

[1] Ganeswara Padhy, [2] Sudam Panda, [3] Santanu Kumar Nayak

[1][2][3] Dept of Electronic Science, Berhampur University, Odisha, India

Abstract:

This paper proposes the weighted median least mean fourth (LMF) adaptive filters for image restoration. LMF filters suffer stability problems due to noise variance and hike in input noise power, which can be prevented by using the Normalized LMF (NLMF) procedure by normalizing weight update terms. Here the proposed filters are utilized to restore noisy images corrupted salt and pepper noise. LMF based weighted median (WMLMF) order-statistics filters are useful in preserving non-homogeneous reason like edge and eliminating streaking.

Keywords:

Weighted median, LMF, LMS, NLMS, NLMF

1. INTRODUCTION

Median filtering techniques have been widely used for impulsive noise removal purposes in case of the image and signal processing application. In case of standard median filtering helps in noise rejection cases but provides poor performances in preservation of the details and the edges of the images. Whereas considering the larger window size, better performance of noise removal occurs .Weighted median filtering [1], techniques have been devised improve the quality of noise filtering with preservation of certain features. The weighted values of input vector have been considered in case of weighted median filter[9],,which helps in preserving the edge and details. Other types filters like cascaded median filters which is nothing but a combination of sub-windows with different orientation, have been derived for this purposes .Stack filters[4,9] provide the better noise suppression and detail preservation with the help of mean absolute error criterion[3].The LMF [11] and NLMF[12,13] filters, improve the quality of picture with detail as well as edge preservation[11-13].Some researchers[14] have been extended the weighted median filters ro weighted order static filter(WOS),which is nothing but an asymmetric median filter, helps in eliminating the positive and negative edge from the images.

Adaptive Weighted Median filters with Least Mean forth Criterion

Here we have been considering the continuous-value of the noisy image matrix. Least mean fourth(LMF) based weighted median filter for non constant signal **s(t)** corrupted with salt and pepper noise n(t) which can be mathematically represented.

$$\mathbf{x}(t) = \mathbf{s}(t) + \mathbf{n}(t) \tag{1}$$

Here $\mathbf{x}(t)$ is corrupted image of size $p \times q$ and $\mathbf{n}(t)$ is a salt & pepper noise added to pixels. Where $t = (t_1, t_2)$ are presents the pixel co-ordinate. We have taken a filter window of size $I_1 \times I_2$ around the neighbourhood of the pixel t in, $I_1 = 2i_1 + 1$ and $I_2 = 2i_2 + 1$ and $i_1 = i_2 = 1,2.....$

The image window can be represented as

$$\mathbf{x}(t) = \begin{bmatrix} x(t_1 - i_1, t_2 - i_2) & x(t_1 - i_1, t_2 - i_2 + 1) & ..... & x(t_1 - i_1, t_2 + i_2) \\ . & . & . & . \\ . & . & . & . \\ x(t_1 + i_1, t_2 - i_2) & x(t_1 + i_1, t_2 - i_2 + 1) & ..... & x(t_1 + i_1, t_2 + i_2) \end{bmatrix}$$

We can arrange the window data into a row matrix format as

$$\mathbf{x}(t) = \left[x(t_1 - i_1, t_2 - i_2) \quad , x(t_1 - i_1, t_2 - i_2 + 1) ... \quad ..... \quad x(t_1 + i_1, t_2 + i_2)\right]^T \tag{2}$$

Where $I_1 \times I_2 = n$ i.e. numbers data available in the window.

Equation (2) can be written as

$$\mathbf{x}(t) = \left[x_1(t), x_2(t), ... x_n(t)\right]^T \tag{3}$$

Using median operation on input noisy as given in equation(3) vector we obtain

$$\mathbf{x}_m(t) = Sort\left[(x_1(t), x_2(t), ... x_n(t))^T\right]$$
$$\mathbf{x}_m(t) = \left[x_{(1)}(t), x_{(2)}(t), ... x_{(n)}(t)\right] \tag{4}$$

Where, $x_{(1)}(t) \le x_{(2)}(t) \le ..... \le x_{(n)}(t)$

The corresponding output of the WM filter can be represented as the weighted sum of the ordered inputs

$$y(t) = \sum_{i=1}^{n} w_i(t) x_m(t) = w^T x_m \quad . \tag{5}$$

Where, $\mathbf{w}(t) = (w_1(t), w_2(t), ... w_N(t))^T$, weight vector of WM filter such that

The cost function of LMF algorithm is considered

$$E(t)=\sum_{t} e^4(t) \tag{6}$$

Where, $\mathbf{e}(t)=\mathbf{s}(t)-\mathbf{y}(t)$ .Here **s**(t) is non corrupted image signal at pixel t and e(t) is the error signal at pixel *t*. The weight updation procedure for this algorithm can be expressed as

$$\mathbf{w}(t+1)=\mathbf{w}(t)+4\mu e^3(t)\mathbf{x}_m(t) \tag{7}$$

Where, μ is the step size parameter. For normalized LMF (NLMF) algorithm step size parameter can be written as

$$\mu'=\frac{\mu}{\left(\|\mathbf{x}(t)\|^2\times\left(\|\mathbf{x}(t)\|^2+e^2(t)\right)+\delta\right.}$$

For better stability, where δ is small number added in the denominator to rectify, when zero value comes into play in the denominator.

Hence for the NLMF algorithm, the weight updation formula can be written as

$$\mathbf{w}(t+1)=\mathbf{w}(t)+4\mu' e^3(t)\mathbf{x}_m(t) \tag{8}$$

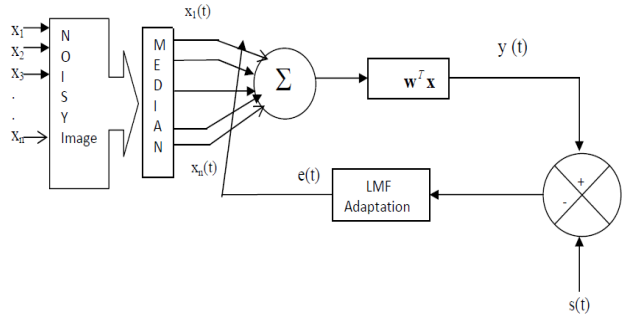

Fig.1 Block diagram for LMF based weighted median filter

2. ALGORITHM

Step-1: Let the input image size be $m_1\times m_2$ *, where* t_1 *and* t_2 *are numbers of rows and columns.*

Step-2: The weight matrix w and step size parameter η are to be initialized. The Initial cost function has been taken to be zero i.e. E=0.

Step-3: The original image s is corrupted with Gaussian or non-Gaussian noise 'n(c)' on each pixel. So the intensity of corrupted image becomes $\mathbf{x(t)}=\mathbf{s(t)}+\mathbf{n(t)}$.

Step-4: By choosing a small cellular window of the image to be input for the proposed algorithm. The size of the window be $I_1\times I_2$. *Where* $I_1=2\times i_1+1$, $I_2=2\times i_2+1$ *and* $i_1=i_2=1,2,3....$

Step-5: The cellular window data is to be converted for the input vector as N×1.Where,

$N=I_1\times I_2$ *as*

$$\mathbf{x}(c)=\left[x_1(t),x_2(t),.....x_N(t)\right]^T$$

Step-6: $\mathbf{x}(t)$ *vector is arranged in ascending order as* $\mathbf{x}_m=\left\lfloor x_{(1)}(t),x_{(2)}(t),.....<x_{(N)}(t)\right\rfloor$,

Weight vector w(c) for Median filter is as: $\mathbf{w}(t)=\left\lfloor w_1(t),w_2(t).....w_{(N)}(t)\right\rfloor$

Step-7: Numbers of iteration is to be specified (say max).

Step-8: For each pixel, a cellular window is framed, the number of windows for the whole image is $r=m_1\times m_2$.

Step-9: For the training process, the evaluation is carried out at each pixel 't' until the rth of pixels and means forth error is calculated.

The output and Parameters are calculated as:

$$y(c)=\sum_{i=1}^{N} w_i(t)x_i(t)=\mathbf{w}^T\mathbf{x}_m$$

$e(t)=d(t)-y(t)$, $E=E+e^4(t)$

Step-10: Weight vector is updated according to formulas for adaptive WLMF filter as

$\mathbf{w}(t+1)=\mathbf{w}(t)+4\mu e^3(t)\mathbf{x}(t)$ and

$\mathbf{w}(t+1)=\mathbf{w}(t)+4\mu' e^3(t)\mathbf{x}(t)$ for NLMF filter.

Step-11: If the mean fourth error for total numbers of pixels is calculated, than goto step-12.

Step-12: If the MFE satisfies the termination criteria, then proceed to step-13, else goto step-5.

Step-13: The following parameters for the evaluation of images, like MFE, MSE, PSNR, and SSIM [15], are to be calculated

$$MFE=\frac{E}{m_1\times m_2}\quad PSNR=10\log_{10}\left(\frac{255^2}{MSE}\right)$$

$$SSIM=\left(\frac{(2\mu_x\mu_y+\tilde{c}_1)(2\sigma_{xy}+\tilde{c}_2}{(\mu_x^2+\mu_y^2+\tilde{c}_1)(\sigma_x^2+\sigma_y^2+\tilde{c}_2)}\right)$$

Step-14: Restored image is to be obtained by convolving updated weight vector on a noisy image.

Step-15: The graph between mean fourth errors versus number of iteration is plotted.

3. SIMULATION RESULTS

In this paper, the simulation is carried out on Lena image with the availability of reference images. The image of Lena is distorted by salt and pepper noise of different strengths of signal to noise ratio 10, 5, 0 dB.The filter coefficients are initialized randomly such that their sum is unity. A small portion of noise image is used in training of adaptive filter using WMLMF median and WMNLMF median algorithm and with respect to iteration loss parameter Mean square error(MSE) and measuring parameter PSNR and SSIM are recorded as listed in Table-1. It is observed that Normalized version of weighted median Least mean fourth algorithm is (WMNLMF) is stable as compared to WMLMS and WMNLMS median

 ISBN: 978-93-90214-20-4

filters. After few numbers of iteration, WMLMS diverges with PSNR 31.74 and SSIM 0.81, while WMNLMS converges with PSNR 31.93and SSIM 0.81, whereas WMLMF converges with the better result with PSNR 32.24 and SSIM 0.83, but the normalized version of weighted median LMF gives the best result among these filters with PSNR 32.87 and SSIM 0.84 with better stability throughout the iterative process of restoration for SNR of 10dB. Reduced PSNR and SSIM are observed for higher noise strength of SNR 5dB and 0dB as tabulated in Table-1.

TABLE-1: Tabulation for mean square error, Peak signal to noise ratio and structural similarity index for different filters for Salt & pepper noisy Lena image.

FILTER TYPE	SNR=10dB			SNR=5dB			SNR=0dB		
	MSE	PSNR	SSIM	MSE	PSNR	SSIM	MSE	PSNR	SSIM
WMLMS	9.7e-04	31.74	0.81	2.8e-04	27.23	0.67	7.1e-03	21.11	0.37
WMNLMS	9.5e-04	31.93	0.81	2.8e-04	27.32	0.68	6.9 e-03	21.16	0.38
WMLMF	9.3e-04	32.24	0.83	2.7e-04	27.57	0.69	6.8 e-03	21.88	0.40
WMNLMF	9.1e-04	32.87	0.84	2.6e-04	27.76	0.71	6.6 e-03	21.97	0.42

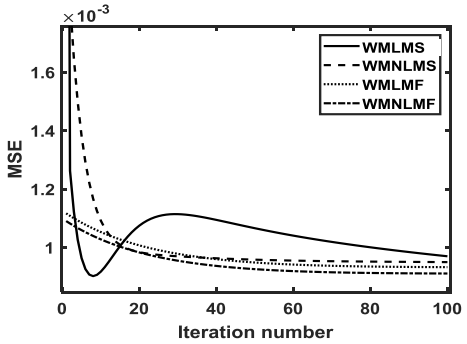

Fig.2. Mean square error (MSE) for different filters

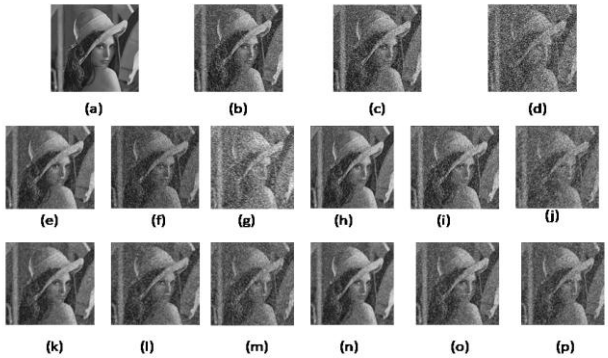

Figure-2. Pure, noisy and restored images. (a)pure image, noisy image of SNR (b)10dB,(c)5dB,(d)0dB. Restored image using WMLMS filter for SNR (e) 10dB, (f)5dB, (g) 0dB. Restored image using WMNLMS filter for SNR (h) 10dB, (i)5dB,(j)0dB. Restored image using WMLMF filter for SNR (k) 10dB, (l) 5dB, (m) 0dB. Restored image using WMNLMF filter for SNR (n) 10dB, (o) 5dB, (p) 0dB.

4. CONCLUSION:

Order statistic Weighted median filtering operation with LMS as well as LMF adaptive filters are applied on Lena image with different noise strength i.e SNR of 10db, 5dB and 0dB. Parameters are tabulated in Table-1, outputs are shown in the Figure-2.Among all the filters normalized version of weighted median LMF(WMNLMF)performs better with good stability and restored images are better other restored images with good PSNR and SSIM.

REFERENCE

[1]Lin Yin, Ruikang Yang,Yrjo Neuvo,"Weighted Median Filters,"IEEE Trans. on Circuit and Syatem-11: Analog and digital signal processing, Vol. 43, No. 3, March 1996.

[2] G. R. Arce and R. E. Foster, "Detail preserving ranked-order based filters for image processing," *IEEE Trans. Acoust., Speech, Signal Processing*,vol. 37, pp. 83–98, Jan. 1989.

[3] E. J. Coyle and J.-H. Lin, "Stack filters and the mean absolute error criterion," *IEEE Trans. Acoust., Speech, Signal Processing*, vol. 36, pp.1244–1254, Aug. 1988.

[4] D. Petrescu, "Optimal design and image processing applications of Boolean, stack and morphological filtering," Ph.D. dissertation, Tampere Univ. Technol., Tampere, Finland, 1997.

[5] A. Nieminen, P. Heinonen, and Y. Neuvo, "A new class of detai lpreserving filters for image processing," *IEEE Trans. Pattern Anal. Machine Intell.*, vol. PAMI-9, pp. 74–91, Jan. 1987.

[6] I. T˘abu¸s, D. Petrescu, and M. Gabbouj, "A training framework for stack and Boolean filtering—Fast optimal design procedures and robustness case study," *IEEE Trans. Image Processing, Spec. Issue Nonlinear Image Processing*, vol. 5, pp. 809–826, June 1996.

[7] X. Wang, "Generalized multistage median filter," *IEEE Trans. Image Processing*, vol. 1, pp. 543–545, Oct. 1992.

[8] P. D. Wendt, E. J. Coyle, and N. C. Gallagher, Jr., "Stack filters," *IEEE Trans. Acoust., Speech, Signal Processing*, vol. 34, pp. 898–911, Aug. 1986.

[9] R. Yang, Y. Lin, M. Gabbouj, J. Astola, and Y. Neuvo, "Optimal weighted median filtering under structural constraints," *IEEE Trans. Signal Processing*, vol. 43, pp. 591–604, Mar. 1995.

[10] X. Yang and P. S. Toh, "Adaptive fuzzy multilevel median filter," *IEEE Trans. Image Processing*, vol. 4, pp. 680–682, May 1995.

[11].walach and B widrow,"The least mean forth (LMF)adaptive algorithm and its family",IEE Trans.Inf.Theory,vol.IT-30,pp.275-283,March 1984.

[12]A.Zerguine,"Convergence behaviour of Normalized least mean forth algorithm",Proc.34th Ann.ASILOMARconf.signals,syst,Compu,PacificGrive,CA,oct.29-Nov1.2000,pp.275-27

[13]E.Eweda,"Global Stabilization of Least mean forth algorithm ",IEE trans Signal processing,vol.60,pp.1473-1477,March 2012.

[14].P.D wendt.E.J.Coyle,and N.C. Gallgher,Jr.,"Stack filter,"IEE.Trans.Acoust.,speech,signal process.vol.ASSP-34,pp.898-911,Aug.1986.

[15] Zhou Wang, A. C. Bovik, H. R. Sheikh, and E. P. Simoncelli, "Image quality assessment: from error visibility to structural similarity," *IEEE Trans. Image Process.*, vol. 13, no. 4, pp. 600–612, Apr. 2004, doi: 10.1109/TIP.2003.819861.

A Generalized Study on Progressive Collapse Resisting Mechanism in R.C Structure

[1] Rohit Ravikumar, [2] Dr. Beena K P

[1][2] Department of Civil Engineering, College of Engineering Trivandrum, India

Abstract:

The term progressive collapse is defined as the collapse of all or a large part of a structure precipitated by damage or failure of a relatively small part of it. The awareness about progressive collapse was highlighted in 1968 with the collapse of the Ronan Point building in the United Kingdom. According to the latest technical standards, the design capacity to survive extraordinary events such as explosion, impact and consequences of human errors is left to the owner. However, the low probability of such events actually occurring means it is uneconomical to spend extreme resources to design every building against progressive collapse. A more feasible solution would be to consider alternative parameters such as secondary load carrying mechanisms, effects of Masonry Infill (MI) walls that are usually neglected in analysis. In reality these resisting mechanism in multistorey building can help to reduce the severity of the collapse, should it actually occur. In the first part of this paper a 3 storey, 3 bay, 9 slab multistory framed structure is designed. Loads from slabs, walls are considered but their design is not included. In the second part of this paper to quantify the effectiveness of each progressive collapse resisting mechanisms six specimens corresponding to the building model is analysed in SeismoStruct. The failure modes and load-displacement relationships are obtained and the contributions of each of the mechanism (Compressive Membrane Action, Compressive Arch Action, Tensile Membrane Action, Tensile Catenary Action) and effect of masonry wall is considered and discussed.

Keywords:

Compressive Arch Action, Compressive Membrane Action, Progressive collapse, SAP2000, SeismoStruct, Tensile Catenary Action, Tensile Membrane Action

1. INTRODUCTION

The term progressive collapse is defined as the collapse of all or a large part of a structure precipitated by damage or failure of a relatively small part of it. It is sometimes also called a disproportionate collapse, which is defined as a structural collapse disproportionate to the cause of the collapse. Reference [1] defines the progressive collapse as "the spread of an initial local failure from element to element resulting, eventually, in the collapse of an entire structure or a disproportionately large part of it". As the small structural element fails, it initiates a chain reaction that causes other structural elements to fail in a domino effect, creating a larger and more destructive collapse of the structure. Progressive collapse is one of the most devastating types of building failures, most often leading to costly damages, multiple injuries, and possible loss of life.

The 1968 Ronan Point collapse has been instrumental in making engineers aware of the possibility of a chain reaction or progressive collapse. Its importance, however, has been growing because of the spread of many tragic collapses: The Murrah Federal Building in Oklahoma (1995), the Giotto Avenue Building in Foggia (1999), and World Trade Centre in New York (2001).

The importance of building structures has increased in the modern times due to the increasing complexity in the buildings increased demands in terms of functional requirement, aesthetics and height. This project requirement as well as many external factors has increased the risk and chances of accidents. Unsafe practices and ignorance of structural design and good construction practices has resulted in many building collapses past as well as in recent times. Some of these are Progressive collapses which resulted in large number of causalities. Progressive collapses results in severe causalities and economic losses which are much more in magnitude than that of the local failure which is small. Therefore, it is very sensible and essential to control Progressive collapses by appropriate structural design and detailing.

The main point is to ensure multiple load path in the structure in case of failure of a member so that failure (say of a column) do not progress from the local area near the failed columns to areas away from the failure location the progressive collapse. As such the effect of progressive collapse and the inherent resisting mechanism may be studied to arrive at an efficient method of designing the building against possible progressive collapses. Study of inherent resisting mechanism can also act as foundation of progressive collapse mitigation schemes.

When a multistorey building is subjected to sudden column loss, the ensuing structural response is dynamic, typically characterized by significant geometric and material nonlinearity. When the failure of vertical members under extreme events, such as blast and impact, is a highly dynamic phenomenon, sudden column loss represents a more appropriate design scenario, which includes the dynamic influences yet is event-independent. Although such a scenario is not identical in dynamic effect to column

damage resulting from impact or blast it does capture the influence of column failure occurring over a relatively short duration to the response time of the structure. It is therefore truly unsurprising that sudden column loss is used as the principal design scenario in the two most recent guidelines ([2] & [3]) produced in the USA for progressive collapse analysis.

2. PROGRESSIVE COLLAPSE RESISTING MECHANISM

In the design against progressive collapse, consideration of secondary load carrying mechanisms can be an effective alternative. These secondary load carrying mechanisms include compressive arch action (CAA) and tensile catenary action (TCA) developed in beams as well as compressive membrane action (CMA) and tensile membrane action (TMA) developed in slabs. In the case of a column local failure, to transfer the load from the collapsed column to the nearby ones, loads and thrusts should travel around the building because these paths imply a strain energy dissipation lower than that relevant to paths in which loads move only in the floor slabs activating their shear-bending behavior. Fig. 1 illustrates the idealized response for a two-way slab panel that is fully restrained at its edges and contains continuous two-way reinforcement that is well anchored at its edges. After that the initial bending failure has occurred, and after that large deflections have taken place, membrane action provides a secondary resisting mechanism which is capable of providing a significant resistance. The final collapse will occur after the steel reinforcement ruptures.

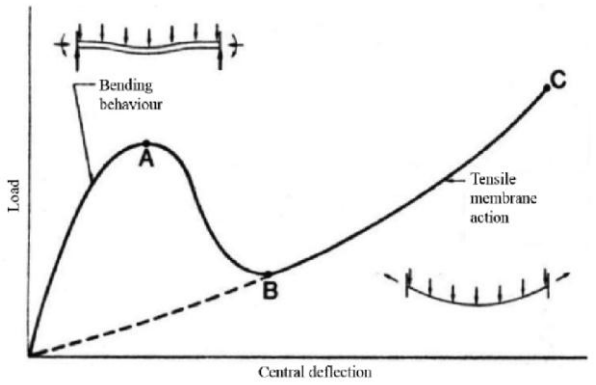

Fig. 1. Load -Deflection Showing CMA and TMA [4]

Due to the membrane behaviour of floor slabs, these slabs are able to provide an elasto plastic behaviour and provides maximum dynamic deformations under gravity load by exhibiting Compressive Membrane Action (CMA) and Tensile Membrane Action (TMA). Similar to slabs, beams can also exhibit both Compressive Arch Action (CAA) and Tensile Catenary Action (TCA).

Several researchers [5], [6], [7], [8], [9] have studied CAA and TCA in resisting progressive collapse. Reference [10] discussed TMA developed in RC slabs to resist progressive collapse in detail The effects of CAA, TCA, CMA, and TMA on the vulnerability of RC structures in resisting progressive collapse were discussed by [11].

The remarkable increase in bending moment and shear force due to missing columns can result in severe damage to the building, especially if the building has an irregular layout or the initial damage leads to the loss of several columns. Hence other than these secondary load resisting mechanisms the masonry infilled (MI) walls, which are taken as non-structural components in conventional design, can also be relied on to prevent the collapse of a building. The effects of MI walls on the load resisting capacity of RC frames to mitigate progressive collapse was evaluated experimentally by [12]

3. BUILDING SPECIFICATION

The specifications of the building designed is as follows:

Number of Storey	:	3
Number of Bays	:	3
Number of Slabs / Floor	:	9

Beams: 400 mm x 600 mm, having Effective Length of 4 m.
Columns: 400 mm x 400 mm, having Effective Length 3 m.
Slab: 0.15 m thick and a floor finish of 0.05 m thickness.
Loads Acting:

- Dead Load: 25 kN/m for Beams & 3.75 kN/m2 for Slabs
- Live Load: 15 kN/m for Beams &2 kN/m2 for Slabs
- Floor Finish Load (1.25 kN/m2 for Slabs)

Materials: M25 Concrete, Fe500 Steel.

The Line Sketch of elevation and plan of the building are given Fig. 2(a) & 2(b) respectively. The 3-D Frame modelled is as shown in Fig. 2(c).

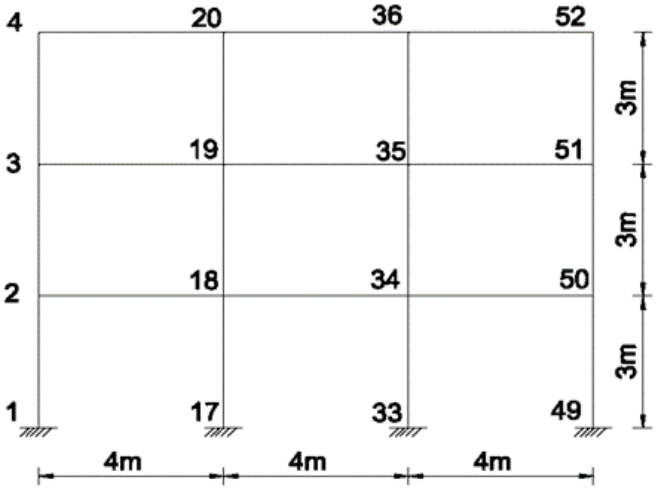

Fig. 2(a). Elevation of Building (X-Z Plane)

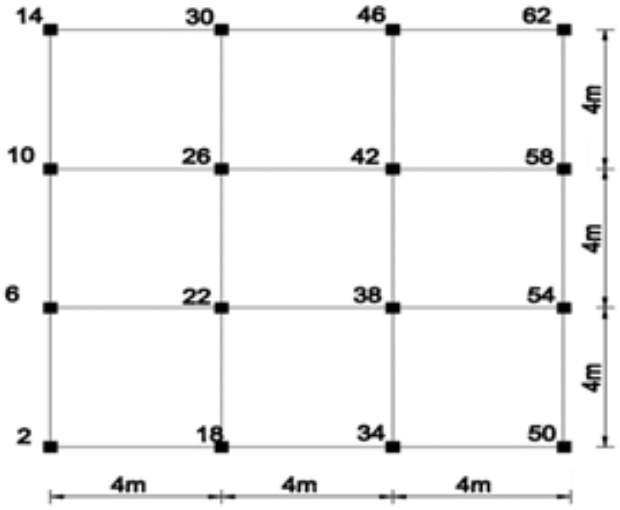

Fig. 2(b). First Floor Plan of Building (X-Y Plane)

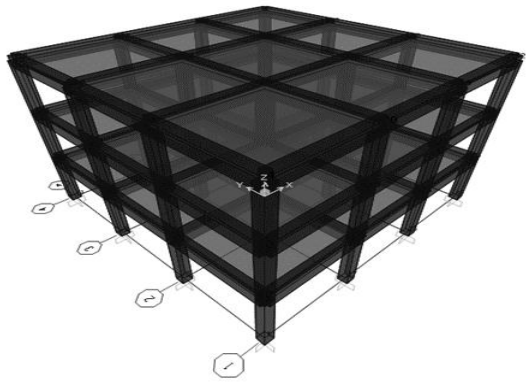

Fig. 2(c). 3D Frame

The Reinforcement obtained was tabulated as shown in Table I.

Table I. Reinforcement of Beams & Columns

Beam (B) Or Column (C)	Area of Longitudinal Reinforcement Obtained (mm^2)		Area of Longitudinal Reinforcement Provided (mm^2)		Provided Shear Reinforcement
	Top	Bottom	Top	Bottom	
B1	576	576	T16 - 3Nos	T16 - 3Nos	2 Legged T8 Stirrups @ 150mm c/c
B2	624	576	T16 - 4 Nos	T16 - 3Nos	2 Legged T8 Stirrups @ 150 mm c/c
B3	584	576	T16 - 3 Nos	T16 - 3Nos	2 Legged T8 Stirrups @ 150 mm c/c
B4	604	576	T14 - 4 Nos	T16 - 3Nos	2 Legged T8 Stirrups @ 150 mm c/c
C1	4151		T25 - 4 Nos & T12 – 4 Nos		Lateral Ties T8 @ 100 mm c/c
C2	1280		T16 - 8 Nos		Lateral Ties T8 @ 100 mm c/c

For the building designed B1 represents all the edge beams (36 Nos) of the building, B2, B3, B4 (each 12 Nos) represents all interior columns of ground floor, first floor, second floor respectively. C1 represents the four interior columns on the ground floor (21-22, 25-26, 37-38 ,41-42), while C2 represents all the other columns. Since the software –SAP2000 performs all the necessary checks while designing, the provided reinforcement is sufficient and the structure as a whole is safe.

4. ANALYTICAL STUDY

Progressive collapse resisting mechanism is determined by performing a nonlinear static pushover (down) using the software SeismoStruct. That is, in this method of analysis the model is first prepared and the required column is removed. Analysis is performed by applying a pseudo static displacement at the collapsed column location and by using the displacement control strategy for the incrimination of the loading factor as shown in Fig.3 (a), (b) &(c). The limit failure of the beam considered in this work is the fracture of reinforcement steel.

Fig. 3(a). Beam Modelled in SeismoStruct

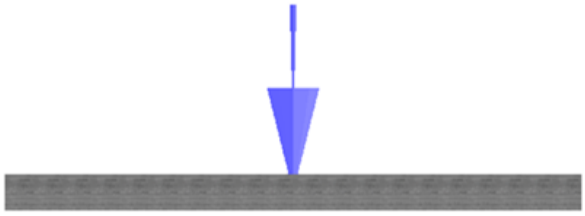

Fig. 3(b). Application of Displacement Controlled Load in SeismoStruct

Fig. 3(c). Beam Failed by Reinforcement Fracture in SeismoStruct

A. Model Validation

The beam modelled is validated based on the experiment data by [11]. The specification of the specimen considered is summarized in Table II.

 ISBN: 978-93-90214-20-4

Table II. Specimen Specification [11]

Size of Beam (mm)	100 x 180
Main Reinforcement	4T10 at Top & Bottom
Stirrups	2 Legged 6 mm Stirrups @140 mm C/C
Clear Cover (mm)	7 mm
Length (m)	4200 mm (after column failure)
Concrete	Average Compressive Strength (f_c'): 19.9 MPa
Steel	Yield Strength (f_y): 437 MPa

i. Parametric Study

In this study an extensive parametric investigation was carried out to find the optimum configuration of beam subjected to interior column support failure. The various parameters considered are

- Number of Sectional Discretization:

SeismoStruct provides the facility to select the number of sectional discretization of the beam section. Its value is usually 150 by default. It was varied from 100 to 300 in this study and analysis was carried out and compared with the experimental data. It was found that the optimum sectional discretization was 150, which gave a result nearer to the experimental data. The Sectional discretization used in this study is given in Fig.4.

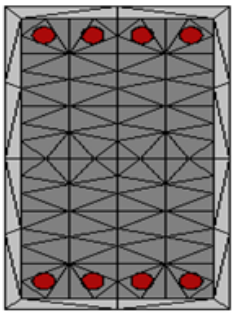

Fig. 4. Beam Sectional Discretization [13]

- Material Model:

SeismoStruct consists of different material models for modelling concrete and steel reinforcement. These material model consists of different parameters which has to varied for the material used. For Commonly used materials such as reinforcement with yield strength of 500 MPa and concrete with average compressive stresses such as 20 MPa, 25 MPa .,etc. are available. Since the material property of the experiment is different, it was varied accordingly.

For concrete various models such as Mander et al. nonlinear concrete model (con_ma), Trilinear concrete model (con_tl) , Chang-Mander nonlinear concrete model (con_cm) were investigated and the model "con_ma" was selected. Typical material model is given in Fig. 5.

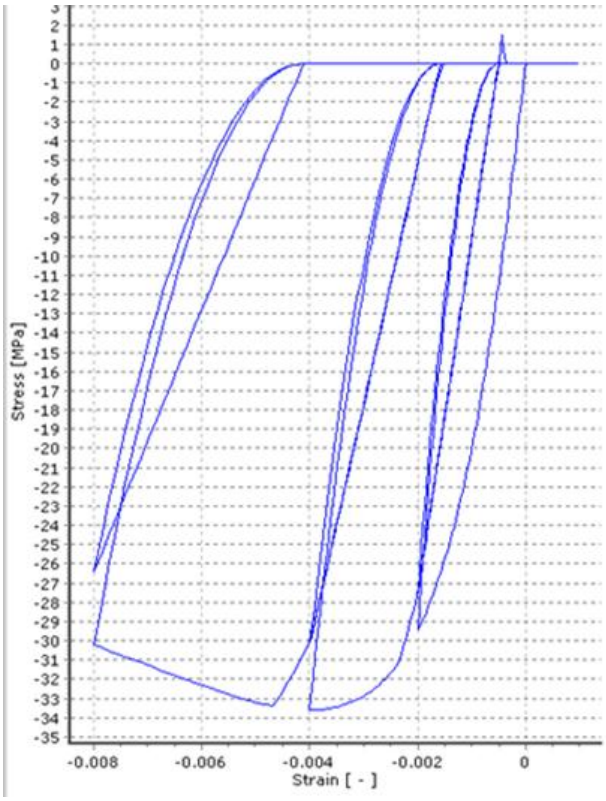

Fig. 5. Material Model for Concrete [13]

For reinforcement various models such as Menegotto-Pinto steel model (stl_mp) , Monti-Nuti steel model (stl_mn) Ramberg-Osgood steel model (stl_ro) were investigated and the model "stl_mn" was selected. Typical material model is given in Fig. 6.

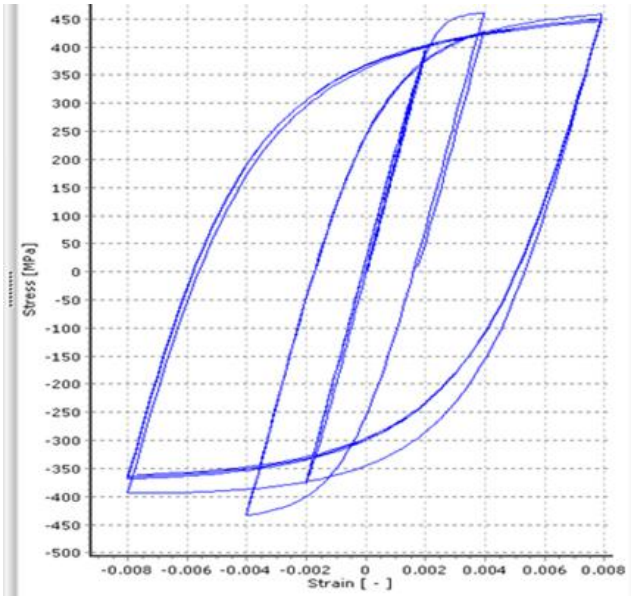

Fig. 6. Material Model for Steel [13]

 ISBN: 978-93-90214-20-4

- Number of Nodes:

Number of nodes was varied to find optimum beam element length. Beam Element lengths of 100,150,210,300,350,420 mm was considered. Optimum was found to be Beam Element Length of 210 mm or 21 Nodes. The Nodes, Element and Element Connectivity of beam modelled in SeismoStruct is shown in Fig. 7.

Fig. 7. Nodes, Element and Element Connectivity of beam

ii. *Result*

The beam is modelled as shown in Fig.8, using the optimum parameters discussed. Static Pushdown Analysis was conducted at the interior column joint where displacement of 1.5 m was applied in 1500 steps. The Load – Displacement graph obtained is given in Fig.9. The result obtained from this analysis was compared with the experimental data obtained from [11] and is tabulated in Table III. Performance criteria (or stages) such as yielding, crushing, and failure of members throughout the structure are set by SeismoStruct is used to calculate the CAA and TCA for this beam.

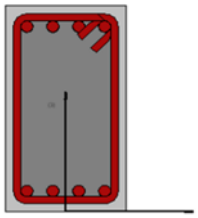

Fig. 8. Beam Modelled in SeismoStruct

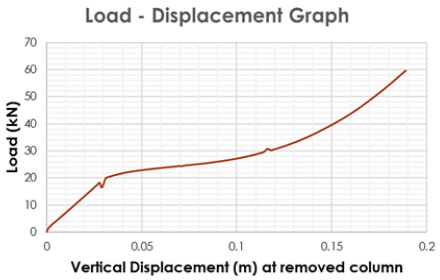

Fig. 9. Load –Displacement Graph of Beam

Table III. Model Validation Results

Parameter	Experimental Data*[11]	Analysis Data
Yield Load (kN)	24	18.35
First Peak Load (kN)	32	30.77
Failure Load	47	59.72
Displacement at first Rebar fracture (mm)	191	189
Failure Type	Rebar Fracture	Rebar Fracture

* Experimental data obtained from [11] in text format

Here the Yield load and First Peak Load found by analysis is comparable with that of the experimental data. This value is found to be less due to the uncertainties in the steel modelling. It was also found that the first rebar fracture occurred in the experiment and analysis coincides. However, analysis was stopped at this point as most of the reinforcement in the beam fractured and the beam is not able to take up any more load. However, in the experiment the steel reinforcement was found to failed gradually from 191 mm to 370 mm. This may have been the reason for the reduced failure load in experiment compared to the analysis. Hence it is safe to assume that the models analysed will be valid.

B. Longitudinal Beam

Longitudinal Beam (LB) is a 2D beam-column assemblage has span of 8,000 mm due to assuming a mid-column had lost. The size of this beam is 400 x 600 mm, having Reinforcement 4T16 at Top & 3T16 at Bottom. Stirrups are provided as 8 mm @ 150 mm c/c as shown in Fig.10.

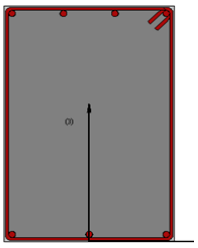

Fig. 10. LB Modelled in SeismoStruct

The load-displacement curve of LB is shown in Fig.11.The first cracks were formed in the beam end near to interior column (BENI) at the loads of 184.27 kN. The measured yield load and first peak load were 165.2 and 232.5 kN, respectively. Since effects of strain hardening, and stirrup confinements are less at this displacement stage the load variation is mostly due to CAA. Hence CAA increased the load carrying capacity by 40.76%. Furthermore, rebar fracture was observed at the 40.52 kN at a displacement of 405 mm. hence there is no significant effect of TCA in increasing the load. Its failure pattern is shown in Fig.12.

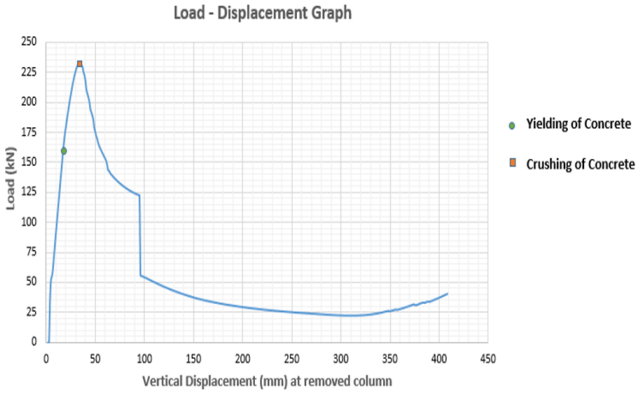

Fig. 11. Load –Displacement Graph of LB

 ISBN: 978-93-90214-20-4

Fig. 12. Failure model of LB

C. Longitudinal Beam & Transverse Beam

Longitudinal & Transverse Beam (LTB) is a combination of transverse and longitudinal beam of span of 8,000 mm (each) due to assuming a mid-column had lost as shown in in Fig.13. The size and reinforcement of this beam is same as that of LB.

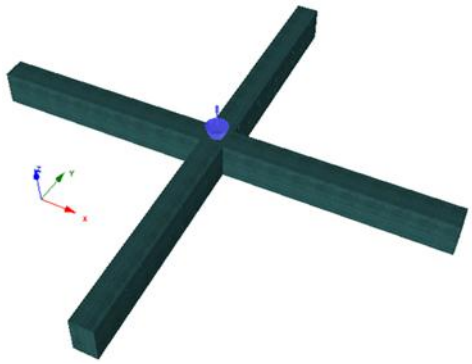

Fig. 13. LTB Modelled in SeismoStruct

The load-displacement curve of LTB is shown in Fig.14. The results obtained was very much identical to LB, but approximately doubled due to symmetry. The first cracks were formed in the beam end near to interior column (BENI) at the loads of 379.78 kN. The measured yield load and first peak load were 345.19and 465.1 kN, respectively. Hence CAA increased the load carrying capacity by 34.73%. Furthermore, rebar fracture was observed at the 81.04 kN at a displacement of 405 mm. Hence here also there is no significant effect of TCA in increasing the load. Its failure pattern is also shown in Fig.15.

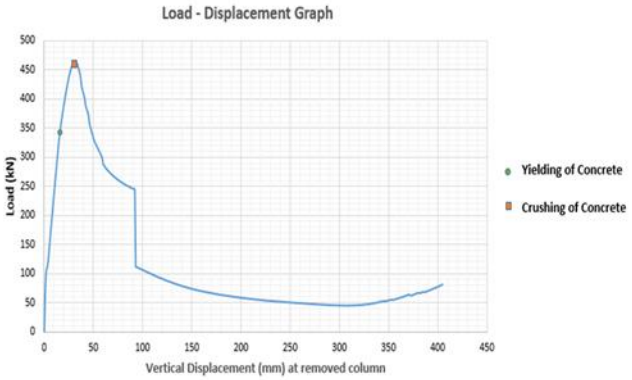

Fig. 14. Load –Displacement Graph of LTB

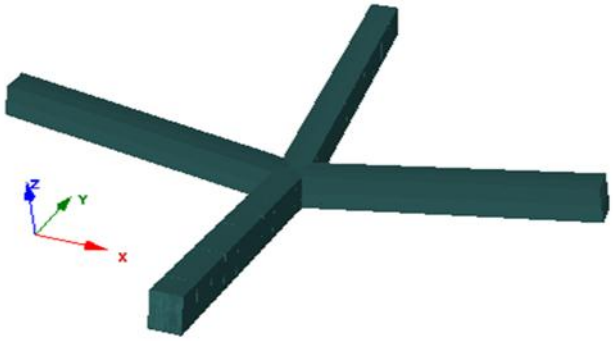

Fig. 15. Failure model of LTB

D. 2D Bare Frame

2D Bare Frame (2DBF) consists of a three storey, three bay bare frame of building designed as shown in Fig.16. Corner columns was modelled in all three stories, whereas the middle one was only modelled for the upper two stories to simulate the removal of the ground center column. The beams were same as LB, while the columns of height 3000 mm, size 400 x 600 mm, having reinforcement 8T16 placed symmetrically. Lateral ties are provided as 8 mm @ 100 mm c/c.

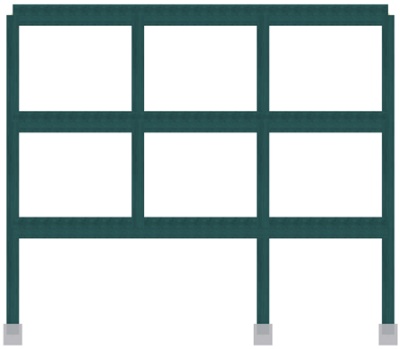

Fig. 16. 2DBF Modelled in SeismoStruct

The load-displacement curve of 2DBF is shown in Fig.17. In this specimen the first crack was formed at beam end near to interior column similar to LB & LTB. However, this cracking load was 436.778 kN which was found to be less than the yield load of the specimen measured as 668.26 kN. This explains the sudden deviation in the load – displacement graph at this load. Moreover, it was observed that these cracks occurred in the first floor earlier than those in the third floors. Crack pattern also indicated that the bays adjacent and above the lost columns were more severely affected.

For this specimen the first peak load was 893.07 kN. This indicated that the contribution of CAA in this specimen was 33.64%. Furthermore, rebar fracture was observed at the 692.51 kN at a displacement of 79 mm. Hence here there is a small TCA of 3.62% in increasing the load. Its failure pattern is also shown in Fig.18.

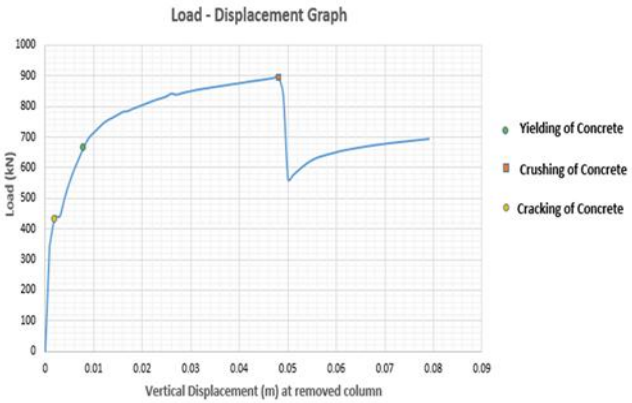

Fig. 17. Load –Displacement Graph of 2DBF

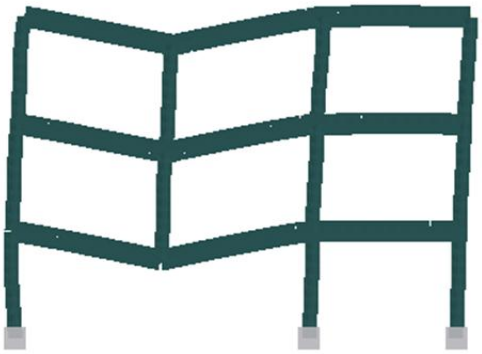

Fig. 18. Failure model of 2DBF

E. 2D Bare Frame with Infill Wall

2D Bare Frame with Infill Wall (2DBFIW) consists of 2DBF with infill walls as shown in Fig.19. Infill walls are modelled in SeismoStruct using Inelastic infill panel element. For this various parameters entered are given in Table IV.

Table IV. Infill Panel Element Parameters

Parameter	Value
Panel Thickness (m)	0.23
Width of strut (m)	0.5
Horizontal offset (X_0) (m)	5.55
Vertical offset (Y_0) (m)	12.50
Specific Weight (kN/m^3)	20

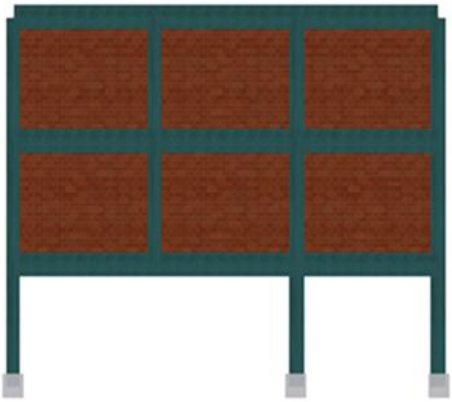

Fig. 19. 2DBFIW Modelled in SeismoStruct

The load-displacement curve of 2DBFIW is shown in Fig.20. In this specimen the first crack was formed at beam end near to adjacent column (BENA) rather than in LB, LTB, 2DBF. This suggested that the MI walls acted as Load transfer path and carried the loads faster to BENA. Moreover, the load – displacement graph has an initial high load resisting capacity of 671.31 kN. This initial load resisting capacity of the specimen is mainly attributed to the MI walls, rather than the RC frame. On further increasing the displacement, cracks might have developed in the MI walls and as a result the load resisting capacity dropped significantly. From then onwards the load -displacement graph was similar to that of 2DBF. At the end of this graph the load resisting capacity is dropping in various stages. This might be because of slippage of the bed joint of MI walls. Moreover, similar to 2DBF, it was observed that cracks occurred in the first floor earlier than those in the third floors and cracks progressed from the adjacent bays to the end bays.

For this specimen, the yield load was 923.091 kN and the first peak load was 1166.06 kN. This indicated that the contribution of CAA in this specimen was 26.32%. Furthermore, rebar fracture was observed at the 827.14 kN at a displacement of 74 mm. Hence here also there is no significant effect of TCA in increasing the load. Its failure pattern is also shown in Fig.21.

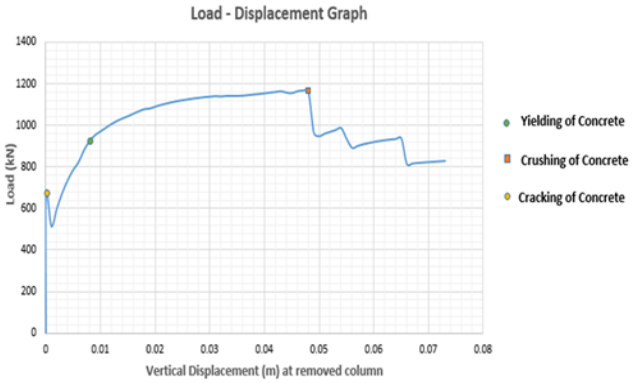

Fig. 20. Load –Displacement Graph of 2DBFIW

 ISBN: 978-93-90214-20-4

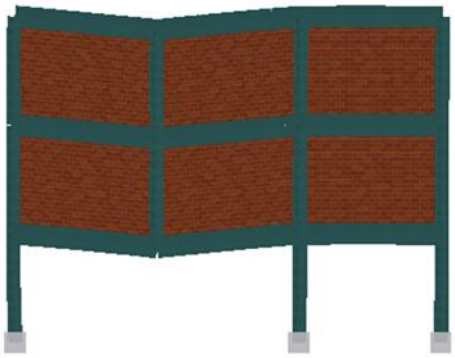

Fig. 21. Failure model of 2DBFIW

F. 3D Frame with Slab

3D Frame with Slab (3DFS) consists of a three storey, three bay building designed as shown in Fig.22 (a) &(b). This is a 3 –D frame based on the building designed with the ground floor interior column removed for analysis. Beams and columns are modelled based on the size and reinforcement data available. Since there are no separate provisions of slabs in SeismoStruct they are modelled as rigid diaphragms by defining a master control node and connecting it to its corresponding slave nodes.

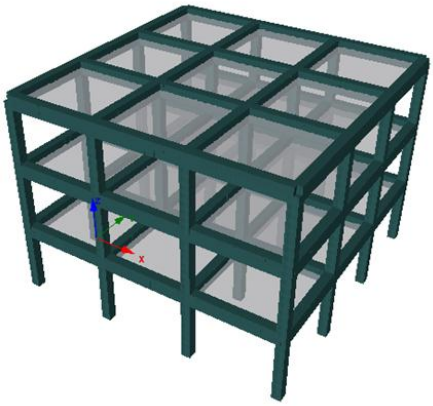

Fig. 22(a). 3DFS Modelled in SeismoStruct

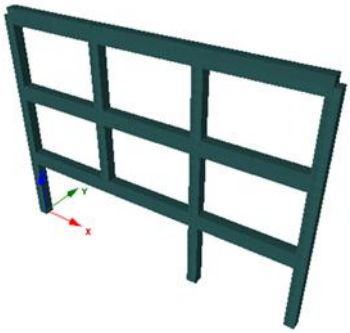

Fig. 22(b). 3DFS Frame Section with Column Removed

The load-displacement curve of 3DFS is shown in Fig.23. In this specimen the first crack was formed at BENA at a cracking load was 2370.25 kN. Cracks first being formed at BENA instead of BENI in this specimen compared to 2DBF, may be because of rigid action of slab. The Cracking loads was found to be less than the yield load of the specimen measured as 3579.54 kN. This explains the sudden deviation in the load – displacement graph at this load. Moreover, it was observed that these cracks occurred in the first floor earlier than those in the third floors, similar to that of 2DBF.

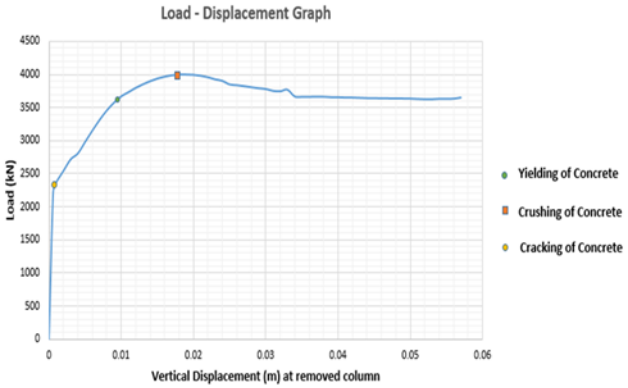

Fig. 23. Load –Displacement Graph of 3DFS

For this specimen the first peak load was 4006.43 kN. This indicated that the combined contribution of CAA and CMA in this specimen was 11.92%. Furthermore, rebar fracture was observed at the 3657.58 kN at a displacement of 57 mm. Hence here there is a small increase in the load of 2.18% due to the presence of TCA & TMA. This values even though small, are significant as they are compared to such a high yield load. A major difference between the Load – displacement graph of 2DBF & 3DFS suggests that the CMA is relatively low and hence didn't contribute much compared to CAA, while TMA has caused the descending part of curve to rise again and remain nearly constant till rebar fracture. Its failure pattern is also shown in Fig. 24 (a) & (b).

Fig. 24(a). Failure Model of 3DFS

 ISBN: 978-93-90214-20-4

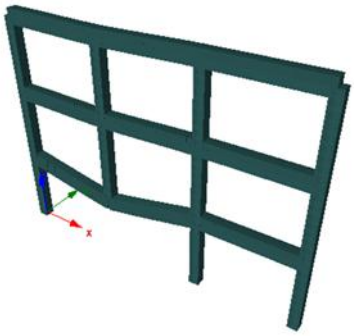

Fig. 24(b). Failure Model of 3DFS Frame Section

G. 3D Frame with Slab and Infill Wall

3D Frame with Slab & Infill Wall (3DFSIW) consists of 3DFS with infill walls as shown in Fig. 25. Infill walls are modelled in SeismoStruct using Inelastic infill panel element. For this various parameters are to be entered as shown in Table -4. Similar to 2DBFIW, infill walls are provided only at the upper two floors.

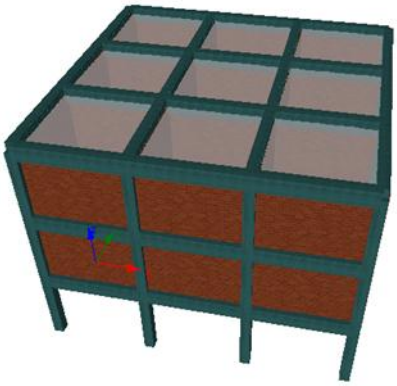

Fig. 25. 3DFSIW Modelled in SeismoStruct

The load-displacement curve of 3DFSIW is shown in Fig.26. In this specimen the first crack was formed at beam end near to adjacent column (BENA) similar to 2DBFIW & 3DFS. This suggested that the MI walls also acted as Load transfer path along with rigid slab and carried the loads faster to BENA. Moreover, the load – displacement graph has an initial high load resisting capacity of 4882.237 kN. This initial load resisting capacity of the specimen is mainly attributed to the MI walls, rather than the RC frame. On further increasing the displacement, cracks might have developed in the MI walls and as a result the load resisting capacity dropped significantly. From then onwards the load -displacement graph was similar to that of 3DFS.

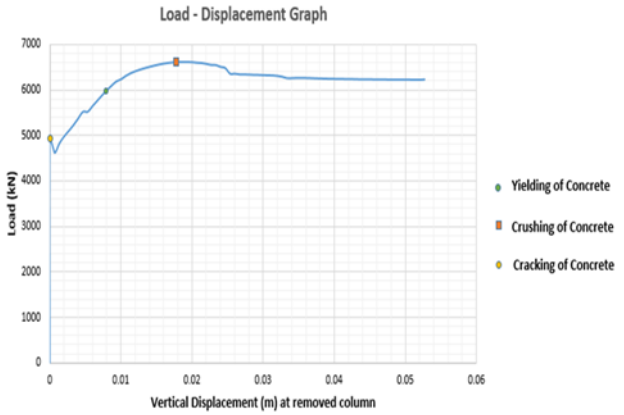

Fig. 26. Load –Displacement Graph of 3DFSIW

For this specimen, the yield load was 5996.9 kN and the first peak load was 6623.09 kN. This indicated that the combined contribution of CAA & CMA in this specimen was 10.44%. Furthermore, rebar fracture was observed at the 6236.57 kN at a displacement of 53 mm Hence here there is a small increase in the load of 3.94% due to the presence of TCA & TMA. This values even though are small, are significant as they are compared to such a high yield load. Similar to 3DFS, here also CMA is relatively low and hence didn't contribute much compared to CAA, while TMA has caused the descending part of curve to rise again and remain nearly constant till rebar fracture. Its failure pattern is also shown in Fig. 27.

Fig. 27. Failure Model of 3DFSIW

5. RESULTS & DISCUSSIONS

A Multistorey building having 3 storey, 3 bay having beams of size 400 x 600 mm, having length 4 m and columns of size 400 x 400 having length 3 m was designed & analysed for progressive collapse analysis using SeismoStruct Software.

The results of LB, LTB, 2DBF & 2DBFIW is compiled in Table V.

Table V. Results of Analysis of LB, LTB, 2DBF & 2DBFIW

Parameter (kN)	Values			
	LB	LTB	2DBF	2DBFIW
Cracking Load (kN)	184.2	379.78	436.778	671.31
Location of First Crack	BENI	BENI	BENI	BENA
Yield Load (kN)	165.2	345.19	668.26	923.091
First Peak Load (kN)	232.5	465.1	893.07	1166.06
Failure Load	40.52	81.04	692.51	827.14
Percentage Increase in Load Carrying capacity due to CAA	40.76	34.73	33.64	26.32
Percentage Increase in Load Carrying capacity due to TCA	-	-	3.62	-
Maximum Displacement before Failure (mm)	405	405	79	74
Failure Type	Rebar Fracture	Rebar Fracture	Rebar Fracture	Rebar Fracture

From Table V, it is found that the Specimens were able to develop significant CAA varying from 26.32 % to 40.76 %. The amount of CAA developed depends on the specimen itself. That is in LB, a beam which had no restraint developed maximum CAA, compared to 2DBFIW, a frame with infill walls. This was because the load was redistributed in 2DBFIW through the infill walls creating a high load resistance. This high load resistance overshadowed the effect of CAA in the initial stage. Nevertheless, by comparing 2DBF and 2DBFIW it is evident that the presence of infill walls increased the yield load by 38.19%, first peak load by 30.56%, failure load by 19.44%, which is a significant improvement. However, there isn't much change in ultimate deformation.

In these specimens it was observed that the effect of TCA is very less. Since the ultimate load is lesser than yield load their effect won't have any effect when column is lost. This is because the specimen cannot provide the load carrying capacity which was required at the earlier stage of collapse. By referring with the results of other experiments conducted by Qian et al.,2015, there is possibility of developing TCA and it can be inferred that it depends on the material and size of beams in Specimen.

The results of 3DFS & 3DFSIW are compiled in Table VI.

Table VI. Results of Analysis of 3DFS & 3DFSIW

Parameter (kN)	Values	
	3DFS	3DFSIW
Cracking Load (kN)	2370.25	4882.23
Location of First Crack	BENA	BENA
Yield Load (kN)	3579.54	5996.9
First Peak Load (kN)	4006.43	6623.09
Failure Load	3657.58	6236.57
Percentage Increase in Load Carrying capacity due to CAA & CMA	11.92	10.44
Percentage Increase in Load Carrying capacity due to TCA & TMA	2.18	3.94
Maximum Displacement before Failure (mm)	57	53
Failure Type	Rebar Fracture	Rebar Fracture

By comparing 3DFS & 3DFSIW it is evident that the presence of infill walls increased the yield load by 105.97%, first peak load by 65.31%, failure load by 70.51%, which is a very significant improvement. However, there isn't much change in ultimate deformation. Furthermore, Infill walls was able to provide this high initial strength throughout. Since 3DFSIW incorporated the effects of all resisting mechanism discussed, it can represent the behavior of an "Ideal" building subject to progressive collapse by loss of a interior column. However, in actual cases provisions should be made for wall openings.

6. CONCLUSION

Each specimen part of a multistorey building when analysed for progressive collapse gave an idea how each individual member can take up the excess loads and deform accordingly. In all these specimens CAA is mainly the progressive collapse resisting mechanism. TCA even though theoretically is a prominent resisting mechanism, its effect is not significant in this case. This may be because of the beam size and materials used in this analysis. Moreover, the effect of Infill walls has significantly increased the load carrying capacity of building. Hence its effect has to be considered when considering any problems related to

progressive collapse, provided proper allowances made for wall openings.

Also by studying progressive collapse resisting mechanism, a concept of "Progressive Collapse Mitigation Technique" can be derived. The main concept of this is based on the fact that the ultimate load is always less than the first peak load, but the specimen is able to take some more deflection before failure by rupture of rebar. So by providing a mechanism to take the load from the specimen at the exact point when the structure loses its initial load carrying capacity, we will be able to sustain the high load as well as keep the structure intact till ultimate deflection is reached. That is the structure will have both high load carrying capacity and the ability to have high deformation. By doing so progressive collapse of a building can be delayed to the extent that the occupants of the building can safely escape from the collapsing building.

In some cases, there will not be any need of progressive collapse mitigation techniques. This is because sudden column loss, which is the extreme case of column damage is considered as the initiation of progressive collapse. Hence structures, if found to have adequate resisting mechanism will be safe against progressive collapse. However further study needs to be conducted on the effect loss of corner columns and simultaneous column losses that can occur in the structure..

REFERENCE

[1] ASCE (American Society of Civil Engineers) (2010) ASCE 7-10 Minimum design loads for buildings and other structures.

[2] General Services Administration (2003). Progressive collapse analysis and design guidelines for new federal office buildings and major modernization projects, Washington, DC, USA.

[3] Department of Defense (2009). Unified facilities criteria, design of buildings to resist progressive collapse (UFC 4-023-03), Department of Defense, Washington, DC, USA

[4] Palmisano, F. (2017) "Improving the robustness of r.c. buildings by the activation of the elasto-plastic catenary behavior", International Journal of Structural Engineering, Vol. 8, No. 1, pp.63–75.

[5] Yi, W., He, Q., Xiao, Y., and Kunnath, S. K. (2008). "Experimental study on progressive collapse-resistant behavior of reinforced concrete frame structures." ACI Struct. J., 105(4), 433–439.

[6] Sasani, M.,and Kropelnicki, J.(2008)."Progressive collapse analysis of an RC structure." Struct. Des. Tall Spec. Build., 17(4), 757–771.

[7] Tian, Y., and Su, Y. P. (2011). "Dynamic response of reinforced concrete beams following instantaneous removal of a bearing column."J.Concr. Struct. Mater., 5(1), 19–28.

[8] Qian,K.,and Li,B.(2013)."Performance of three-dimensional reinforced concrete beam-column substructures under loss of a corner column scenario." J. Struct. Eng., 10.1061/(ASCE)ST.1943-541X.0000630, 584–594.

[9] Yang, B., and Tan, K. (2013). "Robustness of bolted-angle connections against progressive collapse: experimental tests of beam-column joints and development of component-based models." J. Struct. Eng., 10.1061/(ASCE)ST.1943-541X.0000749, 1498–1514.

[10] Mitchell, D., and Cook, W. D. (1984). "Preventing progressive collapse of slab structures." J. Struct. Eng., 10.1061/(ASCE)0733-9445(1984) 110:7(1513), 1513–1532.

[11] Qian, K., Li, B., and Ma, J. (2015). "Load-carrying mechanism to resist progressive collapse of RC buildings." J. Struct. Eng, Vol 141, No.2,

[12] Qian, K., and Li, B. (2017). "Effects of Masonry Infill Wall on the Performance of RC Frames to Resist Progressive Collapse." J. Struct. Eng, Vol 143, No.9,

[13] Seismosoft [2020] "SeismoStruct 2020 – A computer program for static and dynamic nonlinear analysis of framed structures," available from https://seismosoft.com/ Available at: www.seismosoft.com [accessed on 01/03/2021]

Determination of Critical Column in Progressive Collapse Analysis using MATLAB

[1] Rohit Ravikumar, [2] Dr. Beena K P

[1][2] Department of Civil Engineering, College of Engineering Trivandrum, India

Abstract:

The term progressive collapse is defined as the collapse of all or a large part of a structure precipitated by damage or failure of a relatively small part of it. The conventional method of progressive collapse analysis is done using the method of sudden column loss. Hence the study of progressive collapse depends on the column selected to be removed. Removing each column of a multistorey structure sequentially is time consuming and quite difficult. Hence to simplify the procedure, progressive collapse can be analysed by removing a critical column (i.e. a column whose removal causes the maximum damage in shortest time.). This is based on the fact that, if a structure is safe after loss of critical column, then it is safe against the loss of any other column in the structure. Since there isn't any commercial software developed explicitly for this purpose, the analysis can be performed by coding in MATLAB. In this paper, A 3 storey, 3 bay, 9 slab multistorey framed structure is analysed to find critical column.

Keywords:

Critical Column, MATLAB, Progressive collapse, RCC framed structure

1. INTRODUCTION

The term progressive collapse is defined as the collapse of all or a large part of a structure precipitated by damage or failure of a relatively small part of it. It is sometimes also called a disproportionate collapse, which is defined as a structural collapse disproportionate to the cause of the collapse. Reference [1] defines the progressive collapse as "the spread of an initial local failure from element to element resulting, eventually, in the collapse of an entire structure or a disproportionately large part of it". As the small structural element fails, it initiates a chain reaction that causes other structural elements to fail in a domino effect, creating a larger and more destructive collapse of the structure. Progressive collapse is one of the most devastating types of building failures, most often leading to costly damages, multiple injuries, and possible loss of life.

The 1968 Ronan Point collapse has been instrumental in making engineers aware of the possibility of a chain reaction or progressive collapse. Its importance, however, has been growing because of the spread of many tragic collapses: The Murrah Federal Building in Oklahoma (1995), the Giotto Avenue Building in Foggia (1999), and World Trade Centre in New York (2001).

Reference [2] issued Progressive Collapse Analysis and Design Guidelines for New Federal Office Buildings and Major Modernization Projects. Reference [3] issued Unified Facilities Criteria for Design of Buildings to Resist Progressive Collapse (UFC 4-023-03). Both these guidelines were the foundation for progressive collapse analysis. They recognized instantaneous/sudden column loss as a suitable event-independent scenario for assessing structural robustness and suggested using it for progressive collapse analysis. Reference [4] showed how progressive collapse can be evaluated using sudden column loss phenomenon as suggested by [2] & [3]. They compared the ductility demands in multi-storey buildings arising from sudden column loss on, and column damage by blast on the other, by considering a planar sub-frame representing the affected bays to prove that sudden column loss can be used for progressive collapse analysis. [5] compared the different cases of progressive collapse of a 7 storey RC structure due to different column failures to study the resisting mechanism of concrete structures and the effects of initial damage locations using software SAP2000.

A Simplified Procedure for determining critical column in progressive collapse analysis of RC structures was presented by [6]. This method involves using SAP2000 to check the various column loss individually using time – history analysis. Even though this gives a reasonable judgement of critical column, the process is still tedious. By using MATLAB and inputting the algorithm used by [6] in an iterative process, it is possible to find the critical column with less human effort. Moreover, a criterion to measure damage can be inputed using crack width calculated by [7].

2. MATLAB

MATLAB is a commercial software and a trademark of the MathWorks, Inc., USA. It is an integrated programming system, including graphical interfaces and a large number of specialized toolboxes. The MATLAB programming language is useful in illustrating how to program the finite element method due to the fact it allows one to very quickly code numerical methods and has a vast predefined mathematical library and built in graphics functions. This is also due to the fact that matrix, vector and many linear algebra tools are already pre-defined and the user is only required to develop the algorithm and not defining these data structures and the corresponding graphic visualization. That is, a simple two dimensional finite element program in

MATLAB need only be a few hundred lines of code compared to a few thousand in Fortran or C++.

The two important parts of a MATLAB code are M-files & Functions. A M-file is a plain text file with MATLAB commands, saved with extension ".m" (eg. File.m). The M-files can also be scripts of functions. M-files are useful when the number of statements is large, or when you want to execute it at a later stage, or frequently, or even to run it in background. Functions act like subroutines in fortran where a particular set of tasks is performed. In a typical function, in the first line we should name the function and give the input parameters (m,n,p) in parenthesis and the output parameters (a,b,c) in square parenthesis. Eg: function [a,b,c] =File (m,n,p)

3. BUILDING SPECIFICATION

The building considered is same as in [6]. The specifications of the building designed is as follows:

Number of Storey : 3
Number of Bays : 3
Number of Slabs / Floor : 9

Beams: 400 mm x 600 mm, having Effective Length of 4 m.
Columns: 400 mm x 400 mm, having Effective Length 3 m.
Slab: 0.15 m thick and a floor finish of 0.05 m thickness.
Loads Acting:

- Dead Load :25 kN/m for Beams & 3.75 kN/m2 for Slabs
- Live Load :15 kN/m for Beams &2 kN/m2 for Slabs
- Floor Finish Load (1.25 kN/m2 for Slabs)

Materials: M25 Concrete, Fe500 Steel.

The Line Sketch of elevation and plan of the building are given Fig. 1(a) & 1(b) respectively

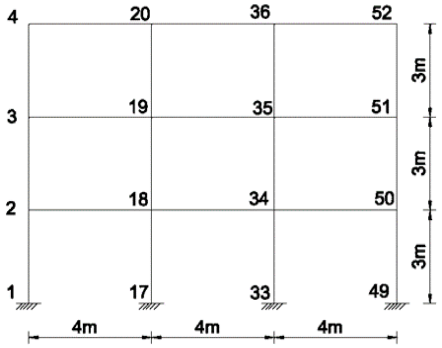

Fig. 1(a). Elevation of Building (X-Z Plane)

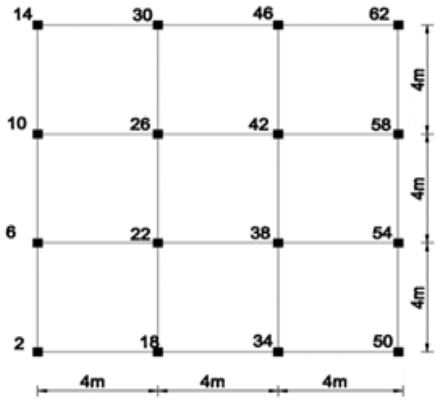

Fig. 1(b). First Floor Plan of Building (X-Y Plane)

The reinforcement provided is shown in Table I.

Table I. Reinforcement of Beams & Columns

Beam (B) Or Column (C)	Area of Longitudinal Reinforcement Provided (mm^2)		Provided Shear Reinforcement
	Top	Bottom	
B1	T16 - 3Nos	T16 - 3Nos	2 Legged T8 Stirrups @ 150mm c/c
B2	T16 - 4 Nos	T16 - 3Nos	2 Legged T8 Stirrups @ 150 mm c/c
B3	T16 - 3 Nos	T16 - 3Nos	2 Legged T8 Stirrups @ 150 mm c/c
B4	T14 - 4 Nos	T16 - 3Nos	2 Legged T8 Stirrups @ 150 mm c/c
C1	T25 - 4 Nos & T12 – 4 Nos		Lateral Ties T8 @ 100 mm c/c
C2	T16 - 8 Nos		Lateral Ties T8 @ 100 mm c/c

For the building designed B1 represents all the edge beams (36 Nos) of the building, B2, B3, B4 (each 12 Nos) represents all interior columns of ground floor, first floor, second floor respectively. C1 represents the four interior columns on the ground floor (21-22, 25-26, 37-38 ,41-42), while C2 represents all the other columns.

4. CRITICAL COLUMN

In the work done by [6], a Model A which contains the entire structure, including the column to be removed was first analysed. The internal axial forces on the column which is to be removed is then found out. Then Model B is then modelled with the column removed. The axial force, obtained during the analysis of Model A was then applied at the top joint of removed column to simulate its presence. This equivalent column load was applied together with the dead. The removal of the column was then simulated by running a time-history analysis in which these equivalent column load was reduced to zero over a short period of time of 10 secs [Fig. 2]. This was done for all column removal scenarios and at each case, the maximum vertical displacement at the joint of column removal, and the time taken was tabulated. The column whose loss caused maximum displacement in the shortest time was taken as critical column.

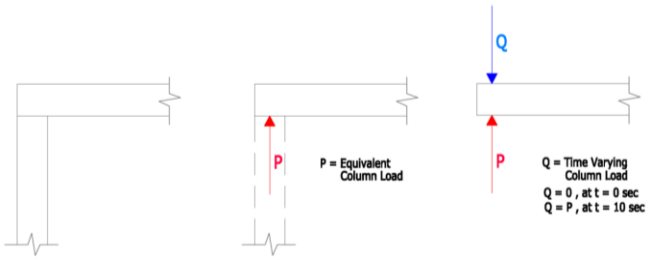

Fig. 2. Time dependent column removal: (a) before column removal (b) column removed & equivalent column load provided (c) column removal in 10 secs [6]

A. MATLAB Coding

In MATLAB, the input data regarding the structure was entered using excel file for ease of entering. Similarly, MATLAB was coded to give output in an excel sheet. The various figures such as graphs, deformed and undeformed shapes of the structure was obtained as "Figures" in MATLAB. The various M-files, Input & Output Excel Data Sheets used in this program is displayed in Table II.

TABLE II . M-files, input & output data sheets

Input Data Sheet	M-Files	Output Data Sheet
Input1.xlsx Input2.xlsx	Discretize.m NAxis.m TFR.m Structure_plot.m Increment_load.m formStiffness3D.m LU_decomposition.m Deformed.m Crack_width.m DPlot.m	Critical_Column.xlsx

i. Input1.xlsx

Every data regarding the structure is input into MATLAB using Excel file. This input file has five sheets –Intro, Nodes, Elements, Restraints, Load. In "Nodes" the various nodes are numbered and their X, Y, Z coordinates are entered. In "Elements" the node connectivity data, reinforcement section data and geometrical properties of elements such as dimensions (B, D, L), modulus of elasticity (Ex, Ey, Ez), moment of inertia (Ix. Iy, Iz) are entered. In "Restraints" the various restraints such as displacement and rotation in the three axis applied for each node are entered. In "Load" the nodal loads corresponding to each nodes and element loads (concentrated & UDL) corresponding to each member element are to be entered. By entering in this format, MATLAB can be coded to extract data from the required sheet of Input file.

ii. Input2.xlsx

In this excel sheet, the various data such as dimensions, cover, bar size, shear reinforcement & spacing of each member (beam & column) are entered from Table II. Each reinforcement section is mapped to the element through "Input1.xlsx" > "Element" Sheet >" Reinforcement Section data" column.

iii. Discretize.m

This M-file is used to discretize each beams element. This makes the analysis more accurate. In this study each beam elements were divided into ten. Hence each beam element had additional nine loads and ten elements, based on this, "Input1.xlsx" was edited to add additional nodal & elemental data.

iv. NAxis.m

This M-file is used to find the depth of neutral axis of each element section from "Input2.xlsx", is found out by considering moments of areas of the cracked transformed section about the neutral axis as shown in (1).

$$b.x^2 + (m-1).A_{Sc}.(x-d') = m.A_{st}.(d-x) \qquad (1)$$

Here "b" is the width of beam, "d" is the effective depth of beam, "d' " is the effective cover of compression reinforcement, "x" is the depth of neutral axis, "m: is the modular ratio (here m = 8), A_{Sc} is the area of compression steel & A_{st} is the area of tension steel.

v. TFR.m

This M-file is used to find effective flexural rigidity based on [7] for all sections defined on "Input2.xlsx". For this effective moment of ineria (I_{eff}) is obtained as in (2).

$$I_{eff} = \frac{I_r}{1.2-\frac{M_r}{M}.\frac{z}{d}.(1-\frac{x}{d})} \qquad (2)$$

$$M_r = \frac{f_{cr}.I_{gr}}{y_t} \qquad (3)$$

Here "M_r" is the cracking moment given by (3), "M" is the maximum moment, "z" is the lever arm, "x" is the depth of neutral axis, "d" is the effective depth, "f_{cr}" is the modulus of rupture of concrete (here f_{cr} = 3.5 N/mm^2), "I_{gr}" is the moment of inertia of gross section, "y_t" is the distance from centroidal axis to extreme fibre in tension.

"TFR.m" assigns True Flexural Rigidity (TFR) to each section such that TFR = E.I_r for M < M_r & TFR = E.I_{eff} for M > M_r .

vi. Strucutere_plot.m

This M- file, makes use of the built in "Plot function" to connect nodes, based on element data from "Input1.xlsx". The structure plotted is displayed as a "Figure" in MATLAB.

vii. Increment_load.m

This M- file is the fundamental part of the MATLAB code. This M- file operates in a two-level iterative process. After preliminary analysis, the equivalent column load (P) of each column of structure is found out. In the first level, the first column of the structure is selected and its data is deleted from "Input1.xlsx", and the equivalent load of that column is applied at the joint to simulate presence of that column.

In the next level of iteration, a time varying load (Q) is varied from zero to maximum (P) to simulate a column failure in 10 load steps as shown in Fig. 2. The deflection at the joint in each load step is entered into "Critical_Column.xlsx". This process is again repeated for the next column and the next, until all the columns are removed and analysed, one at a time.

viii. formStiffness3D.m

This is a function developed to obtain stiffness of element in 3-D, assemble them to form the global stiffness matrix and finally multiply the element stiffness with nodal displacement to get nodal forces. This is also a two-level process in which the function is called two times- firstly on getting global stiffness matrix and then secondly to obtain nodal force vector. This function is first called to provide the preliminary analysis for "Increment_load.m", and it is repeated for every iterative process with the modified nodes, elements & loads.

For using this function 2-Noded element, with six degrees of freedom (3 – Translation & 3- rotation) at each node are considered. Here the element is inclined with respect to the global axis. The element degrees of freedom are shown in Fig. 3. The various standard equations involved are shown in (4), (5), (6), (7), (8) & (9).

$$U^T = [U_1\ U_2\ U_3\ U_4\ U_5\ U_6\ U_7\ U_8\ U_9\ U_{10}\ U_{11}\ U_{12}] \quad (4)$$

$$K'^e = \begin{bmatrix} \frac{EA}{L} & 0 & 0 & 0 & 0 & 0 & -\frac{EA}{L} & 0 & 0 & 0 & 0 & 0 \\ & \frac{12EI_z}{L^3} & 0 & 0 & 0 & \frac{6EI_z}{L^2} & 0 & -\frac{12EI_z}{L^3} & 0 & 0 & 0 & \frac{6EI_z}{L^2} \\ & & \frac{12EI_y}{L^3} & 0 & -\frac{6EI_y}{L^2} & 0 & 0 & 0 & -\frac{12EI_y}{L^3} & 0 & -\frac{6EI_y}{L^2} & 0 \\ & & & \frac{GJ}{L} & 0 & 0 & 0 & 0 & 0 & -\frac{GJ}{L} & 0 & 0 \\ & & & & \frac{4EI_y}{L} & 0 & 0 & 0 & \frac{6EI_y}{L^2} & 0 & \frac{2EI_y}{L} & 0 \\ & & & & & \frac{4EI_z}{L} & 0 & -\frac{6EI_z}{L^2} & 0 & 0 & 0 & \frac{2EI_z}{L} \\ & & & & & & \frac{EA}{L} & 0 & 0 & 0 & 0 & 0 \\ & & & & & & & \frac{12EI_z}{L^3} & 0 & 0 & 0 & -\frac{6EI_z}{L^2} \\ & & & & & & & & \frac{12EI_y}{L^3} & 0 & \frac{6EI_y}{L^2} & 0 \\ & & & & & & & & & \frac{GJ}{L} & 0 & 0 \\ & & & & & & & & & & \frac{4EI_y}{L} & 0 \\ Sim. & & & & & & & & & & & \frac{4EI_z}{L} \end{bmatrix} \quad (5)$$

$$R = \begin{bmatrix} r & 0 & 0 & 0 \\ 0 & r & 0 & 0 \\ 0 & 0 & r & 0 \\ 0 & 0 & 0 & r \end{bmatrix} \quad (6)$$

$$K_e = R^T K'_e R$$
$$F_e = k'_e R U \quad (7)$$

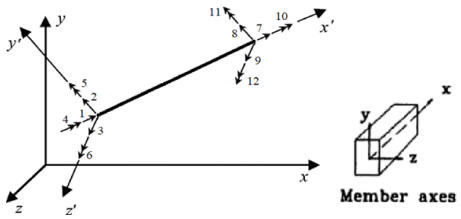

Fig. 3. Element DOF of 3-D element

Here to define rotation a P Node is defined as: x_p, y_p, z_p. The coordinates of P Node were selected in such a way that, it lied on the plane of element, but never on the axis of the element. Hence MATLAB was coded to automatically generate its own P-Node of each element by adding twice the length of element to the coordinates of the end nodes of the element. This was done only for the coordinates in the plane of the element.

Then,

$C_x = \frac{(x2-x1)}{L}$ $C_y = \frac{(y2-y1)}{L}$ $C_z = \frac{(z2-z1)}{L}$

$C_{xz} = (C_x^2 + C_z^2)^{0.5}$

$$\begin{bmatrix} C_x & C_y & C_z \\ \frac{-C_x.C_y.Cos\omega - C_z.Sin\omega}{C_{xz}} & C_{xz}.Cos\omega & \frac{-C_y.C_z.Cos\omega + C_x.Sin\omega}{C_{xz}} \\ \frac{C_x.C_y.Sin\omega - C_z.Cos\omega}{C_{xz}} & -C_{xz}.Sin\omega & \frac{C_y.C_z.Sin\omega + C_x.Cos\omega}{C_{xz}} \end{bmatrix} x_{ps} =$$

$x_p - x_1$ $y_{ps} = y_p - y_1$ $z_{ps} = z_p - z_1$

r =

$$y_{2p} = \frac{-C_x.C_y}{C_{xz}}.x_{ps} + C_{xz}.y_{ps} - \frac{C_y.C_z}{C_{xz}}.z_{ps} x_{2p} = C_x.x_{ps} + C_y.y_{ps} + C_z.z_{ps} \quad (8)$$

Where,

$$Cos\omega = \frac{y_{zp}}{\sqrt{y_{2p}^2 + z_{2p}^2}} Sin\omega = \frac{z_{2p}}{\sqrt{y_{2p}^2 + z_{2p}^2}} z_{2p} = \frac{-C_z}{C_{xz}}.x_{ps} + \frac{C_x}{C_{xz}}.z_{ps}$$

This is the case generally. But for vertical members such as columns, the "r" matrix is different.

$$r = \begin{bmatrix} 0 & C_y & 0 \\ -C_y.Cos\omega & 0 & Sin\omega \\ C_y.Sin\omega & 0 & Cos\omega \end{bmatrix} ; \quad (9)$$

$$Sin\omega = \frac{z_{ps}}{\sqrt{x_{ps}^2 + z_{ps}^2}} \quad ; \quad Cos\omega = \frac{-x_{ps}.C_y}{\sqrt{x_{ps}^2 + z_{ps}^2}}$$

ix. LU_decomposition.m

This M- file is used to solve linear equations to find nodal displacement in "formStiffness3D.m". This uses concept of LU decomposition.

x. Deformed..m

This M-file is a modification of "Structure_plot.m". When the column is completely removed at the end of the last load step of "Increment_load.m", the X,Y,Z displacements at each nodes amplified ten times are added to its corresponding nodal coordinates to obtain the deformed shape of the structure. This gives the deformed shape of the structure, when that column is removed. This is also

displayed as "Figure" in MATLAB and is applicable to all column loss scenarios. Moreover, the joint with the column removed is highlighted as a separate "Figure" by showing only the immediate elements connected to the joint.

xi. Crack_width..m

This M-file is used to compute the maximum crack width of the structure using Annex F of [7]. Crack width is computed only at the end of load step, when column is removed completely. The crack width at the corner and at bottom face of beam is found for all the elements of the structure, and only the maximum among these & it's corresponding element is reported in "Critical_Column.xlsx".

xii. DPlot..m

This M-file is used to get a graphical representation of column loss in the structure. After analysis at each load step, the displacement at node where the column was connected is measured. i.e. the displacement from the time the column was intact to completely removed. This is plotted against the load step to give a graphical representation on the effect of column loss. This is also displayed as a "Figure" in MATLAB.

xiii. Critical_Column.xlsx

This analysis for each column loss is finally tabulated in this excel file. The information shown is the detail of the column removed, the node it was connected to, the vertical displacement at the node in each load step and the maximum crack width obtained from "Crack_width.m".

5. RESULTS & DISCUSSION

After analysing the structure using MATLAB code, the structure was plotted as shown in Fig. 4.

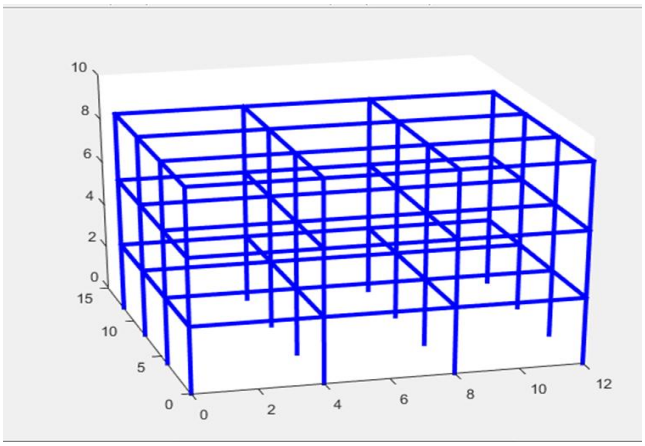

Fig. 4. 3D structure Plotted in MATLAB

The interior column in ground floor, column 16 (Node 21-Node 22), was found to be critical column. This was because it produced max vertical displacement in shortest time. i.e. weighted average displacement at node 21 = 4.376 mm and the maximum cracks of 0.508 mm was formed at Element 53 (Node 22-38) when column 21-22 was completely removed. This results also coincide with [6].

The displacement at node 22 at each load step is shown in Fig. 5. These displacement values were found to vary almost linearly due to the material properties remaining constant. However, there is a slight non linearity in the beginning. This may be due to the beam sections transforming from uncracked to cracked. The displacement Vs load step obtained from MATLAB is shown in Fig. 6. The deformed shape of the structure and the joint amplified ten times corresponding to Column 21-22 removal (Element 16) is shown in Fig. 7(a) & 7(b).

	A	B	C	D	E	F	G	H	I	J	K	L	M	N	O
1	Case No.	Node	Deflection											Maximum Crack Width (mm)	Beam
2			T=0	T=1	T=2	T=3	T=4	T=5	T=6	T=7	T=8	T=9	T=10		
18	16	22	0	1.028216	1.867519	2.706823	3.546127	4.385431	5.224735	6.064039	6.903343	7.742647	8.581951	0.508440	53

Fig. 5. "Critical_Column.xlsx" Data for Elemnt 16 Removal

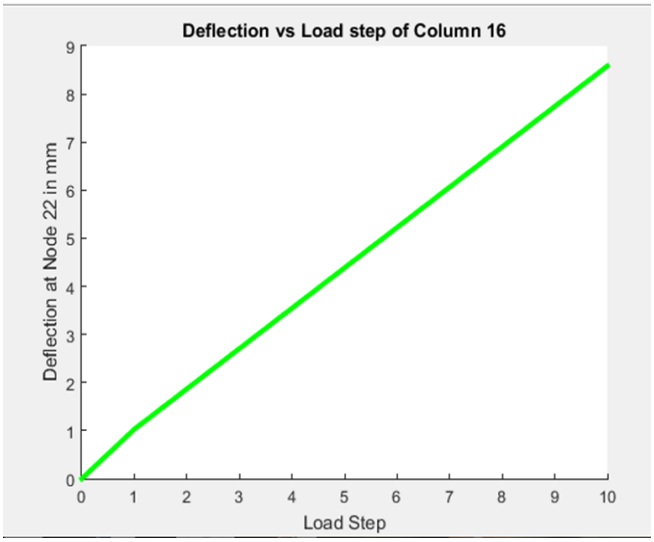

Fig. 6. Displacement Vs Load Step for Elemnt 16 Removal

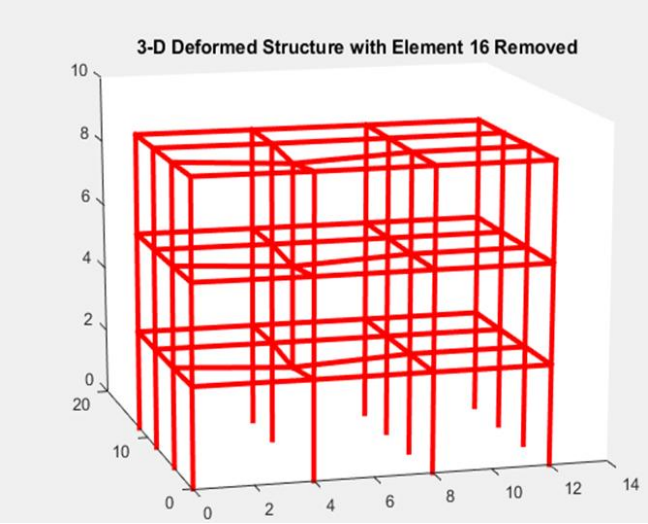

(a)

 ISBN: 978-93-90214-20-4

(b)

Fig. 7. Deformed Structure & Joint Plotted in MATLAB

6. CONCLUSION

Critical column of a RC framed structure was found by coding in MATLAB. It was found that the interior column of the ground floor was the critical column of the structure considered. The concept used for this analysis is a simplified version to simplify the progressive collapse analysis. For more accurate results, the MATLAB code can be expanded with additional codes. This includes, replacing direct stiffness with finite element method, increasing the element discretization, adding material and geometrical non linearity etc.

Moreover, the current analysis didn't consider the load of failed structures and its impact. But the results obtained in this study is accurate as the removal of this interior column affects all the three floors above it so it amplifies the damage scenario calculated. Further studies are also required regarding effect of multiple column loss or removal.

REFERENCE

[1] ASCE (American Society of Civil Engineers) (2010) ASCE 7-10 Minimum design loads for buildings and other structures.

[2] General Services Administration (2003). Progressive collapse analysis and design guidelines for new federal office buildings and major modernization projects, Washington, DC, USA.

[3] Department of Defense (2009). Unified facilities criteria, design of buildings to resist progressive collapse (UFC 4-023-03), Department of Defense, Washington, DC, USA

[4] Gudmundsson, G.V. and Izzuddin, B.A. (2009). "The 'sudden column loss' idealisation for disproportionate collapse assessment", The Structural Engineer, Vol. 88, No. 6, pp. 22–26.

[5] Sagirolu, S. and Sasani, M. (2014). "Progressive collapse – resisting mechanism of concrete structures and effects of initial damage locations", Journal of Structural Engineering, Vol.140, No. 3, pp. 33-47.

[6] Rohit Ravikumar, Beena K P. (2021)."A simplified procedure for determining critical column in progressive collapse analysis of RC structures", International Journal for Research in Applied Science and Engineering Technology (IJRASET), Volume 9, Issue III, Page No: 623-628,

[7] IS456-2000: Indian Standard Plain and Reinforced Concrete Code of Practice. Bureau of Indian Standards, New Delhi.

IoT- Based Vehicle Parking System

[1] Susandhika M, [2] Helanvidhya T, [3] Saranya J

[1] PG Student, Department of ECE, Rajalakshmi Engineering College, Chennai, India
[2][3] Assistant Professor, Department of ECE, Rajalakshmi Engineering College, Chennai, India

Abstract:

Due to the extreme growing number of cars everywhere, parking vehicles in cities has recently become a major problem that is only getting worse. Here, we suggest an IoT-based framework for controlling and tracking available parking spaces, which offers an intelligent solution. The Internet of Things (IoT) can connect billions of devices and services with a variety of applications at any time and in any place. In this paper, we created a mobile application to track a vehicle's parking space and receive real-time updates, resulting in an intelligent solution. Here sensor node is placed under every parking slot and effective communication of devices is done across arduino nano and node MCU. Furthermore, the sensor detects the status of the parking slot and sends the information to the end user.

Keywords:

Node MCUEsp8266, Sensor node, arduino Nano

1. INTRODUCTION

Traffic congestion caused by vehicle is an alarming problem at a global level and it has been growing exponentially. Car parking problem is a major contributor and has been, still a major problem with increasing vehicle size in the luxurious segment and confined parking spaces in urban cities. Searching for a parking space is a routine activity for many people in cities around the world. This search burns about one million barrels of the world's oil every day. As the global population continues to urbanize, without a well-planned, convenience-driven retreat from the car these problems will worsen.Smart Parking systems typically obtain information about available parking spaces in a particular geographic area and process is real-time to place vehicles at available positions.[1]It involves using low-cost sensors, real-time data collection, and mobile-phone-enabled automated payment systems that allow people to reserve parking in advance or very accurately predict where they will likely find a spot. When deployed as a system, smart parking thus reduces car emissions in urban centers by reducing the need for people to needlessly circle city blocks searching for parking. It also permits cities to carefully manage their parking supply.

Limitation of a driver's capability of finding a vacant parking spaces and absence of efficient management are also at fault causing this problem.So we are going to design a system which aims to improve parking facilities by the introducing IoT based vehicle parking system. The system will automatically assign a vacant space to the patrons for parking their vehicles.[3]

2. IMPORTANCE OF SMART PARKING

- Accurately predict and sense vehicle occupancy in real-time.
- Guides residents and visitors to available parking.
- Optimize Parking Space Usage
- Simplifies the parking experience and adds value for parking stakeholders, such as drivers and merchants
- Help traffic in the city flow more freely leveraging IoT technology.
- Enables intelligent decisions using data, including real–time status applications and historical analytics reports
- Smart Parking plays a major role in creating better urban environment by reducing the emission of CO2 and other pollutants[1]
- Smart Parking enables better and real time monitoring and managing of available parking space, resulting in significant revenue generation
- Provides tools to optimize workforce management

3. INTERNET OF THINGS

The internet of things describes the network of physical object, thingsthat are embedded with sensors, software, and other technologies for the purpose of connecting and exchanging data with other devices and systems over the Internet.In the consumer market, IoT technology is most synonymous with products pertaining to the concept of the "smart home", including devicesand appliances such as lighting fixtures, thermostats, home security systems and cameras, and other home appliances that support one or more common ecosystems, and can be controlled via devices associated with that ecosystem, such as smartphones and smart speakers. IoT can also be used in healthcare systems.[1]

There are a number of serious discussions about dangers in the growth of IoT, especially in the areas of privacy and security, and consequently industry and governmental moves. To address these concerns have begun including the development of international standards.

4. HARDWARE IMPLEMENTATION

Recently, with the increase of automobiles incities, parking problems are serious .
The aim of the project is to design and provide:-

- A simple mobile application for parking vehicles.
- Getting approximate about the availability of parking space.
- Can search nearby places using google map.
- It is an efficient time saving system.
- It reduces traffic problems mainly in cities.

User can search their destination parking facilities and accordingly and reach their destination without any confusion.

A. Node MCU base board

This base board is Breakout Board for ESP8266 Node MCU V3 Lua CH340 WiFi Development Board. All the I/O ports are easily accessible through the 2.54mm pin header for easy prototyping. Accept power input of 5~12V through 5.5mm power from wall plug adapter.

- Small and handy module.
- Supply Voltage: 6~24Vdc.
- The spacing between headers pin is 2.54 mm.
- Lead-out all the I/O ports of the ESP-12E development board.
- Lead out the pins of 5V and 3.3V power supply.
- Easy to connect with peripheral modules with jumper wires.
- It is anOnboard 5V/1A DC-DC step-down converter circuit.
- Onboard power-on LED indicator.
- Board Dimension: 60x60 mm

B. Esp8266 microcontroller

The ESP8266 is the name of a micro controller designed by Expressive Systems. The ESP8266 itself is a self-contained Wi-Fi networking solution offering a bridge from existing micro controller to Wi-Fi and it is capable of running self-contained applications. This module comes with a built in USB connector and a assortment of pin-outs. With a micro USB cable, you can connect NodeMCU to laptop and flash it without any trouble;itis immediately breadboard friendly like Arduino.[5]
The basic way to use the ESP8266 module is by using serial commands, as the chip is basically a Wi-Fi/Serial transceiver. However, this is not convenient. What we recommend is using the very cool Arduino ESP8266 project, which is a modified version of the Arduino IDE .we can install this to computer. This makes it convenient to use the ESP8266 chip.

C. Arduino nano

The Arduino Nano is a small, complete, and breadboard-friendly and it is a board basedon the ATmega328P . It offers the same connectivity and specifications of the Arduino Uno board in a smaller form factor.[5]
The Arduino Nano has number of facilities for communicating with computer, other Arduino, or other microcontrollers. The ATmega328 provide UART TTL (5V) serial communication, which is available on digital pins 0 (RX) and 1 (TX). An FTDI FT232RL on the board channels this serial communication over USB and the FTDI drivers provide a virtual comfort to software on the computer. The Arduino software includes a serial monitor which allows simple textual data to be sent to and from the Arduino board. The RX and TX LEDs on the board will flash when data is being transmitted via the FTDI chip and USB connection to the computer but not for serial communication on pins 0 and 1. A Software Serial library allows serial communication on any of the Nano's digital pins. The ATmega328 also support I2C and SPI communication. The Arduino software includes a Wirelibrary to simplify use of the I2C bus. This Arduino is then inbuilt codedthat connects with a LCD display.

Fig. 1 Arduinonano

D. LCD display

Liquid crystal displays (LCDs) have materials which combine the properties of both liquids and crystals. Rather than having a melting point, they have a temperature range within which the molecules are almost as mobile as they would be in a liquid, but are grouped together in an ordered form similar to a crystal.
The principle behind the LCDs is that when an electrical current is applied to the liquid crystal molecule, the molecule tends to untwist. This causes the angle of light which is passing through the molecule of the polarized glass and also causes a change in the angle of the top polarizing filter. As a result, a little light is allowed to pass the polarized glass through a particular area of the LCD.Thus that particular area will become dark compared to others. The LCD works on the principle of blocking light. While constructing the LCDs, a reflected mirror is arranged at the back. An electrode plane is made of indium-tin-oxide which is kept on top and a polarized glass with a polarizing film is also added on the bottom of the device. The complete region of the LCD has to be enclosed by a common electrode and above it should be the liquid crystal matter.Next comes the second piece of glass with an electrode in the form of the rectangle on the bottom and, on top, another polarizing film. It must be considered that both the pieces are kept at the right angles. When there is no current, the light passes through the front of the LCD it will

be reflected by the mirror and bounced back. As the electrode is connected to a battery the current from it will cause the liquid crystals between the common-plane electrode and the electrode shaped like a rectangle to untwist. Thus the light is blocked from passing through. That particular rectangular area appears blank. Crystalonics dot–matrix liquidcrystal displays are available in TN, STN types, with or without backlight. The use of C-MOS LCD controller and driver ICs result in low power consumption. These modules can be interfaced with a 4-bit or 8-bit micro processor /Micro controller.[5]

The controller IC has two 8 bit registers, an instruction register (IR) and a data register (DR). The IR stores the instruction codes and address information for display data RAM (DD RAM) and character generator RAM (CG RAM). The IR can be written, but not read by the MPU.The DR temporally stores data to be written to /read from the DD RAM or CG RAM. The data written to DR by the MPU, is automatically written to the DD RAM or CG RAM as an internal operation.

When an address code is written to IR, the data is automatically transferred from the DD RAM or CG RAM to the DR. data transfer between the MPU is then completed when the MPU reads the DR. likewise, for the next MPU read of the DR, data in DD RAM or CG RAM at the address is sent to the DR automatically. Similarly, for the MPU write of the DR, the next DD RAM or CG RAM address is selected for the write operation.

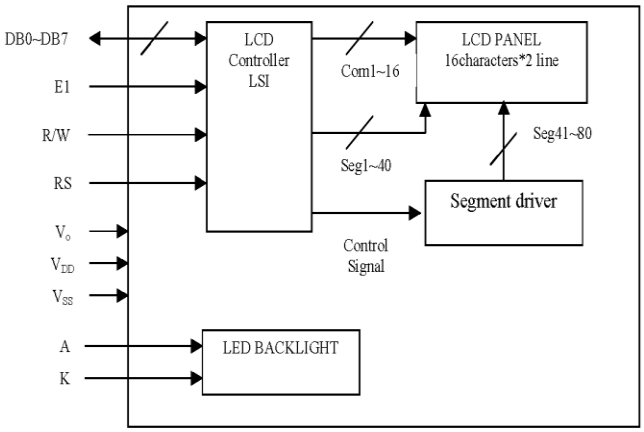

Fig. 2LCD driver Block Diagram

E. IR sensor

The Multipurpose Infrared Sensor is an add-on for your line and obstacle avoider that gives you the ability to detect lines or nearby objects. The sensor works by detecting reflected light coming from its own infrared LED. By measuring the amount of reflected infrared light, it can detect light or dark lines or even objects directly in front of it. An onboard GREEN LED is used to indicate the presence of an object or detect line. Sensing range is adjustable with inbuilt variable resistor.The sensor has a 3-pin header which connects to the microcontroller board or Arduino board via female to female or female to male jumper wires. [9]

Features:

- 5VDC operating voltage.
- I/O pins are 5V and 3.3V compliant.
- Range: Up to 20cm.
- Adjustable Sensing range.
- Built-in Ambient Light Sensor.
- 20mA supply current.
- Mounting hole.

There are different types of infrared transmitters depending on their wavelengths, output power and response time. Infrared Transmitter is a light emitting diode (LED) which emits infrared radiations called as IR LED's. Even though an IR LED looks like a normal LED, the radiation emitted by it is invisible to the human eye.

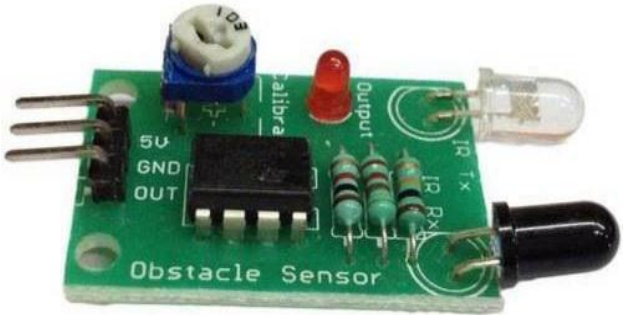

Fig. 3 IR sensors with transmitter and receiver

Infrared receivers or infrared sensors detect the radiation from an IR transmitter. IR receivers come in the form of photodiodes and phototransistors. Infrared Photodiodes are different from normal photo diodes as they detect only infrared radiation. Below image shows the picture of an IR receiver or a photodiode. Different types of IR receivers exist based on the wavelength, voltage, package, etc. When used in an infrared transmitter – receiver combination, the wavelength of the receiver should match with that of the transmitter.[9]

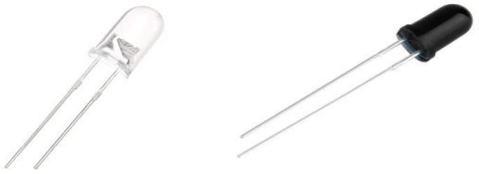

Fig. 4 IR Transmitter and Receiver

The emitter is an IR LED and the detector is an IR photodiode. The IR photodiode is sensitive to the IR light emitted by an IR LED. The photo-diode's resistance and output voltage change in proportion to the IR light received. This is the underlying working principle of the IR sensor.

5. SOFTWARE IMPLEMENTATION

The most basic way to use the ESP8266 module is to use serial commands, as the chip is basically a WiFi/Serial transceiver. However, this is not convenient. What we

recommend is using the very cool Arduino ESP8266 project, which is a modified version of the Arduino IDE that you need to install on your computer. This makes it very convenient to use the ESP8266 chip as we will be using the well-known Arduino IDE. Following the below step to install ESP8266 library to work in Arduino IDE environment.[4]

IDE stands for "Integrated Development Environment" that is mainly used for editing, compiling and uploading the code in the Arduino Device. Almost all Arduino modules are compatible with this software that is an open source and is readily available to install and start compiling the code on the go. A range of Arduino modules available includes Arduino Uno, Arduino Mega, Arduino Leonardo, Arduino Micro and many more. Each of them contains a microcontroller on the board that is actually programmed and accepts the information in the form of code. The main code, also known as a sketch, created on the IDE platform will ultimately generate a Hex File which is then transferred and uploaded in the controller on the board.The IDE environment mainly contains two basic parts: Editor and Compiler where former is used for writing the required code and later is used for compiling and uploading the code into the given Arduino Module. This environment supports both C and C++ languages.

6. RESULTS AND DISCUSSIONS

By the help ofArduinoIDE Software, Embedded C is programmedand effectively communicated with the help of ArduinoNano based on that, results are shown below.

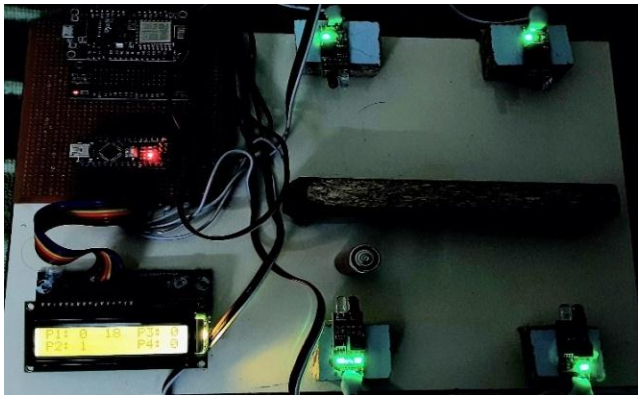

Fig. 5 Parking slot 2

In the above result an object (battery) is taken as example. When the object reaches the parking slot 2 the sensor emits IR radiation and sense the object and it is received by IR receiver .Thus the LED display as 1 ,leaving remaining slot to 0 .

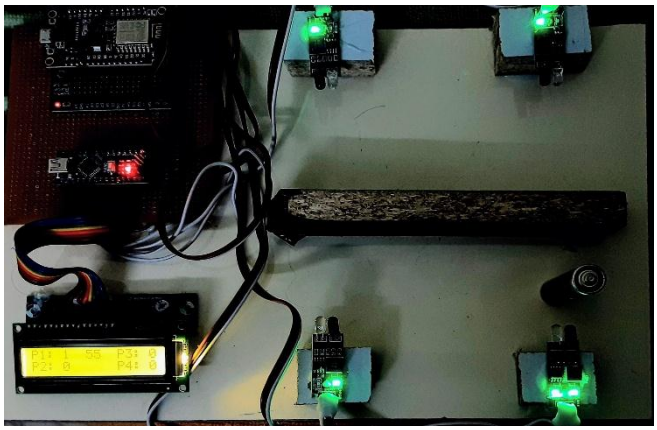

Fig. 6 Parking slot 1

Then now, in theabove result object is removed from the parking slot 2 and kept in parking slot 1.Again the sensor notice the empty slot and turn the parking slot 2 to 0.The sensor present in parking slot1 senses the object and set the parking slot 1 as 1 remaining slot to zero.This information is immediately updated without any delay. The Parking slot availability is shown in the following table.

Table 1: Parking Slot availability

Parking slot 1	Parking slot 2	Parking slot 3	Parking slot 4	Mobile application
0	0	0	0	0,0,0,0
1	0	0	0	1,0,0,0
0	1	0	0	0,1,0,0
0	0	1	0	0,0,1,0
0	0	0	1	0,0,0,1
1	1	0	0	1,1,0,0
1	0	1	0	1,0,1,0
1	0	0	1	1,0,0,1
0	1	1	0	0,1,1,0
0	1	0	1	0,1,0,1
0	0	1	1	0,0,1,1
1	1	1	1	1,1,1,1

7. CONCLUSION

In this work we have reduced the effort of parking vehicle in traffic by building hardware inbuilt with Arduino coding thereby developing mobile software where the user can search from any place with the help of network service provider.

By this much of user time is saved and it avoid uneven parking leading to heavy traffic in urban areas.This system will reduce unnecessaryfuel waste.The node MCU with esp8226 consumes less power and it can work with 3.3mv which makes it very easy for use.Moreover implementing of this setup in all parking slot is cost efficient and energy consuming.

REFERENCE

[1] M. Handte, S. Foell, S. Wagner, G. Kortuem, and P. J. Marron, "An internet-of-things enabled connected navigation system for urban busriders," *IEEE internet of things journal*, vol. 3, no. 5, pp. 735–744,2016.

[2] I. Samaras, N. Evangeliou, A. Arvanitopoulos, J. Gialelis, S. Koubias,and A. Tzes, "Kathodigos-a novel smart parking system based onwireless sensor network," in *Intelligent Transportation Systems*, vol. 1, pp. 140–145, 2013.

[3] R. Kannadasan, A. Krishnamoorthy, and N. Prabakaran, "RFIDbased automatic parking system,"*Australian Journal of Basic and Applied Sciences*10(2):186-191 2016.

[4] S. Hanche, P. Munot, P. Bagal, K. Sonawane, and P. Pise, "Automated vehicle parking system using RFID," *Sinhgad Institute of Technology and Science*,Volume-1, Issue-2, 2013.

[5] K. T. Dorjee, D. Rasaily, and B. Cintury, "RFID-based automatic vehicleparking system using microcontroller,"*international Journal of Engineering Trends and Technology* (IJETT)2016.

[6] M. Wang, C. Perera, P. P. Jayaraman, M. Zhang, P. Strazdins, R. Shyam-sundar, and R. Ranjan, "City data fusion: Sensor data fusion in theinternet of things," in *The Internet of Things: Breakthroughs in Researchand Practice*. IGI Global, 2017, pp. 398–422.

[7] A. Zaslavsky, C. Perera, and D. Georgakopoulos, "Sensing as a serviceand big data," arXiv preprint arXiv:1301.0159, 2013.

[8] M. A. Razzaque, M. Milojevic-Jevric, A. Palade, and S. Clarke, "Middle-ware for internet of things: a survey," *IEEE Internet of Things Journal*,vol. 3, no. 1, pp. 70–95, 2016

[9] L. Baroffio, L. Bondi, M. Cesana, A. E. Redondi, and M. Tagliasacchi,"A visual sensor network for parking lot occupancy detection in smartcities," *in Internet of Things (WF-IoT), 2015 IEEE 2nd World Forumon*. IEEE, 2015, pp. 745–750.

[10] T. N. Pham, M.-F. Tsai, D. B. Nguyen, C.-R. Dow, and D.-J. Deng, "Acloud-based smart-parking system based on internet-of-things technologies," *IEEE Access*, vol. 3, pp. 1581–1591, 2015.

[11] M. Suresh, P. S. Kumar, and T. Sundararajan, "Iot based airport parkingsystem," *in Innovations in Information, Embedded and CommunicationSystems* (ICIIECS), 2015 International Conference on. IEEE, pp. 1–5,2015.

Electronics Sensor and Alarm System based Pressure Cycled Emergency Ventilator for Covid- 19

[1] Thillaikkarasi R, [2] Deepa K, [3] Gokla M, [4] Saranya S, [5] Surya E

[1] Faculty of Bio Medical Engineering, Department of Bio Medical Engineering, Salem College of Engineering and Technology, Salem, India
[2][3][4][5] Students of Bio Medical Engineering, Department of Bio Medical Engineering, Salem College of Engineering and Technology, Salem,India

Abstract:

Many organizations have developed low-cost emergency ventilators in response to anticipated ventilator shortages caused by the COVID-19 pandemic. Many of these devices are pressure-cycled pneumatic ventilators, which are simple to make but lack the sensing and warning features that some of the commercial ventilators having now a days. This paper describes a low-cost, simple-to-make electronic sensor for pressure-cycled ventilators, a sensor and alarm system that estimates clinically useful metrics including pressure, respiratory rate and sounds an alarm when the ventilator malfunctions. A pair of nonlinear recursive envelope trackers are used in a low-complexity signal processing algorithm to control the signal from an electronic pressure sensor attached to the patient's airway. This algorithm, gives high accuracy and sensitivity to use in hearing aids and having a very little memory. It also performs a few calculations on each sample, making it suitable for use on almost any microcontroller.

Keywords:

Biomedical control, biomedical signal processing, envelope detectors, pressure measurement, ventilator

1. INTRODUCTION

THE COVID-19 crisis could result in a scarcity of ventilators, which are used to treat patients with serious respiratory symptoms patients with COVID-19 can develop acute respiratory distress syndrome (ARDS), which causes severe breathing difficulties as a result of blood overflowing through the lungs. By supplying oxygen, mechanical ventilation may aid in the treatment of these patients. As the underlying condition progresses. Appropriate oxygen supply is a vital component since the number of COVID-19 cases is expected to rise, hundreds of businesses, university research teams, and other organizations have created emergency ventilators under the supervision of a special authorization of critical care, and it can help COVID-19 patients avoid death due to ARDS and hypoxemia. Regulators' special permissions. Pressure-cycled pneumatic ventilators, such as the Illinois Rapidvent, built by the authors' institutions, are particularly appealing for this emergency because they can be produced quickly and cheaply. They work without the use of electronic components since they are operated by pressurized gas and driven by a mechanical modulator. However, they lack the sensors found in more-expensive commercial ventilators that provide closed-loop control, monitoring, and alarm capabilities. Clinicians rely on these electronic systems to adjust ventilator settings and to alert them to ventilator malfunctions or patient activity that require their attention. Without sensing and alarm features, clinicians must constantly monitor each patient and cannot be sure that ventilator settings are correct.

Fig. 1 Pressure cycled emergency ventilator setup.

They do not, however, have the sensors used in more costly commercial ventilators that allow for closed-loop control, tracking, and alarming. These electronic devices are used by clinicians to change ventilator settings and to alert them to ventilator malfunctions or patient activity that requires their attention. Clinicians must continuously track each patient without the use of sensing and warning features. It's impossible to know if the ventilator settings are right. An electronic sensor and alarm system for pressure-cycled emergency ventilators is defined in this paper. This system, like the pneumatic ventilators it is meant to complement, must be low-cost and simple to manufacture using readily available components. When the breathing cycle is irregular, the device's most important feature is to sound an alarm. Pressure-cycled ventilators create distinct pressure waveforms since they use pressure levels to switch between inhalation and exhalation modes. This pressure signal can be evaluated by the sensor and warning system to see if the ventilator is cycling normally. The same pressure signal can

be used to detect sudden pressure loss due to disconnection and pressure spikes due to mechanical failure, as well as to calculate clinically useful parameters like PIP, PEEP, and respiratory rate (RR). Much of the functionality of similar commercial control devices is replicated by these sensing and warning features. A comprehensive monitoring system will also track tidal volume, or the amount of air delivered with each breath, as well as oxygen levels. Concentration in the air, and it will set off alarms based on that concentration. A mechanical plan for stream control, rate control, and different controls are worked upon here, over an electronic sensor-based model, as the intricacy in plan and trouble in the acquisition of segments can impede organization of adequate ventilators during a plague. It must be referenced that numerous plans for quickly prototyped ventilators being grown at present for use in this plague depend on the change of an AMBU (Artificial Manual Breathing Unit) sack, with a robotized pressure component. On introductory thought, this gives off an impression of being a feasible choice, yet thinking about that exact volume control of ventilator yield is a basic prerequisite while ventilating an intubated patient, the AMBU sack configuration presents issues. Because of the actual shape varieties (because of the plan varieties among brands) in the accessible AMBU packs, changes would need to be made to the mechanical framework to oblige the distinctions in them. Thus, as we would see it, the utilization of a normalized air supply (as a chamber) can smooth out end-client preparing, improving ease of use and consistence, which can be basic for use in crises. [1] Like the pneumatic ventilators

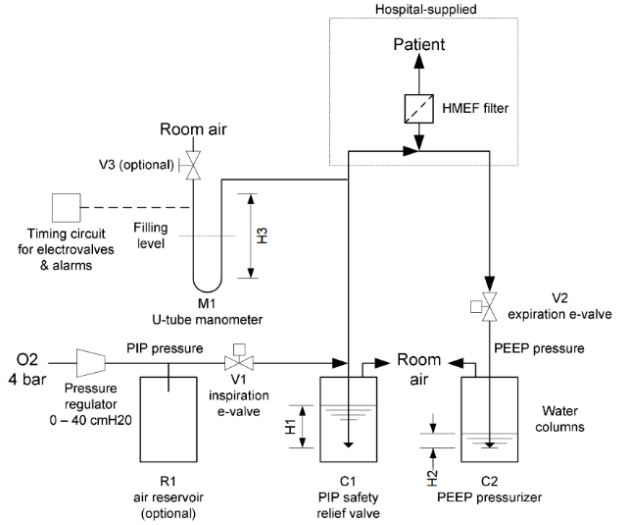

Fig. 2 Schematic diagram for emergency ventilator

It is intended to complement, must be low-cost and simple to manufacture using readily available components. When the breathing cycle is irregular, the device's most important feature is to sound an alarm. Since, like the pneumatic ventilators it is meant to complement, this system must be inexpensive and simple to manufacture. [5] Since the variables shown at the ventilator only address the data for the combination of both related patients, a treating therapist has no knowledge of the tidal volume obtained from each patient, nor of the actual patient's compliance. [7] The required ventilator strength, restrictive losses, compliance, and other factors have been determined using an electromechanical model for respiration, which can be used to improve the Automatic Bag Mask Valve(ABMV) emergency ventilator design. A spring factor is used to model the lung compliance. [9] The relation size was chosen to keep the inspiratory-to-expiratory (I: E) time ratio constant at 1:2. By adding a function to change the position of the rocker tip to regulate the tidal volume from 100 ml to 600 ml of oxygenated air per breath, the kinematic linkage design has been kept modular. [10] Its greatest flaw is that it doesn't have a way to bind to a ventilating circuit in an emergency. With Chevalier Jackson's metal tracheostomy tube, we explain a simple and efficient ventilation technique.

2. METHODOLOGY

Pressing factor cycled pneumatic ventilator, Gas is permitted to stream into the lungs until a current aviation route pressure limit is reached, at which time a valve opens permitting exhalation to follow. The volume conveyed by the ventilator fluctuates with changes in aviation route obstruction, lung consistence, and trustworthiness of the ventilator circuit.

Pressing factor cycled ventilators produce trademark pressure waveforms, during compulsory breathing, the aviation route compel ascends from PEEP to PIP during motivation, at that point drops from PIP to PEEP during exhalation. During helped breathing, the fundamental shape is something similar, however the pressing factor may fall underneath PEEP when the patient starts inward breath. The pressing factor sign can be utilized to assess the PIP, PEEP (or least pressing factor for helped breathing), and Respirtory Rate.

Since pressure-cycled ventilators produce very much characterized pressure waveforms during typical activity, the pressing factor sign can likewise be utilized to distinguish breakdowns. On the off chance that the gas circuit becomes impeded or disengaged, the modulator will quit cycling among inward breath and exhalation modes, causing the compel sign to stay steady. The proposed caution framework utilizes low-intricacy pressure condition signal preparing calculations to identify this steady pressing factor condition. The gas pressure in the patient's airway is monitored by an electronic pressure sensor (Fig. 3). Measurements and alarms are generated by a low-power microcontroller that processes the pressure signal Measurements and alarms are generated by a low-power microcontroller that processes the pressure signal. Any kind of ventilator can be integrated with it. It is, instead, a stand-alone component that can be connected to any pressure-cycled ventilator. The design prioritises cost and ease of production because it is designed to address an immediate shortage. The system is made up of low-cost, easily

available components that can be assembled on a two-layer printed circuit board using through-hole or surface-mount components and runs on a standard 5 volt power supply. Figure 3 illustrates the sensor and alarm system. Standard respiratory tubing adapters are attached to the patient side of the ventilator to connect the device to the patient's airway. A microcontroller, a display module, push buttons, a buzzer, and a pressure sensor comprise the electronic system. The ATmega328 8-bit microcontroller was chosen for its ease of use and wide availability. It does not need an external n by an internal 8 MHz clock. Because the proposed algorithm has low computational requirements, as outlined in Section VII, almost any microcontroller with an analog-to-digital converter and multiple digital inputs and outputs should be suitable for the sensor and alarm module. The open-source firmware includes a C implementation of the monitoring algorithm that is hardware agnostic and can be ported to other systems.

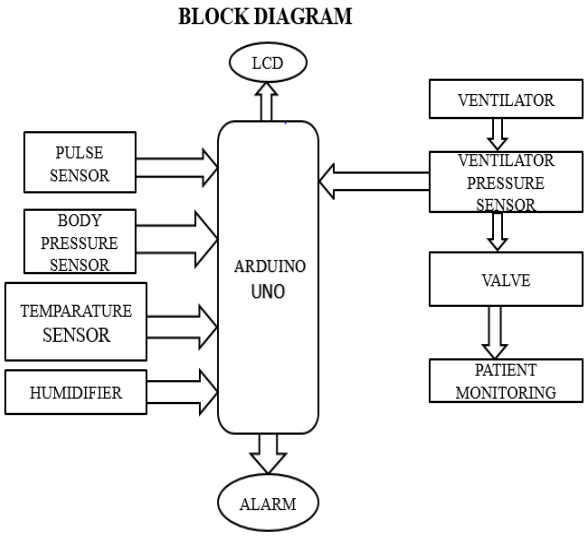

Fig. 3. Block diagram of emergency ventilator

3. VENTILATION CYCLED BY PRESSURE

Since they are low cost, easy to produce, and need no electronic components for basic operation, pressure-cycled pneumatic ventilators, which are operated by pressurised gas, are useful in the current emergency.

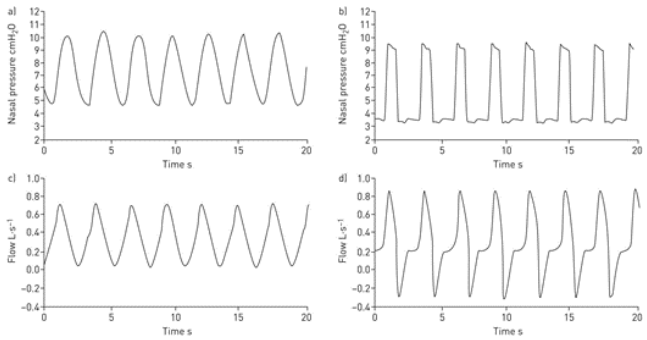

Fig. 4. Pressure cycled waveform

They deliver pressurised gas to the patient's airway and, using a pressure-switching mechanism operated by pneumatic logic, cycle between inhalation and exhalation modes. High-pressure gas is pumped into the patient's lungs during inhalation. The pressure in the airway rises as the lungs expand until it exceeds the Peak Inspiratory Pressure (PIP), a maximum pressure level that the user can change. As PIP is reached, the modulator opens a path to the atmosphere, allowing air from the lungs to escape the ventilator. During exhalation, the pressure in the airway gradually reduces, but it does not fully vanish. not suffocate in the atmosphere Instead, as it falls below PEEP, a spring closes the valve. Through inhaling, the patient lowers the pressure below the PEEP threshold. A PIP dial and a rate dial, which defines expiratory time, can also be set by the clinician to monitor flow. The PEEP threshold in pneumatic ventilators is a fixed fraction of PIP determined by the mechanical nature of the system. Since COVID-19 patients can need PEEP of 10–15 cm H2O and PIP of 30–40 cm H 2O [4,] some COVID-19 emergency ventilators are equipped with lower PIP-to-PEEP ratios than commercial ventilators. The Illinois RapidVent, for example, has a PIP-to-PEEP ratio of about 2.4. The airway pressure increases from PEEP to PIP during inspiration and then falls from PIP to PEEP during exhalation during mandatory breathing. The basic shape remains the same during assisted breathing, but when the patient initiates inhalation, the pressure can fall below PEEP. PIP, PEEP (or minimum pressure for assisted breathing), and RR can all be calculated using the pressure signal. The pressure signal can be used to detect malfunctions since pressure-cycled ventilators emit well-defined pressure waveforms during normal operation. The modulator will avoid cycling between inhalation and exhalation modes if the gas circuit becomes obstructed or disconnected, resulting in a continuous pressure signal. We used the NXP MPXV5010 piezoresistive pressure sensor in our implementation, which has a pressure range of about 0 to 100 cm H2O and output voltages of about 0 to 5 volts.

4. MONITORING OF VENTILATION

Three metrics are calculated by the control system: PIP, PEEP (or minimum pressure of the breath period for assisted breathing), and RR. The pressure envelopes are used to monitor all three of these parameters by detecting inhalation and exhalation cycles**.** During each inhalation period, the two envelope trackers each store the most recent pressure sample that triggered their attack mode. The high-pressure envelope has multiple attack-mode samples in a row. Several attack-mode samples for the low-pressure envelope are taken in a row during exhalation.

5.1 PIP AND PEEP

The previous attack value is retained when a mode switch occurs. The corresponding PIP or PEEP estimate is updated with this information. This is the case. The PIP monitor is enabled when a low-pressure attack occurs. The most recent high-pressure attack value has been added to the table. The

PEEP monitor is changed when a high-pressure attack happens. the importance of the most recent low-pressure attack.

5.2 LEVEL OF RESPIRATION

The machine also keeps track of how long it takes for these mode-switch events to happen. The length of a full breath period is calculated between peaks of high pressure The average is smoothed after smoothing. There are a certain number of samples per breath. .

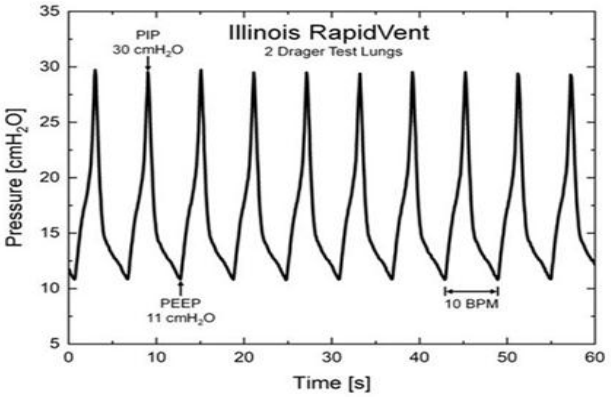

Fig. 5. RapidVent alarm sound wave

5.3 ALARM CONDITIONS

The monitoring device triggers alarms in several conditions that indicate the ventilator is not working properly, as shown in Table I. The alarm thresholds may vary between patients and between ventilator devices and so they are configurable by the user. The table shows the range of values that users of the Illinois RapidVent may select; these were chosen in consultation with local intensive-care experts.

5.4 APPLICATION OF ALGORITHM

The monitoring algorithm is simple to implement and takes up little memory. Algorithm 1 shows the algorithm's fundamental loop. The algorithm state consists of seven floating-point values, the vhigh and vlow envelopes, and a binary inhalation/exhalation state vector. and the estimated PIP, PEEP, and RR; and the three integer counters Tpeak, Thigh, and Tlow. The program must also store the user-configurable alarm thresholds in memory. For every observed sample, the envelopes are updated acccording to (1) and (2) and the alarm conditions from TableI are checked. Breaths are monitored by a state variable that switches from inhalation to exhalation at the first low-pressure attack value in each breath period, and from exhalation to inhalation at the first high-pressure attack value in each cycle. Thigh and Tow counters keep track of how long it's been since the last assault on each envelope.

Result, the time-based non cycling alarm conditions described in Table I can be implemented. Teak, a second counter, counts the samples after the previous high-pressure peak (circles in Fig. 6), allowing the machine to calculate the time between breath cycles. Regardless of the sample rate, the PIP, PEEP, and RR metrics are modified once per breath cycle. The execution time of the algorithm was calculated on the ATmega328 to determine the system's computational complexity. If the sensor senses a pressure beyond the permissible range, the high- and low-pressure warnings go off immediately. The pressure in a pressure-cycled ventilator should never exceed the user-defined PIP value. A pressure reading that exceeds the PIP dial's range signifies a mechanical failure. The low-pressure threshold pmin, that is, atmo, can be set close to zero.

5. CONCLUSION

The proposed sensor and alert framework can improve the usefulness of pressing factor cycled crisis ventilators. While it is not as strong as a full-highlighted business ventilator framework, it gives basic observing highlights that are not accessible on absolutely mechanical ventilators. The recursive envelope-following calculation permits the framework to follow breathing, estimate metrics, furthermore identify glitches with a couple of figuring for each example what's more, a minuscule memory impression In this manner, the framework can be constructed rapidly utilizing almost any minimal effort microcontroller and a couple other electronic segments.

6. RESULT

Electronic sensor and caution based pressing factor cycled crisis ventilator was effectively planned. Volume control mode, intermitted required ventilation, and consistent positive aviation route pressure are largely highlights of the crisis ventilator. It can deliver flowing volumes of 300 to 800 ml with a 10% blunder, with pressing factor, volume, and waveforms that are almost indistinguishable from those of current business ventilators.

7. DISCUSSION

The RapidVent was planned by the requirements of basic consideration doctors and respiratory advisors, and we imagine that a profoundly prepared individual would oversee its utilization. The Rapid Vent is intended for use with 50 psig gas, which could by unadulterated oxygen, air, or a gas blend. At the point when associated with oxygen, the RapidVent can convey either 100% oxygen or half oxygen utilizing an entrainment spout. There is an assortment of industrially accessible entrainment spouts that could be utilized to set the oxygen blend at an alternate proportion. While 50 psig oxygen is broadly accessible in North America and some different pieces of the world, a few locales of the world use clinic oxygen or air supply at a lower pressure. The RapidVent can without much of a stretch be altered for an alternate pressing factor setting, by tuning the consistence of the stomach and the spring steady of the coordinated spring.

REFERENCE

[1] Corey, Ryan M., Evan M. Widloski, David Null, Brian Ricconi, Mark A. Johnson, Karen C. White, Jennifer R. Amos et al. (2020), “Low-Complexity System and

Algorithm for an Emergency Ventilator Sensor and Alarm". IEEE Transactions on Biomedical Circuits and Systems, Vol.14, No. 5 pp. (1088-1096).

[2] Iyengar, Karthikeyan, Shashi Bahl, Raju Vaishya, and Abhishek Vaish, (2020), "Challenges and solutions in meeting up the urgent requirement of ventilators for COVID-19 patients", Research Gate article in Diabetes & Metabolic Syndrome Clinical Research, Vol. 14, No. 4 pp. (499-501).

[3] King, William P., Jennifer Amos, Magdi Azer, Daniel Baker, Rashid Bashir, Catherine Best, Eliot Bethke et al. (2020), "Emergency ventilator for COVID-19", Research Gate article in PLoS ONE, Vol. 15, No.12, pp. (1-11).

[4] Szlosarek R, Teichert R, Wetzel A, Reuter F, (2021), "Design construction of a simplified, gas driven, pressure controlled emergency ventilator", ScienceDirect African journal emergency medicine, Vol. 7, No. 11, pp. (175-181).

[5] . Peter Reinacher, Thomas E. Schlaepfer, Martin A. Schick, Juergen Beck, Hartmut Buerkle, and Stefan Schumann, (2020), "When Resources Are Scarce-Feasibility of Emergency Ventilation of Two Patients with One Ventilator", Research Gate journal, Vol. 7, No. 11, pp. (1-9)

[6] Dr. Rajeev Chauhan, Vivek chaudari, Akash gaddamwar, Eshan dhar, (2020), "Mathematical modelling of an automatic bag valve emergency ventilator", research Gate international research journal, Vol. 7, No. 9, pp. (1677-1685).

[7] Lorenzo Florence, Francesco savario, Florence, Federio rotini, (2020), "Challenging COVID-19 with creativity: supporting design space exploration for emergency ventilators", Research Gate article in applied science, Vol. 10, No. 66, pp. (453-477).

[8] Jocob knorr, Megansheehan Danial C, Santana, (2020), "Design and performance testing of a novel emergency ventilator for in hospital use", research Gate article in candian journal of respirator theory, Vol. 3, No. 5, pp. (1-11)

[9] Tarion J, Kapil S, Muthu N, Kanagaraj S, (2020), "Rapid manufacturable ventilator for respiratory emergencies of COVID-19 disease", Springer Vol. 22, No. 34, pp. (1-9).

[10] Kamran A. Syed, Roshna R. Paul, Ajoy M. Vardhese, Neenu A. Joseph, "Emergency ventilator with a chevalier Jacksons metal tracheostomy tube", (2014), ScienceDirect International Journal of Paediatric Otorhinolaryngology, Vol. 8, No. 78, pp. (888-890).

Lane Detection to Prevent Trajectory in Curved Roads and Primary Security

[1] Susari venkata MuraliKrishna, [2] Sandhya Devi.RS

[1][2] EEE.Kumaraguru College of Technology, Kumaraguru College of Technology, Coimbatore, India

Abstract:

Bend is the auto collision inclined territory in the rush hour gridlock arrangement of the primary roads How to successfully distinguish the lane line and give the traffic data ahead for drivers might be a troublesome point for the safe driving. The conventional lane discovery innovation isn't truly material inside the bended road conditions. Along these lines a bend discovery calculation which depends on straight-bend model is proposed in this paper and this technique has a decent materialness for most bend street conditions. To begin with, the strategy separates the road picture into region of interest and along these lines the street foundation district by investigating the fundamental qualities of the road picture. At an identical time, the straight-bend numerical model is set up. The numerical condition of the straight model is acquired by utilizing the improved Hough transform. The polynomial curve model is set up as indicated by the progression of the road lane line and the digression connection between the straight model and bend model, the recognition and distinguishing proof of the straight and in this way the bend are acknowledged individually and the road lane line is recreated. As of late GPS and GSM module used to theft location and vehicle global positioning framework. we added innovation like, a secured face acknowledgment dependent on vehicle theft tracking and discovery framework. In this module we will utilize python programming to prevent the bypassing of the face id and unique finger impression of e-vehicle which are the essential primary security by utilizing the lock application which distinguished by the vehicle.

Keywords:

Straight bend model, Curve, Region-of -interest, hough transform, bend detection, primary security

1. INTRODUCTION

With the quick development of the great transportation framework, the quantity of vehicle has risen quite a long time after year which is bring about genuine traffic conditions [1]. Specifically, the rate of bended streets and the justification mishaps stay high. At the point when the vehicle is turning, there will be a visually blind zone of sight which is joined by expanded centrifugal force. The turning range will diminish and the horizontal sliding will happen effectively, which is caused for event of mishaps [4]. In Japan, the car crash rate on the bended areas of the street surpassed 41.01% of the absolute mishap rate , while the quantity of auto collisions on the bended street in China represented 7.84% of the complete mishap. [9]Judging from the seriousness of the mishap, the deadly mishaps of the bend involves 16.3% of all lethal mishaps [11]. Different insights show that the fundamental reasons of mishaps in the bended locales are the over-speeding of the turning vehicles during turning, unpredictable overwhelming lane changes and lane inhabitance [15].During driving, numerous mishaps happened because of absence of driver's mindfulness or newness to the street ahead, particularly at the bended street which is the spot of the great frequency of mishaps. Thusly, in the event that it is feasible to identify and perceive the street ahead before the appearance of bended street conditions, caution the driver ahead of time and keep away from crash ahead of time, numerous superfluous mishaps can be dodged and the wellbeing of life and property can be ensured. In the security module we will utilize Python programming to forestall the bypassing of the face id and finger impression of e-vehicle which are utilized as the essential security by add an extra layer of safety by utilizing a frequency of code emitted from the lock application which is distinguished by the receiver of the vehicle.

A. Need For The Project

To identify the bends in a lane line and forestall the direction and produce the better outcomes about the design of the streets during any sort of environment and produce the satisfactory aftereffects of the street. Preventing face acknowledgment sidestep utilizing an extra layer of safety, for example, unique mark acknowledgment and installing versatile application in portable stage for 2 factor confirmations Problem recognizable proof. The proposed framework can recognize the bend lane line, give powerful traffic data. The recognition and ID of the straight and the bend are acknowledged individually and the street lane line is reproduced. The technique partitions the street picture into the region of interest and the street foundation area by investigating the fundamental attributes of the street picture utilizing color clustering method. To keep the vehicle from digital assault the extra component will assist with keeping from all the conceivable digital assaults. All the information that is in the encrypted form by utilizing the AES calculation.

B. Prior Knowledge

1. Lane expectation

Lane recognition ordinarily requires the utilization of applicable calculations to extricate the pixel highlights of the lane line, and afterward the proper pixel fitting calculation is utilized to finish the lane location. Customary lane location utilizes Canny edge extraction calculation or Sobel edge extraction calculation to get lane line up-and-comer focuses and use Hough change for lane include recognition, however most activities depend on manual component extraction. The most recent exploration depends on deep neural networks to make thick forecasts rather than artificial feature extraction.

2. Security Verification

To prevent the bypassing of the face id and finger impression of e-vehicle which are utilized as the essential security by add an extra layer of safety by utilizing a recurrence of code emitted from the lock application which is distinguished by the beneficiary of the vehicle.

2. ROAD REGION DIVISION AND MODEL

A. Straight area bend region division

The design and development of organized streets have exacting industry guidelines. Plane direct plan generally incorporates: straight, roundabout curvilinear and delicate bends, or single-circle bends or joined bends, and so forth

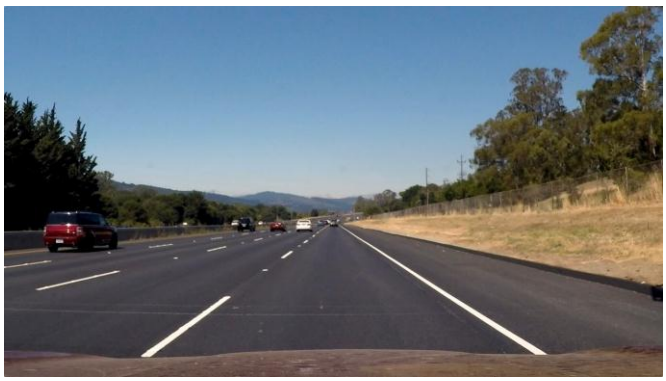

(a) Straight

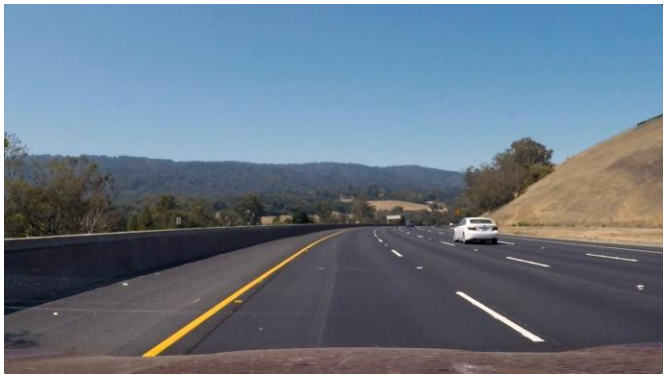

(b) Curve

At the point when the line is a straight line, the street lane is a straight line as demonstrated in Fig.1 (a). At the point when the line is a bend, the street lane can't be just described by a straight-line model as demonstrated in Fig.1 (b). Bend straight design is fundamentally as per the balance of force when the vehicle is driving on a roundabout bend, while dependent on the assessing the driving safety, the driving control's convenience, the fuel utilization and tire wear's economy, the comfort level and different components to decide the bend plan standard in plane direct plan, as demonstrated in Fig. 2. During the running of the vehicle and as indicated by its relating driving speed, the plan of the cutoff least turning sweep should leave a specific edge as per the security of turning about the vehicle.

B. Lane fitting

To assess the lane example, figure out which pixel has a place with which lane, we need to change over every one of them into a boundary portrayal. To this end, we utilize the generally utilized fitting calculation. As of now, the broadly utilized lane fitting models are essentially cubic polynomials, sp line curve or circular segment curves. Inverse perspective transformation is utilized to change the picture into a "bird's-eye view" to improve the quality of the fitting while at the same time keeping up the computational effectiveness, and afterward receive the strategy for curve fitting. The fit lines in the " bird's-eye view " can be re-projected into the first picture through a inverse transformation matrix. By and large, the inverse perspective transform computes the transformation matrix on a single image and can stay fixed, yet on the off chance that the street plane changes, the fix is not, at this point legitimate, causing lane focuses close to the horizon to be projected to endlessness, which influences lane line recreation absolute exactness. To tackle the present circumstance, we apply a converse point of view change to the picture prior to fitting the bend, and uses a uses a loss function customized for lane fitting problem to optimize. A custom function network is utilized to produce a changeable framework and change the lane pixels, at that point use bend fitting polynomials to perform pixel fitting on the changed over pixels, lastly convert the fitted pixels into the info picture.

The advantage of this network is that the identification calculation can fit the pixels of far off lanes with great power when the street surface changes, and better adjust to lane changes. The camera on the vehicle gathers the picture and sends it to the cloud information handling focus. After the picture is exposed to parallel division and inserted division, the grouping activity is performed and joined with the changeable framework produced by the custom organization to create the last lane recognition picture.

3. MODULE DESCRIPTION

A. Structural Road

The model-based strategies first utilize reasonable mathematical model to portray the lane line, and afterward

acquire the boundaries of the mathematical model by numerous techniques, for example, Random Sample Consensus, Least Square Method Transform to fit the comparing lane lines. The regular lane line models incorporate direct model illustrative model hyperbola model, etc. The literature extracted the short line in the street picture to rough the lane line, it delivered better outcomes however it can't adjust the situation when the lane line is the bend. During the driving interaction, as far as possible turning sweep will increases the vehicle's speed speeds up comes to, as far as possible turning span is 650m and the general minimum radius reaches.

B. Multinomial model

At the point when the line is a straight line, the street lane is a straight street as demonstrated in Fig.1 When the line is a bend, the street lane can't be just portrayed by a straight line model as demonstrated in Curve direct plan is principally as indicated by the equilibrium of power when the vehicle is driving on a round bend, while dependent on the assessing the driving wellbeing, the driving control's accommodation, the fuel utilization and tire wear's economy, the comfort level and different elements to decide the roundabout bend range The cutoff least sweep .As demonstrated in we accepts that the street bend span, and the length of circular segment 60m the camera shooting distance is the close to field because of the point of camera establishment and the bend length is thought to be 60m as per the boundary overflow speculation and the circle's focal point which is compared to the circular segment length is the digression of bend is the digression point and is the convergence of the augmentation and digression.

C. Lane location

The technique joined the versatile shrewd edge location to expand the edge data of the lane line, it can successfully decrease the effect of commotion edges and adjust to an assortment of unforgiving street conditions. Yet, it's not useful for various lighting circumstances. The writing utilized the enlightenment invariance to remove white and yellow substitute lane lines, and afterward understood the discovery of lane line by utilizing grouping calculation in the other lane lines. The strategy has a decent identification impact for night or the light changes.

As demonstrated in we expect that the street bend sweep and the length of curve the camera shooting distance is the close to field because of the point of camera establishment and the circular segment length is thought to be as per the boundary overflow theory and the circle's focal point which is compared to the circular segment length is the digression of curve digression point and is the convergence of the expansion and digression.

D. Lane recognition innovation

With the fast development of the thruway transportation framework, the quantity of vehicle proprietorship has risen quite a long time after year which is bring about genuine traffic conditions specifically, the occurrence of bend mishaps and the reality of mishaps stay high. At the point when the vehicle is turning, there will be a visually impaired zone of sight which is joined by expanded diffusive power. The turning range will diminish and the sidelong sliding will happen effectively, which is caused impact.

E. Canny edge identification

Watchful edge identification to amplify the edge data of the lane line, it can adequately lessen the effect of clamor edges and adjust to an assortment of unforgiving street conditions. Be that as it may, it's not useful for a wide range of lighting circumstances. The writing utilized the enlightenment invariance to remove white and yellow substitute lane lines, and afterward understood the recognition of lane line by utilizing bunching calculation in the other lane lines. The strategy has a decent identification impact for night or the light changes. Be that as it may, obscured or lowered by the shadow, the impact of identification isn't acceptable.

F. Security verification

To forestall the bypassing of the face id and unique mark of e-vehicle which are utilized as the essential security by add an extra layer of safety by utilizing a recurrence of code transmitted from the lock application which is recognized by the recipient of the vehicle.

4. METHODOLOGY

For more intricate lane recognition, it tends to be better addressed with other related advances. The writing proposed a layered lane location calculation by grouping lane sort of lane lines and afterward the comparing lane discovery calculations are utilized. The writing proposed the technique that convolutional neural organization (CNN) joined with help vector machine (SVM)algorithm to recognize the lane line. The strategy is a novel idea for lane identification field and it effectively kills the impedance lines, and furthermore it has better execution contrasted and CNN calculation. During any sort of environment circumstance the proposed lane location framework will track down the exact picture of the specific lane and cycle the picture utilizing the CNN and SVM modules and caution the driver Preventing face acknowledgment sidestep utilizing an extra layer of safety, for example, finger impression acknowledgment and installing portable application in versatile stage for security verification.

5. RESULT AND DISCUSSION

This chapter will deal with the simulation results for the lane detection and the 2-factor security authentication of the vehicle. The captured video will be processed video will undergone into several steps such as color filtering, edge detection, region of interest, canny edge detection process, detecting the lane line, and with line filtering and regressing each step will give the outcomes accordingly The OpenCV and pillow module will be doing the image processing art of the captured video that is done during the initial process. the captured video will be converted into the pixels that is

where the image will be converted in to the binary format then the converted numbers will be processed as the output image that which shows on the dash board of the car.

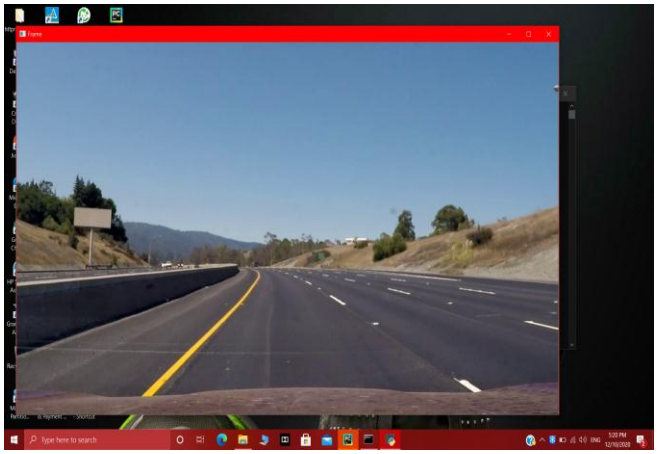

Fig.2. Captured image

The above Fig.2 shows that the image that which is been captured the camera that has already built in the vehicle.

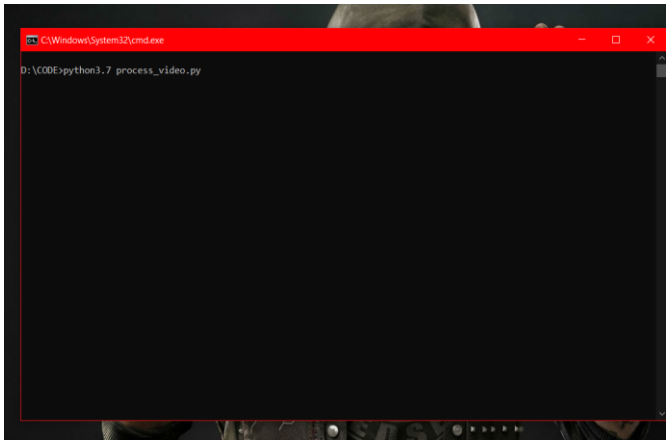

Fig.3. The process undergone with perspective transformation.

The above Fig.3 shows that the captured image that which is processed through the filtering process and perspective transformation of the lane with the canny edge detection by using the opencv module.

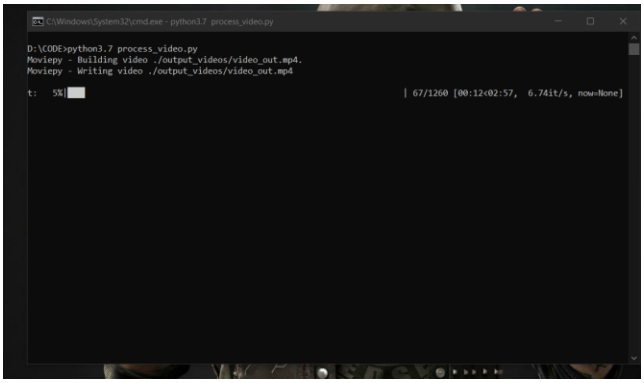

Fig.4. Building and writing of the image that captured

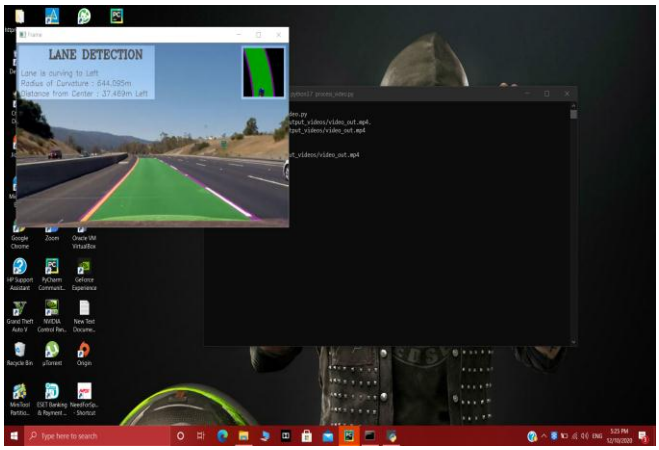

Fig.5. The output image

The above shows the final outcome of the processed video that has captured and produce the lane-line of the road that which has to be followed on the structural lane line of the roads.

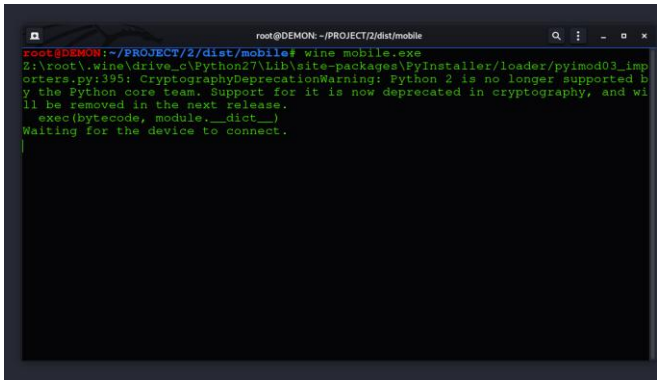

Fig.6. Building communication with vehicle

The above shows the mobile application that which has been under the frequency region of the vehicle it waits for the connectivity with the vehicle.

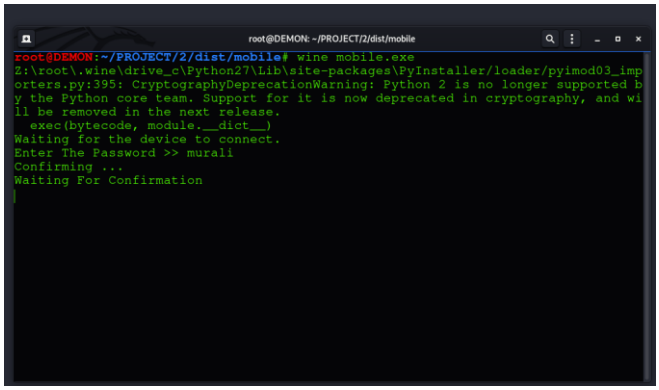

Fig.7. Initializing setup with a password

The above figure shows the set up of the security with the initial stage for setting up some password for the vehicle to get access.

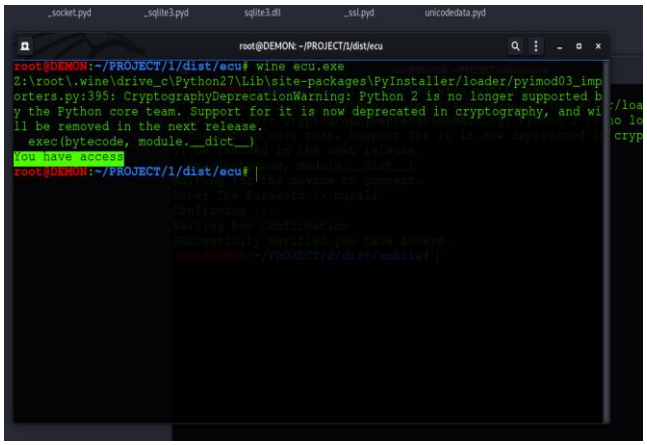

Fig.8. Authentication of the vehicle

The above figure shows the access for the vehicle with the password protection method.

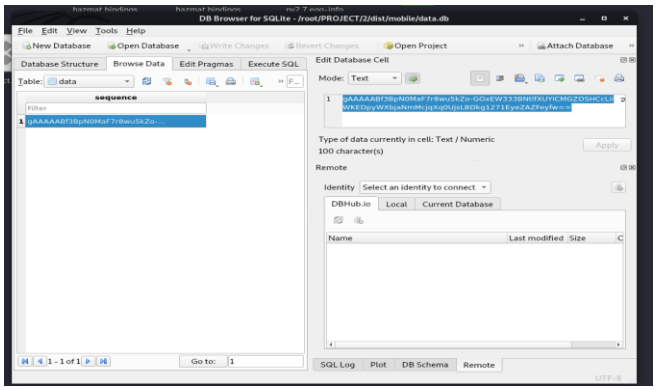

Fig.9. Encrypted data

The above shows that the entered data will be in the encrypted form so that there will be no man in the middle (MITM) threats can occurs.

6. CONCLUSION

This paper proposed the lane line's discovery calculation which depends on the straight-bend model by setting up the model of the straight and bend and breaking down the qualities of the street picture. It can more readily settle the exact identification of lane lines and it has extraordinary importance in functional applications. The exploratory outcomes show that the calculation can precisely distinguish the street lane line and give the strayed data of vehicle and the course of the bend. It has incredible importance to improve the dynamic wellbeing driving and helped driving of the vehicle which is in the bended street conditions. This technique gives an extra security to the vehicle which forestalls the bypassing of the bypassing of the essential highlights.

REFERENCE

[1] HuifengWang, YunfeiWang, Xiangmo Zhao, Guiping Wang, He Huang, Jiajia Zhang, “Lane Detection of Curving Road for Structural High-way with Straight-curve Model on Vision,”,2019.

[2] Yue dong,Jintao Xiong,Liangchao Li, “Robust lane detection and tracking for lane departure warning”, 2012.

[3] Yong Chen , Mingyi He, “Sharp curve lane boundaries projective model and detection,” 2012.

[4] Tomader MAZRI,Mehdi FENICHE “Lane Detection and Tracking For Intelligent Vehicles: A Survey,”2019.

[5] Aoxue Li , Haobin Jiang , Jie Zhou, And Xinchen Zhou, “Learning Human-Like Trajectory Planning on Urban Two-Lane Curved Roads From Experienced Drivers,”2019.

[6] P.Wu,C.Chang,and C.Lin, “Lane-mark extraction for automobiles under complex conditions,”*Pattern Recognition*,vol. 47, no. 8, pp. 2756-2767,Aug. 2014.

[7] Hong Peng,Jinsheng Xiao,Xian Cheng,et al, “Lane detection algorithm based on extended Kalmanfilter,”*Journal of Optoelectronics Laser*, vol. 26, no. 3, pp. 567-574, Mar. 2015.

[8] M.B.Paula,and C.R.Jung, “Real-time detection and class-ification of road lane markings,”*XXVI Conference on Graphics,Patterns and Images,IEEE Computer Society*,2013,pp. 83-90.

[9] J.Huang,H.Liang,Z.Wang,et al, “Lane marking detection based on adaptive threshold segmentation and road classification,”*IEEE International Conference on Robotics and Biomimetics*,2014,pp. 291-296.

[10] R.Gopalan,T.Hong,M.Shneier,et al, “A learning approach toward detection and tracking of lane markings,”*IEEE Trans on International Transportation System*,vol. 13,no. 3,pp. 1088-1098, Mar. 2012.

[11] D.C.Hernandez,V.D.Hoang,and K.H.Jo, “Vanishing point based image segmentation and clustering for omni-directional image,”*Intelligent Computing Theories and Technology*,vol.16,no.3, pp. 541-550, Mar. 2013.

[12] Yongzhong Wang,Xiaoyun Wang,and Chenglin Wen, “Gradient-pair constraint for structure lane detection,”*Journal of Image and Graphics*,vol.17,no.6,pp. 657-663,Jun. 2012.

[13] F.You,R.H.Zhang,L.S.Zhong,et al, “Lane detection algorithm for night-time digital image based on distribution feature of boundary pixels,”*Journal of the Optical Society of Korea*, vol. 17,no. 2,pp. 188-199, Feb. 2013.

[14] H.Yoo,U.Yang,and K.Sohn, “Gradient-enhancing con-version for illumination-robust lane detection,” *IEEE Transactions on Intelligent Transportation Systems*,vol. 14, no. 3, pp. 1083-1094, Mar. 2013.

[15] J.Son,H.Yoo,S.Kim,and K.Sohn, “Real-time illumination invariant lane detection for lane departure warning system,”*Expert System with Applications*, vol. 42, no. 4,pp. 1816-1824, Apr. 2015.

Brain Tumor Detection of CT Scan Image Analysis Using Image Mining Algorithms

[1] J. Karthikeyan*, [2] Dr. C. Jothi Venkateswaran

[1] Research Scholar, Presidency College, Chennai, Tamil Nadu, India
[2] Regional Joint Director, Directorate of Collegiate Education, Tamil Nadu, India

Abstract:

The detection of Brain tumor at early stage is extremely tedious task for medical surgeons and doctors. CT scan brain images have lots of noisy data and other ecological interferences. Therefore, the medical surgeons and doctors having struggle to identify the causes of brain tumor. So here we decided to operate with the system to detect brain tumor from CT scan images. CT scan plays an important role in diagnosing brain tumor images with better ionizing radiation, faster acquisition speed, higher contrast and spatial resolution. Image mining is an extension of data mining to image domain. In this paper, the analysis of image segmentation with k-means clustering algorithm and feature extraction of an image is the efficient way of edge detection process and the result of segmented image conclude that diagnosis of brain tumor. The method of this research paper is helpful in data or information retrieval from CT scan Brain images, using image mining techniques the accuracy of tumour detection is improved.

Keywords:

CT SCAN, Brain Tumor, Image Mining, Clustering, Image Segmentation, K-means algorithm

1. INTRODUCTION

CT imaging is preferred over MRI due to wider availability, lower cost, and sensitiveness to early stoke. Computed tomography (CT) and magnetic resonance imaging (MRI) are the two modalities that are regularly used for brain imaging. While MRI is the preferred clinical modality for imaging the anatomy of the brain, due to its lack of ionizing radiation and a higher contrast resolution. In addition, CT can be used in the presence of metallic implants and tattoos with metallic ink, for which MRI is contraindicated due to the dangers imposed by the high magnetic fields required. CT is also better suited for the evaluation of penetrating brain injuries and other trauma and acute neurological emergencies. Computed tomography (CT) is a type of scan that are used in computers to create detailed pictures of the brain. CT scan is the most powerful types of tests used to diagnose brain tumors.

A formation of abnormal cells within the brain that can interrupt the function of the human brain is termed as Brain Tumor. Every year approximately 40,000- 50,000 persons are diagnosed with brain tumor in India. Traditionally, doctors and medical radiologist manually find out and compute the size of the human brain tumor from CT Scan images during consistent screening.

A brain tumor occurs when infrequent cells shape appears inside the cerebrum, which has two main types, namely, benign tumors and malignant tumors. Malignant tumors can be categorized into basic tumors, and secondary tumors that spread elsewhere. Automated brain tumor detection through MRI can offer a valued outlook and earlier accurate detection of the brain tumor. The tumor detection is performed in several stages, namely, enhancement, segmentation, classification. Depending on the tumorous tissue origin and its behavior, it is classified from less aggressive (benign: grades I and II) to aggressive (malignant: grades III and IV). The clinicians diagnose brain tumors using medical imaging techniques like magnetic resonance imaging(MRI) and computerized tomography (CT).

A computer system which is capable for browsing, searching, retrieving and processing the images from large databases is called as an image retrieval system [3]. The image compression method reduces the transmission requirements and storage space for a given input data [4].New development in digital and medical technologies give birth to various types of medical images like X-rays, CT, MRI, ECG, fMRI etc and they are the standard for various diagnosis and treatment purposes [5].Image mining includes the extraction of knowledge or patterns or relationships, which are not directly stored in image format or in the images [6]. In the paper of [7] mining of images and its associations have done using blobs. Image mining commonly use two methods. Latter approach mine knowledge from huge dataset which consist of only image data and the former approach, they mine the collective set of images along with their correlated data. In the paper [8] has used rule mining to learn the associations between structures, size and role of human brain images. Use of different image compression methods help to condense the amount of data required to represent an image.

Image mining has led to tremendous growth significantly to large and detailed image databases. The most important areas belonging to image mining are: image acquisition, image knowledge extraction, image preprocessing, feature extraction, image segmentation and unsupervised clustering algorithms like k-means clustering algorithm. Here we gives the input of CT scan brain tumor images. The image

is converted into gray scale image for further processing. The denoising method is to remove noisy data and other ecological inconsistent data are removed from image. Image pre-processing and filtering techniques are applied on image. Then the CT scan brain tumor images are segmented by using k-means clustering algorithm, watershed algorithm, region based segmentation, and threshold based segmentation. Finally the canny edge detection applied to diagnosis whether the brain tumor is present or not.

2. RELATED WORK

As an interdisciplinary research field, image mining has its own following characteristics: Dependence on spatial information is vital for interpretation of image content but there isn't such requirement in traditional data mining. Interpretation of image contents is achieved through high level semantic that is generated by knowledge reasoning. Complexity of the image mining process not only analyzes and discovers a mode, but it also has to deal with the operations related to mining system such as image retrieval, indexing, and storing, which play important roles in the final mining results and all these processes add difficulties to image mining [Rajendran et al., 2009]. The main characteristics of image mining system in literature are: color, shape and texture features. The color feature extraction procedure includes color image segmentation.

For this purpose ideas from the procedure described in image retrieval by color semantics with incomplete knowledge are adopted [Corridoni et al., 1998]. First the standard RGB image is converted as L*u*v* image, where L* is luminance, u* is redness greenness, and v* is approximately blueness yellowness [Zaiane et al., 1998]. In the process of image analysis and information extraction, segmentation algorithms are used to partition the image into regions which are spatially continuous, disjoint and homogenous. A region is defined as a set of continuous pixels, with two dimensional distributions, representing uniformity related to some attribute. A segmentation algorithm uses primarily region growing, edge detection or combination of both [Marcelino Pereira Dos Santos Silva et al., 2008]. The fundamental challenge in image mining is to determine how low-level pixel representation contained in an image or an image sequence can be effectively and efficiently processed to identify high-level spatial objects and relationships. Typical image mining process involves preprocessing, transformations and feature extraction, mining, evaluation and interpretation and obtaining the final knowledge. Various techniques from existing domains are also applied to the image mining and include the object recognition, learning, clustering and classification [Hassan 2005].

This noise free image is the input to the K-means segmentation process, which uses approximate reasoning, for calculating shape and position of the tumor [Lakshmi et al., 2015]. Image processing can be defined as an active research area where MR image processing is a very challenging field. Medical imaging technologies can be used for imaging different parts of the human body for medical diagnosis. Brain tumor is a very serious and life-threatening disease. Image segmentation plays an important role in image processing as it is used in the extraction of suspicious parts from the MRI (magnetic resonance imaging) images. The paper proposed segmentation of the human brain MRI image using K-means clustering algorithm followed by the morphological filtering which is used to avoid the misclustered regions formed after segmentation[Joseph et al., 2014]. [Roy et al., 2015] proposed automatic brain tumor detection approach using symmetry analysis. The sequence of the methodology proposed in this paper shows the detection of tumor at the beginning and then segmenting the area of interest followed by area of tumor calculation.

3. PROPOSED METHOD

In this research paper, the systematic user friendly approach of CT scan brain image segmentation for detection of brain tumor and it can be computed by k-means clustering algorithm with the edge detection has been proposed using python. The below diagram shows an block diagram of each process which are described in figure 1

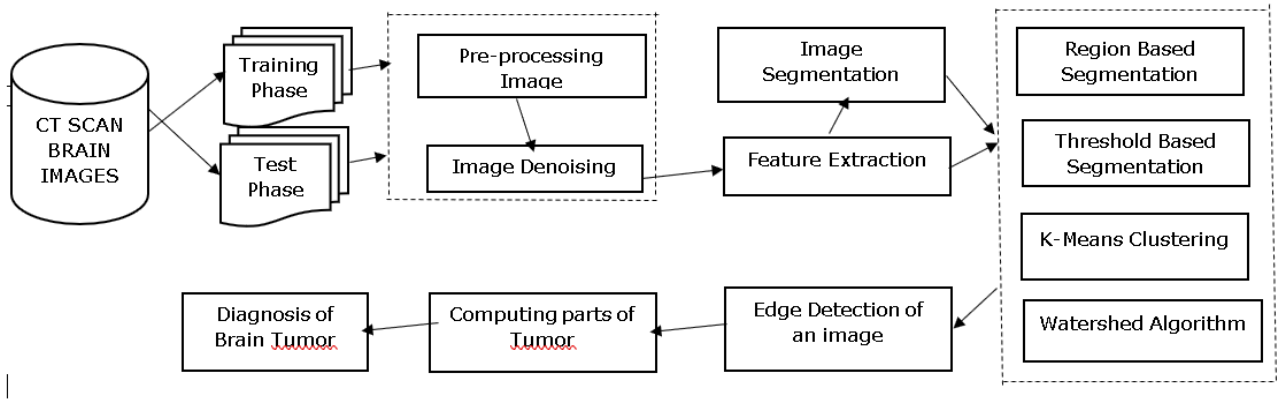

Figure 1. Block Diagram

 ISBN: 978-93-90214-20-4

3.1. CT SCAN BRAIN IMAGE

CT scan is better suited for the evaluation of penetrating brain injuries and other trauma and acute neurological emergencies. The dataset used is BRATS 2015 dataset. It consists of 4 modalities(different types of scans) namely T1, T1C, T2 and T2-FLAIR. For each patient and each modality, we get a 3D image of brain. For patients with brain tumor, physical symptoms vary from patient to patient. Some patients don't even show general symptoms. CT scans of patients are more reliable than physical symptoms.

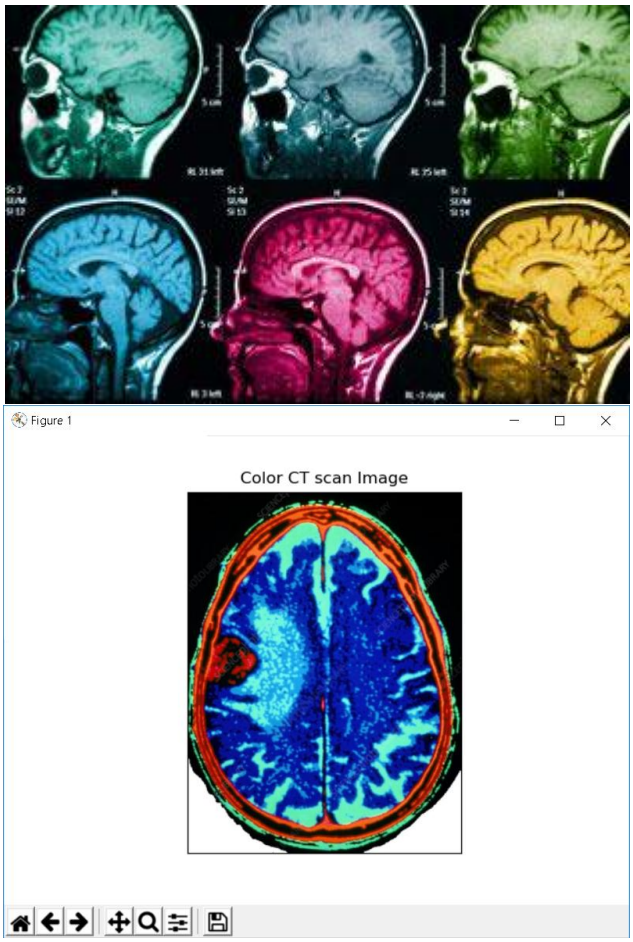

Figure 2. CT Scan Brain Image

3.2. PRE-PROCESSING IMAGE

The CT scan of the human brain tumor image are initially converted into Gray scale image. The image pre- processing step helps to improve the quality of an image. In image mining, the data cleaning process involved in pre-processing of an image.

Image denoising Algorithm

Image denoising is to pre process the original image by cleaning noise from the image. Image noise may be caused by different sources (from sensor or from environment) which are often not possible to avoid in practical situations. Therefore, image denoising plays an important role in a wide range of applications such as image restoration, visual tracking, image registration, and image segmentation.

There are two main types of noise in the image:

1. Salt and pepper noise - Pixels in the image are different in color or intensity from their surrounding pixels
2. Gaussian noise: Each pixel in the image will be changed from its original value by a (usually) small amount.

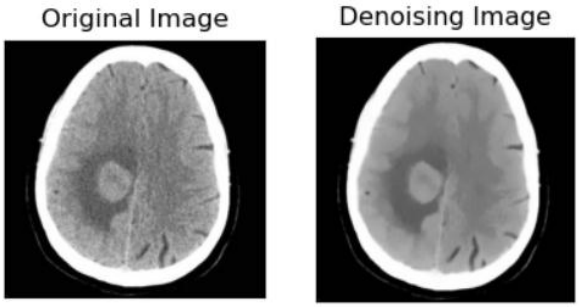

Figure 3. Image pre-processing

3.3. FEATURE EXTRACTION

The Coloured CT scan images of RGB are converted into gray scale images. The intensity of an image information is to improve the brightness or contrast of the images. The quality can be increased by feature extraction of the CT scan brain tumor images. In feature extraction, thresholding contains the extraction of the CT scan brain image cluster displays the forecasting tumor at the output of segmentation with k-means clustering algorithm. Then the thresholding can be extracted by each cluster is completed. Feature extraction is done by threshold based image segmentation.

3.4. IMAGE SEGMENTATION

Image segmentation is the process of partitioning an image into multiple different regions (or segments). The goal is to change the representation of the image into an easier and more meaningful image. To detect Brain Tumor in CT scan image by applying the following 4 different Segmentation techniques - Region Based Segmentation, Threshold Based Segmentation, K means clustering based segmentation, watershed Segmentation.

3.4.1. Region Based Segmentation

Adaptive thresholding uses the algorithm that calculates the threshold for a small regions of the brain tumor image so that we can get different thresholds for different regions of the same image and it gives us better results for images with varying light conditions.

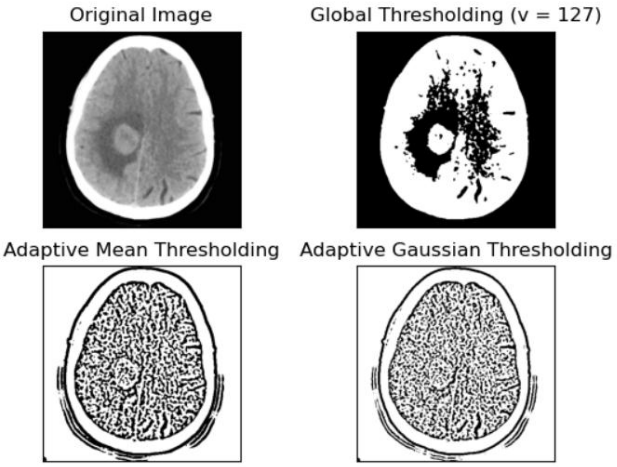

Figure 4. Region based Image Segmentation

3.4.2. Threshold Based Segmentation

The threshold calculates for binary values to be zero, to zero inverted, threshold binary, threshold binary inverted and truncated image has the small regions of the brain tumor image.

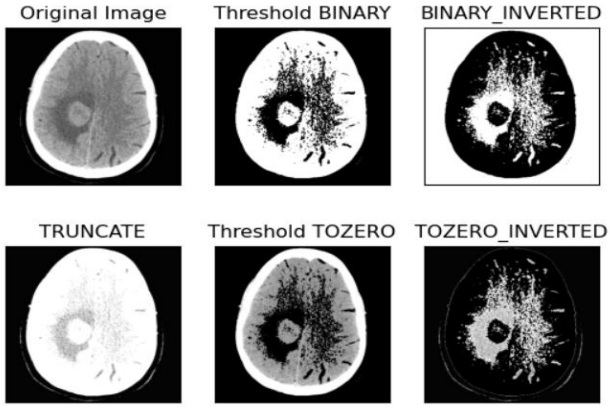

Figure 5. Threshold based Image Segmentation

3.4.3. K- Means Clustering based segmentation

K-Means clustering is unsupervised machine learning algorithm that aims to partition N observations into K clusters in which each observation belongs to the cluster with the nearest mean. A cluster refers to a collection of data points aggregated together because of certain similarities. The process of K-Means clustering based segmentation is first to read the Ct scan brain tumor image and convert RGB to Gray scale image. Reshape the original image to a 2D array of pixels and 3 color values (RGB) .Convert to float then find out the pixels to define stopping criteria. Then initialize the number of clusters (K). Thus the image is convert back to 8 bit values and flatten the labels array. Again, convert all pixels to the color of the centroids. Reshape back to the original image dimension. Now the segmented image occurred. Display the segmented image to further process.

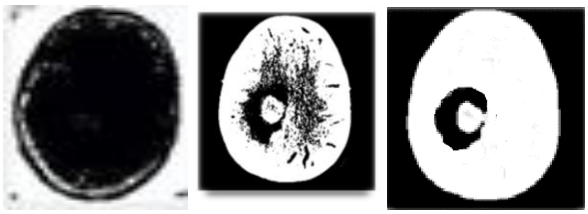

Figure 6. K-Means cluster based Image Segmentation

3.4.4. Watershed Algorithm

The image segmentation with marker-based watershed algorithm is to specify the pixel points are merged by regions. The marker-based means labeling where the region is a foreground or a background, and give different labels for original image. Using one color or intensity is label the region which are foreground or background with another color. Then, for the region we are not sure of anything, label it with 0. That is named as marker. After that, we apply watershed algorithm. Then our marker will be updated with the labels we gave, and the boundaries of objects will have a value of -1.

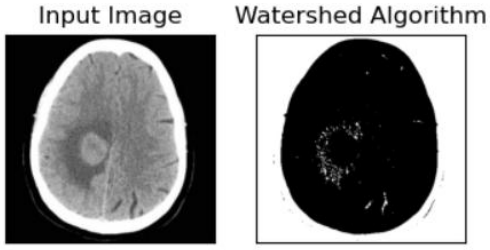

Figure 7. Watershed Algorithm based Image Segmentation

3.5. EDGE DETECTION OF AN IMAGE

Canny edge detection is the basic operations for image processing. It helps us reduce the amount of data (pixels) to process and maintains the structural aspect of the image. From canny edge detection, the result will get clean, thin edges that are well connected to nearby edges.

The canny edge detector is a 4-step detection process. The steps are:

Noise Reduction - 5x5 Gaussian filter, Calculating gradients - Finding Intensity Gradient of the Image, Nonmaximum suppression - upper threshold, Thresholding with hysterysis - upper/lower threshold

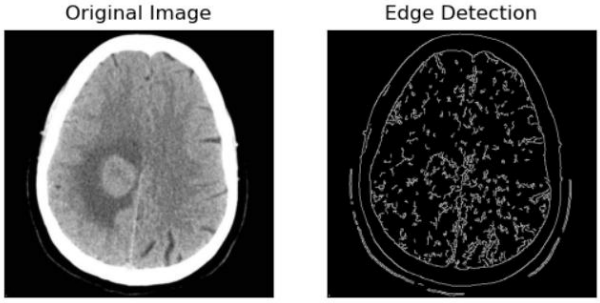

Figure 8. Edge Detection of an Image

 ISBN: 978-93-90214-20-4

3.6. COMPUTING PARTS OF TUMOR

The CT scan brain tumor image is computed by the binary images of number of white pixels(0). This binary method can be used for computing part of tumor. The final image , that is edge detection of binary image only have the pixels of black and white. The maximum size of the black and white pixels are 256 X 256. A black pixel has the value of 0 and a white pixel has the value of 1.

f (0) = black pixel (value 0)

f (1) = white pixel (value 1)

The tumor area computation is as follows:

Tumor Size is TS= [(√px)*0.264] mm2

Where,

px = number of white pixels and value of 1 pixel = 0.264 mm.

4. RESULTS AND DISCUSSION

Brain tumours are triggered by wild and irregular cell development or cell partition inside the brain. Exact brain tumour finding is a stimulating zone in medical image processing. The manual proof of identity in brain tumours from CT scan images is a monotonous procedure as individual patient has consequently various images.

In this Research, The CT scan brain tumor images can be detected by using systematic approach of machine learning python. CT imaging is preferred over MRI due to wider availability, lower cost, and sensitiveness to early stoke. CT scans save lives. But they can also cause cancer. And of the 70 million scans done last year double the number a decade ago. Now, at least 23 million were unnecessary. Therefore we can do to avoid CT scan of human brain for future risks.

The block diagram of each process which are described in figure 1. Preliminary input images are occupied and the annoying data slice, noise and intensity matching were done in pre-processing step. The CT Scan Brain Image was shown in the figure 2. Image denoising is to pre process the original image by cleaning noise from the image is shown in the figure 3. The Region based Image Segmentation was done by the original image to global thresholding , Adaptive mean thresholding and Adaptive gaussian thresholding are shown in figure 4.

The threshold calculates for binary values to be zero, to zero inverted, threshold binary, threshold binary inverted and truncated image has the small regions of the brain tumor image. Figure 5 Shows the Threshold based Image Segmentation. The process of K-Means clustering based segmentation is first to read the Ct scan brain tumor image and convert RGB to Gray scale image. K-Means cluster based Image Segmentation were shown in the Figure 6. The image segmentation with marker-based watershed algorithm is to specify the pixel points are merged by regions. The Figure 7 shows the Watershed Algorithm based Image Segmentation. From canny edge detection, the result will get clean, thin edges that are well connected to nearby edges. The Edge Detection of an Image is shown in Figure 8.

A confusion matrix stretches the conception of quantity of accurate and inappropriate predictions completed by the perfect related with the genuine classifications of the original data. The Figure 9 shows the final result. The knowledge and proficiency of medical experts to estimate and complete with a result. Then the computerised system by their skill will decrease the time of action for a specific patient. The medical experts are able to accomplish the same task in a reduced amount of time with an exact result.

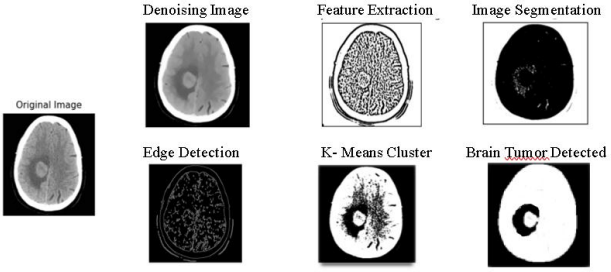

Figure 9. Results

5. CONCLUSION

In Medical imaging field, everywhere commonly research is happening with the purpose of generate or pretend interrelated with human and structurally vital images to recognize, study or to recover possible data for the improvement of manhood.

The Image Mining analysis of CT scan brain tumor images are preprocessed using Image Denoising algorithm. It can be feature extracted by the image calculated using a threshold value. To detect Brain Tumor in CT scan image by applying the four different types of Segmentation techniques like Region Based Segmentation, Threshold Based Segmentation, K means clustering based segmentation, watershed Segmentation. Then, Canny edge detection operations helps to reduce the amount of pixels. Using python, the brain tumor detection of CT scan image and its segmentation calculated by K – means clustering algorithm. The detection of brain tumor clearly displayed and more precise results to be produced. This detected brain tumor can also calculate for different sets of CT scan brain images from BRATS datasets. The Tumor detection from the brain images was ended by an accuracy of 91.06%.

REFERENCE

[1] N. Varuna shree and T.N.R. Kumar. Identification and classification of brain tumor MRI images with feature extraction using DWT and probabilistic neural network. (2018)

[2] Vani, V. (2015). Review on Automated Brain Tumor Segmentation and classification from Brain MRI. International Journal of Advanced Scientific and Technical Research.

[3] R.Venkata Ramana Chary, Dr.D.Rajya Lakshmi and Dr. K.V.N Sunitha,2012, “Feature extraction methods for colour image similarity, advanced Computing, ” An International Journal (ACIJ).

[4] Vamsidhar Enireddy and Kiran Kumar Reddi, 2012, "A Data Mining Approach for Compressed Medical Image Retrieval," International Journal of Computer Applications.
[5] A. Hema, E. Annasaro,2013, "A Survey in Need of Image Mining Techniques," International Journal of Advanced Research in Computer and Communication Engineering," Vol. 2.
[6] Megalooikonomou, Davataikos C. and Herskovits, 1999, "Mining lesion-deficit associations in a brain image database," KDD, San Diego, CA USA.
[7] Zhang Ji, Hsu, Mong, Lee,2001, "Image Mining: Issues, Frameworks and Techniques," Proceedings of the Second International Workshop on Multimedia Data Mining (MDM/KDD'2001), in conjunction with ACM SIGKDD conference. San Francisco, USA.
[8] Zaiane, O., Han J., et al, ,1998, "Mining MultiMedia Data. CASCON'98," Meeting of Minds,Toronto,Canada,pp 83-96.
[9] Hong Huang et al., Brain image segmentation based on FCM clustering algorithm and rough set.(2019)
[10] Arun kumar ray et al., Image analysis for MRI based brain tumor detection and feature extraction using biologically inspired BWT and SVM. (2017)
[11] G.Sethuram rao and D.Vydeki. Brain tumor approaches – A review.(2018)
[12] Saini, P. K., & Singh, M. Brain Tumor Detection in Medical Imaging Using Matlab. (2015)
[13] Debnath bhattacharyya. Brain tumor detection using MRI image analysis. (2011)
[14] Kavitha angamuthu rajasekaran et al., Advanced brain tumor segmentation from MRI image.
[15] Parasuraman Kumar and B. VijayKumar. Brain Tumor MRI Segmentation and Classification Using Ensemble Classifier.(2019)
[16] Rafael M. Luque-Baena. MRI segmentation of the human brain: challenges, methods and applications. (2015)

Design and Optimization of Electric Go-Kart

[1] More Abhishek Vivek, [2] Idris Press Wala, [3] Vighnesh Nair

[1][2][3] Student, Vishwakarma University, India

Abstract:

The main objective behind this is to design an electric Go-kart that can withstand all types of external forces, wear and tear, and traction without any damage. To design and analyze an efficient racing Go-kart, an electric vehicle instead of an IC engine, which should also be low cost,durable and environment friendly while also being safe and easy to maintain.

With the ever increasing fuel prices and skyrocketing pollution levels, we have designed this electric Go-kart which will be pocket friendly as well as eco friendly. Reducing carbon footprint was our major area of focus. Due to this we worked on improving the efficiency of our kart. Safety of the driver, reliability and durability were the key factors in mind while designing this electric Go-kart.

Keywords:

Electric Go-kart, Powertrain, Braking System, Steering System, Chassis, Steel, Electronics, Hydraulic, Ackerman Geometry, Safety, Current, Voltage, Impact Test, Strength, Weight

1. INTRODUCTION

The future of go-karts pushes innovation to new levels by making them completely electric while maintaining and increasing safety standards for people of all ages.

The current demand for electric go karts is increasing as compared to gasoline powered go-karts for a number of reasons, like Electric go karts require lower maintenance, And they include reduced labor costs.

The use of electric go karts provides improved safety standards like better track control and fail safes for any contingency, Since they are electric, they are also environmentally friendly.

The biggest revolution brought by electric go-karts is that they can be used both indoors as well as outdoors since they emit no smoke and they are safer as they do not run on gasoline which is highly flammable.

2. CHASSIS DESIGN

The chassis is the load-bearing framework of an artificial object which structurally supports the object in its construction and function. The chassis design needs to be prepared for impacts created in any certain crash or rollover. It must be strong and durable taking always in account the weight distribution for better performance.

2.1 MATERIAL DESIGN:

As per International standards, the chassis material must have at least 0.18% carbon content. The following materials which are commercially available and are currently being used for the chassis of a racing vehicle are shortlisted. They are as follows:

Table 1: Comparative study of material specification

Material specification	AISI 4130	AISI 4140
Density (gm/cc)	7.85	7.85
Poisson's ratio	0.27-0.30	0.27-0.30
Young's modulus (GPa)	190	190-210
Carbon content(%)	0.280-0.330	0.380-0.430
Tensile strength yield(MPa)	560	655

The material used in the cage must meet certain requirements of geometry as set by international championships, and other limitations. As the frame is used in a racing vehicle, weight is an important factor and must be considered. The proper balance of fulfilling the design requirements and minimizing the weight is crucial to a successful design.

The rules define that the chassis should be made with materials equivalent to or better than the bending strength and stiffness of 4130 steel. A key factor in this statement is that only steel members are allowed in the construction of chassis. However the alloy of the steel is allowed as long as the equivalency of the minimum requirement is achieved. These values are to be calculated about the axis which gives the lowest value. Calculating the strength and stiffness ensures that tubes with a non-circular cross section will sustain even in the worst of conditions. The required values of the steel used in the chassis have been included in the adjoining table.

After reviewing each of these factors, it is evident that the best choice will be AISI 4140 steel.

3. ANALYSIS

Each impact test is a worst case scenario that could potentially occur to the vehicle. There are three tests:

1. Front impact test
2. Rear impact test
3. Side impact test

3.1 Front Impact Test

The front collision test is designed to stimulate a head-on collision between two cars, the vehicle is designed to handle crash damage at 54km/hr. This is the maximum top speed the vehicle is expected to reach.

For the front impact test, the force is calculated using the change in momentum equation.

Consider car crashes to the wall and come to a stop in 0.4 seconds.

Change in momentum= F×t

Or mv-mu=F×t

Where;

m= mass of whole vehicle = 250kg

v= final velocity of vehicle= 0 m/s

u=initial velocity of vehicle=15 m/s

t= impulse time= 0.4 (for front impact)

mv= final momentum (the one it ended up with).

mu=initial momentum (the one it started with).

The change in momentum = mv-mu

=(250×0) - (250×15)

Change in momentum= -3750kg m/sec.

(The negative sign shows that the car lost momentum)

Change in momentum = F ×t

3750= F × 0.4

F= 9375 N

Hence for front impact test, the 9375 N force is applied in front of the chassis by constraining all mounting positions with appropriate constraints.

The position of applied force and the appropriate constraints are shown in the following figure:

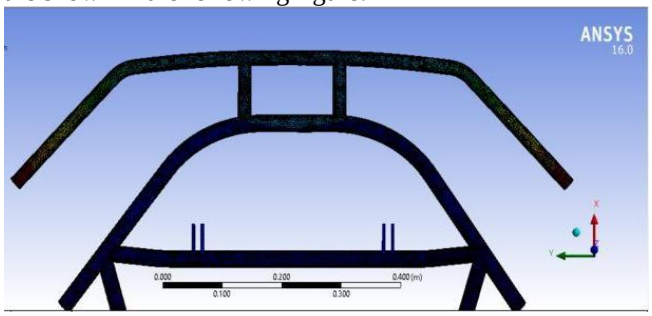

Fig 1. Front impact test

3.2 Side Impact Test

The side impact simulates the vehicle is hit by another vehicle of the same weight from the side . For Side impact, a force equivalent to 2G is applied on the side portion of the vehicle.

Where; G = m×g

m= total weight of vehicle = 250 kg

g= acceleration due to gravity

F=2G = 2×250×9.81

F= 4905 = 5000N

Hence the calculated force was placed on one side of the model of frame while keeping proper constraints and the stresses were simulated. The images are shown below.

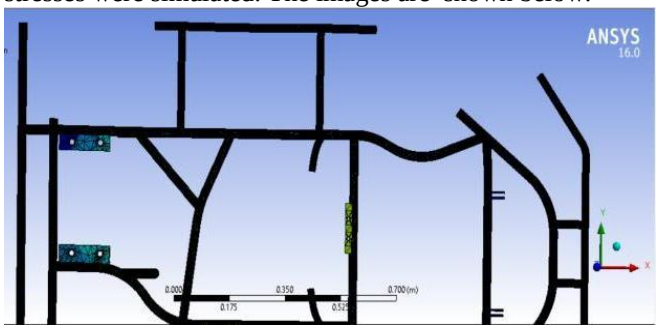

Fig 2.side impact test

3.3 Rear impact test

Rear impact test reproduces the effect that an impact would have on the rear part of the vehicle, at moderate speed.

For Rear impact, a force equivalent to 4G is applied on the rear portion of the vehicle.

where; G= m×g

m= Total weight of the vehicle=250 kg

g= acceleration due to gravity

F= 4G= 4×m×g

F= 4×250×9.81

F= 9810 N =10000N

Hence the calculated value of the rear impact force was divided into two parts. 70% of the load is applied on the bottom rail of the rear bumper where the impact is the highest and 30% load is applied on the upper part of the rear rail where the impact is not much. The analysis is shown in the following figure:

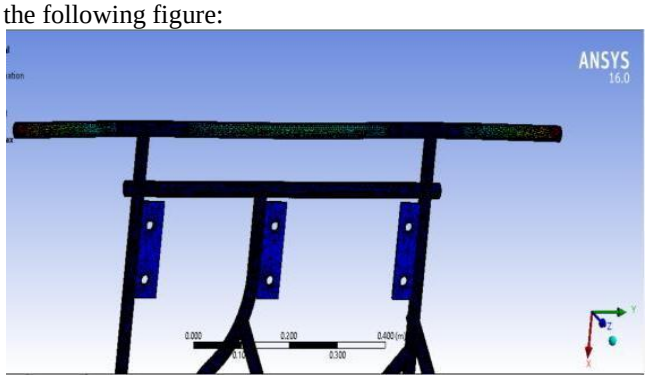

Fig 4. Rear impact test

3.4 Bending Analysis-

For calculating bending in the chassis, the maximum force is applied on the CG, node connected to the chassis by rigid connectors.

The CG, node is calculated from the CAD model.

Maximum force = m × g

where ,
m = total mass of the Go-kart (250 kg)
g= gravitational acceleration(m/s^2)

Maximum Force = 250 × 9.81
= 2452.5 N
The loading diagram is shown in the following figure:

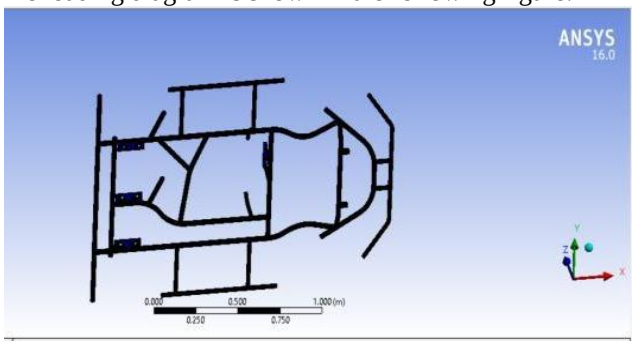

Fig 5. Bending stresses

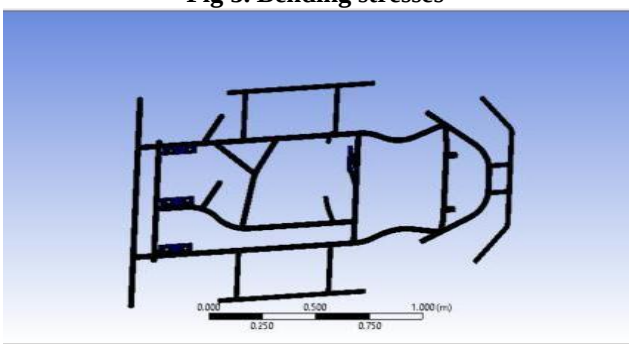

Fig 6. Bending strains

4. STEERING:

WORKING:
When a vehicle is turning, the inner front wheel needs to turn at a different angle to the outer because they are turning on different radii. The Ackermann steering mechanism is a geometric arrangement of linkages in the steering of a vehicle designed to turn the inner and outer wheels at the appropriate angles.

OBJECTIVE:
The steering system converts the rotation of the steering wheel into a swivelling movement of the road wheels in such a way that the steering-wheel rim turns a long way to move the road wheels a short way. Positive and precise wheel movement is expected while steering(none of the wheels must lose traction or as such).

DESIGN:
Calculations:
The front wheel configuration 0° angle and 3° angle.
1) Wheelbase(b) = 1070mm=1.070 m
2) Track Width(a) = 1105mm=1.105 m
3) $Tie\ rod\ length(c) = track\ width/2$
=1105/2
=552.5 m =55.25 m
(55.25-10) cm=45.25 cm
Half tie rod= 0.4525 m
c=0.4525×2
=0.905 m
4) Inner wheel maximum turning angle(ɵ) = 16.75°
5) Outer wheel maximum turning angle(ϕ) = 23.61°
6) Steering Ratio=1:1
7) For inner wheel radius(front)

$$R(in) = b/sin\,ɵ + (a-c)/2$$

R(in)= 1.070/0.288 + (1.105-0.905)/2
R(in)= 3.81m
8) For outer wheel radius(front)

$$R(out) = b/sin\,\phi + (a-c)/2$$

R(out)=1.07/o.400 + (1.105-0.905)/2
R(out)=2.77m
9)$For\ inner\ wheel\ radius(rear)$

$$= b/tan\,ɵ + (a-c)/2$$

=1.07/0.300+ (1.105-0.905)/2
=3.65m
10)$For\ outer\ wheel\ radius(rear) = b/tan\,\phi + (a-c)/2$
=1.07/0.437 + (1.105-0.905)/2
=2.547 m

5. BRAKING SYSTEM

Hydraulic braking system
A hydraulic braking system transmits brake-pedal force to the wheel brakes through pressurized fluid, converting the fluid pressure into useful work of braking at the wheels.

5.1 Objective
The braking system is designed in such a way that it locks the rear wheels and halts at a safe distance.

5.2 Design
The braking system used is a hydraulic disc brake system with two independent hydraulic circuits, working with Pulsar 220 master cylinder and KBX(dual piston) calipers to provide braking force. One port actuates the brake calipers and one is connected to the switch for brake light indication.

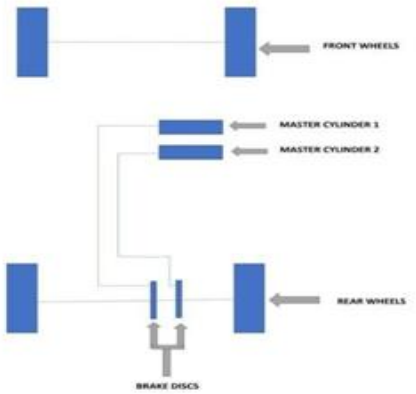

Fig 7.Braking system (schematic)

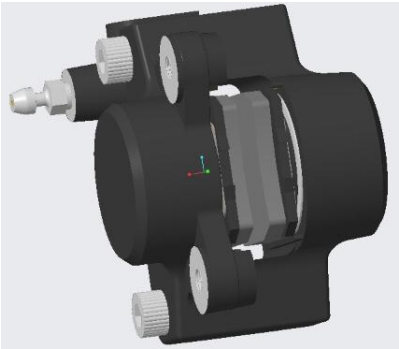

Fig 8.Braking Caliper

Table 2: Specification table

Type	Specification
Brake disc diameter	140mm
Master cylinder diameter	8.5mm
Caliper diameter	30mm
Brake pedal leverage	4:1
Top speed	80km/hr

5.3Calculation:
Weight(m)=250kgs (with driver)
Force on pedal (PR)=350N
Leverage(L)=4:1

Force on master cylinder(F):
PR×L=350×4=**1400N**

Area(A)= (3.14× 8.5×8.5)/4
=**56.75**mm^2

Brake Line Pressure(P)
P=F/A
=1400/56.75
=**24.66**× 10^6 **pa**

Pressure on caliper=24.66× 10^6 **pa**
Force on Caliper:
BLP×A=F
Where, A=(3.14×30×30× 10^{-6})/4
=706.86× 10^{-6}
F=BLP×A
=17431.16N
Total Force on Caliper
Force=2×17431.15 **(because of 2 pistons)**
=**34862.33N** (Normal Force)
Frictional Force (B.F)
=0.8N
=0.8 × 34862.33
=**27889.8N**
Diameter of brake disc= 0.14m
Radius=0.07m
Braking Torque (B.T)
=B.F×Radius
=27889.8×0.07
=**1952.286Nm**
Braking force on tyre
=B.T/Radius of tyre
=1952.286Nm/0.1397
=13974.8461
=13974.8461×2 **(for 2 calipers)**
=**27949.7N**
Deceleration
B.F=m×a
a= 27949.7/250
a=111.8m/s^2
Stopping distance(S)
Max speed=80KMPH
u=22.22m/s ,v=0
v^2 -u^2= 2(a× s)
0-493.78=2×111.8×s
s= 493.78/223.6
s=2.21m
Stopping time(t)
v=u + a×t
0-22.22=111.8×t
t=0.20sec.

6. Drive Train:
OBJECTIVE:
The Objective of drive train is to transmit the power generated by the motor to the driving wheels which as a result propels the vehicle

6. DESIGN

The drive train uses the belt drive system to connect the drive shaft and the motor shaft . there are two parallel pulleys one on the motor shaft and other on the drive shaft and have a V belt running across them to transmit the power from one to other.

6.1 SPECIFICATION OF POWER TRAIN:
Motor Specifications:
Rated Power=2.5kW
Max power 5.2 KW
Rated Torque=7.7NM
Peak Torque 23NM
Rated Speed=3000rpm
Rated Voltage : 48V
Under Voltage : 38.5 +- 0.5V
Rated current :- 59.3 A

Motor Controller Specifications:
Rated Voltage : 48V
Rated Current : 72A
Throttle Voltage : 1.2-4.3V
CAN BUS : 2.0b 500kbps

Battery Specifications :
Configuration : 13s10p
Battery selected : Panasonic (formerly SANYO) NCR18650GA 3300mAh 10A CDR
Battery Chemistry : Li-ion NCA
Max Voltage : 54.6V (4.2V per cell)
Nominal Voltage : 46.8V (3.6V per cell)

Cut off Voltage : 32.5V (2.5V per cell)

Belt Drive Specifications :
Driving Pulley Diameter : 1.25inch
Driven Pulley Diameter : 5inch
Reduction Ratio : 4:1
Belt Type : V-Belt.

The reasons for selecting these cells is because they have a very good power efficiency for 5A current usage (3160mAh in real world tests) and as it's rated for 10A Continuous Discharge Rating it will stay well below its maximum temperature, allowing for easy cooling.

7. BEARINGS AND JOINTS

7.1 Bearing selection:

From the standard chart, selecting the rolling contact bearing as internal diameter is d = 20mm and the static load capacity of maximum load is 879.1524N. Therefore selecting the bearing of bearing number as 6004 .
Internal diameter = 20mm
Outer diameter = 42mm
Breadth = 12mm
Dynamic load capacity = 9.95KN
Static load capacity = 5KN

7.2 Bearings:

Bearing ensures free rotation of shaft or the axle with minimum friction. It supports the shaft or the axle and holds it in the correct position. It takes up the forces that act on the shaft or the axle and transmits to the frame or a foundation. Ball bearings are used mostly for radial loads acting on the vehicle. The life of the bearing depends on a number of revolutions. Bearings used are selected from standard charts by considering appropriate designations such as: Type Quantity Ball bearing (6003) 8 Ball bearing (S6004RS) 1 Pillow block (P206) 2.

7.3 Heim Joints:

Heim bearings produce the industry's widest range of rod ends type and sizes. Heim products range includes rod-ends with brass race inserts in standard, precision, and high capacity designs; High strength, two piece designs; self lubricating rod-ends with engineered thermoplastic races or Teflon liners; and military standard rod-ends for the ultimate in rod-end performance. Heim rod-ends are also available with a variety of plating's, coatings and materials and with a wide range of optional features such as lubrication, fittings, left hand threads and keyway slots.

Fig 9. Heim Joint

Fig 10.Ball Bearing

8. SAFTEY

In the event of a hazardous accident ,the cockpit is securely layered with shock absorbing foam in all the tubing to protect the driver. SAE rated brake lights have been installed to maintain high safety standards. The remaining standard safety equipment, including fire extinguishers and kill switches were all placed for easy access and use, as well as maximum optimization of their function during an emergency. A driver's suit has also been used during the testing of the Go-kart.

Fig 11. Drivers Suit

9. RIMS & TIRES

OBJECTIVE:
The rims and tires perform the work of converting the torque created by the drivetrain into a push force which results in acceleration of the vehicle.

DESIGN:
The Go-kart is designed to work with 10'' front and 11'' rear diameter tires. This allows the vehicle to reach a higher top speed by sacrificing some push force.
The wheels selected are made of aluminum , which gives enough strength to endure rough terrain while reducing the weight considerably.

10. ELECTRIC SYSTEM:

Emergency stop kill switches and brake lights are included in the electric system.
There are 3 kill switches in the vehicle, one over the wheel reach of the driver, second one outside the body of the car and third is the brake over travel switch. The second location is easily accessible to the driver and Pit-Crew in case of emergency.
The working of the kill switch is pretty simple. It just kills the energy provided by the motor by opening the circuit resulting the motor to stop immediately
Kill switch doesn't affect the working of any other electronic component.
We have used relays to switch to the shutdown circuit in case of overcurrent/overvoltage occurring.We have used fuses for accumulators to prevent current overload, with a central main fuse at a lower rating than the parallel set cell fuses so that in case the fuse does trip we only have to replace the central main fuse rather than all parallel sets.

 ISBN: 978-93-90214-20-4

Motors can be controlled by the analog throttle voltage or the CANBUS system that communicates with the AMS to control the appropriate current required.

11. FASTENERS:

OBJECTIVE:
Threaded joints are used to hold two or more machine parts together. These parts can be dismantled, if required, without any damage to machine parts or fastening.

BOLTS:
We have majorly used bolts of size M6, M8, M10, M12, M16 and M20. Since all tensile bolts can sustain axial, compressive and tensile loads, we have only designed for 4 bolts in one plane bearing mounting.

NUTS:
We have used Nylon lock nuts everywhere so that connections do not get loose due to vibrations.

12. OVERALL VEHICLE DETAILS

Table 3: Overall vehicle details

Length	1.72m
Width	1.28m
Wheel base	1.070m
Track width	1.105m
Ground clearance	1.8 inch
Front tire size	10 inch
Rear tire size	11 inch
Max speed	80km/hr
Max acceleration	0.27m/s^2
Stopping distance	2.21m
Kerb weight	170kgs
Weight distribution	60%at rear and 40% at front

13. CONCLUSION

Our prime goal is to design Go-kart which matches the SAE criteria for safety, durability and efficiency as well as provide features that will have mass market appeal to the general Go-kart enthusiasts.
Design decisions were made with each of these parameters kept in mind. We relied on our individual knowledge and experience of Go-kart vehicles, as a tool for developing the initial subassembly designs of the kart. Wherever applicable, selection of components for each subassembly of the kart was based on engineering knowledge of UG level coursework.
Computational design and software were used to verify each part of a subassembly which met or exceeded its stated objectives. Use of these design tools also allowed to address and rectify conflicts between interfacing sub-assemblies before fabrication and machining, saving both time and money. Every day we had our prime attention and focus in rectifying the finest design possible for the Go-kart. This design is the fruit of our hard work and many restless days and nights.

REFERENCE

[1] Smith, C. (1978). Tune to win. Carroll Smith Consulting.
[2] Gillespie, T. D. (1992). Fundamentals of vehicle dynamics. SAE International.
[3] Singh, K. (2004). Automobile engineering, Vol Ii,(automobile engines, including electrical equipment).
[4] (n.d.). Wikipedia. Retrieved July 13, 2020, from https://www.wikipedia.org/
[5] (n.d.). Google Scholar. https://scholar.google.com/
[6] Singh, K. (2021). Automobile Engineering Vol-1 PB. STANDARD PUBLISHING.
[7] Crolla, D. (2021). Encyclopedia of Automotive Engineering by Crolla, David(March 23, 2015) Hardcover. Wiley.
[8] Lee, H. (2018). Finite Element Simulations with ANSYS Workbench 19 (1st ed.). SDC Publications.

Performance Analysis of Single Phase Multilevel Inverter for Islanded Grid Application

[1] C.Pavan Kumar, [2] Akhila Manthena, [3] YerabatiLasyapriya, [4] Kamutam Varenya, [5] Potharaju Sampath

[1] Assistant Professor, EEED, Kakatiya Institute of Technology and Science, Warangal, India
[2][3][4][5] Student, EEED, Kakatiya Institute of Technology and Science, Warangal, India

Abstract:

Multilevel inverters (MLI) are being preferred for high power and medium voltage applications over conventional two level inverters. The conventional topology of inverter requires more number of power semiconductor switches and has more harmonic distortion with higher switching losses and so these are limited to wide range of applications. In this project work, the comparative performance analysis of multi- level reduced switch count hybrid inverter and cascaded multilevel inverter for Islanded grid applications, in terms of number of semiconductor switches and total harmonic distortion (THD) will be discussed. Reduced switch count hybrid multilevelinverter(RSHMLI)topology, integration with solar PV system is designed for Islanded grid applications. Further, to decrease the harmonic distortion, switching losses and to enhance the performance of hybrid multilevel inverter configuration, the power semiconductor switches (IGBTs) gate switching operation is carried out with level shifted pulse width modulation technique. Design, simulation and comparison of cascaded inverter and hybrid inverter are carried out in MATLAB/Simulink software tool for5 and 7 levels of output voltages.

Keywords:

THD-Total Harmonic Distortion, MLI- Multi Level Inverter

1. INTRODUCTION

The multilevel inverter (MLI) has been used as an alternative in high power and medium voltage situations. A multilevel inverter is a power electronic device which is capable of providing desired alternating voltage level at the output using multiple lower level DC voltages as an input. Usually 2 level inverter is used to generate the AC voltage from DC voltage. The concept to multilevelinverter(MLI) is kind of modification of two-level inverter. The MLI technology is on high demand and on rise in field of industrial electronics with advancement in power quality etc.Inmultilevel inverters we don't deal with the 2 level voltage instead ,in order to create a smoother stepped output waveform,more than 2 voltages levels are combined together and the output waveform obtained in this case has lower dv/dt and also lower harmonic distortions.it is also well known that switching frequency is reduced with reduced number of switches. This paper gives a clear description about the topologies of Cascaded H bridge MLI and Hybrid MLI along with their output different levels and with usage of suitable PWM techniques.There are some novel methods recommended, where low switching frequency and high power devices are used. A small change is required to decrease the output voltage distortion, with the drawback of considerable amount of low order current harmonics. The accurate magnitude of O/P voltage cannot be obtained because Pulse width modulation technique is utilized. Multilevel inverters improve quality of power by means of output waveforms ,which eventually decrease the level of harmonics .The properties of staircase waveform are it has very low THD,small amount of common mode voltage,least dv/dt stress and electromagnetic compatibility.A specific optimization technique is used to control the switching angle of semiconductor switches (IGBT) of hybrid MLI and cascaded H bridge cascaded H-bridge multilevel inverter and hybrid MLI.

2. MULTILEVEL INVERTER AND THEIR TOPILOGIES

Multilevel inverters have three types. Diode clamped multilevel inverters, flying capacitor multilevel inverters and cascaded H-bridge multilevel inverter. The choice of topology for each inverter should be based on what is the usage of the inverter. Each topology has some advantages and disadvantages. By expanding the quantity of levels, the THD will be diminished yet then again cost and weight will be expanded too. Likewise since the exchanging plots for switches are not the equivalent, the drive circuit for each switch is isolated from different switches.. The THD will be diminished by expanding the quantity of levels. Clearly a output voltage with low THD is desired , however expanding the quantity of levels needs more equipment, likewise the control will be more scrambled. It is an adjustment between value, weight, intricacy and a generally excellent yield voltage with lower THD. The mentioned different categories of MLIs are compared on the basis of THD and switching patterns. By comparing these MLIs we would like to choose the Cascaded H bridge MLI and hybrid MLI because of their low THD.

3. SWITCHING OPERATIONS OF HYBRID MLI AND CASCADED H BRIDGE MLI:

The switching operations of 5and 7 levels of Cascaded H Bridge and Hybrid multilevel inverters are as given in the tables 1,2,3,4 along with their switching diagrams.

5 LEVEL CASCADED H BRIDGE MLI:

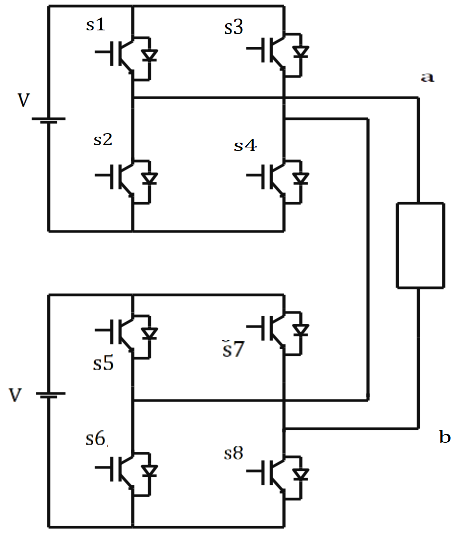

Fig 1: Switching diagram of 5 level cascaded H bridge MLI.

Switching operation:

O/P Voltages	Switching Conditions							
Vab	S 1	S 2	S 3	S 4	S 5	S 6	S 7	S 8
2Vdc	1	0	0	1	1	0	0	1
Vdc	1	0	0	1	1	1	0	0
0	1	1	0	0	0	0	1	1
-Vdc	0	1	1	0	1	1	0	0
-2Vdc	0	1	1	0	0	1	1	0

Table 1: switching operation of 5 level cascaded H bridge MLI

7 LEVEL CASCADED H BRIDGE MLI:

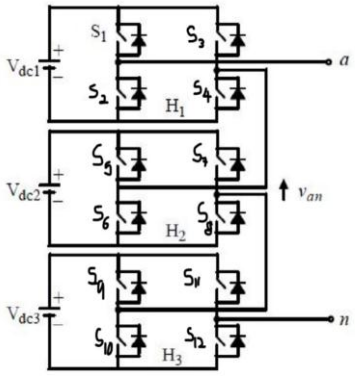

Fig 2: Switching diagram of 7 level cascaded H bridge MLI.

Switching operation:

Output voltage	S 1	S 2	S 3	S 4	S 5	S 6	S 7	S 8	S 9	S 10	S 11	S 12
3Vdc	**1**	**0**	**0**	**1**	**1**	**0**	**0**	**1**	**1**	**0**	**0**	**1**
2Vdc	**1**	**0**	**0**	**1**	**0**	**0**	**1**	**1**	**1**	**0**	**0**	**1**
Vdc	**1**	**0**	**0**	**1**	**0**	**0**	**1**	**1**	**0**	**0**	**1**	**1**
0	**1**	**0**	**1**	**0**	**1**	**0**	**1**	**0**	**1**	**0**	**1**	**0**
-Vdc	**0**	**1**	**1**	**0**	**1**	**1**	**0**	**0**	**1**	**1**	**0**	**0**
-2Vdc	**0**	**1**	**1**	**0**	**0**	**1**	**1**	**0**	**1**	**1**	**0**	**0**
-3Vdc	**0**	**1**	**1**	**0**	**0**	**1**	**1**	**0**	**0**	**1**	**1**	**0**

Table 2: Switching operation of 7 level cascaded H bridge MLI

5 LEVEL HYBRID MLI:

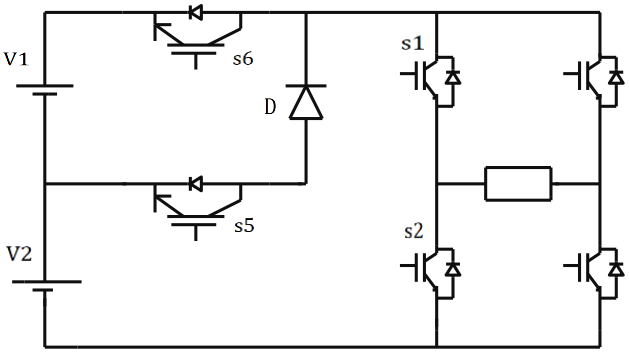

Fig 3: Switching diagram of 5 level Hybrid MLI

Switching operation:

Output voltage	S1	S2	S3	S4	S5	S6
Vdc	**1**	**0**	**0**	**1**	**1**	**1**
Vdc/2	**1**	**0**	**0**	**1**	**1**	**0**
0	**1**	**0**	**0**	**1**	**0**	**0**
-Vdc/2	**0**	**1**	**1**	**0**	**1**	**0**
- Vdc	**0**	**1**	**1**	**0**	**1**	**1**

Table 3: Switching operation of 5 level Hybrid MLI

7 LEVEL HYBRID MLI:

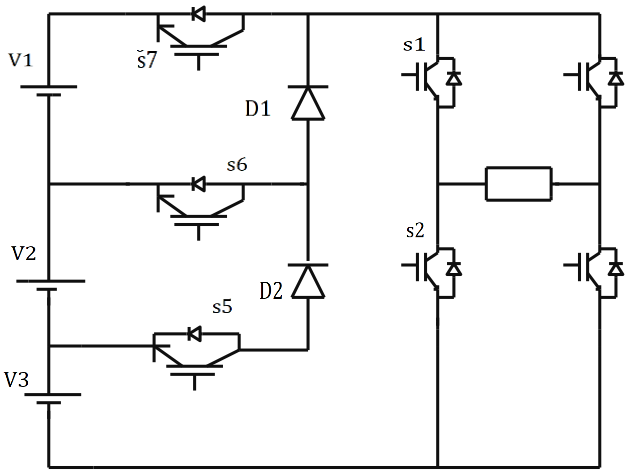

Fig 4: Switching diagram of 7 level Hybrid MLI

 ISBN: 978-93-90214-20-4

Switching operation:

Output voltage	S 1	S 2	S 3	S 4	S 5	S 6	S 7	D 1	D 2
3Vdc	**1**	**1**	**0**	**0**	**0**	**0**	**1**	**.**	**.**
2Vdc	**1**	**1**	**0**	**0**	**0**	**1**	**0**	**.**	**1**
Vdc	**1**	**1**	**0**	**0**	**1**	**0**	**0**	**1**	**1**
0	**1**	**1**	**0**	**0**	**0**	**0**	**0**	**.**	**.**
-Vdc	**0**	**0**	**1**	**1**	**1**	**0**	**0**	**1**	**1**
-2Vdc	**0**	**0**	**1**	**1**	**0**	**1**	**0**	**.**	**1**
-3Vdc	**0**	**0**	**1**	**1**	**0**	**0**	**1**	**.**	**.**

Table 4: Switching operation of 7 level Hybrid MLI

4. CASCADED H BRIDGE MLI at 5 and 7 levels:

Simulation result at 5 level:

For simulation of 5-level cascaded H bridge MLI, two DC sources of 100v each are taken. Unequal DC sources are also chosen for testing. S1,S3,S4,S7 operate always in positive half cycles during ON condition of switch T1 and during ON condition of switch T2 ,S1,S2,S5,S6 operate in negative half cycles.The O/P voltage, I/P voltage and current waveforms. The input voltage, output voltage and current waveforms are determined by using FFT analysis and THD, the results are given below.

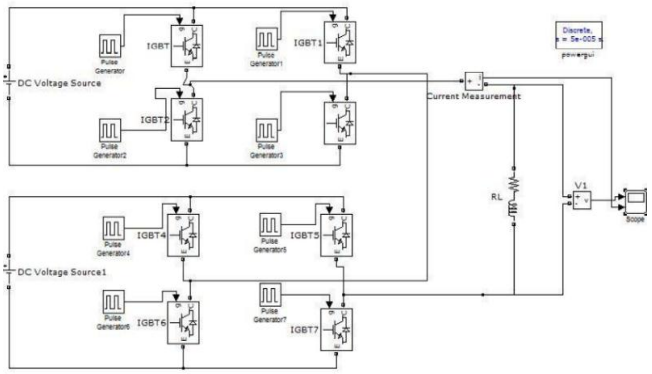

Fig 5: Simulation of single phase 5 level cascaded H bridge MLI.

Result:

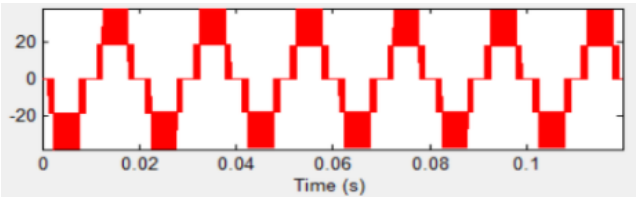

Fig 5.1: O/P voltage waveform of single phase 5 level cascaded H bridge MLI.

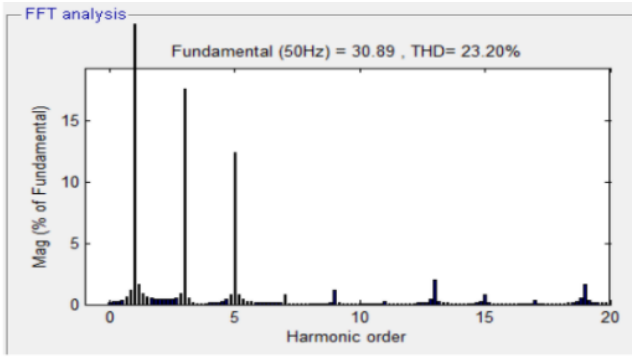

Fig 5.2: FFT analysis of single phase 5 level cascaded H bridge MLI.

Simulation result at 7 level:

For simulation of 7-level cascaded H bridge MLI, two DC sources of 100v each are taken. In this simulation 0.002 is taken as one time span in which during positive half cycle with switches T1, T2, T3 are in activity, S1, S3, S4, S7, S11 and S10 works consistently and in negative half cycle with T1, T2, T3 turned ON where S1, S2, S5, S6, S8 and S9 works periodically.The input voltage, output voltage and current waveforms are determined by using FFT analysis and THD, the results are given below in Fig 6.1, Fig6.2.

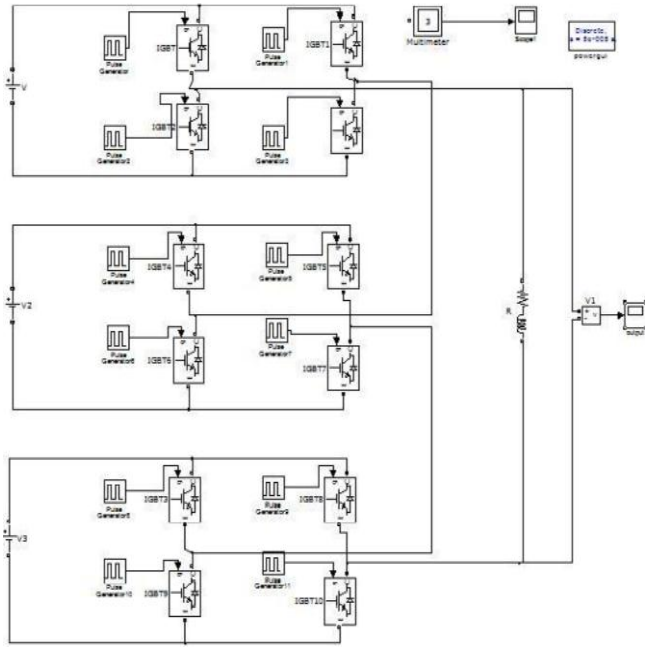

Fig 6: Simulation of single phase 7 level cascaded H bridge MLI

 ISBN: 978-93-90214-20-4

Result:

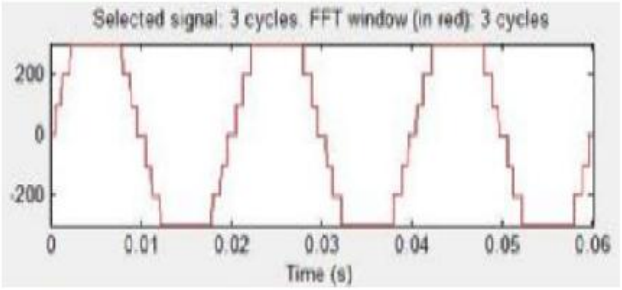

Fig 6.1:O/P voltage waveform of single phase 7 level cascaded H bridge MLI.

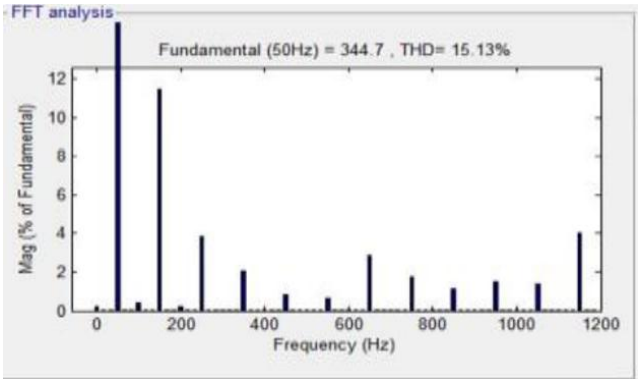

Fig 6.2:FFT analysis of single phase 7 level cascaded H bridge MLI.

5. HYBRID MLI at 5 and 7 levels:

Simulation result at 5 level:

wo DC sources are utilized for the recreation of 5-level Hybrid MLI. Additionally, in this composition, two 100 V DC sources are taken. It tends to be finished with inconsistent dc sources moreover. FFT analysis is done, with the aim that THD can be determined as demonstrated underneath. At the point when switch T1 will be in ON condition, the switches S1 and S2 consistently work in positive half cycle and when T2 will be ON the switches S3 and S4 will be worked in negative half cycle.The input voltage, output voltage and current waveforms are determined by using FFT analysis and THD, the results are given below.

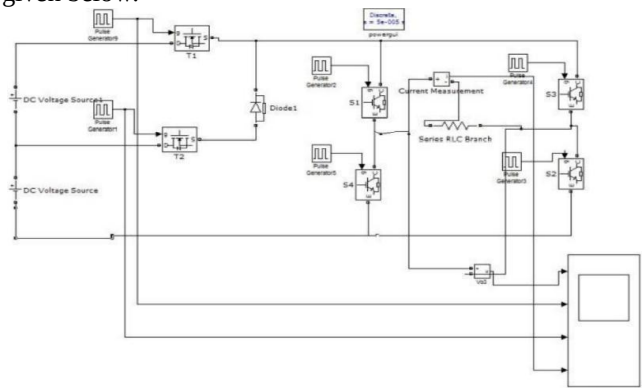

Fig 7: Simulation of single phase 5 level Hybrid MLI.

Result:

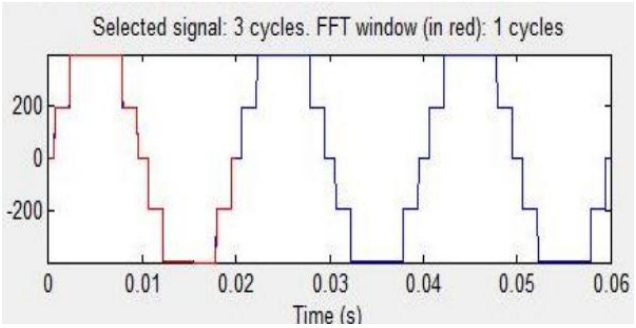

Fig 7.1: O/P voltage waveform of single phase 5 level Hybrid MLI

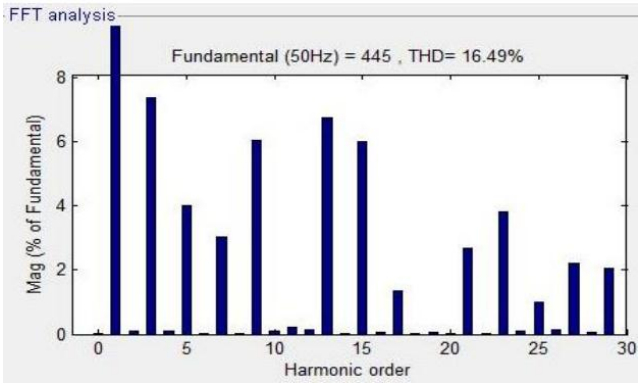

Fig 7.2:FFT analysis of single phase 5 level Hybrid MLI

Simulation result at 7 level:

Three sources (100V) are utilized for the simulation of 7-level hybrid MLI in this paper. At the point when three switches T1, T2 and T3 work, just S1 and S2 will work in positive half cycle and furthermore S3 and S4 will be in negative half cycle periodicallyThe input voltage, output voltage and current waveforms are determined by using FFT analysis and THD, the results are given below.

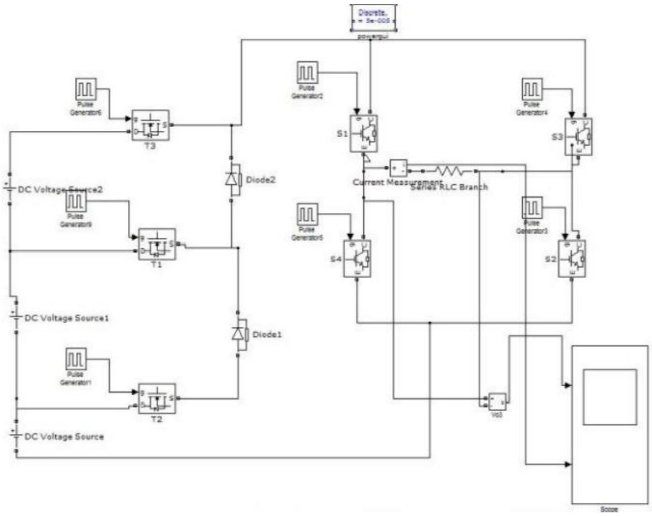

Fig 8: :Simulation of single phase 7 level Hybrid MLI

Result:

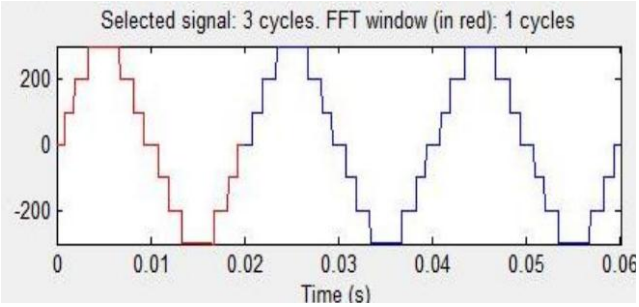

Fig 8.1: O/P voltage waveform of single phase 7 level HybridMLI

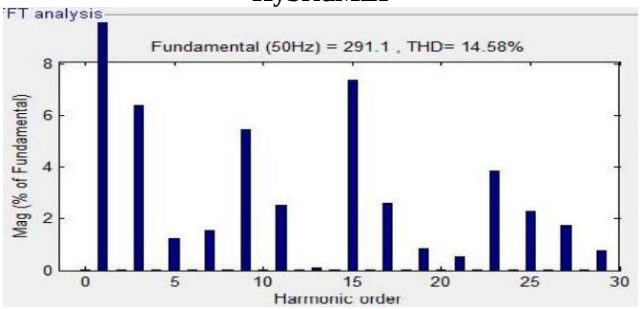

Fig 8.2: FFT analysis of single phase 7 level Hybrid MLI

6. COMPARISON BETWEEN CASCADED & HYBRID MULTILEVEL INVERTER:

The comparative analysis is carried out between 5th level and 7th level hybrid and cascaded type multilevel inverter regarding number of semiconductor switches and total harmonic distortion (THD). In the level 5 the cascaded inverter, 8 number of switches are used. The total harmonic distortion (THD) from FFT analysis is to be 18.46% where as in level -5 the hybrid inverter uses only 6 number switches and the THD is 16.49%. The 7th level cascaded inverter has 12 active switches and the THD is 15.13% but in 7th level hybrid inverter only 7 semiconductor switches are used with THD of 14.58%. So, 7-level hybrid topology is more advantageous than other types given in Table 1.

Model	*No. of Switches*	*THD%*
5 Level Cascaded Inverter	*8*	*18.46*
5 Level Hybrid Inverter	*6*	*16.49*
7 Level Cascaded Inverter	*12*	*15.13*
7 Level Hybrid Inverter	*7*	*14.58*

Table 5: Comparison of no. of switches used in hybrid and cascaded H-Bridge inverter

7. CONCLUSION

Cascaded H bridge multilevel inverter and Hybrid multilevel inverters are compared at 5 and 7 voltage levels. This idea, just as providing every cell with a one of a kind DC voltage, can bring about a high number of voltage levels.. However, it is shown that in some cases, the power quality must be lowered slightly in order to ensure that the current drawn from transformer/rectifier sources remains positive. The new 7-level inverter is experimentally verified. The experimental results match with the simulation results. In this 7-level hybrid inverter only 7 switches are required for its smooth operation. The voltage stresses across different switches are shown in tabular form. The installation area and cost also reduces compared to 7-level cascaded topology.

REFERENCE

[1] Rodriguez,J.;Jih-ShengLai;FangZhengPeng;,"Multilevelinverters:asurveyoftopologies, controls, and applications," Industrial Electronics, IEEE Transactions on , vol.49, no.4, pp. 724- 738, Aug2002.

[2] Jih-Sheng Lai; Fang ZhengPeng; , "Multilevel converters-a new breed of power converters," IndustryApplicationsConference,1995.ThirtiethIASAnnualMeeting,IAS'95.,Conference Record of the 1995 IEEE , vol.3, no., pp.2348-2356 vol.3, 8-12 Oct1995.

[3] Panagis, P.; Stergiopoulos, F.; Marabeas, P.; Manias, S.; , "Comparison of state of the art multilevel inverters," Power Electronics Specialists Conference, 2008. PESC 2008. IEEE , vol., no., pp.4296- 4301, 15-19 June2008.

[4] Malinowski, M.; Gopakumar, K.; Rodriguez, J.; Pérez, M.A.; , "A Survey on Cascaded Multilevel Inverters," Industrial Electronics, IEEE Transactions on , vol.57, no.7, pp.2197- 2206, July2010.

[5] Tolbert, L.M.; Fang ZhengPeng; Habetler, T.G.; , "Multilevel converters for large electric drives," Industry Applications, IEEE Transactions on , vol.35, no.1, pp.36-44, Jan/Feb1999.

[6] Fang ZhengPeng; , "A generalized multilevel inverter topology with self-voltage balancing," Industry Applications, IEEE Transactions on , vol.37, no.2, pp.611-618, Mar/Apr2001.

[7] T.A.MeynardandH.Foch,"Multi-levelchoppersforhighvoltageapplications,"inProc.Eur. Conf. Power Electron. Appl., 1992, vol. 2, pp. 45-50.

[8] Liu, Y.; Luo, F.L.; , "Multilevel inverter with the ability of self-voltage balancing," Electric Power Applications, IEE Proceedings - , vol.153, no.1, pp. 105- 115, 1 Jan.2006.

[9] A. Rufer, M. Veenstra, and K. Gopakumar, "Asymmetric Multilevel Converter for High Resolution Voltage Phasor Generation", in Proceedings of the European Power Electronics and Applications Conference (EPE 1999),1999.

Performance Analysis of EV charger with Cuk Converter and ABC Algorithm

[1] Venugopal Dugyala, [2] Thirupathi Allam, [3] T Pavani

[1][2][3] Department of EEE, Kamala Institute of Technology & Science, Singapur, Huzurabad, Karimnagar, Telangana, India

Abstract:

In this paper, an enhanced performance of Electric Vehicle (EV) charger (battery) by adopting Bridge Less (BL) Cuk converter and Artificial Bee Colony (ABC) algorithm is investigated. Minimum numbers of switches are employed in this proposed methodology to charge the battery with optimum cost. Steady state input voltages and currents are obtained even though the EV charger operates with unbalanced load i.e. operated in underload, nominal load, or overload. It maintains constant battery parameters even under unbalance in input supply also. Robustness is achieved by operating BL-Cuk converter with ABC algorithm even with variation of 50% rise or decay in input voltage. Proposed technique reduces the conduction losses in switches and no need of DC link capacitor. Hence, balance voltage appears across capacitor over the conventional EV charging approaches. Fly back converters are introduced to synchronize the AC supply, Cuk converter and EV charger.

Keywords:

EV charger, ABC algorithm, unbalanced load, power quality

1. INTRODUCTION

There is a rapid growth is going on in transportation sector since a decade to fulfil its needs and battery based Electric Vehicles (EVs) are playing a crucial role. EVs are leading over the traditional mechanical-gasoline vehicles because of its numerous advantages [9],[18] such as EVs are ecofriendly, savage of fuel, flexibility to employ GPS, GSM or IoT based smart systems to control the speed of the EV with optimum cost.

In Battery Electric Vehicles (BEVs), the utilisation of AC-DC and DC-DC converters are more significant to charge the battery. The efficient operation of EV is always dependents upon battery. EV charger parameters i.e. battery voltage/current must be maintained constant irrespective of its loaded condition and interruptions of input supply. To get steady state EV charger response, operation of power converters in Continuous-Conduction Mode (CCM) is highly required. This can be achieved by employing proposed ABC algorithm-based BL Cuk converter fed EV.

The design of BEVs have been already presented by various authors by employing different control strategies such as on-board/off-board converter topologies [7], [14], Where in on-board EVs have high power controllability but its cost is more. Off-board based EVs suppress the weight of the vehicle, easy to recharge and efficient. In [20],[12] zero voltage switching based power converters are employed to control the EVs, in this operation the ripple content in output waveforms are more around 45% of THD. This ripple harmonic content has been mitigated by adopting interleaved two phase converters [8], in this obtained power density is less. In [10],[5], diode-based bridge converters are considered to charge the battery, but its dynamic response of the system is sluggish. In [17],[11], single stage and two stage series and parallel operated power converters are used to enhance the performance of EV charger, but they operate at low power factor.

To enhance performance of the EV charger, the modelling of uni-directional DC-DC converter is important. These are available in different configurations such as zeta converter [2], SEPIC converter [6], buck-boost [4], and Cuk converters [1]. In these topologies, Cuk converter provides the continuous output voltages and currents. Hence, in this article bridge less Cuk converter is utilised to get better performance of EV charger. It contains less components, cost is less, and improving power factor and efficiency of the EV charger.

The next sections of this manuscript is summarized as follows, BL Cuk converter and fly back converter fed EV charger configuration is discussed in section 2, proposed ABC control scheme provided in section 3, MATLAB/simulations are illustrated in section 4 and conclusions are given in section5.

2. IISYSTEM CONFIGURATION

The Bridge Less (BL)-Cuk converter and fly back converter based EV charger topologies have been discussed in this section. The modelling and mathematical formulation have been adopted from [13].

BL Cuk Converter

Proposed BL Cuk converter does not have body diodes. Hence, its conduction losses are zero and improvement of efficiency. It is operating in three modes as depicted below.

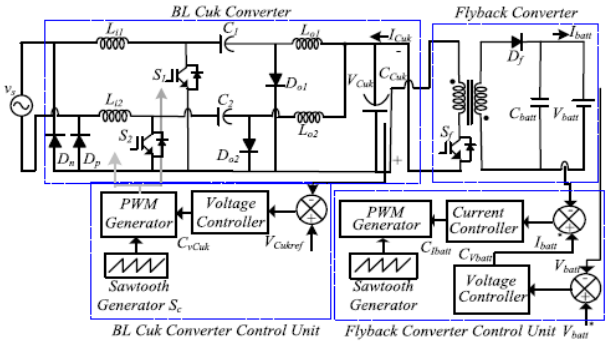

Fig. 1. Structure of BL Cuk converter based EV charger

Mode-I:

In this mode of operation, switch (S1) is fed with positive half cycle (P1) of AC mains, so switch (S1) is triggered. In this, inductor (L01) is charges up to its peak value i.e. Vs/ Li1. Conduction path is depicted as Vs(+ve)- Li1-S1- Diode (Dp)-Vs(-ve) and represented in Fig. 2. The maximum current across switch (S1) is mathematically expressed as

$$I_s = \frac{V_s D T_s}{L_{eq}} \quad (1)$$

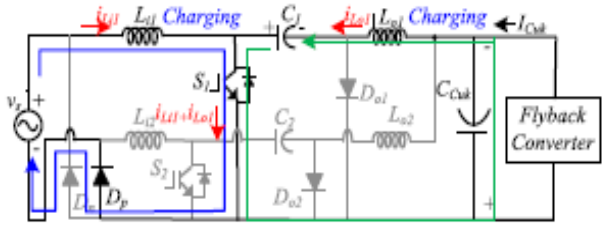

Fig. 2. Configuration BL Cuk converter in Mode-I

Mode-II:

In this mode of operation, switch (S1) is turned and Diode (D01) starts conducting because inductor releases its storage energy. The conduction path of BL Cuk converter in this mode is depicted as Vs(+ve)-Li1-D01- Diode (Dp)-Vs(-ve) and configuration represented in Fig. 3. The current through inductor is expressed as

$$\frac{di_L}{dt} = \frac{V_0}{L_{eq}} \quad (2)$$

Where V_0 is the output voltage appear across Cuk converter. The off-time period is expressed as (T_{off})

$$T_{off} = \frac{V_s T_{on}}{V_o} \quad (3)$$

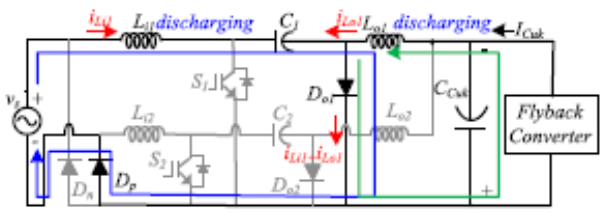

Fig. 3. Configuration BL Cuk converter in Mode-II

Mode-III:

This mode is configured the Dis-Continuous Mode (DCM) operation of BL Cuk converter. In this mode, current stored in inductor in mode-I is same as current released by the inductor in mode-II, hence no current flows in the inductor in this time period. Inductor current zero causes the output voltage across output diode (D01) is zero. The operation of BL-Cuk converter in DCM mode is configured in Fig. 4. Inductor needs new current settings to conduct from mode-III to mode-I and switch (S1) is to be triggered.

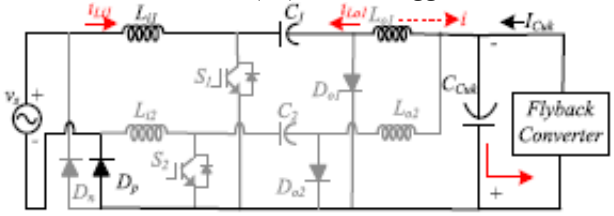

Fig. 4. Configuration BL Cuk converter in Mode-III

Fly back converter

To synchronize the BL Cuk converter and EV charger, fly back converter plays a vital role[3],[14]. To match input and output quantities, fly back converters composed of a linear transformer (LT). Based on BL Cuk converter operation, fly back converter operates in three modes.

In mode-I, S1 is turn-on and magnetising inductor (Lmf) is charged to its peak value. The magnitude of current in switch (Sf) is expressed as

$$I_{sf} = \frac{V_0}{L_f}(t_1 - t_2) + I_{Lf}(0) \quad (4)$$

The maximum current across switch (Sf) is

$$I_{sfm} = \frac{V_0 D}{L_f f_s} + I_{Lf}(0) \quad (5)$$

where fs is the switching frequency fs = 1/Ts

In mode-II, S1 is turn-off and inductor (Lmf) discharges and releases the energy. The current through switch (Sf) is zero [15],[16]. So, it acts as open circuit, which means switch (Sf) is turned off. In this operation

$$I_{sf} = 0 \quad (6)$$

The current through inductor (Lmf) is expressed as

$$I_{Lmf} = \frac{V_{batt}}{L_f}(t_3 - t_2) + I_{sf} = \frac{V_0}{L_f}(t_1 - t_2) + I_{Lf}(0) \quad (7)$$

where Vbatt is output voltage of the charger.

In mode-III, it is DCM mode operation switch (Sf) is still in off position and there no release energy from inductor (Lmf) so output current is zero.

$$I_{sf} = I_0 = 0 \quad (8)$$

In this mode battery does not charge, battery always charge in CCM mode of operation only.

3. DESIGN OF PROPOSED CUK CONVERTER AND ABC ALGORITHM

In modern electrical industries almost 90-95% industries are involved with PI controllers to operate power converter switches in efficient manner. It is a challenge to all the engineers to extract PI parameters exactly and to improve the dynamic performance. In conventional control methods such as Genetic Algorithm (GA), Relative GA (RGA), Particle Swarm Optimization (PSO), etc., an error is considered as an objective function in terms of PI controller values. The PI controller parameters are then computed such that the objective function is minimized. These

approaches provide best tracking response but speed of recovery response with any disturbances is low. Such limitation may be overcome by expert control algorithms.

ABC algorithm is a hybrid expert-based control approach; this approach enhances the closed loop performance. This is done by adopting an intelligent system to track optimum PI values; it prohibits good supervisory control regulatory response, disturbance rejection and robust performance of the system.

In this ABC control approach, to calculate PI gain parameters, artificial honeybees considered are employee bee, onlooker bee and scout bee. In this, error is predicted/ estimated in very advance and PI gain values are varied. The dynamic error of the network is taken as function of food source and fitness of the bees is the solution to the source. This algorithm needs a data of initialization of number of parameters, maximum/minimum number of cycles and colony dimensions. Initialization of high population size is better to track optimum PI values. Fitness parameters are varied based on the error. It is expressed as

$$\text{Fitness} = \sum_{k=0}^{n} e^2(t) \quad (9)$$

Where e (t) is the dynamic error of the system, the proposed ABC algorithm flow chart is shown in Fig. 5.

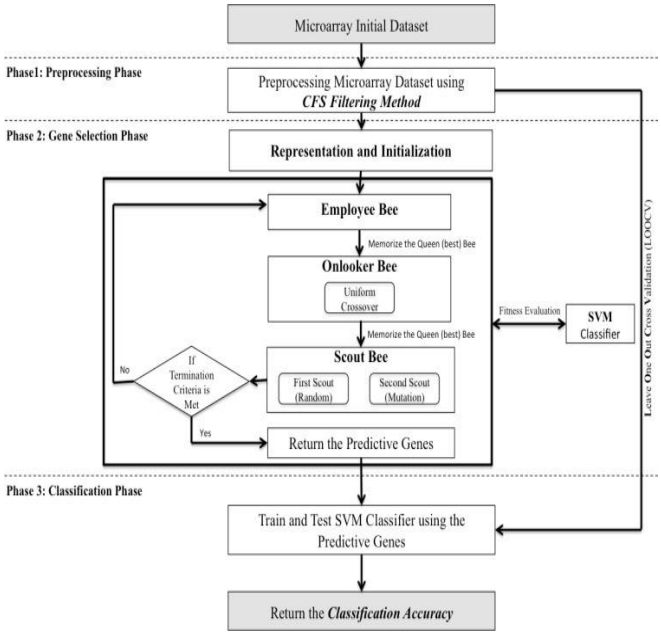

Fig. 5. Proposed ABC flow chart

4. SIMULATION RESULTS AND ANALYSIS

The Simulink model of BL Cuk converter EV charger is shown in Fig. 6.

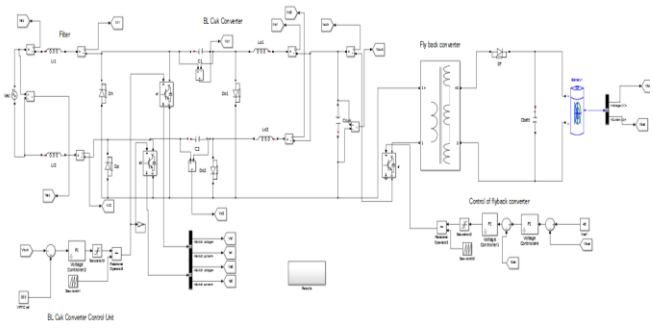

Fig. 6. Simulink model of EV charger

Performance of EV charger with balanced input

The enhanced performance parameters such supply voltage (Vs), current (Is) and battery voltage (Vbat) and current (Ibat) is shown in Fig. 7.These output results are obtained, if the BL Cuk converter is operated under steady state Continuous Conduction Mode (CCM). Observe that battery is constant charging at around 45Vand 8 A.

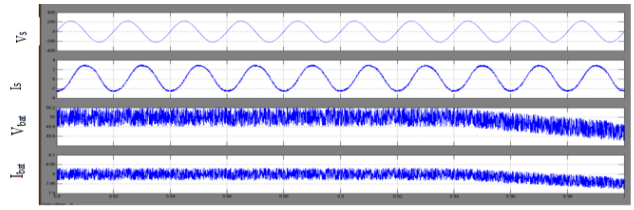

Fig. 7. EV Charger supply and battery parameters

The constant voltage of 277.5 V appears across at DC link and is shown in Fig. 8. Voltage is regulated as constant and corrected power factor hence enhanced performance of EV charger with proposed ABC control technique.

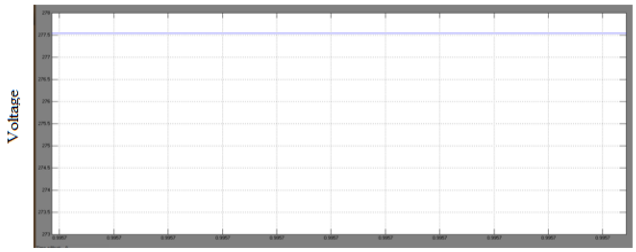

Fig. 8. Voltage at DC Link

The switching quantities, switching voltages (V_{s1}, V_{S2}), currents (I_{s1}, I_{S2}) are described in Fig. 9. There is negative drop in voltage and current waveforms so there is no conduction loss in the proposed network.

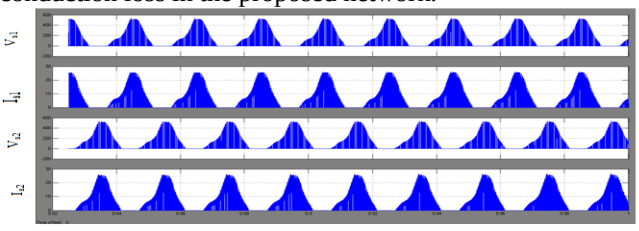

Fig. 9. output waveforms of switching parameters at different zero crossing

The current in inductor at different zero crossing i.e. 24A is shown in Fig. 10. From the waveform, it is evident that there is no production of circulating currents in the proposed BL Cuk converter topology.

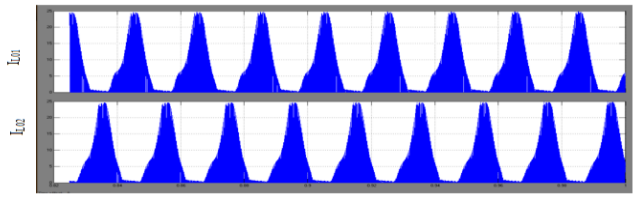

Fig. 10. Output waveform of inductor current at different zero crossing switching action

The output voltages of capacitors Vc1, Vc2 and currents across inductors IL1 and IL2 at different zero cross switching is shown in Fig. 11. It is shown that there is no return in inductor to negative cycle means corrects the PF.

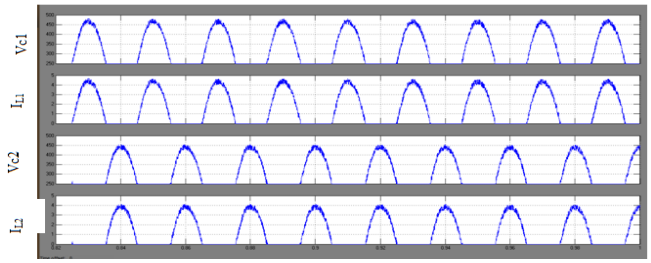

Fig. 11. Voltage across capacitor and current in inductor

Performance of EV charger with unbalanced input

In this condition a wide range of unbalanced line voltage is fed to the EV charger. This is condition is examined for two scenarios. In first scenario, rise in line voltage transient is created in at t=0.4 sec, initially supply voltage is 110V at t = 0s to t = 0.4s, at t = 0.4s rapidly the line voltage is increased to 220 V then the corresponding supply current is varied that is shown in Fig. 12. Even also there is no alteration, fluctuations in battery voltage and battery currents are shown in Fig. 13 and Fig. 14. Proposed ABC control technique produces the robustness and tracks the battery voltage and current is constant.

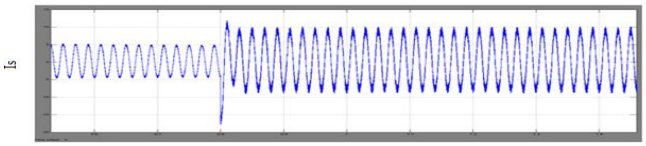

Fig. 12. Transient variation of input current waveform

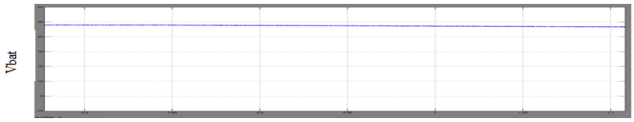

Fig. 13. Battery Voltage

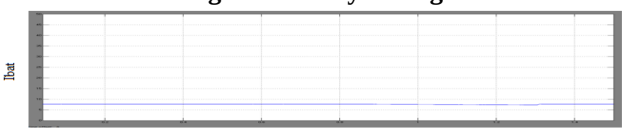

Fig. 14. Battery current

In next scenario, dip in line voltage is created at t=0.4 sec, initially consider the supply voltage is 220V at t=0s to t=0.4, at t=0.4s suddenly the voltage is suppressed to 110 V then corresponding supply current is reduces that is shown in Fig. 15. Even though there is no alteration, fluctuations in battery voltage and battery currents are shown in Fig. 16 and Fig. 17. Proposed ABC control technique prohibits the robustness to tracks the battery voltage and current is constant.

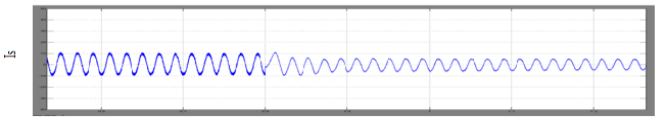

Fig. 15. Transient variation of input current waveform

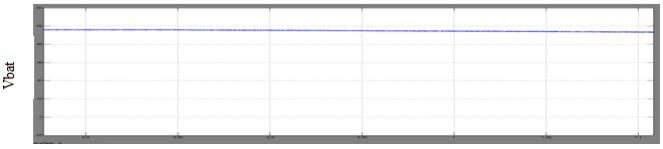

Fig. 16. Battery Voltage

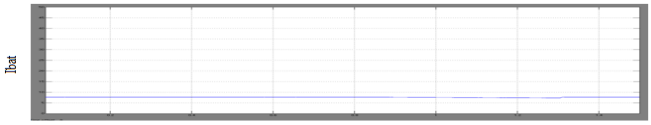

Fig. 17. Battery current

From the above discussion it is summarized as even a wide variation in supply parameter due to any abnormal conditions there is no variation in battery charging quantities means. The proposed ABC control technique-based BL Cuk converter enhance the PQ.

Performance of EV charger with variable loads

The load variation on EV charger how the supply quantities are suffered to reach the load demand is presented here. In this, load variation on EV is composed as underload, nominal load, and overload.

Underload:

In this, load is suddenly removed on the EV the output voltages and current are varied that is shown in Fig.18. As decay in load the input current offers from supply terminals are suppressed as shown in Fig.18. From the waveforms it is observes that supply voltage is mismatch with the supply current, so it leads to poor PF, voltage regulation and sluggish the overall performance of the system.

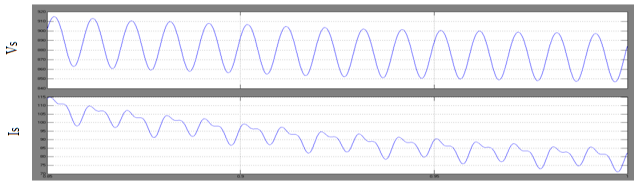

Fig. 18. Variation of input Voltage and current in under load

The non-sinusoidal current harmonic current and voltages are creating at source side its harmonic content (THD) is obtained as 4.06% is shown in THD plot in Fig.19.

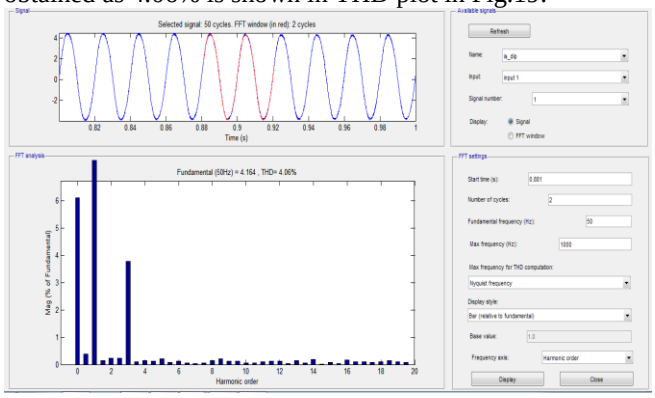

Fig. 19. THD plot

Nominal load:

In this rated voltage is applied on the EV so there is no variation in input voltages and currents in source side. It improves the PF of the system and overall dynamic response of the system. The variation of input parameters at nominal load is shown in Fig. 20.

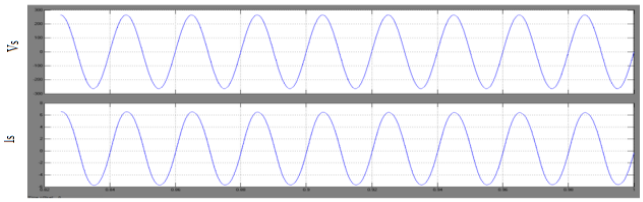

Fig. 20. Variation of input Voltage and current in under load

By operating EV at rated load obtained almost sinusoidal voltages and currents at source side is almost steady state. Its harmonic content (THD) is obtained as 2.33% is shown in THD plot in Fig. 21.

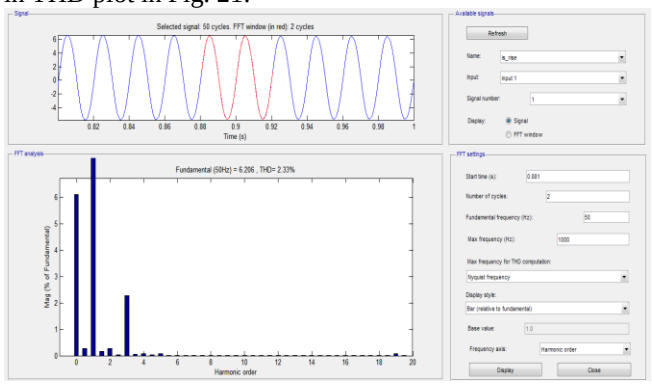

Fig. 21. THD plot

Overload:

In this load is suddenly inserted on EV the output voltages and current variation is shown in Fig. 22. As increment in the load, input current from main terminals are increases that is shown in Fig. 22. From the waveforms it is observes that supply voltage is mismatch with the supply current, so it leads to poor PF, voltage regulation and sluggish the overall performance of the system.

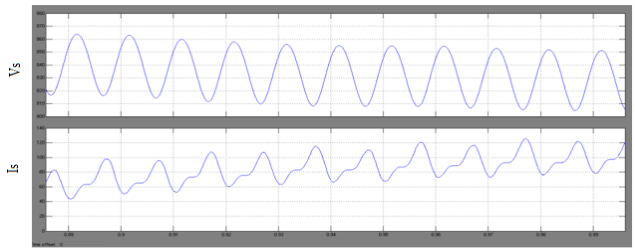

Fig. 22. Variation of input Voltage and current in overload

The non-sinusoidal harmonic current and voltages are created at source side its harmonic content (THD) is obtained as 3.70% is shown in THD plot in Fig. 23.

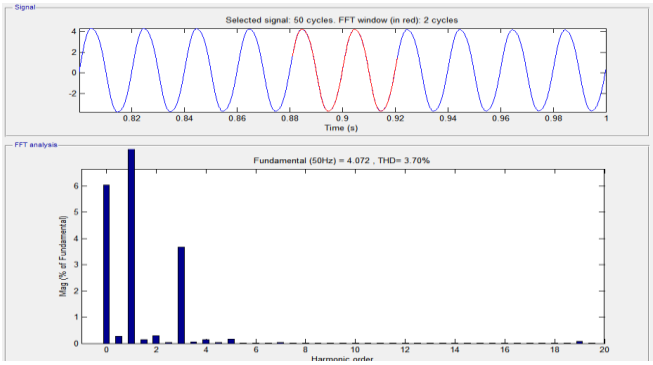

Fig. 23. THD Plot

The summary is EV is operates at under load, overload or at rated load almost constant performance of EV charging is obtains. At nominal load, obtained less THD value compared to underload and overload scenarios.

5. CONCLUSION

Enhance PQ of EV charger with BL Cuk converter and ABC algorithm is discussed in this paper. Obtained simulation results for different conditions of EV charger such as performance EV charger with balanced input, performance of EV charger with unbalanced input, performance of EV charger with unbalanced load i.e. under load, rated load and over load and proven in each condition EV charger parameters prohibits steady state output. Even EV charger is examined for variation in source side quantities or variation on load side parameters above or below of 50% obtained constant battery parameters and enhance the PQ. Improved PF and robustness also achieved in output waveforms with proposed ABC based BL Cuk converter fed EV charger.

REFERENCE

[1] A. A. Fardoun, E. H. Ismail, A. J. Sabzali, and M. A. Al-Saffar, “New efficient bridgeless Cuk rectifiers for

PFC applications," IEEE Trans. Power Electron., vol. 27, no. 7, pp. 3292–3301, Jul. 2012.

[2] A. Jha and B. Singh, "Bridgeless zeta PFC converter for low voltage high current LED driver," in Proc. IEEE CERA, 2017, pp. 539–544

[3] A.V.V. Sudhakar, D. Rajababu, B. Sathyavani, "Analysis of the Power Losses in Both DC Side and AC Side Cascaded Converters", International Journal of Recent Technology and Engineering (IJRTE), ISSN: 2277-3878,Volume-8, Issue- 1C2, May 2019, pp. 897-899.

[4] B. Zhao, A. Abramovitz, and K. Smedley, "Family of bridgeless buckboost PFC rectifiers," IEEE Trans. Power Electron., vol. 30, no. 12, pp. 6524–6527, Dec. 2015

[5] C. Li and D. Xu, "Family of enhanced ZCS single-stage single-phase isolated AC–DCconverter for high-power high-voltage DC supply," IEEE Trans. Ind. Electron., vol. 64, no. 5, pp. 3629–3639, May 2017.

[6] D. S. L. Simonetti, J. Sebastian, F. S. dos Reis, and J. Uceda, "Design criteria for SEPIC and Cuk converters as power factor preregulators in discontinuous conduction mode," in Proc. Int. Conf. Ind. Electron., Control, Instrum., Autom., 1992, vol. 1, pp. 283–288.

[7] F. Musavi, M. Edington, W. Eberle, and W. G. Dunford, "Evaluation and efficiency com- parison of frontend AC-DC plug-in hybrid charger topologies," IEEE Trans. Smart Grid, vol. 3, no. 1, pp. 413–421, Mar. 2012.

[8] H. Choi, "Interleaved boundary conduction mode (BCM) buck power factor correction (PFC) converter," IEEE Trans. Power Electron., vol. 28, no. 6, pp. 2629–2634, Jun. 2013.

[9] Kuperman, U. Levy, J. Goren, A. Zafransky, and A. Savernin, "Battery charger for electric vehicle traction battery switch station," IEEE Trans. Ind. Electron., vol. 60, no. 12, pp. 5391–5399, Dec. 2013.

[10] Limits for Harmonics Current Emissions (Equipment current ≤ 16Aper Phase), International standards IEC 61000-3-2, 2000.

[11] L. Petersen and M. Andersen, "Two-stage power factor corrected power supplies: The low component-stress approach," in Proc. IEEE Appl. Power Electron. Conf., 2002, vol. 2, pp. 1195–1201.

[12] M. Yilmaz and P. T. Krein, "Review of battery charger topologies, charging power levels, and infrastructure for plug-in electric and hybrid vehicles," IEEE Trans. Power Electron., vol. 28, no. 5, pp. 2151–2169, May 2013.

[13] Radha Kushwaha, and BhimSinghA Power Quality Improved EV Charger With Bridgeless Cuk Converter, IEEE Transactions on Industry Applications, Vol. 55, No. 5, September/October 2019, pp. 5190-5203.

[14] Rajababu D. and Raghu Ram K., "Load current observer and adaptive voltage controller for standalone wind energy system with linear and non-linear loads", International Journal of Engineering and Advanced Technology, vol. 9, no. 1, 2019, pp. 5491-5496.

[15] Rajababu D. and Raghu Ram K., "Voltage control of isolated wind energy conversion system using adaptive voltage controller for non-linear loads", International Journal of Recent Technology and Engineering, vol. 8, no. 3, 2019, pp. 3214-3219.

[16] Rajababu D. and Raghu Ram K., "Voltage control strategy for three-phase inverter connected standalone wind energy conversion systems", International Journal of Innovative Technology and Exploring Engineering, vol. 8, no. 11, 2019, pp. 2164-2168.

[17] S. Chen, Z. R. Li, and C. Chen, "Analysis and design of single-stage AC/DC LLCresonant converter," IEEE Trans. Ind. Electron., vol. 59, no. 3, pp. 1538–1544, Mar. 2012

[18] S. G. Li, S. M. Sharkh, F. C.Walsh, and C. N. Zhang, "Energy and battery management of a plug-in series hybrid electric vehicle using fuzzy logic," IEEE Trans. Veh. Technol., vol. 60, no. 8, pp. 3571–3585, Oct. 2011.

[19] S. S. Williamson, A. K. Rathore, and F. Musavi, "Industrial electronics for electric transportation: Current state-of-the-art and future challenges," IEEE Trans. Ind. Electron., vol. 62, no. 5, pp. 3021–3032, May 2015.

[20] Y. Hsieh, T. Hsueh, and H. Yen, "An interleaved boost converter with zero-voltage transition," IEEE Trans. Power Electron., vol. 24, no. 4, pp. 973–978, Apr. 2009

A Polytomous Item Response Analysis of Job Stress Scale-Short Version by Using Partial Credit Model

[1] Pooja Patidar, [2] Dr. Sandeep Arya, [3] Dr. Abhishek Shukla

[1] Research Scholar, Jaypee University of Engineering & Technology, Guna, India
[2][3] Jaypee University of Engineering & Technology, Guna, India

Abstract:

The purpose of this study was to perform an item response theory (IRT) analysis for evaluation of job stress measurement scale short version. The sample consisted of 400 retail employees from India. Partial credit model for five ordered categories was applied using construct map. Results showed that the Job stress scale items had good discrimination, threshold parameters and high item information values. This study suggested that some items showed irregular ICC patterns, can have the scope of further improvement of Job stress scale with desirable psychometric properties.

Keywords:

Job Stress, Item response theory, Item characteristic curve, Polytomous response category, Role Stress

1. INTRODUCTION

Job stress is defined as the harmful physical and emotional responses that occur when job requirements do not match the employees capabilities, resources, and needs (National Institute of Occupational Safety and Health 1999). The 21st century is a time of globalization, the revolution of information, and speed (Cascio, 2001). Change is only a factor appears to be constant in the organization (Mossholder, Settoon, Armenakis & Harris, 2000). In this rapidly changing environment, characterized by intensified competition and escalating demands for flexibility and adjustment, organizations have taken to organizational activities such as outsourcing, downsizing, and mergers in order to adapt to the new situation (Hellgren and Sverke, 2003). Job stress is being created in the organization due to changes in the global economy. Job stress among employees are not a common phenomenon. There are many studies referred to the job stress and their consequences. Stress can evoke the negative emotional feelings like fear, frustration, sadness, anger etc. (Cavanagh,1988) of Job stress exists stressors such as workload, working conditions and expectation from management cause strain (Beehr & Glazer, 2001) and can lead to poor health of employees. Even, it was found that job stress increases with reference to ethical ideology (Shukla & Srivastava, 2017)

The organizational stress framework includes sources of work stress, such as job factors, role conflict, role ambiguity, work overload, and expectations. The demographic variables such as age, sex, occupation, health status, education, and social support also can influence it (Matteson & Ivancevich 1989). Men and women experience many of the same stressors (Desmarais, 2005). Work stress studies in India have been conducted on various groups such as teachers (Aggarwal ,1972; Negi ,1974; Wadhwa ,1977; Kulsum ,1985; Dixit ,1986; Padmanabhaiah ,1986; Bajaj, N.,1988, Malik ,1996; Kumar ,2001), banking sector (Bhatnagar and Bose, 1985), retail sector (Shukla & Srivastava, 2016).

The Job stress measurement scale (Pareek,1981) has been used in numerous studies. These include in the area of Information Technology (Sunetra Bhattacharya and Jayanti Basu,2007), schools (K. Dubat, S. Punia and Rashmi Goyal,2007), Nursing (Geetika Tankha,2006), Supervisory personnels (Srivastava,1991). These all studies used the original full form of job stress scale. However, there is a concern related to the missing data. Whereas missing data for particular item is a problem in measuring the overall stress. When several item comprises a scale, the missing data is only a minor problem, typically handled by inserting the mean of other item reponses. The original role stress scale comprises 50 items measuring 10 different dimensions of job stress. Although, the long version of scale consists of several issues for example, respondents felt monotonous whilefilling the questionnaire, due to interest lost by respondents the issue comes with accuracy of the results. Therefore, it is always encouraged to use shorter version of questionnaire. With shorter scales, the advantage is of not consisting missing data and it is easy for respondents to give quick response with high accuracy. We designed modified Job stress scale comprises 20 items with the highest mean total correlation to measure global job stress with ten role dimensions. It is adopted from the full form of job stress scale (Pareek,1981).

The study represents the most thorough psychometric investigation of the job stress scale till date and also the first IRT modeling effort in the field of job stress. IRT offers some advantages over classical methods for analyzing job

 ISBN: 978-93-90214-20-4

stress in the organization. In the field of job stress, the application of advanced psychometric methods like IRT is very rare which gives us a cause of concern. IRT can provide information about measurement precision across the range of a latent trait at both the item and test level rather than providing only a single reliability estimate for all participants. This can assist greatly in the identification of items that may contribute little to measurement precision. IRT models explicitly map the relations between person and item parameters on the same latent trait scale. IRT models can also facilitate important psychometric applications, such as examining differential item and test functioning across groups, and computerized adaptive testing (see Reise &Henson, 2003)

2. THEORETICAL BACKGROUND

2.1 Item Response Theory

Item response theory is a probabilistic model that attempts to explain the response of a person to an item (Hambleton, Swaminathan, & Rogers, 1991; Lord, 1980). Item response theory (IRT) provides a good approach in scale measurement (Bjorner et al., 1998; Raczek et al., 1998). Item Response Theory (IRT) is a psychometric theory that represents mathematical functions which relate respondent and item parameters to the probability of the responses. IRT can provide information about measurement scale precision across the range of a latent trait of the respondent at the item level as well as a test level rather than providing only a single reliability estimate for all participants. IRT can assist in the identification of items that may contribute little to measurement precision. IRT model exclusively map relations between item and person on the same scale. In IRT, the underlying latent trait is commonly designated by the Greek letter theta (θ) and is most often scaled to have a mean of zero and standard deviation of one. Item characteristic curve (ICC) represents the relation between the response to an item and latent trait (θ). The model shown in Fig.1 is called a partial credit model. According to response criterion the IRT models are categorized in two types i.e. dichotomous and polytomous. Items with only two alternative responses are called dichotomous and response alternatives with more than are called polytomous. The psychometric assessment scales are generally polytomous scored. In dichotomous reponse the probability of a correct response for the respondent can be described by 3 parameter logistic (3PL) IRT model, where the items are multiple choice.

$$p_i(\theta) = c_i + \frac{1 - c_i}{1 + e^{-a_i(\theta - b_i)}}$$

Where θ indicates that the person's abilities are modeled as a sample from a normal distribution for the purpose of estimating the item parameters. After the item parameters have been estimated, the abilities of individual people are estimated for reporting purposes , b_i, and c_i are the item parameters which represents discrimination level, difficulty level and pseudo guessing respectively.

In polytomous response, the probability of respondent correct response can be described by Partial credit model (Masters, 1982) or generalized partial credit model (Muraki, 1992), graded response model (Samejima, 1969, 1972).
The partial credit model equation,

$$P_{ix}(\theta) = \frac{\exp \sum_{k=0}^{x} (D(\theta - b_{ik}))}{\sum_{h}^{m_i} \exp \sum_{k=0}^{h} (D(\theta - b_{ik}))}$$, x= 1, 2, …, mi.

where *Pix(θ)* refer to the probability of an examinee at latent ability θ scoring x.The function of equation is also known as score category response function (SCRF).

3. RESEARCH METHODOLOGY

3.1 Participants

The sample consisted of 400 retail employees (284 males, 116 females), ranging in age from 20 to 60 years and other demographic description as shown in sample descriptive statistics (table 1) . The participants were obtained from retail industry from Indore located in Madhya Pradesh, India through non-probability purposive sampling (Cohen, Manion, & Morrison, 2000). All respondents were treated in accordance with the "Ethical principles of Psychologists and Code of Conduct" (American Psychological Association, 2002).

3.2 Instrument

Occupational Role Stress short version, adopted from original job stress scale by Pareek (1981) was used to measure the occupational stress of the respondents. We can use job stress word interchangeable from role stress. The full form of occupational role stress scale was used to generate a 20-item scale which was designed to measure the role stress of the individuals in the organization. The modifications for local consideration were made after interviewing a total of 100 employees of retail sector of Madhya Pradesh before the final designing of questionnaire. We accepted only those items which indicated good internal consistency i.e. alpha >0.65 (George, D., & Mallery, P. ,2003). Role stress scale short form consist of 20 items, in which it measure 10 type of stressors. Each dimension is measured by 2 items of job stress scale. This scale measures the stress among employees in workplace. The response scale has been five point Likert scale ranging from one (strongly disagree) to five (strongly agree). The reliability index ascertained by the Cronbachs alpha - coefficient for the modified scale as a whole were found to be 0.89 also shows a reliable scale. Further, to ensure the content validity of the modefied scale, the view points of experts in the area and from retail sector regarding the modified role stress scale were taken which ensured about its face validity.

3.3 Factor Analytic Approach

In order to identify the different role dimensions contributing to the role stress of employees in retail Industry. The Factor analysis statistical technique is used for examining the relationships among various interrelated variables. The scale was analyzed using principle

component analysis with varimax rotation with the help of SPSS package version 21.0 response category 1, 2,3, 4, 5 have been assigned to all items. Initially, tests for adequacy of the data for the application of factor analysis (Stewart, 1981) were conducted. It was found that the value of the Kaiser-Meyer-Okin (KMO) measure of sampling adequacy statistic was 0.724, which is quite high. Moreover, the correlation matrix revealed that there was enough correlation for the application of factor analysis. Besides, the Bartlett's Test of Sphericity value was found to be 5534.313 which was also highly significant ($p<0.001$).

The ten dimesions are adopted from original role stress scale (Pareek,1981), the statement labels, and the respective factor loadings are summarized in table 1. The relationship between the original variable and its factor is represented by the factor loading.

3.4 Data Analysis

The limitations of classical test methods for studying issues relevant to Job stress scale make it crucial to determine whether existing scale is adequate from an IRT perspective. Specifically, it is necessary to study whether the existing scale of Job stress has a high and evenly distributed degree of measurement precision. As the job stress scale has a polytomous response format, We have used Partial credit IRT model (Masters, 1982). The partial credit model (Masters, 1992) is an extension of the Rasch model to polytomous items. Thus, item slopes are assumed to be equal across items. The partial credit model represents the probability of a person responding in category x as a function of the difference between their trait level and a category intersection parameter. The graded response model (GRM) (Samejima, 1969) is based on the cumulative log-odds principle, whereas the generalized partial credit model (GPCM) (Muraki, 1992) is based on the adjacent log-odds principle. In the graded response model, Item discrimination parameter does not depend on the number of response categories. However, the cumulative category response functions of the models that belong to the heterogeneous case are not identical. Therefore, it also makes sense that we obtained the result that indicates the a-parameter of the PCM depends on the number of response categories.

A partial credit model assessment of unidimentionallityfor five ordered response categories was applied by (Masters, 1982) using Construct Map (Wilson, 2005). Construct map generates item parameter, standard error, mean square and t statistic along with the item. The maximum number of EM iterations is set to be 2000. The t-statistic is a transformation of the mean square into a standard normal distribution. Values above 2.0 (or below -2.0) are generally considered significant. We used Gaussian quadrature method of integration. There are 15 quadrature nodes that are used during E-M algorithm. The logits range is used for item estimation during EM algorithm which vary from -6 to 6. The EM Convergence criterion is set for 0.5.

4. RESULTS

Table 1 Descriptive Statistics and scale dimentionality

Variable	Job Stress
N	400
M	63.09
SD	3.96
Cronbach's Alpha	0.89
Skewness	0.089
Kurtosis	0.067

Table 1 presents the statistics relevant to scale dimentionality. The sample size, mean , standard deviation, Cronbach alpha, skewness and kutosis for Job stress scale for 400 respondents. Cronbach's alpha values were high. Skewness and kurtosis absolute values of 0 to 2, and 0 to 7, respectively, can be taken as demonstrating sufficient univariate normality (Curran et at,1996).

4.1 Item Estimates and Fit graph

Partial credit response model was caliberated for job stress scale. This section helps to analyze how well the items are fitting the model. Table 2. Shows the parameter estimates, their standard errors, the outfit (unweighted) and infit (weighted) mean squares and associated t-statistics. Step parameters are displayed according to the measurement model. Table 4 showed item statistics for individual item of job stress scale short version with with ordered response category, ability parameter, step difficulty, thresholds and error.

The Item difficulty parameter estimated for I1 is -0.226 with standard error 0.045. All Item difficulty level seems moderate except item I2 (-0.667) and I4 (-0.510). Table 3 & 4 also revealed that the category threshold values were somewhat skewed toward the negative range of logits. Fig. 1 indicated the infit mean square parameter.The infit mean square for an item is defined as the ratio of the variance of the observed residuals over the variance of the expected residuals. All the item values are close to 1.5 except I2 (1.66). Item I2 shows variance in observed residual to expected residual. Item I2 exhibits higher value of mean square shows less contribution to latent trait.

Item Estimates
(by item)
Item Set: base
Variable: Construct 1

Item difficulties:

item	Estimate	Error	Outfit -Unwghted- MnSq	Outfit -Unwghted- t	Infit -Weighted- MnSq	Infit -Weighted- t
1 I1	-0.226	0.045	1.19	2.5	1.13	1.9
2 I2	-0.667	0.035	1.66	7.8	1.38	5.0
3 I3	0.150	0.046	0.58	-7.0	0.60	-6.7
4 I4	-0.510	0.034	1.19	2.6	1.00	0.0
5 I5	0.474	0.042	1.40	5.1	1.32	4.3
6 I6	0.275	0.041	1.64	7.6	1.52	6.8
7 I7	0.157	0.046	1.55	6.7	1.49	6.4
8 I8	0.025	0.042	1.45	5.7	1.39	5.1
9 I9	-0.073	0.048	0.46	-9.8	0.46	-10.4
10 I10	0.094	0.047	1.53	6.4	1.47	6.1
11 I11	-0.006	0.043	1.30	3.9	1.22	3.1
12 I12	0.235	0.044	1.24	3.2	1.16	2.2
13 I13	0.165	0.044	1.58	7.0	1.29	3.8
14 I14	0.102	0.044	1.58	7.1	1.28	3.6
15 I15	0.027	0.043	1.45	5.6	1.11	1.6
16 I16	0.100	0.043	1.43	5.4	1.17	2.3
17 I17	0.290	0.039	1.07	1.0	0.87	-1.9
18 I18	-0.186	0.043	1.45	5.6	1.07	1.0
19 I19	-0.294	0.043	1.49	6.1	1.18	2.5
20 I20	-0.132		0.75	0.3	0.86	0.5
Average	0.000		1.30	3.6	1.15	1.9

Figure 1 :Item Parameter (Standard error) for Job stress scale-Short version.

According to Adams and Khoo (1996) suggest 0.75 and 1.33 as bounds of acceptable mean score values. Figure 1 and 2 showed that Items I2 (1.66), I3 (0.58), I5 (1.40), I6 (1.64), I7 (1.55), I8 (1.45), I9 (0.46), I10 (1.53), I13 (1.58) and I14 (1.58) showed a higher value from the acceptable mean score values, which depicts that these items are higher in difficulty level as per the sample ability.

Item Estimates
Item Set: base
Variable: Construct 1
Infit Mean Squares

	0.58	0.67	0.75	0.83	0.92	1.00	1.08	1.17	1.25	1.33	1.42	1.5
I1			.			*		.				
I2			.					.	*			
I3		*	.					.				
I4			.			*		.				
I5			.					*.				
I6			.					.				*>
I7			.					.			*	
I8			.					.	*			
I9		<*	.					.				
I10			.					.		*		
I11			.				*	.				
I12			.			*		.				
I13			.					*	.			
I14			.					*	.			
I15			.			*		.				
I16			.				*	.				
I17			.	*				.				
I18			.			*		.				
I19			.				*	.				
I20			.	*				.				

Fig 2 shows a Infit Mean Square graph of all items.

4.2 Item Characteristic Curve

Figure 3 displays the Item characteristic curve for the Job stress scale- short version. These curves indicate the area on the logits (theta) continuum of range -6 to 6, in which the ability and probability of correct response provide the high discrimination among the respondents. The items showed high discrimination across values of the latent trait and that have largely nonoverlapping response option categories. Also Fig 2 showed some irregular ICC for items (I2,I4,I5&I9) which suggested that items are poor.

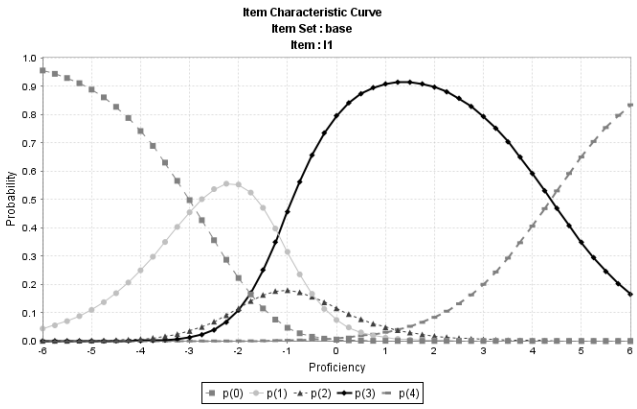

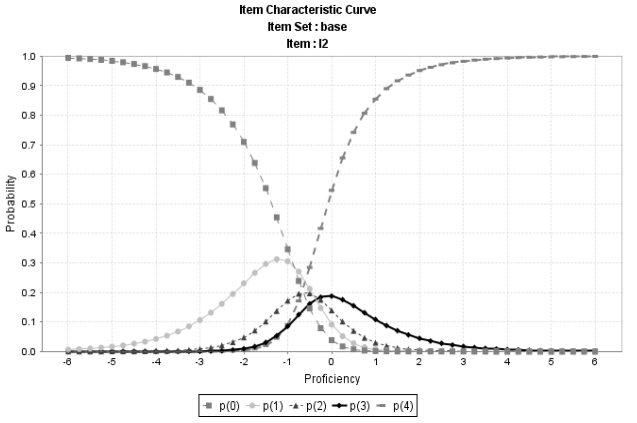

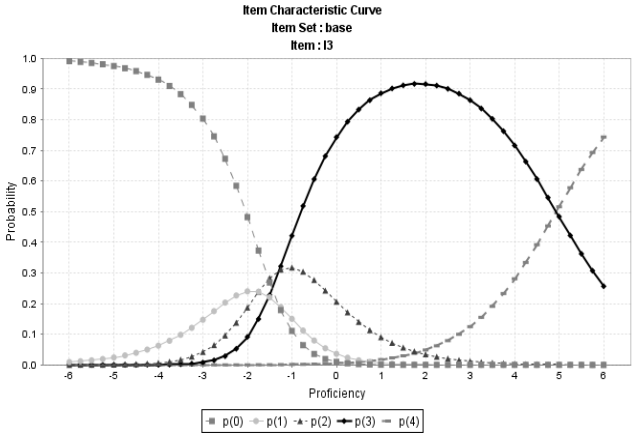

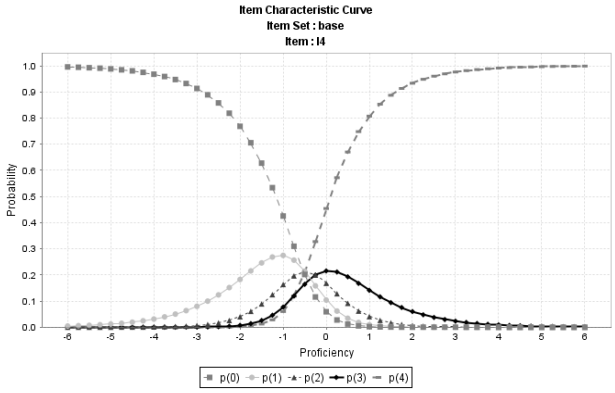

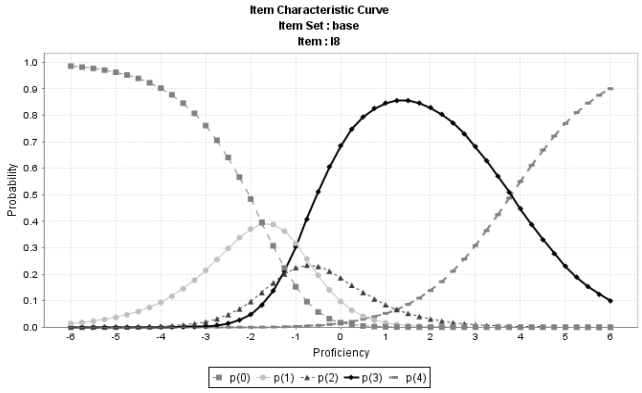

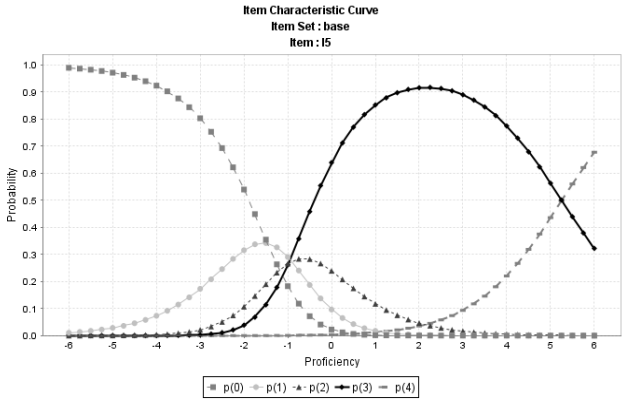

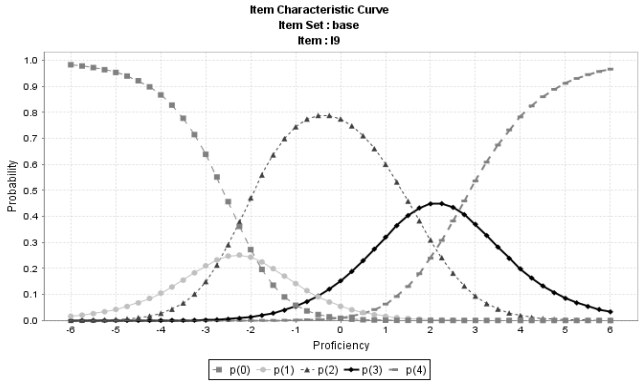

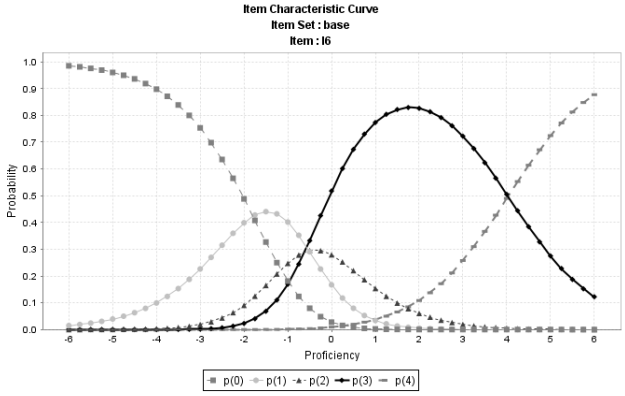

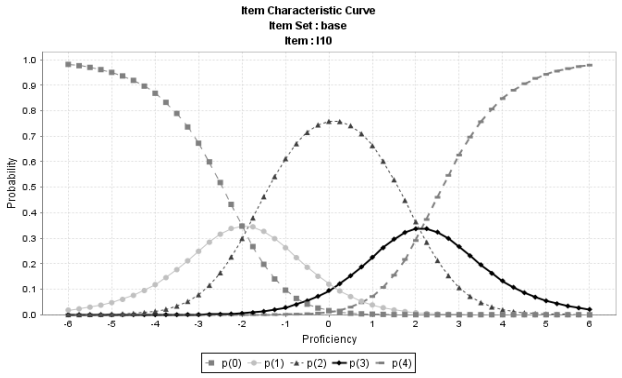

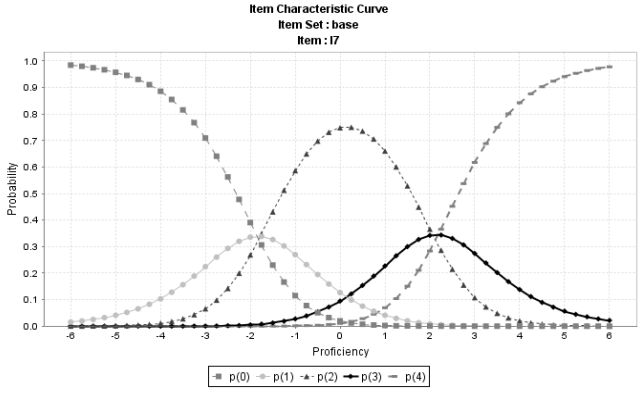

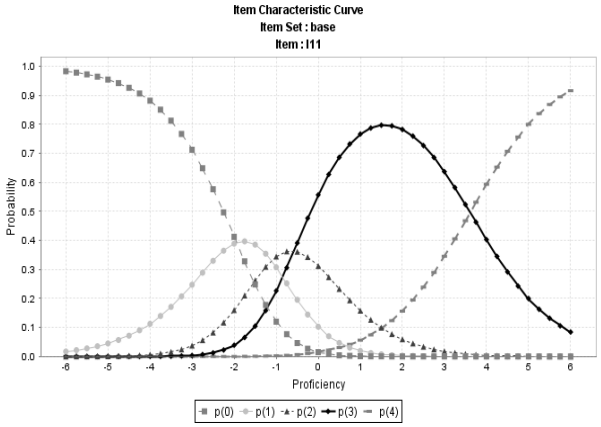

 ISBN: 978-93-90214-20-4

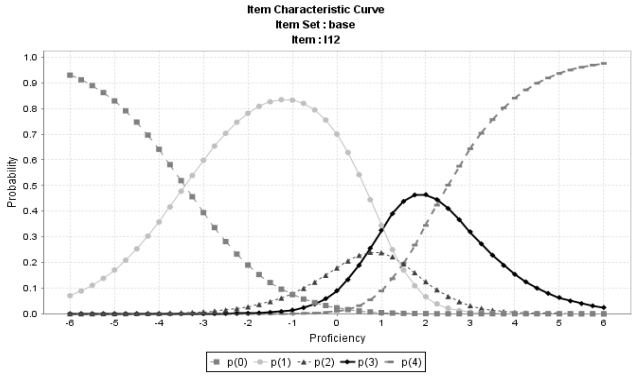

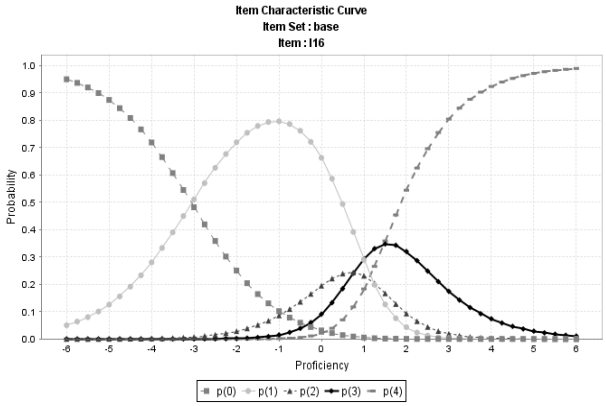

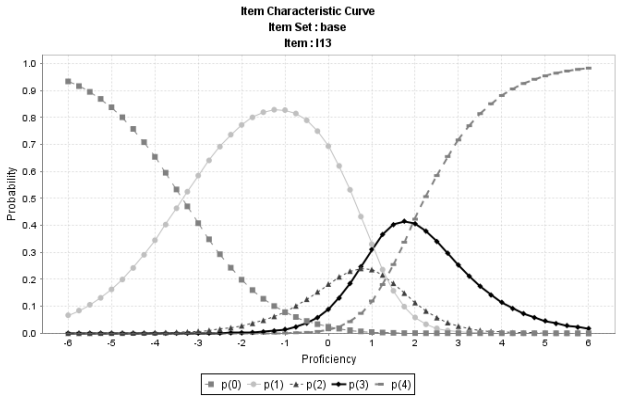

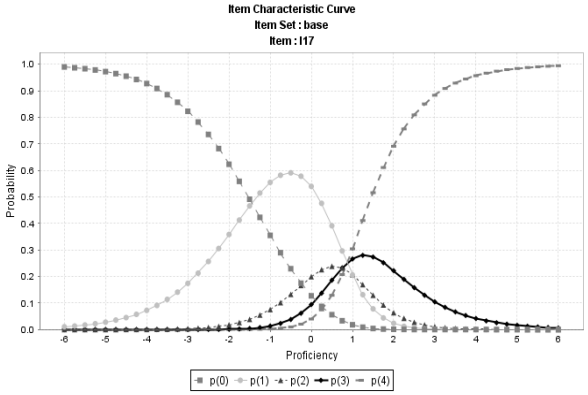

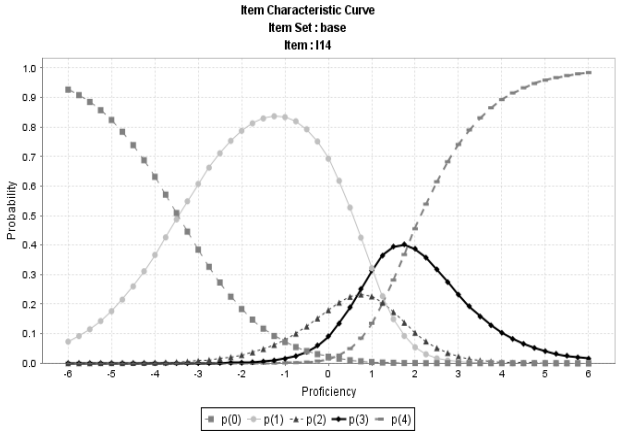

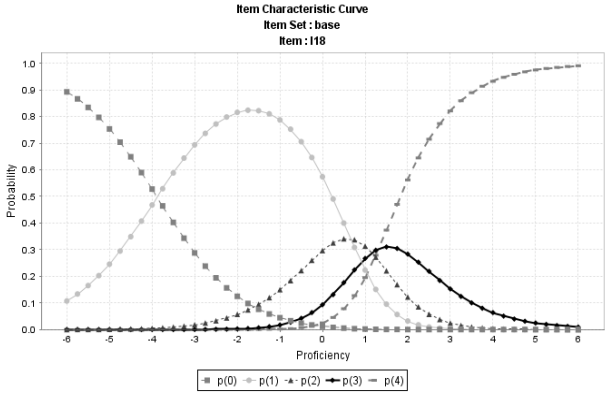

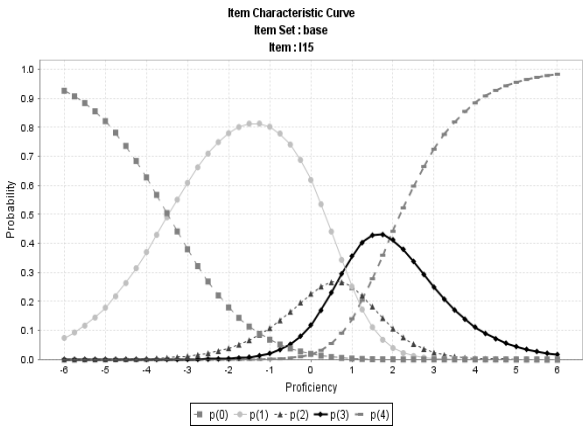

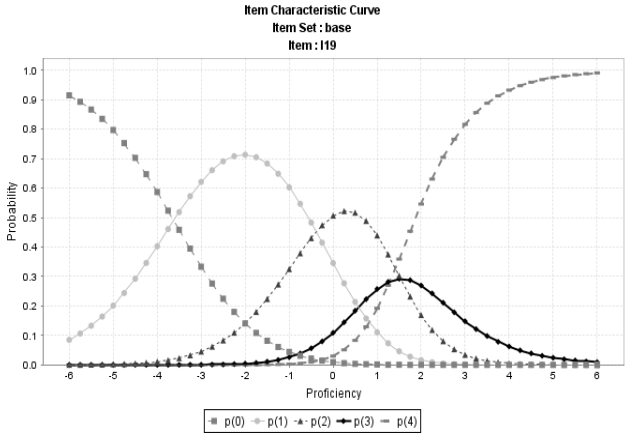

 ISBN: 978-93-90214-20-4

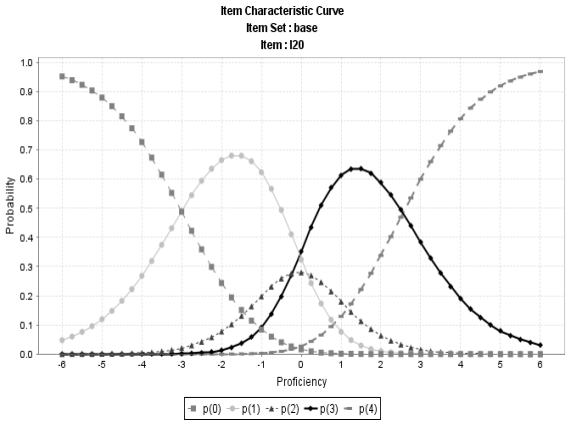

Figure 3. Item response properties for a Twenty-item job stress scale-short version, using the Partial credit model

4.3 Test Information Curve

A test information index computed from the standard error of measurement for a specific proficiency estimate to ascertain the sensitivity of the instrument relative to a respondent's proficiency. A given instrument can be compared by providing more information about respondents at one range of proficiency than at another range. Figure 4 displayed the test information curve, which shows that items of the job stress scale are good at distributing its precision equally across the proficiency region between -1.0 to 1.0. The overall degree of information is high for different respondents.

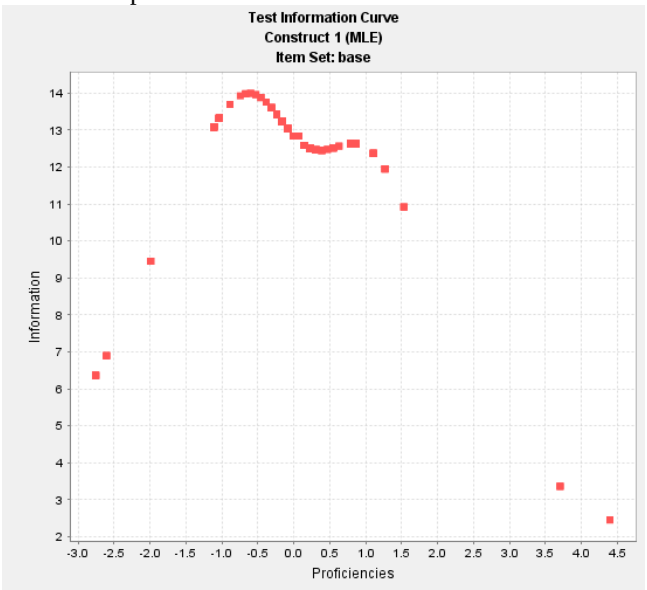

Fig 4:- Test Information Curve

5. DISCUSSION

The purpose of this research was to use IRT to examine the psychometric properties of the Job stress scale short version (Pareek, 1981) across samples of participants. The study investigates the psychometric properties of every item of job stress scale short form by using IRT method. IRT methods can be especially helpful in the context of evaluating items individually and recommend to develop a new scale from an existing scale from which items are not performed among the different demographic sample.

The results of the IRT analysis suggests the job stress has good psychometric properties. Many of the items have high discrimination parameters (Figure 3), indicating they are effective at discriminating individuals across the range of the latent trait. Furthermore, category estimate values (Table 1) were mostly skewed toward the negative range of logits. In other words, the item threshold values were concentrated in a narrow region of the trait range, that is, toward the negative end. The test information curve also suggests that the respondents having high information and distributed its precision between a low range of proficiency.

Despite the encouraging outcomes of the IRT analysis, there are some potential issues that could be addressed in future revisions of the scale. There were some items that had relatively poor psychometric properties. For example, Items 2 ("I'm afraid I'm not learning enough in my present job for taking up higher responsibility"), I4 ("I do not have adequate knowledge to handle the responsibilities in my job"), I5 ("I'm not clear on the scope and responsibilities of my job") and I9 ("I do not get enough resources to be effective in my job") etc., had irregular ICC patterns shows low discrimination parameter values across the entire range of the latent trait. In fig 2 shows the item which is not performed and does not lie in the acceptable range, i.e. 0.33 to 1.75 (Adams and Khoo, 1996).

The Implication of this analysis will be first the improvement of items which are showing low parameter estimation. We have analyzed twenty items of the job stress scale short version , that can be improve and further develop a new short version scale which consist 13 items with good psychometric performance. Seven of the items can be reframed , so that the items difficulty parameter would be appropriate and give high information values. This suggestion would certainly be amenable to future empirical work with the scale.

In gerenal terms, the improvement of the scale will be important according to the sample and Industry. The study converged to show that the job stress yields precise measurement across most of the latent trait range and that 13 items showed good psychometric properties and seven of the items showed poor properties which has to improve for future studies. Overall, the findings of the study suggest clearly that the revised Job stress measurement scale showed fair psychometric properties and for future studies it can be recommended for the rapid assessment of individual differences in the Industry.

REFERENCE

[1] Adams, R. J. & Khoo, S. T. (1996). Quest: The Interactive Test Analysis System. Melbourne: ACER.

[2] Aggarwal, J.C. (1972). A Study of Adjustment Problems and there Related to More effective and

Less Effectives Teachers. New Delhi. Vikas Publisher.

[3] American Psychological Association (2002). Ethical principles of psychologists and codes of conduct. Washington, DC: Author.

[4] Bajaj, N. (1988) "Job involvement in four occupational groups", Journal of Educational Psychology, 42 (12): 263-269.

[5] Beehr, T. A., & Glazer, S. (2001). A cultural perspective of social support in relation to occupational stress. In P. L. Perrewe & D. C. Ganster (Eds.), Research in occupational stress and well being .Volume 1: Exploring theoretical mechanisms and perspectives (pp. 97-142). New York: JAI Press.

[6] Bhatnagar, D., & Bose, K. (1985, October-December). Organisations role stress and branch managers. Prajnam Journal of Social and Management Sciences, XIV (4), 349-360.

[7] Bjorner J., Kreiner S., Ware J., Damsgaard M., Bech P. (1998)Differential item functioning in the Danish translation of the SF-36. Journal of Clinical Epidemiology, 51, 1189–1202, DOI: 10.1016/S0895-4356(98)00111-5.

[8] Cascio WF (2001). Knowledge creation for practical solutions appropriate to a changing world of work. South African Journal of Industrial Psychology. 27(4): 14–16.

[9] Cavanagh, M E (1988) 'What you don't know about stress?' Personnel Journal, July 53-59.

[10] Cohen, L., Manion, L., & Morrison, K. (2000). Research methods in education (5th ed.). NY: RoutledgeFalmer.P.99.

[11] Curran, P. J., West, S. G., & Finch, J. F. (1996). The robustness of test statistics to nonnormality and specification error in confirmatory factor analysis. Psychological Methods, 1, 16–29.

[12] Desmarais, S. & Alksnis, C. (2005). Gender issues. In J. Barling, E. K. Kelloway, & M. R. Frone (Eds). Handbook of work stress. (pp. 455-485). Thousand Oaks, CA: Sage

[13] Dixit, M. (1986) . "A Comparative Study of Job Satisfaction among Primary School Teachers" Survey of Research in Education by M.B. Buch (1983-88), N.C.E.R.T.

[14] Geetika Tankha (2006). A Comparative Study of Role Stress in Government and Private Hospital Nurses. Journal of Health Management April 2006 vol. 8 no. 1 11-22. doi: 10.1177/097206340500800102.

[15] George, D., & Mallery, P. (2003). SPSS for Windows step by step: A simple guide and reference. 11.0 update (4th ed.). Boston: Allyn & Bacon.

[16] Hambleton, R. K., Swaminathan, H., & Rogers, H. J. (1991). Fundamentals of item response theory. Newbury Park, CA: Sage.

[17] Hellgren,J and Sverke,M.(2003)"Does job insecurity impaired well or vice versa? Estimation of cross-lagged effect using latent variable modeling", Journal of Organizational Behavior,24(215).

[18] J. Juliet gladies & Dr. Vijila kennedy(2011).Impact of organizational climate on job stress for women employees in IT sector in India.Asia pacific journal of research in Business Management. Vol 2. ISSN 2229-4104.

[19] K. Dubat, S. Punia and Rashmi Goyal (2007). A Study of Life Stress and Coping Styles among Adolescent Girls. J. Soc. Sci., 14(2): 191-194.

[20] Kulsum, U. (1985). "Job Satisfaction among Teachers Working in Corporation, Government, Private-Aided and Private Unaided Schools", Journal of Educational Psychology, 36(23): 451-459.

[21] Kumar, M. (2001). "A Comparative Study of Adjustment Level of Primary School Teachers in Ambala District", M.Ed. Dissertation, Department of Education, K.U., Kurukshetra.

[22] Lawrence Erlbaum Associates.

[23] Malik, K. (1996). "A Comparative Study of Achievement of B.Ed. male and female pupil teachers in relation to their adjustment and reading interest", M.Ed. Dissertation. Department of Education, M.D.U., Rohtak.

[24] Masters GN (1992). A Rasch model for partial credit scoring. Psychometrika.1992;47:149–174.

[25] Masters, G.N. (1982). A Rasch model for partial credit scoring.Psychometrika,47,149-174.

[26] Matteson, M. T. & Ivancivich, J. M. (1989). Controlling work stress. San Francisco: Jossey-Bass.

[27] Mossholder, KW, Settoon, RP, Armenakis, AA & Harris, SG 2000, 'Emotion during organizational transformations: An interactive model of survivor reactions', Group and Organization Management, 25 (3), 220-243.

[28] Murarki, E.(1992). A generalized partial credit model:Application of EM algorithm. Applied Psychological Measurement,16,159-176.

[29] National Institute for Occupational Safety and Health (NIOSH). 1999. Stress…at Work. Centers for Disease Control and Prevention, U. S. Department of Health and Human Services. Publication no. 99-101, 26 p.

[30] Negi, N.S. (1974). "A Study of the Factors related to Job Satisfaction of Science Teachers in Higher Secondary Schools in Delhi", Unpublished M.Ed. Dissertation, Delhi: Delhi University.

[31] Norkiah Abdul Kadir. (1980). Relation of stress and job satisfaction among teachers. Unpublished dissertation, Universiti Kebangsaan Malaysia and Universiti Putra Malaysia.

[32] Padmanabhaiah, S. (1986). "Job Satisfaction and Teaching Effectiveness of Secondary School Teachers" 4th Survey of Research in Education by M.B. Buch (1983-88), N.C.E.R.T.

[33] Pareek,U. (1981), "Role Stress Scales", Research Report, Indian Institute of Management, Ahmedabad.

[34] Raczek A., Ware J., Bjorner J., Gandek B., Haley S., Aaronson N., Apolone G., Bech P., Brazier J., Bullinger M., Sullivan M. (1998) Comparison of Rasch and summated rating scales constructed from SF-36 physical functioning items in seven countries: results from the IQOLA Project. International Quality of Life Assessment. Journal of Clinical Epidemiology, 51, 1203–1214, DOI: 10.1016/S0895-4356(98)00112-7.

[35] Reise, S. P., & Henson, J. M. (2003). A discussion of modern versus traditional psychometrics as applied to personality assessment scales. Journal of Personality Assessment, 81, 93–103.

[36] Rosli Mat Taib. (1997). Work satisfaction among teachers: Research in two district in Selangor. M.Ed. diss., Universiti Malaya, Kuala Lumpur.

[37] Samejima,F.(1969).Estimation of latent ability using response pattern of graded scores.Psychometrika Monograph Supplement, No17.

[38] Samejima,F.(1972).A general model of free response data.Psychometrika Monograph, No18.

[39] Shukla, A., & Srivastava, R. (2016). Examining the effect of emotional intelligence on socio-demographic variable and job stress among retail employees. Cogent Business & Management, 3(1), 1201905.

[40] Shukla, A., & Srivastava, R. (2017). Influence of ethical ideology on job stress. Asian Journal of Bsiness Ethics, 6(2), 233-254.

[41] Srivastava, A. K(1991). A study of role stress-mental health relationship as moderated by adopted coping strategies. Psychological Studies, Vol 36(3), Nov, 192-197.

[42] Sunetra Bhattacharya and Jayanti Basu (2007). Distress, Wellness and Organizational Role Stress among IT Professionals: Role of Life Events and Coping Resources. Journal of the Indian Academy of Applied Psychology, July 2007, Vol. 33, No.2, 169-178.

[43] Suseela Malakolunthu. (1994). A study of teacher's stress and it's correlates. M.Ed. diss., Universiti Malaya, Kuala Lumpur.

[44] Wadhwa, S. (1977). "A Study of Some Background Factors of Graduate Teachers'Adjustment", 2nd Survey of Research in Education by M.B. Buch (1973-78), Baroda.

[45] Wilson, M. (2005). Constructing measures: An item response modeling approach. Mahwah, NJ:

Voltage Sag and Swell Mitigation in a Transmission Line using DVR for Balanced and Unbalanced Faults

[1] G.Manideep, [2] R.Manvith, [3] T.Teja, [4] J.Venkata sai Pawan Kalyan, [5] Dr.V.Prakash

[1][2][3][4] B.Tech, EEE, Kakatiya Institute of Technology and Science, Warangal, India
[5] Assistant Professor, EEE, Kakatiya Insitute of Technology and Sceince, Warangal, India

Abstract:

This paper gives the detailed description of the modeling and simulation of a Dynamic Voltage Restorer (DVR) for power quality problems like voltage sag and swell based on the technique Sinusoidal Pulse Width Modulation (SPWM). In today's world power quality has become one of the major concerns in the field of electrical engineering. The common problems are voltage Sags and voltage swells, they can result in the failure of equipment at end user. Thus, maintaining voltage quality in the power distribution network is very essential and important. DVR is regarded as one of the most efficient custom power electronics devices used in power system network. The device consists of Voltage Source Inverter (VSC) with a suitable switching circuit to mitigate any sag or swell formed in the power distribution network. Sinusoidal Pulse Width Modulation is the mostly used technique for producing switching pulses to the VSC. The SPWM technique is obtained by using either PI Controller. The DVR is connected in series to the network through an injection transformer. In this work the DVR is modeled and simulated using MATLAB/SIMULINK software. The switching pulse to the DVR is provided from suitable technique and the outputs of different networks are compared. The simulation aims to improve voltage quality by mitigating faults such as Voltage sag and Voltage swell.

Keywords:

Dynamic Voltage Regulator (DVR), Voltage sag, Voltage swell, Voltage Source Converter (VSC), PI Controller, ANN, MATLAB/SIMULINK

1. INTRODUCTION

Electrical energy is very simple and regulated form of energy and can be easily transformed into other forms. Power quality has become major problem for today's industries and consumers. Power quality issues are caused by increasingly usage of electronic equipment's and usage of non-linear loads. The electronic devices are very sensitive to disturbances and become less tolerant to power quality problems such as voltage sags, voltage swells, transients, harmonic contents and voltage. This degrades the efficiency and decreases the lifetime of end user equipment, economic losses to both utility and consumers. It also causes data and memory loss of electronic equipment's. One of the most common power quality problems we are facing today is voltage dips. A voltage dip is a short time (10 m-sec to 1 min) during which a decrease in magnitude of r.m.s.voltage occurs. This is due to sudden disconnection of loads, fault within the system. voltage swell is due to single L-G fault this leads in voltage rise of un-faulted phases.

In order to provide pure and clean power (pure sinusoidal voltage waveform) we use devices for voltage control are: (a) By using Flexible AC transmission Systems (FACTS) devices, (b) By reactive power injection, (c) By using tap changing transformer. For improving power quality, custom power devices (CPDs) are mostly recommended, among which the Dynamic Voltage Restorer (DVR) and Distribution Static Compensator (D-STATCOM) are considered as the best and cost-effective solutions..DVR is widely considered in mitigating faults such as Voltage sag and voltage swell since the cost size and complexity of DVR when compared to other devices is small when compared to other Custom Power Devices (CPD).

This paper tries to provide a way of simulating the working of DVR on balanced and unbalanced voltage sags and swells through MATLAB.A way of simulating fault conditions on the power distribution network is also carried out through MATLAB.

2. INTRODUCTION TO POWER QUALITY ISSUES

Any power problem manifested in voltage, current or frequency deviations from the first value end in failure or mal-operation of customer electric devices. The quality of electric power is characterized by parameters by continuity of supply, voltage, current, frequency and harmonic contents in electrical signal.

There are wide ranges of power quality problems each of those may have a spread of various causes, different effects and different solutions which will be wont to improve the power quality and equipment performance.

2.1 Importance of power quality improvement:

The power quality expresses the degree of similarity of ideal power supply with practical power supply. A system is said to have good power quality if the loads connected to

the system/network run efficiently without decreasing its performance. The deficiency in power quality can lead to either failure of equipment or decrease in the performance and lifetime of the appliance. In order to prevent such consequences and improve the operating condition of the system the power quality control is employed. Hence Power Quality is considered as utmost importance

2.2 Types of Power Quality Issues :

1. Voltage Swell
2. Voltage Sag
3. Voltage Interruptions
4. Transients
5. Wave distortion.

Power quality issues such as voltage sag and voltage swell are discussed in this paper.

2.1.1 Voltage Sag:

- Voltage sags are occurred due to presence of huge currents and large drop in the transmission lines.
- A reduction within the RMS voltage of the load in the range 0.1 to 0.9 of the first value.
- Duration: greater than half a main cycle and less than 1 minute.
- Causes: explosion in loads, Faults on the transmission lines.

2.1.2 Voltage Swell:

- An increase within the RMS voltage of the load in the range of 1.1 to 1.8 the original value.
- Duration of the voltage swell is bigger than half a main cycle and fewer than 1 minute.
- Causes: Sudden reduction in loads, Energizing large Capacitor banks.
- Voltage swell is subdivided as:
  - Instantaneous swells
  - Momentary swells
  - Temporary swells

2.3 Dynamic Voltage Restorer

DVR is a voltage source converter connected in series with the load to be protected, it injects required amount of voltage into the system to compensate for the fault, which can either sag or swell. The DVR is connected to the system through a injection transformer. The DVR consists of a VSC connected to the injection transformer primary side through a low pass filter A battery is used as input to the VSC.

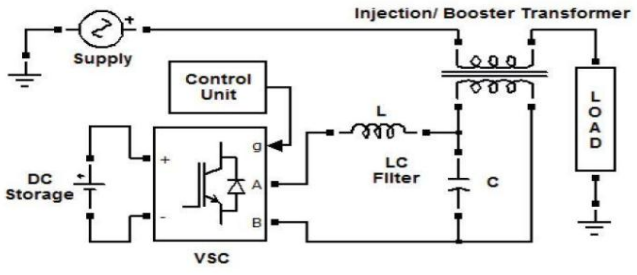

Fig 1. Basic schematic of a DVR

DVR operates in 3 modes. This is based on the condition of the transmission lines.

- Protection mode
- Standby mode
- Injection mode

2.4 Construction of a DVR:

DVR have different blocks. They are VSC:

VSI converts fixed supply voltage to variable supply voltage. The converted voltage is nearly equal to sinusoidal voltage. The output voltage is developed such that it has the same phase sequence as the system voltage. The magnitude of the output voltage is desirable and controlled through suitable PWM scheme. The output is passed through a passive filter to remove the harmonics.

Injection transformer:

The AC voltage supplied by the VSC is stepped up and supplied to load bus using the injection transformer. The injection transformer also separates the two systems electrically. The amount of voltage compensated depends on the rating of the transformer.

Energy storage device:

Devices such as lead acid batteries, flywheels, dc capacitors are used as energy storage. They are the input supply to the voltage source converter. For areas with large power requirement an ac to dc converter is used in the place of energy storage unit. If a flywheel is used as energy storage unit then AC to AC conversion required.

3. WORKING AND SIMULATION MODELS

3.1 Working scheme of the DVR:

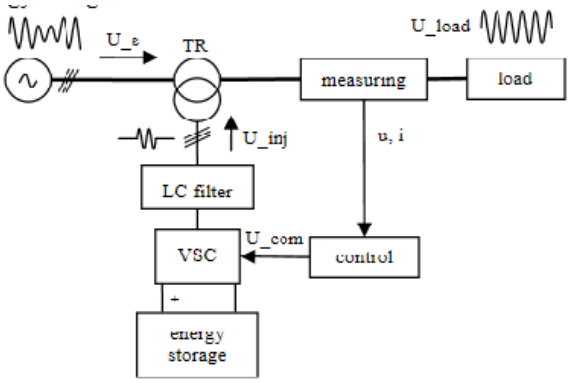

Fig. 1. Simplified scheme of a DVR

Fig.2 Working scheme of a DVR

The DVR is connected in series to the load and hence it can be called a series connected FACT controller. A DVR; s primary function is to mitigate any voltage sag or swell on the power system network. The DVR is usually installed between the source and the load that is to be protected. The measuring unit gives the values of voltage and current of the system. These values are compared with the actual values of the system by the control unit and a respective

signal is generated by the control unit to be sent to the VSC. This process is repeated at every moment by the control unit.

The difference between the actual value of the system and measured value of the system is called the Reference voltage and this voltage is used to generate the pulses required for generating the voltage to be injected by the DVR. The reference signal is mostly proportional to the value of the voltage to be injected by the DVR. The power output of the DVR depends on the amount of energy that can be stored in the storage device (BATTERY). DVR s are generally installed in places where the chances of sudden loading is high and the place usually has large electricity consumers.

3.2 Reference voltage generation :

There are several voltage reference techniques which can be used in DVR, which are

- Peak value method
- RMS method
- Fourier transform method
- DQ method

In this method the reference voltage for the controller is generated by using the DQ technique. It is based on DQ transformation. DQ actually means dq0 – direct quadrature 0 axis. It is a mathematical transformation used in simplifying the analysis of three phase circuits. The two quantities d and q are at quadrate with each other and they rotate at a frequency of (w). The advantage of using dq transformation is that the three quantities from the three-phase system are reduced to two quantities. At ideal conditions the value of d=1 and q=0.For any other condition the value of d,q and 0 are not equal to zero. The reference voltage is generated by first converting the measured values in abc to dq0 and then comparing them with the ideal d1 values. The output signal is passed through a controller and then again converted back to abc. The final signal so generated is the reference signal and this is used to create pulses for the VSC.A phase locked loop is created to synchronize the frequency of the compensating voltage with the line voltage. DQ transformation is calculated as follows:

3.3 Controller scheme in MATLAB:

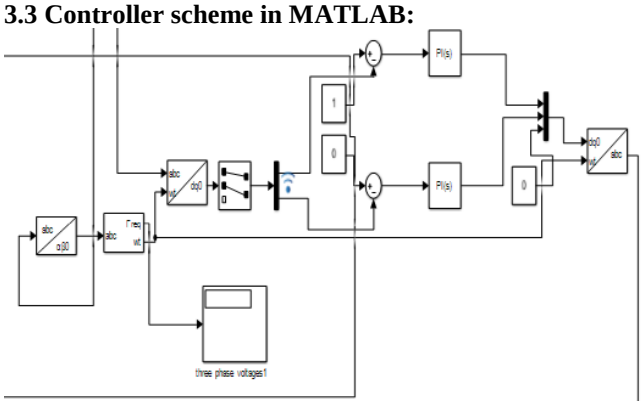

Fig.3.Subsystem PI Controller in MATLAB

The three phase voltage levels of the grid are measured are taken in as abc input.These abc values are given to the abv to dq0 conversion block in matlab.TO achieve the same frequency for the dq values,The abc values are passed through a PLLL to produce the frequency input for the abc/dq0 bloc.The converted values are then compared with the actual dq0 values(in this case d=1,q=0) and the ouput is passed through a PI controller and then the values are again converted back to the abc domain.

The voltage generated is called the reference voltage and it is used to create pulses for VSC in DVR.To generate Pulses the Reference voltage is given as a input to PWM generator block in matlab.The ouput consists of six pulses which are given as input to the VSC gate.

3.4 Creating the fault in matlab

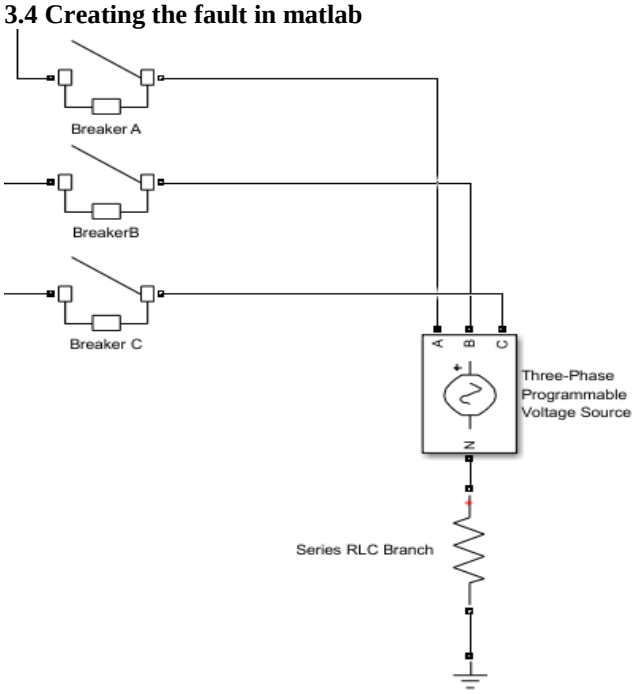

Fig.4. Subsystem Fault block in MATLAB

To achieve the correct simulation of different faults such as sag, swell and interruption on the power system, A model of power system is created and a suitable voltage is injected by connected a programmable voltage source parallel with the grid to achieve the fault.

3.4 Creating balanced fault: The level of fault voltage that should be injected is set in the programmable voltage source and all the breakers are closed.

3.4.1Creating unbalanced fault*:* The level of fault voltage that should be injected is set in the programmable voltage source and any two breakers are closed.

 ISBN: 978-93-90214-20-4

3.5 Complete MODEL and design specifications

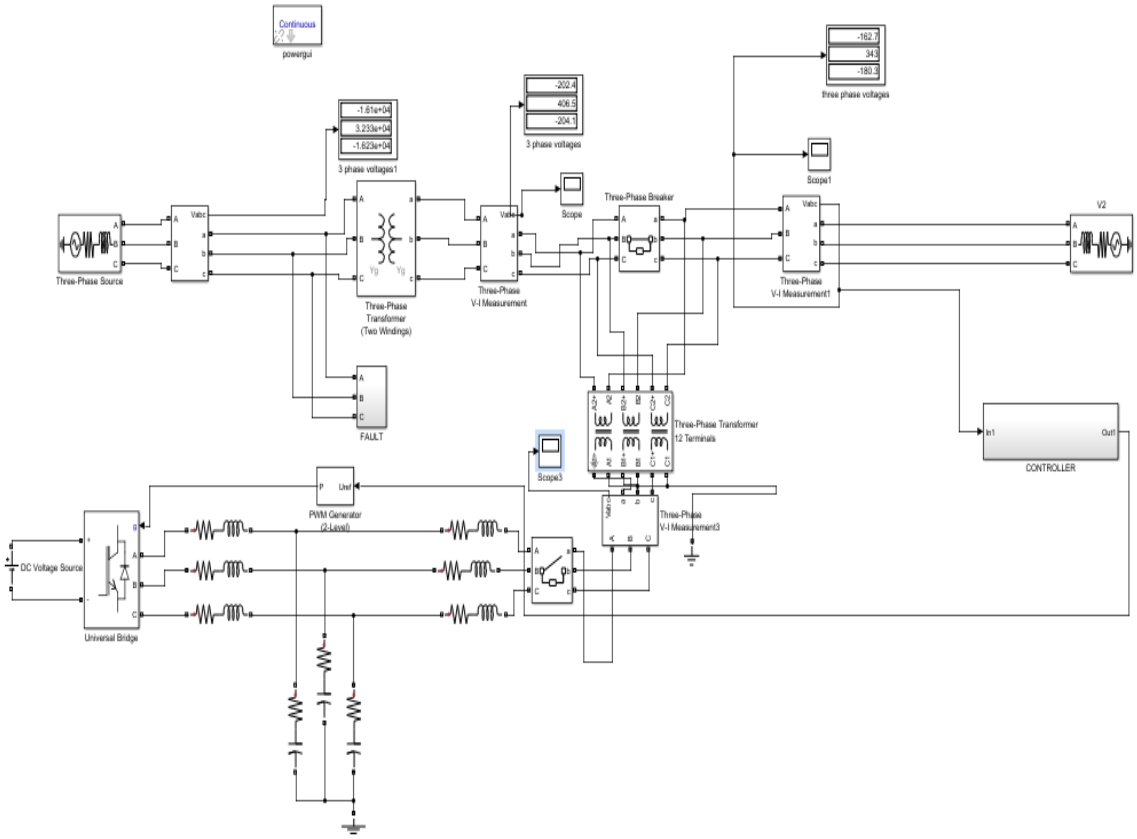

Fig.5. Simulink model of DVR

A power system grid consisting of two voltage sources is constructed in Simulink. The voltage source V1 generates 33kv and the voltage source at load generates 415V.A step down transformer is used to make the grid function on a single voltage level. The voltage is injected by the DVR through Injection Transformer.

4. SIMULATION RESULTS

4.1 Balanced Sag:

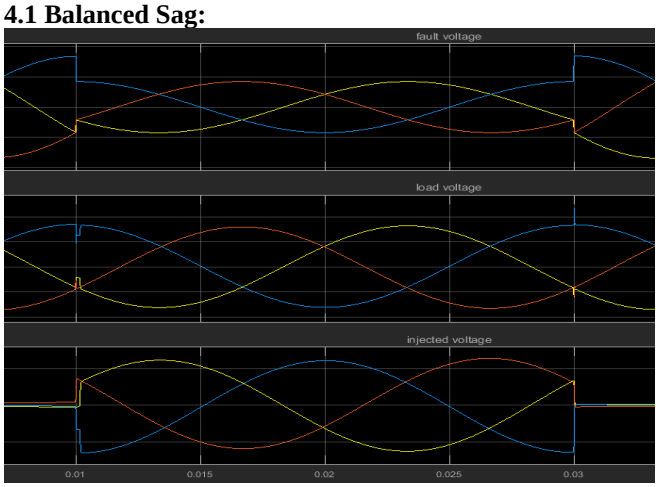

Fig.6. (a). voltage waveform of a balanced system with sag, rectified signal, DVR injected signal.

In the above fig.6. (a) the first signal shows the voltage sag for a balanced system. The sag is from 10msec to 30 msec. during this period the DVR get activated and start supplying the power from the DC energy source. The second signal is the scenario where the DVR is turned on and started supplying the power into the system. Third signal in the fig shows the amount of power supplied by the DVR into the system.

2. Balanced Swell:

In the figure 6. (b) shows the balanced system with voltage swell in the first signal. The swell is from 10msec to 30 msec. in the second signal this is the rectified signal. The required amount of power is injected into the system by DVR which is shown in the third signal.

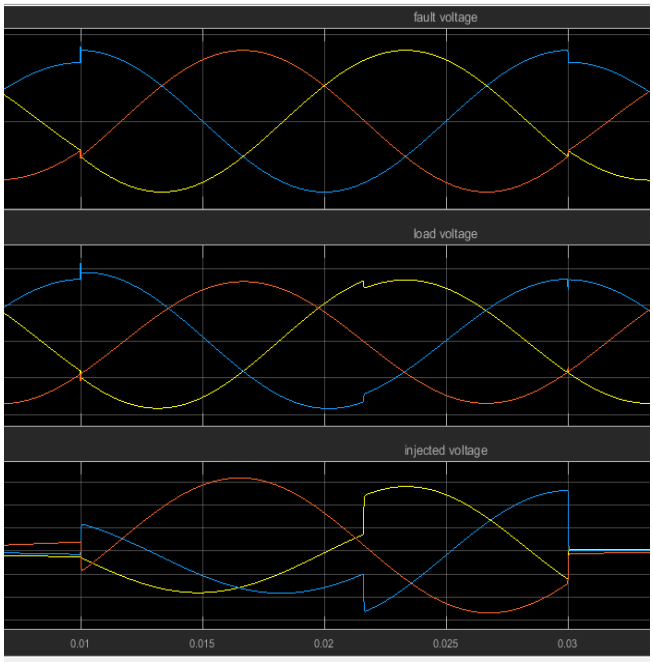

Fig.6. (b) voltage waveform of balanced swell

3.Unbalanced sag:

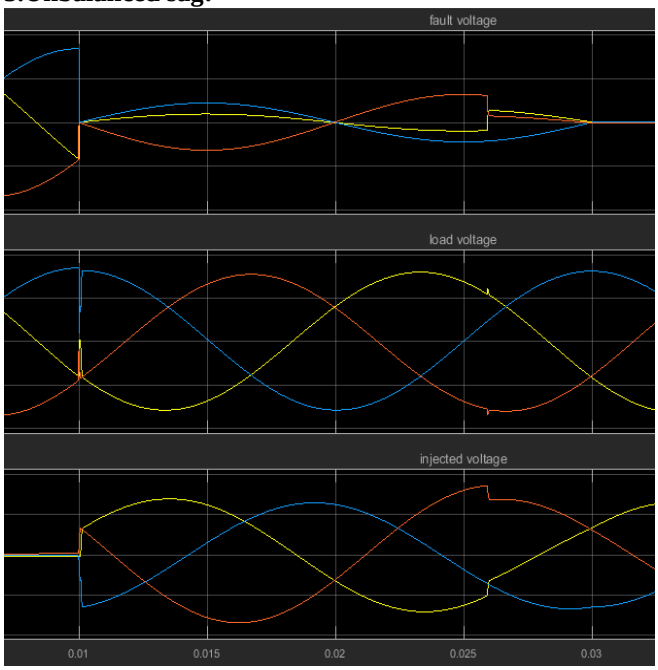

Fig.6. (c) voltage waveform of unbalanced sag

The Fig.6 (c) shows the unbalanced system with sag. Unbalanced system is formed by giving the unequal voltages to the system by using fault block, this gives the unbalanced system with sag. The second signal is the corrected signal, sag is reduced by inducing the voltage into the system by DVR. Signal three is the voltage signal that is induced into the system by DVR.

4. Unbalanced swell:

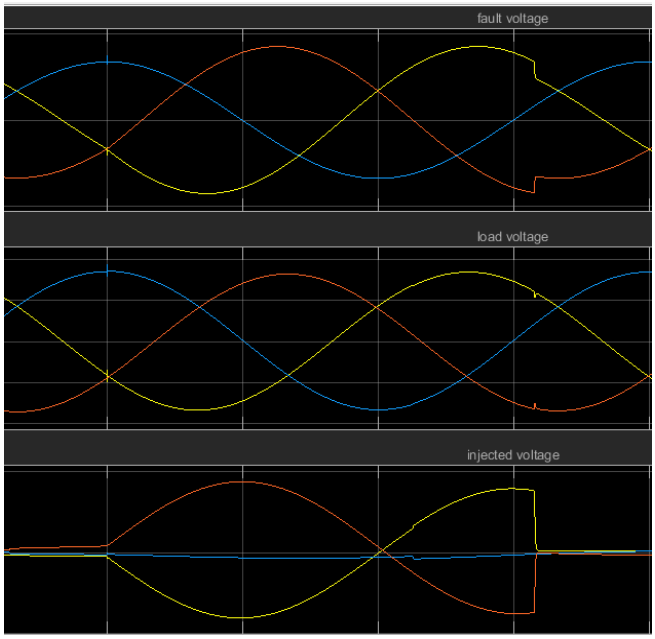

Fig.6. (d) voltage waveform of unbalanced swell

In the figure 6. (d) shows the unbalanced system with voltage swell in the first signal. The swell is from 10msec to 30 msec. in the second signal this is the rectified signal. The required amount of power is injected into the system by DVR which is shown in the third signal.

5.Voltage Interruption:

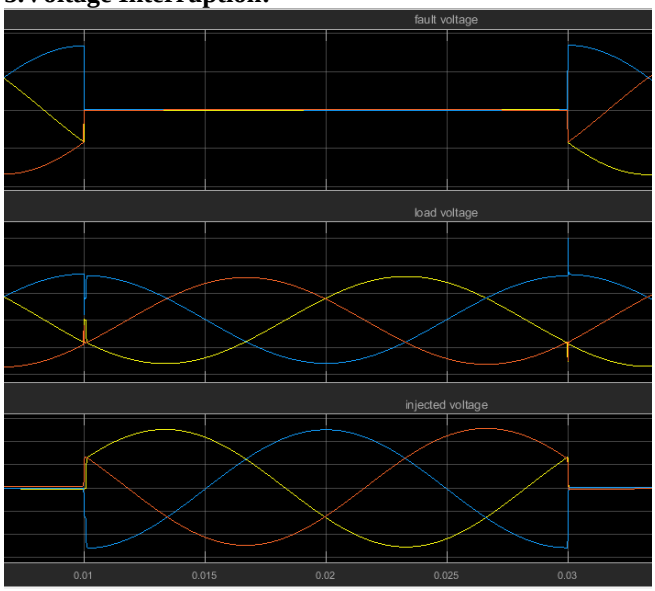

Fig.6 (e) voltage waveform of an interrupt

The above Fig.6 (e) shows the signal which has a voltage interrupt occurred in the system from 10m sec to 30m sec. when adding the DVR to the system the amount of voltage required for the system is supplied by the DVR. After

successful injection of required voltage, we get the second waveform.

5. CONCLUSION

In this paper we have seen the mitigation of the power quality issues present in the system such as voltage sag, voltage swell, voltage interruptions for both balanced and unbalanced system. We have compensated these errors is done by using DVR (Dynamic Voltage Restorer) in the MATLAB Simulink with the help of PI controller. We have considered both balanced and unbalanced voltages and simulation results are shown in this paper. These results from the simulation shows DVR gives a good voltage regulation for voltage swell, sag and interruptions present in the system..

REFERENCE

[1] S.V Ravi Kumar and S. Siva Nagaraju "SIMULATION OF D-STATCOM AND DVR IN POWER SYSTEMS" in ARPN Journal of Engineering and Applied Sciences, VOL. 2, NO. 3, JUNE 2007.

[2] Ali Moghassemi and Sanjeevikumar Padmanaban "Dynamic Voltage Restorer (DVR): A Comprehensive Review of Topologies, Power Converters, Control Methods, and Modified Configurations" Published: 11 August 2020.

[3] M. A. Kabir and U. Mahbub control of shunt active power IEEE Power and Energy Confb, "Synchronous detection and digital r filter in power quality improvement", ference at Illinois (PECI), Feb. 2011.

[4] S. Singh, V. Rai, A. Kumar and K. B. Sahay, "Simulation and comparison of DVR and D-STATCOM for voltage sag mitigation," 2016 IEEE 6th International Conference on Power Systems (ICPS), New Delhi, 2016, pp. 1-6, doi: 10.1109/ICPES.2016.7584238.

Enhancing the Performance of a Single Phase UPQC System Using Combined Super Capacitor and Fuel Cell Unit

Dr. Vodapalli Prakash

Kakatiya Institute of Technology & Science, Warangal, Telangana, India

Abstract:

The distribution network usually composed of mixed loads of different nature. As a customer experiencing many difficulties, when using different types of devices. Most of the modern devices are using latest semiconductor based technology may create some impact while using those devices. The custom power device Unified Power Quality Conditioner (UPQC) is a truly efficient device to improve the conditions in the system. The combined execution of supercapacitor and fuel cell integrated UPQC to mitigate the power quality problems for mixed loads. This system reduces the harmonic content of the system as per the IEEE definitions.

Keywords:

Power problems, super capacitor, fuel cell, capacity, harmonic distortion, IEEE standard, power filter

1. INTRODUCTION

The customers are of the different categories and their demands are also different. The higher rating machines are equipped with different power electronic converters of at most importance. Due to the usage of these, the non-linearity in the system increases. It will disturb the entire system. The rural areas become urban proportionately the demand with different load requirements. With the expansion of existing units, the demand is increased. [1].

These equipments are electronic type and inject harmonic constituents and damage the network. With the involvement of these devices continuously may disturb the network leads to damage and non-working of equipment or malfunctioning at user side [2-3]. To rectify those problems in the network, Custom power devices play an important duty in reducing the problems [4-6]. There are plenty of reasons for the power quality problems in the systems and also whenever faults occurred, damage of machines and winding faults etc.

In the series of the custom devices, UPQC is one of the most efficient devices in mitigating the problems. UPQC uses the series and shunt filters are connected back to the back with the dc side. The series filter is responsible for managing the voltages & harmonics. Shunt filter [7-8] and [16] is for currents compensation. Fuel cells are capable of transforming chemical energy into electrical energy. These are efficiently used in military applications, combined electric vehicles and industrialization purpose and remote applications etc.

Due to the inherent characteristics of supercapacitors such as quick charge and discharge rate, power density, they can employed in electric vehicles, electric trains etc. With the addition of supercapacitor is reduces the load burden increases the working capability [11-15]. In the most peak conditions, fuel cell supplies the current along with supercapacitor supports the system.

The DC to DC converter acts like a buck boost converter incorporated in the system to support voltage sag & swells [9-10]. This combined unit supports working functionality of UPQC, DC- to- DC converter and checked in MATLAB. The significance in power quality explained in Section 1 and Section 2; analyse about supercapacitor and fuel cell combined UPQC, Section 3; explains about series and shunt filters. Section 5; demonstrates results, Section 6; conclusions.

2. SC-FC BASED UPQC

The circuit diagram of the SC-FC based UPQC configuration shown in Fig 1. The filters adopting a dc link supplied to a fuel cell – supercapacitor unit given to the dc capacitor, whereas supercapacitor unit used for backup unit for short span. The shunt filter is tried to eliminate the harmonics in the source currents and regulate the load conditions. To maintain the proper magnitudes of voltages, transformer is used for and also used to decrease the harmonic content in the series filter. The Figure.2 shows the arrangement in the simulation for the executed method.

In this approach, d-q method is employed for the combined UPQC along with a DC to DC converter to control the voltages for the achieved performance. Park's- Inverse Park's transformations employed for the production of the reference signal.

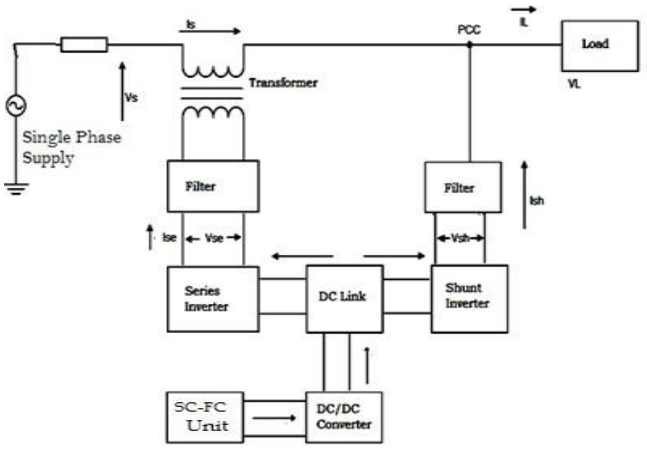

Fig.1.Circuit Diagram of SCFC integrated UPQC.

3. CONTROL METHOD OF SERIES AND SHUNT CONVERTER

i. Series APF

The target of the series active filter is to eliminate harmonics, shown in Fig.2, is employed to suppress voltage harmonics. The phase locked loop is used to engage the harmonize with the supply voltage [17]. Three phase disturbed supply voltages are collected and given to point of common coupling which generates two unit vectors (sinθ, cosθ).

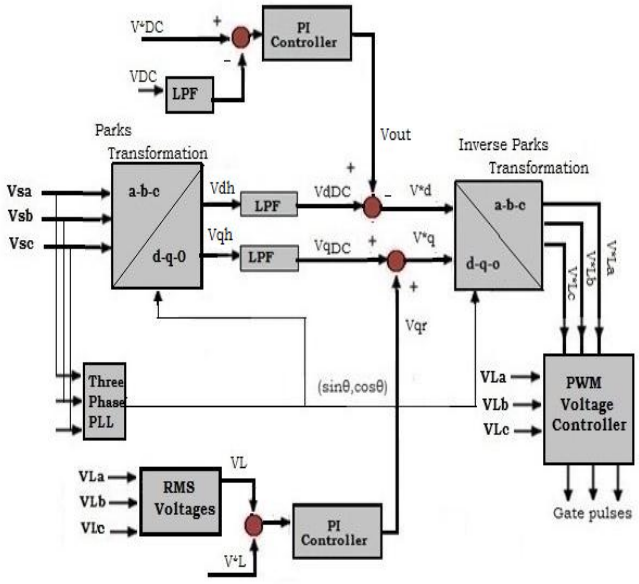

Fig 2. Control method of Series APF [18].

The source voltages V_{sa}, V_{sb}, V_{sc} are changed into d-q-0 from abc, given in (3.1).

$$\begin{bmatrix} V_{sd} \\ V_{sq} \\ V_0 \end{bmatrix} = \frac{2}{3}\begin{bmatrix} \cos\theta & \cos\left(\theta-\frac{2\Pi}{3}\right) & \cos\left(\theta+\frac{2\Pi}{3}\right) \\ -\sin\theta & -\sin\left(\theta-\frac{2\Pi}{3}\right) & -\sin\left(\theta-\frac{2\Pi}{3}\right) \\ \frac{1}{2} & \frac{1}{2} & \frac{1}{2} \end{bmatrix}\begin{bmatrix} V_{sa} \\ V_{sb} \\ V_{sc} \end{bmatrix} \quad (3.1)$$

The low pass filters (LPFs) are filters the harmonic components. The components of voltages in d- and q-axes are shown in equation (3.2) and (3.3).

$$V_{dh} = V_{dDC} + V_{dAC} \quad (3.2)$$
$$V_{qth} = V_{qDC} + V_{qAC} \quad (3.3)$$

V_{dh}, V_{qh} are d axis and q axis voltages consist of DC (fundamental), ripple (harmonic) components and V_{dDC}, V_{qDC} are direct-axis and quadrature-axis fundamental DC voltages. To retain the DC bus voltage of the series filter, a proportional–integral controlling mechanism is used, output is considered as the voltage (V_{out}).

The ref. d-and q-axis voltages are V^*_d, V^*_q are given by,

$$V^*_d = V_{dDC} - V_o \quad (3.4)$$
$$V^*_q = V_{qDC} + V_{qr} \quad (3.5)$$

Reference and actual source voltage will produce the three phase RMS voltage. This will helps to introduce the suitable injected voltage by the same for the compensation of voltage losses. To get the required compensation reactive component of voltage, use Average RMS voltage and reference voltage from the PI controller.

V_{qDC} (reactive component) and with V_{qr} values are maintained to get the suitable voltage at the converter of series active filter, so that it can be needful to retain the RMS voltage at point of interconnection due to RMS voltage loss by load reactive power. The two reference voltage values (V^*_d, V^*_q) are used to generate the reference load voltages, to adjust the amount of voltage at series APF. The Inverse Park transformation is applied for producing the reference voltages which is given in equation (3.6) is to change reference load voltage (V^*_{Labc}) are transform d-q-0.

$$\begin{bmatrix} V^*_{La} \\ V^*_{Lb} \\ V^*_{Lc} \end{bmatrix} = \frac{2}{3}\begin{bmatrix} \cos\theta & -\sin\theta & 1 \\ \cos\left(\theta-\frac{2\Pi}{3}\right) & -\sin\left(\theta-\frac{2\Pi}{3}\right) & 1 \\ \cos\left(\theta+\frac{2\Pi}{3}\right) & -\sin\left(\theta-\frac{2\Pi}{3}\right) & 1 \end{bmatrix}\begin{bmatrix} V_d \\ V_q \\ V_0 \end{bmatrix} \quad (3.6)$$

ii. Control method for Shunt Converter

Shunt APF is shown in Fig4, targeted to manage the link voltage as well and to remunerate the load current under reactive, non-linear loads.

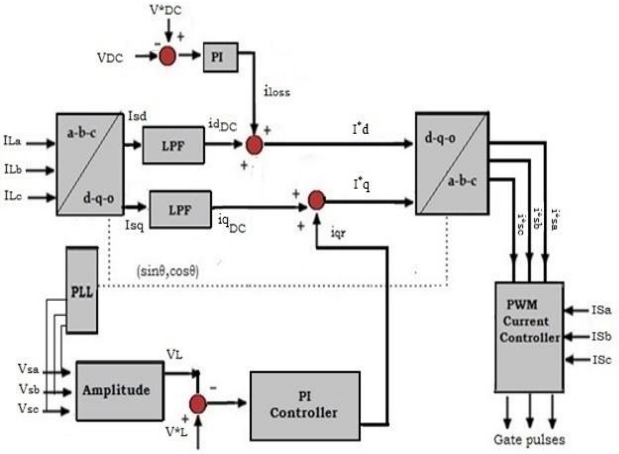

Fig 3. Control method of Shunt APF [18].

The source currents should be sinusoidal irrespective of the load conditions with the help of shunt APF by the current controller design. Three phase disturbed currents are sensed and added to point of common coupling which produce two quadrature unit vectors (sinθ, cosθ). The reference currents of direct axis, quadrature axis are I^*_d, I^*_q values are shown in equation in (3.7), (3.8).

$$I_d^* = i_{dDC} + i_{out} \quad (3.7)$$
$$I_q^* = i_{qDC} + i_{qr} \quad (3.8)$$

Where i_{dDC}, i_{qDC} direct-axis and quadrature-axis fundamental currents, i_{out} is the output of the PI controller. The load currents in the three phases are transformed into d-q-0 from abc using the mentioned equation (3.9):

$$\begin{bmatrix} i_{ld} \\ i_{lq} \\ il_0 \end{bmatrix} = \frac{2}{3}\begin{bmatrix} \cos\theta & \cos\left(\theta - \frac{2\Pi}{3}\right) & \cos\left(\theta + \frac{2\Pi}{3}\right) \\ -\sin\theta & -\sin\left(\theta - \frac{2\Pi}{3}\right) & -\sin\left(\theta - \frac{2\Pi}{3}\right) \\ \frac{1}{2} & \frac{1}{2} & \frac{1}{2} \end{bmatrix}\begin{bmatrix} i_a \\ i_b \\ i_c \end{bmatrix} \quad (3.9)$$

The two reference currents (i^*_d, i^*_q) are used to generate the reference load currents, to correct the current magnitude at shunt APF. The reference source currents are produced by Inverse Park transformation given by equation 3.10.

$$\begin{bmatrix} i_{sa}^* \\ i_{sb}^* \\ i_{sc}^* \end{bmatrix} = \frac{2}{3}\begin{bmatrix} \cos\theta & -\sin\theta & 1 \\ \cos\left(\theta - \frac{2\Pi}{3}\right) & -\sin\left(\theta - \frac{2\Pi}{3}\right) & 1 \\ \cos\left(\theta + \frac{2\Pi}{3}\right) & -\sin\left(\theta - \frac{2\Pi}{3}\right) & 1 \end{bmatrix}\begin{bmatrix} i_d \\ i_q \\ i_0 \end{bmatrix} \quad (3.10)$$

The control strategy of shunt active filter senses the current values and is examined with the reference currents to obtain switching pulses.

4. SINGLE PHASE FUEL CELL - SUPERCAPACITOR UNIT WITH DC-DC CONVERTER

Fuel cells are the sources of generating electricity receiving chemical agents. PEMFC are using most of the applications due to its startup and where less temperatures can be employed [19-20].

The DC-DC converter with 2 full-bridges [9] also employed in two directions. The working voltage of the fuel cell varies between 60-70V, while the dc link voltage is about 650V. The converter increases the fuel cell unit voltage to the DC link voltage in released mode.

5. RESULT

(a) Sag Compensation

A sag is produced in the source end-voltage from 0.2 to 0.4 sec displayed in below figure.4. The UPQC can rectify the voltage related problems to make the load voltage is normal.

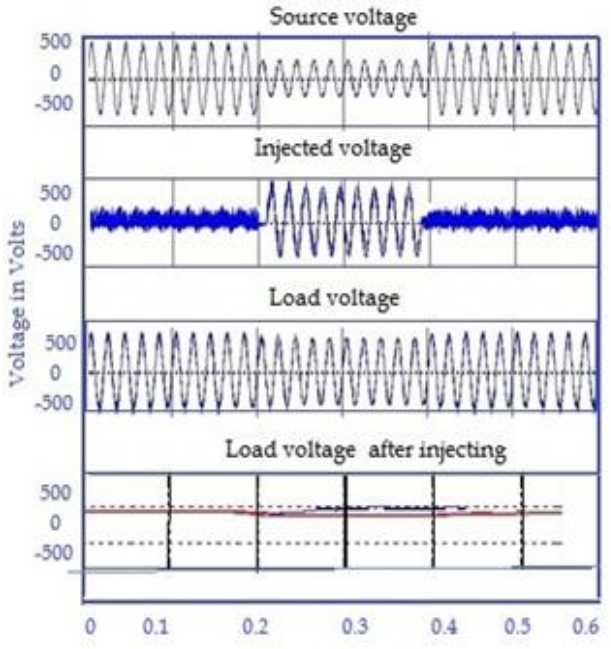

Fig 4. Sag compensation.

Similarly voltage swell is observed from 0.2 to 0.4 sec is in the source end-voltage and the after mitigation the load voltage is maintained constant, it is shown in Fig.5.

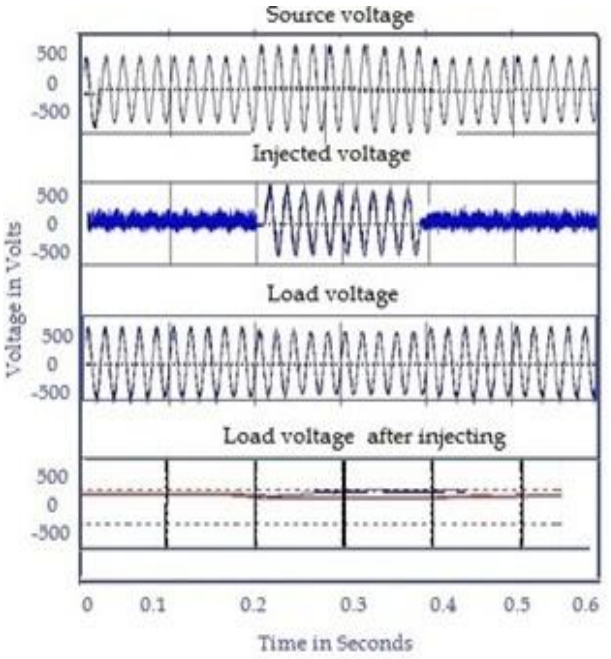

Fig.5 Swell compensation.

To support the load voltage, the fuel cell with supercapacitor is supplies the required remunerating power through the series compensator and it can be monitored that the load voltage retains the same.

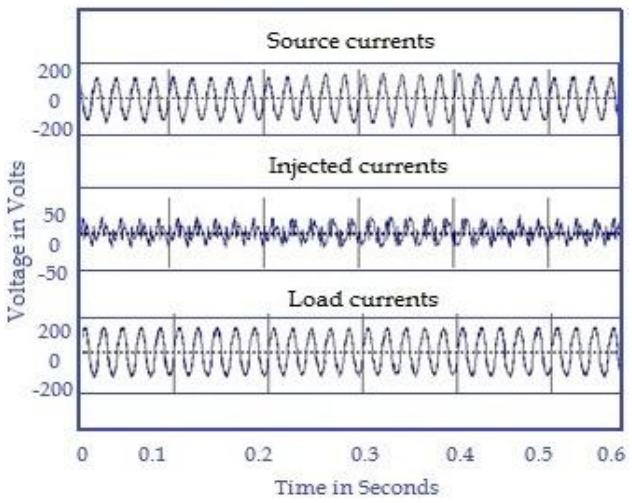

Fig 6. Swell analysis

Fig. 7 (a) & (b), represents the harmonic analysis of source current and load voltage. The THD of the Source current and load voltage values are $^{0.82}$ and 1.62. Due to misuse of equipment and not proper functioning.

The THD spectrum of analysis of source current, load voltage when UPQC combined with super capacitor analysed in Figure.12 (a) and (b).

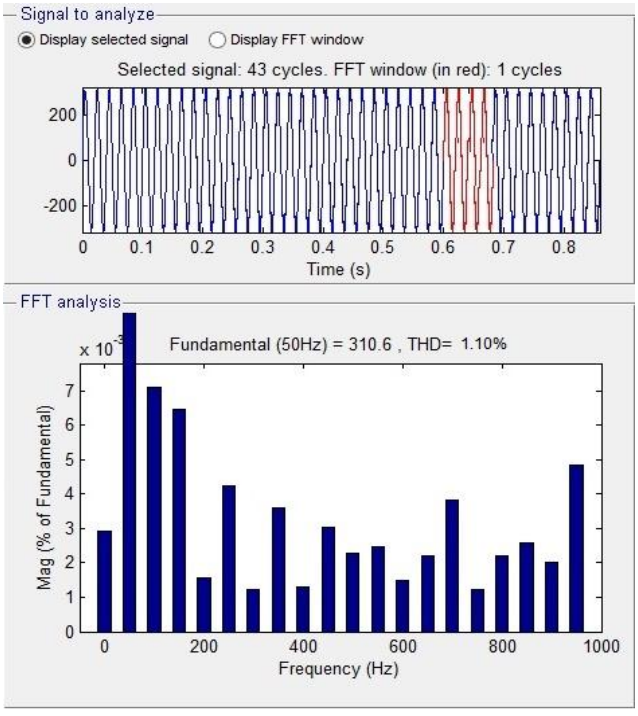

(a).

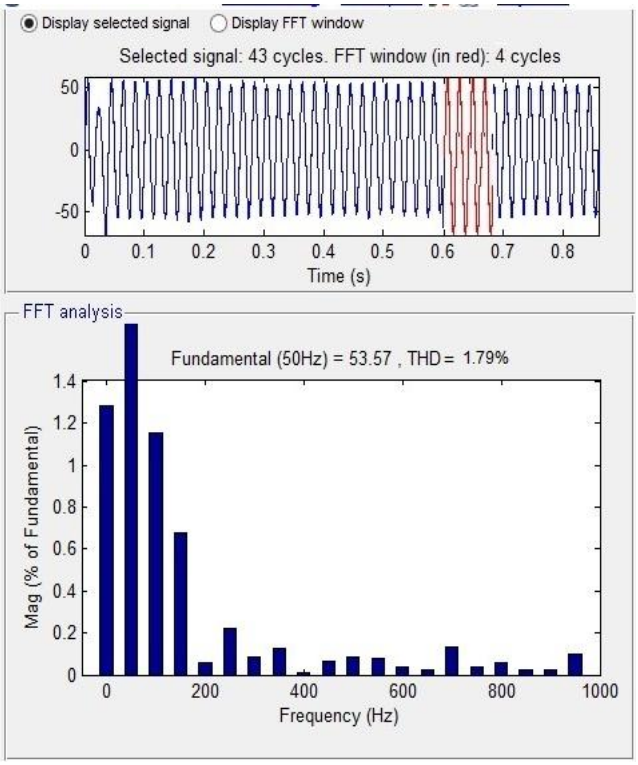

(b)

Fig. 7 (a) Source current. (b) Load voltage.

6. CONCLUSION

This paper worked on the execution of combined effect of fuel cell-supercapacitor combined with single phase UPQC, which rectifies the different problems. Here, the combined unit working good in mitigating voltage sag, swells. This composition perfectly handles the problems associated with voltage and currents. The obtained values are as per IEEE dictionary and the same executed through MATLAB systems.

Acknowledgment

I was very much thankful to Head Dr. C.Venkatesh and Principal Professor Dr. K. Ashoka Reddy, for their support and motivation. Also my gratitude to Management KITS-Warangal for providing wonderful facilities to do my research.

REFERENCE

[1] Buang M Han, B. Bae, "Unified power-quality conditioner with super-capacitor energy storage," Euro. Trans. Electr. Power 2008; 18, pp.327–343

[2] Metin Kesler, Engin Ozdemir, "Simplified Control Method for Unified Power Quality Conditioner (UPQC)," International Conference on Renewable Energies and Power Quality Vol. 1, No.7, April 2009, pp. 474-478.

[3] Argyrou, Maria & Christodoulides, Paul & Marouchos, Christosa & Kalogirou, Soteris. (2018). Hybrid battery-supercapacitor mathematical

modeling for PV application using Matlab/Simulink. 10.1109/UPEC.2018.8541933.

[4] S.Khalid & Bharti Dwivedi "POWER QUALITY ISSUES, PROBLEMS, STANDARDS & THEIR EFFECTS IN INDUSTRY WITH CORRECTIVE MEANS," in International Journal of Advances in Engineering & Technology, May 2011. Vol. 1,Issue 2,pp.1-11.

[5] Vanessa Paladini, Teresa Donateo, Arturo de Risi *, Domenico Laforgia," Super-capacitors fuel-cell hybrid electric vehicle optimization and control strategy development", Elsivier,Energy Conversion and Management 48 (2007), pp. 3001–3008.

[6] Víctor M. Moreno, Alberto Pigazo, Marco Liserre and Antonio Dell'Aquila, "Unified Power Quality Conditioner (UPQC) with Voltage Dips and Over-voltages Compensation Capability" DOI: 10.24084/repqj06.28, March 2008.

[7] Sanjib Ganguly "Impact of Unified Power-Quality Conditioner Allocation on Line Loading, Losses, and Voltage Stability of Radial Distribution Systems", IEEE TRANSACTIONS ON POWER DELIVERY, Vol. 29, Issue. 4, AUGUST 2014, pp.1859-1867.

[8] Iurie Axente, Jayanti Navilgone Ganesh, Malabika Basu, Michael F. Conlon, Kevin Gaughan "A 12-kVA DSP-Controlled Laboratory Prototype UPQC Capable of Mitigating Unbalance in Source Voltage and Load Current", IEEE TRANSACTIONS ON POWER ELECTRONICS, VOL. 25, NO. 6, JUNE 2010, pp. 1471-1479.

[9] Prakash Vodapalli, T. Rama Subba Reddy, S. Tara Kalyani, P.B. Karandikar, "Application of supercapacitor in enhancing power quality of UPQC for three phase balanced/unbalanced loads", Journal of Electrical Engineering, 2014, ISSN No:1582-4594, Issue no 4, vol.14, 2014, Edition: 4, Article 14.4.50.

[10] Yang Zhang, Shengfa Zhang and Jiahong Chen, "The applications of bidirectional full-bridge DC-DC isolated converter in UPQC," *International Conference on Electrical Machines and Systems*, Wuhan, 2008, pp. 1916-19.

[11] Bei Gou, Woon Ki Na, Bill Diong,"FUEL CELLS Modeling, Control and Applications", CRC Press, 2010, pp 02.

[12] NADA ALLOUI, DEKHINET ABDELMALEK, CHERIF FETHA "Analysis of Electric disturbances in the quality of electric energy using the ABC method of classification for the application to voltage dips and short interruptions", Journal of Electrical Engineering, ISSN No:1582-4594, vol.16, edition: 4, issue no 4, Article 16.4.12, 2016.

[13] M. STANLEY WHITTINGHAM, ROBERT F. SAVINELL, AND THOMAS ZAWODZINSKI, GUEST EDITORS, "BATTERIES AND FUEL CELLS", Volume 104, Issue 10,October 13, 2004.

[14] Jayalakshmi N. S., Pramod Bhat Nempu and Shivarudraswamy.R."CONTROL AND POWER MANAGEMENT OF STAND-ALONE PV-FC-UC HYBRID SYSTEM" Journal of Electrical Engineering · May 2016.

[15] O.C. Onar, M. Uzunoglu, M.S. Alam, "Modeling, control and simulation of an autonomous wind turbine/photovoltaic/fuel cell/ultra-capacitor hybrid power system", Journal of Power Sources 185 (2008) 1273–1283.

[16] X. Yu, M. R. Starke, L. M. Tolbert and B. Ozpineci, "Fuel cell power conditioning for electric power applications: a summary," in *IET Electric Power Applications*, vol.1, issue no. 5, Sept. 2007, pp.643-656.

[17] Govindasamy SUNDAR, Rangaswamy ASHOK "Dynamic Protection of Power Converters Associated with the Grid Using Shunt Active Filter And Thyristor Switched Capacitor for Power Quality Enhancement", Journal of Electrical Engineering, ISSN No:1582-4594, issue no 4, vol.19, Edition: 4, Article 19.9.33, 2019.

[18] Bhim Singh, Ambrish Chandra, Kamal Al-Haddad - Power Quality: Problems and Mitigation Techniques, WILEY, February 2015, ISBN: 978-1-118-92205-7.

[19] Ali M. Eltamaly, Yehia Sayed, Abou-Hashema M. El-Sayed and Amer Nasr A. Elghaffar, "Voltage Sag Compensation Strategy Using Dynamic Voltage Restorer for Enhance the Power System Quality", Journal of Electrical Engineering, ISSN No : 1582-4594, Issue no 3, vol.19, 2019, Article 19.3.31.

[20] Fuel Cell Handbook (Fifth Edition) By EG&G Services Parsons, Inc. Science Applications International Corporation, October 2000, pp.1-3.

Challenges of Restructured Power Engineering and Power Exchange

Dr. Vodapalli Prakash

Kakatiya Institute of Technology & Science, Warangal, Telangana, India

Abstract:

Re-regulation is the modification of the system procedures and methods that manages the power flow in the existing, It also provides a platform for smooth conduction of the available rules and instructions that controls the electric industry to provide consumers the option of electricity providers those are manage the business of trading by changing competitiveness. Reregulation changes the productive working capacity of the production. Power exchanges working for the power market and the consumers.

Keywords:

Reregulation, competition, power market, Power Exchange, efficiency

1. INTRODUCTION

There are different issues are placed in each and every part of the power system. The cost of each unit of consuming increasing day by day, It is a burning issue throughout the world, there which is a unsettling concern about re-define and re-design of the power market. The contention in the wholesale generation market and the retail market combined with the open access to the supply circuit can combine many benefits to the end consumers, such as less tariff and with many benefits. However, these struggles also accompany various production issues and impediment to the operation of re-modelled power system.

To have a fruitful and reliable power system maintenance, there are lot many challenges inside the system, it also offers additional challenge of the coordination of controls between the various independent bodies, each one having with different targets and dynamic objectives and goals.

The re-defining of the electricity Sectors is bracing by the economic opportunities to society resulting from the re-regulation of other groups.

The important scenario of restructuring is wholesale and retail market power. Wholesale market power is the power of whole generators to access supply systems and to contention in for wholesale markets including discoms and independent markets. On the other hand, retail power note to the capacity of marketers to get entry to distribution systems in order to sell electricity to users. Contrarily, end users will be able to pick a marketer to acquire electricity from. The condition for retail market is wholesale market.

The need of remodeling of the existing power market:

- To give electricity for every one with their utmost satisfaction at reasonable tariff.
- To promote the revalry in the generation and supply of electricity.
- To supply electricity to all consumers without interruption with good quality.
- To improve efficiency and economy of the power system.
- Also provides strong buyers and new producers.

The target of re-regulation is to enable competitiveness based upon tropical environmental conditions and efficiencies.

2. POWER EXCHANGES

A Power Exchange (PX) is a place, where efficient trading takes place. The PX build an environment, it provides an easy access to the markets. It is an interface in which generators and consumers bid to sell and buy energy.

It is an anonymous, translucent, reliable and stable to have transactions in the trading, to sell or purchase the power from power producer to other power producer or the unit will transmit to the distributors in a comfortable zone.

The primary goal is to provide forums to contest electricity energy supply and demand in the current and forward energy markets. The market range may vary from a half hour to a few months but the most useful scenario is a day-ahead market.

3. DESIGN ISSUES OF POWER EXCHANGE

Based on the market design, the day-ahead market may be predate by a longer term market and supplemented by an hour-ahead market. The so called ‘hour ahead assign energy trading opportunities up to one or two hours before the operating hours. Depending on the market design and activity rules the energy bids may include several price components or a Unique price component.

A multi market bid may offers separate price unit tag, no-load operation and energy. A single part bid also includes all the costs which adds fixed and variable cost in either case the energy bid may included.

The market design, bidding rules and bid section process flow, impacts on the computer applications needed to support the Power Exchange.

The type of market structure and procedures to be adopted and the using software using, these all points will helps in determining a successful or winning bid.

Basically, the work flow of the PX is:

- get bids from power producers and customers.
- compare the bids, decide the market last clearing rate, prepare scheduling plan.
- provide schedules to the Independent System Operator (ISO).
- adjust the scheduling plan when the system overloaded.

The PX manages the electric power pool, which provides an association to match electric energy supply and demand based on bid prices.

Benefits:

- create liquidity
- encourage competition
- standard Contracts
- creates a feasible market
- Unbiased
- national

4. CONCLUSIONS

Deregulation is an critical issue in the restructured electrical power system. It is one of the powerful tool. This paper presented the problems associated in the power system and how to get benefit from the Re-Regulation and how Power exchanges plays a critical role between the power producers and customers in a better way.

REFERENCE

[1] Wu Shan, Mei Tianhua, Gong Jianrong, Gan Deqiang. Voltage Fluctuation and Flicker Caused by Distributed Generation [J]. Energy Engineering, 2006(4) : 54-58.

[2] Vora Animesh," Congestion Management in Degulated Power System- A Review", International Journal of Science and Research vol.3 Issue 6, June 2014, pp 2237-2240.

[3] K. Uhlen, L. Warland and O.S. Grande, "Model for Area Price Determination and Congestion Management in Joint Power Market," IEEE International Symposium CIGRE, 5-7 Oct.2005,pp 100-109.

[4] L.A.Taun, K.Bhattacharya and J.Daalder, "A Review On Congestion Management Methods in Deregulated Electricity Market", PES-2004'

[5] A. J. Wood and B. E. Wollenberg, Power generation, operation and control, 2nd ed., New York: Wiley Interscience, 1996..

Multi Level H Bridge Inverter

Dr. Vodapalli Prakash

Kakatiya Institute of Technology & Science, Warangal, Telangana, India

Abstract:

In this paper concentrated on the design of a multilevel inverter and increase number of levels with low number of switches at the output without adding any complexity to the power circuit. Advantage of this implementation is to reduce the total harmonic distortion and increase output voltage. The simulation is done by Matlab2017 software.

Keywords:

Cascaded H- bridge multilevel inverter, pulse width modulation

1. INTRODUCTION

Power electronic converters, especially dc/ac PWM inverters have been extending their range of use in industry because they provide reduced energy consumption, better system efficiency, improved quality of product, good maintenance, and so on. For a medium voltage grid, it is troublesome to connect only one power semiconductor switches directly . As a result, a multilevel power converter structure has been introduced as an alternative in high power and medium voltage situations such as laminators, mills, conveyors, pumps, fans, blowers, compressors, and so on. As a cost effective solution, multilevel converter not only achieves high power ratings, but also enables the use of low power application in renewable energy sources such as PV, wind and fuel cells which can be easily interfaced to a multilevel converter system for a high power application.

The most common basic application of multilevel converters has been in traction, both in locomotives and track-side static converters. More recent applications have been for power system converters for VAR compensation and stability enhancement , active filtering , high-voltage motor drive , high-voltage dc transmission , and most recently for medium voltage induction motor variable speed drives . Many multilevel converter applications focus on industrial medium-voltage motor drives , utility interface for renewable energy systems , flexible AC transmission system (FACTS) , and traction drive systems . The inverters in such application areas as stated above should be able to handle high voltage and large power. For this reason, two-level high-voltage and large-power inverters have been designed with series connection of switching power devices such as gate-turn-off thyristors (GTOs), integrated gate commutated transistors (IGCTs), and integrated gate bipolar transistors (IGBTs), because the series connection allows reaching much higher voltages. However, the series connection of switching power devices has big problems, namely, non equal distribution of applied device voltage across series-connected devices that may make the applied voltage of individual devices much higher than blocking voltage of the devices during transient and steady-state switching operation of devices. As alternatives to effectively solve the above-mentioned problems, several circuit topologies of multilevel inverter and converter have been researched and utilized. The output voltage of the multilevel inverter has many levels synthesized from several DC voltage sources. The advantages of cascade multilevel inverters were prominent for motor drives and utility applications.

A multilevel converter can be implemented in many different ways. The simplest techniques involve the parallel or series connection of conventional converters to form the multilevel waveforms . More complex structures effectively insert converters within converters . The voltage or current rating of the multilevel converter becomes a multiple of the individual switches, and so the power rating of the converter can exceed the limit imposed by the individual switching devices.

The elementary concept of a multilevel converter to achieve higher power is to use a series of power semiconductor switches with several lower voltage dc sources to perform the power conversion by emphasizing a staircase voltage waveform. Capacitors, batteries, and renewable energy voltage sources can be used as the multiple dc voltage sources. The commutation of the power switches aggregate these multiple dc sources in order to achieve high voltage at the output; however, the rated voltage of the power semiconductor switches depends only upon the rating of the dc voltage sources to which they are connected.

Multilevel converters do have some disadvantages. One particular disadvantage is the greater number of power semiconductor switches needed. Although lower voltage rated switches can be utilized in a multilevel converter, each switch requires a related gate drive circuit. This may cause the overall system to be more expensive and complex.

Multilevel Inverters (MLI) comprises an array of power semiconductor device and DC/capacitor voltages, which generates output voltage level with stepped waveform.

The aim of MLI is to generate a near sinusoidal voltage waveform with several steps by utilizing the proper switching signal of the semiconductor devices and isolated or non-isolated DC voltage sources . Increasing the number

of level in output waveform leads to attain pure sinusoidal voltage without expensive passive filters and bulky transformers . High frequency multilevel inverter waveform requires less passive filter when compared to other waveform.

MLI topologies are a cost effective solution for many industries because of their various benefits. It consists of DC sources and semiconductor devices whose count depends on the structure of configuration and output voltage level.

Multilevel inverters are classified as

• Diode clamped multilevel inverter • Flying capacitors multilevel inverter • Cascaded H- bridge multilevel inverter

The main concept of Diode clamped MLI is to use diodes and provides the multiple voltage levels through the different phases to the capacitor banks which are in series. A diode transfers a limited amount of voltage, thereby reducing the stress on other electrical devices. The maximum output voltage is half of the input DC voltage. It is the main drawback of the diode clamped multilevel inverter. This problem can be solved by increasing the switches, diodes, capacitors. Due to the capacitor balancing issues, these are limited to the three levels. This type of inverters provides the high efficiency because the fundamental frequency used for all the switching devices.

In Flying capacitor MLI, switching states are like in the diode clamped inverter. Clamping diodes are not required in this type of multilevel inverters. The output is half of the input DC voltage. It is drawback of the flying capacitors multi level inverter. It also has the switching redundancy within phase to balance the flying capacitors. It can control both the active and reactive power flow. But due to the high frequency switching, switching losses will takes place.

The voltage across the capacitors is considered to be half of DC source voltage Vdc . The output voltage consists of five different voltage levels Vdc, (+Vdc/2),0, (-Vdc/2) and Vdc

Phase redundancies are available for balancing the voltage level of the capacitors.

2. MODELLING

The main objective of this topology is to increase number of levels with a reduced number of switches without adding any complexity to the power circuit. The main objective of this topology is to increase number of levels with a reduced number of switches without adding any complexity to the power circuit. In this project, various carrier pulse width modulation techniques are proposed, which can minimize the total harmonic distortion and enhances the output voltages from proposed work of five level inverter. The output of each H- bridge can have three discrete levels, results in a staircase waveform that is nearly sinusoidal even without filtering. A single H-bridge is a three-level inverter. Each single-phase full-bridge inverter generates three voltages at the output: +Vdc , 0 and – Vdc.

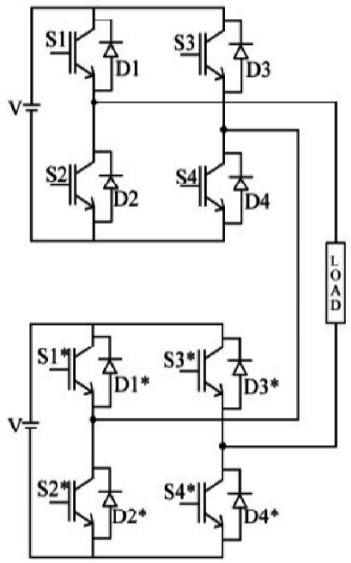

Fig:1 Cascaded H-Bridge Multilevel Invereter

For phase opposition disposition modulation all carrier waveforms above zero reference are in phase and are 180° out of phase with those below zero. The rules for the phase opposition disposition method, when the number of level N = 5

1. The N –1 = 4 carrier waveforms are arranged so that all carrier waveforms above zero are in phase and are 180 out of phase with those below zero
2. The converter is switched to + Vdc when the reference is greater than both carrier waveforms.
3. The converter is switched to zero when the reference is greater than the lower carrier waveform but less than the upper carrier waveform.
4. The converter is switched to +2Vdc when the reference is less than both carrier waveforms.
5. When the modulation signal is greater than both the carrier waveforms, S1 and S2 are turned on and the converter switches to positive node voltage and when the reference is less than the upper carrier waveform but greater than the lower carrier, S2and S1 are turned on and the converter switches to neutral point. When the reference is lower than both carrier waveforms, S1an and S2an are turned on and the converter switches to negative node voltage.

IN PHASE DISPOSITION :

There in, the a-phase modulation signal is compared with two triangle waveforms. The rules for the in phase disposition method, when the number of level N = 5, are

1. The N –1 = 5-1= 4 carrier waveforms are arranged so that every carrier is in phase. 2. The converter is switched to +Vdc when the reference is greater than both carrier waveforms.

3. The converter is switched to zero when the reference is greater than the lower carrier waveform but less than the upper carrier waveform.
4. The converter is switched to 2Vdc when the reference is less than both carrier waveforms

Calculation of switching angles:

The number of H-bridges N=(m-1)/2

$\alpha i = (i*180)/m$, where i=1,2,….(m-1)/2

where m=level of output voltage

α= switching angle

where α1=36°, α2=72°, α3=180°-72°, α4=180°-36°, α5=180°+36°, α6=180°+72°, α7=360°-72°, α8=360°-36°

50 cycles……1 second

I cycle= 0.02 seconds

3. RESULTS AND ANALYSIS

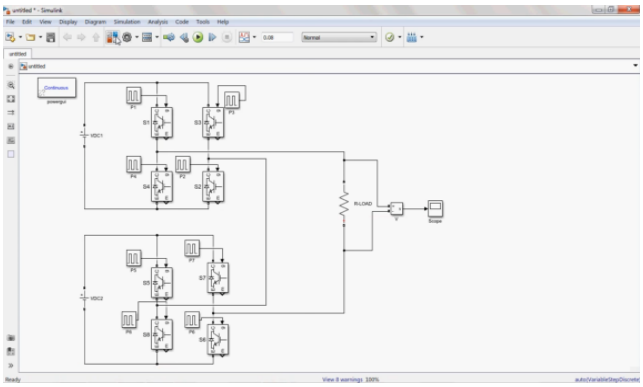

Fig.2 Five Level H bridge Inverter with 8 Switches

Fig.3 Switching table and wave forms

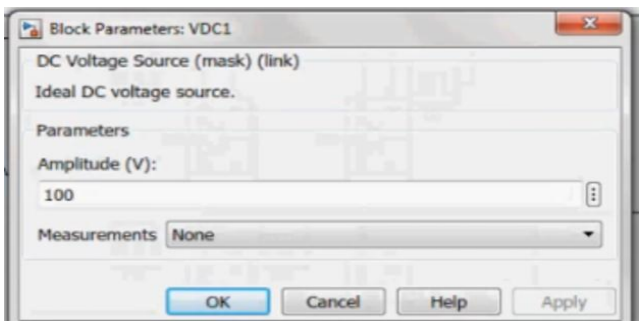

Fig.4 Input Parameters

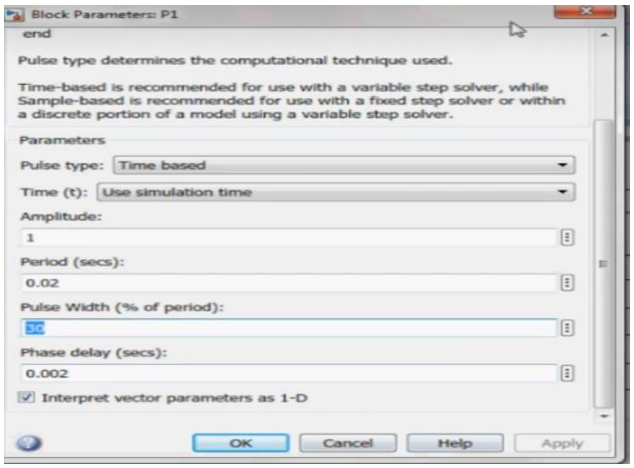

Fig. 5 Pulsewidth

Fig. 6 Output waveform

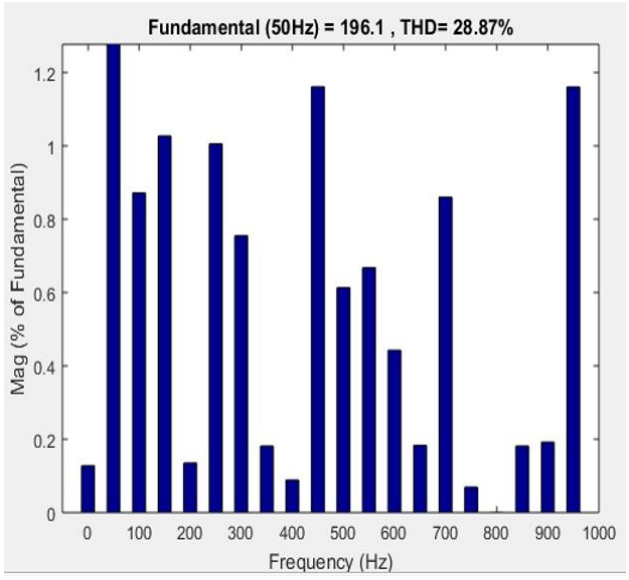

Fig.7 THD of Five Level H bridge with 8 Switches using PWM

 ISBN: 978-93-90214-20-4

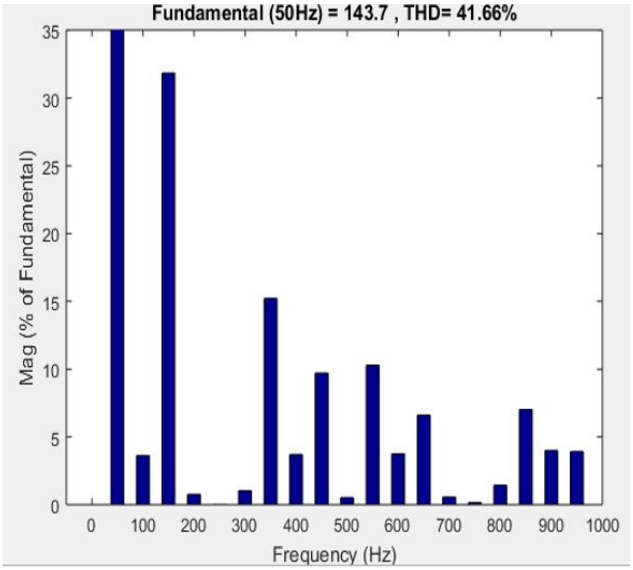

Fig. 8 THD of Five Level H bridge with 8 Switches using PWM

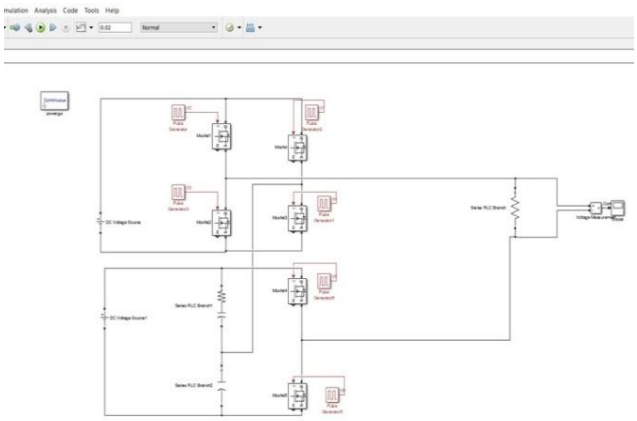

Fig. 9 With six switches

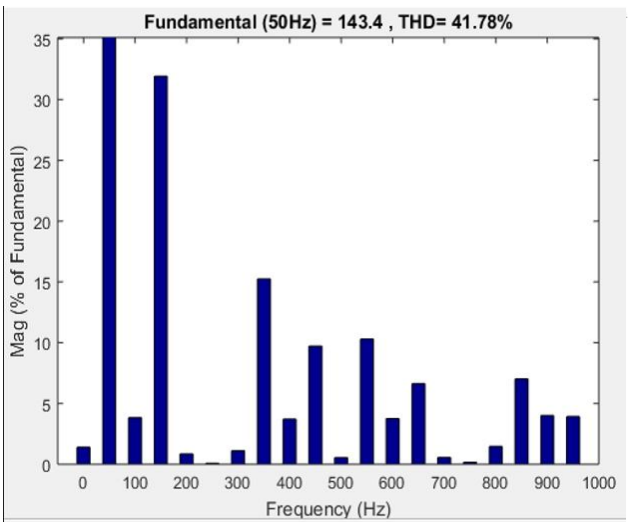

Fig. 10 THD of Five Level H bridge with 6 Switches

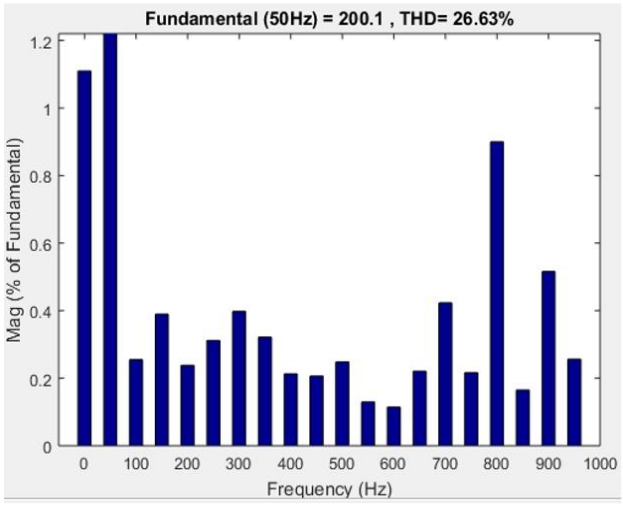

Fig.11 THD of Five Level H bridge with 6 Switches (PWM)

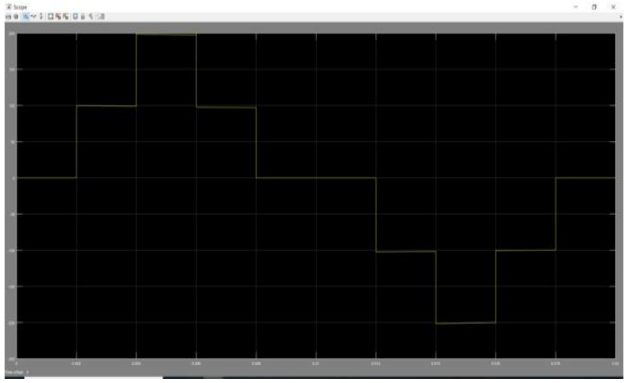

Fig.12 Output waveform with reduced(6) switches

4. CONCLUSIONS

The proposed work of five level multilevel cascade inverter output voltage total harmonics distortion is reduced and improve the efficiency of system compare with other methods.The THD is low compared to other. This topology minimized in terms of cost, losses and filter size.

REFERENCE

[1] M. F. Escalante, J. C. Vannier, and A.Arzande “Flying Capacitor Multilevel Inverters and DTC Motor Drive Applications,” IEEE Transactions on Industry Electronics, vol. 49, no. 4, Aug. 2002, pp. 809-815.

[2] Krishna Kumar Gupta, Alekh Ranjan, Pallavee Bhatnagar, Lalit Kumar Sahu, and Shailendra Jain,“ Multi Level Inverter Topologies” IEEE transactions on power electronics, January 2016 ,vol. 31, no.1.

[3] M.Kavitha,A.Arun Kumar,N.Gokulnath, “ New Cascaded H- Bridge Multilevel Inverter with Reduced number of Switches”, Sep 2012, IOSR – JEEE.

[4] J. Rodriguez, J.-S. Lai, and F. Z. Peng, "Multilevel inverters: a survey of topologies, controls, and applications," IEEE Trans. Ind. Electron.,2002, vol. 49, pp. 724-738.

[5] Kureve D. Teryima , Agbo O. David and Samuel T. Awuhe ," THD Analysis of SPWM For a 5 Level Cascaded H-bridge Multilevel Inverter", International Journal of Advanced Science and Technology Vol.87 (2016), pp.47-56.
[6] M. E. Kathar, prof. S .M.Kulkarni "Comparative study of Multilevel Inverter Topologies" International journal of Engineering Sciences & Research Technologies, April 2017.
[7] Jainil K. Shah, Manish S. Patel "Comparative Analysis of Single Phase Cascaded H-Bridge Multilevel inverter" International Journal of innovative research in Electrical, Electronics, Instrumentation and Control Engineering Issue 4, April 2015, Vol. 3, Issue 4.

Image Segmentation and Lung Cancer Classification through Neural Network for CT Scan Images

[1] Paramjit Singh, [2] Dr. Pankaj Nanglia, [3] Vikrant Shokeen, [4] Dr. Aparna N Mahajan

[1] Research Scholar, Maharaja Agrasen University, Himachal Pradesh, India
[2][4] Assistant Professor, Maharaja Agrasen University, Himachal Pradesh, India
[3] Assistant Professor, MSIT, Delhi, India

Abstract:

Lung cancer is the most common cause of death in the world. The total 5-year survival rate for lung cancer, which combines all stages, is approximately 20%. Early detection of Lung cancer can save a lot of number of lives. An image processing technique is being developed to classify the stages of lung cancer. Manual computation of Lung Cancer is a time taking process. In the medical industry, Computer Aided Detection (CAD) aims to optimize the classification process. This paper proposes Lung Cancer Detection for computed tomography (CT) images. It uses Speed up robust feature (SURF) for feature extraction, Cuckoo search(CSA), Fire fly algorithm(FFA) for feature optimization and Feed Forward Back Propagation Neural Network (FBBPNN) for classification. The training mechanism utilizes 500 cancerous images and the proposed method results in 96.5% classification accuracy and 94.8% sensitivity. This paper also discusses the possible future modifications in the presented work.

Keywords:

Medical Engineering, Lung Cancer, Image Processing, Feature Extraction, Classification, CAD, SURF, CT, GA, FFBPNN

1. INTRODUCTION

Lung Cancer has caused thousands of deaths in the last couple of years. The process of detection of cancer is not easy (Holzinger et al., 2014). The accurate detection of most of the patient is done at advanced stages (Kuruvilla and Gunavathi, 2015) [1-4] SAD can be very useful for early detection of lung cancer. SAD divides the detection process into two phases namely Training and Classification. Figure 1 illustrates the working of SAD.

Figure 1 shows two adjoined processes namely training and classification. The classification process is often termed as detection process as well (Braga et al., 2008) [5-7] It starts with the training mechanism. The training involves feature extraction, followed by optimization. The optimized feature vector is passed to the learning model of the classification algorithm. As shown in Figure 1, after training, the trained set is stored in a database. There are several feature extraction and optimization algorithms. Some of them are listed in the literature (Farag et al., 2011),[8-9] utilized geometric feature descriptors namely scale-invariant feature transform (SIFT) and SURF is utilized to extract feature vectors (Camarlinghi et al., 2012). These extracted feature vectors are then utilized in a ratio by the proposed algorithm. Later, the classification is done using k-Nearest Neighbour (k-NN) (Krishnaiah et al., 2013). The proposed algorithm has used data-driven template-matching approach over the CT images (Han et al., 2010),[10-13] utilized SURF and presented a neighbourhood selection algorithm for the optimization of key points. The extracted features are utilized for the automated registration process. It took scaled data in the first step.

The extracted feature set is optimized using GA and then a hyperplane selection algorithm for Support Vector Machine (SVM)[14-17] is applied. The training and classification both the activities are performed by SVM (Hemamalini et al., 2016), utilized both Magnetic Resonance Imaging (MRI) and CT images for the analysis (Kureshi et al., 2016). SIFT and SURF is used for feature vector extraction (Ma et al., 2017). The evaluated results show that SURF depicts a number of key-points as compared to SIFT and it gets an edge over SIFT in this comparison. (Huang and Wang, 2006), utilized GA for the betterment of feature vector.[18-22]

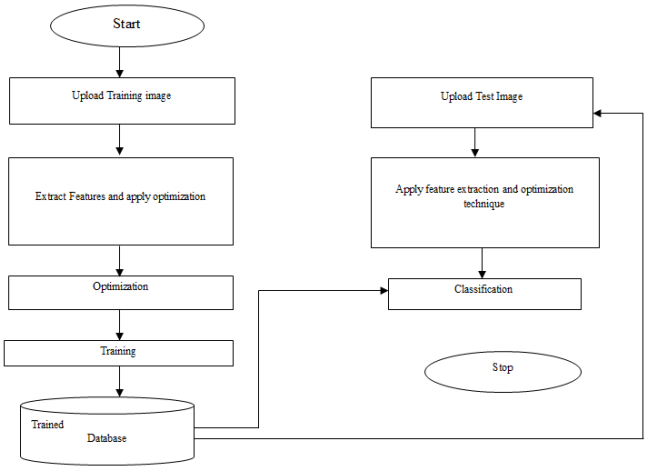

Figure 1 Working of CAD

The optimized vector is passed to the Radial Basis Function (RBF) of SVM for classification. The performance evaluation is done on the basis of accuracy weight, true positive (tp), and false positive (FP) ratio (Lee et al., 2001) also utilized GA for optimization of feature vectors. Further, the work is carried out for template matching (Gunavathi and Premalatha, 2015), proposed lung cancer classification mechanism using k-NN and cuckoo search. The utilized fitness function aims to reduce the complexity of classification (Kuruvilla and Gunavathi, 2015), proposed the classification mechanism using Artificial Neural Fuzzy Inference System (ANFIS). The proposed work is compared with the Fuzzy Inference System (FIS) and it uses Principal Component Analysis (PCA) for feature extraction.[23-24]

2. PROPOSED SOLUTION

The proposed solution uses SURF for feature vector extraction. As per the literature, optimization is necessary for feature vectors and therefore, GA is applied for the same. The proposed solution trains the optimized feature set using the FFBP Neural Network. The trained set is then passed for the classification.

2.1 Feature Extraction and Training

SURF results in key point feature vector. A total of 100 affected lung cancer images are binarized and then passed as input to it.

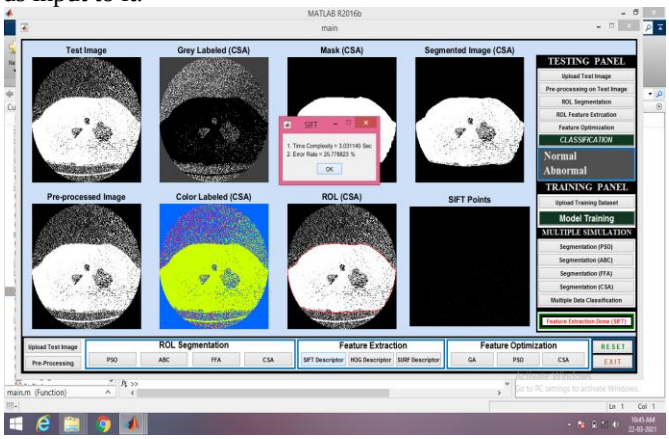

Figure 2 shows different stages of binarization of the CT image (Choi et al., 2012).

Table 1 Feature vector of SURF, SIFT and PCA

Image	PCA->Principle Eigen Vector)	SIFT-> Key Points	SURF -> Key Points
Image 1(255 * 394)	256 *1	252*252	221*64
Image 2 (194*259)	256 *1	253*252	166*52
Image 3 (182*276)	256 *1	252*252	169*28
Image 4 (193*200)	256 *1	253*252	192*52

Table 1 illustrates the feature vectors extracted by SIFT, PCA, and SURF. Figure 3 shows the feature vector extracted by SIFT, SURF, and PCA.

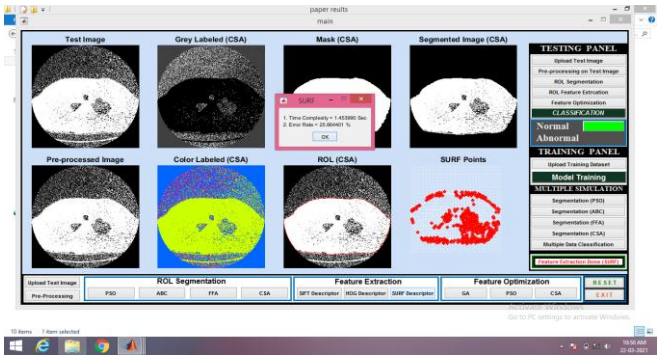

Figure 3 Feature extraction algorithms

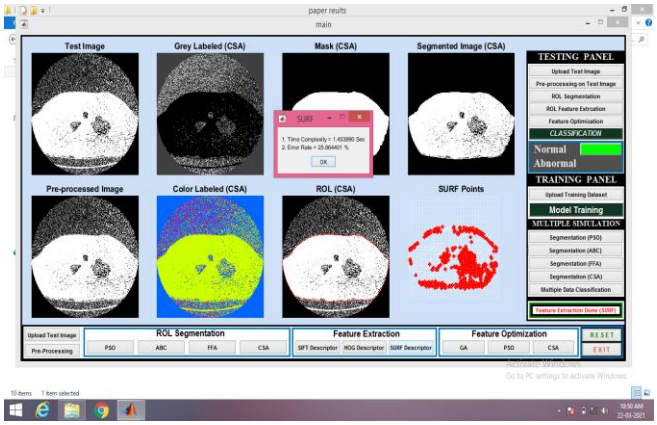

Figure 3 Feature vectors of feature extraction by SURF, SIFT and HOG algorithms

SURF key points maps to most of the ROI part extracted in Figure 2 whereas, for the same input image, the key points of other algorithms do not provide close competition to SURF (Nanglia et.al, 2021).

The proposed work has tested the key points by adding some noise to all the key features of each algorithm. How much any feature is pronto noise, can be evaluated by Peak Signal to Noise Ratio (PSNR). Each feature set is passed with the white Gaussian noise of intensity 0.1 followed by the PSNR evaluation.

$$\text{PSNR} = 10 * \text{Log10}\left(\frac{256^2}{\text{MSE}}\right) \quad (1)$$

Table 2 PSNR with white Gaussian Noise

PCA---- Average PSNR	SIFT----- Average PSNR	SURF---- Average PSNR
42.24	44.25	44.56

The PSNR of SURF is recorded to be the highest among all the three feature extraction technique. Hence SURF is finally selected as the key feature holder for further processing.

The extracted feature set is passed to GA for the optimization and the following fitness function is utilized for the processing.

Table 3 Used Genetic Fitness Function

GA Fitness	if f(r) > $f(t)$ 0 otherwise

Where f(r) is current feature vector and f(t) is the threshold of selection. The SURF features are reduced by 20-25% after implementing GA.

The optimized feature set is passed to FFBP NN for training. FFBP NN is a multiclass classifier with Feed forwarding in order to satisfy the stopping constraints and it back propagates in order to validate the Mean Square Error (MSE). NN mainly encompasses the three-layer mechanism. A brief description of layers of NN is as follow.

- Input Layer: Takes the feature vector as input. No processing is done at this layer other than forwarding the data to the intermediate layer with 'n' number of neurons.
- Hidden Layer: The hidden layer utilizes weight function to convert data into a format, which is understandable by the architecture of machine learning. The weight function may be of the following types:

Linear: $w = ax + b$ (2)

Quadratic: $w = ax^2 + bx + c$ (3)

Polynomial: $w = (ax + b)^k$ (4)

Where w is the converted weight of the input set. a, b and c are the arbitrary constants. k is the polynomial power constraint.

The simulation is performed by using MATLAB's Neural Network Toolbox. The toolbox helps in the selection of the type of weight function depending upon the type of data utilized.

- Output Layer: It can be further divided into two sub-categories namely the output layer for the training data and output layer for the test data. The training architecture of utilized Feed Forward Back Propagation Neural Network is as follow.

Algorithm Train_NN(N1, Opt_set1, N2, Opt_set2)

Where N1= Total number of cancerous images

Opt1= Optimized Feature vector for N1

N1= Total number of cancerous images

Opt1= Optimized Feature vector for N1

1. gcount=1; Train_set=[ ]; //group count
2. Foreachfvec in Opt1.Row
3. Train_set(gcount,:)= Opt1_set1.Row.Value // Placing feature vector
4. Group(gcount)=1;
5. Gcount=gcount+1;
6. End For
7. Foreach fvec1 in Opt_set2.Row
8. Train_set(count,)=Opt_set.Row.Value
9. Group(count)=2
10. End For
11. Net=newff(Train_set, Group,20) // Initializing Neural Network(NN) Machine Learning with the train set, its target set named as a group and 20 Neurons. The neurons will help the hidden layer to initiate the weight machines.
12. Net.trainingparameters.addparameters(total iteration)=50; // Initialized neuron framework with 50 iteration at max. If the provided set of iterations is 50 even, then it is not necessary that it will have to complete 50 iterations. It depends upon the validation parameter value that how much iterations are required to process.
13. Train.Machine(Net); // Performing Training

The train set is initialized as empty and groupset is accordingly set. The train set will contain both the values of the cancerous and the non-cancerous feature set. This data is passed to Neural training with varying weight function and the following training architecture is obtained.

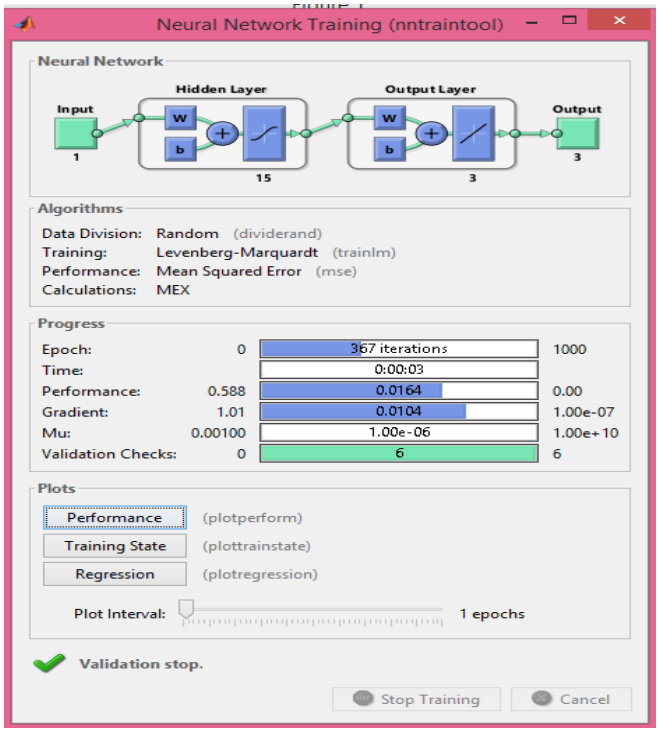

Figure 4 FFBPNN Training

Figure 4 demonstrates the complete working of the Neural Network training mechanism. The parametric architecture for Neural Network is as follows:

i. Total Iterations Max=500;
ii. Validation Parameters: 4
iii. Passed Number of Neurons:15
iv. Attained Iteration: 300-400
v. Numbers of Times Training done: 100

The utilization of NN gives an edge of checking the back-propagation mechanism. Figure 5 demonstrates the results of back propagation.

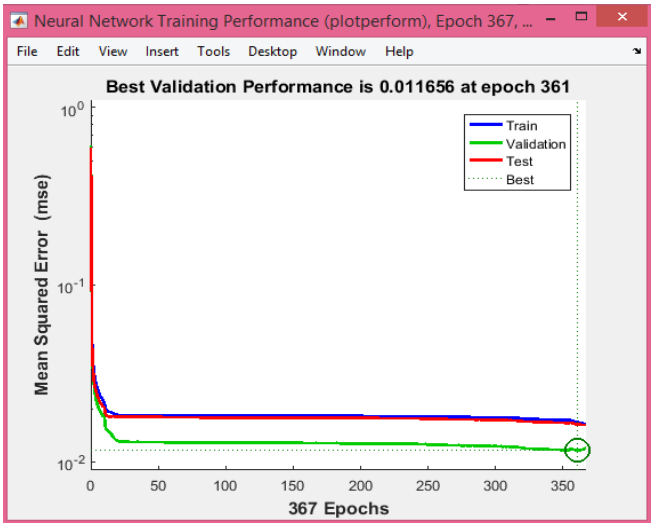

Figure 5 Back Propagation (BP)

Figure 5 represents the back propagation of NN. Out of 8 iterations, the structure of 2nd iterations are selected. This is because of the cross-reference of train data and validation data generated by the tool itself.

3. EXPERIMENTAL RESULTS

The train set contains around 76% of the total data and rest is used as a test set. Sensitivity and accuracy are calculated and is compared with (Kuruvilla and Gunavathi, 2015).

Sensitivity is the measure of true classified images out of true-labeled images.

$$\text{Sensitivity} = \text{True Positive} / (\text{True Positive} + \text{False Negative}) \quad (5)$$

Accuracy is the measure of performance in terms of true classification. In other words, how efficiently a classifier judges the affected samples, can be measured by accuracy.

$$\text{Accuracy} = (\text{True Positive} + \text{True Negative}) / (\text{True Positive} + \text{True Negative} + \text{False Positive} + \text{False Negative}) \quad (6)$$

True Negative= Left not affected samples out of total samples

False Negative = Left affected samples out of total samples

True Positive = True classified samples out of total samples

False Positive= False classified samples for true samples

The average classification accuracy obtained by the proposed algorithm is 96.5 %. The average sensitivity of the proposed algorithm is 94.8%. Compared to (Kuruvilla and Gunavathi, 2015), the percentage growth is about 1-2.5%."

4. CONCLUSION

"This paper proposed a software aided detection supported by SURF, GA, and FFBP-NN. The proposed algorithms also tested SIFT and PCA for feature vector in the preliminary phases. The PSNR after adding the white Gaussian noise to the feature vectors stood 41.23 43.15 and 44.65 namely for PCA, SIFT, and SURF.70% of the entire data is used for the training and rest for the classification. The feature vectors obtained by SURF are modified using GA. GA results into a reduced set of SURF feature vector by 20%. The optimized feature set is then trained by FFBP-NN. The classification parameters are sensitivity and classification accuracy. The proposed algorithm obtains a classification accuracy of 96.5% whereas the obtained average sensitivity is 94.8%. It is then compared with previous implemented Kuruvilla's algorithm and stands a growth of 1-2.5 % for both the parameters.

The future possibilities may include variation in the fitness function in the present work. The future research workers may also try their hand at varying neuron count for training."

REFERENCE

[1] Braga, P. L., Oliveira, A. L., & Meira, S. R. (2008, March). A GA-based feature selection and parameters optimization for support vector regression applied to software effort estimation. In Proceedings of the 2008 ACM symposium on Applied computing (pp. 1788-1792). ACM.

[2] Camarlinghi, N., Gori, I., Retico, A., Bellotti, R., Bosco, P., Cerello, P., & Fantacci, M. E. (2012).Combination of computer-aided detection algorithms for automatic lung nodule identification. International journal of computer assisted radiology and surgery, 7(3), 455-464.

[3] Choi, W. J., & Choi, T. S. (2012). Genetic programming-based feature transform and classification for the automatic detection of pulmonary nodules on computed tomography images. Information Sciences, 212(1), 57-78.

[4] Farag, A., Ali, A., Graham, J., Farag, A., Elshazly, S., & Falk, R. (2011, March). Evaluation of geometric feature descriptors for detection and classification of lung nodules in low dose CT scans of the chest.In Biomedical Imaging: From Nano to Macro, 2011 IEEE International Symposium on (pp. 169-172). IEEE.

[5] Gunavathi, C., & Premalatha, K. (2015). Cuckoo search optimisation for feature selection in cancer classification: a new approach. International journal of data mining and bioinformatics, 13(3), 248-265.

[6] Han, X. (2010). Feature-constrained nonlinear registration of lung CT images. Medical image analysis for the clinic: a grand challenge, 63-72.

[7] P. Nanglia, S. Kumar, A. N. Mahajan, P. Singh and D. Rathee, "A hybrid algorithm for lung cancer classification using SVM and Neural Networks," *ICT Express Science Direct*, vol. 3, no. 2, pp. 1-7, 2020.

[8] P. Nanglia, A. N. Mahajan, P. Singh and D. Rathee, "Detection & Classification of Lung Cancer at an

Early Stage by Applying Feature Extraction Optimization and Neural Network on Hybrid Structure," International Journal of Innovative Technology and Exploring Engineering (IJITEE) Scopus, vol. 9, no. 2, pp. 3737-3745, 2019.

[9] P. Singh, P. Nanglia and A. N. Mahajan, "Improved Lung Cancer Segmentation Using K-Means and Cuckoo Search," International Journal of Innovative Technology and Exploring Engineering (IJITEE) Scopus, vol. 9, no. 2, pp. 3746-3758, 2019.

[10] P. Nanglia, S. Kumar, D. Rathee and P. Singh, "Comparative Investigation of Different Feature Extraction Techniques for Lung Cancer Detection System," in International Conference on Advanced Informatics for Computing Research (ICAICR) Springer, Himachal Pradesh, 2018.

[11] Shallu, P. Nanglia, S. Kumar and A. K. Luhach, "Detection and Analysis of Lung Cancer Using Radiomic Approach," in International Conference on Computational Strategies for Next Generation Technologies Springer, Punjab, 2017.

[12] P. Nanglia, A. N. Mahajan, D. S. Rathee and S. Kumar, "Lung cancer classification using feed forward back propagation neural network for CT images," International Journal of Medical Engineering and Informatics, vol. 12, no. 5, pp. 447-456, 2020.

[13] Juan, L., & Gwun, O. (2009). A comparison of sift, pca-sift and surf. International Journal of Image Processing (IJIP), 3(4), 143-152.

[14] Burger, W., Burge, M. J., Burge, M. J., & Burge, M. J. (2009). Principles of digital image processing (p. 221). London: Springer.

[15] Pang, Y., Li, W., Yuan, Y., & Pan, J. (2012). Fully affine invariant SURF for image

[16] matching. Neurocomputing, 85, 6-10. Huijuan, Z., & Qiong, H. (2011, September). Fast image matching based-on improved SURF algorithm.

[17] In Electronics, Communications and Control (ICECC), 2011 International Conference on (pp. 1460-1463). IEEE.

[18] Whitley, D. (1994). A genetic algorithm tutorial. Statistics and computing, 4(2), 65-85.

[19] Houck, C. R., Joines, J., & Kay, M. G. (1995). A genetic algorithm for function optimization: a Matlab implementation. Ncsu-ie tr, 95(09).

[20] Karaboga, D., & Basturk, B. (2007). A powerful and efficient algorithm for numerical function optimization: artificial bee colony (ABC) algorithm. Journal of global optimization, 39(3), 459-471.

[21] Fourie, P. C., & Groenwold, A. A. (2002). The particle swarm optimization algorithm in size and shape optimization. Structural and Multidisciplinary Optimization, 23(4), 259-267.

[22] Narayanan, B. N., Hardie, R. C., Kebede, T. M., & Sprague, M. J. (2017). Optimized feature selection-based clustering approach for computer-aided detection of lung nodules in different modalities. Pattern Analysis and Applications, 1-13.

[23] Hawkins, S. H., Korecki, J. N., Balagurunathan, Y., Gu, Y., Kumar, V., Basu, S., ... & Gillies, R. J. (2014). Predicting outcomes of nonsmall cell lung cancer using CT image features. IEEE Access, 2, 1418-1426.

[24] Westaway, D. D., Toon, C. W., Farzin, M., Sioson, L., Watson, N., Brady, P. W., ... & Gill, A. J. (2013). The International Association for the Study of Lung Cancer/American Thoracic Society/European Respiratory Society grading system has limited prognostic significance in advanced resected pulmonary adenocarcinoma. Pathology-Journal of the RCPA, 45(6), 553-558.

[25] Hawkins, S. H., Korecki, J. N., Balagurunathan, Y., Gu, Y., Kumar, V., Basu, S., ... & Gillies, R. J. (2014). Predicting outcomes of nonsmall cell lung cancer using CT image features. IEEE Access, 2, 1418-1426.

An Efficient and Secure Electronic Payment Protocol through E Commerce

[1] Dr.V.Geetha, [2] Dr.C.K.Gomathy, [3] HemanthReddy, [4] M.ChaitanyaKumar Reddy

[1][2] Assistant Professor/CSE SCSVMV University, Kanchipuram, India
[3][4] UG Scholar /CSE SCSVMV University, Kanchipuram, India

Abstract:

E-commerce implies an electronic purchasing and marketing process online by using typical Web browsers. As e-commerce is quickly developing on the planet, particularly in recent years, many areas of life are affected, particularly the improvement in how individuals regulate themselves non-financially and financially in different transactions. In electronic payment or e-commerce payment, the gateway is a major component of the structure to assure that such exchanges occur without disputes, while maintaining the common security over such systems. Most Internet payment gateways in e-commerce provide monetary information to customers using trusted third parties directly to a payment gateway. Nonetheless, it is recognized that the cloud Web server is not considered a protected entity. This article aims to develop an efficient and secure electronic payment protocol for e-commerce where consumers can immediately connect with the merchant properly. Interestingly, the proposed system does not require the customer to input his/her identity in the merchant's website even though the customer can hide his/her identity and make a temporary identity to perform the service. It has been found that our protocol has much improved security effectiveness in terms of confidentiality, integrity, non-repudiation, anonymity availability, authentication, and authorization.

Keywords:

e-commerce; electronic payments system; payments gateway

1. INTRODUCTION

E-commerce was introduced to the consumer and business worlds as a unique approach in 1990. E-commerce is becoming very popular nowadays since the customer can spend from home; solutions are affordable, with items delivered to the home with no hassle. The popularity of e-commerce is mainly because of its online business perspective. It makes it possible to gain and sell goods online, to provide various services and information through the Internet, and to exchange money immediately between businesses.In the electronic payment system, the payment gateway is an essential component of the infrastructure to confirm that such exchanges happen with no concerns and to ensure that the common security over electronic systems is maintained.Such a system will help secure a purchase along with a person's transaction information. A payment gateway defends transaction information by encrypting personal information, such as credit/debit card details, to guarantee that information is transferred securely between a consumer and the transaction processor. Each online exchange should go through a managed transaction gateway.The e-payment system must be harmless for online transaction applicants, for instance, fee gateway server, bank account server, and merchant server.

2. LITERATURE REVIEW:

Electronic payment systems have continued to grow over recent years because of the increase of online banking and shopping.Specifically, online buyers have to feel comfortable that their personal information and banking details are protected and cannot be seen by hackers. Thus, a connection that is secure it needed to assure payment transactions. Identity theft and phishing fraud are the two most popular types of fraud found within the Internet store.To mitigate both types of fraud, a new secure electronic payment gateway to offer authorization was proposed.

The main objective of this proposed method was to provide authorization confidentiality, integrity, and availability for transactions. In their study, the authors utilized the Triple Data Encryption Standard (TDES, more often referred to as 3DES) cryptosystem to encrypt the transaction information and accomplish a greater speed of transactions within the payment gateway. The 3DES algorithm utilizes the data encryption standard (DES) cipher three times to encrypt its information.As a symmetric crucial cipher, it applies a similar element for both encryption and decryption processes. The Feistel cipher can make both processes almost precisely the same, whichresults in an algorithm that is more effective to put into action.3DES was created as a safe option due to DES's small crucial length. In 3DES, the DES algorithm is operated three times with three secrets and is regarded as safe in the event that three individual keys are used. To protect vulnerable cardholder information during transmission, good cryptographic and security protocols must be used. They encourage cryptographic libraries, such as certified AES and 3DES.However, the most recent improvement, referred to as AES, isslow. Therefore, 3DES is safer and faster. The 3DES algorithm utilizes the data encryption standard (DES) cipher three times to encrypt its information

3. PROPOSED SYSTEM

In previous work, a secure electronic payment gateway for e-commerce was proposed. we propose a secure protocol in e-commerce to enhance the security of the e-commerce process, which can also improve the security of existing work. Interestingly, the proposed system does not require the customer to input his/her identity in the merchant website even though the customer can hide his/her identity and make a temporary identity to process a request for the service. The proposed system is made up of five entities: client (C), merchant (M), payment gateway (PG), user bank (B), and merchant bank.The user initiates the transaction by mailing his short-term identity to the server. Be aware that the public key pair continues to be accredited through the certification authority.

SECURE ELECTRONIC TRANSACTION SET is an open encryption and security specification designed to protect credit card transactions on the Internet. The current version, SETv1, emerged from a call for security standards by MasterCard and Visa in February 1996. A wide range of companies were involved in developing the initial specification, including IBM, Microsoft, Netscape, RSA, Terisa, and Verisign. Beginning in 1996. SET is not itself a payment system. Rather it is a set of security protocols and formats that enables users to employ the existing credit card payment infrastructure on an open network, such as the Internet, in a secure fashion. In essence, SET provides three services:

• Provides a secure communications channel among all parties involved in a transaction

• Provides trust by the use of X.509v3 digital certificates

• Ensures privacy because the information is only available to parties in a transaction when and where necessary. SET Overview: A good way to begin our discussion of SET is to look at the business requirements for SET, its key features, and the participants in SET transactions. Requirements: The SET specification lists the following business requirements for secure payment processing with credit cards over the Internet and other networks:

• Provide confidentiality of payment and ordering information: It is necessary to assure cardholders that this information is safe and accessible only to the intended recipient. Confidentiality also reduces the risk of fraud by either party to the transaction or by malicious third parties. SET uses encryption to provide confidentiality.

• Ensure the integrity of all transmitted data: That is, ensure that no changes in content occur during transmission of SET messages. Digital signatures are used to provide integrity.

• Provide authentication that a cardholder is a legitimate user of a credit card account: A mechanism that links a cardholder to a specific account number reduces the incidence of fraud and the overall cost of payment processing. Digital signatures and certificates are used to verify that a cardholder is a legitimate user of a valid account.

• Provide authentication that a merchant can accept credit card transactions through its relationship with a financial institution: This is the complement to the preceding requirement. Cardholders need to be able to identify merchants with whom they can conduct secure transactions. Again, digital signatures and certificates are used.

• Ensure the use of the best security practices and system design techniques to protect all legitimate parties in an electronic commerce transaction: SET is a well-tested specification based on highly secure cryptographic algorithms and protocols.

• Create a protocol that neither depends on transport security mechanisms nor prevents their use: SET can securely operate over a "raw" TCP/IP stack. However, SET does not interfere with the use of other security mechanisms, such as IPSec and SSL/TLS.

• Facilitate and encourage interoperability among software and network providers: The SET protocols and formats are independent of hardware platform, operating system, and Web software. Key Features of SET To meet the requirements just outlined, SET incorporates the following features:

• Confidentiality of information: Cardholder account and payment information is secured as it travels across the network. An interesting and important feature of SET is that it prevents the merchant from learning the cardholder's credit card number; this is only provided to the issuing bank. Conventional encryption by DES is used to provide confidentiality.

• Integrity of data: Payment information sent from cardholders to merchants includes order information, personal data, and payment instructions. SET guarantees that these message contents are not altered in transit. RSA digital signatures, using SHA-1 hash codes, provide message integrity. Certain messages are also protected by HMAC using SHA-1.

• Cardholder account authentication: SET enables merchants to verify that a cardholder is a legitimate user of a valid card account number. SET uses X.509v3 digital certificates with RSA signatures for this purpose.

• Merchant authentication: SET enables cardholders to verify that a merchant has a relationship with a financial institution allowing it to accept payment cards. SET uses X.509v3 digital certificates with RSA signatures for this purpose. Note that unlike IPSec and SSL/TLS, SET provides only one choice for each cryptographic algorithm. This makes sense, because SET is a single application with a single set of requirements, whereas IPSec and SSL/TLS are intended to support a range of applications.

4. 3DES METHODOLOGY:

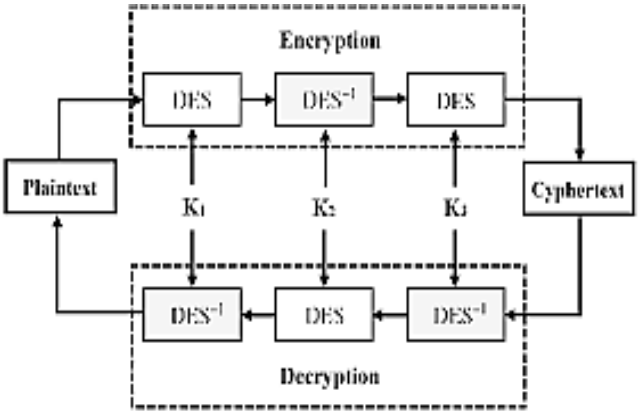

As mentioned above, all the public-key encryption and digital signature used in SET are based on the RSA scheme. RSA requires a relatively large computational cost and large message overhead. Based on \squareand-multiply" and \simultaneous multiple exponentiation,the main computational cost for one public-key encryption or one digital signature generation is estimated to be 1:5 4 jnj modulo multiplications where n is a composite of the RSA scheme. For PReq generation, for example, one public-key encryption and one digital signature generation are required, therefore the computational cost is estimated to be 768 modulo multiplications (jnj = 1024bit). Part of Table 9 shows computational costs for message generations and verications in SET, respectively. Turning now to message or communication over- head, digital signatures and public-key encrypted session keys are regarded as the main overhead. In addition, the hash variables (160bit) for message linking are also regarded as message overhead. The message over- head for one digital signature or public-key encrypted session key is estimated to be jnj.

5. CONCLUSION

Clients need such a secure system, because it satisfies all specifications and is a sufficient system. We proposed a secure electronic payment system for e-commerce environments on the basis of these requirements. In our proposed method, the transaction gateway functions as a proxy to communicate between the client/merchant and the bank. The security analysis demonstrated that the proposed plan has better protection effectiveness in terms of confidentiality, non-repudiation, integrity, availability, and anonymity. The extension of this article will focus on the utilization of our proposed framework in real-world applications by proving its ability to avoid various attacks and determine the time necessary for electronic payment.

REFERENCE

[1] Miva. The History of Ecommerce: How Did It All Begin?—Miva Blog. Available online: https://www.miva. com/blog/the-history-of-ecommerce-how-did-it-all-begin/ (accessed on 16 June 2020).

[2] Bezhovski, Z. The Future of the Mobile Payment as Electronic Payment System. Eur. J. Bus. Manag. 2016, 8, 2222–2839.

[3] Masihuddin, M.; Islam Khan, B.U.; Islam Mattoo, M.M.U.; Olanrewaju, R.F. A Survey on E-Payment Systems: Elements, Adoption, Architecture, Challenges and Security Concepts. Indian J. Sci. Technol. 2017, 10, 1–19.

[4] Hajira Be, A.B.; Balasubramanian, R. Developing an enhanced high-speed key transmission (EHSKT) technique to avoid fraud activity in E-commerce. Indones. J. Electr. Eng. Comput. Sci. 2018, 12, 1187–1194.

[5] Izhar, A.; Khan, A.; Sikandar, M.; Khiyal, H.; Javed, W.; Baig, S. Designing and Implementation of Electronic Payment Gateway for Developing Countries. J. Theor. Appl. Inf. Technol. 2011, 26, 3643–3648. [CrossRef] 13. European Union Agency for Cybersecurity. Algorithms, Key Sizes and Parameters Report—2013; European Union Agency for Cybersecurity: Eracleon, Greece, 2013;

A Spam Discovery Using Linguistic and Spammer Behavioural System

[1] Dr.V.Geetha, [2] Dr.C.K.Gomathy, [3] Palle Anurag Kashyap, [4] NalladimmuVenkatAniketReddy

[1][2] Assistant Professor/CSE SCSVMV University, Kanchipuram, India
[3][4] UG Scholar /CSE SCSVMV University, Kanchipuram, India

Abstract:

Online review systems play an important role in affecting consumers' behaviors and decision making, attracting many spammers to insert fake reviews to manipulate review content and ratings. To increase utility and improve user experience, some online review systems allow users to form social relationships between each other and encourage their interactions. In this paper, we aim at providing an efficient and effective method to identify review spammers by incorporating social relations based on two assumptions that people are more likely to consider reviews from those connected with them as trustworthy, and review spammers are less likely to maintain a large relationship network with normal users. The contributions of this paper are two-fold: (1) We elaborate how social relationships can be incorporated into review rating prediction and propose a trust-based rating prediction model using proximity as trust weight, and (2) We design a trust-aware detection model based on rating variance which iteratively calculates user-specific overall trustworthiness scores as the indicator for spamicity. Experiments on the dataset collected from Yelp.com show that the proposed trust-based prediction achieves a higher accuracy than standard CF method, and there exists a strong correlation between social relationships and the overall trustworthiness scores.

Keywords:

Spam, Linguistic, Spammer

1. INTRODUCTION

What Is A Social Network?

Wikipedia defines a social network service as a service which "focuses on the building and verifying of online social networks for communities of people who share interests and activities, or who are interested in exploring the interests and activities of others, and which necessitates the use of software."

A report published by OCLC provides the following definition of social networking sites: "Web sites primarily designed to facilitate interaction between users who share interests, attitudes and activities, such as Facebook, Mixi and MySpace."

Examples of Social Networking Services

Examples of popular social networking services include:

Facebook: Facebook is a social networking Web site that allows people to communicate with their friends and exchange information. In May 2007 Facebook launched the Facebook Platform which provides a framework for developers to create applications that interact with core Facebook features

MySpace: MySpace is a social networking Web site offering an interactive, user-submitted network of friends, personal profiles, blogs and groups, commonly used for sharing photos, music and videos.

Twitter: Twitter is an example of a micro-blogging service. Twitter can be used in a variety of ways including sharing brief information with users and providing support for one's peers.

Note that this brief list of popular social networking services omits popular social sharing services such as Flickr and YouTube.

Opportunities and Challenges

The popularity and ease of use of social networking services have excited institutions with their potential in a variety of areas. However effective use of social networking services poses a number of challenges for institutions including long-term sustainability of the services; user concerns over use of social tools in a work or study context; a variety of technical issues and legal issues such as copyright, privacy, accessibility; etc.

Institutions would be advised to consider carefully the implications before promoting significant use of such services.

2. LITRATURE SURVEY

A google wave-based fuzzy recommender system to disseminate information in University Digital Libraries 2.0

Nowadays Digital Libraries 2.0 are mainly based on the interaction between users through collaborative applications such as wikis, blogs, etc. or new possible paradigms like the *waves* proposed by Google. This new concept, the *wave*, represents a common space where resources and users can work together. The problem arises when the number of resources and users is high, then tools for assisting the users in their information needs are necessary. In this case a fuzzy linguistic recommender system based on the Google Wave capabilities is proposed as tool for communicating

researchers interested in common research lines. The system allows the creation of a common space by means a *wave* as a way of collaborating and exchanging ideas between several researchers interested in the same topic. In addition, the system suggests, in an automatic way, several researchers and useful resources for each wave. These recommendations are computed following several previously defined preferences and characteristics by means of fuzzy linguistic labels. Thus the system facilitates the possible collaborations between multi-disciplinar researchers and recommends complementary resources useful for the interaction. In order to test the effectiveness of the proposed system, a prototype of the system has been developed and tested with several research groups from the same university achieving successful results.

A hybrid fuzzy-based personalized recommender system for telecom products/services

The Internet creates excellent opportunities for businesses to provide personalized online services to their customers. Recommender systems are designed to automatically generate personalized suggestions of products/services to customers. Because various uncertainties exist within both product and customer data, it is a challenge to achieve high recommendation accuracy. This study develops a hybrid recommendation approach which combines user-based and item-based collaborative filtering techniques with fuzzy set techniques and applies it to mobile product and service recommendation. It particularly implements the proposed approach in an intelligent recommender system software called Fuzzy-based Telecom Product Recommender System (FTCP-RS). Experimental results demonstrate the effectiveness of the proposed approach and the initial application shows that the FTCP-RS can effectively help customers to select the most suitable mobile products or services.

3. RECOMMENDER SYSTEMS BASED ON SOCIAL NETWORKS

The traditional recommender systems, especially the collaborative filtering recommender systems, have been studied by many researchers in the past decade. However, they ignore the social relationships among users. In fact, these relationships can improve the accuracy of recommendation.

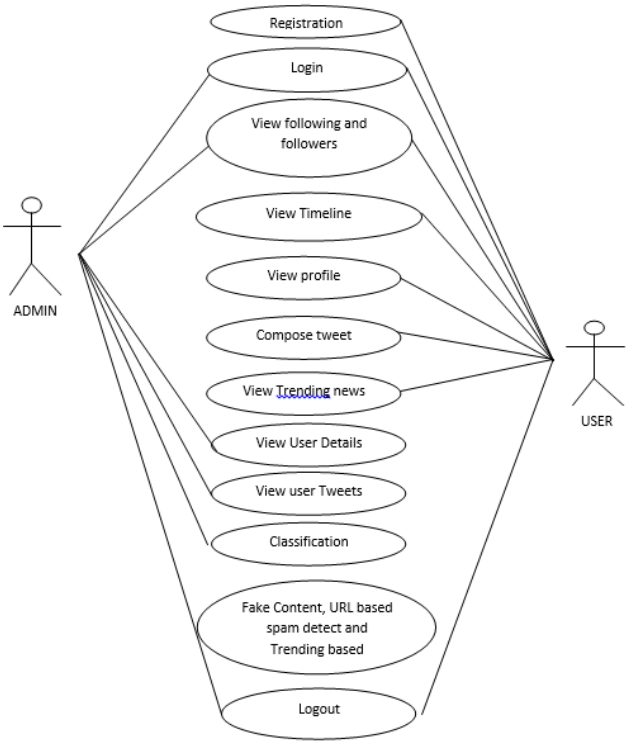

Fig 1:Use Case Diagram.

In recent years, the study of social-based recommender systems has become an active research topic. In this paper, we propose a social regularization approach that incorporates social network information to benefit recommender systems. Both users' friendships and rating records (tags) are employed to predict the missing values (tags) in the user-item matrix. Especially, we use a biclustering algorithm to identify the most suitable group of friends for generating different final recommendations. Empirical analyses on real datasets show that the proposed approach achieves superior performance to existing approaches.

4. SPAM REVIEW DETECTION (SRD) USING THE SPAMMER BEHAVIORAL METHOD

Spam review detection using the spammer behavioral method finds the unusual spammer patterns and relationships between different spammers. Only a few studies have explored spam review detection using the spammer behavioral method to date. For example, Mukherjee et al. developed a spam review detection method using a clustering technique by modelling the spamicity of the reviewer to identify spammer and not-spammer clusters. Heydari et al. have proposed a model incorporating only time series feature of the reviewer on an Amazon real dataset. Kc and Mukherjee offered a text mining model by using the unsupervised approach and features, relying upon the time integration among multiple time durations. In addition, this model was integrated with the semantic

language model for spotting spam reviews and used a Yelp dataset.3 Li et al. have suggested that the author spamicity unsupervised model has been based on features such as the review posting rate and temporal pattern. The model produced two clusters: spammers and truthful users. The datasets were gathered from the Chinese website Dianping4 to train the proposed model. Dematis et al. have observed a network model for spam review detection. In their work, the correlation among users and products was captured and the algorithm was used to recognize the spam reviews. Based on the review of spammer behavioral models, it has been observed that most of existing studies have only utilized time series-based spammer behavioral feature. It is analyzed that utilizing rich set of behavioral features can help in improving the accuracy of spammer identification. Therefore, the proposed behavioral framework utilizes thirteen spammer behavioral features to calculate spam score in spam review identification.

5. SPAM REVIEW DETECTION (SRD) USING THE LINGUISTIC METHOD

The spam review detection problem was first studied in 2007 by Jindal and Liu [18]. They analyzed 5.8 million reviews from Amazon.com. The key focus of this research was on review text. The authors have found many duplications of review content and analyzed that a spammer mostly copies the review content for a different purpose after a little modification. The authors trained the model by using the logistic regression classifier. Lau et al.have applied the semantic language model to identify spam reviews. The authors used the Support Vector Machine classifier to train the proposed method. Li et al. used a supervised learning approach with a co-training method to highlight spammers based on linguistic features. Fusilier et al. proposed a classification method that used N-gram characters as a linguistic feature. Moreover, the proposed method used the Naïve Bayes to classify spam and not-spam reviews. Ott et al. have designed a dataset for spam review detection, employing a crowd source through AMT (Amazon Mechanical Turk). The authors found that the classifier performed better by adding elements such as psycholinguistic features. Hazim et al. used statistically based features for the Extreme Gradient Boost Model and Generalized Boosted Regression Model to evaluate multilingual datasets (i.e., the Malay and English languages). It was observed by the experimental results that the Extreme Gradient Boost Model performed better for the English review dataset and the Generalized Boosted Regression Model performed better for the Malay dataset. Kumar et al. have proposed a hierarchical supervised-learning method. This method analyzed reviewer's behavioral features and their interactions using multivariate distribution. Zhang et al recommended a supervised model based on reviewer features to identify spam reviews. Ahmed and Danti used various rule-based machine learning algorithms. Moreover, the authors compared the effectiveness of the proposed method through a Ten-Fold cross-validation training model for sentiment classification. Lin et al. performed different experiments using the threshold-based method to identify spam reviews. The authors proposed different time-sensitive features to find spam reviews as early as possible and trained the model by using the SVM classifier. Li et al. used the feature-based sparse additive generative model and the SVM classifier to discover the general rule for spam review detection. Based on the literature review, it has been observed that most of the existing studies did not incorporate a number of important linguistic features while designing linguistic feature-based SRD models and utilized only one classifier to train their proposed models. The current study, therefore, extends the SRD domain to design a linguistic model utilizing several features, including stemming and N-gram techniques. These features have significantly improved the accuracy of the proposed model in spam review identification. Moreover, the proposed model utilizes and compares the accuracy of four different classifiers, including Naïve Bayes (NB), Logistic Regression (LR), Support Vector Machine (SVM) and Random Forest (RF) to further improve the accurate prediction of spam review.

6. CONCLUSION

In this paper, we performed a review of techniques usedfor detecting spammers on Twitter. In addition, we also presented a taxonomy of Twitter spam detection approachesand categorized them as fake content detection, URL basedspam detection, spam detection in trending topics, and fakeuser detection techniques. We also compared the presented techniques based on several features, such as user features,content features, graph features, structure features, and timefeatures. Moreover, the techniques were also compared interms of their specified goals and datasets used. It is anticipatedthat the presented review will help researchers findthe information on state-of-the-art Twitter spam detection techniques in a consolidated form.Despite the development of efficient and effective approaches for the spam detection and fake user identification. Twitter, there are still certain open areas that requireconsiderable attention by the researchers. The issues arebriefly highlighted as under:False news identification on social media networks isan issue that needs to be explored because of the seriousrepercussions of such news at individual as well as collectivelevel. Another associated topic that is worthinvestigating is the identification of rumor sources on socialmedia. Although a few studies based on statistical methodshave already been conducted to detect the sources ofrumors, more sophisticated approaches, e.g., social networkbasedapproaches, can be applied because of their proveneffectiveness.

REFERENCE

[1] C. Chen, S. Wen, J. Zhang, Y. Xiang, J. Oliver, A. Alelaiwi, and M. M. Hassan, ''Investigating the deceptive information in Twitter spam,'' Future Gener. Comput. Syst., vol. 72, pp. 319–326, Jul. 2017.

[2] I. David, O. S. Siordia, and D. Moctezuma, ‘‘Features combination for the detection of malicious Twitter accounts,’’ in Proc. IEEE Int. Autumn Meeting Power, Electron. Comput. (ROPEC), Nov. 2016, pp. 1–6.

[3] M. Babcock, R. A. V. Cox, and S. Kumar, ‘‘Diffusion of pro- and anti-false information tweets: The black panther movie case,’’ Comput. Math. Org. Theory, vol. 25, no. 1, pp. 72–84, Mar. 2019.

[4] S. Keretna, A. Hossny, and D. Creighton, ‘‘Recognising user identity in Twitter social networks via text mining,’’ in Proc. IEEE Int. Conf. Syst., Man, Cybern., Oct. 2013, pp. 3079–3082.

[5] C. Meda, F. Bisio, P. Gastaldo, and R. Zunino, ‘‘A machine learning approach for Twitter spammers detection,’’ in Proc. Int. Carnahan Conf. Secur. Technol. (ICCST), Oct. 2014, pp. 1–6.

[6] T. Ong, M. Mannino, and D. Gregg, ‘‘Linguistic characteristics of shill reviews,’’ Electron. Commerce Res. Appl., vol. 13, no. 2, pp. 69–78, Mar. 2014.

[7] I. Dematis, E. Karapistoli, and A. Vakali, ‘‘Fake review detection via exploitation of spam indicators and reviewer behavior characteristics,’’ in Proc. Int. Conf. Current Trends Theory Pract. Inform. Cham, Switzerland: Edizioni Della Normale, 2018, pp. 581–595

[8] H. Li, Z. Chen, A. Mukherjee, B. Liu, and J. Shao, ‘‘Analyzing and detecting opinion spam on a large-scale dataset via temporal and spatial patterns,’’ in Proc. Int. Conf. Web Social Media, 2015, pp. 634–637.

[9] B. Liu and L. Zhang, ‘‘A survey of opinion mining and sentiment analysis,’’ in Mining Text Data. Boston, MA, USA: Springer, 2012, pp. 415–463

[10] S. Zhou, Z. Qiao, Q. Du, G. A. Wang, W. Fan, and X. Yan, ‘‘Measuring customer agility from online reviews using big data text analytics,’’ J. Manage. Inf. Syst., vol. 35, no. 2, pp. 510–539, Apr. 2018.

[11] L. Chen, L. Chun, L. Ziyu, and Z. Quan, ‘‘Hybrid pseudo-relevance feedback for microblog retrieval,’’ J. Inf. Sci., vol. 39, no. 6, pp. 773–788, Dec. 2013. [12] C. Lin, Z. Huang, F. Yang, and Q. Zou, ‘‘Identify content quality in online social networks,’’ IET Commun., vol. 6, no. 12, pp. 1618–1624, 2012

Doping and Doping Less III-V Tunnel FETs: Investigation on Reasons for ON Current Improvement

[1] N. Anjani Devi, [2] Ajay kumar Dharmireddy, [3] Sreenivasa Rao Ijjada

[1] Research Scholar, Department of Electronics and Communication Engineering, GITAM Deemed to be University, Vishakapatnam, Andhra Pradesh, India
[2] Assistant Professor, SIR C.R.Reddy College of Engineering, Eluru, Andhra Pradesh, India
[3] Department of Electronics and Communication Engineering, GITAM Deemed to be University, Vishakapatnam, Andhra Pradesh, India

Abstract:

The low band gap material Tunnel FETs shows fundamentally different mechanism than conventional Si TFETs. InAs/Si TFETs are designed in this work. And ON current I_{ON}=1.0 X 10^{-5} A/µm is attained. This drain current does'nt meet ITRS requirements. The random dopant fluctuation (RDF) is limiting the ON current by effecting V_{TH}. Hence doping less InAs/Si TFET is designed by employing charge plasma to induce the carriers into source and drain. The RDF effects are hence removed and ON current of 2.6X10^{-3} A/µm and subthreshold slope SS of 19.5 mV/dec are obtained.

Keywords:

Doping, Tunnel FET

1. INTRODUCTION

To overcome the theoretical constraints and limitations like short channel Effects, Tunnel field effect transistor (TFET) shows enhances performance and replaces conventional MOSFET. However, still random carrier fluctuations show degradation of device performance by increasing I_{OFF}. To overcome this problem doping less Tunneling FET are also studied. Gate field plate structure is introduced in Si TFETs and ON current improvement is noted in compared to Si TFETs [1]. The effect of using high K dielectric and its induced fringing fields improves the ON current in Si TFETs [2]. The operating principle and its designing are described in [10]. The designs are trying to improve gate controlling tunneling by that ON current can be improved. But the I-V characteristics shows very weak temperature dependence [3]. The variation in performance parameters ON current, OFF current, Subthreshold swing are due to variations in gate oxide K value, material, oxide thickness. The effect geometrical variations are discussed in [4-5]. But another significant effect to be considered with device scaling is "Random dopant Fluctuations (RDF)". The RDF impacts the I-V characteristics which is non negligible. The double gate TFET is investigated for RDF effects and threshold voltage variations, transconductance shifts, subthreshold shifts are reported in [6]. Hence, without doping, charge plasma TFETs are designed and analysed [7-9]. This paper investigates the reasons for ON current improvement and also subthreshold slope shifts by designing and simulating both doping, doping less III-V Tunnel FTES.

Keywords: FTES, TFET, RDF, Device specifications and simulations:

i. Conventional InAs/Si TFET:

For the simulation InAs/Si hetero junction dual gate Tunnel FET is designed with HFO_2 gate oxide. Chanel thickness is 1.2nm, gate thickness is 1.6nm, Silicon thickness t_{si} is 20nm, gate length is 40nm. Technology computer aided design (TCAD) is used to simulate both designs. InAs is considered as source material to ensure low bandwidth and high tunneling probability. But channel and drain are Si only which makes the device hetero junction. The Si on drain side makes the device more sustain with ambipolar current. The 40nm InAs/Si HTFET is shown in figure 1. The drain current can be continuously evaluated without any deviations in geometrical measurements using dynamic non-local BTBT model [4].

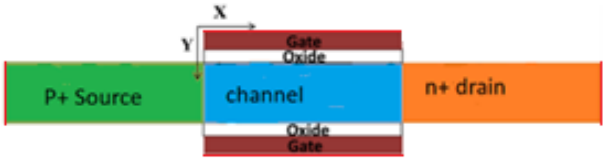

Fig 1: Dual gate hetero InAs/Si TFET

Fermi dirac distributions of source and channel f_s, f_{ch} has much effect on tunneling probability and hence on drain current I_D or I_{ON}. The total tunneling current is given as equation 1.[10]

$$I_T \propto \int_{CB(ch)}^{VB(s)} P_T(E)[f_s(E) - f_{ch}(E)]dE \qquad [1]$$

 ISBN: 978-93-90214-20-4

And the SS depends on and exhibits different trends with fermi dirac distributions [11]. To attain desirable SS value, let us consider source valance band maximum is very much greater than E $F_{p,s} + 3k_bT$. In this condition SS shows progressively increasing from 0mV/dec. and it given as equation 2.

$$SS \propto ln(10).\frac{E_{fp,s} - CB_{ch,min}}{q} \quad [2]$$

The channel conduction band lies within $3k_BT < C\ B_{ch,min} < V\ B_{s,max} - 3k_BT$. Which leads to SS value to 60mV/dec at 300K. Hence, Fermi-Dirac distribution in doped TFTEs have considerable impact and large source doping leads to larger gate voltage sweep. Thus, the sub 60mV/dec values for subthreshold swing can be attained by double gate Tunnel FETs. Using nonlocal band to band tunneling algorithm the drain current is extracted from I-V characteristics. The transfer characteristics are shown in fig.2.

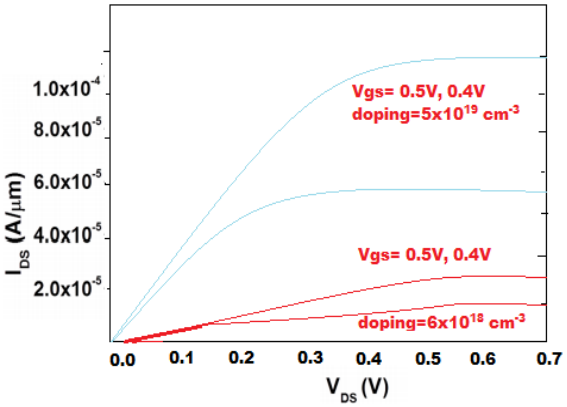

Fig 2: simulated output characteristics in TCAD and captured saturation

The Transfer characteristics obtained with two different BTBT models is shown in fig 3. The non-local tunnelling path model and dynamic barrier tunnel model are used to analyse the characteristics. The barrier height can be effectively changed using barrier tunnel model and so the characteristics are improved over nonlocal BTBT model.

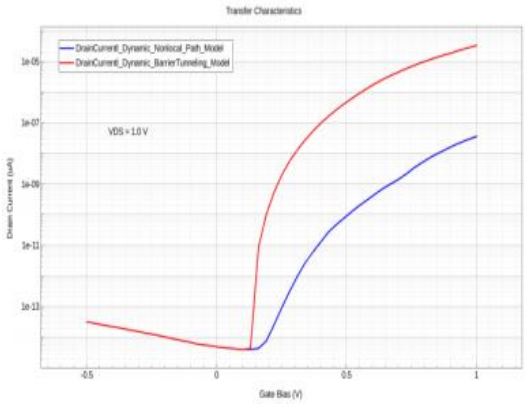

Fig 3: V_{GS} vs I_D at V =1.0V for two different BTBT models

ii. Doping less Charge plasma InAs/Si TFET:

In the process of attaining large ON currents with TFETs, many architectures were described [12-15]. The hetero junction InAs/Si doping less charge plasma dual gate TFET is shown in figure 4.

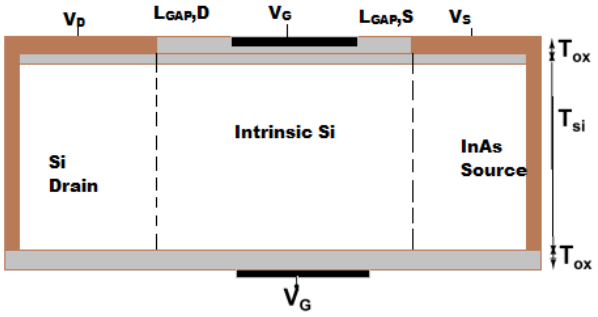

Fig 4: The cross-sectional view of charge plasma dual gate Tunnel FET

The charge plasma TFET without doping is demonstrated in this work. To avoid random dopant fluctuations effect and so that to overcome V_{TH} variations charge plasma induced TFET is considered. The L_{GAP} is the spacer oxide thickness at source an drain side. L_{GAP}, S is 3nm and L_{GAP}, D is 15nm. Gate workfunction plays important role in improving characteristics and workfunction $\boldsymbol{\phi}$=4.5 for both gates. At the channel length of 50nm, the T_{ox}=3nm, T_{Si}= 10nm are considered. All the simulation parameters are same as the device in fig 1. except the carrier concentration of n_i=1.0x10^{15}cm^{-3}. The Drain characteristics at V_{GS}=1.0v to 1.3V at the intervals of 0.1V are shown in figure 6.

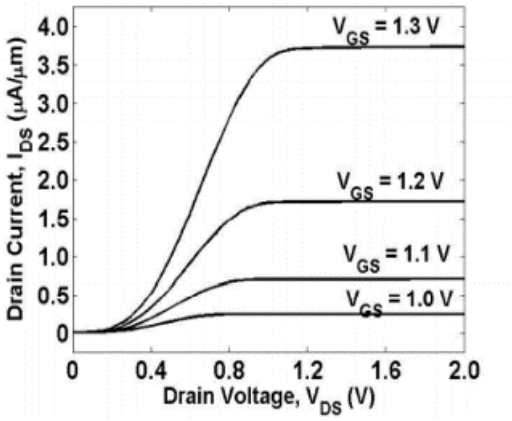

Fig 6: The output characteristics of charge plasma InAs/Si TFET

2. RESULTS AND DISCUSSION:

In the conventional InAs/Si the source and drain regions are uniformly doped and source doping profile should be sharp to improve the tunneling probability. Whereas in doping less TFET the metal electrodes used to induce carriers are only on top side makes the carrier distribution asymmetric. The metal electrodes can be further extended to opposite side to ensure uniform carrier concentration. At V_{DS}=1.0V

 ISBN: 978-93-90214-20-4

and V_{GS} of 0V the ON current of conventional and doping less TFETs are nearly $1.1x10^{-5}$ A/μm. But in doping less TFET the drain current depends on following factors.

i. L_{GAP}, spacer between gate and drain, gate and source
ii. $\boldsymbol{\phi}$, Workfunction of source, drain, gate metal electrodes.
iii. The metal electrode length

Hence by varying above factors the drain current in doping less TFET is improved. At L_{GAP} of 3nm,15nm for source and drain and work function of 4.5eV the ON current I greatly improved to 54%. The comparison of performance parameters for conventional and doping less charge plasma TFET are shown in table 1.

Table 1: comparison of performance parameters

Design	I_{ON}(A/μm)	I_{OFF}(A/μm)	SS (mV/dec)
Conventional InAs/Si TFET	$1.0x10^{-5}$	$1x10^{-17}$	41.54
Doping less InAs/Si	$2.6x10^{-3}$	$3.64x10^{-15}$	19.5

3. CONCLUSION

The low band gap material InAs greatly improves tunneling probability and ON current is improved in InAs/Si conventional TFET compared to Si TFET. Random dopant fluctuations (RDF) is one of constrain to ON current improvement. V_{TH} variations can be overcome by supressing RDF. Hence doping less charge plasma InAs/Si dual gate TFET is designed to avoid RDF effects. Even though the drain current characteristics are very much similar in both the devices, by varying spacer thickness and metal electrode work function I_{ON} of $2.6x\ 10^{-3}$ A/μm is achieved and SS of 19.5mV/dec is obtained. Hence the novel technique charge plasma facilitates to improve device performance by varying geometrical parameters.

REFERENCE

[1] XIANGZHAN WANG, ZHOUQUAN TANG, "Gate Field Plate Structure for Subthreshold Swing Improvement of Si Line-Tunneling FETs," IEEE Trans. On Device and Materials Reliability, vol. 9, no. 3, pp. 490-495, oct. 2010.

[2] Krishna K. Bhuwalka, Martin Sauter "Fringing-Induced Drain Current Improvement in the Tunnel Field-Effect Transistor with High-κ Gate Dielectrics", IEEE Trans. 2015.

[3] M. Born, K. K. Bhuwalka, M. Schindler, U. Abelein, M. Schmidt, T. Sulima, and I. Eisele, "Tunnel FET: A CMOS device for wide temperature range," in Proc. 25th Int. Conf. MIEL, Belgrade, Serbia, May 14–17, 2006, pp. 124–127.

[4] S. Saurabh and M. J. Kumar, "Estimation and Compensation of ProcessInduced Variations in Nanoscale Tunnel Field-Effect Transisitors for Improved Reliability," IEEE Trans. On Device and Materials Reliability, vol. 10, no. 3, pp. 390-395, Sep. 2010.

[5] L. Zhang and M. Chan, 'The Impact of Device Parameter Variation on Double Gate Tunneling FET and Double Gate MOSFET," IEEE EDSSC, 2010.

[6] Numerical Study on Effects of Random Dopant Fluctuation in Double Gate Tunneling FET Ying Zhul , Yun Yel , Yu Caol , 2 , Jin Hel , 3 , Aixi Zhangl , 3 , Hongyu Hel , Hao Wangl , Chenyue Mal , Yue Hul , Mansun Chan3 , and Xiaoan Zhu3, 978-1-4673-2523-3/13/$31.00 ©20 13 IEEE

[7] L. De Michielis, L. Lattanzio, and A. M. Ionescu, "Understanding the superlinear onset of tunnel-FET output characteristic," IEEE Electron Device Lett., vol. 33, no. 11, pp. 1523–1525, Nov. 2012.

[8] J. Knoch, M. T. Bjork, H. Riel, H. Schmid, and W. Riess, "One dimensional nano electronic device—Toward the quantum capacitance limit," in Proc. Device Res. Conf., Jun. 2008, pp. 173–176.

[9] J. Knoch, S. Mantl, and J. Appenzeller, "Impact of the dimensionality on the performance of tunneling FETs: Bulk versus onedimensional devices," Solid-State Electron., vol. 51, no. 4, pp. 572–578, Apr. 2007.

[10] K. K. Bhuwalka, J. Schulze, and I. Eisele, "A simulation approach to optimize the electrical parameters of a vertical tunnel FET," IEEE Trans. Electron Devices, vol. 52, no. 7, pp. 1541–1547, Jul. 2005.

[11] Tunneling and Occupancy Probabilities: How Do They Affect Tunnel-FET Behavior? Luca De Michielis, Livio Lattanzio, Kirsten E. Moselund, Heike Riel, and Adrian M. Ionescu. IEEE ELECTRON DEVICE LETTERS, VOL. 34, NO. 6, JUNE 2013

IFERP International Conference
IFERP Explore

https://icrcest.com/ | info@icrcest.com

UPCOMING CONFERENCES

Technoarete® Group

Integrating Researchers to Incubate Innovation

SUPPORTED BY

ALL CONFERENCE ALERT
Academics conferences at a glance

ECA
Get World wide Engineering Conferences Update..

Conference Alerts
Global Academic Conferences

INTERNATIONAL CONFERENCE ALERTS